

Communication 3

LABORATOIRE DE CONSTRUCTIONS HYDRAULIQUES

Département de Génie Civil

Ecole Polytechnique Fédérale de Lausanne



EXPANDING STILLING BASIN

Roger BREMEN

Directeur du Laboratoire :
Prof. R. Sinniger

LAUSANNE, 1990

PREFACE

An unknown large number of stilling basins of different types have been built over a period of many decades in relation to hydropower, flood control, irrigation facilities and urban water systems. Not only have many model tests been performed in connection with these constructions but also fundamental studies were undertaken to search for general applicable laws as an aid for the design engineer.

One may ask therefore if today a further study can add something new in this particular field. After three years of thorough theoretical and experimental analysis the answer is *yes*.

As regards the *sequent depths* ration for expanding basins, in equation (5.26) for the first time a simple expression including all essential parameters is established.

As an answer to the often encountered problem of *asymmetric flow* in sudden expanding basins, a characterization of three main flow domains is represented in figure 5.27, permitting the judgement of the flow character in the early design phase.

With the aim to establish rules for the design of economic and satisfactorily functioning stilling basins, a number of devices were tested, searching for the most performant one. General applicable rules have then finally been found for the design of a sill geometry and its position, leading to a symmetric flow, keeping the basin length within reasonable limits.

Professor Richard Sinniger

RESUME

Dans le domaine des constructions hydrauliques, les ouvrages de dissipation d'énergie occupent une place prépondérante. Ces structures doivent permettre une restitution de l'eau à la rivière sans engendrer d'érosions.

Pour permettre cette dissipation d'énergie, une des solutions envisageables consiste en la mise en place d'un bassin amortisseur. Le fonctionnement de ces bassins se base sur le phénomène du ressaut hydraulique permettant de dissiper une importante quantité de l'énergie cinétique de l'eau. Les caractéristiques de l'écoulement à l'intérieur du dissipateur dépendent d'une part des conditions à l'entrée du bassin (vitesse et débit d'eau), des conditions à l'aval (niveau du plan d'eau) ainsi que de la forme du dissipateur.

Le présent travail traite de bassins amortisseurs comportant un élargissement de la section transversale. La largeur du dissipateur s'accroît donc de l'amont vers l'aval. Comparé à un dissipateur prismatique, ce type de bassin amortisseur présente un certain nombre d'avantages, notamment :

- hauteur conjuguée nécessaire inférieure pour des conditions à l'entrée identiques, et
- adaptabilité de la forme du dissipateur aux caractéristiques de la rivière.

D'autre part, les bassins amortisseurs avec élargissement présentent un certain nombre d'inconvénients parmi lesquels il faut citer :

- le risque d'écoulement asymétriques dans le dissipateur et à l'aval,
- le manque de méthodes de calcul confirmées par des essais sur prototypes, et
- un volume global du ressaut supérieur à celui d'un dissipateur prismatique.

En raison de ces inconvénients, la diffusion des dissipateurs avec élargissement reste aujourd'hui assez limitée.

L'objectif de cette recherche était donc d'une part de mieux connaître le comportement de ce type d'ouvrage et d'autre part de proposer des solutions permettant de pallier à ces inconvénients majeurs. Une vaste étude expérimentale a donc été conduite dans le Laboratoire de Constructions Hydrauliques de l'EPFL. Après une description des différents types d'écoulements pouvant se présenter dans un tel dissipateur, une première partie de l'étude a été consacrée au développement d'une méthode de calcul permettant d'évaluer les caractéristiques essentielles du ressaut

dans un tel bassin. Cette méthode permet donc de prévoir à partir des conditions à l'entrée du dissipateur et de sa géométrie,

- les hauteurs conjuguées,
- la position du ressaut par rapport à l'expansion,
- la longueur du ressaut, et
- la symétrie de l'écoulement.

La deuxième partie de l'étude a été consacrée à la recherche et l'optimisation de moyens constructifs permettant d'améliorer les écoulements dans ce type d'ouvrage. Ces éléments doivent notamment permettre une réduction de sa longueur, un écoulement symétrique ainsi qu'une répartition des vitesses uniformes à l'aval du dissipateur. Après une comparaison qualitative de différentes solutions envisageables, un seuil central fixé sur le fond du dissipateur s'est révélé comme le plus efficace. Une étude détaillée a donc été consacrée à l'optimisation de la position et de la géométrie du seuil, ceci en fonction des conditions à l'entrée du bassin amortisseur et de sa géométrie. Sur la base de la méthode de calcul d'une part et de l'optimisation du seuil central d'autre part, un nouveau dissipateur avec élargissement est finalement proposé.

SUMMARY

The present research deals with stilling basins involving diverging side walls. The purpose of the study was to investigate hydraulic jumps located in expanding stilling basins and to propose devices by which the characteristics of this jump may be improved.

Based on both a theoretical and an experimental approach, a computational procedure for the design of expanding stilling basins was developed. This procedure may be used for a preliminary evaluation of the main dimension of the stilling basin. A central sill turned out as the most effective device to shorten the basin length and improve the flow symmetry. Several numerical examples illustrates the computational procedure outlining thereby the influence of the expansion on the overall jump characteristics.

ZUSAMMENFASSUNG

Die vorliegende Forschungsarbeit befasst sich mit seitlich aufweitenden Tosbecken. Es wird einerseits das Verhalten des Wassersprunges in seitlich aufgeweitete Tosbecken beschrieben, und andererseits werden verschiedene Einbauten vorgeschlagen anhand derer die Fliesseigenschaften wesentlich verbessert werden können.

Auf der Grundlage umfangreicher Modellversuche und theoretischer Erkenntnisse, sind mehrere Beziehungen entwickelt worden, die eine einfache Vordimensionierung dieser Tosbecken ermöglichen. Eine zentrale Schwelle erwies sich als vorteilhafteste Einbaute um die Länge des Wassersprunges zu reduzieren und einen stabilen, symmetrischen Abfluss sicherzustellen. Das vorgeschlagene Dimensionierungsverfahren wird anhand zahlreicher numerischer Beispiele erläutert wobei der Einfluss der seitlichen Aufweitung auf die Fliesseigenschaften jeweils beschrieben wird.

SOMMARIO

Oggetto della presente ricerca è lo studio di bacini di smorzamento con sezione trasversale crescente. Particolare attenzione è rivolta alla determinazione del comportamento del risalto idraulico in questo tipo di bacini e alla ricerca di soluzioni costruttive tali da migliorarne sensibilmente le caratteristiche di funzionamento

Sulla base di una ricerca teorico-sperimentale, viene sviluppato e presentato un modello di calcolo per il dimensionamento del bacino. In quest'ambito si rivela di particolare importanza la presenza di una soglia centrale capace di ridurre la lunghezza del dissipatore creando contemporaneamente un flusso stabile e simmetrico. Numerosi esempi numerici illustrano il modello di calcolo proposto, mettendo in evidenza l'influenza dell'espansione sulle caratteristiche del risalto.

TABLE OF CONTENTS

1.	INTRODUCTION.....	1
1.1	Preliminary remarks.....	1
1.2	Application domains of expanding energy dissipators	1
1.3	Scope of the present research project	4
1.4	Description of the investigation.....	5
2.	DESCRIPTION OF FLOW PHENOMENA.....	7
2.1	Introduction.....	7
2.2	Sudden expansion.....	8
2.2.1	Cyclic flow phenomenon	8
2.2.2	Repelled hydraulic jump in sudden expansion (R-jump).....	12
2.2.3	Spatial hydraulic jump in sudden expansion (S-jump)	14
2.2.4	Transitional hydraulic jump in sudden expansion (T-jump).....	15
2.3	Gradual linear expansion	17
2.3.1	Cyclic flow phenomena	17
2.3.2	Repelled hydraulic jump in gradual linear expansion (R-jump).....	19
2.3.3	Spatial hydraulic jumps in gradual linear expansion (S-jump)	21
2.3.4	Transitional hydraulic jumps in gradual expansion (T-jump).....	22
2.4	Domain of investigation.....	23
2.5	Conclusions.....	24

3.	LITERATURE REVIEW	27
3.1	Introduction.....	27
3.2	Sudden expansions	27
3.2.1	Notation.....	27
3.2.2	Spatial hydraulic jump (S-jump).....	29
3.2.3	Repelled hydraulic jumps (R-jumps).....	36
3.2.4	Transitional hydraulic jumps (T-jump)	39
3.2.5	Comments on hydraulic jumps in sudden expansions	43
3.3	Gradual expansions	45
3.3.1	Spatial hydraulic jump (S-jumps).....	45
3.3.2	Repelled hydraulic jumps (R-jumps).....	48
3.3.3	Comments on hydraulic jumps in gradual expansions.	58
3.4	Diverging stilling basin.....	58
3.5	Conclusions.....	61
4.	EXPERIMENTAL INSTALLATIONS.....	63
4.1	Introduction.....	63
4.2	Installation LCH1.....	63
4.3	Installation LCH2.....	66
4.3.1	Inlet tank.....	67
4.3.2	Test channel.....	69
4.4	Measuring devices.....	71
4.4.1	Instrument supporting devices.....	71
4.4.2	Flow depth and pressure head.....	73
4.4.3	Velocity measurement.....	74
4.5	Discharge measurement.....	77
4.6	Computation of small flow depths	80
4.6.1	Assumptions	80
4.6.2	Method of computation	81
4.7	Conclusions.....	82

5.	SUDDEN EXPANSION.....	85
5.1	Introduction.....	85
5.2	Description of experiments	85
5.3	Toe position X_1	89
5.4	Conventional momentum approach.....	92
5.5	Sequent depths	97
	5.5.1 Introduction	97
	5.5.2 Effect of shape factor ω_1	98
	5.5.3 Limit conditions.....	98
	5.5.4 Effect of X_1	100
	5.5.5 Discussion of results	103
	5.5.6 Energy dissipation.....	107
	5.5.7 Volume and efficiency of jump	108
5.6	Comparison with experimental results	111
	5.6.1 Introduction	111
	5.6.2 Computational models	111
	5.6.3 Unny's experimental investigation	112
	5.6.4 Herbrand's experimental investigation.....	113
	5.6.5 Experiments of Sethuraman and Padmanabhan.....	115
	5.6.6 Comments on present experiments	115
5.7	Length of transitional jump	118
	5.7.1 Introduction	118
	5.7.2 Experimental investigation.....	118
	5.7.3 Computational model.....	121
5.8	Symmetry of jump.....	122
5.9	Numerical example	126
5.10	Conclusions	128
6.	EFFECT OF NEGATIVE STEP	131
6.1	Introduction.....	131
6.2	Description of experiments	131
6.3	Conventional momentum approach.....	133

6.4	Sequent depths.....	137
6.4.1	Introduction	137
6.4.2	Sequent depth ratio in a prismatic channel with a negative step	138
6.4.3	Sequent depth in sudden expansion with negative step.....	141
6.5	Jump length.....	144
6.6	Jump symmetry	145
6.7	Numerical example	149
6.8	Conclusions.....	151
7.	EFFECT OF DEFLECTORS, BLOCKS AND SILLS.....	153
7.1	Introduction.....	153
7.2	Deflectors.....	154
7.3	Sills	159
7.3.1	Introduction	159
7.3.2	Experiments.....	159
7.3.3	Conclusions.....	168
7.4	Baffle piers	168
7.5	Conclusions.....	172
8.	SUDDEN EXPANSION WITH CENTRAL SILL.....	175
8.1	Introduction.....	175
8.2	Stilling basin performance	175
8.3	Experimental investigation.....	177
8.4	Sequent depths ratio	179
8.5	Jump length with central sill.....	180
8.6	Jump symmetry	182
8.6.1	Effect of sill position.....	182
8.6.2	Effect of the sill height.....	186
8.7	Experiments with erodible channel bed.....	189

8.7.1	Stilling basin without baffle elements	189
8.7.2	Stilling basin with central sill	191
8.7.3	Gradual expansion with central sill	192
8.7.4	Basin length and dissipator volume	193
8.8	Cavitation aspects.....	195
8.9	Numerical example	196
8.10	Conclusions.....	198
9.	CONCLUSIONS	201
9.1	Preliminary remarks.....	201
9.2	Jump patterns in expanding channels.....	202
9.3	Prediction of main jump patterns in sudden expansions	203
9.3.1	Introduction	203
9.3.2	Prediction of sequent depths ratio	204
9.3.3	Prediction of jump length	206
9.3.4	Evaluation of the jump symmetry	207
9.3.5	Prediction of sill geometry	208
9.4	Conclusive remarks.....	210

APPENDIX I

APPENDIX II

APPENDIX III

REFERENCES

1. INTRODUCTION

1.1 PRELIMINARY REMARKS

One of the tasks of the hydraulic engineer is the design of energy dissipating structures. The purpose of such a structure is to dissipate part of the kinetic energy of the inflowing stream in order to return safely the flow to the downstream channel or river. Based on the energy dissipating action of hydraulic jumps, stilling basins are one of the possible solutions which may be adopted (Mason, 1982).

The required design information may be grouped in the following three categories:

1. Inflowing and outflowing conditions,
2. Local geological and topographical conditions, and
3. Computational models.

Based on the information at his disposal, the hydraulic engineer should design a safe and economic energy dissipator. The safety of the designed structure depends on the extent of data available for items 1 and 2 on the one hand, and on the accuracy of the computational models on the other hand.

The present study describes a chronological course of works undertaken from 1987-1990 at the «Laboratoire de Constructions Hydrauliques» of the «Ecole Polytechnique Fédérale de Lausanne» (EPFL). Some parts of the study are not directly applicable to the design of dissipating structures since these involved versions incompatible with design requirements. However, the final solution should be an adequate alternative to the actual design of prismatic energy dissipators.

The investigation undertaken illustrate the hydraulic aspects which should be considered in the design of dissipating structures involving a hydraulic jump in an expanding channel. Compared to a prismatic geometry, an expansion modifies not only the sequent depths ratio, but influences significantly several other flow characteristics of the hydraulic jump, such as the jump symmetry and the jump length. In order to predict the flow pattern of hydraulic jumps in expanding channels, particular attention should be paid to those flow phenomena which cannot be observed in prismatic geometries.

The study was limited to hydraulic aspects related to the design of non-prismatic free surface energy dissipators. Other design aspects such as construction procedures will not be discussed hereafter.

1.2 APPLICATION DOMAINS OF EXPANDING ENERGY DISSIPATORS

When a supercritical flow enters a wider channel at the downstream end of which subcritical flow prevails, the hydraulic jump occurs in a non-prismatic channel. The width of the tailwater channel is then larger compared to the supercritical inflow width. In order to illustrate some applications, three examples will briefly be presented in this paragraph.

In the first example, the approaching channel is controlled by a number of gates. If only parts of the gates are in operation, the width of approaching flow is smaller than the width of tailwater channel, and the geometry of jump is non-prismatic.

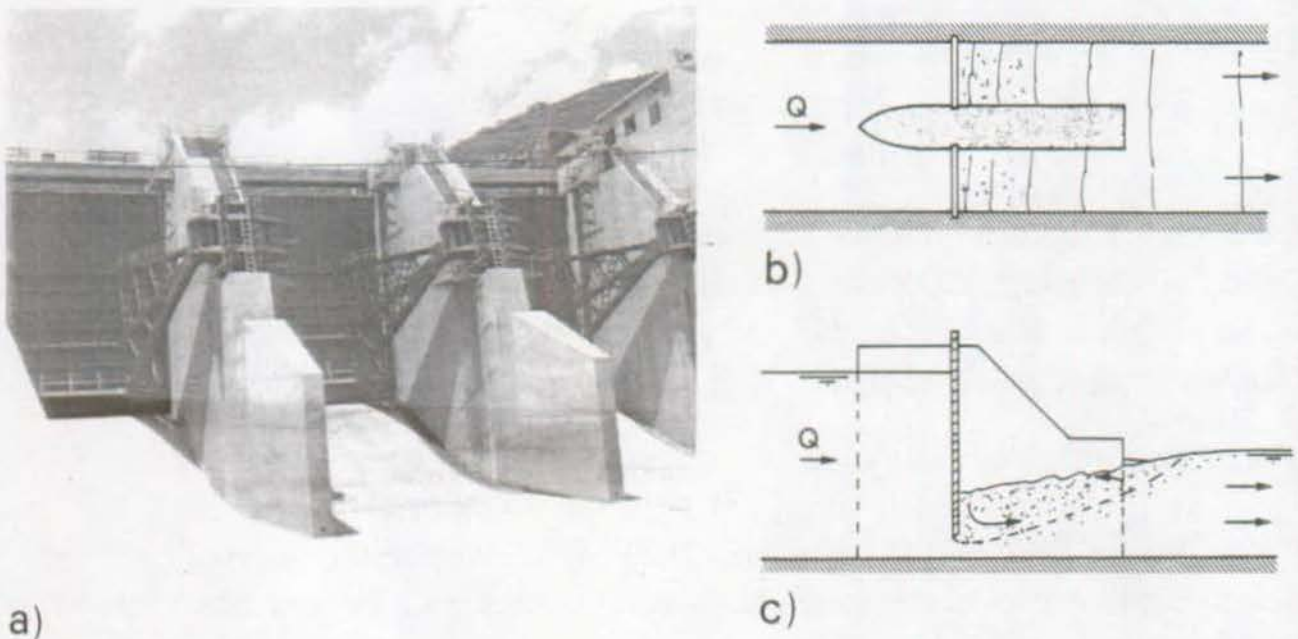


Fig. 1.1 : Example of spillway gates. a) Layout of Kotmale dam (Sri Lanka) ; b) effect of the pier width on the jump expansion. c) submerged hydraulic jump.

The hydraulic jump is either submerged (Fig. 1.1c) or unsubmerged depending on the tailwater conditions. As indicated in Fig. 1.1b), the pier width may also produce an expansion effect on the hydraulic jump. An appropriate computational model is then required to evaluate the position of jump for different inflow and tailwater conditions.

In the second example, shown in Fig. 1.2, a bottom outlet is considered. Therein, the width of the river, downstream from the stilling basin is several times larger than the bottom outlet gate. In order to predict the conditions for which the bottom outlet

would be submerged, an appropriate computational model accounting for the width difference must be used. Furthermore, the risk of asymmetric flows should be evaluated.

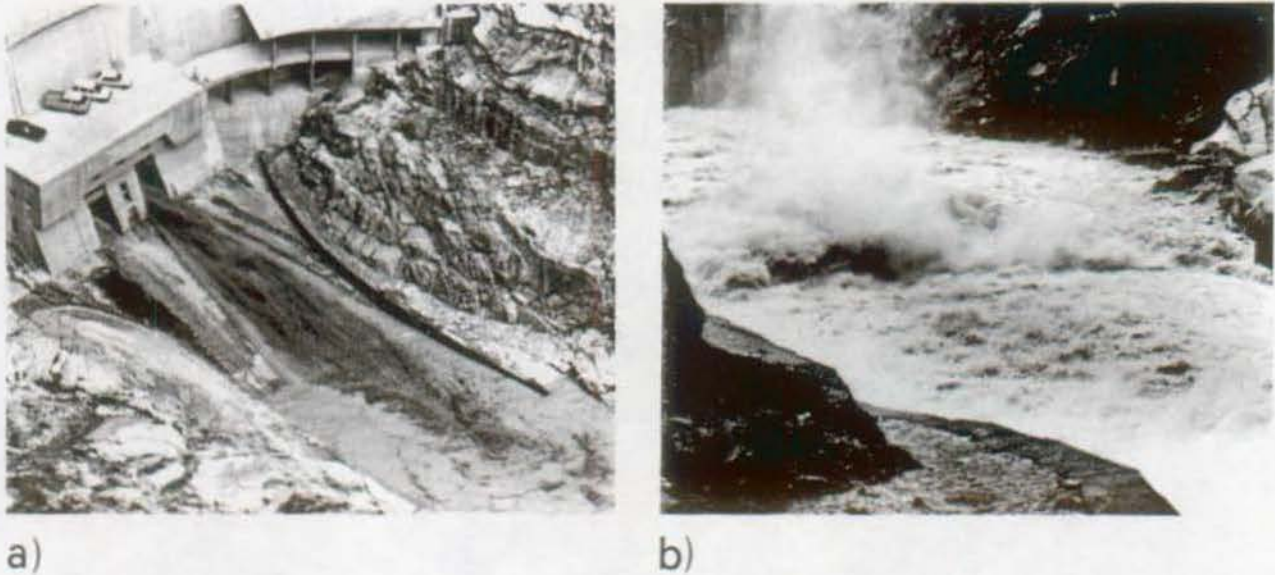


Fig. 1.2 : Hydraulic jump located downstream from the bottom outlet of Gebidem dam (Switzerland) for unsubmerged flow conditions. a) Overall view, b) downstream view.

Finally, Fig. 1.3 shows two examples of dissipators in which sudden expanding stilling basins were provided. For safe and economical design of such structures, the main jump characteristics such as length, front position and symmetry should be predicted as accurately as possible. A computational model accounting for the expansion of flow is necessary.

Particular attention was paid to the risk of asymmetric flows formed downstream from the stilling basin. The model developed in this study allows a preliminary evaluation of this risk, and proposes effective appurtenances avoiding the asymmetry phenomenon. Additionally, a new type of stilling basin is proposed which may be both safe and economic for appropriate site conditions. In general however, the three-dimensional flow conditions occurring in non-prismatic stilling basins are difficult to predict. In order to evaluate site-specific effects on the performance of stilling basin, laboratory tests should be planned for the final design.

The three examples above indicate typical applications of a computational model for predicting the main flow pattern of hydraulic jumps formed in expanding channels.

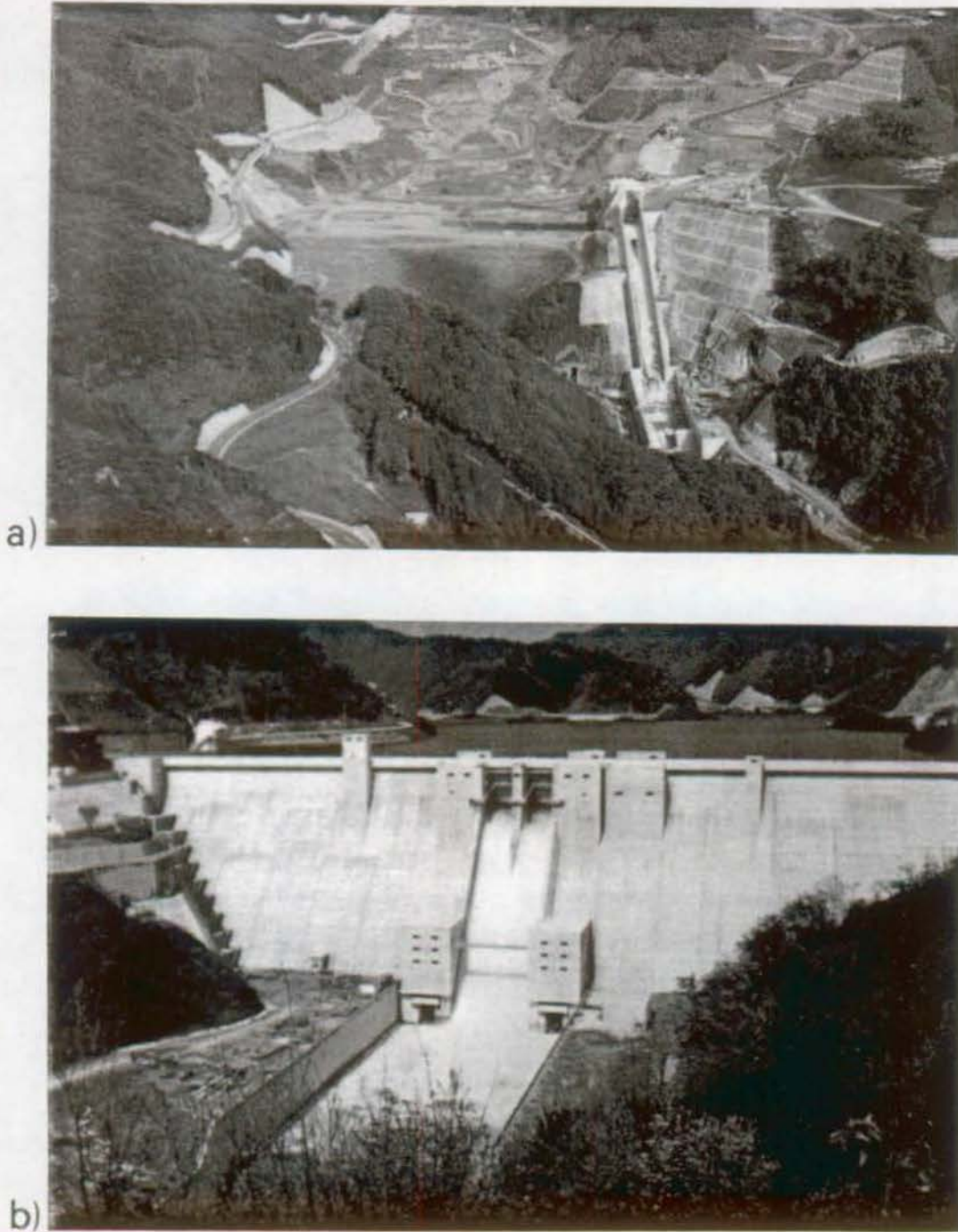


Fig. 1.3 : Stilling basin with sudden expansion. a) Arakawa dam (under construction) and b) Hitokura dam both in Japan.

1.3 SCOPE OF THE PRESENT RESEARCH PROJECT

The purpose of the present investigation is dual. Firstly, a computational method is developed to predict the main flow characteristics of hydraulic jumps in expanding channels. These characteristics are,

- the sequent depths ratio,
- the position of the jump relative to the expansion,
- the jump length, and
- the jump symmetry.

This model is established both by a theoretical approach and an extensive experimental investigation. In order to facilitate the description of the investigation extensive use is made of figures and photographs. Furthermore, numerical examples at the end of some chapters illustrate the application of the equations which have been developed .

The second part of the investigation deals with the evaluation of devices by which the flow pattern in expanding channels may be improved. The main flow problem encountered in such channels is the formation of asymmetric flows in otherwise symmetric channel geometries. Based essentially on an experimental investigation, this part widens the knowledge on asymmetric flow phenomena in expanding channels. A comparison of several devices shows the most effective appurtenance to be selected in order to avoid or prevent the flow asymmetry. In addition to the jump asymmetry, other jump characteristics such as the velocity distribution and the wave action in the tailwater channel, were evaluated.

From the research point of view, extensive use of non-dimensional groups of parameters was made, which involved only two lengths scales, throughout this project. Hence, the parameters involved in the analysis of hydraulic jumps in expanding channels are established by theoretical and experimental means. In order to conduct a reasonable yet realistic study, the geometry of energy dissipators had to be simplified. The number of parameters to be analyzed was still large, such that practical constraints were also accounted for to limit their number. From the point of view of practice different appurtenances and their effect on the flow pattern are extensively described and design recommendations for a type of expanding stilling basin are finally offered.

1.4 DESCRIPTION OF THE INVESTIGATION

In chapter 2, different flow phenomena which may occur in expanding channels are presented, thereby considering two different expansion geometries. Both, gradually and sudden expanding channels are accounted for. The description of these phenomena indicates the significant difference of the flow pattern between hydraulic jumps in prismatic and non-prismatic channels. A classification of jumps, based on

criteria such as front position and jump symmetry is presented in order to facilitate further developments.

After a qualitative description of the flow pattern in expanding channels a quantitative evaluation of the flow phenomena follows. In the literature review, presented in chapter 3, the significant investigations into hydraulic jumps in expanding channels are discussed. A comparison of several computational models outlines discrepancies between different approaches. A particular feature of the present knowledge is that almost no account exists of the problem of jump symmetry. This item will be particularly treated herein as it is closely linked to the dissipator efficiency.

The laboratory installations used for the experimental investigations are described in chapter 4. Therein, attention is paid to the accuracy of the measuring techniques used. The methods for discharge calibration and the evaluation of small flow depths in supercritical flow are also described.

Based on experimental and theoretical means, a computational model for hydraulic jumps in sudden expansions without the presence of appurtenances is presented in chapter 5. For given inflow conditions, the model allows prediction of the sequent depths ratio, the jump length, the jump position relative to the expansion section, and the jump asymmetry in terms of width ratio. The comparison of the present model with other computational methods and published experimental data ends this chapter.

In chapter 6, the effect of a negative step on the jump pattern is evaluated. The computational model developed in the preceding chapter is generalized to include the step. However, the improvement of flow expected with a negative step was only partially obtained.

A qualitative investigation of the effect of other types of appurtenances on the jump pattern is described in chapter 7. Therein the effect of different types of blocks, sills and deflectors fixed on the channel floor is evaluated. Particular attention was paid to their effect on the jump symmetry and length of jump. Based on these experiments, a sill was found to be the most effective device in improving the overall jump symmetry.

In order to design the sill, an experimental investigation which was performed is reported in chapter 8. From this, the optimum sill position and sill height as a function of the inflow conditions and the channel geometry were determined. To evaluate the bed erosion, additional experiments were performed with an erodible channel floor. The main results of the present research project are finally summarized, and design recommendations are given in chapter 9.

2. DESCRIPTION OF FLOW PHENOMENA

2.1 INTRODUCTION

To overcome the confusion encountered in the literature in defining hydraulic jumps, it seems necessary to describe in detail some typical flow configurations in non-prismatic channels. Some of the following definitions are in agreement with prior investigations. In addition, several new definitions are introduced for a better understanding of the flow phenomena. In the first part of this chapter, abrupt symmetrical expansions are considered, whereas the second part is concerned with linear gradual expansions with relatively large expansion angles.

Each flow configuration is defined as accurately as possible and extensively illustrated by photographs and schematic diagrams. Particular attention is paid to qualitative flow descriptions, as regards symmetry of flow, velocity distribution and jump length. The quantitative aspects will be considered in chapter 3 in which a detailed literature review of each flow configuration is presented.

As shown in Fig. 2.1 a channel expansion may be subdivided into three parts. Beginning from upstream, the first part is a prismatic channel referred to as the *approaching channel*. The present study is limited to horizontal approaching channels with a rectangular cross-section. The *expansion section* indicates the transition between prismatic and non-prismatic geometries. This section will be used as a reference position for various length measurements. The *expanding channel* includes the entire domain of non-prismatic geometry and is limited downstream by the *end section* which marks the transition between the non-prismatic and the prismatic channel reaches. The rectangular *tailwater channel* is prismatic and horizontal and has larger channel width than the approaching channel.

The expansion geometry may be completely defined by the expansion ratio $B=b_2/b_1$ and the total expansion angle 2ϕ . In the present chapter, only symmetrical channel geometries will be investigated. For sudden expansions (Fig. 2.1b) the end section is identical to the expansion section without an expansion channel. For such geometries the transition between the approaching and the tailwater channels will be indicated as the *expansion section*.

The present investigation accounts for hydraulic jumps located in non-prismatic channels. A hydraulic jump may be defined as a sudden transition from supercritical to subcritical flow conditions involving significant energy losses. The *toe* of the jump

indicates the upstream limit of the jump. The jump end section as well as the jump length will be defined in chapter 5.

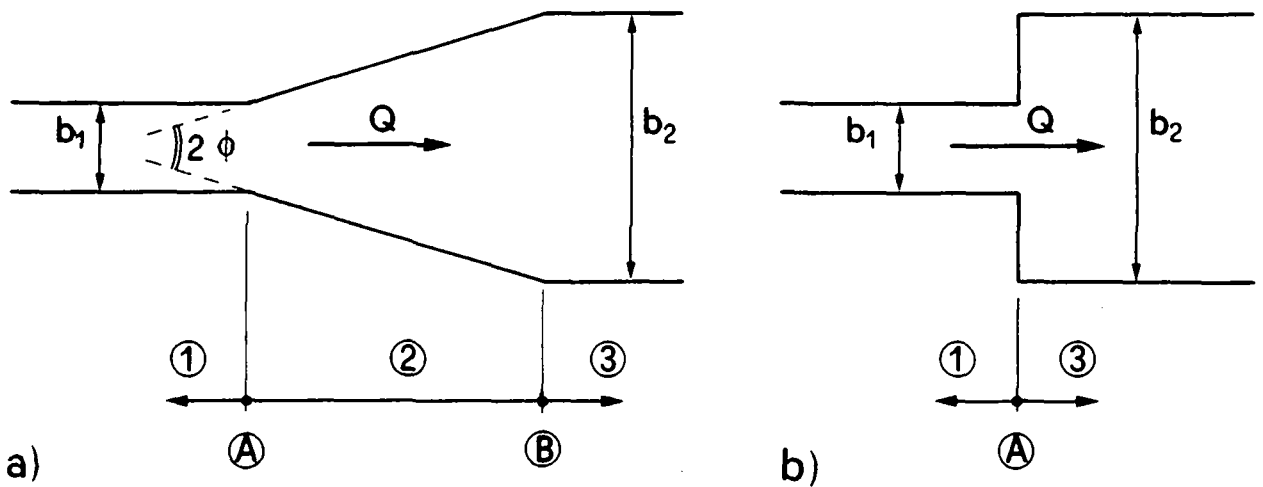


Fig. 2.1 : Notations used to describe the expansion geometry. ① Approaching channel, ② expanding channel, ③ tailwater channel. (A) expansion section, (B) end section for a) gradual linear expansion and b) sudden expansion.

The tailwater characteristics depends on the channel geometry, the inflow conditions, as well as on the toe position relative to the expansion section. Due to the non-prismatic channel geometry, the toe position is equally significant as the inflowing depth and the discharge. The proposed flow classifications are therefore essentially based on the toe position relative to the expansion section.

2.2 SUDDEN EXPANSION

2.2.1 Cyclic flow phenomenon

Consider a supercritical flow in a rectangular sudden expanding channel. For nonsubmerged flow the stream remains supercritical along the entire channel. Downstream from the expansion section, the flow expands until it occupies the full width of the channel. The flow is then reflected on the channel side walls thereby forming oblique cross-waves (Fig. 2.2a).

In order to illustrate the flow pattern for different tailwater conditions, an overflow weir was installed at the downstream end of the tailwater channel (Fig. 4.4). Raising the overflow weir beyond a certain limit, depending on the inflow conditions, made a

hydraulic jump appear somewhere in the proximity of the weir. Due to the non uniform velocity distribution outside and inside of the cross-waves, the front of the jump is V-shaped as shown in Fig. 2.2b). Downstream from the jump, maximum velocities occur near the side walls, whereas the minimum is attained at the channel axis.

Raising the weir further moved the jump upstream, thereby increasing the jump portion inside of the cross-waves. As shown in Fig. 2.2c) the front becomes linear in the central channel part, and remains oblique in the two lateral flow portions. The overall flow characteristics downstream from the jump remained unchanged. Increasing further the tailwater head pushes the jump further upstream and leads to a straight front. As shown in Fig. 2.2d) this jump is located shortly downstream from the first reflection point of the cross-waves. Therefore, its characteristics are mainly influenced by the central flow portion. Note the upper limit position of the jump toe in order that the previously type of jump may establish. If the tailwater head is raised beyond this limit position, the jump front changes abruptly, and a cyclic flow phenomenon is generated as shown in Fig. 2.3. This cyclic phenomenon may only be prevented when the overflow weir is significantly raised or lowered.

Cyclic flow begins with a jump breakdown phenomenon as shown in Figs. 2.3 a) to d). The front of the jump becomes rapidly asymmetric involving a lateral upward stream which spills over the supercritical flow (Fig. 2.3 d). The front of this stream is continuously supplied by the tailwater and attains rapidly the expansion section. Thus, one lateral eddy is filled by mainly stagnant water (Fig. 2.3 d) + e). Due to the highly nonuniform flow condition across the tailwater channel, the flow pattern might be better described as a surface jet than as a hydraulic jump. The inflowing stream is deflected along one channel side, whereas a backward flow establishes at the opposite side (Fig. 2.3d) and g). The backward flow occupies the entire channel length and generates significant surface waves. The flow depth in the lateral eddy decreases slowly and reduces the lateral pressure on the inflowing jet (Figs. 2.3g) and h). After some time, depending on the inflowing conditions, the stagnant water in the eddies is completely drained downstream and the supercritical flow occupies again the entire channel width.

Simultaneously, a hydraulic jump forms further downstream and its front moves steadily upstream (Fig. 2.3i). This movement continues until the front reaches the same position as in Fig. 2.3a) (Fig. 2.3l) and m). The toe becomes again rapidly asymmetric and a new cycle starts (Figs. 2.3n). It should be noted that during one cycle, the inflowing conditions as well as the overflow weir position remain unchanged.

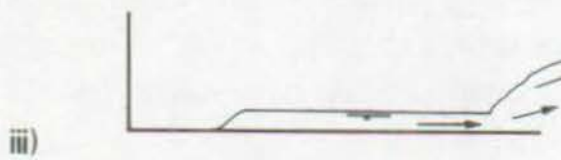
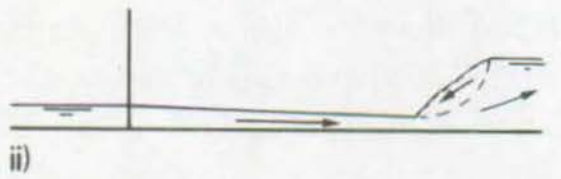
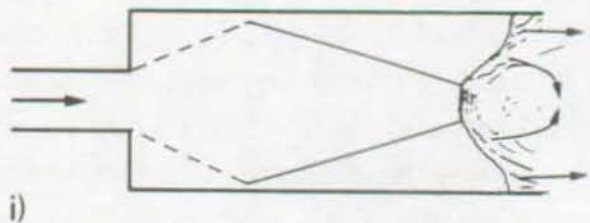
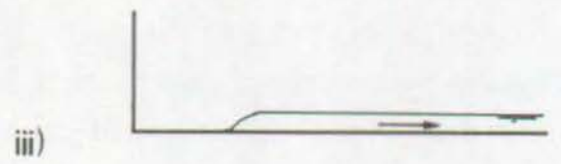
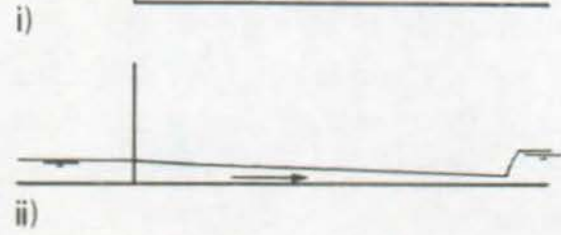
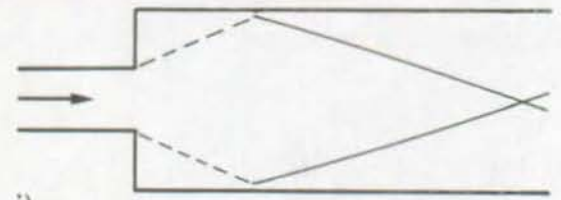


Fig. 2.2 : Flow downstream from abrupt expansion. a) supercritical flow throughout; b) jump in the proximity of overflow weir. i) plan view; ii) axial section; iii) section near side wall.

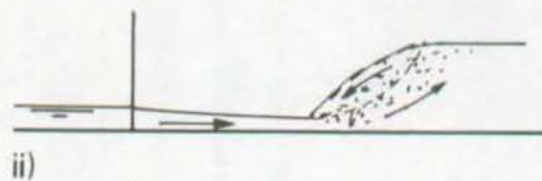
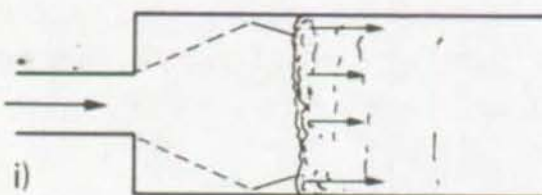
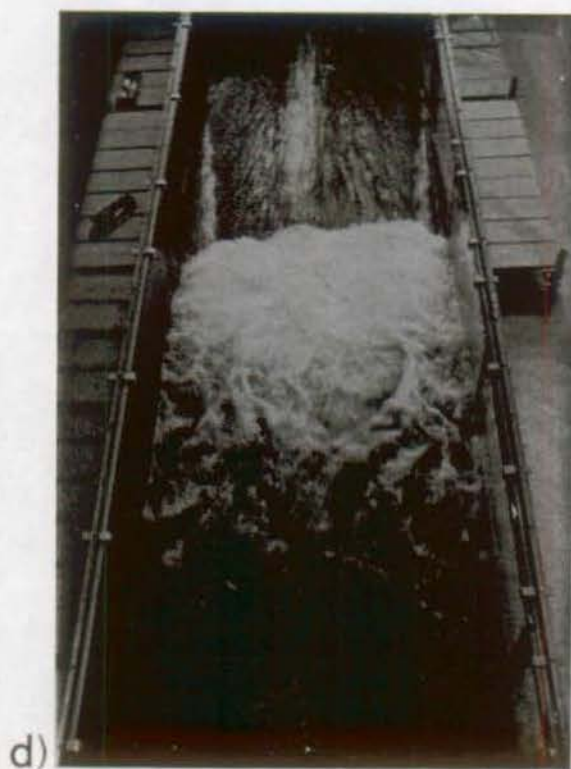
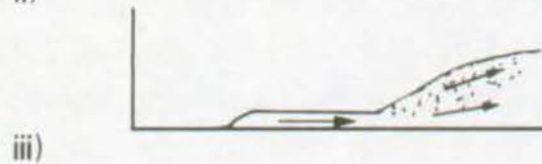
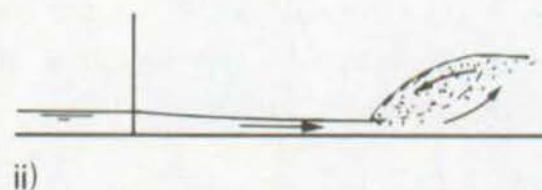
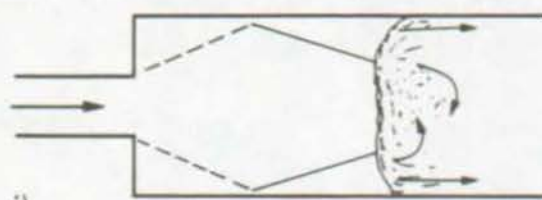


Fig. 2.2 (cont.) : Flow downstream from abrupt expansion. c) central jump position; d) jump near the points of first cross-wave reflection. i) plan view; ii) axial section; iii) section near side wall.

2.2.2 Repelled hydraulic jump in sudden expansion (R-jump)

In the preceding paragraph, the significant influence of the tailwater level on the flow pattern was outlined. Based on the prior description, the **repelled hydraulic jump** may be defined as follows :

Definition 1 : Repelled hydraulic jump in sudden expansion (R-jump).

A hydraulic jump for which the toe is located downstream of the first reflection point of the cross-waves has a limiting toe position. The jump formed under this tailwater condition is termed the repelled jump. Any further increase in tailwater head would cause the jump to break down.

This definition according to Rajaratnam and Subramanya (1968), includes the main flow characteristics. The repelled hydraulic jump is very sensitive to tailwater variations. A slight increase leads to the jump breakdown shown in Fig. 2.3, whereas a decrease moves the front downstream as shown in Fig. 2.2b) + c). The cross waves, as well as the approximate toe position and velocity distribution are presented schematically in Fig. 2.4a), whereas Fig. 2.4b) shows a photograph of a repelled jump.

R-jumps have some characteristics common with classical jumps, such as symmetry and surface roller. Also, they are confined to a relatively short reach, as is clearly seen from Fig. 2.4b). These characteristics disappear abruptly once the tailwater is increased. Then, jumps occur to which the following flow descriptions apply.

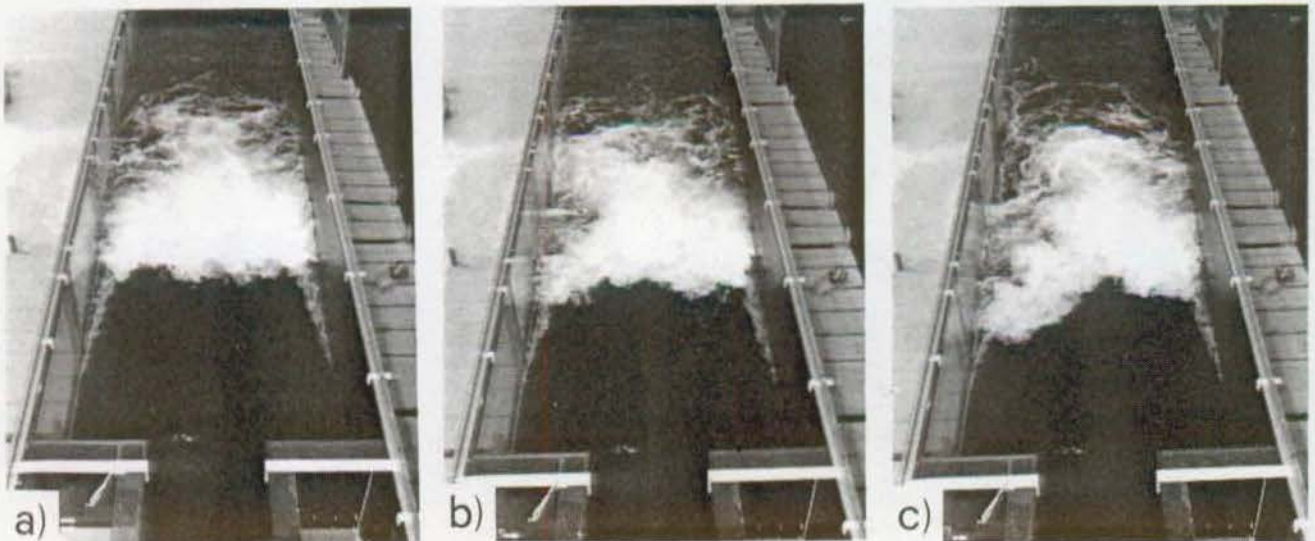


Fig. 2.3 : Cyclic flow phenomena in sudden expansion. a) to c) towards jump breakdown. Continuation on next page.

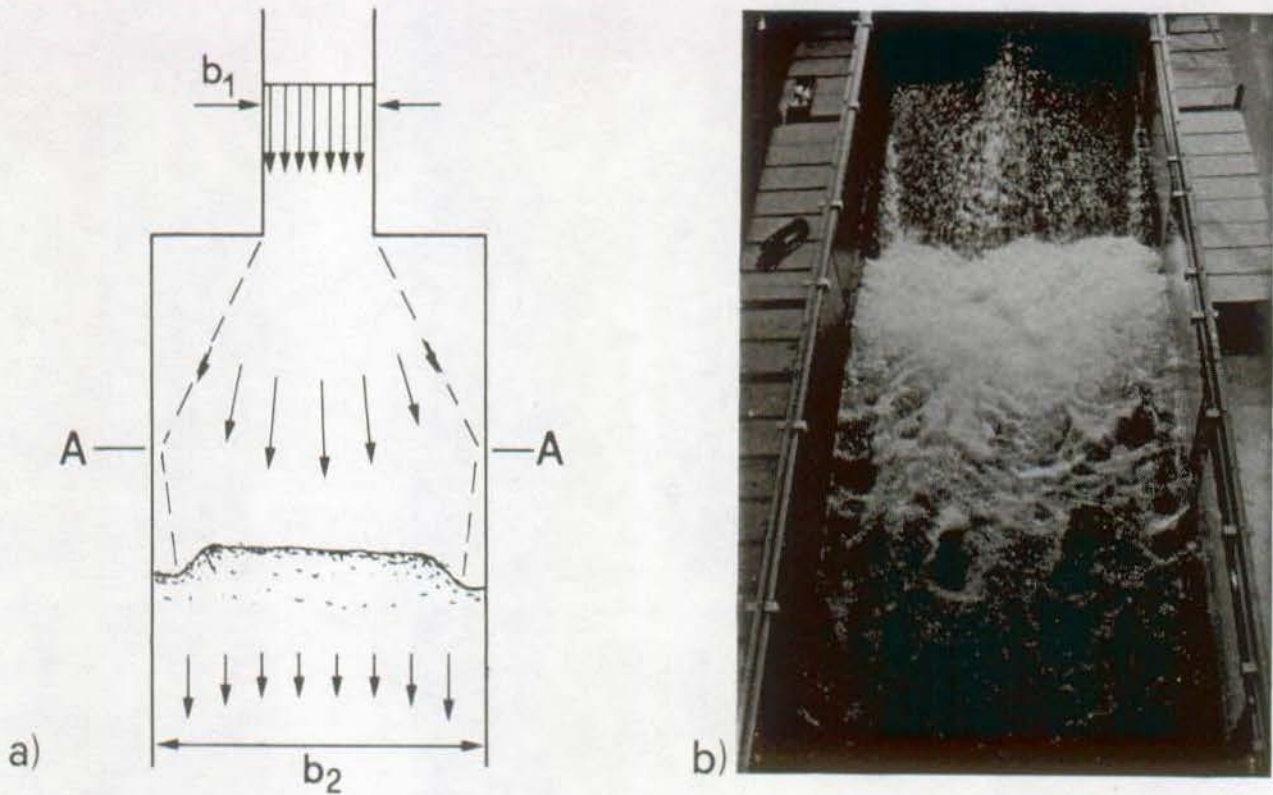


Fig. 2.4 : Repelled hydraulic jump. a) Schematic plot with (--) cross waves and typical transverse velocity distributions, b) photograph. A : point of cross-wave reflection by the side walls.

2.2.3 Spatial hydraulic jump in sudden expansion (S-jump)

The tailwater depth, required for an R-jump is the highest level for which symmetric and stable flow prevails. A slight increase produces the cyclic phenomenon described in paragraph 2.2.1. This phenomenon may only be stopped by significantly raising or lowering the tailwater. When the overflow weir is lowered, the R-jump reappears, whereas raising this weir increases the flow depths in the lateral eddies. Under such tailwater conditions, the supercritical stream is unable to empty the stagnant water zone. The width of the backward flow is stabilized after a short time and overall steady but asymmetric flow conditions prevail.

The **spatial hydraulic jump** may therefore be defined as follows :

Definition 2 : Spatial hydraulic jump in sudden expansion (S-jump).

Consider a jump for which the tailwater is higher than for cyclic flow to appear. It is characterised by a mainly steady asymmetric surface jet without surface roller. The forward flow is continuously supplied by the two lateral eddies. The front is V-

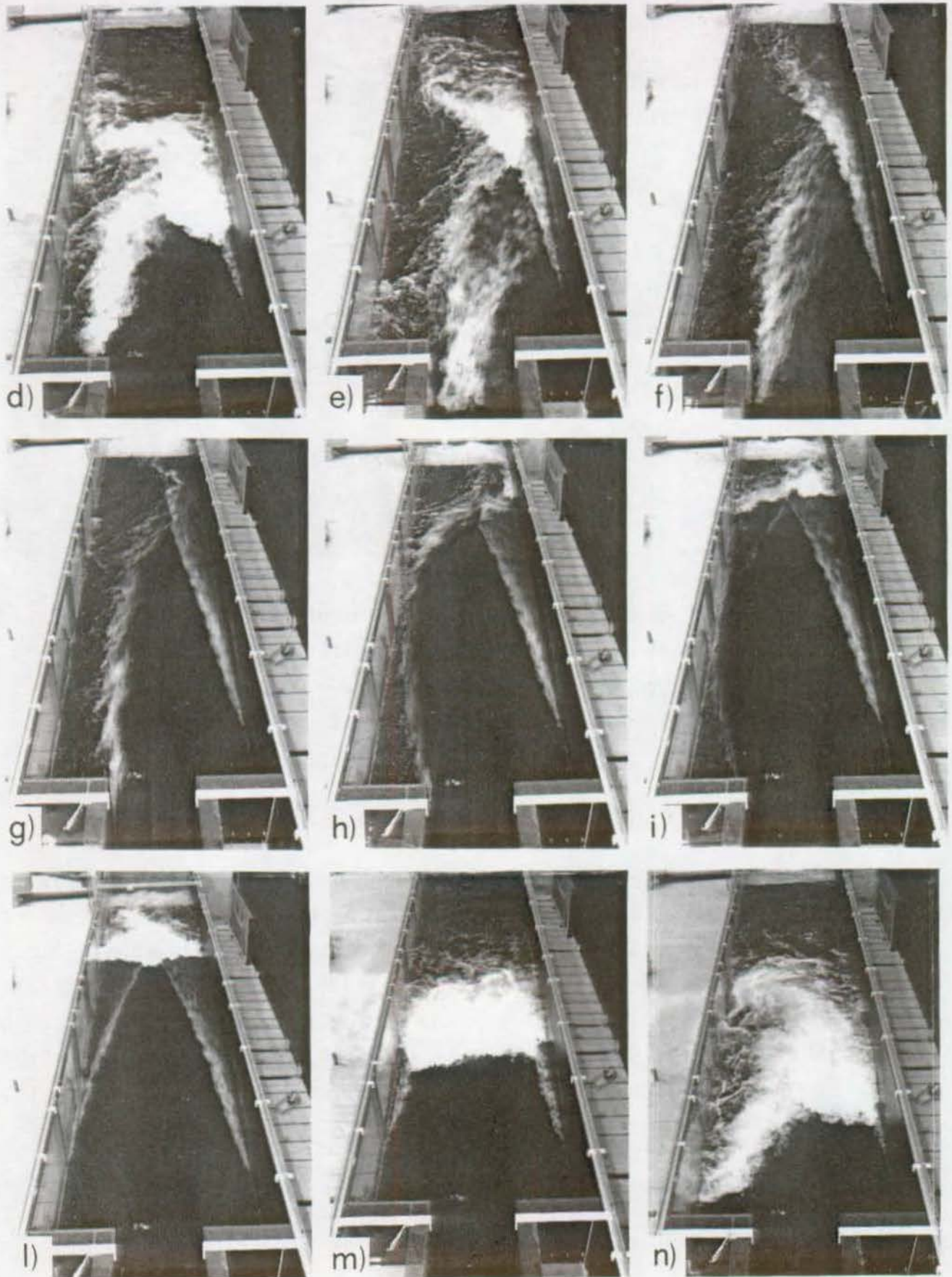


Fig. 2.3 (cont.) : Cyclic flow phenomena in sudden expansion. d) to g) surface flow jet; h) to n) upstream movement and subsequent jump breakdown.

shaped and the average toe position corresponds approximately to the expansion section.

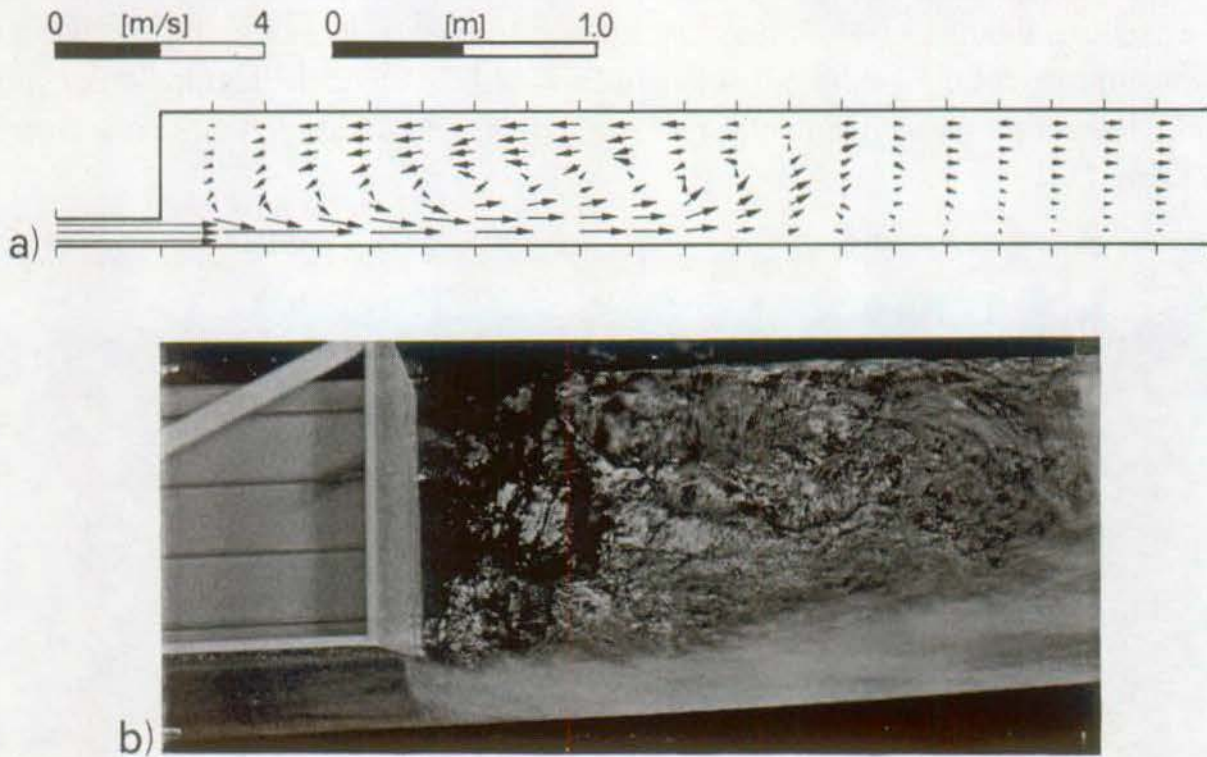


Fig. 2.5 : Spatial hydraulic jump (S-jump) in a half model. a) depth-integrated velocity profiles, b) corresponding photograph.
 $B=b_2/b_1=5$, $F_1=8.21$.

The flow in S-jumps is strongly non-uniform with high velocity concentrations along one side wall and a backward flow along the opposite channel side. Fig. 2.5 shows the velocity distribution measured in a half-model. For the measurement of the velocity distribution, the half-model geometry was preferred to a symmetric channel since a reduction of the flow oscillation could be obtained. Therein the approaching channel was 10cm wide, whereas the tailwater channel width attained 50cm. As outlined in Fig. 2.5a), the expansion of the inflowing stream is poor. There is more similarity to jets rather than to hydraulic jumps. For design purposes, the significant extension of backward flow, and velocity concentrations in the tailwater channel, are evidently unsuitable.

2.2.4 Transitional hydraulic jump in sudden expansion (T-jump)

The flow conditions improve in terms of symmetry and longitudinal extension of jump if the tailwater level is raised above that required for S-jumps. The toe of the

jump rapidly becomes straight as it moves upstream from the expansion section. The length of the backward flow is simultaneously reduced and the jump asymmetry decreases. A small surface roller, which is supplied by the lateral eddies, forms in the approaching channel (Fig. 2.6a). A further tailwater increase moves the toe upstream, reduces the length of backward flow and develops the surface roller (Fig. 2.6b). However, the fundamental characteristics of the flow phenomena remain unchanged.

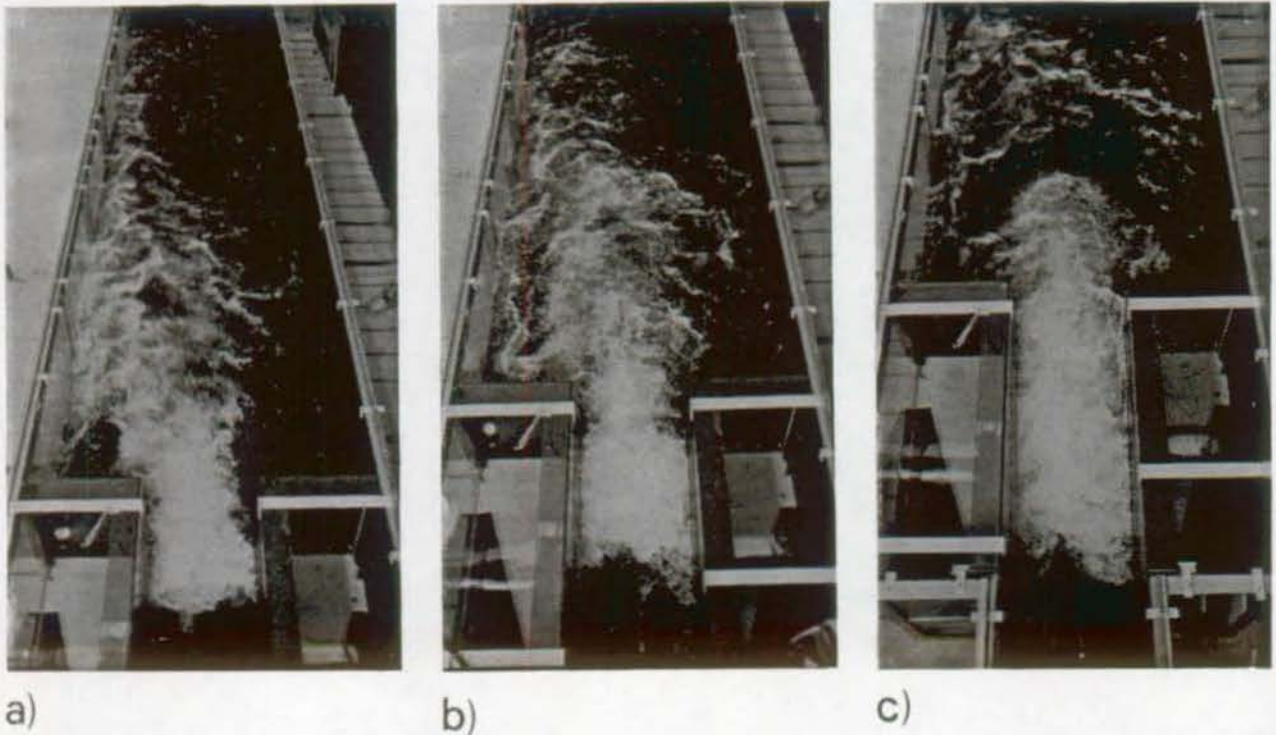


Fig. 2.6 : Transitional hydraulic jump (T-jump). Effect of the toe location on the jump pattern. a) nearly S-jump, b) average jump position, c) nearly classical jump.

Finally, if the submergence is sufficient, the entire jump forms upstream from the expansion section and the flow entering the wider channel is subcritical (Fig. 2.6c).

The **transitional hydraulic jump** may therefore be defined as follows :

Definition 3 : Transitional hydraulic jump (T-jump).

A T-jump is a hydraulic jump characterised by a toe position which is located in the approaching channel. The jump extends partly in the approaching channel and partly in the tailwater channel. The T-jump symmetry and longitudinal extension depend on the toe position relative to the expansion section.

In the case of low submergence the distinction between S-jumps and T-jumps could be difficult since no abrupt changes between the two types of jumps can be observed. The

most suitable parameter seems to be the toe position. The toe of the T-jump is entirely located upstream from the expansion section, whereas for the S-jump the toe is oblique and crosses the expansion section.

2.3 GRADUAL LINEAR EXPANSION

2.3.1 Cyclic flow phenomena

In the second part of this chapter, the flow pattern observed in gradual linear expansions will be described and classified. In order to outline some similarities between this type of expansion and sudden expansions, the description procedure will be identical to paragraph 2.2.

Consider a supercritical flow entering a linearly expanding symmetrical channel. At the expansion section the flow cannot abruptly change direction and local separation results. Further downstream, depending on the expansion geometry and on the inflow

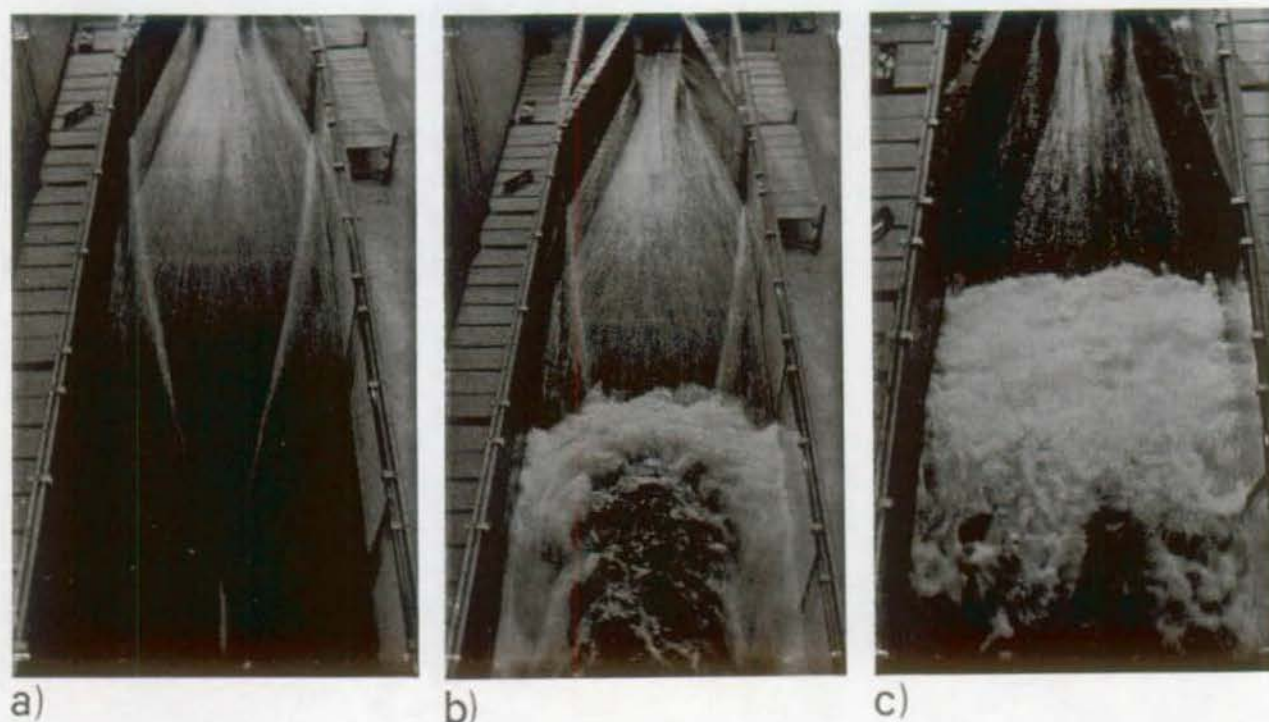


Fig. 2.7 : Flow downstream from gradual linear expansion. a) supercritical flow throughout, b) jump in the proximity of overflow weir, c) jump located partially in the tailwater and partially in the expansion channel ($2\phi=23.8^\circ$).

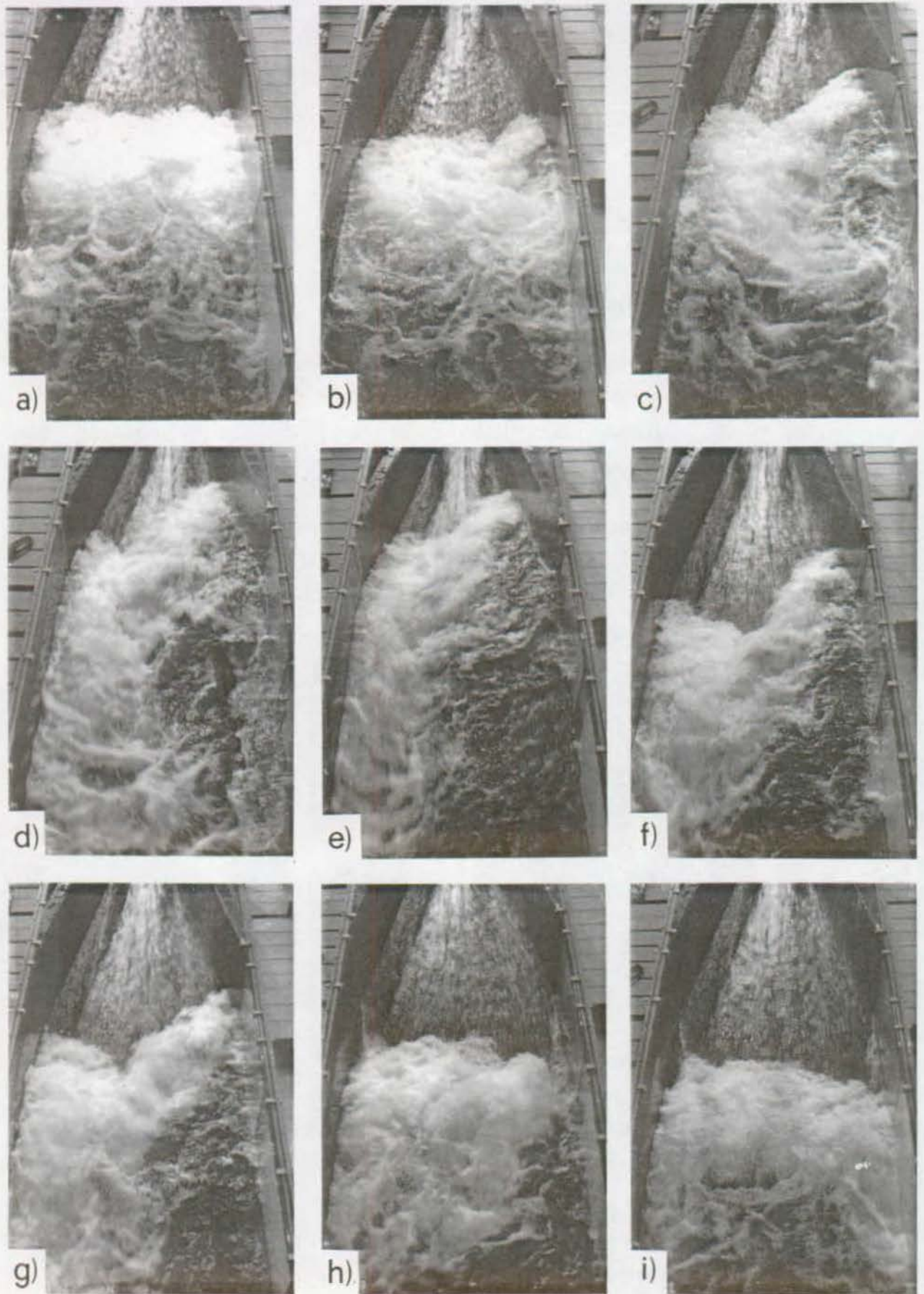


Fig. 2.8 : Cyclic flow phenomena in gradual expansion. a) to c) jump breakdown; d) to g) oblique jump; h and i) upstream movement and jump breakdown ($2\phi=23.8^\circ$).

conditions, the flow would diverge more than the constant boundary angle. At the end section (Fig. 2.1a), oblique cross-waves form (Fig. 2.7a) and as described in paragraph 2.2.1 they reach the channel axis further downstream, and again reflected.

Raising the overflow weir generates a hydraulic jump with a V-shaped front somewhere in the tailwater channel (Fig. 2.7b). Increasing the tailwater level moves the toe upstream into the expansion channel (Fig. 2.7c). The jump is therefore located partially in the prismatic and partially in the expanding channel. The front is straight, the jump appears symmetric and uniform flow conditions prevail downstream from the jump.

As for R-jumps, the front attains a limit position also in gradual linear expansions (Fig. 2.8a). Raising the tailwater head above the limiting level leads to an abrupt change of the jump characteristics (Fig. 2.8b). The front becomes asymmetric and moves upstream along one channel side combined with a reverse flow zone (Fig. 2.8c). As in abrupt expansions this configuration indicates the start of cyclic flow. Since the stagnant water zones are considerably reduced as compared to sudden expansions at corresponding flow conditions, the cyclic phenomenon observed was generally of a shorter period. However, the main flow characteristics, such as asymmetry and backward flow remain practically unchanged.

The upstream movement of the front along one channel side wall due to increasing tailwater attains rapidly a limiting position (Fig. 2.8d to e). For this position the jump asymmetry is well pronounced, and involves a significant backward flow. Then the entire front moves downstream thereby maintaining the flow asymmetry (Fig. 2.8f). This movement continues until the entire jump is located in the tailwater channel (Fig. 2.8h). The flow asymmetry becomes gradually less pronounced. Finally an overall symmetric jump forms again in the prismatic channel (Fig. 2.8i). This jump moves upstream until the starting position is reached again (Fig. 2.8a).

Although similar flow patterns may be observed in both gradual linear and sudden expansions, the magnitude of the cyclic phenomenon is reduced in the gradual linear expansion. It should be outlined that for Fig. 2.8 and Fig. 2.3 identical inflow conditions were considered ($F_0=5.02$, $h_1=5.0\text{cm}$). Therefore, the magnitude of the phenomenon depends significantly on the expansion geometry.

2.3.2 Repelled hydraulic jump in gradual linear expansion (R-jump)

Despite an intensity reduction of the cyclic phenomenon, similar flow patterns may be observed in both gradual and sudden expansions. When considering a gradual linear

expansion with a horizontal channel floor, the **repelled hydraulic jump** may be defined as follows :

Definition 4 : Repelled hydraulic jump in gradual linear expansion (R-jump).

A hydraulic jump located partially or entirely in a linearly expanding channel with a straight front and symmetrical flow conditions is referred to as R-jump. Increasing the tailwater above a limiting position causes an oblique front and pronounced asymmetric and cyclic flow conditions.

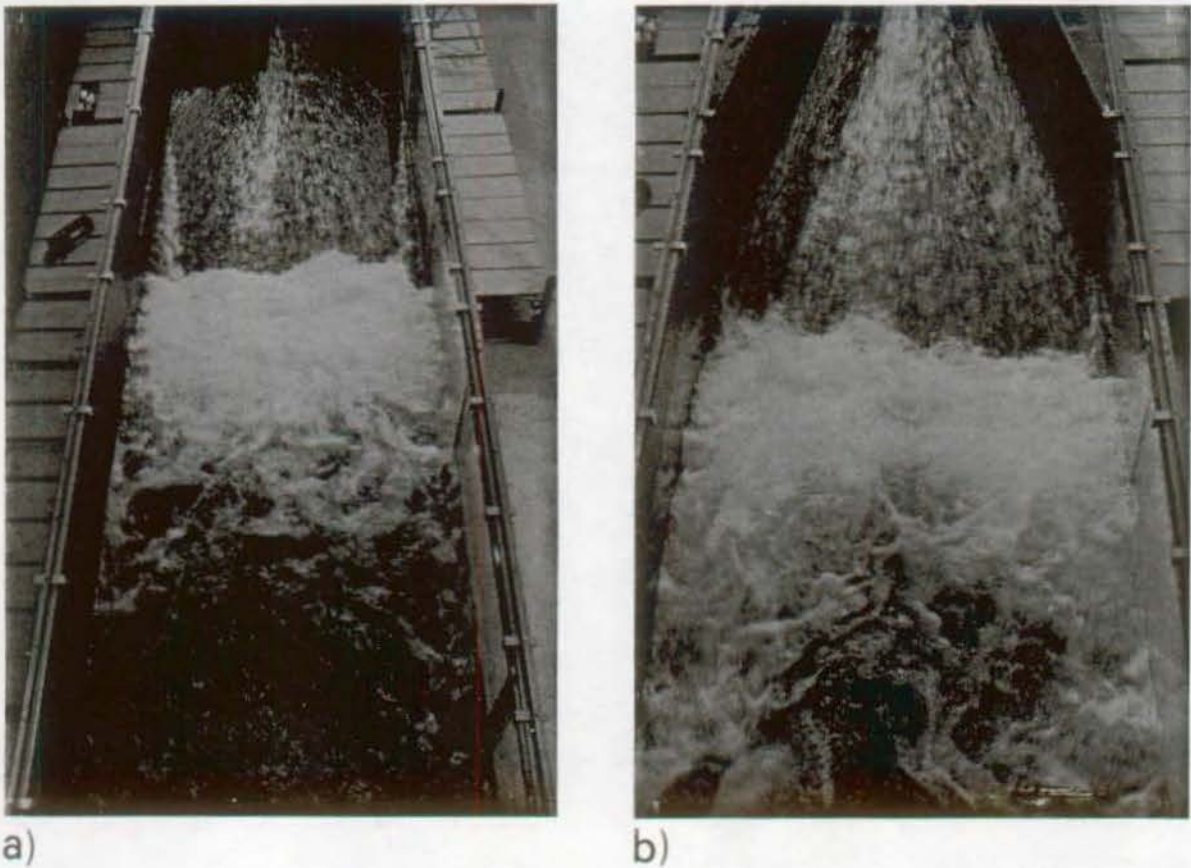


Fig. 2.9 : Comparison between R-jumps in a) sudden and b) gradual linear expansions. $2\phi=23.8^\circ$, $F_1 \approx 5.02$, $b_2/b_1=3$.

In Fig. 2.9 the R-jump in a sudden expansion is compared to the jump pattern observed in a gradual linear expansion. For both cases, the inflow conditions were identical. The high velocity stream near the channel side walls is especially well outlined in Fig. 2.9b). As mentioned in paragraph 2.2.2 R-jumps show some characteristics of the classical jump, namely symmetry, a surface roller and nearly uniform flow conditions in the tailwater.

The position of the R-jump relative to the expanding channel depends on both the channel size and the inflow conditions. The R-jump may be located entirely in the

expanding channel when small jumps (small inflow depth and small inflow Froude numbers) and long expanding channels (small expansion angles) are considered. As shown in Fig. 2.9, the jump may also be located entirely in the tailwater channel.

2.3.3 Spatial hydraulic jumps in gradual linear expansion (S-jump)

The R-jump defined in the preceding paragraph corresponds to the highest tailwater level for which symmetric and steady flow prevails. Raising the overflow weir beyond this level, produces the cyclic phenomenon described in paragraph 2.3.1. In order to stop the cyclic phenomenon, the tailwater level has to be significantly raised, as observed for sudden expansions. Under such tailwater conditions, the jump becomes again steady but remains asymmetric.

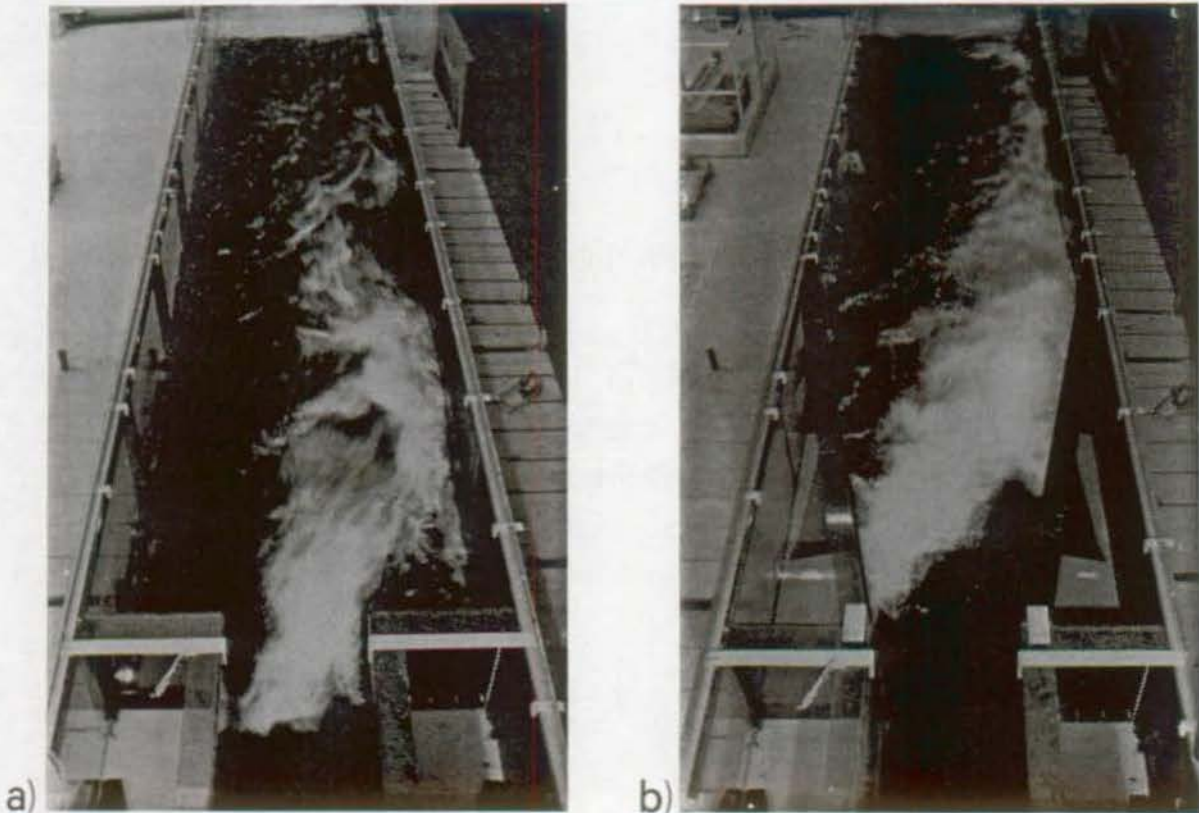


Fig. 2.10 : Comparison between S-jumps in a) abrupt and b) gradual linear expansion. $2\phi=23.8$ deg. $b_2/b_1=3$ and $F_1=5.02$.

The spatial hydraulic jump in a gradual linear expansion may therefore be defined as follows :

Definition 5: Spatial hydraulic jump in a gradual linear expansion (S-jumps).

An S-jump corresponds to a flow configuration for which the tailwater level is above the cyclic flow. It is steady but asymmetric, with an oblique front and a significant backward flow along one channel side. The toe of S-jumps is always located downstream from the expansion section.

Fig. 2.10 compares the spatial jumps for the sudden and the gradual linear expansions. The inflow conditions, and the tailwater level are identical in both channel geometries. As shown in these photographs, the basic characteristics of S-jumps, namely the flow asymmetry and the associated backward flow remain qualitatively unchanged. For a given tailwater variation, the toe displacement for the gradual expansion is larger than for the sudden expansion. For the latter, the toe position remains nearly constant as was already mentioned in paragraph 2.2.3. Therefore, according to the present definition, asymmetric but stable jumps in the gradual linear expansion may be classified as S-jumps provided the front is located in the expanding channel reach.

2.3.4 Transitional hydraulic jumps in gradual expansion (T-jump)

Consider an S-jump of which the front is located somewhere in the expanding channel (Fig. 2.10b). Raising the tailwater level moves the front upstream. For sufficient tailwater height, the front attains the expansion section as is indicated in Fig. 2.1. This level corresponds to the highest tailwater for an S-jump in a gradual linear expansion to appear. A further level increase moves the jump into the approaching channel. The **transitional hydraulic jump** in gradual linear expansions may therefore be defined as follows :

Definition 6: Transitional hydraulic jump in gradual linear expansion (T-jumps).

A T-jump is a hydraulic jump characterized by a toe position located in the approaching channel. The jump extends partially into the approaching channel and partially into the expanding channel.

Fig. 2.11 compares T-jumps in sudden and gradual linear expanding channels. Compared to S-jumps, the front is straight and the flow asymmetry becomes less pronounced, especially for Fig. 2.11b). The flow characteristics of the T-jump depends on the toe position relative to the expansion section. When the toe is located a short distance upstream from the expansion section the S-jump pattern prevails,

whereas the classical jump pattern prevails for jumps located mainly in the approaching channel.

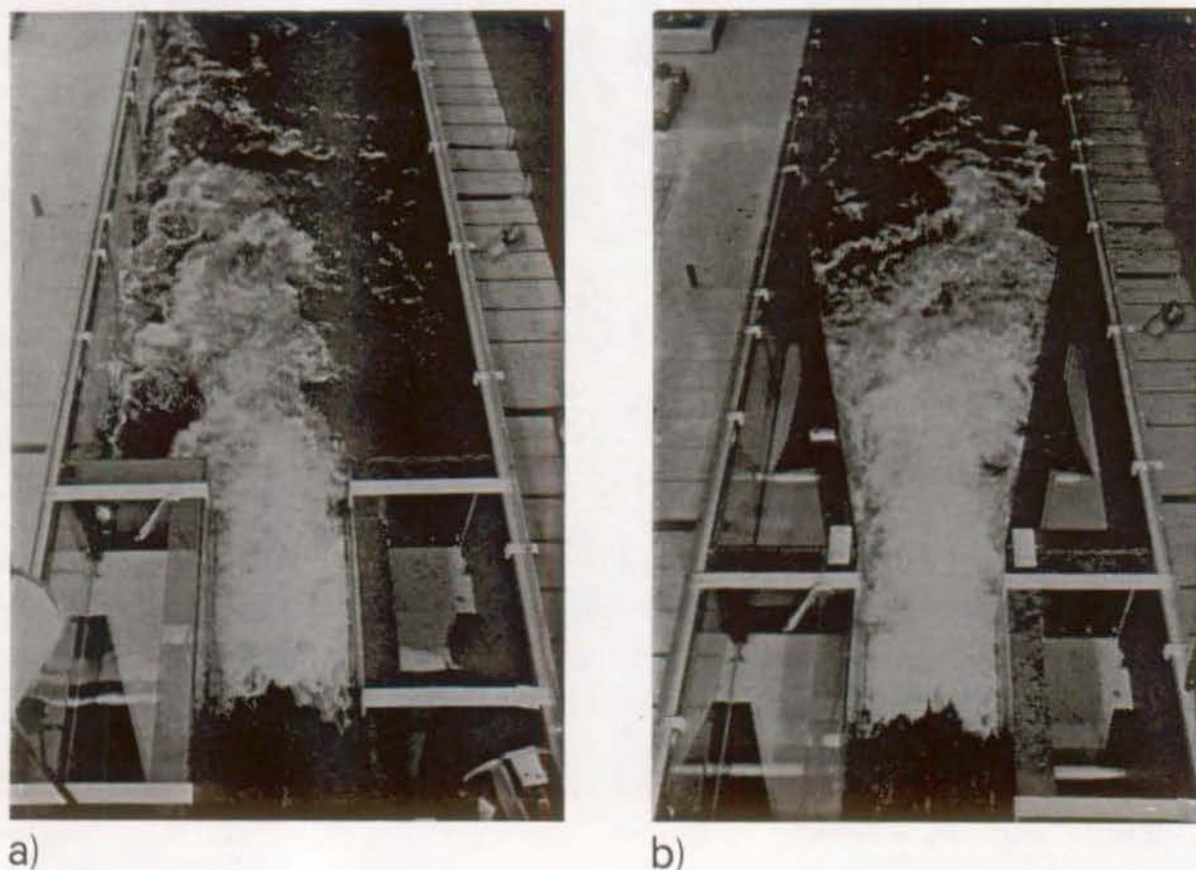


Fig. 2.11 : Comparison between T-jumps in sudden (a) and gradual linear (b) expansion. $b_2/b_1=3$, $F_1=5.02$, $b_1=0.5\text{m}$. $2\phi=23.8^\circ$.

2.4 DOMAIN OF INVESTIGATION

The flow patterns of hydraulic jumps in expanding channels may be quite different as outlined in paragraphs 2.3 and 2.4. A quantitative analysis of the three jump types, and the cyclic flow phenomena in both sudden and gradual expansions would require a large and time-consuming experimental investigation. A selection of the channel configurations to be investigated in the present research project thus became necessary.

Since R-jumps exhibit some major characteristics also encountered by the classical jump as regards symmetry and surface roller, they were excluded from the experimental tests. The main criterion for excluding R-jumps is their extremely limited domain of stability under variable tailwater. Yet, the present knowledge on

the type of jump and the proposed computational models will be described in the next chapter.

A comparison of jumps in sudden and gradual expansions reveals similar flow patterns in both channel geometries in particular as regards to the asymmetry of flow. As the phenomenon of asymmetry has received only scarce attention, attention will be focussed on means to obtain symmetric flow and thus effective energy dissipation. Except for some conclusive experiments presented in chapter 8, the laboratory tests will also be limited to sudden expansions. Two main reasons justify this limitation. First, for an identical ratio b_2/b_1 and identical inflow and outflow conditions, the asymmetry phenomenon is more pronounced in sudden expansions than in gradual expansions. Appurtenances avoiding or limiting the flow asymmetry in sudden expansions should therefore also be effective in gradual expansions. In chapter 8 this assumption will be verified experimentally.

Second, the sudden expansion geometry may be only described by the expansion ratio $B=b_2/b_1$. For gradual linear expansions at least one additional parameter is needed (linear expansion), such that the experimental investigation would require analysis of several different channel geometries. This must be left to future research studies.

The experimental investigation presented in chapters 5,6, and 7 is therefore limited to S and T-jumps in sudden expansion channels. An account for gradual expansions is made in chapter 8.

However, the review of literature presented in the next chapter considers investigations on both abrupt and gradual linear expansions. Therein, particular attention will be paid to computational models proposed for the prediction of the overall jump parameters such as length or the sequent depths ratio.

2.5 CONCLUSIONS

The purpose of this chapter was to illustrate and propose a classification of different types of hydraulic jumps in expanding channels. In order to limit the extent of presentation, a symmetric channel geometry was selected. The first part of the chapter was concerned with the symmetric sudden expansion, whereas the second part dealt with a gradual linear expansion.

The characteristics of hydraulic jumps located in expanding channels may be considerably different from the pattern observed in prismatic channels. For a

particular expansion geometry the flow pattern changes significantly depending on the toe position relative to the channel expansion. In order to classify the flow patterns in expanding channels, three jump types were defined, based on symmetry and front position. Apart from small differences these three types of jumps may be observed in both sudden and gradual linear expansions.

R-jumps are practically not influenced by the channel expansion. Therefore, this type of jump is symmetric, has a well developed surface roller, and the velocity distribution in the tailwater region is nearly uniform. However, its characteristics are very sensitive to slight tailwater level variations.

S-jumps are characterized by asymmetric flow and an oblique toe in the vicinity of the expansion section which significantly increases the jump length as compared to the classical jump. As shown in Fig. 2.10, the flow patterns of jumps in abrupt and gradual expansions are similar. It should be outlined that no improvement of the jump symmetry may be observed in the gradual linear expansion compared to the sudden expansion. This preliminary observation indicates that an improvement of jump pattern is not obtained by reducing the expansion angle.

T-jumps involve characteristics of both S-jumps and classical jumps. T-jumps are characterized by a relatively stable toe position perpendicular to the channel axis, always located upstream from the expansion section. The flow pattern depends on the toe location relative to the expansion section. For low tailwater levels asymmetric flow combined with returning currents prevails. The effect of the toe location on the jump symmetry was outlined in Fig. 2.6. However, for abrupt expansions symmetric flow conditions may only be obtained when the main part of the jump is located in the approaching channel. The gradual expansion geometry seems to slightly improve the flow pattern of T-jumps. However, the velocity distribution in the tailwater remains still highly non-uniform.

In order to limit the extent of the experimental investigation, the following research mainly deals with S- and T-jumps in sudden expanding channels. The performance of appurtenances avoiding the flow asymmetry in sudden expansions has also been tested in gradual linear expansions.

3. LITERATURE REVIEW

3.1 INTRODUCTION

In chapter 2, typical flow patterns observed in expanding channels have been described and extensively illustrated by photographs. The proposed classification based on the toe position and the jump symmetry will facilitate further investigations. Particular attention was paid to the asymmetry observed for S and T-jumps when relative large expanding angles were considered.

The present chapter aims at describing investigations on hydraulic jumps formed in expanding channels. Except for a few contributions (Riegel and Beebe, 1917) the research on this type of hydraulic jumps started only about 30 years ago. In most of the contributions, a computational approach for the prediction of the sequent depths ratio is proposed. Only few investigations describe the flow patterns typical for hydraulic jumps in expanding channels as reported in chapter 2.

After the definition of the relevant notation, the main results of each investigation are summarized and commented. The chapter is subdivided in two main parts. In the first part sudden expansions are considered whereas the investigations related to gradual expansions are described in the second part.

Therein, distinction is made between stilling basins with parallel approaching streamlines (Riegel and Beebe 1917, Cvetkov 1952, Rajnov 1964) and those assuming a radial distribution of the approaching velocity field, such as the contribution of McCorquodale (1979), Nettleton and McCorquodale (1983,1989).

Of major concern are the expressions for the overall jump parameters, including sequent depth, position of toe and length of jump. The application of the momentum approach to expanding channel geometries presents some major problems. First, the momentum contribution of the side walls depends from the jump profile and from the pressure distribution along these walls. Especially for this second parameter only limited measurements are available. The momentum equation allows the computation of the sequent depths, but a supplementary equation is needed to predict the jump position relative to the expansion.

Apart from these computational approaches, descriptions pertinent to jumps in expanding stilling basins will be of interest in order to point at difficulties actually encountered with this type of dissipator.

3.2 SUDDEN EXPANSIONS

3.2.1 Notation

It is useful to define some basic notation used in this chapter, first. The notations adopted in the literature are frequently substituted by the writer's symbols. The comparison between different relations is thus simplified.

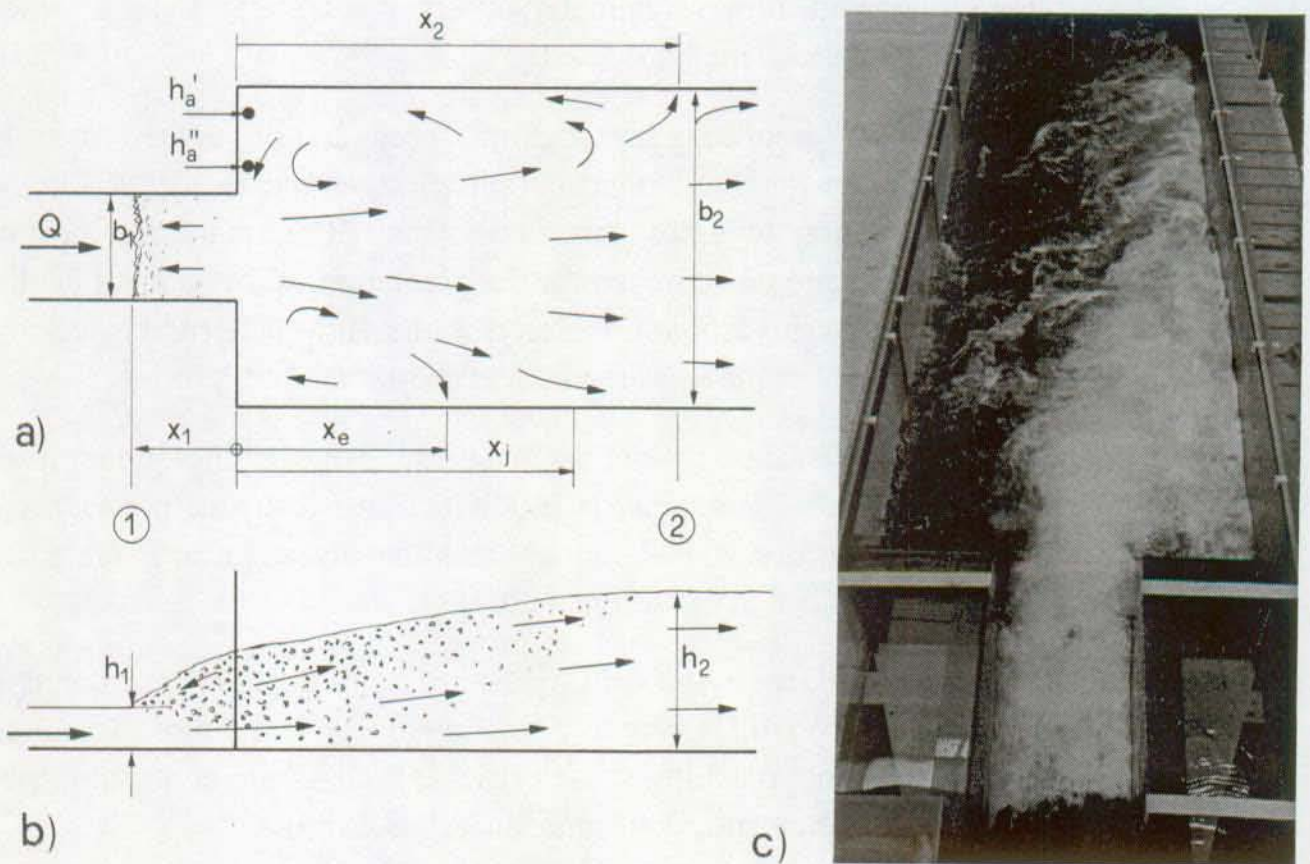


Fig. 3.1 : Relevant notation for sudden expansion and typical T-jump patterns. a) Notation. Index 1: inflow conditions. Index 2: tailwater conditions. a) plan view ; b) axial view ; c) photograph of T-jump ($B=3$, $F_1=9.7$).

Fig. 3.1 shows a typical T-jump configuration with the basic notation. The front of the hydraulic jump defines the position of section 1. This section is located upstream of the expansion section for T-jumps ($x_1 > 0$), at the expansion section for S-jumps ($x_1 = 0$) and downstream of the expansion section for R-jumps ($x_1 < 0$) (chapter 2).

The definitions adopted for section 2 differ considerably from one author to the other. Except for the R-jump, two lateral eddies are formed downstream of the expansion, as described in chapter 2. Only downstream of these eddies (indicated by x_e and x_2) the flow becomes nearly uniform. In Fig. 3.1 section 2 is therefore located at the downstream end of the longer lateral eddy.

3.2.2 Spatial hydraulic jump (S-jump)

Kusnezow (1958) conducted experiments on S-jumps in a 1 m wide channel with a maximum inflow Froude number $F_1=7.25$. Expansion ratios $B=b_2/b_1$ between 1 and 100 were examined. Based on his experimental data, Kusnezow proposed

$$Y = \frac{0.5}{B} K_K \left[\sqrt{1+8BF_1^2} - 1 \right] \quad (3.1)$$

for the sequent depth ratio $Y=h_2/h_1$. The empirical coefficient K_K was adjusted as

$$K_K = 0.8 - \left(0.9 - \frac{1}{B} \right) 0.15 \quad (3.2)$$

It should be noted that the limit condition $B=1$ (prismatic channel) is in disagreement with the Bélanger relation. Furthermore, certain combinations of B and F_1 , lead to sequent depths ratios Y smaller than 1. These are the main reasons why Eq. (3.2) seems inappropriate.

The approach on S-jumps presented by Unny (1960) is based on the turbulence theory as established by Rouse (1951,1957,1958), and Harleman (1951). Fig. 3.2 shows a schematic plot of the flow configuration investigated. All experiments were performed in an asymmetric expanding channel of width ratio $B=2$ (Fig. 3.2). The experimental data include the depths h_1 and h_2 as well as the toe position x_1 . For each run, about five different jump positions were considered. However, only the series with a toe position $0 > x_1 > 6\text{cm}$ were considered for the computational model.

Unny assumed that the separation surface between the main flow and the lateral eddy (line C-D) is vertical and prismatic across the entire jump, starting from point C. This assumption led to the particular choice of the control volume as shown in Fig. 3.2. The position of section ② in which the sequent depth h_2 was measured was not well defined. It seems however that this section was located upstream from the end section

② of the longer lateral eddy. The velocity distribution across section ② was therefore nonuniform with a significant backward flow along the expansion side wall.

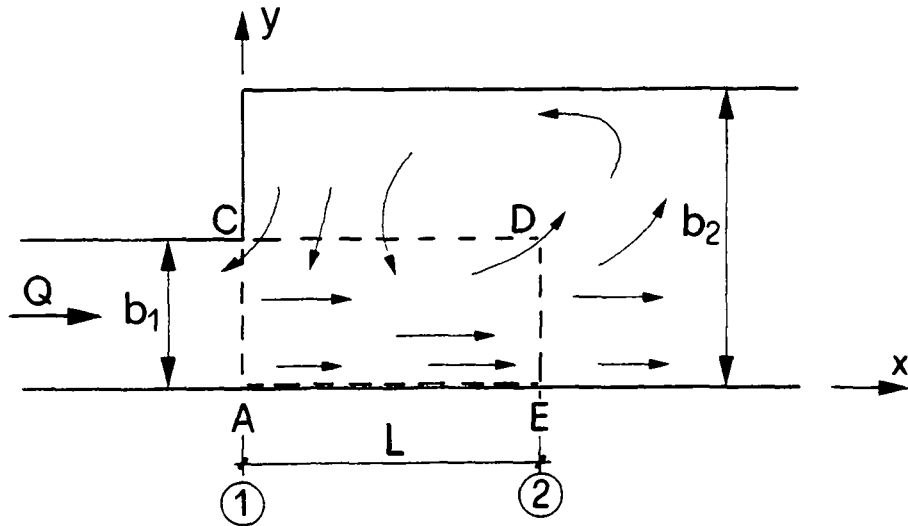


Fig. 3.2 : Experimental setup according to Unny. (--) control volume and schematic flow pattern in asymmetric expanding channel.
 $b_1=0.285\text{m}$; $b_2=0.57\text{m}$

Unny established the generalized sequent depth relation

$$F_1^2 = \frac{0.5Y(Y^2-1) + Y\Psi}{Y\alpha_1 - (\alpha_2 + \alpha_2' + \theta_u - \theta_u')} , \quad (3.3)$$

accounting for the nonuniform and turbulent velocity distribution at the boundaries of the control volume. Ψ accounts for the frictional effects, the momentum correction coefficients α_1 and α_2 for the nonuniform velocity distributions at sections ① and ② (Fig. 3.2), and α_2' the corresponding turbulent shear contribution at section ②. The momentum contribution along line C-D was expressed as

$$\theta_u = \frac{\int_0^L \int_0^{h_2} -uv \cdot dz dx}{b_2 u_{m2}^2 h_2} ; \quad \theta_u' = \frac{\int_0^L \int_0^{h_2} u'v' \cdot dz dx}{b_2 u_{m2}^2 h_2} . \quad (3.4)$$

Herein, u and v are, respectively, the local velocity components in the x and y directions along the surface $L \cdot h_2$ and u_{m2} is the average cross sectional velocity in

section 2. θ'_u accounts for the turbulent momentum contribution of the velocity fluctuations u' and v' . Based on the results of Rouse (1951) and Harleman (1951) on classical jumps, Unny assumed that the effect of Ψ , α_1 , α_2 , and α'_2 were small and could even be neglected. This assumption which was not verified experimentally seems inappropriate since the velocity distribution at section ② is highly nonuniform.

Based on a number of assumptions, Unny obtained an explicit formula of θ_u and θ'_u . Inserting these in Eq. (3.3) gives

$$Y = 0.5K_U \left(\sqrt{1 + \frac{8F_1^2}{K_U^2}} - 1 \right) \quad (3.5)$$

where

$$K_U = 1 + k(1-1/B)^c \omega_1 F_1^2 \quad (3.6)$$

k and c are constants and $\omega_1 = h_1/b_1$ accounts for the inflowing jet geometry. Unny's experiments, which were limited to a half model with an expansion ratio $B=2$, did not allow to define these two constants. Instead, the global value $K_U(B=2)k(1-1/B)^c = 2.2$ was specified.

Macha (1963) considered four expansion ratios $B=2.0$, $B=1.6$, $B=1.4$, and $B=1.2$. The tailwater channel width $b_2=2.0\text{m}$ was thereby kept constant. His analytical approach is based on the same control volume as Unny's. Neglecting frictional and turbulence effects in sections ① and ②, the sequent depth ratio Y is related as

$$F_1^2 = \frac{0.5(Y^2-1)Y}{Y-(1+\theta_M+\theta'_M)} \quad (3.7)$$

to the inflowing Froude number in which $\theta_U = \theta_M$ and $\theta'_U = -\theta'_M$. Fig. 3.3 shows the experimental installation, the control volume considered and the approximate toe position ($x_1 \cong 0$) which was kept constant for all the measurements.

Based on the experimental data and using Eq. (3.7) Macha computed the term $\theta_M + \theta'_M$ as presented in Fig. 3.4 as a function of F_1 and the shape factor ω_1 for two expansion ratios. For S-jumps ω_1 seems to influence significantly the depths ratio Y . Application of the momentum, and the continuity equations across the entire channel section do not reveal this term. No functional relation between $\theta_M + \theta'_M$, F_1 and ω_1 was proposed.

According to Peterka (1958) the jump efficiency η could be defined as the ratio of the dissipated energy $\Delta H = H_1 - H_2$ and the energy head of the inflow stream H_1 . The efficiency η , for non-prismatic rectangular channels with vertical side walls may be expressed as (see paragraph 5.5.6)

$$\eta = \frac{H_1 - H_2}{H_1} = 1 - \frac{Y + \frac{F_1^2}{2B^2 Y^2}}{1 + \frac{F_1^2}{2}} \quad (3.8)$$

Herein, $H = h + Q^2 / (2gb^2h^2)$ is the energy head. This is shown in Fig. 3.5 for the data considered in Fig. 3.4.

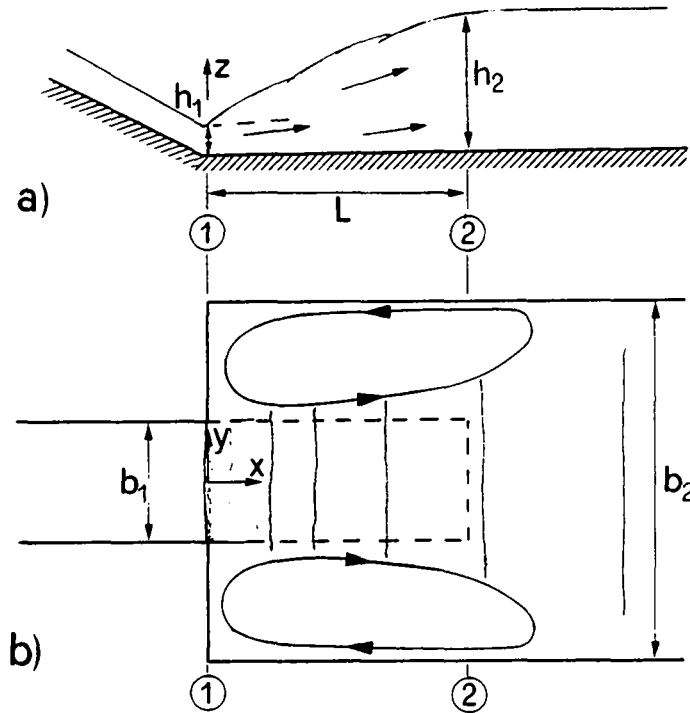


Fig. 3.3 : Experimental setup according to Macha (1963).

(- - -) boundaries of the control volume; $b_2 = 2.0\text{m}$; $1.2 \leq B \leq 2$.

a) longitudinal axial section; b) plan view.

The difference between the computed efficiencies and the efficiency of the classical jump is thereby nearly constant for fixed values of ω_1 and B . Therefore, the additional dissipation seems to depend mainly on the parameters B and ω_1 , but is independent of the inflowing Froude number. This means S-jumps have to be considered especially for low inflow Froude number, since in this case the relative increase of dissipation would be significant.

Macha attributed all additional energy dissipation in a nonprismatic stilling basin to the presence of the lateral eddies. Yet, as was observed by Bretz (1987) when analysing Macha's results pertinent to the sill-controlled basin, his inflow characteristics (h_1, F_1) were considerably influenced by wall frictional effects. Also,

the computational procedure adopted for the evaluation of these basic quantities was found questionable.

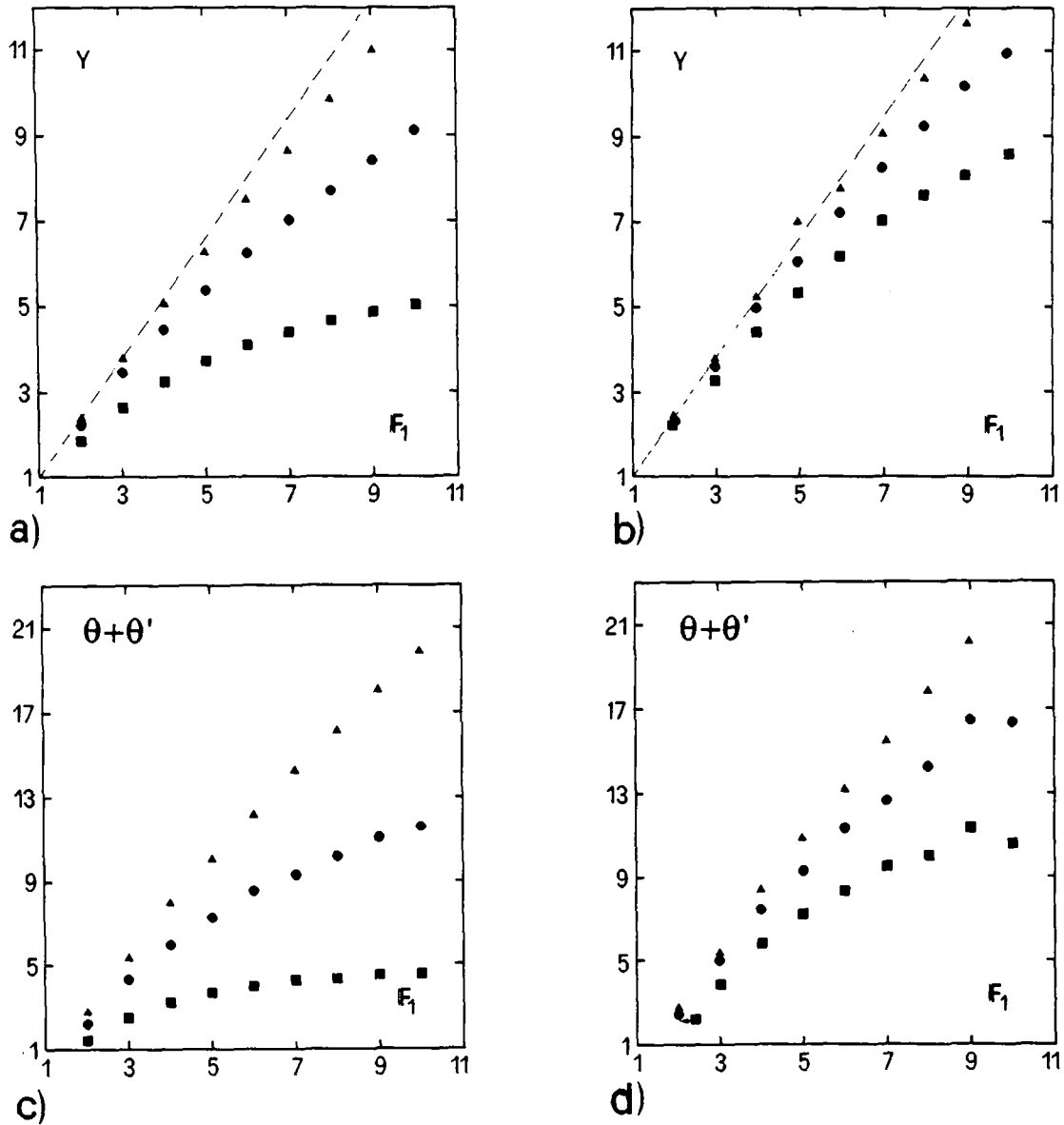


Fig. 3.4 : Typical experimental results of Macha for S-jumps. Sequent depth ratio Y (top) and corresponding terms $\theta_M + \theta'_M$ (bottom) for different shape factors ω_1 . (\blacktriangle) $\omega_1=0.02$; (\bullet) $\omega_1=0.06$; (\blacksquare) $\omega_1=0.15$. (--) classical jump. Expansion ratios a), c) $B=2$ and; b), d) $B=1.4$.

Macha's conclusions are in disagreement with the results of Herbrand (1971), who conducted an experimental study in a 52cm wide sudden expanding channel. The inflow channel of Herbrand was 15cm wide, the inflow Froude numbers ranged between 3 and 8, and expansion ratios $B=3.5$, $B=2$ and $B=1.4$ were investigated. Fig. 3.6 compares the measurements on the S-jump of Unny, Macha and Herbrand for $B=2$.

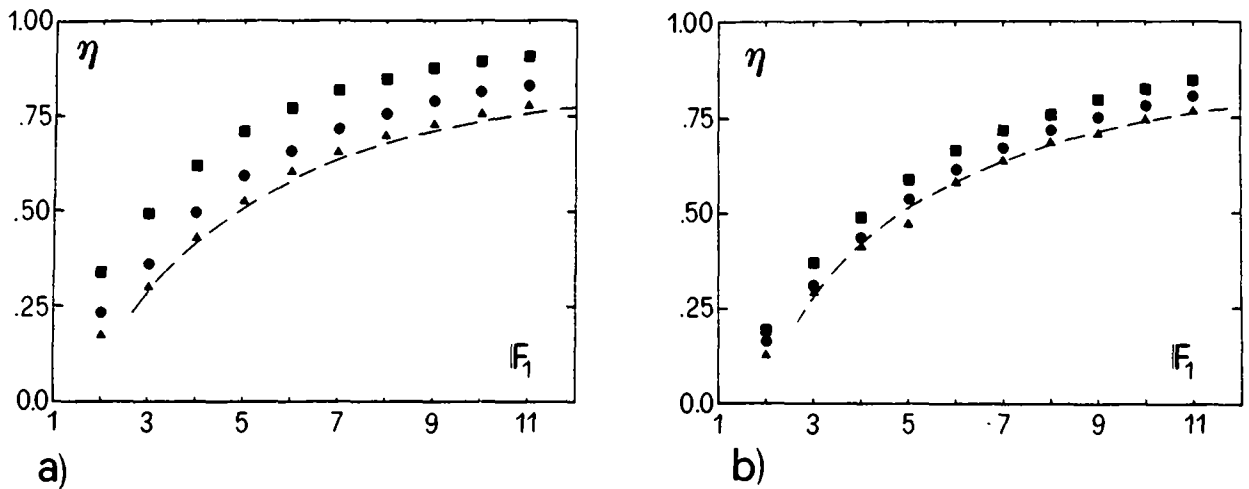


Fig. 3.5 : Efficiency η for a) $B=2$ and b) $B=1.4$. (--) classical jump; notations see Fig. 3.4.

It is seen that the measurements of Macha and Unny are in agreement, whereas the experimental results of Herbrand differ considerably. This difference cannot be justified by experimental means. It seems to indicate that different phenomena were observed. Except Unny, who measured the average toe position x_1 , Macha and Herbrand overlooked this parameter. The effect of x_1 on the sequent depths will be discussed in detail in chapter 5.

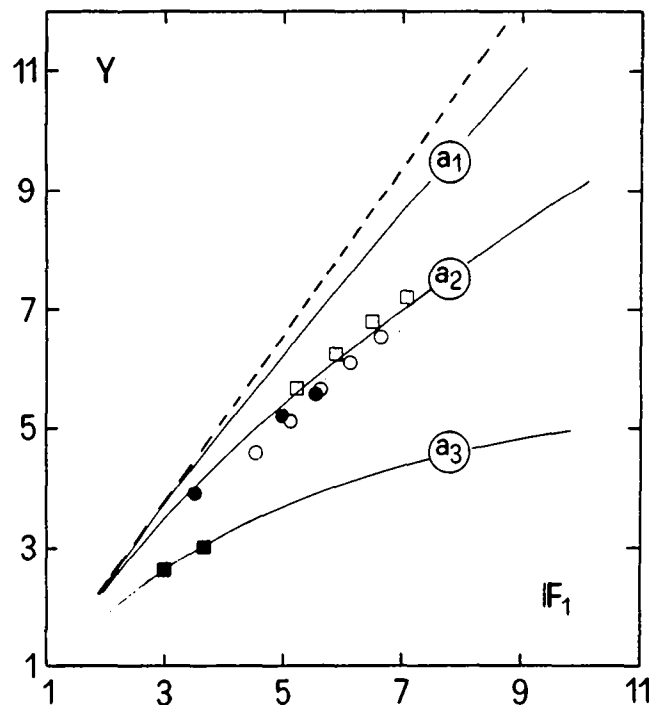


Fig. 3.6 : Sequent depth ratios Y for S-jumps and $B=2$.
 (—) Macha: (a_1) $\omega_1=0.02$, (a_2) $\omega_1=0.06$, and (a_3) $\omega_1=0.15$.
 Unny: (●) $\omega_1=0.06$, and (■) $\omega_1=0.15$. Herbrand: (□) $\omega_1=0.16$, and (○) $\omega_1=0.25$. (--) classical jump.

Based on his experimental data, Herbrand attributed no significant effect of the shape parameter ω_1 on the sequent depth ratio Y . In other words, the lateral eddies are said to have practically no effect on the energy dissipation. Herbrand verified this statement experimentally by inserting an element in the stilling basin which suppressed the formation of the lateral eddy (Fig. 3.7). The difference in Y for configurations with, and without side elements amounted to only 3.5%.



Fig. 3.7 : Side element by which the formation of a lateral eddy is suppressed (Herbrand 1971).

Based on a conventional momentum approach, Herbrand proposed

$$Y^3 - \frac{Y}{B}(1 - C_a^2 + BC_a^2 + 2F_1^2) + \frac{2F_1^2}{B^2} = 0 \quad (3.9)$$

for the sequent depths ratio Y with $C_a = h_a/h_1$. h_a is the average water level along the expansion side wall. Fig. 3.8 shows some typical expansion wall surface profiles and an average flow depth $h_a > h_1$. He concluded that the assumption $h_a = h_1$ involves only a small error. For high inflowing Froude numbers this led to the explicit relation

$$Y = F_1 \sqrt{\frac{2}{B}} - \frac{1}{2B} \quad (3.10)$$

which is in good agreement with his sequent depth measurements. Therein, ω_1 varied between 0.16 and 0.54. Note that Eq. (3.10) differs considerably from Macha.

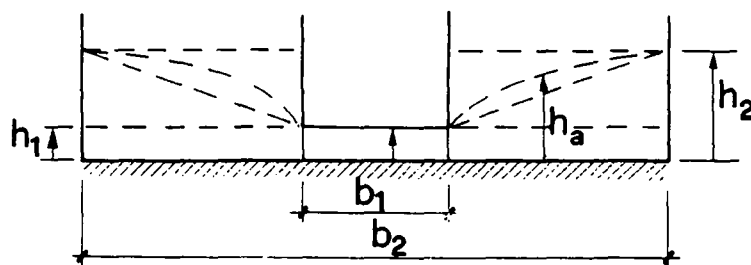


Fig 3.8 : Typical surface profiles along expansion side walls and a corresponding average water level h_a according to Herbrand (1971).

Based on the classical momentum approach across the entire channel width, similar relations were also obtained by Bundschu (1928), and Frank (1943). Bundschu assumed $h_a=h_1$, whereas Frank neglected the streamwise momentum contribution of the expansion side wall at all ($h_a=0$).

3.2.3 Repelled hydraulic jumps (R-jumps)

Probably the first measurements of repelled jumps were conducted by Riegel and Beebe (1917). The inflow conditions were measured in the channel axis shortly upstream from the jump position whereas the sequent depth was measured at the end of the jump. Their purpose was to verify the Bélanger's relation. They assumed that the nonuniform inflow conditions and the radial streamlines across the channel had no effect on Y .

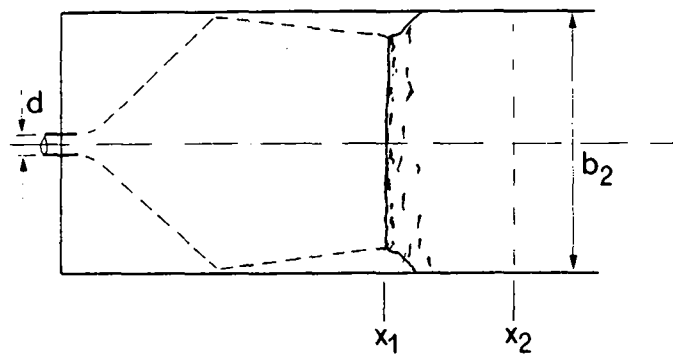


Fig. 3.9 : Riegel and Beebe's (1917) experimental setup. $b_2=3.05\text{m}$,
 $d=0.24\text{m}$.

The discrepancy between the measurements and the prediction was attributed to the nonuniform inflowing depth. Indeed, the measured axial depth is higher than the average across the entire channel. Further experiments conducted by Riegel and Beebe on gradually expanding channels will be described in the second part of the chapter.

The first systematic study on repelled hydraulic jumps was forwarded by Nosedá (1963). The inflow Froude numbers F_1 ranged between 1.97 and 6.42 in an abrupt expanding channel of $B=5$. Fig. 3.10 shows the experimental configuration, the cross waves, and fronts of the hydraulic jump at various tailwater levels.

The flow in the tailwater channel was subdivided into two portions, containing (1) the discharge $Q_c=Q_c(x)$ within the cross-waves, and (2) the discharge $Q_1=Q_1(x)$ between

the cross-waves and the channel side walls. The longitudinal coordinate x is measured from the expansion section. Continuity implies that $Q=Q_c+Q_1$. The widths of the two flow zones are b_c and b_1 respectively, such that $b_c+b_1=b_2$. First, it was found that the ratio Q_c/Q depends exclusively on b_c/b_2 , namely

$$\frac{Q_c}{Q} = \frac{b_c/b_2}{2.7-1.9b_c/b_2} \quad (3.11)$$

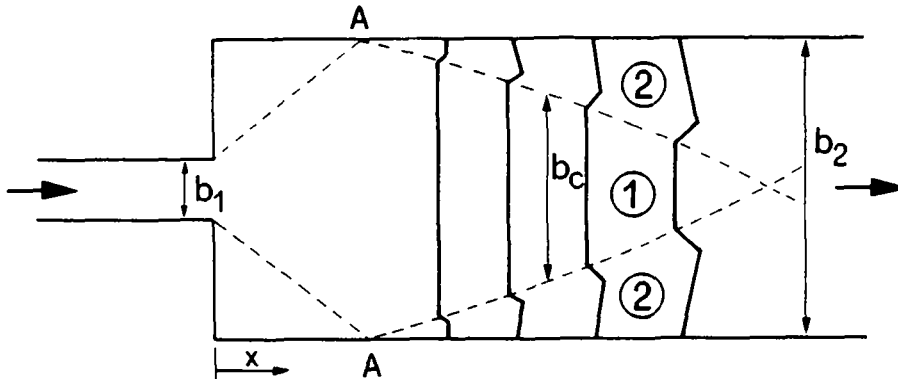


Fig. 3.10 : Experimental configuration of Nosedá (1963). (--) cross waves; (—) schematic jump fronts at various tailwater depths.

Subsequently, the flow depths at the inside of the cross waves h_{1c} and the flow depth between the cross waves and the side walls h_{11} were recorded. These flow depths were measured just upstream from the toe. Further, by observing the corresponding widths b_c and b_1 of each flow portion, the inflow Froude numbers F_{1c} and F_{11} were computed. Now, upon applying Bélanger's Eq. (5.1) separately to each flow portion, the sequent depths h_{2c} and h_{21} were evaluated. Solving Eq. (5.1) for both domains ① and ②, and toe positions located downstream from the toe position of R-jumps, shows that h_{2c} is always smaller than h_{21} . However, when moving the jump towards the critical R-jump position (point A in Fig. 3.10), h_{21} becomes smaller than h_{2c} . The difference $h_{21}-h_{2c}$ then increases rapidly if the jump moves still further upstream. This difference leads to the breakdown of the repelled jump, as described in chapter 2.

The average downstream flow depth h_2 was computed as

$$h_2 = (h_{2c}b_c + h_{21}(b_2-b_c))/b_2 \quad (3.12)$$

This result is in fair agreement with Nosedá's observations. Despite the fair agreement between the predicted and the measured flow depths, the approach presented by Nosedá cannot be used for the prediction of the sequent depths. First, the supercritical flow in the expansion must be computed in order to establish the

functions $h_{1c}(x)$ and $h_{1l}(x)$. Second, the pattern of the cross waves must be known. The effect of the wall roughness and the bottom slope on the supercritical flow remain unspecified. Third, Eq. (3.11) must be verified for other expansion ratios B . Yet, the analyses of the flow patterns inside and outside of the cross waves allow the understanding of the instability of repelled jump, and its breakdown phenomena.

Rajaratnam and Subramanya (1968) conducted an experimental research program in a 0.457m wide sudden expanding channel. The width of the inflow channel was variable in order to obtain expansion ratios ranging from $B=1.2$ to $B=6$. The experimental setup, including the jump and the cross-waves, is shown in Fig. 3.11.

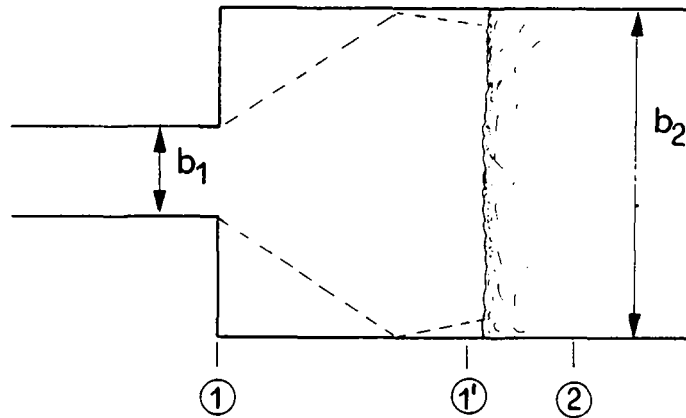


Fig. 3.11 : Repelled jump according to Rajaratnam and Subramanya (1968). (--) cross waves ; (—) toe position.

Their sequent depths relation based on the momentum equation between sections ① and ② assumed that 1) the Bélanger's sequent depth relation may be used, thereby neglecting the effect of the cross-waves; 2) the average velocity may be considered as constant between the sections ① and ① . Thus,

$$F_1'^2 = BF_1^2 \quad \text{with} \quad h_1' = \frac{h_1}{B} \quad . \quad (3.13)$$

Introducing Eq. (3.13) in Bélanger's equation yields

$$Y = \frac{0.5}{B} \left[\sqrt{1 + 8BF_1^2} - 1 \right] \quad . \quad (3.14)$$

This is equivalent to Eq. (3.1) established by Kusnezow (1958) for the spatial hydraulic jump provided $K_K=1$.

Rajaratnam and Subramanya attributed the differences between their measurements and Eq. (3.14) to frictional effects, and proposed the modified relation

$$\frac{Y - 0.75}{F_1 - 0.85} = \frac{1}{B} + 0.3 \quad (3.15)$$

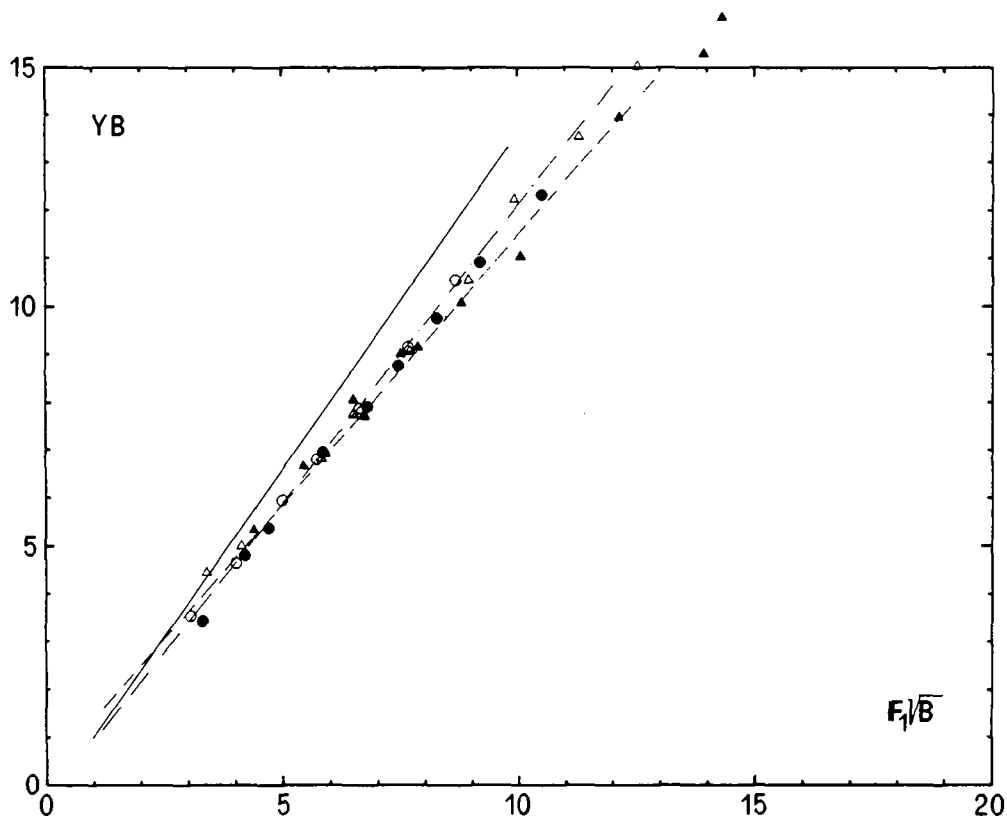


Fig. 3.12 : Experimental results of Rajaratnam and Subramanya (1968).
 (○) $B=1.2$; (●) $B=1.5$; (△) $B=2.0$ and (▲) $B=3.0$;
 (—) Eq. (3.14), Eq.(3.15) for (- -) $B=2$ and (---) $B=1.2$.

This relation is based on the momentum equation applied between sections ① and ② (Fig. 3.11) by accounting for frictional effects. This point of view seems inappropriate because the effect of cross-waves on the R-jump is larger than frictional effects. The deviation between Eq. (3.14) and the experiments should therefore be mainly attributed to the nonuniform inflow conditions. In Fig. 3.12 the experimental results of Rajaratnam and Subramanya, for different expansion ratios B , are compared to Eqs. (3.14) and (3.15).

3.2.4 Transitional hydraulic jumps (T-jump)

It seems that Schröder (1957) has conducted the first systematic investigation on transitional hydraulic jumps. The purpose of his work was to analyze the formation, and the effect of the lateral eddies in nonprismatic stilling basins relative to erosion.

The investigation was therefore directed to the observation of the mechanism of internal energy dissipation .

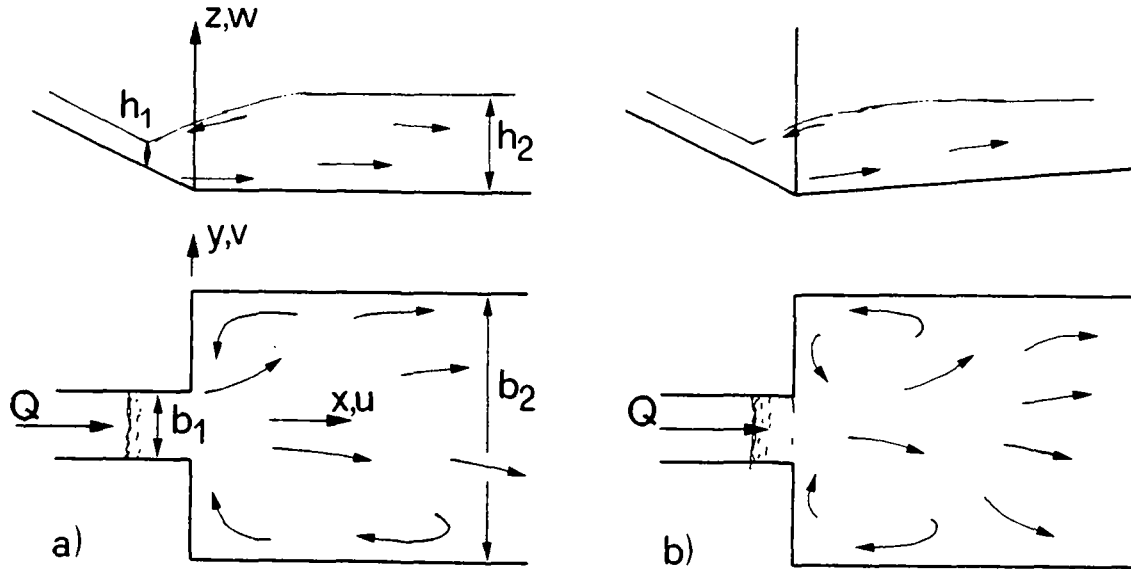


Fig. 3.13 : Schröder's experimental configuration a) horizontal bed; b) negatively sloping bed. Longitudinal section (top) and plan view (bottom). $b_1=0.47\text{m}$; $b_2=1.175\text{m}$.

Schröder observed that the flow remains symmetric to the channel axis in negatively sloping basins. This was not verified with a horizontal bottom (Fig. 3.13). Therefore, an adverse sloping bottom stabilizes the formation of a jump, and Schröder confined the main part of the measurements to this bottom configuration. The supercritical flow was controlled by a vertical plane gate.

The upstream positively sloping channel was 0.47m wide, whereas the maximum downstream width of the stilling basin attained 1.175m. The toe of jump was located on the positively sloping approach channel, yet without indication of its position.

From the analytic point of view, Schröder referred to the approach of Jaeger (1949). The energy and momentum equations were presented taking into account the effects of nonuniform velocity distribution and streamline curvature. The one-dimensional relation for the energy head H_m of a homogeneous fluid is

$$H_m = \alpha \frac{V_m^2}{2g} + \beta \frac{p_m}{\rho g} + z \quad (3.16)$$

when neglecting the thermal and the surface tension contributions. V_m is the average cross-sectional velocity, p_m the average pressure and z the local vertical coordinate relative to a fixed but arbitrarily chosen reference level. The term

$$\alpha = \frac{1}{QV_m^2/2g} \int \frac{V^2}{2g} u dy dz \quad (3.17)$$

accounts for the nonuniform velocity distribution, and the term

$$\beta = 1 + \frac{1}{QP_m/\rho g} \int \frac{p}{\rho g} u dy dz \quad (3.18)$$

involves the streamline curvature effects. Q is the discharge, V the local velocity and u its component in the direction of flow (Fig. 3.13). According to Jaeger (1949), the nonuniformity of the energy distribution across a section can be measured by

$$\varepsilon = \frac{1}{b \frac{p_m}{\rho g} \frac{V_m^2}{2g}} \int \Delta H dy dz \quad \text{with} \quad \Delta H = H - H_m \quad (3.19)$$

b is the local channel width and H the local energy head. Neglecting the streamline curvature ($\beta=1$), Eq. (3.19) may be expressed as

$$\varepsilon = \alpha - \alpha'' \quad (3.20)$$

with

$$\alpha'' = \frac{1}{b \frac{p_m}{\rho g} \frac{V_m^2}{2g}} \int \frac{V^2}{2g} dy dz \quad (3.21)$$

For potential flow the velocity distribution is uniform and the pressure hydrostatic leading to $\varepsilon=0$. In case of nonuniform velocity or pressure distribution ε is always larger than 0.

Schröder measured the velocity and pressure distribution in six sections across the stilling basin for different flow conditions. These measurements allowed the computation of ε , and the energy head H_m . Based on those experimental data, Schröder proposed for the slope of the energy head line in the direction of flow

$$dH_m/dx = H'_m = C\varepsilon \quad \text{with} \quad C = C_0(\Delta H/b)^n \quad (3.22)$$

C_0 and n are functions depending on the ratio B and the inflow water depth h_1 . Fig. 3.14 shows a comparison between experimental results of Schröder and Eq. (3.22).

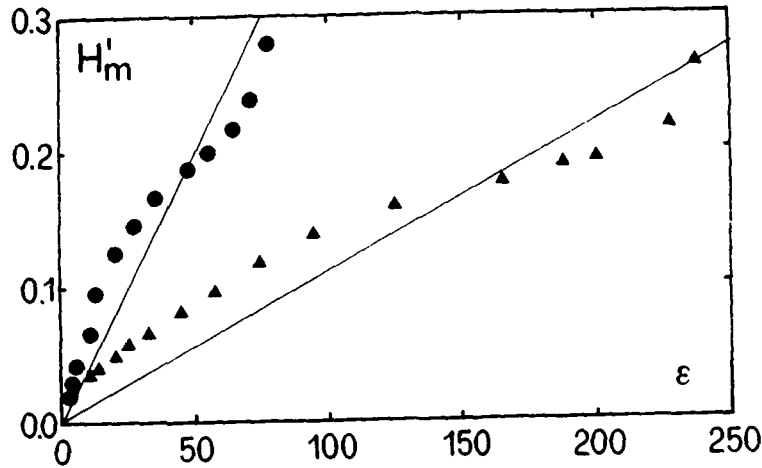


Fig. 3.14 : Relation between H'_m and ϵ . (—) empirical relation according to Eq. (3.22). Schröder's experiments (●) $B=5$; (▲) $B=2.5$

Assuming hydrostatic pressure distribution ($\beta=1$), Eq. (3.22) indicates that the slope of the energy line, or the energy loss per unit length depends linearly on the velocity gradients, as measured by ϵ across a flow section. Therefore, the energy loss per unit width increases with the nonuniformity of the velocity distribution.

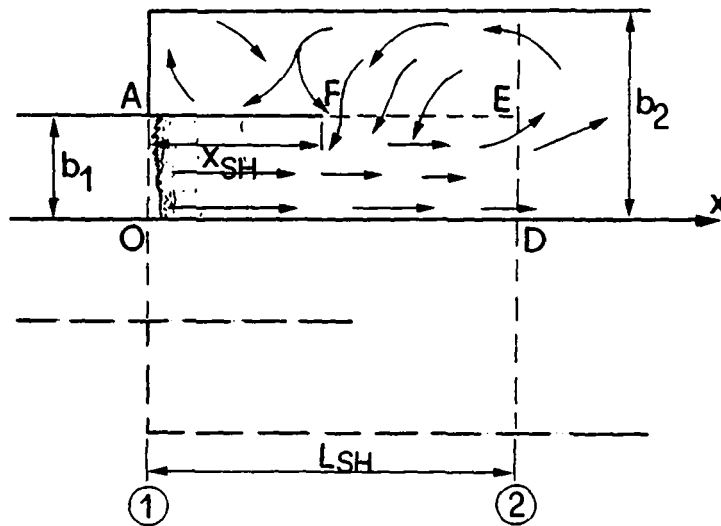


Fig. 3.15 : Sharma's (1964) experimental setup. (--) Control volume boundaries AODE. A-F extended channel side wall. $b_1=1.0\text{m}$ and $b_2=2.0\text{m}$ (same experimental installation as Unny)

A similar result was also obtained by Oosterholt (1947) when considering the energy dissipation of a surface roller in submerged hydraulic jumps. This finding indicates that the two lateral eddies contribute significantly to the energy dissipation; yet, no quantitative measurements are actually available. The investigation of Schröder is

therefore an important contribution to a better understanding of the mechanisms of the energy dissipation in hydraulic jumps. However his results cannot be used for design purposes, mainly because no attempt was made to predict the sequent depth ratio Y , the jump length, or the asymmetry phenomenon.

Sharma (1964) considered a sudden asymmetric expansion (half-model) with a vertical wall extending in the inflow channel width. Fig. 3.15 shows the experimental setup, a typical toe position, and the boundaries of the control volume. Note that section ② was also not defined. Furthermore, as the jump occurred partially in the narrow and partially in the wide channel portions Sharma's flow configuration was a transitional jump (chapter 2).

Based on a new parameter $X_{SH}=x_{SH}/L_{SH}$ accounting for the toe position relative to the end of the protruding side wall (point F in Fig. 3.15), Sharma extended Unny's approach (1960) as

$$C_1 Y^3 + C_2 Y^2 + C_3 Y + C_4 = 0 \quad (3.23)_1$$

for the sequent depth ratio Y with

$$\begin{aligned} C_1 &= 1 - X_{SH} , \\ C_2 &= 1 + K_{SH}\omega_1(1 - X_{SH})F_1^2 , \\ C_3 &= X_{SH} - 2(1 - X_{SH})F_1^2 , \text{ and} \\ C_4 &= -2X_{SH}F_1^2 . \end{aligned} \quad (3.23)_2$$

L_{SH} is the transitional jump length measured from the expansion section. Eq. (3.23)₁ is valid only for $B=2$ for which $K_{SH}=1.886$ was found from the experiments. The sequent depths computed with Eq. (3.23) for $x_{SH}=0$ are similar to those obtained by Macha and Unny.

3.2.5 Comments on hydraulic jumps in sudden expansions

This review shows that the analysis and the computational models for sudden expanding channels differ considerably from author to author. The discrepancy of approaches is particularly significant for S-jumps, where experimental deviations up to 100% may result (Fig. 3.6). It seems that insufficient attention was paid to the toe

position relative to the expansion section. Except of Unny, who measured the jump position, Herbrand indicated only "*the toe is approximately at the beginning of the expansion section*". Especially for large expansions ratios, a variation of the tailwater level modifies only slightly the toe position. Furthermore, Unny, Macha and Herbrand neglected the frictional effect on the inflowing supercritical flow when investigating S-jumps, thereby overestimating F_1 . However, this neglect cannot justify the significant experimental deviations. The position of section ② as considered by Unny and Macha was upstream from the end of jump. Therefore, their tailwater depths were smaller than at the end of the longer lateral eddy. Furthermore, the asymmetric flow phenomenon in channel expansions was not mentioned. The character of these studies seems strongly simplified compared to what will be reported in chapter 5.

The experimental data of Rajaratnam and Subramanya, and Nosedá on repelled hydraulic jumps are in agreement, although different approaches were adopted.

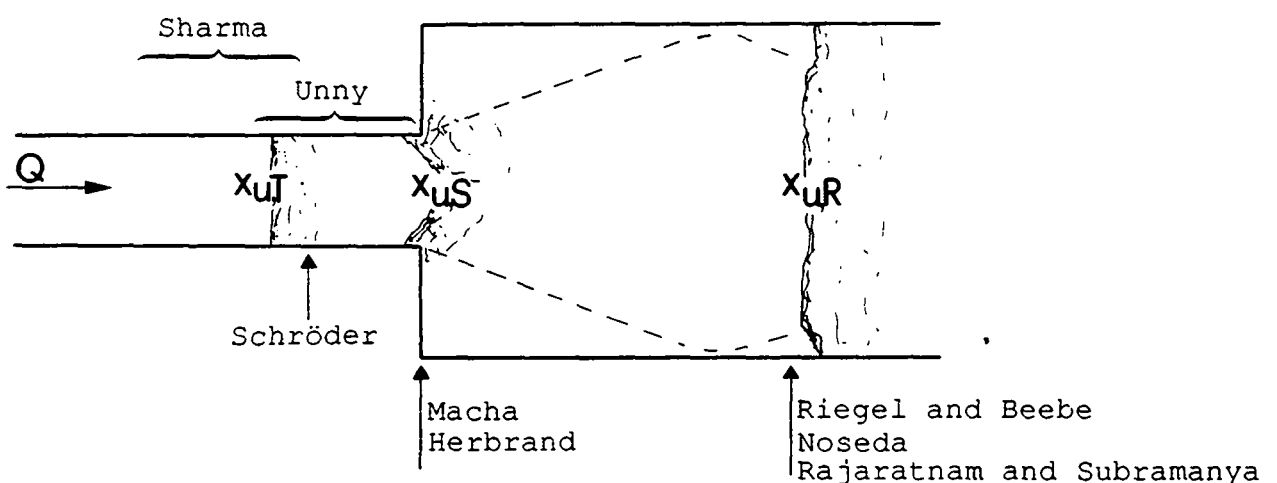


Fig. 3.16 : Classification of hydraulic jumps in sudden expanding channels according to chapter 2.

x_{uT} : toe position for T-jumps; x_{uS} : toe position for S-jumps and x_{uR} : toe position for R-jumps.

The purpose of investigations on the T-jump presented by Schröder and Sharma differ fundamentally so that a comparison becomes impossible. Schröder analyzed the internal energy dissipation mechanism, whereas Sharma related the inflow conditions to the channel geometry and tailwater parameters by ignoring the internal mechanisms. Sharma's experiments included thirtyfive runs without any systematic change of toe position. These data are not sufficient to establish a general sequent depths relation. Finally, no attempt was made to investigate the flow asymmetry,

especially for S-jumps. A visualisation of flow asymmetry had of course required a symmetric channel expansions.

Fig. 3.16 shows the toe positions considered in the previously reported investigations.

3.3 GRADUAL EXPANSIONS

3.3.1 Spatial hydraulic jump (S-jumps)

S-jumps satisfying the definition of chapter 2 are generally analysed by parallel streamline models. Such flow configurations are frequently encountered in linear expansions with large expanding angles.

Riegel and Beebe conducted in 1917 a series of experiments in a gradually expanding stilling basin. The purpose of their investigation was to establish an optimal stilling basin geometry for the Miami Flood Control Project.

The measurements of series 1, described in paragraph 3.2.3, were conducted in a 3.3m wide sudden expanding channel, whereas in series 2 a gradually expanding channel with a diverging angle of $2\phi=8.54^\circ$ was considered. In this series the inflowing flow depth, the tailwater level and the toe position were measured. Since the channel geometry was described only superficially, a comparison of the experimental data with computation involves some uncertainties.

Further experiments (series 3) were carried out by adding some small blocks on the bottom of the stilling basin. The authors concluded that the bottom velocities below the jump are then reduced, and that the jump occurs more upstream.

Furthermore, when the tailwater level was increased, the main stream was deflected along one side of the channel, in much the same way as in the smooth channel.

For the final design, the authors proposed a gradually expanding stilling basin of sloping bottom covered with negative steps as shown in Fig. 3.17. The jump position was stabilized by two additional submerged sills. Although the comparison between the experimental and the computed data is not conclusive from the qualitative point of view, Riegel and Beebe gave some useful informations on the effect of blocks, sills and steps on the main flow properties.

Cvetkov (1952) presented the first computational model for the sequent depths ratio in gradually expanding stilling basins. The toe of the jump was assumed straight, and was located at the expansion section ① as shown in Fig. 3.18. No account was made for the possible formation of lateral eddies between the main flow and the side walls. Fig. 3.18a) shows the boundaries of control volume for the computational model, and Fig. 3.18c) the assumed pressure distribution along the side walls.

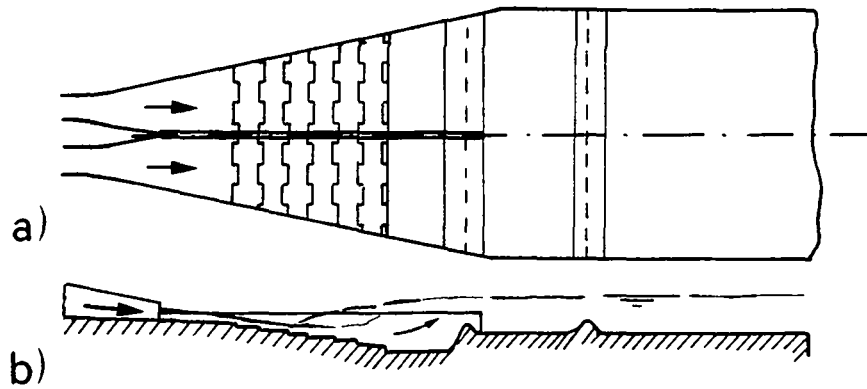


Fig. 3.17 : Miami Flood Control Project. Final design of stilling basin.
a) plan view ; b) longitudinal cross section.

Upon assuming $L_j = 6(h_2 - h_1)$ for the jump length, the conventional momentum approach led to

$$C_1 \cdot Y^4 + C_2 \cdot Y^3 + C_3 \cdot Y^2 + C_4 \cdot Y + C_5 = 0 \quad (3.24)$$

in which

$$C_1 = 48\omega^2 \text{tg}^2\phi,$$

$$C_2 = 16\omega \text{tg}\phi - 72\omega^2 \text{tg}^2\phi,$$

$$C_3 = 1 - 2\omega \text{tg}\phi,$$

$$C_4 = 1 - 24F_1^2 \omega \text{tg}\phi - 14\omega \text{tg}\phi + 24\omega^2 \text{tg}^2\phi, \text{ and}$$

$$C_5 = -2F_1^2$$

with $\omega_1 = h_1/b_1$ and ϕ is the expansion angle. For $\phi=0$ Eq. (3.24) becomes equivalent to the Bélanger's relation. For gradual expansions, the shape parameter ω_1 results from the momentum contribution of the side wall pressure. For sudden expanding channels, ω_1 was introduced empirically.

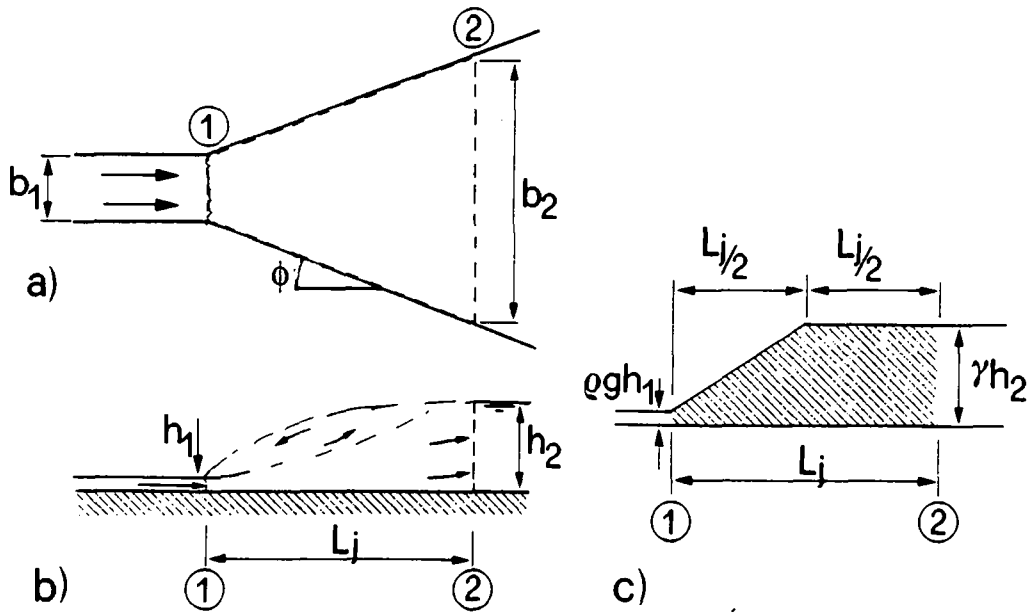


Fig. 3.18 : Cvetkov's computational model. a) Plan view including (--) control volume; b) side view and c) assumed pressure distribution along the lateral side walls ①-②.

Rajnov (1964), proposing a similar approach, considered that the pressure on the side walls increase linearly from h_1 to h_2 . This led to sequent depth ratios Y slightly smaller than those of Cvetkov.

Rajaratnam (1967), assuming parallel streamlines and a linearly increasing side wall pressure as Rajnov, proposed for the momentum contribution of the side walls

$$P = \frac{\rho g}{3} \cdot \tan\phi \cdot \frac{h_2 - h_1}{m} (h_1^2 + h_1 h_2 + h_2^2). \quad (3.25)$$

Introducing this relation in the classical momentum approach, and with the modified parameters

$$\bar{F}_1^2 = \frac{Q^2}{4gb_1^2 h_1^3} \quad ; \quad \bar{\omega}_1 = \frac{1}{m} \cdot \tan\phi \cdot \frac{h_1}{b_1} \quad (3.26)$$

led to

$$1 + \frac{1}{3}\bar{\omega}_1(Y-1)(1+Y+Y^2) - (1+\bar{\omega}_1(Y-1))Y^2 = 2\bar{F}_1^2 \left[\frac{1}{Y} \cdot \frac{1}{1 + \bar{\omega}_1(Y-1)} - 1 \right] \quad (3.27)$$

Assuming $m=(h_2-h_1)/L_j=6$ for the average slope of the jump profile, Rajaratnam's relation is in agreement with the measurements of Riegel and Beebe. Yet he remarked that further extensive experiments were needed for testing the basic assumptions made in developing Eq. (3.27).

3.3.2 Repelled hydraulic jumps (R-jumps)

R-jumps satisfying the definition of chapter 2 are generally approached by a radial streamline model as shown in Fig. 3.19. Such flow configurations are encountered in expansions with small expanding angles. Assuming a radial streamline distribution across the entire channel (Fig. 3.19), and hydrostatic pressure distribution, Rubatta (1963) proposed

$$x = \frac{Q}{2\phi h \cdot \sqrt{2g(H-h)}} \quad (3.28)$$

for the surface profile $h=h(x)$ across a gradual expansion, thereby neglecting frictional effects, that is $H=H_1$ for the energy head. x is the radial coordinate, and 2ϕ the total expanding angle. Eq. (3.28) is only valid if the angle ϕ is small enough to avoid separation between the main flow and the side walls. The limit expansion angle for which Eq.(3.28) may be used is given in paragraph 3.4

Unlike the hydraulic jump in prismatic channels, the computation of the sequent depths in gradually expanding channels is related to the jump length L_j . Applying the momentum equation on the control volume shown in Fig. 3.19 yields for perfectly symmetric flow

$$\int_0^\phi \frac{1}{2}\rho g(h_1^2 x_1 - h_2^2 x_2) \cos\phi d\phi + F \sin\phi = \int_0^\phi \rho (x_2 y_2 V_2^2 - x_1 y_1 V_1^2) \cos\phi d\phi \quad (3.29)$$

$F \sin\phi$ is the longitudinal momentum contribution exerted by the side walls which depends on the wall pressure distribution and the jump profile. Assuming small diverging angles, Rubatta neglected this force at all and thus eliminated the jump length parameter. With the nondimensional parameters

$$\mu = \frac{H_2}{H_1} \quad \text{and} \quad \zeta = \frac{Q}{2\phi \sqrt{gH_1^5}} \quad (3.30)$$

and assuming $x_0=x_1=x_2$ the sought quantities h_1 and h_2 could be computed with

$$h_1 = H_1 \cdot C_1 \quad , \quad h_2 = H_1 \cdot C_2 \quad (3.31)_1$$

and

$$x_0 = H_1 \zeta \frac{1}{C_1 \sqrt{2 \cdot (1 - C_1)}} \quad (3.31)_2$$

with

$$C_1 = \frac{13 - \mu}{18} - \frac{1}{9} \cdot \sqrt{41 - 10\mu - 31\mu^2} \operatorname{Ch} \left(\frac{\theta_1}{3} \right) \quad , \quad (3.31)_3$$

$$C_2 = \frac{13\mu - 1}{18} + \frac{1}{9} \cdot \sqrt{31 + 10\mu - 41\mu^2} \operatorname{Sh} \left(\frac{\theta_2}{3} \right) \quad , \quad (3.31)_4$$

where

$$\operatorname{Ch} \theta_1 = \frac{299 + 3 \cdot \mu - 255\mu^2 - 47\mu^3}{(41 - 10\mu - 31\mu^2)^{3/2}} \quad , \quad (3.31)_5$$

and

$$\operatorname{Sh} \theta_2 = \frac{47 + 255\mu - 3\mu^2 - 299\mu^3}{(31 + 10\mu - 41\mu^2)^{3/2}} \quad . \quad (3.31)_6$$

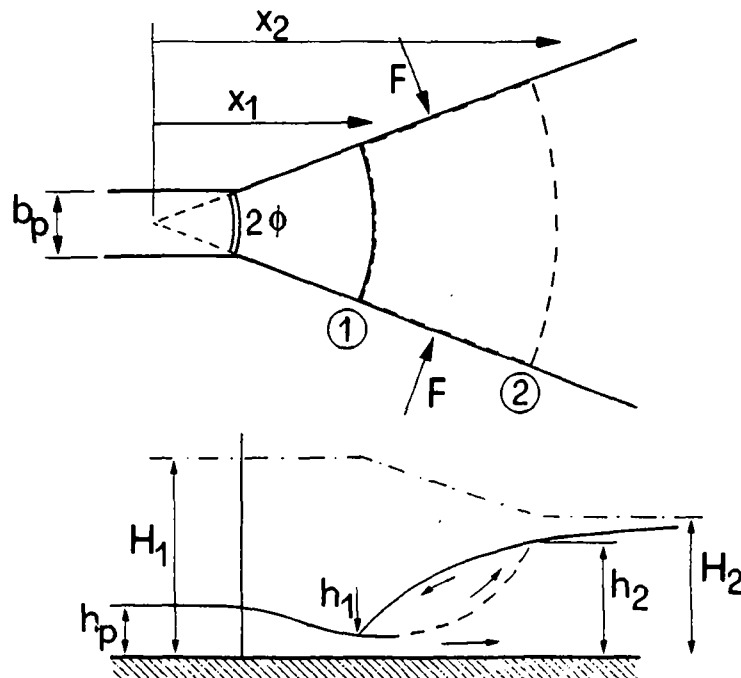


Fig. 3.19 : Schematic R-jump representation.

(--) Boundaries of the control volume, and notation

Herein, $\text{Sh}(i)$ and $\text{Ch}(i)$ are the sine and the cosine hyperbolic functions. The upstream channel width b_0 varied between 20 and 30cm, whereas the expanding angle ranged between $2\phi=2^\circ$ and $2\phi=24^\circ$ with discharges Q up to 128 l/s. Apart from the sequent depths, Rubatta measured the toe position x_1 , and the coordinate x_2 of the jump. Rubatta proposed for the jump position

$$\frac{x_1}{H_1} = \zeta^{0.335} \bar{C}_1 \left(\frac{\mu}{\zeta^{0.318}} \right), \quad (3.32)_1$$

and

$$\frac{x_2}{H_1} = \zeta^{0.335} \bar{C}_2 \left(\frac{\mu}{\zeta^{0.318}} \right) \quad (3.32)_2$$

where \bar{C}_1 and \bar{C}_2 depend on μ and ζ and could easily be estimated by a plot. The experimental data are in agreement with Eqs. (3.32). For given values of Q , H_1 and H_2 , the computation of the jump position, the sequent depths and the jump length is straightforward. The average slope m of the jump profile was found to be independent of ζ and could be approximated as

$$m = 8\mu + 3.6 \quad (3.33)$$

The contribution of Rubatta has to be considered as a semi-empirical approach and the model should therefore be verified by other measurements.

Starting from Eq. (3.29) and introducing

$$F_P = \frac{\rho g}{2} (x_2 - x_1) \left(\frac{h_1^2 + h_2^2}{2} \right) \quad (3.34)$$

for the momentum contribution of the side walls, Paderi (1964) obtained

$$\frac{1}{4} (1 - \bar{Y}^2) \bar{X}^2 + \left[\frac{1}{4} (1 - \bar{Y}^2) + F_2^2 \right] \bar{X} - \frac{F_2^2}{\bar{Y}} = 0 \quad (3.35)_1$$

for the sequent depth ratio $\bar{Y}=h_1/h_2$ with $\bar{X}=x_1/x_2$ and

$$F_2^2 = \frac{Q^2}{g(2\phi)^2 x_2^2 h_2^3} \quad (3.36)_1$$

The additional relation

$$1 - \bar{X} = m \frac{h_2}{x_2} (1 - \bar{Y}) \quad (3.37)_1$$

was needed to solve Eq. (3.35)₁. For the average slope m of the jump profile Paderi proposed $m=10\bar{Y}+5.6$. This approach allows the computation of h_1 and x_1 starting from the known values x_2 , h_2 and Q . Accordingly for given inflow conditions H_1 and Q , the sequent depth can be established by an iterative procedure.

De Magalhaes (1976), using the usual parameters Y and $X=x_2/x_1$ transformed Eqs.(3.35)₁ and (3.36)₁ into

$$(1 + X)XY^3 - [X(1+X) + 4F_1^2X]Y + 4F_1^2 = 0 , \quad (3.35)_2$$

and

$$X - 1 = m(Y - 1)\frac{h_1}{x_1} , \quad (3.37)_2$$

respectively, with

$$F_1^2 = \frac{Q^2}{g(2\phi)^2 x_1^2 h_1^3} . \quad (3.36)_2$$

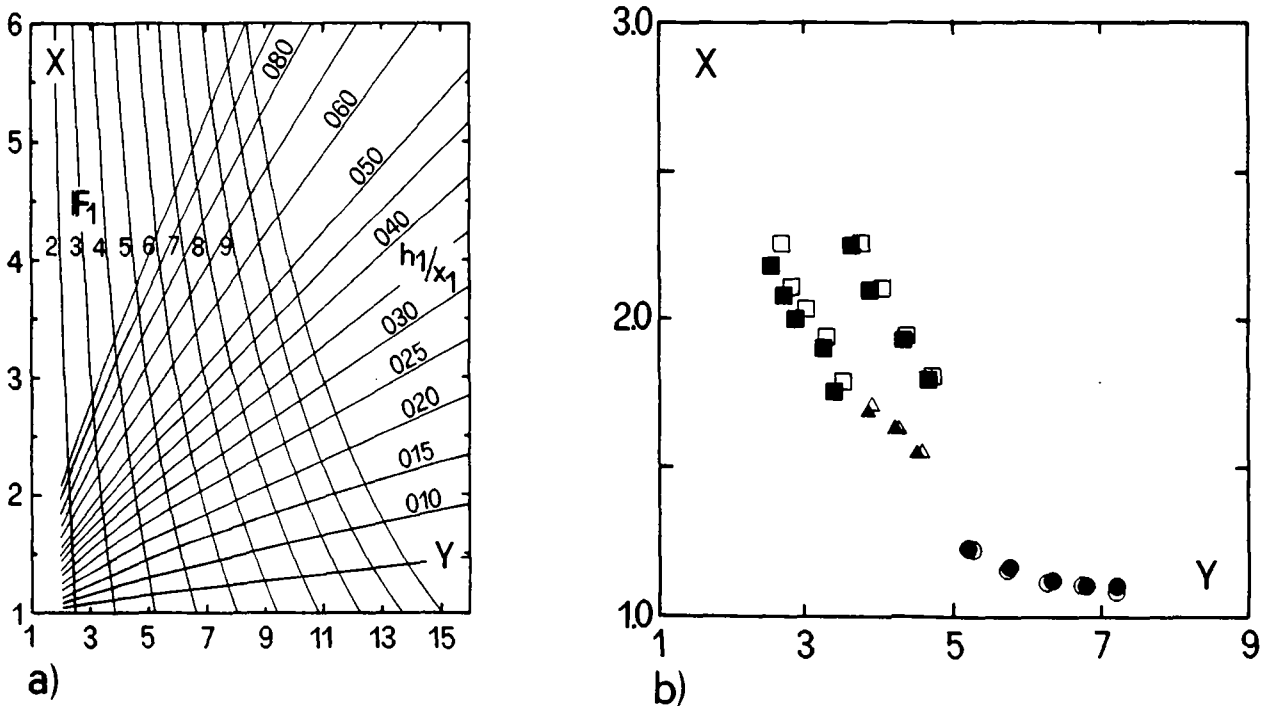


Fig. 3.20 : Prediction of Magalhaes. a) proposed plot b) comparison with experimental results of Rubatta. Open signs: prediction, full signs: Rubatta's measurements. (●) $2\phi=2^\circ$, (▲) $2\phi=8^\circ$ and (■) $2\phi=16^\circ$.

For the solution of these equations Magalhaes proposed a plot shown in Fig. 3.20a). Starting with the inflow conditions x_1 , h_1 and F_1 the sequent depth and the final jump

section could be established. Fig. 3.20b) shows the comparison between the prediction of Magalhaes (and Paderi) and the experimental results of Rubatta.

A significant contribution to the hydraulic jump in gradually expanding channels was presented by Arbhahirama and Abella (1971). Their approach was fundamentally based on the research of Koloseus and Ahmad (1969) which consider a circular jump created by a vertical jet striking a horizontal plane surface. The jump profile, was considered as the quarter-ellipse

$$\frac{(h - h_1)^2}{(h_2 - h_1)^2} + \frac{(\bar{x} - L_j)^2}{L_j^2} = 1 \quad (3.38)$$

where the horizontal major semi-axis is equal to the jump length. \bar{x} is the local coordinate with the origin at $x(\bar{x}=0)=x_1$. This equation is verified experimentally for two inflow Froude numbers F_0 (measured upstream from the expansion) and a diverging angle $2\phi=22.9^\circ$.

As indicated in Fig. 3.21, the comparison of the Eq. (3.38) with the experimental data indicates that the assumed water surface profile is too high for $\bar{x}/L_j < 0.5$. In this figure the flow depths h indicate the measured depths at the coordinate \bar{x} . Furthermore the plot shows that the assumption of a linear profile seems to involve only a small error.

Arbhahirama and Abella assumed a hydrostatic pressure distribution and radial streamlines. The application of the momentum and the continuity equations led to

$$XY = \frac{1}{2} (\sqrt{1 + 8F_e^2} - 1) \quad (3.39)$$

with

$$F_e^2 = F_1^2 X + C_p \quad (3.40)$$

and

$$C_p = \frac{XY(X - 1) \left(X \left[\frac{Y^2}{3} + 0.118Y + 0.048 \right] + \frac{1}{2} \right)}{(XY - 1)} \quad (3.41)_1$$

where

$$F_1^2 = \frac{Q^2}{g(2\text{tg}\phi)^2 x_1^2 h_1^3} \quad (3.42)$$

This formulation is similar to the Bélanger relation. Assuming a linear jump profile and a hydrostatic pressure distribution led to

$$C_p = \frac{XY(X-1) \cdot [X(Y^2 + Y + 1) + 3]}{6(XY - 1)} \quad (3.41)_2$$

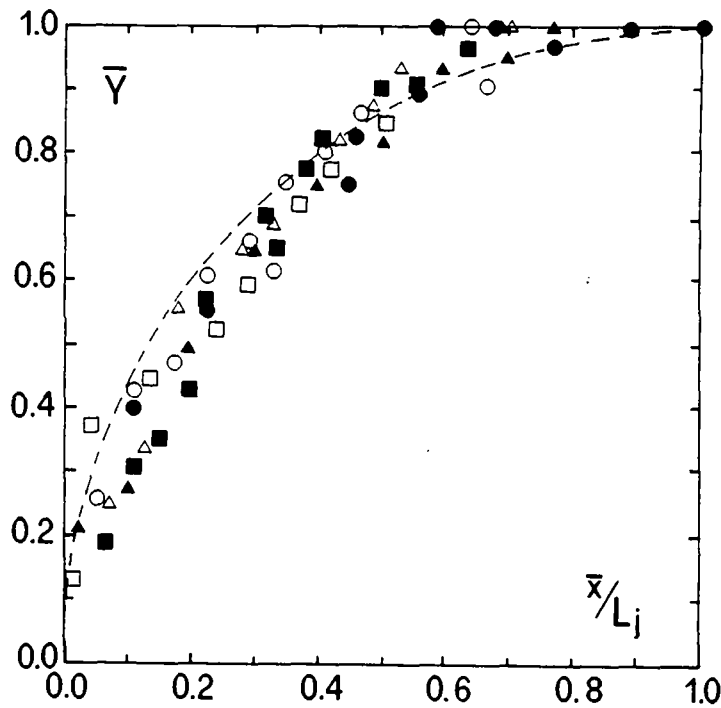


Fig. 3.21 : Nondimensional jump profiles $\bar{Y}=(h-h_1)/(h_2-h_1)$ as a function of \bar{x}/L_j according to Eq.(3.38).of Arbhahirama and Abella (1971). Open signs $F_0= 4.8$; Solid signs $F_p=7.27$. (○) $x_1=26in, x_2=44in$; (△) $x_1=18in, x_2=36in$; (□) $x_1=11in, x_2= 33in$; (●) $x_1=26in, x_2=60in$; (▲) $x_1=17in, x_2=56in$ (■) $x_1=3in, x_2=48in$.

The dimensionless head loss across the jump obtains

$$\eta = \frac{\Delta H_{12}}{h_1} = \frac{F_1^2}{2} \cdot \frac{X^2Y^2 - 1}{X^2Y^2} \quad (3.43)$$

where $\Delta H_{12} = H_1 - H_2$. Using Eq. (3.39), the jump length L_j is given as

$$\frac{L_j}{x_1} = \frac{1}{2Y}(\sqrt{1 + 8F_e^2} - 1) \quad (3.44)$$

The experiments were carried out in a 0.457m wide, 0.686m high and 6.49m long flume. Incorporated therein was a short, 0.1m wide element with a sluice gate (Fig. 3.22). Six different diverging angles ranging from $2\phi=10.34^\circ$ to $2\phi=26.08^\circ$ were considered. The measured sequent depths are in good agreement with Eq. (3.39). This close agreement indicates that the difference between the predicted and the measured jump surface profiles has only an insignificant effect.

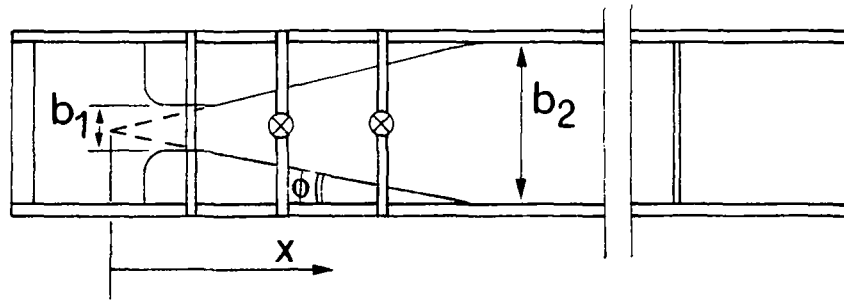


Fig. 3.22 : Experimental setup of Arbhahirama and Abella (1971).
 $b_1=0.457\text{m}$, $b_2=0.686\text{m}$, and $10.34^\circ < 2\phi < 26.08^\circ$.

The lengths measurements scattered and the measured data are generally lower than predicted according to Eq. (3.44).

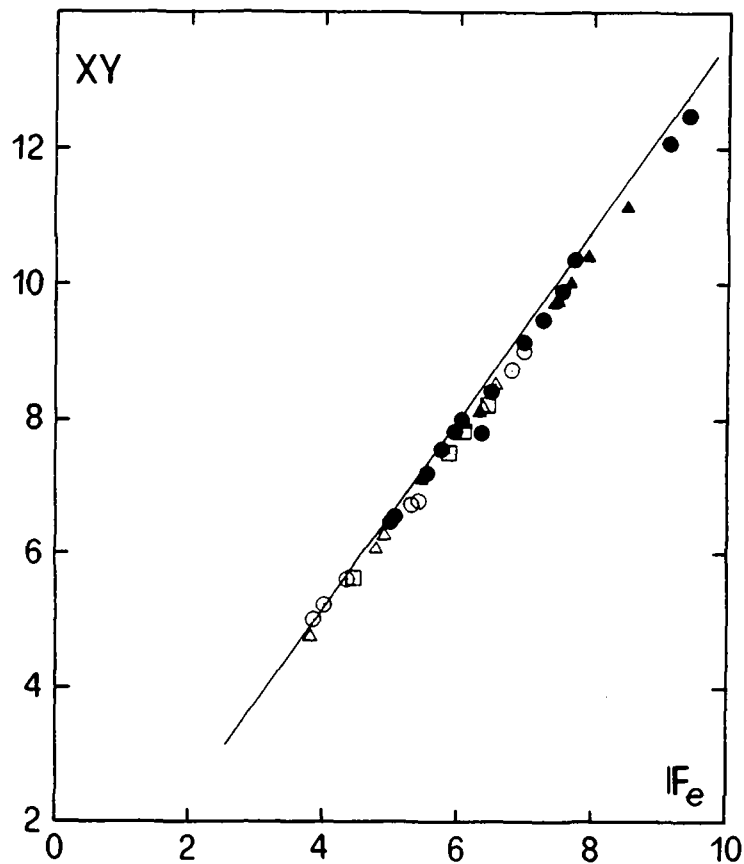


Fig. 3.23 : Measurements of Rubatta (1963) assuming a surface profile according to Eq. (3.41)₁. Comparison between prediction according to Eq.(3.39) and experiments. (●) $2\phi=2^\circ$; (▲) $2\phi=4^\circ$; (○) $2\phi=8^\circ$; (△) $2\phi=16^\circ$ and (□) $2\phi=24^\circ$.

In Fig. 3.23, Eq. (3.39) is compared with the experimental data of Rubatta. As regards the location of the toe, Arbhahirama and Abella further proposed the semi-empirical relation

$$\frac{F_0 h_0}{h_2} = 0.829 + 0.132 \frac{x_1 \phi}{h_0} \quad (3.45)$$

where index 0 indicates the flow conditions at the expansion section.

The effect of air entrainment in radial jumps was considered theoretically and experimentally by Khalifa and McCorquodale (1979). The surface profile along the side walls was assumed as

$$\bar{Y} = C_1 \bar{X}^2 + C_2 \bar{X} \quad (3.46)$$

$$\text{where } \bar{Y} = \frac{h - h_1}{h_2 - h_1} \quad \text{and} \quad \bar{X} = \frac{\bar{x} - x_1}{x_2 - x_1} .$$

C_1 and C_2 are functions of the inflowing Froude number and the entrained air quantity. Applying the momentum and the continuity equations on a radial flow element led to

$$Y^3(X^2 - C_3 X) + Y^2(2XC_3 - C_4 X) + Y(C_4 X - C_3 X - X^2 - 2X\beta_1 F_1^2) + 2F_1^2 \beta^2 = 0 \quad (3.47)$$

involving seven variables. β represents the momentum correction coefficient. To establish these functions, an experimental study was conducted in a 11.0m long, 0.46m wide and 0.6m deep plexiglas flume. The expanding angle was $2\phi = 27^\circ$ and a gate, located between the expanding walls produced a radial supercritical flow. Inflowing Froude numbers between 1.5 and 9 were considered.

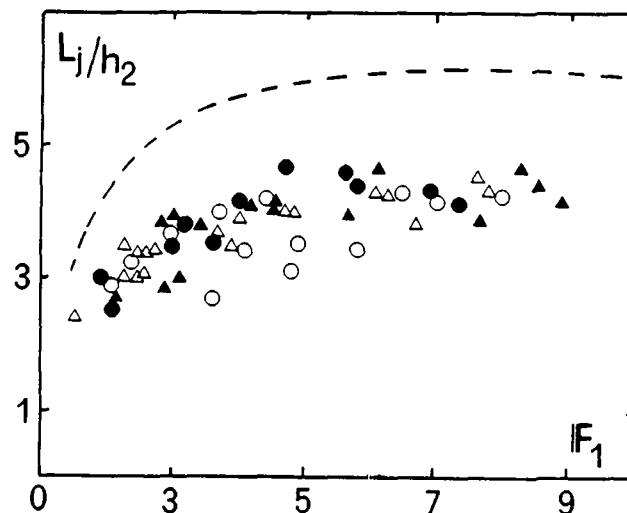


Fig. 3.24 : Jump lengths L_j according to Khalifa and McCorquodale (1979). (\circ) $X=1.2-1.4$; (\triangle) $X=1.41-1.6$; (\blacktriangle) $X=1.61-1.8$; (\bullet) $X=1.81-1.85$. (--) according to USBR for classical jump.

The measurements included informations on the sequent depths, the jump profile as well as the jump length L_j defined as the point *where the surface profile becomes approximately horizontal*. Unfortunately, their experimental data are only presented graphically instead of numerically. Furthermore, the ratio X was given only approximately. As shown in Fig. 3.24, a significant reduction of the jump length was obtained with the expanding channel in comparison to the jump length measured in USBR Basin I.

Fig. 3.25 shows that the jump surface is shifted towards a linear curve when the inflow Froude number F_1 increases. Khalifa and McCorquodale explained this tendency by the increased air entrainment for high Froude numbers and proposed two relations for $\bar{Y}(\bar{X})$, depending only on the range of F_1 . However, it is well known that

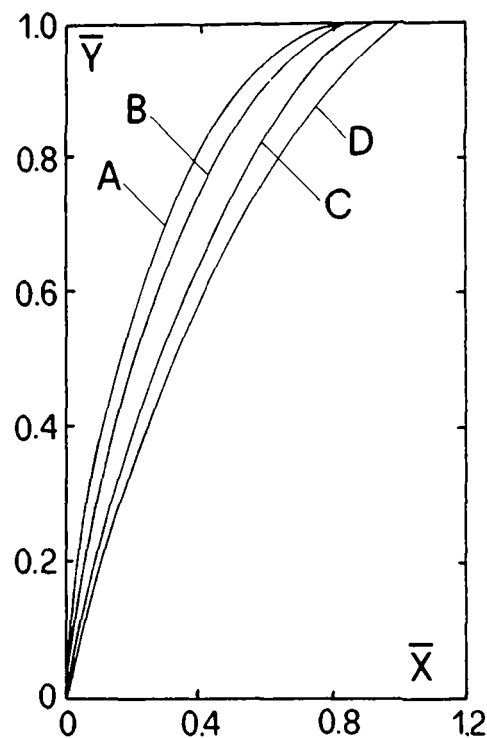


Fig. 3.25 : Average measured surface profiles for different inflow Froude numbers according to Khalifa and McCorquodale (1979). (A) $F_1=2.4$; (B) $F_1=3.0$; (C) $F_1=4.75$ and (D) $F_1=7.1$.

the air entrainment must also be related to scale parameters like the Reynolds number. Hydraulic jumps with high inflow Froude numbers at reduced air entrainment can be obtained for low inflow Reynolds numbers (small inflow depth).

The validity of observations for other inflow Reynolds numbers R_1 than those considered by Khalifa and McCorquodale ($2.8 \times 10^4 < R_1 < 4.2 \times 10^4$) was not verified. Velocity measurements indicated $\beta_1=1$ and that β_2 ranged between 1.2 and

1.7. For computations, the average value of $\beta_2=1.5$ was retained. The functions C_3 and C_4 could then be computed from C_1 and C_2 .

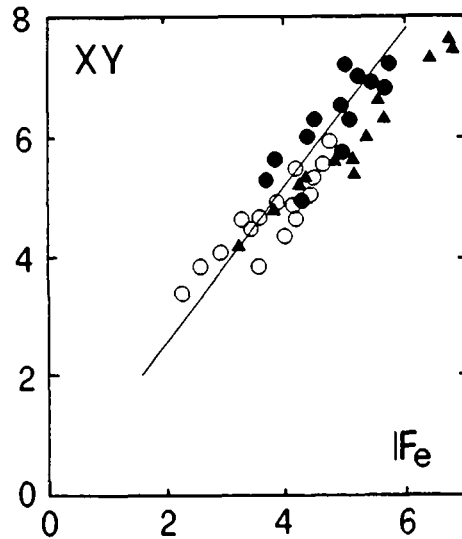


Fig. 3.26 : France's experimental data compared with (—) Eq. (3.39) by assuming a linear surface profile. (○) $2\phi=3.85^\circ$; (●) $2\phi=7^\circ$; (▲) $2\phi=8.7^\circ$.

France (1981) presented a series of experiments in a 10m long, 0.3m wide and 0.3m high channel. The flow was controlled by a vertical 0.1m wide gate. The experimental results are compared with Eq. (3.41)₂ and Eq. (3.39) as established by Arbhahirama and Abella for the sequent depths computation assuming a linear surface profile (Fig. 3.26).

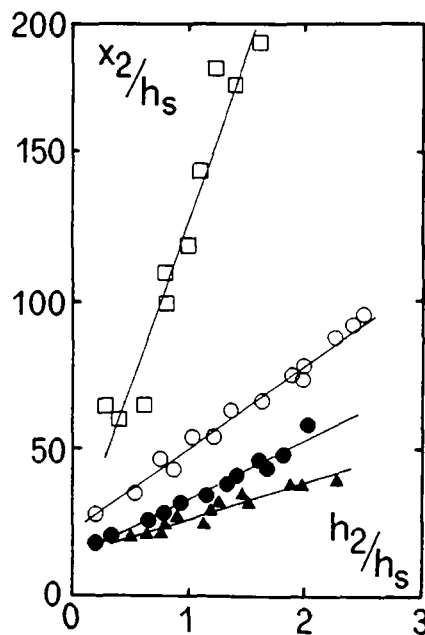


Fig. 3.27 : Jump sensitivity (notation see Fig. 3.26). (□) classical jump. (—) Average experimental curve

Fig. 3.27 shows the jump sensitivity defined as *the change in toe location per unit change in tailwater level*. It is seen to depend strongly on the diverging angle ϕ . Furthermore, France observed that the length of the jump in diverging channels is significantly smaller than in prismatic channels.

3.3.3 Comments on hydraulic jumps in gradual expansions.

This review reveals that the flow patterns, and the proposed computational models depend on the considered diverging angle ϕ . For small ϕ the flow does not separate from the side walls and could be modelled by radial streamlines. For such expansions, the effect of jump surface profile on the sequent depth relation remains small. It seems, therefore that a linear profile as adopted for example by Paderi, accounts satisfactorily for the momentum contribution of the side walls. As shown by Khalifa and McCorquodale, a more detailed surface description involves the effects of inflowing Froude number and air entrainment.

It is difficult, however, to define the flow conditions and channel geometry for which this model is valid, that is to define the transition between radial and spatial jumps. This condition depends on the inflow characteristics, the channel geometry, as well as on the toe position relative to the expansion. For high inflow Froude numbers a radial flow needs excessively long expansion walls with small diverging angles in order to avoid a separation of the supercritical flow from the side walls.

3.4 DIVERGING STILLING BASIN

The investigations presented so far include no description of the disadvantages of hydraulic jumps in expanding channels (chapter 2). In the present paragraph, an account will be given on such investigations in expanding stilling basins, including a description of the main flow patterns.

Nettleton and McCorquodale (1983, 1989) investigated gradual linearly expanding stilling basins as shown in Fig. 3.28. A tendency for bi-stable flow configuration was noted particularly at larger expanding angles. "The flow separates from one side wall and attaches to the opposite wall, this causing an asymmetrical jump with a dead zone or side eddy on the separation side and a strong effluent jet on the other side". The study of Nettleton and McCorquodale shows that this disadvantage may be removed

when providing the basin with baffle blocks. A series of experiments were conducted with the standard USBR baffle block configuration.

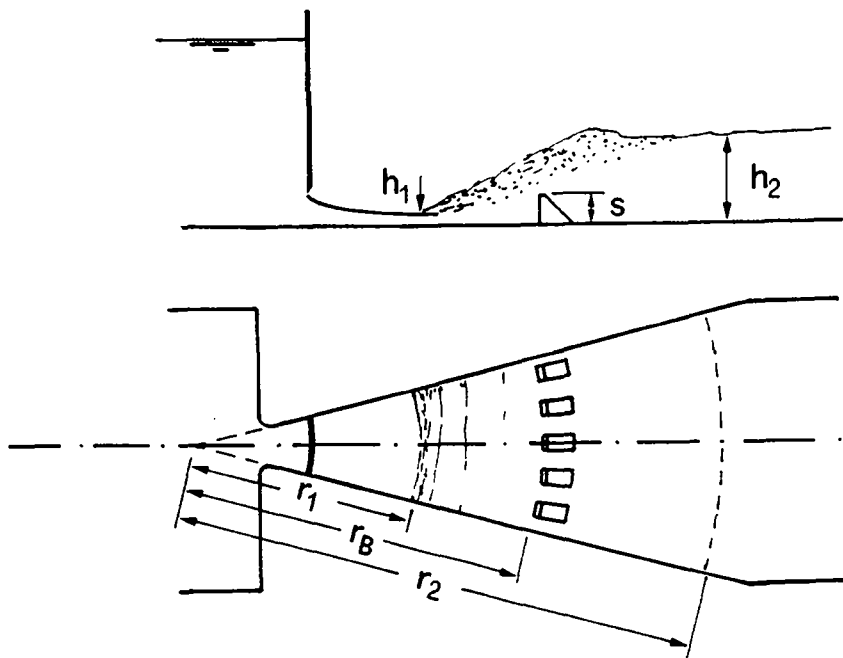


Fig. 3.28 : Experimental setup of Nettleton and McCorquodale (1983, 1989). a) axial view; b) plan view.

Based on the experimental investigation, explicit relations for the sequent depths ratio, the jump length and the jump profile were developed. Investigations on expanding channels conducted by McCorquodale (1986) indicated that the flare angle ϕ should be smaller than

$$\phi < \tan^{-1} \left(\frac{1}{C_{\phi} F_0} \right) \quad (3.48)$$

where F_0 is the inflow Froude number at the toe of the jump and C_{ϕ} a constant which depends on the inflow patterns. When a curved gate is used, a value of $C_{\phi}=1.5$ may be adopted, whereas $2 < C_{\phi} < 3$ when the expansion occurs downstream from a prismatic channel.

Despite the bi-stable flow phenomenon, Nettleton and McCorquodale (1983) mentioned the following advantages of expanding stilling basins :

- the dimensions and costs of control gates or tunnels can be significantly reduced if a definite tailwater velocity is strived for,

- the required tailwater depth is less than for the classical jump at identical approach conditions;
- the diverging basin can be used similar as sloping basins, to contain the jump when the tailwater level is uncertain; and
- the diverging basin seems to be superior to the prismatic basin for velocity reduction in low Froude numbers jumps ($F_1 < 4$).

Herbrand and Knauss (1973) conducted a series of model tests on gradual and sudden expanding stilling basins. The sequent depths ratio was predicted according to Eq. (3.10), corresponding to the S-jump configuration. The main dimensions of the stilling basins investigated are given in Table 3.1.

Table 3.1 : Main dimensions of the investigated expanding stilling basins.

Example	Name of dam	Scale of model	H [m]	Q [m ³ /s]	b ₁ [m]	b ₂ [m]	B [-]	F ₁ [-]
1	Langenprozelten	1:33	33.5	33	5.0	10	2.0	13.8
2	Wondreb	1:25	14	95	3.5	11.5	3.3	3.0
3	Eixendorf	1:30	30	257	7.0	17.5	2.5	4.8
4	Mauthaus	1:25	63	63	3.1	15.5	5.0	9.0
5	Kardamakis	1:50	103	1325	9.7	32	3.3	4.4

In all stilling basins considered, appurtenances were fixed on the floor of the dissipator in order to improve its efficiency and compactness. For four basins, the appurtenances consisted of two rows of baffle blocks, as shown in Fig. 3.29.

It should be noted that if the second row of blocks is located in the openings of the first row leads to nearly 100% of obstruction. For one stilling basin (Mauthaus), a continuous sill turned out as the most effective device to shorten the stilling basin.

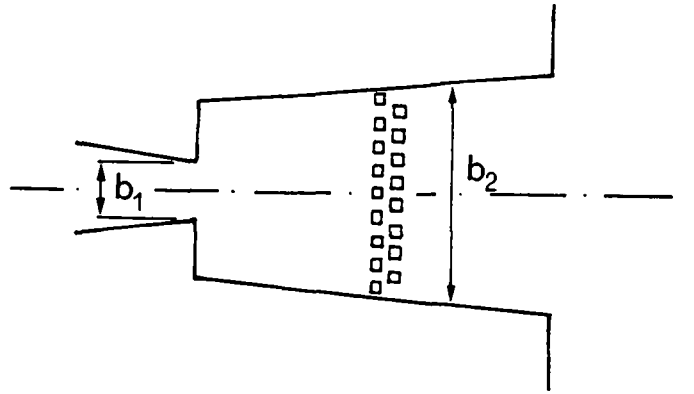


Fig. 3.29 : Stilling basin of Langenprozelten with two rows of baffle blocks. $b_1=5.0\text{m}$, $b_2=10.0\text{m}$, $Q=33\text{m}^3/\text{s}$.

3.5 CONCLUSIONS

In the present chapter, investigations accounting for hydraulic jumps in expanding channels were reported. In the first part sudden expansions were considered, whereas the second part deals with gradual expanding channels.

Investigations on repelled jumps (**R-jumps**) in sudden and gradual expansion are usually in agreement. For gradual expansions, this type of jump is investigated by assuming radial flow conditions. The computational models include usually an evaluation of the toe position relative to the expansion section and the jump length. However, no attempt was made to limit the application domains in order to insure symmetric flow in the tailwater channel. As shown in chapter 2, the symmetry of the jump depends on both the inflow and tailwater conditions, and on the channel geometry.

Since no definite criteria were proposed, the application of these approaches should be limited to small expansion angles (typically less than 10 degrees). For sudden expansions, the model proposed by Rajaratnam (1968) may be used to predict the sequent depths ratio, but no attempt was made to determine the jump position.

Spatial hydraulic jumps (**S-jumps**) are investigated assuming parallel streamlines upstream and downstream from the hydraulic jump. As regards sudden expansions, the equation proposed by Herbrand allows a straightforward evaluation of the sequent depths ratio. However, the flow asymmetry, a significant phenomenon for S-jumps sudden expansions was even not mentioned. Therefore, particular interest will be paid

to the asymmetry of jumps in order to widen the knowledge of hydraulic jumps in expansions.

Despite a large application domain, only few investigations were published on transitional hydraulic jumps (**T-jumps**). The investigation reported by Schröder contributes to a better understanding of the phenomena of energy dissipation in hydraulic jumps, but may not be used for design purposes.

Despite several investigations on particular sudden expanding stilling basins, no systematic research was conducted in order to develop a general design procedure for the preliminary evaluation of the main dissipator dimensions. The purpose of the following chapters is therefore to offer a computational model for the evaluation of the main jump characteristics in sudden expanding channels. Based on this model a sudden expanding dissipator provided with a central sill and an end sill is finally proposed.

4. EXPERIMENTAL INSTALLATIONS

4.1 INTRODUCTION

The experimental study was carried out at the Laboratoire de Constructions Hydrauliques of the Ecole Polytechnique Fédérale de Lausanne (EPFL). This laboratory is equipped with 8 parallel flow circuits connected to a main basin of about 800 m³. Each circuit includes a pump installed just over the main basin, an electromagnetic discharge measuring device, two butterfly valves and supply conduits to the test facilities. From the experimental setup, the water is generally returned to the main basin by collectors. The maximum discharge per pump is either 125 l/s or 250 l/s with pressures between 3 and 6 bars depending on the pump features. The water temperature varies between 18°C and 20°C. A detailed description of the laboratory installations was presented by Bretz (1987).

This chapter aims to describe the experimental facilities such as the channels, the instruments and other measuring devices. Furthermore, the pump calibration will be described in detail. The last paragraph accounts for the computational method used for the determination of small inflowing depths to hydraulic jumps.

4.2 INSTALLATION LCH1

Fig. 4.1 shows the main dimensions of this multiple purpose experimental channel. The 17 m³ upstream basin was supplied by two conduits of 0.30 m diameter (max. total discharge 375 l/s). A 0.5 m wide and 10.8 m long prismatic rectangular and horizontal channel was connected to the basin. At the upstream channel extremity a standard shaped 0.50 m wide and 0.70 m high spillway of design head $H_D=0.2$ m (Fig. 4.1.d) controlled the channel inflow. This spillway was necessary since the accuracy of the electromagnetic discharge measuring device was considered as insufficient. The head on the spillway was measured by a 10cm diameter stilling well (± 0.2 mm) shown in Fig. 4.2a) and connected with a flexible PVC tube to the inflow basin. The approach to the spillway contained floats to dampen surface waves (Fig. 4.1d).

The channel had a glass wall on the right side, whereas the bottom and the left side were made of 10mm thick smooth PVC elements (Fig. 4.1). The channel height in the domain of spillway was 1.20m, and 0.70m further downstream. Two rails placed at

the top of the channel side walls carried various trolleys. Measuring devices such as point gauges, propeller velocity meters and Pitot tubes could easily be fixed onto these trolleys. Fig. 4.1.c) shows a photograph of the channel including a trolley onto which a point gauge is fixed.

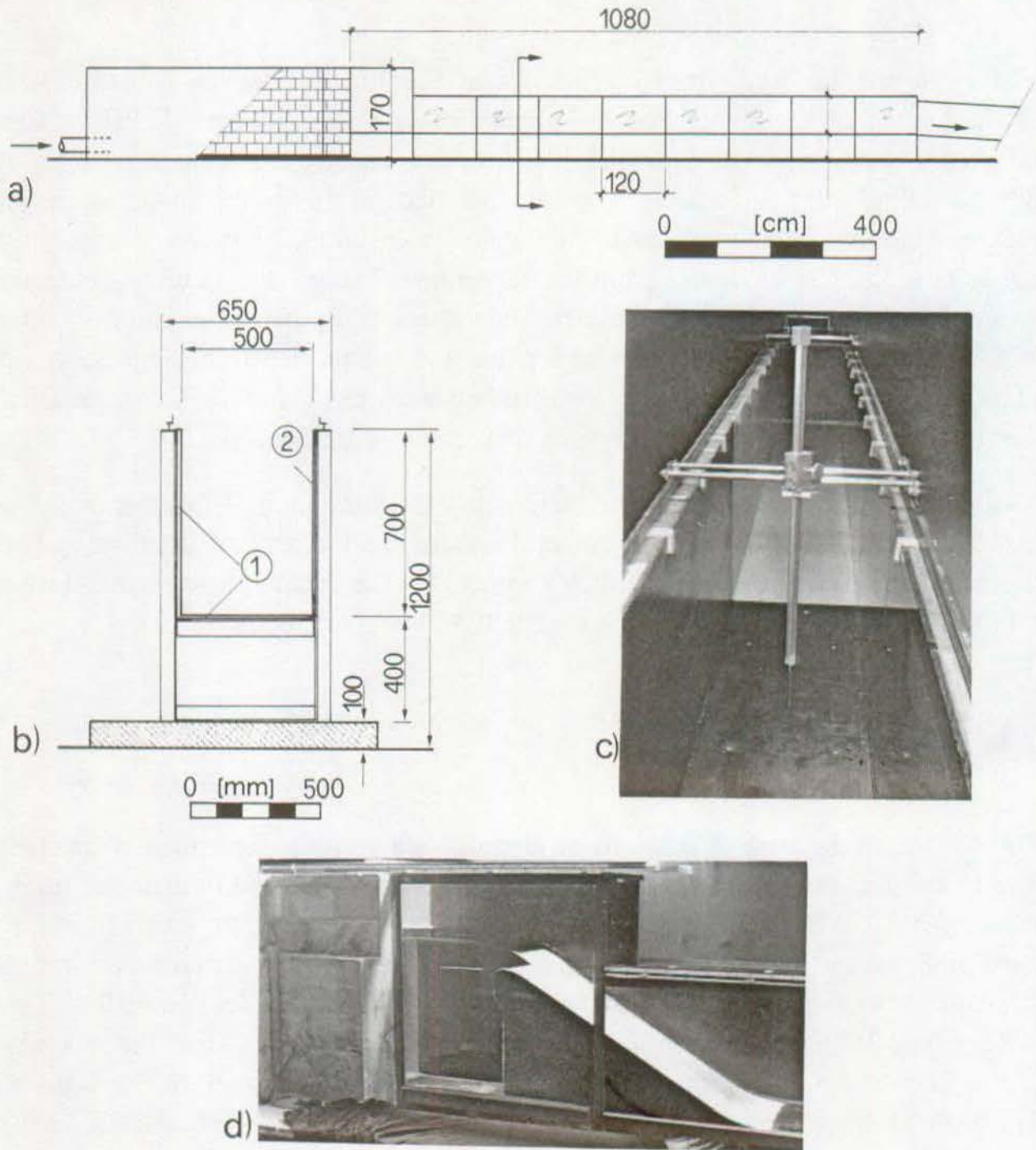


Fig. 4.1 : Test channel LCH1. a) longitudinal section with overall dimensions ; b) channel cross section ; c) downstream view including trolley with suspended point gauge; d) view of the upstream channel with the spillway used for discharge measurement. ① PVC walls ; ② Glass wall.

A vertical sharp-crested gate made of PVC could be placed at any channel position and fixed onto the channel rails (Fig. 4.2b and c). The channel portion upstream from the gate was thereby used as an intermediate basin. The maximum head on the gate was 0.7 m. The depth of the supercritical outflow was adjusted by the gate opening. However, wide ranges of inflow Froude number were only obtained with relatively small gate openings. To improve the approaching flow conditions, two foam screens were installed upstream from the gate (Fig. 4.2b). The resulting outflow from the gate was perfectly level and free of cross-waves.

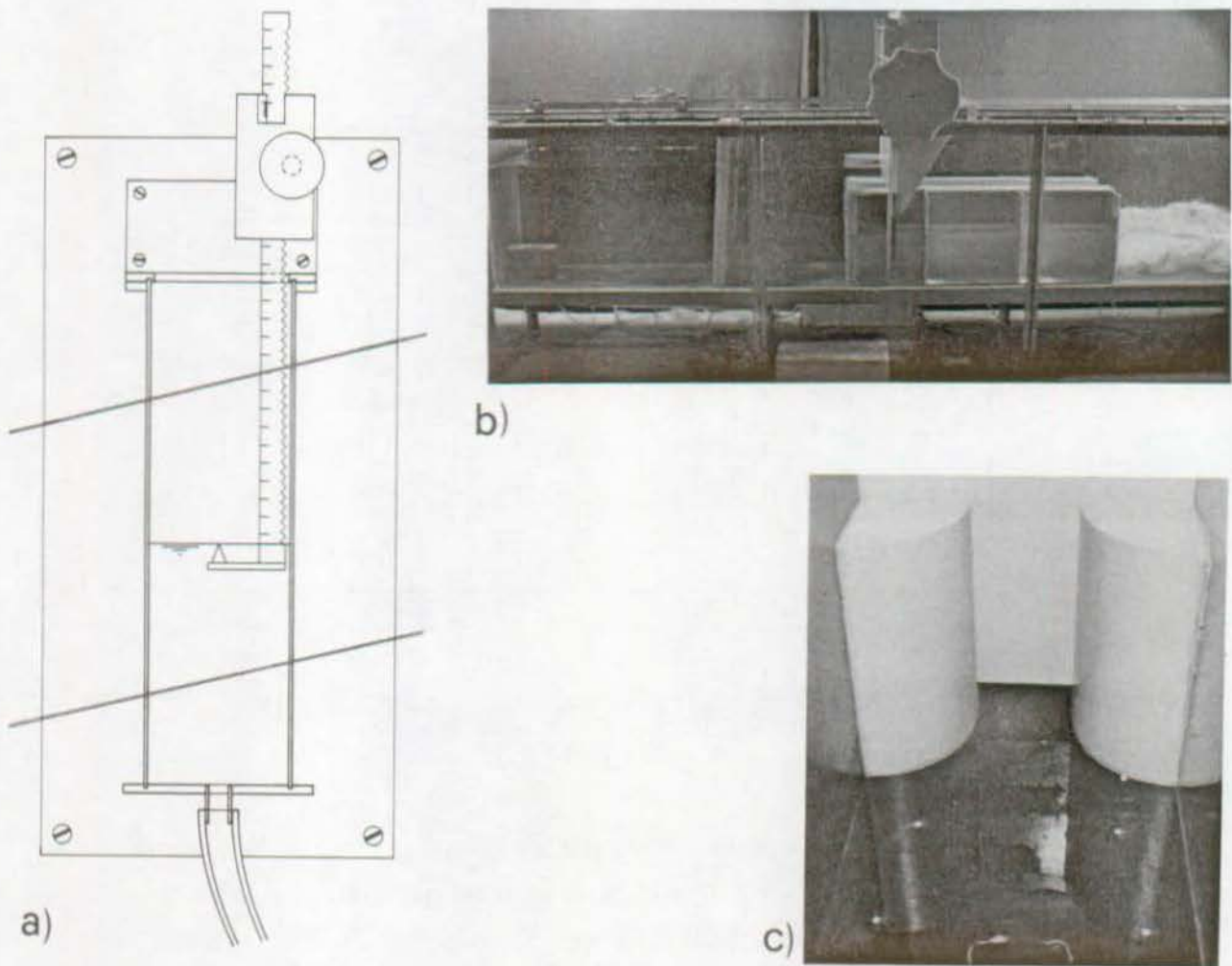


Fig. 4.2 : a) spillway head measuring device. b) vertical gate with two foam screens (left) and PVC elements for non-prismatic channel geometries (right). c) vertical quarter circular cylinders improving the approaching flow conditions to gate.

Various non-prismatic test geometries were obtained by PVC elements fixed on the channel bottom (Fig. 4.2b). These elements reduced the original channel width for a

length L_e of 0.90 m. Upstream from the gate, quarter circular PVC cylinders improved the approaching flow conditions (Fig. 4.2c). Fig. 4.3 shows some asymmetric, and symmetric abrupt expansions installed in LCH1.

The head at the gate H_g as well as the flow depth downstream from the hydraulic jump were generally measured by point gauges. For some preliminary runs the observations were verified by pressure taps. The agreement between the two were always better than 1mm. Details on the computation of the inflow depth h_1 will be given in paragraph 4.6. An overflow structure located at the downstream channel end allowed the adjustment of the tailwater level.

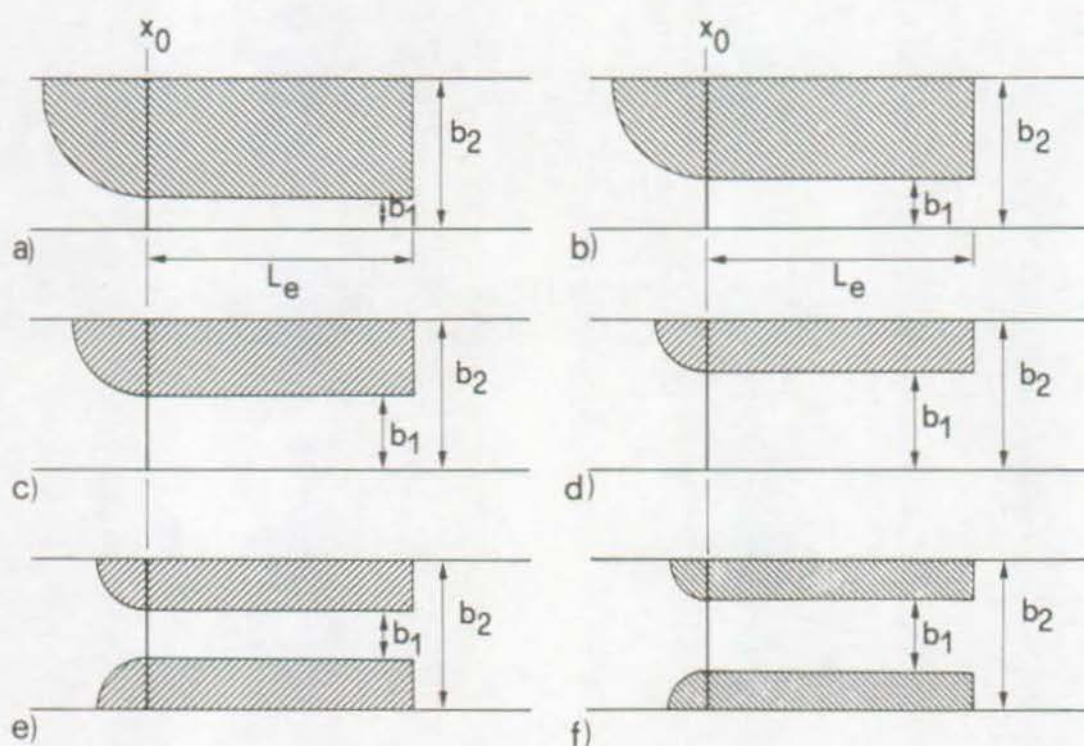


Fig. 4.3 : PVC elements considered for abrupt expansions in channel LCH1 with $b_2=0.5$ m; x_0 : gate position; $L_e=0.90$ m ; Asymmetrical: a) $B=5$; b) $B=3$; c) $B=2$; d) $B=1.5$. Symmetrical: e) $B=3$; f) $B=2$.

4.3 INSTALLATION LCH2

The second experimental installation was purposely designed for flows in non-prismatic channels. This model, of larger dimensions than LCH1, was composed of an

inlet steel tank connected to a rectangular horizontal channel. Fig. 4.4 shows its main dimensions.

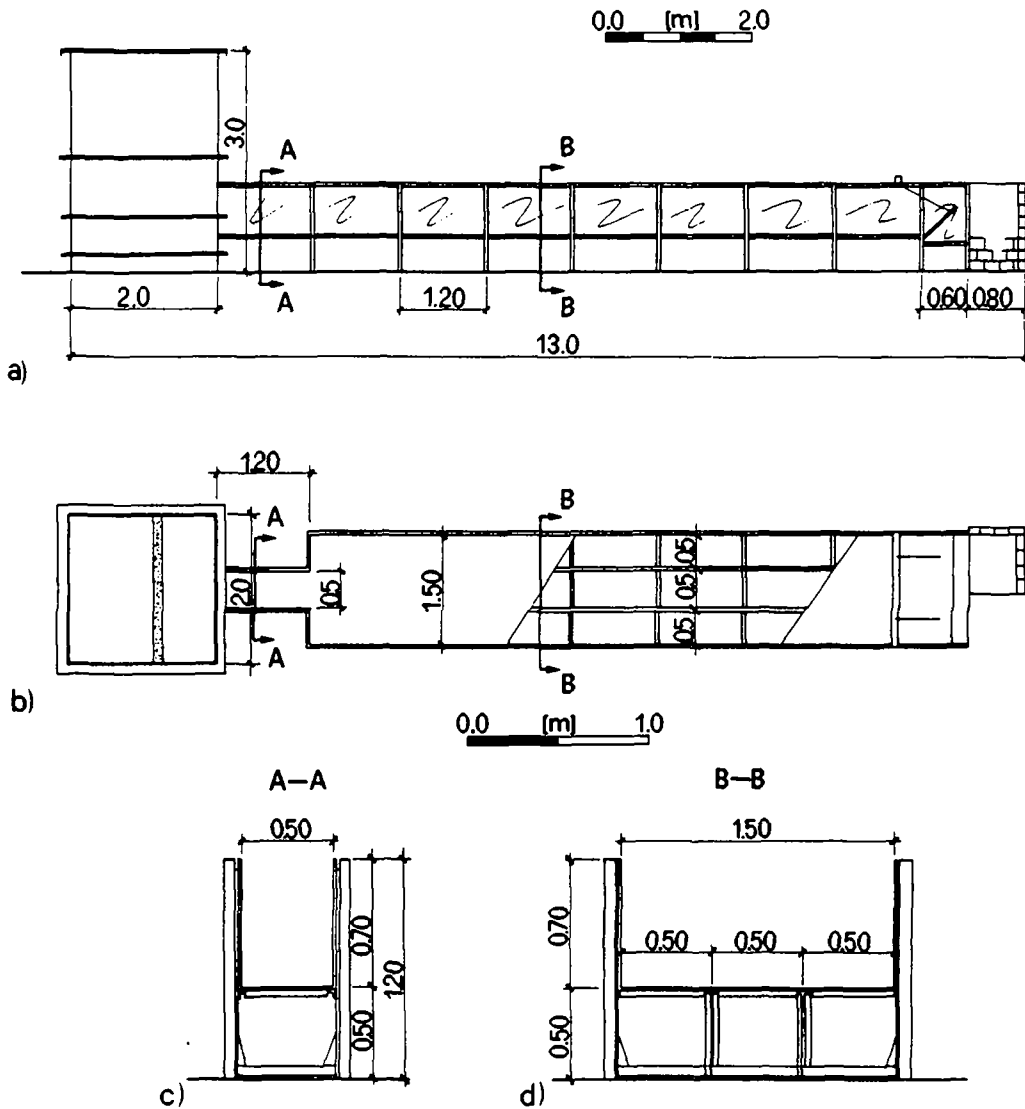


Fig. 4.4 : Test channel LCH2. a) longitudinal section ; b) plan view; c) upstream channel cross-section ; d) downstream channel cross section.

4.3.1 Inlet tank

The tank was made of 5mm thick steel plates reinforced with rolled beams. The internal square section measured 2.0m \times 2.0m and the total height was 3.0m. For basins of this height the optimal design in terms of economy and safety was found to

be a steel structure. The tank was supplied by a horizontal conduit with a maximum flow capacity of 250 l/s.

The water level in the tank was measured by a scaled transparent vertical tube fixed at the external basin wall. The tank inflow devices included a 1 m long conduit element in which holes of 30mm were drilled (Fig. 4.5a). To improve the outflow into the tank, this conduit was covered with a 20mm thick foam mattress. This latter porous material provided an almost uniform and smooth tank inflow.

A vertical 40mm thick porous screen was installed across the tank to further improve the outflow (Fig. 4.5b). This device was necessary to obtain a uniform high velocity tank outflow. Without it, the supercritical flow was irregular and occasionally even led to some vortex formation.

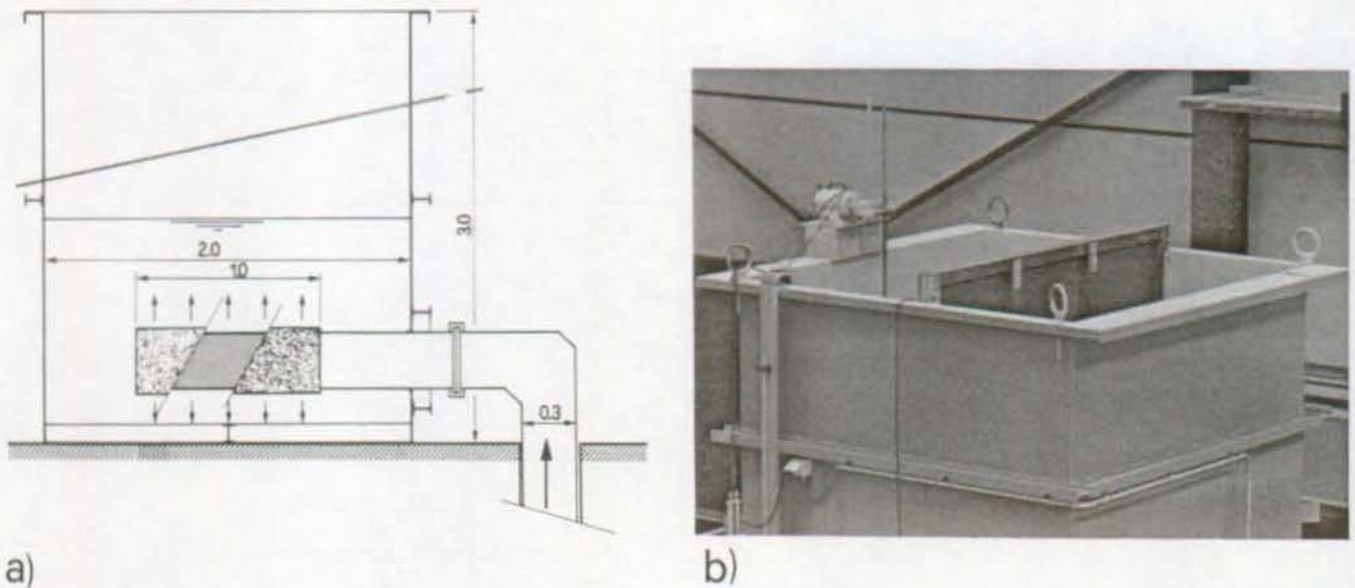


Fig. 4.5 : Improvement of the tank flow. a) vertical section of the tank inflow conduit, b) top of the tank including the vertical porous screen (center) and the motor for the adjustment of the gate opening (left).

At a height of 0.5m above the tank bottom, a square opening of 0.5m \times 0.5m connected the tank to the test channel. This opening was reinforced peripherically by steel plates. The latter were subsequently used as gate slots.

The tank outflow was controlled by a vertical 25mm thick PVC gate (Fig. 4.6a). The position of the gate lip could be adjusted by an electric motor fixed on the top of the tank (Fig. 4.5b). It became necessary to provide the tank outflow with various flow improving devices. Particular attention was thereby paid to the disruptive effect of the gate slots.

First of all, a quarter circular element was fixed between the bottom and the outflow section of the tank. Further, two similar elements were placed vertically on each side of the tank opening (Fig. 4.6b). However, these devices reduced only partially the disturbance of the flow due to the gate slots. Therefore, a slightly inclined guide plate was installed on the downstream gate side (Fig. 4.6a). The contraction coefficient of the gate was reduced by a half circular cylinder fixed upstream of the gate (Fig. 4.6a). This device insured positive pressures on the gate guide plate. These additional devices improved significantly the outflowing jet.

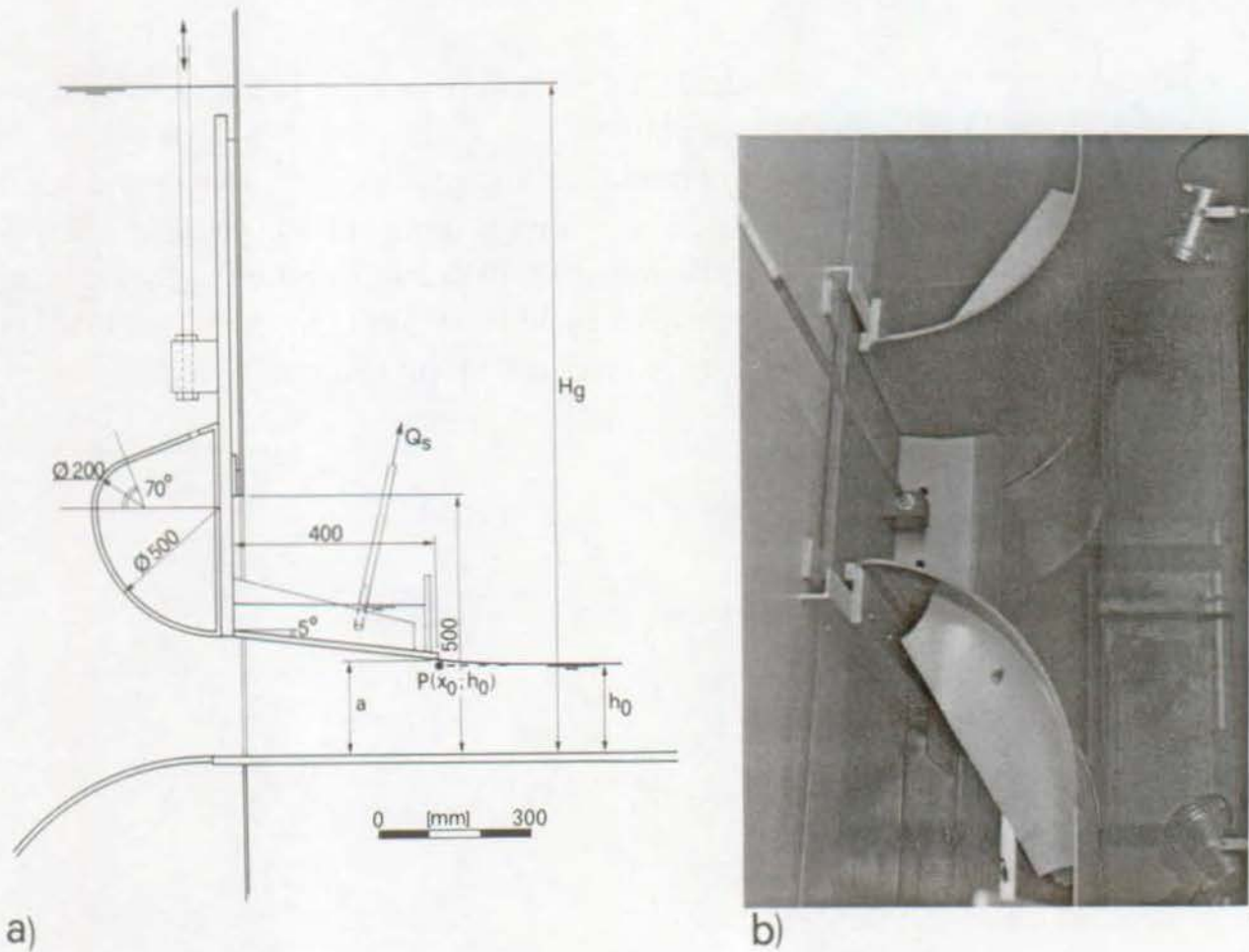


Fig. 4.6 : Transition from tank to channel. a) longitudinal section showing gate and connecting element, b) view of the final gate installation from above with the cylindrical PVC elements (flow direction from right to left).

A drainage fixed on the gate guide plate collected the gate losses. Volumetric discharge measurements indicated siphon discharges of the drainage Q_s ranging between 0.1 and 0.6 l/s depending on the water level in the supply tank.

4.3.2 Test channel

The channels of the installations LCH1 and LCH2 were similar. Channel LCH2 was also horizontal, rectangular and 0.7m high. The glass wall was installed along the left side whereas the bottom and the right channel side were covered with smooth PVC. The channel was divided into two parts: the upstream portion was 0.5m wide and 1.2m long. The downstream portion was 1.5m wide and 8.4m long. The downstream end of the channel was equipped with an overflow weir by which the tailwater could be adjusted. The flow then fell in a collecting channel and was fed back to the main basin.

With the exception of the investigation presented in chapter 8, the expansion ratio used for channel LCH2 was kept constant to $B=3$. This geometry was chosen because of a major interest in this configuration. The abrupt expansion geometry could be transformed into a gradual expansion by using additional PVC elements. Fig. 4.7 shows some of the geometrical configurations considered. Accordingly, a wide range of expansion ratios and expanding angles could be analyzed by quite simple means. However, the usual expansion geometry investigated was abrupt.

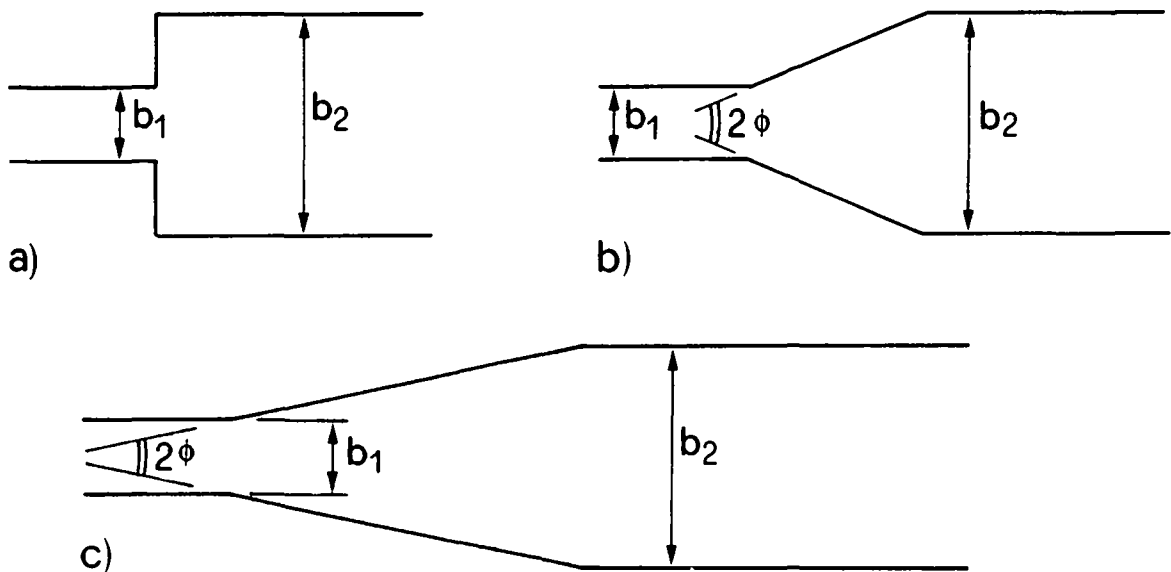


Fig. 4.7 : Expansions geometries considered in LCH2. $b_1=0.5\text{m}$, $b_2=1.5\text{m}$ ($B=3$). a) sudden expansion. Gradual linear expansions, b) $2\phi=45.2^\circ$ and c) $2\phi=23.5^\circ$.

Pressure taps were installed along the channel axis at a spacing of 0.25m. They were connected to water manometers which allowed accurate pressure readings ($\pm 1.0\text{mm}$).

Two steel rolled angles were fixed at the top of the channel side walls and used as trolley rails (Fig. 4.8). Trolleys moving on three wheels supported the various instruments to be described in paragraph 4.4.

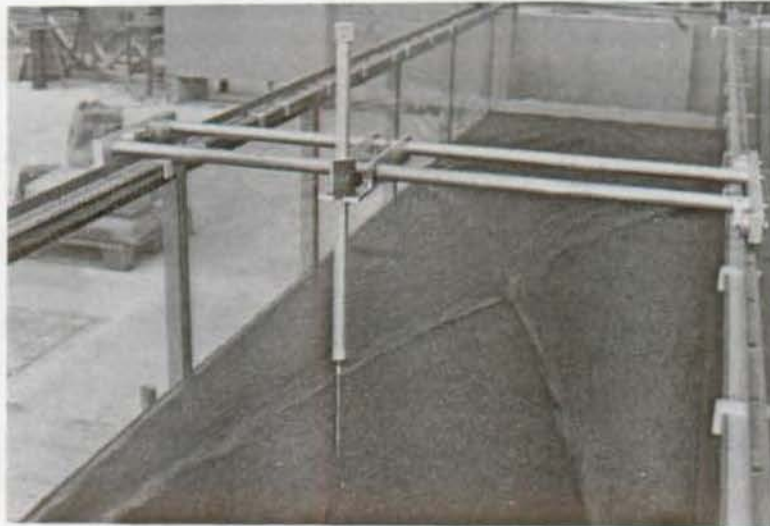


Fig. 4.8 : View of the trolley on the rails supporting a point gauge in channel LCH2.

After 1 year of operation the following maximum deviations to the original design were measured:

- $\pm 1. \text{ mm}$ vertical deviation of the channel bottom, due to PVC undulations
- $\pm 0.5\text{mm}$ horizontal deviation of the channel sides at the bottom level, and
- $\pm 3.0\text{mm}$ horizontal deviation of the channel width at the top of the channel.

These verifications were made with 60cm of stagnant water in the channel.

4.4 MEASURING DEVICES

4.4.1 Instrument supporting devices

Detailed descriptions of prototypes developed at LCH were presented by Bretz (1987), and Hager and Bretz (1986). Herein only the main characteristics of the instruments will be described.

The installations LCH1 and LCH2 were both equipped with horizontal rails parallel to the channel bottom. As shown in Fig. 4.9, these rails were used to support wheeled trolleys composed of two parallel steel axels and one rotating support plate. A scale fixed on one axle allowed rapid horizontal positioning of the measuring probe. The probes were fixed on oval aluminium profiles by which vertical positioning was possible within ± 1 mm.

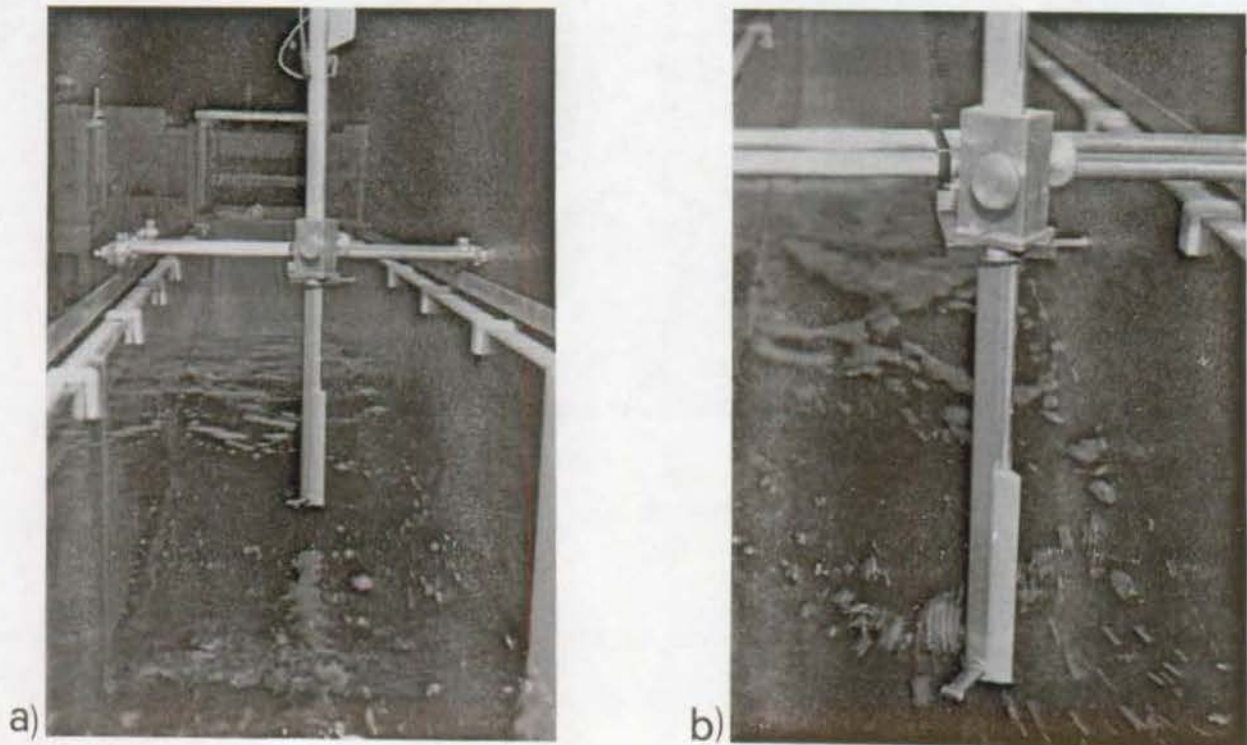


Fig. 4.9 : Instrument supporting devices : a) trolley supporting a propeller meter in channel LCH1, b) detail of support device to set the vertical probe position. Also visible are (from bottom to top) the propeller meter casing, the scated suspension rod with the streamlined rear portion and the horizontal trolley axels.

To link the aluminium tube to the trolley, a special supporting device was designed (Fig. 4.9a). By turning the positioning wheel of the device, the probe (propeller meter, angle probes etc.) could be positioned accurately at any desired location above the channel bottom. A scale, fixed to the aluminium tube and calibrated to the channel bottom allowed immediate reading of the distance between the probe and the channel bottom.

As shown in Fig. 4.9a) the lower portion of the aluminium tube was equipped with a PVC element. Its streamlined shape prevented air entrainment from the low pressure zone at the rear of the tube. Without this device air was entrained at the wake and thus

modified the flow conditions on the measuring probe. For velocity measurements, the rotating speed of the propeller was significantly reduced by the presence of air. For angle measurement an air pocket formed over the flag-type element and significantly modified the angle of streamline. A description of the device used to avoid air entrainment, and the effect of air on the probes was presented by Hager and Bretz (1986).

4.4.2 Flow depth and pressure head

To measure flow depths, standard point gauges and pressure taps were used. The latter were considered for low velocity flow with significant wave generation, as typically occur at the downstream portion of hydraulic jumps. The pressure taps were composed of vertical steel tubes fixed on the channel bottom (3mm internal diameter) and connected to a flexible PVC tube. This latter tube was connected to a vertical glass pipe (5 mm internal diameter) equipped with a calibrated scale. A 0.2m long compressed foam element in the PVC tube reduced the level fluctuations. This

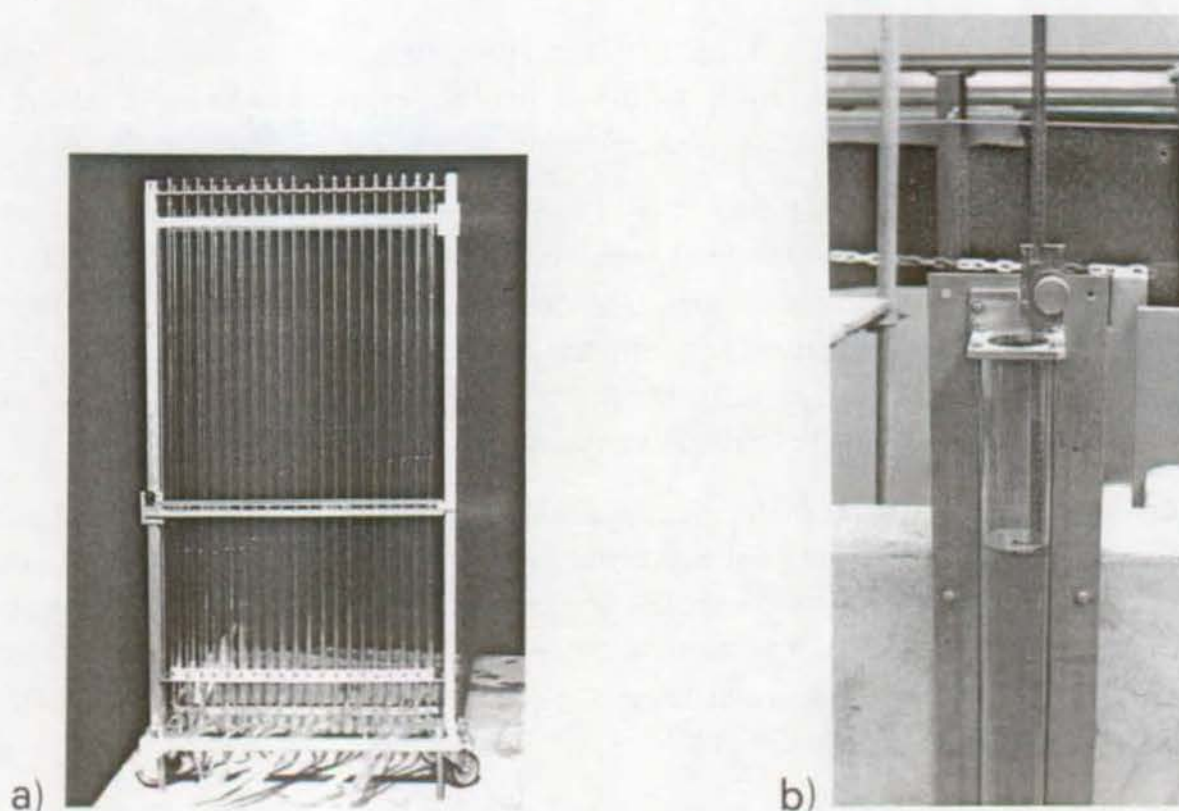


Fig. 4.10 : a) View of the manometer battery used for channel LCH2,
b) Cylinder for gauging used for discharge calibration in LCH2.

device was particularly efficient for fluctuations at frequencies higher than 0.5 to 1 Hz, whereas the fluctuations were reduced only partially at lower frequencies. Fig. 4.10 shows the calibrated glass pipes used for the pressure reading.

The point gauges were fixed on a scaled aluminium tube which was supported by the trolley. The rack fixed on the tube allowed rapid surface recording. Supercritical as well as subcritical flows with low wave generation were typically measured with this device. The accuracy of the two flow depth measuring devices depended both on the local bottom deviations, and on the flow surface fluctuations.

The maximum absolute deviation in depth measurement could reasonably be estimated to $\pm 1.0\text{mm}$ for supercritical flow and to $\pm 2.0\text{mm}$ for measurements downstream from hydraulic jumps. For small supercritical flow depths the relative deviation could become significant. This experimental error influenced the inflowing Froude number as well as the sequent depths ratio Y . Therefore, small flow depths were generally computed rather than observed by direct measurement. The computational method will be presented in paragraph 4.6.

4.4.3 Velocity measurement

Velocity is a vector and needs 3 independent values to define it. Therefore, it was necessary to measure the horizontal and the vertical angles relative to some reference direction, as well as the local velocity magnitude.

To measure the directions of the local velocity vector, first the horizontal angle (θ_1) was determined with the experimental probe as shown in Fig. 4.11b). It consists of a rigid flag fixed on a vertical steel axis. The deviation θ_1 of the direction relative to the channel axis was mechanically transmitted to a calibrated angle meter located at the top of probe. The entire instrument was fixed on an aluminium tube and supported by the trolley, as described in paragraph 4.4.1.

The vertical angle probe was then placed at the same measuring point and rotated such that the orientation of the flag corresponded to the previously measured horizontal angle. This second probe was composed of a balanced rigid flag rotating around a horizontal axis (Fig. 4.11a). The vertical angle θ_2 was electrically transmitted to a potentiometer and registered on an angle meter. At zero water velocity, the probe was adjusted to the horizontal direction.

For velocities smaller than 5m/s, a propeller meter of 10mm internal diameter was placed at the measuring point, thereby accounting for the previously defined direction θ_1 , and θ_2 of local streamline.

The propeller meter used for 3D measurements was mounted on a rotating horizontal axle, as shown in Figs. 4.12d) and e). The vertical angle could be set externally from the top of the aluminium tube whereas the horizontal angle was set by turning the supporting device on the trolley's plate. For subcritical flow conditions and velocity measurements limited in horizontal planes, the propeller meter shown in Figs. 4.12b) and c) was used.

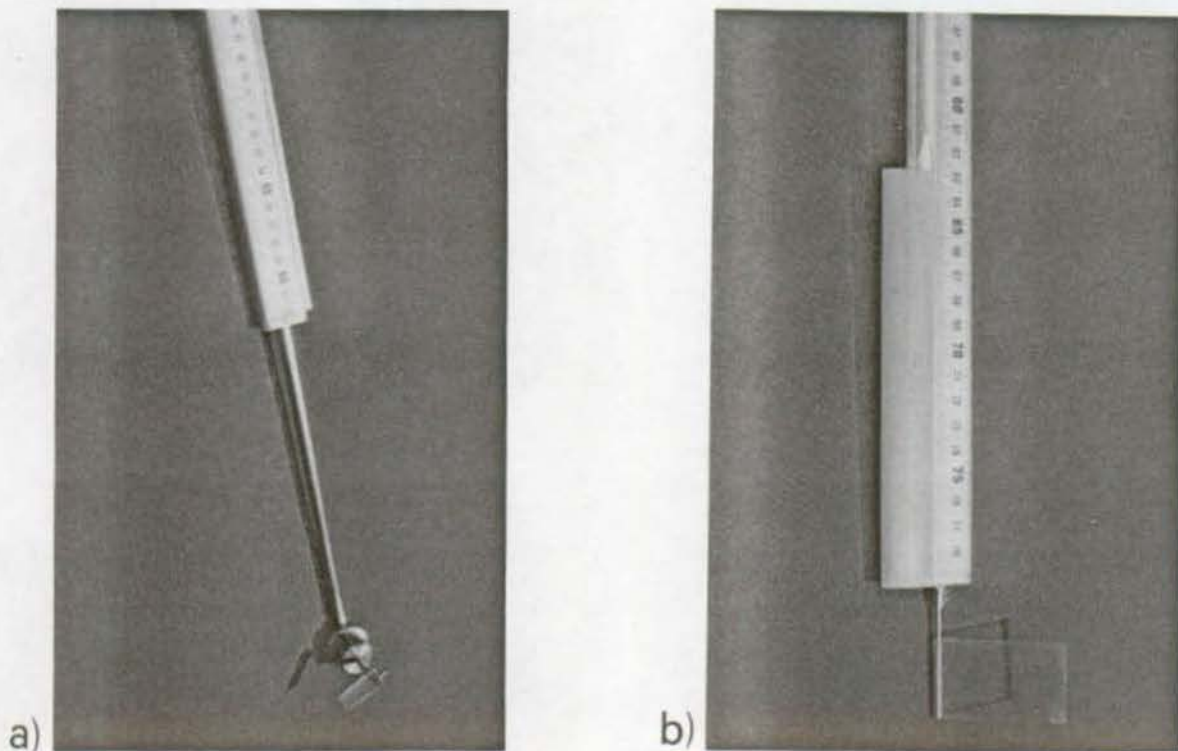
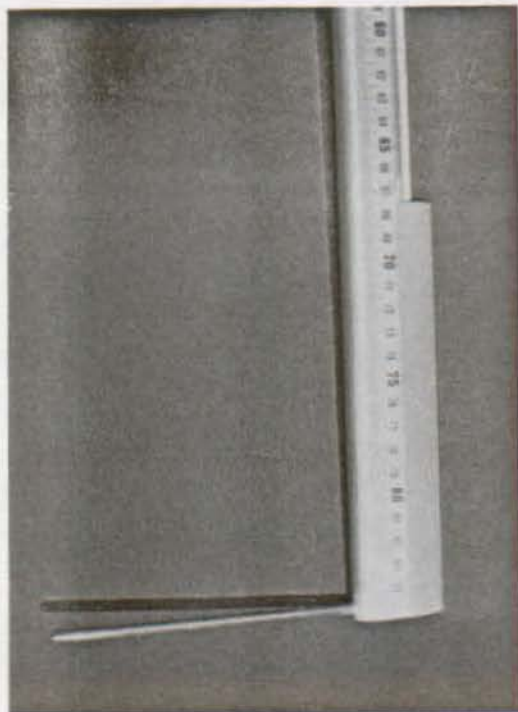


Fig. 4.11 : Angle probes including meter for depth location. a) vertical and b) horizontal angle probes. Note streamlined shape to avoid air entrainment.

The upper velocity limit of 4-5m/s was not imposed by use of the propeller meter, but by air entrainment. For lower velocities this disadvantage was suppressed by a PVC element fixed on the downstream side of the aluminium tube (Fig. 4.12d). It was found that the element was essential for correct velocity measurements. For velocities larger than 5m/s, or small flow depths (<15mm) the velocity was measured by a 3 mm diameter Pitot tube, which could be turned only horizontally, however.



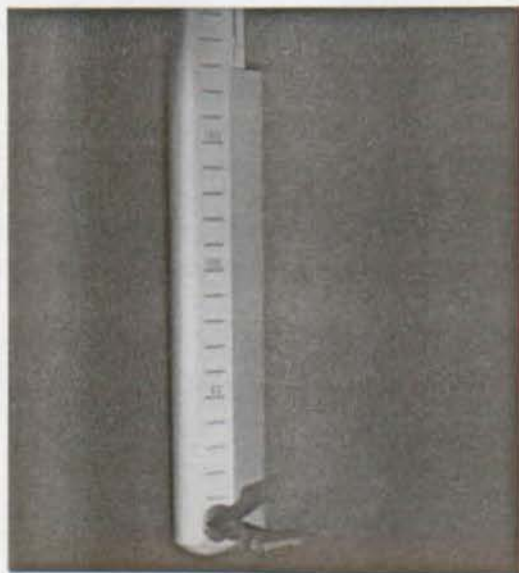
a)



b)



c)



d)



e)

Fig. 4.12 : Velocity measurement devices. a) Pitot tube of 3mm external diameter, b) and c) propeller velocity meter for relatively low velocities, d) and e) propeller meter used for relatively high velocities.

4.5 DISCHARGE MEASUREMENT

The electromagnetic discharge measuring device had a maximum deviation of ± 1.2 l/s or ± 2.5 l/s depending on the capacity discharge of pump. This deviation was considered too large for this project, especially for low discharges. A more accurate discharge measurement method became necessary.

Installation LCH1 was equipped with a 0.7m high, 0.5m wide PVC standard-shaped spillway of design head $H_D=0.20$ m. To calibrate this spillway for discharges up to 15 l/s, a 0.45m high 90 degrees V-notch sharp-crested weir was temporarily installed in the downstream portion of channel (Fig. 4.13a). For larger discharges a vertical sharp-crested weir was inserted which allowed discharge calibration up to 50 l/s (Fig. 4.13b).



a)



b)

Fig. 4.13 : Discharge measuring devices used in LCH1. a) 90 deg. V-notch sharp-crested weir; b) rectangular sharp-crested weir.

The discharge coefficient C_d of the standard spillway

$$C_d = \frac{Q}{b\sqrt{2gH_s^3}} \quad (4.1)$$

could be expressed as (Hager and Bremen 1988)

$$C_d = \frac{2}{3\sqrt{3}} \left(1 + \frac{4\chi}{9 + 5\chi} \right) \quad \text{with} \quad \chi = H_s/H_D \quad (4.2)$$

where H_s is the head on the spillway and b the spillway width. The accuracy obtained with this measuring method could be estimated as:

- less than 0.2 l/s for $Q < 20$ l/s, and
- less than 1% of the actual discharge for $Q \geq 20$ l/s.

Fig. 4.13 shows the two types of weirs used in LCH1. In order to reduce the wave action, two foam screens were placed 1m and 1.5m respectively upstream from the weir plate.

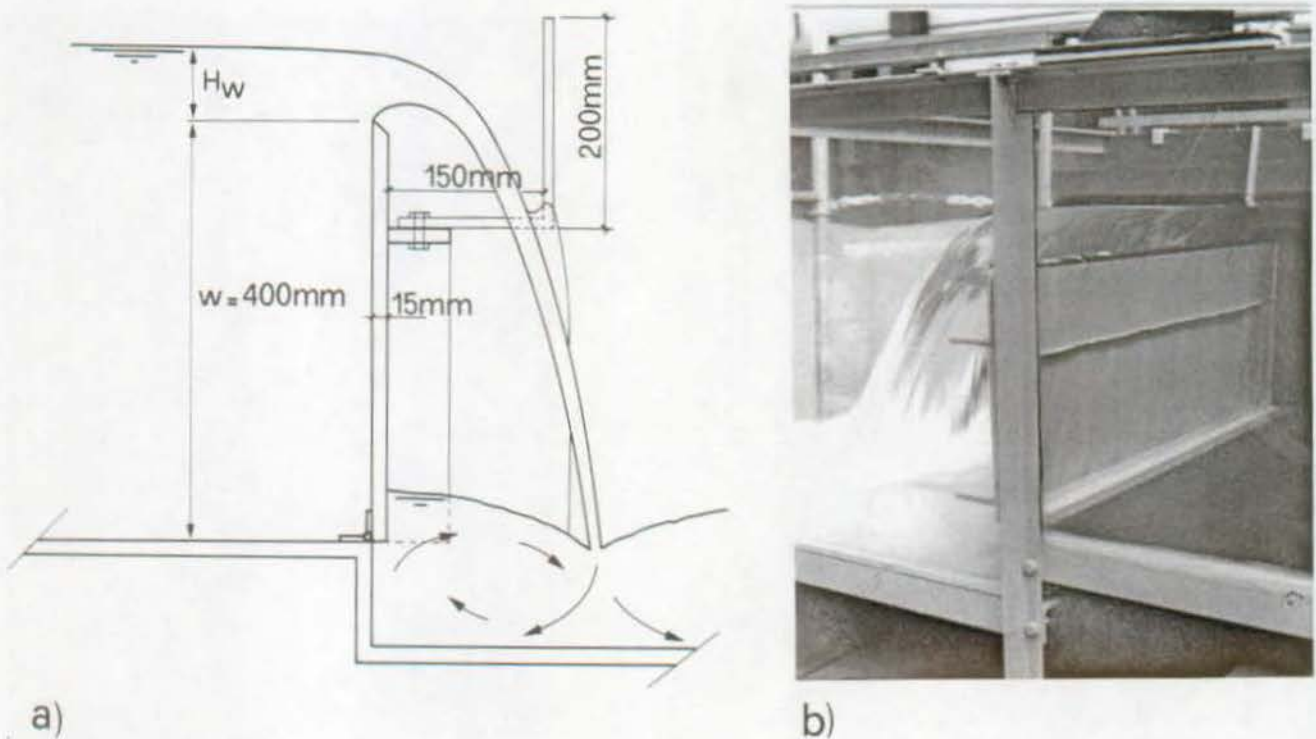


Fig. 4.14 : Sharp-crested weir of the installation LCH2 for pump calibration. a) Notation and dimensions. b) Photographic view.

The electromagnetic discharge measuring device used for LCH2 was calibrated using the inclined weir at the channel end. Placed vertically, it could be used as a sharp crested 1.5m wide and 0.4m high vertical weir. The aeration of the nappe was guaranteed by 3 air supply holes drilled on the PVC side wall and by two jet breakers fixed downstream from the weir. Fig. 4.14 shows the main dimensions of the

overflow weir in the vertical position. The head was measured with a point gauge 0.90 m upstream from the weir section (Fig. 4.10b).

The discharge coefficient for a full width rectangular weir is defined as

$$C_{dw} = \frac{Q}{b\sqrt{2gH_w^3}} \quad (4.3)$$

in which b is the weir width and H_w is the head on the weir. To select an equation for C_{dw} , some of the relations proposed in the literature were compared. Since only the relative deviations are of interest, these relations were normalized by

$$\bar{C}_{dw} = 0.4023 \left[1 + \frac{0.0011}{H_w} \right]^{3/2} \left(1 + 0.135 \frac{H_w}{w} \right) \quad (4.4)$$

according to Rehbock(1929). Fig. 4.15 shows the ratio C_{dw}/\bar{C}_{dw} as a function of the weir head H_w for a weir height of $w=0.40$ m. It is seen that the discharge coefficients proposed by Rehbock (1913 and 1929) lie above the other values, in case of small heads. However, for heads H_w above 60mm, the deviations between the relations of Rehbock (1913), Rehbock (1929), SIA (1924), Sarginson

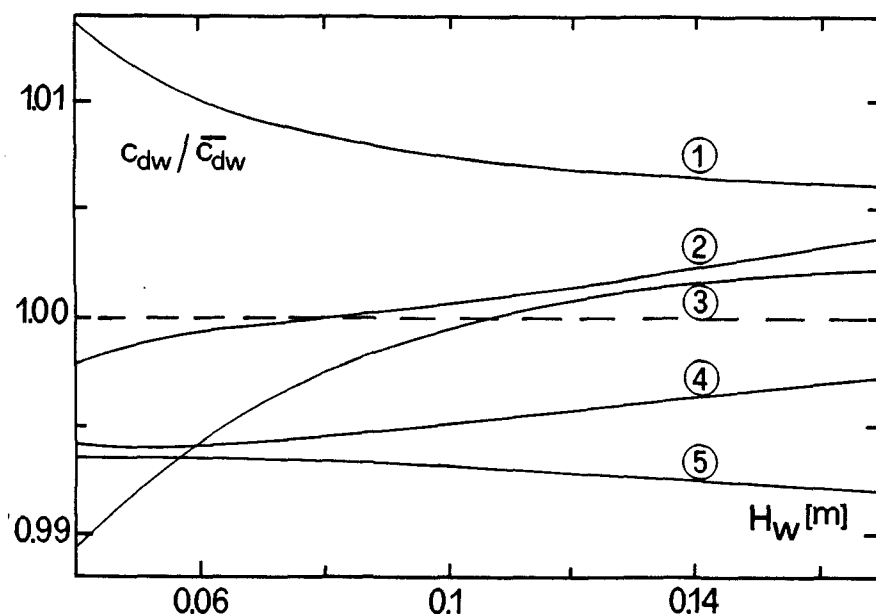


Fig. 4.15 : Comparison of discharge coefficients, normalized to Eq. (4.4). ① Rehbock (1913) ; ② SIA(1924); ③ Kindsvater and Carter (1957) ; ④ Sarginson (1972) (water temperature 18° C) and ⑤ Hydraulic Research Station (1980). (--) Rehbock (1929).

(1972) and the Hydraulic Research Station (1980) are smaller than 1% and even decrease for higher heads.

Eq. (4.4) was finally selected for the computation of the discharge

$$Q = C_{dw} b \sqrt{2gH_w^3} \quad (4.5)$$

in which $b=1.50\text{m}$. Accounting for an error $\pm 0.3\text{mm}$ in the head measurement and 1% in C_{dw} , the discharge accuracy can be estimated as less than

- 0.5 l/s for $Q < 50$ l/s,
- 1% of the actual value for 50 l/s $< Q < 100$ l/s, and
- 1.0 l/s for $Q > 100$ l/s.

4.6 COMPUTATION OF SMALL FLOW DEPTHS

4.6.1 Assumptions

As described in paragraph 4.4.1 the absolute deviation between observed and exact flow depths was estimated to $\pm 1.0\text{mm}$. In case of small flow depths ($< 20\text{mm}$), such as in supercritical flows, the measurement by point gauge or pressure taps turned out as inaccurate. The combined error on the inflowing depth, the inflowing Froude number and on the measured sequent depth could become significant. It was therefore preferred to compute small flow depths with a classical backwater curve analysis. The relative error involved in calculating small inflow depths using the measurement of the inflow discharge Q , and of the head on the gate H_g were significantly lower.

Fig. 4.16 shows the supercritical flow considered in channel LCH1 as well as the notation used. The computational procedure is based on the following assumptions

- the head losses across the gate are negligible,
- the channel could be considered as hydraulically smooth (Bretz 1987),
- a simplified surface profile (Fig. 4.16b) could be considered instead of the effective contraction profile,

- the origin of computation is at a distance «a» downstream from the gate, with «a» as gate opening, and
- the inflowing depth h_1 at the toe of jump may be computed by a conventional backwater curve, starting at (x_0, h_0) .

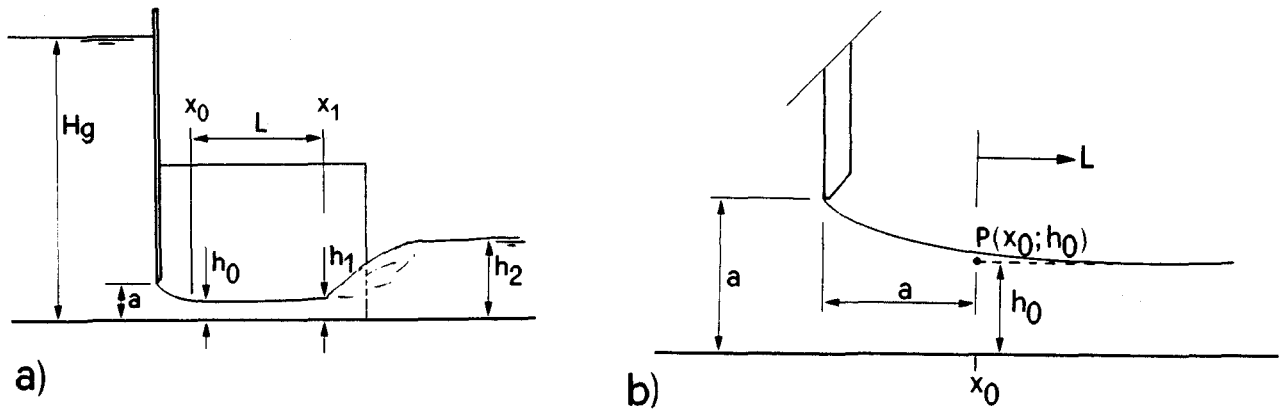


Fig. 4.16 : Approaching flow to jump in channel LCH1. a) Notation, b) simplified surface profile for the computation of head losses (—) surface profile ; (•) starting point for computation of (---) backwater curve.

For channel LCH2, the starting point $P(x_0, h_0)$ of the backwater curve is located at the downstream end of the gate cover (Fig. 4.6a). The head loss across the gate and the gate cover were neglected. The same PVC wall and floor elements were used in LCH2 as in LCH1, hence both channels were considered as hydraulically smooth.

4.6.2 Method of computation

Assuming potential flow across the gate yields

$$H_g = h_0 + \frac{Q^2}{2gb_1^2h_0^2} \quad (4.8)$$

according to Bernoulli's equation. Flow depths h_0 downstream of the gate may thus be computed in the first step, provided H_g and Q are experimentally determined and head losses across the gate may be neglected (paragraph 4.6.1). Secondly, the backwater curve between x_0 and x_1 (Fig. 4.16a) is determined. The slope of the surface profile may be expressed as (Chow, 1959)

$$\frac{dh}{dx} = \frac{S_f - S_0}{1 - F^2} \quad (4.9)$$

where F is the local Froude number and S_0 the local bottom slope. $S_0=0$ was assumed for both channels LCH1 and LCH2. The local friction slope

$$S_f = \frac{f}{4R_h} \cdot \frac{V^2}{2g} \quad (4.10)$$

is established by the Colebrook-White relation for smooth channels

$$\frac{1}{\sqrt{f}} = -2 \cdot \log \left[\frac{2.51}{R\sqrt{f}} \right] \quad (4.11)$$

Therein, $R=4Q/((b+2h)v)$ is the local Reynolds number and $R_h=(bh)/(b+2h)$ is the local hydraulic radius, both for rectangular cross sections.

Solving Eq. (4.8) led to the initial condition $h(x_0)=h_0$. In order to solve Eq. (4.9) a conventional Runge-Kutta 4th-order integration method was selected. The distance $L=x_1-x_0$ was subdivided into 100 identical intervals. Numerical verifications show that for the flow conditions considered (h_1 , F_1 and L) an increase in the number of intervals (up to 10'000) modified the flow depth h_1 at the jump toe by less than 0.2 %. In comparison to the error involved in the discharge measurement, the accuracy of the computational method selected was considered satisfactory. The flow depth h_1 obtained served as the basis to compute quantities such as H_1 , F_1 , and Y^* .

4.7 CONCLUSIONS

In this chapter, the main characteristics of the experimental equipment used for the laboratory investigations have been described. The measuring devices used, as well as the observational techniques employed were also presented. Particular attention was paid to the evaluation of the observational accuracy. The relative error of the electromagnetic discharge measurement device was considered as too large for discharges smaller than 20 l/s. With a calibration of the electromagnetic discharge measuring device using sharp-crested weirs, the discharge accuracy was reduced to 1%.

In order to reduce the error involved in the flow depth measurements, point gauges and manometers (pressure tabs) were used simultaneously. Particular attention was

paid to an accurate determination of the supercritical inflow depths at the toe section. The precise determination of the inflow depth h_1 is essential for the analysis of the experimental data since several normalizing quantities are derived from h_1 such as for the inflow Froude number F_1 , the experimental sequent depths ratio Y_{ex} , or the experimental jump length $L_{j,ex}$. Therefore, for small inflow depths, (typically less than 20mm) a backwater curve defined the flow depth just upstream from the toe. This procedure turned out to be more accurate in comparison to a direct depth measurement by point gauge.

The installations and measurement techniques described in this chapter will be referred to extensively in the next chapters.

5. SUDDEN EXPANSION

5.1 INTRODUCTION

In this chapter sudden expansions in rectangular and horizontal channels will be investigated by theoretical and experimental means. The simple geometry was investigated since only the ratio B of channel expansion has to be considered. Once the jump characteristics could be predicted for this geometry, more complex flow configurations will be investigated in the forthcoming chapters.

After a description of the experiments, the applicability of a conventional momentum approach to jumps in sudden expansions is verified by the experimental data. A new non-dimensional parameter describing the toe position relative to the expansion section is then defined. Based on this parameter, a computational model is established which allows the prediction of the sequent depths ratio as well as of the flow depth along the side walls of the expansion section. The computational results are compared with the data of Unny, Herbrand, and Sethuraman and Padmanabhan.

An expression for the jump length L_j in sudden expansions is obtained from the experimental data. As shown in chapter 2, L_j is very long for S-jumps, and is gradually reduced if the toe moves further upstream.

Hydraulic jumps located in sudden expansions are characterized by asymmetric and oscillating flows. The jump asymmetry could be evaluated quantitatively by measuring the difference of flow depths between the right and the left lateral eddies. Based on these measurements, the effect of jump position as well as of the expansion ratio B on the jump symmetry will be investigated.

Finally, in paragraph 5.9 a numerical example illustrates the computational model.

5.2 DESCRIPTION OF EXPERIMENTS

The experiments were carried out in the installations LCH1 and LCH2. The experimental facilities were described in paragraphs 4.2 and 4.3.

Table 5.1 shows the characteristics of the six series to be presented. Column 2 indicates the downstream channel width b_2 (Fig. 5.2), and column 3 the width ratio $B=b_2/b_1$. The domains of F_1 and of $\omega_1=h_1/b_1$ are given in columns 5 and 6, whereas column 7 indicates the number of runs conducted for each series. As shown in this

table, five series were carried out in installation LCH1. Asymmetrical expansions were considered in four series. Particular attention was paid to the expansion ratio $B=3$ which was considered in three series, two of which had a symmetric and one an asymmetric expansion geometry.

Table 5.1 : Sudden expanding channels: Overall characteristics of experiments.

Series	b_2 [m]	B [-]	channel shape	F_1		ω_1		No of runs
				from	to	from	to	
1	2	3	4	5		6		7
1.1	0.50	5	asym	2.65	8.12	0.13	0.61	238
1.2	0.50	3	asym	2.62	8.15	0.076	0.38	240
1.3	0.50	3	sym	2.63	8.05	0.073	0.37	221
1.4	0.50	2	asym	2.67	8.18	0.052	0.24	236
1.5	0.50	1.5	asym	2.65	8.13	0.036	0.19	209
1.6	1.50	3	sym	2.99	10.60	0.044	0.12	172

Based on the literature review (chapter 3) and on some preliminary runs, it may be assumed that the sequent depths ratio Y for jumps in rectangular sudden expansions depends on

- the width ratio $B = b_2/b_1$,
- the inflowing Froude number F_1 ,
- the toe position x_1 relative to the expansion section, and
- the shape factor $\omega_1 = h_1/b_1$.

The effect of the inflow Reynolds number R_1 is thereby neglected because relatively large inflow depths h_1 were considered (Hager and Bremen, 1989).

To investigate the effect of each parameter, it was necessary to obtain experimental results in which three parameters were kept constant and only one parameter varied. Fig. 5.1 shows the organization of the experimental test program.

For each channel geometry, four to five different gate openings were considered. For each gate opening, in turn, five different discharges were investigated. Rising progressively the overflow weir led to about ten toe positions for each discharge. Due to frictional effects on the inflowing depth h_1 it was impossible to keep F_1 constant for different jump locations, as indicated in paragraph 4.7.

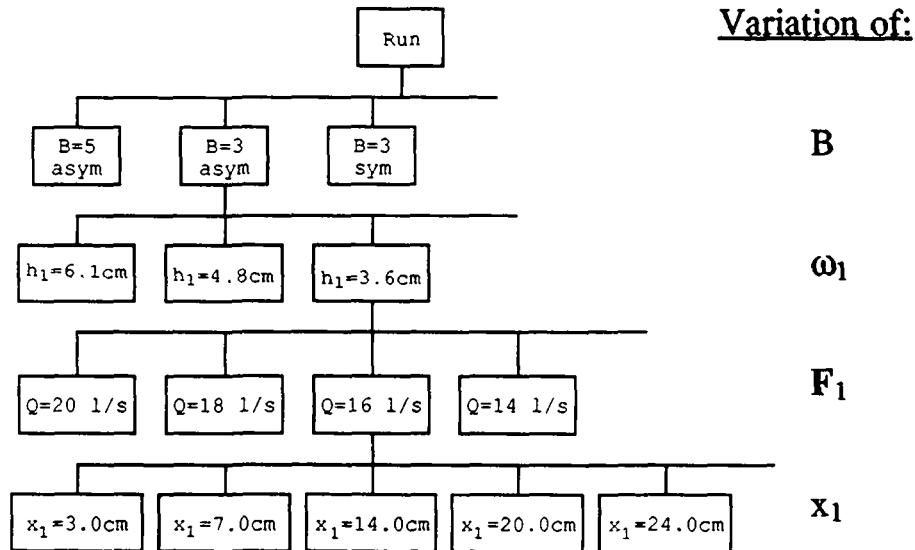


Fig. 5.1 : Organization of the experimental test program.

For each run, the following parameters were measured (Fig. 5.2):

- inflow and tailwater depths h_1 and h_2 ,
- flow depths h_{a1} and h_{a2} along the expansion side walls,
- toe position x_1 and jump end section x_j , and
- end sections x_2 and x_e of the lateral eddies.

As described in chapter 2, a fundamental difference between hydraulic jumps in prismatic and non-prismatic channels is the formation of two lateral eddies. Due to this phenomenon, particular attention must be paid to section 2 where the flow is again nearly uniform and the flow depth is h_2 . Due to the formation of lateral eddies the assumption of strictly uniform flow, as considered by a conventional momentum approach, is not satisfied. It was therefore decided to measure h_2 at the downstream end of the longer lateral eddy (Fig. 5.2), as the surface profile is approximately horizontal beyond this section. It should be noted, however, that the distance between section 2 and the toe of the jump may become significant, especially when low tailwater levels prevail, as indicated in Chapter 2.

Besides the flow depth h_2 , attention was paid to the average water levels h_{a1} and h_{a2} along the side walls of the expansion. On each channel side, these levels were measured at two points (Fig. 5.2a) and the average value $h_a = (h'_a + h''_a)/2$ of each side was retained. Evidently, these levels could be measured only along one channel side wall for asymmetric expansions.

The inflow depth h_1 was measured at the toe section with a point gauge and compared to the computed value as described in paragraph 4.7. The deviation between the

computed and the measured depth was usually smaller than 1mm. The inflow parameters F_1 and ω_1 were established on the basis of the computed flow depth h_1 .

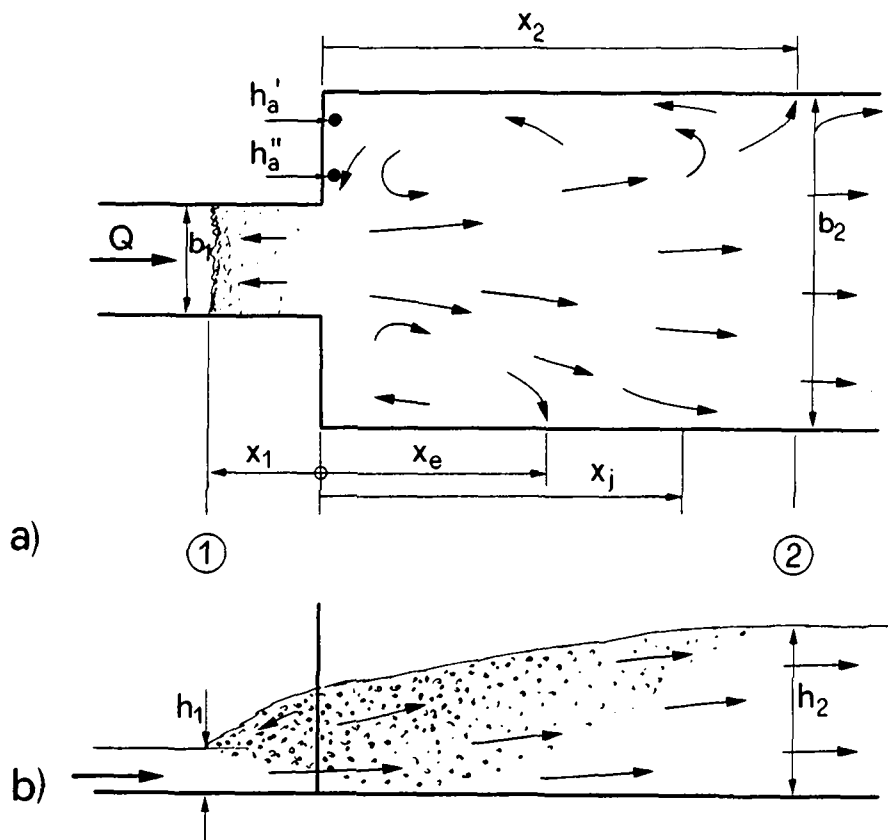


Fig. 5.2 : Sudden expansions : parameters measured for T- and S-jumps. a) plan view; b) axial section with typical air bubble distribution.

The toe position x_1 was measured starting from the expansion section (Fig. 5.2). Positive values indicate that the toe is located upstream of the expansion. Due to turbulent fluctuations of the toe, the experimental measurement of x_1 involved some deviations particularly for small x_1 . Comparing three independent measurements of x_1 involves a deviation between 1 to 4cm, depending on the flow characteristics.

x_e and x_2 indicate, respectively, the end section of the shorter and the longer lateral eddy, starting from the expansion section. The larger value coincides with the section at which h_2 was measured. Deviations up to 50cm should be expected for the length of the longer eddy. The measurement of these parameters became particularly difficult for small x_1 .

The length x_j corresponds to the distance from the expansion section to the jump end section. Adding this value to x_1 gives the jump length L_j . The criterion adopted for the measurement of x_j was based on the air detrainment.

The jump end section corresponds to the section where only small air bubbles are contained in the upper flow portion. Beyond the end of the jump, the turbulence has greatly diminished and the flow is almost uniform, although there may still be some action of the side eddies.

Fig. 5.3 shows a typical T-jump in which the position x_j is indicated.

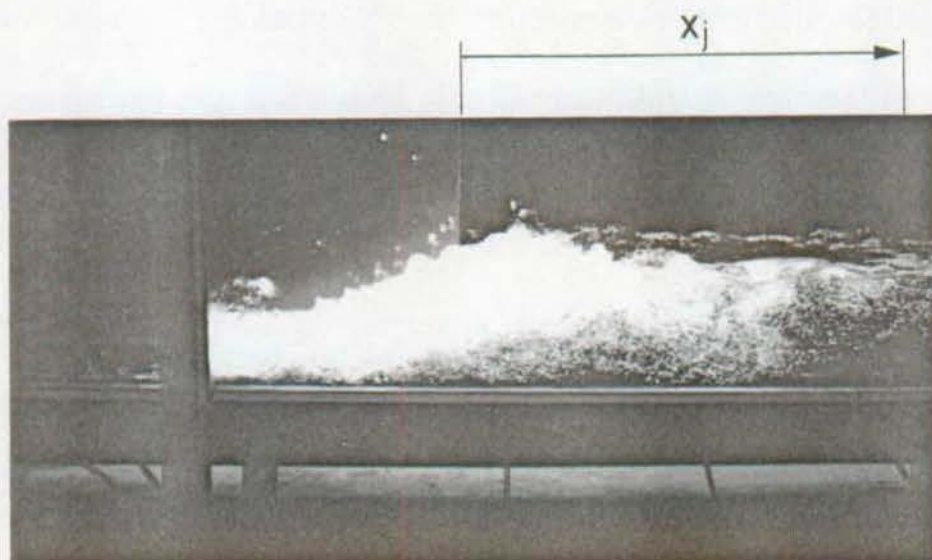


Fig. 5.3 : Jump end section x_j for typical T-jump (Series 1.2 with $h_1=1.4\text{cm}$, $F_1=8.21$, $x_1=25\text{cm}$, $x_j\cong 62\text{cm}$).

The experimental data as well as some parameters defined later (X_1 , F_1 , L_j^*) are listed in Appendix 2. Herein Y indicates the sequent depths ratio, and $Y^*=h_2^*/h_1$ the depths ratio according to the Bélanger's relation

$$Y^* = 0.5(\sqrt{1 + 8F_1^2} - 1) \quad (5.1)$$

Indices "ex" and "p" refer to experimental observation and prediction, respectively. The data are subdivided depending on the channel geometry. The notation used as well as the channel geometry are summarized on a head page. The units are indicated at the top of each column.

5.3 TOE POSITION X_1

As indicated in paragraph 5.2, it may be assumed that

$$Y = Y(B ; F_1 ; x_1 ; \omega_1) . \quad (5.2)$$

Unlike the parameters B , F_1 and ω_1 , the toe position x_1 is a dimensional quantity. This quantity should be normalized in a way that it becomes of physical significance. The correct normalizing length must satisfy the conditions:

1. For $x_1=0$ (S-jump) the sequent depths ratio Y attains the minimum value.
2. If the entire jump is shifted upstream away from the expansion, Y attains a maximum corresponding approximately to the sequent depths ratio for the prismatic channel (Bélanger's equation). The expansion ratio B has then no effect on Y .

It should be noted that the position x_1 for which $Y \cong Y^*$ depends on the inflow characteristics F_1 and h_1 . The normalizing length should therefore include these parameters. Accordingly, the non-dimensional toe position parameter X_1 is defined as

$$X_1 = \frac{x_1}{L_r^*} \quad (5.3)$$

in which L_r^* is the length of the surface roller of a classical jump.

Bretz (1987) conducted an experimental investigation on the length of the surface roller. His observations were made in the modified installation LCH1 (prismatic channel geometry). Based on his experimental data he proposed the linear relation

$$\lambda_r^* = \frac{L_r^*}{h_1} = 6.29F_1 - 3.59 \quad (5.4)$$

provided $4 < F_1 < 12$. Fig. 5.4 compares Eq. (5.4) with the data of several experimental investigations. The data are seen to follow quite closely Eq. (5.4), although the average deviation in L_r^* amounts to roughly $\pm 5h_1$.

According to Hager, et al. (1990) the roller length of the classical jump depends not only on F_1 and h_1 but also on ω_1 and on the modified inflow Reynolds number $R_1^* = Q/(b_1v)$. The effect of these additional parameters should be considered if $F_1 > 8$. For the purpose of this study the accuracy of Eq. (5.4) was considered as sufficient. In

context with jumps in expanding channels L_r^* should be regarded primarily as a scaling length. The role of λ_r^* is comparable to Y^* as a scaling for vertical lengths. Both Y^* and λ_r^* are not measurable quantities in expanding hydraulic jumps but represent simple functions of F_1 .

The jump length L_j^* in prismatic channels may be estimated by the relation

$$\lambda_j^* = \frac{L_j^*}{h_1} = 220 \operatorname{th} \left(\frac{F_1 - 1}{22} \right) \quad (5.5)$$

in which $\operatorname{th}(i) = [\exp(i) - \exp(-i)] / [\exp(i) + \exp(-i)]$. Eq. (5.5) is based on the experimental investigation conducted by Bradley and Peterka (1957) in Basin 1 (see also Peterka (1983)). The length of the surface roller was preferred to the jump length since L_r^* was investigated in more detail and may be defined with better accuracy. As an approximation, the length of roller may also be given as $L_r^* = 4.5h_2^*$. Thus, the ratio of length of jump to length of roller is approximately $L_j^*/L_r^* \approx 1.3$.

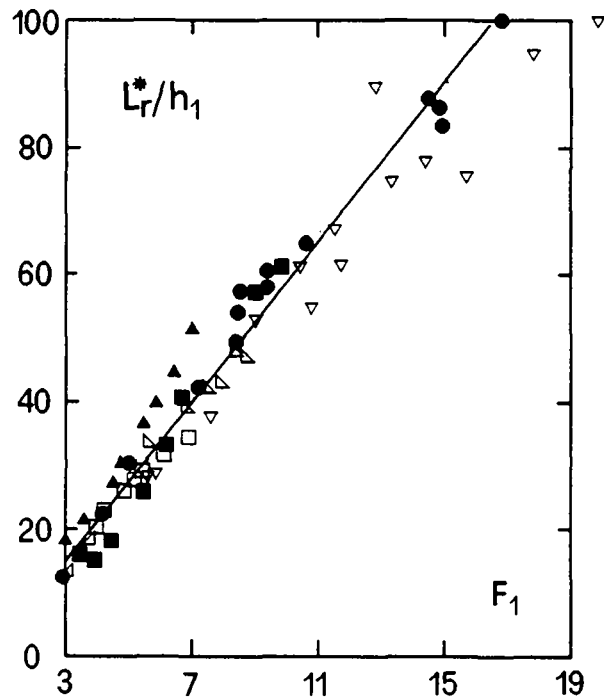


Fig. 5.4 : Length of roller L_r^* : Comparison of Eq. (5.4) with the data of (●) Safranez (1929); (▲) Einwachter (1932); (▽) Pietrkowski (1932); (◄) Bakhmeteff and Matzke (1936); (□) Schröder (1963); (■) Rajaratnam (1965); (◄) Sarma and Newnham (1973).

It should be noted that L_r^* becomes small both for low inflowing Froude numbers and small inflow depths h_1 . For such cases the relative accuracy of X_1 due to an observational error in x_1 may thus become significant.

For S-jumps the toe position is $X_1=0$ since the toe is located at the expansion section ($x_1=0$). For jumps in which the entire surface roller is located upstream of the expansion the toe position is $X_1>1$.

Fig. 5.5 shows jumps for three different values of X_1 and the same inflow conditions h_1 and F_1 . These were obtained when the tailwater level was gradually raised. In Fig. 5.5a) the toe is located shortly upstream from the expansion section generating a strongly asymmetric jump and high waves. In Fig. 5.5b) the tailwater level was increased, and moved the toe of the jump further upstream. The jump asymmetry and the wave height are thereby reduced. However, the main stream is still deflected on the left channel side and a significant backward flow along the opposite side wall is induced. Only in Fig. 5.5c) an overall symmetric flow could be obtained. Therein 90 % of the surface roller is located in the upstream channel.

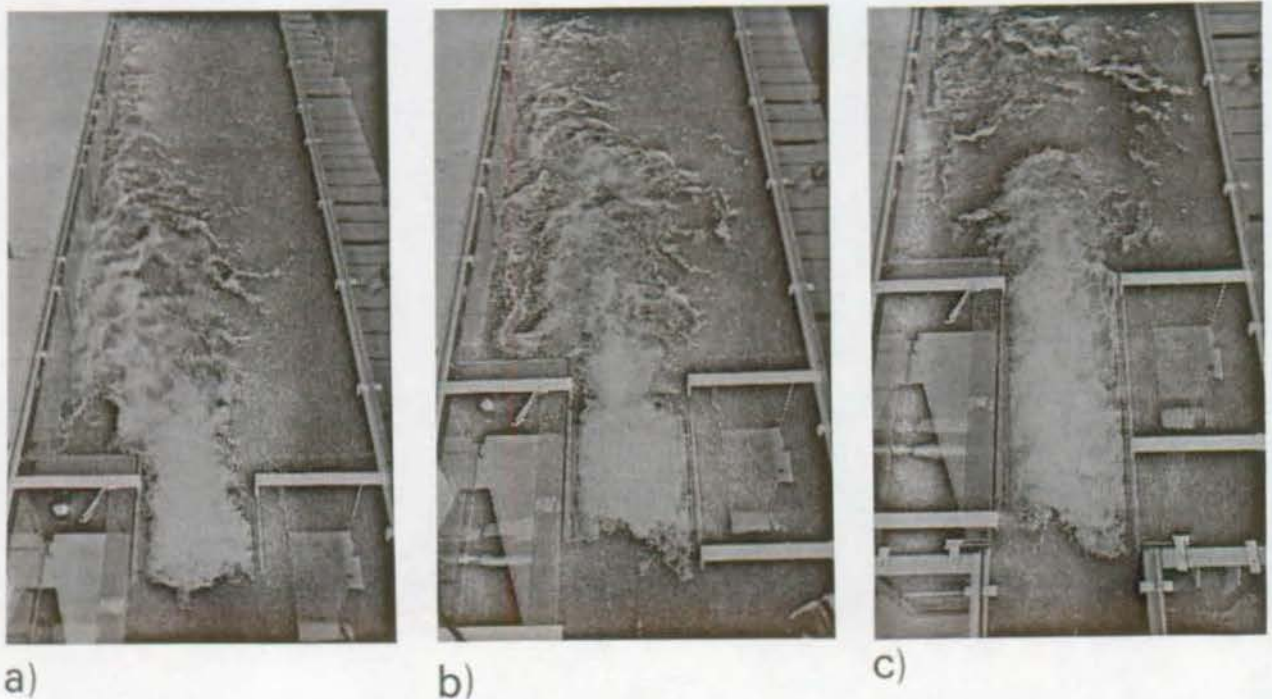


Fig. 5.5 : Overall jump characteristics for different values of X_1 .
 $F_1=5.02$, $h_1 \approx 5.0\text{cm}$. a) $X_1=0.1$; b) $X_1=0.4$ and c) $X_1=0.9$.

The toe position parameter X_1 is a measure of jump extension in the approaching channel. For $X_1=0$ the entire jump is located in the wide tailwater channel, whereas the jump occurs partly in the narrow approaching channel otherwise.

5.4 CONVENTIONAL MOMENTUM APPROACH

The sequent depths ratio Y of hydraulic jumps in prismatic channels could be predicted by a conventional momentum approach. The deviations between the theory and the experiment must mainly be attributed to wall frictional effects.

According to Hager and Bremen (1989), the modified sequent depths equation reads

$$\bar{Y} = Y_0^* [1 - 3.25\omega_1 \cdot \exp(F_1/7) \cdot \log(R_1^*)^{-3}] \quad (5.6)_1$$

in which

$$Y_0^* = Y^* [1 - 0.70 \log(R_1^*)^{-2.5} \cdot \exp(F_1/8)] \quad (5.6)_2$$

with $R_1^* = V_1 h_1 / \nu$. Eq. (5.6) accounts for the wall friction between the toe and the end of the jump. With $\nu \cong 10^{-6} \text{ m}^2/\text{s}$ the discharge per unit width must be larger than $0.1 \text{ m}^2/\text{s}$ for $Y^*/\bar{Y} > 0.95$.

As outlined by Harleman (1951) nonuniform velocity distribution has only a small effect on Y since the velocity distribution coefficient α_2 at the jump end section is always smaller than 1.05. Therefore it seems worthwhile to verify if the assumptions made in prismatic channels could be used for non-prismatic geometries. Assuming hydrostatic pressure and uniform velocity distributions, the momentum approach leads to (Herbrand (1971)

$$\frac{b_1 h_1^2}{2} + (b_2 - b_1) \frac{h_a^2}{2} + \frac{Q^2}{g b_1 h_1} = \frac{b_2 h_2^2}{2} + \frac{Q^2}{g b_2 h_2} \quad (5.7)$$

Using the continuity equation, and introducing the parameters

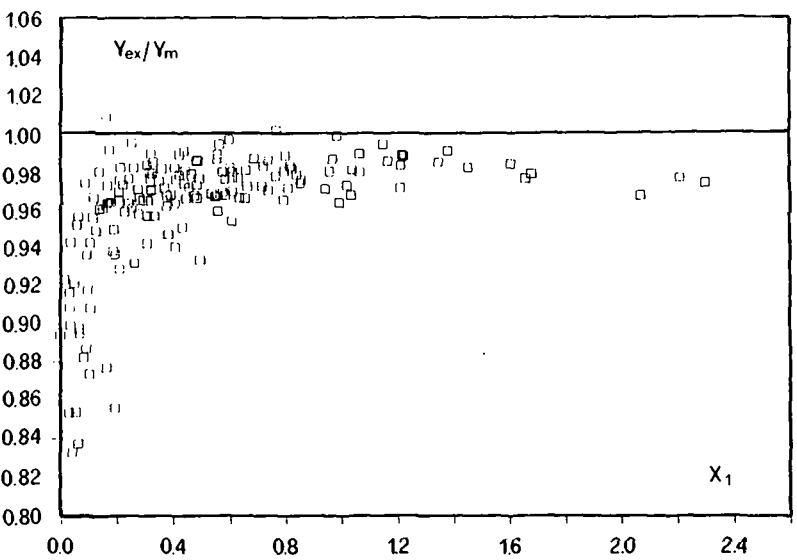
$$Y = \frac{h_2}{h_1} ; Y_a = \frac{h_a}{h_1} ; B = \frac{b_2}{b_1} ; F_1^2 = \frac{V_1^2}{g h_1}$$

yields

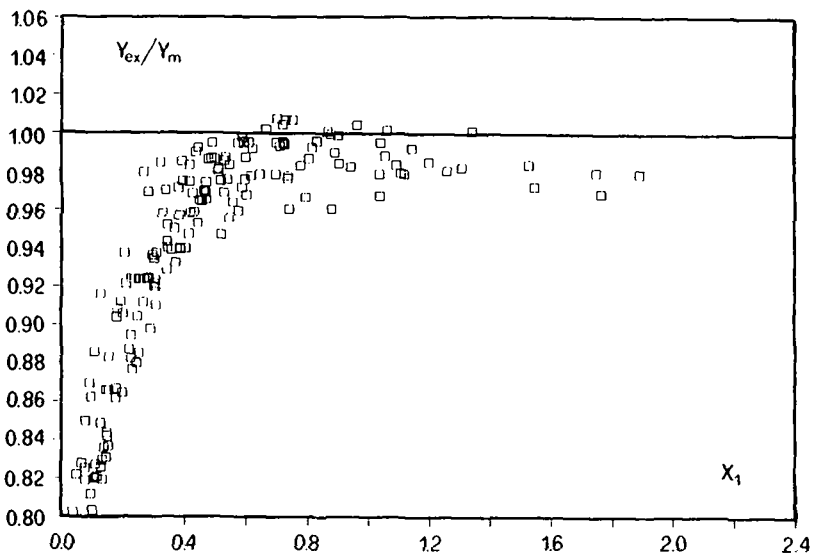
$$Y^3 - \frac{Y}{B} (1 - Y_a^2 + B Y_a^2 + 2 F_1^2) + \frac{2 F_1^2}{B^2} = 0 \quad (5.8)$$

Herein the frictional effects are neglected and the channel bottom is assumed horizontal. According to Herbrand (1971), Eq. (5.8) could be linearized to yield

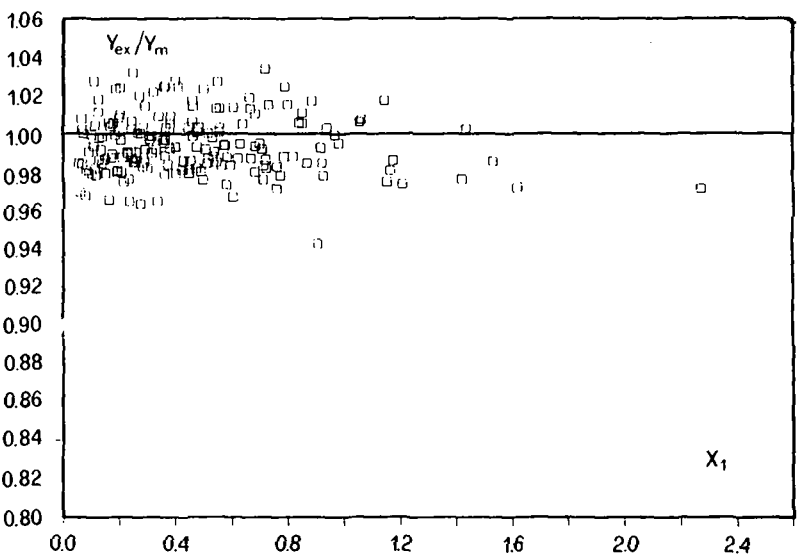
$$Y = \sqrt{\frac{2}{B} \cdot F_1} + \frac{1}{2B} , \text{ if } 1 \leq Y_a \leq Y , \quad (5.9)$$



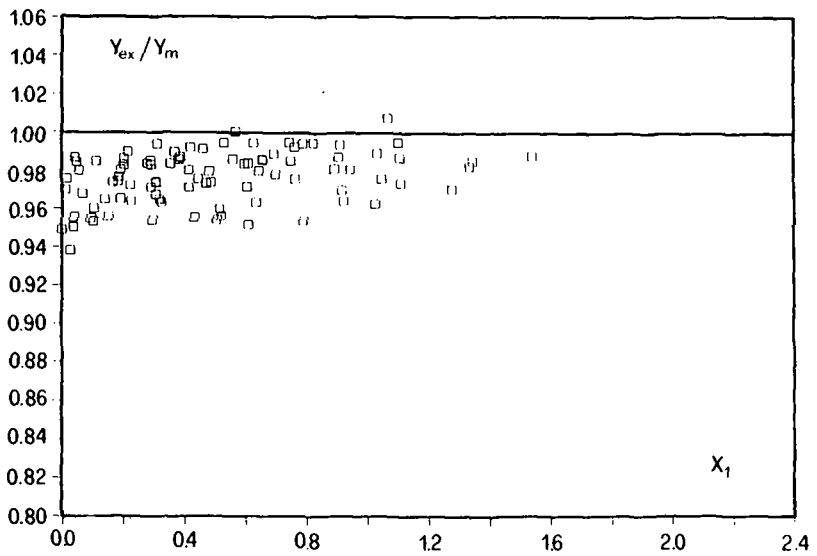
a)



b)



c)



d)

Fig. 5.6 : Sequent depths ratio: Y_{ex}/Y_m as a function of X_1 . a) $B=5$ asymmetric, channel LCH1. b) $B=3$ symmetric, channel LCH2, $B=3$ symmetric, channel LCH1 and $B=1.5$ asymmetric, channel LCH1.

and

$$Y = \sqrt{2} \cdot F_1 + \frac{1}{2B}, \quad \text{if } Y_a = Y \quad (5.10)$$

$Y_a < 1$ occurs if the toe is located at the expansion section (S-jumps), whereas $1 < Y_a < Y$ when the toe moves upstream. As outlined in chapter 3, the experiments conducted by Herbrand were in agreement with Eq. (5.9).

Eq. (5.8) involves the parameters Y , B , F_1 , and Y_a as described in paragraph 5.2. Once the experimental values of B , F_1 and Y_a are introduced in Eq. (5.8), it can be solved for Y . The sequent depths ratio obtained by this approach will be indexed with "m" (momentum). Y_m was computed for all runs and is listed in Appendix 2 together with Y_{ex} according to the experiments.

$Y_{ex}/Y_m = 1$ indicates that the experimental results satisfy Eq. (5.8) perfectly. Fig. 5.6 shows the ratio Y_{ex}/Y_m as a function of X_1 for all channel geometries considered. For $X_1 > 0.2$ the average value of Y_{ex}/Y_m becomes slightly smaller than one, depending on the series considered. This indicates that the experimental results satisfy Eq. (5.8) for $X_1 > 0.2$.

The conventional momentum approach could therefore be applied for the analysis of sudden expansions provided $X_1 > 0.2$ since wall friction becomes significant otherwise.

The deviation of 1 to 2% can be attributed to frictional effects as for the classical jump. For the series 1.1, 1.2 and 1.3 the deviation between Y_{ex} and Y_m becomes significant if $X_1 < 0.2$ to 0.3. Two reasons explain this deficiency.

The first reason is related to the limited length of the experimental installations. For $X_1 < 0.2$, the flow is strongly asymmetric and leads to a long lateral eddy along one channel side (chapter 2). Since x_2 could exceed 10 times the channel width, section 2 was located in the vicinity of the overflow weir. For such flow configurations, the test reach was too short and it was therefore impossible to attain a horizontal surface profile. This situation was particularly met in installation LCH2 when X_1 was small. This explains that the deviation is more pronounced in LCH2 (series 1.6) than in LCH1.

The friction force could be expressed as

$$F_f = \rho g \int_0^L A \cdot S_f \cdot dx \quad \text{with} \quad A(x) = b(x) \cdot h(x) \quad (5.11)$$

in which

$$S_f = \frac{V^2}{2g} \cdot \frac{f}{4R_h} \quad (5.12)$$

is the local frictional slope and L the distance between sections 1 and 2. The hydraulic radius for a rectangular channel of width b and height h is

$$R_h = \frac{bh}{b + 2h} \quad (5.13)$$

Eq. (5.11) could be approximated by

$$F_f \cong C_f \rho \cdot g \cdot b_2 \cdot h_2 \cdot L \cdot S_f \quad (5.14)$$

in which C_f is an integration coefficient. Assuming f constant yields

$$F_f \cong C_f \rho (b_2 + 2h_2) \frac{Q^2}{b_2^2 h_2^2} \cdot L \quad (5.15)$$

To investigate the variation of F_f with the toe position parameter X_1 , Eq. (5.15) could be normalized by the sum S_2 of static and dynamic forces in section 2

$$S_2 = \rho g \left(\frac{h_2^2}{2} b_2 + \frac{Q^2}{g b_2 h_2} \right) \quad (5.16)$$

Fig. 5.7 shows the ratio $F_f/(S_2 C_f)$ as a function of X_1 . For low values of X_1 (<0.20) the frictional contribution to the momentum equation is more than 10 times larger than for $X_1 \geq 0.5$.

Therefore, the portion of frictional force in the momentum equation depends on the toe position X_1 . For low values of X_1 this force influences the sequent depths ratio and should be included in momentum considerations.

For $X_1 > 0.2$ the scatter of Y_{ex}/Y_m (Fig. 5.6) is approximately $\pm 2\%$. This is larger than generally observed for classical hydraulic jumps (Hager and Bremen 1989), and should be attributed to the additional error involved by the measurement of the ratio Y_a . In case of classical hydraulic jumps only F_1 is needed to apply the momentum equation.

The significant results may be summarized as follows:

1. A conventional momentum approach may be used to investigate hydraulic jumps in sudden expansions if the position x_2 of the sequent depth is defined. In this study h_2 was measured downstream from the longer lateral eddy. Otherwise then in

prismatic channels, the momentum equation involves two unknowns (for example Y and Y_a) and two known parameters (for example B and F_1). The additional equation needed to solve Eq. (5.8) will be developed in paragraph 5.5

2. The deviation between Y_m due to Eq. (5.8), and Y_{ex} according to the experiments must mainly be attributed to frictional effects. These are insignificant for $X_1 > 0.2$. For smaller values of X_1 , the frictional force has to be included.
3. The measurements in the installations LCH1 and LCH2 are in fair agreement except for $X_1 < 0.4$. The larger deviation between Y_{ex} and Y_m recorded in LCH2 for $0.2 < X_1 < 0.4$ should be attributed to the limited length of the latter channel.

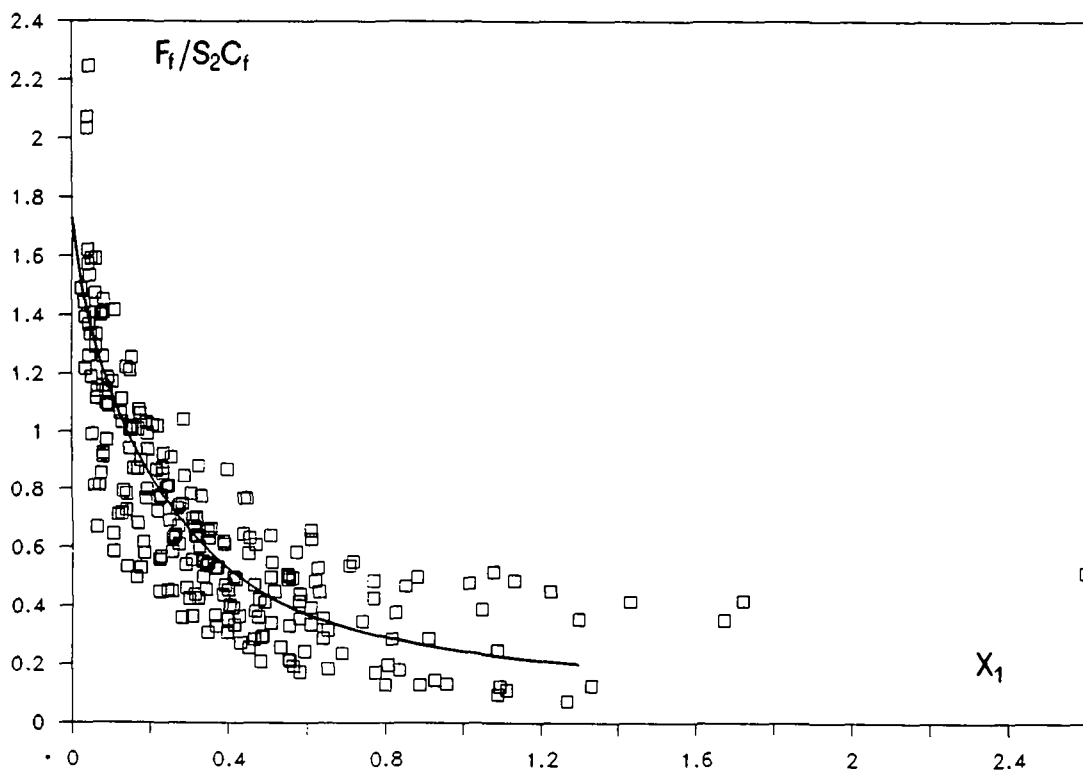


Fig. 5.7 : Effect of wall friction on sequent depths: Variation of the ratio $F_f/(S_2 C_f)$ with the toe position parameter X_1 . Series 1.2. (—) Average experimental curve.

5.5 SEQUENT DEPTHS

5.5.1 Introduction

To solve Eq. (5.8) for either Y or Y_a , an additional equation is needed. In a first step it should be verified if all the parameters of Eq. (5.2) have to be considered or if their

number could be reduced. In particular, as shown in chapter 3, the effect of ω_1 on Y should be investigated.

In a second step the parameters selected have to be analyzed separately in a way that some empirical relations could be established.

Based on the inflow conditions F_1 , h_1 , and X_1 , the relations which will be derived allow the prediction of Y and Y_a . In the next paragraph, the model will then be compared to some published experimental data.

5.5.2 Effect of shape factor ω_1

To investigate the effect of $\omega = h_1/b_1$ on the sequent depths ratio Y , it would be ideal to keep the remaining parameters F_1 , B and X_1 constant. However, due to the frictional effects on the inflowing depth h_1 , small variations on F_1 , and ω_1 could not be avoided during the experiments.

Fig. 5.8 shows some typical experiments conducted in channel LCH1 for an asymmetric expansion ratio $B=3$ (series 1.2). Y_{ex} is plotted as a function of F_1 , thereby considering different values of X_1 . In this series, five gate openings were investigated for which five domains of ω_1 resulted.

Fig. 5.8 reveals no systematic influence of ω_1 on Y_{ex} . However, Y_{ex} depends significantly on the position parameter X_1 as well as on F_1 . This observation, which was already presumed by Herbrand for S-jumps is of fundamental significance since the effect of the shape factor ω_1 may be dropped.

The sequent depths ratio Y in sudden expanding channels depends only on the expansion ratio B , the inflowing Froude number F_1 and on the toe position parameter X_1 .

5.5.3 Limit conditions

The relation to be established for Y should satisfy the following limit conditions:

1. $Y = Y(F_1) = Y^*$ according to (Eq. 5.2) for $B=1$,
2. $Y = Y^*$ for $X_1 \gg 1$ and any expansion ratio B , and
3. Considering the linear relation

$$Y = m \cdot F_1 + n \quad (5.17)$$

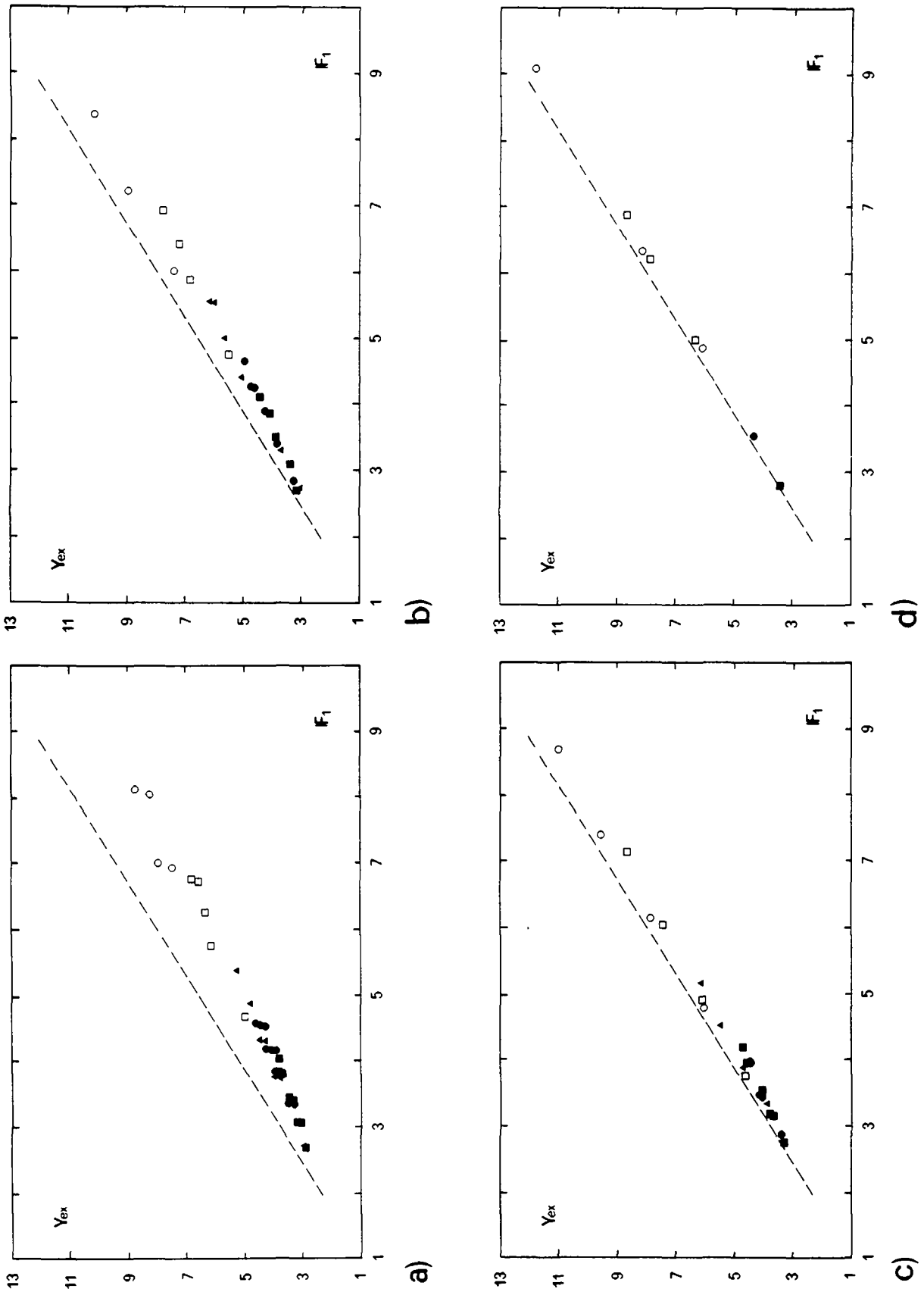


Fig. 5.8 : Effect of ω_1 on sequent depth ratio. Y_{ex} as a function of F_1 for four values of X_1 and five domains of ω_1 . a) $0.15 < X_1 < 0.25$; b) $0.35 < X_1 < 0.45$; c) $0.55 < X_1 < 0.65$; d) $0.75 < X_1 < 0.85$. (--) Sequent depths according to Bélanger. (■) $\omega_{11} \cong 0.377$; (●) $\omega_{12} \cong 0.305$; (▲) $\omega_{13} \cong 0.230$; (○) $\omega_{14} \cong 0.146$; (□) $\omega_{15} \cong 0.085$.

according to the conventional momentum approach as presented in § 5.4, m should be included in the domain

$$m_{\min} = \sqrt{\frac{2}{B}} < m < \sqrt{2} = m_{\max} . \quad (5.18)$$

The value $m=m_{\min}$ applies when the toe is located at the expansion section (S-jump), whereas $m=\sqrt{2}$ when the jump is entirely in the prismatic channel.

5.5.4 Effect of X_1

As is indicated in the preceding paragraph, the slope m depends only on X_1 and ranges between

$$\sqrt{\frac{2}{B}} < m < \sqrt{2} \quad (5.19)$$

for a particular expansion ratio B considered. Further, Fig. 5.8 reveals that the curves $Y(F_1)$ for different B and X_1 intersect at one common origin $(F_1; Y)=(1; 1)$. Therefore the equation for $Y(F_1)$ may be written as

$$(Y - 1) = (Y^* - 1) \cdot (1 - \Delta Y) \quad (5.20)$$

in which Y^* is the sequent depths ratio according to Eq. (5.1) and ΔY a factor of proportionality independent of F_1 .

Inserting the limit conditions in Eq. (5.20) yields

$$0 \leq \Delta Y \leq 1 - \frac{1}{\sqrt{B}} . \quad (5.21)$$

Fig. 5.9 shows the experimental values of ΔY as a function of X_1 for series 1.3 (Table 5.1). Based on this figure, the following remarks apply :

1. For $X_1 \rightarrow 0$, ΔY attains the maximum values ranging between 0.34 and 0.44. The upper limit is attained for $X_1=0$ and amounts for $B=3$ to

$$\Delta Y_{\max} = 1 - \frac{1}{\sqrt{B}} = 0.442 . \quad (5.22)$$

Eq. (5.21) is thus verified experimentally.

2. As mentioned previously, the scatter of experimental data is significant and should mainly be related to the difficulty of measuring exactly the toe position. Assuming that 5% of the experimental data could be deleted, the remaining 95% of the measurements are included in a domain of $\pm 0.06 \Delta Y$.
3. Fig. 5.9 shows that $\Delta Y \approx 0$ for $X_1 > 1.3$ which indicates that Y becomes independent of B if the entire jump is located upstream from the expansion (§ 5.3).

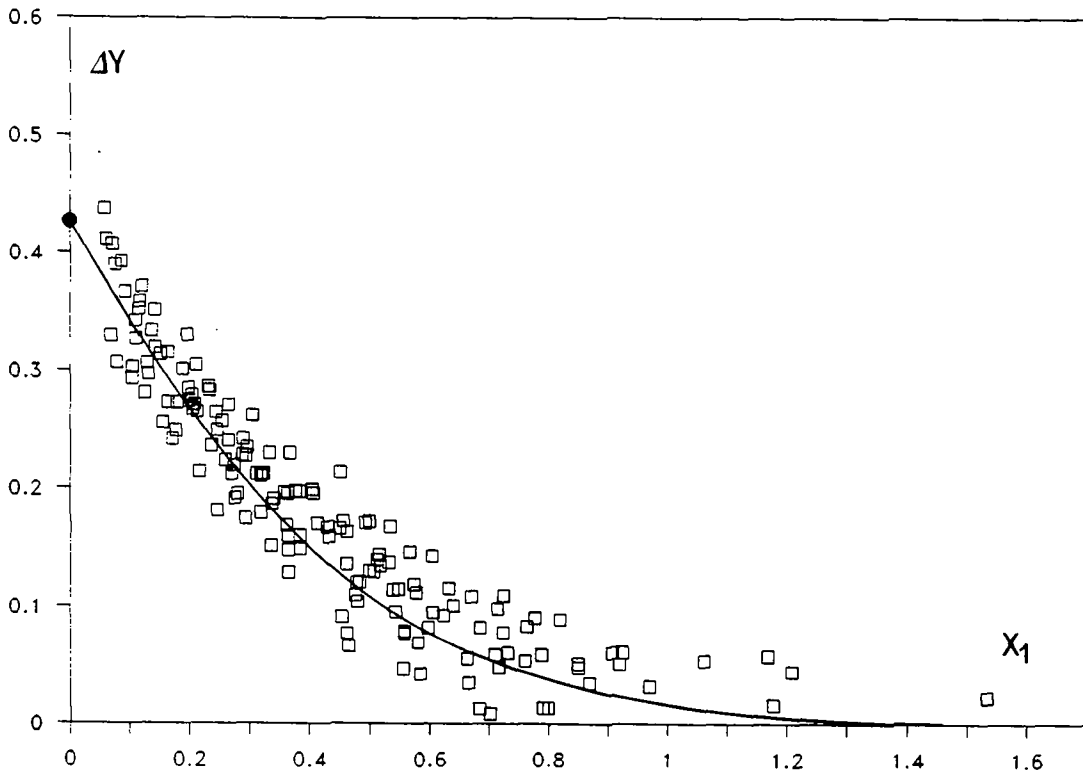


Fig. 5.9 : ΔY as a function of the toe position parameter X_1 for series 1.3. (\square) experimental values ; (—) prediction according to Eq. (5.23) with (\bullet) ΔY_{\max} according to Eq. (5.22).

The effect of X_1 on ΔY may now be studied for one particular expansion ratio B . According to Eq. (5.21), one could write

$$\Delta Y = \Delta Y_{\max} \cdot f(X_1) \quad (5.23)$$

in which ΔY_{\max} depends exclusively on B , and $0 \leq f(X_1) \leq 1$. Using the data of series 1.3, it was found that

$$f(X_1) = [1 - \text{th}(\bar{C}X_1)] \quad (5.24)$$

in which $\text{th}(i) = [\exp(i) - \exp(-i)] / [\exp(i) + \exp(-i)]$ and the constant \bar{C} was set to $\bar{C} = 1.9$.

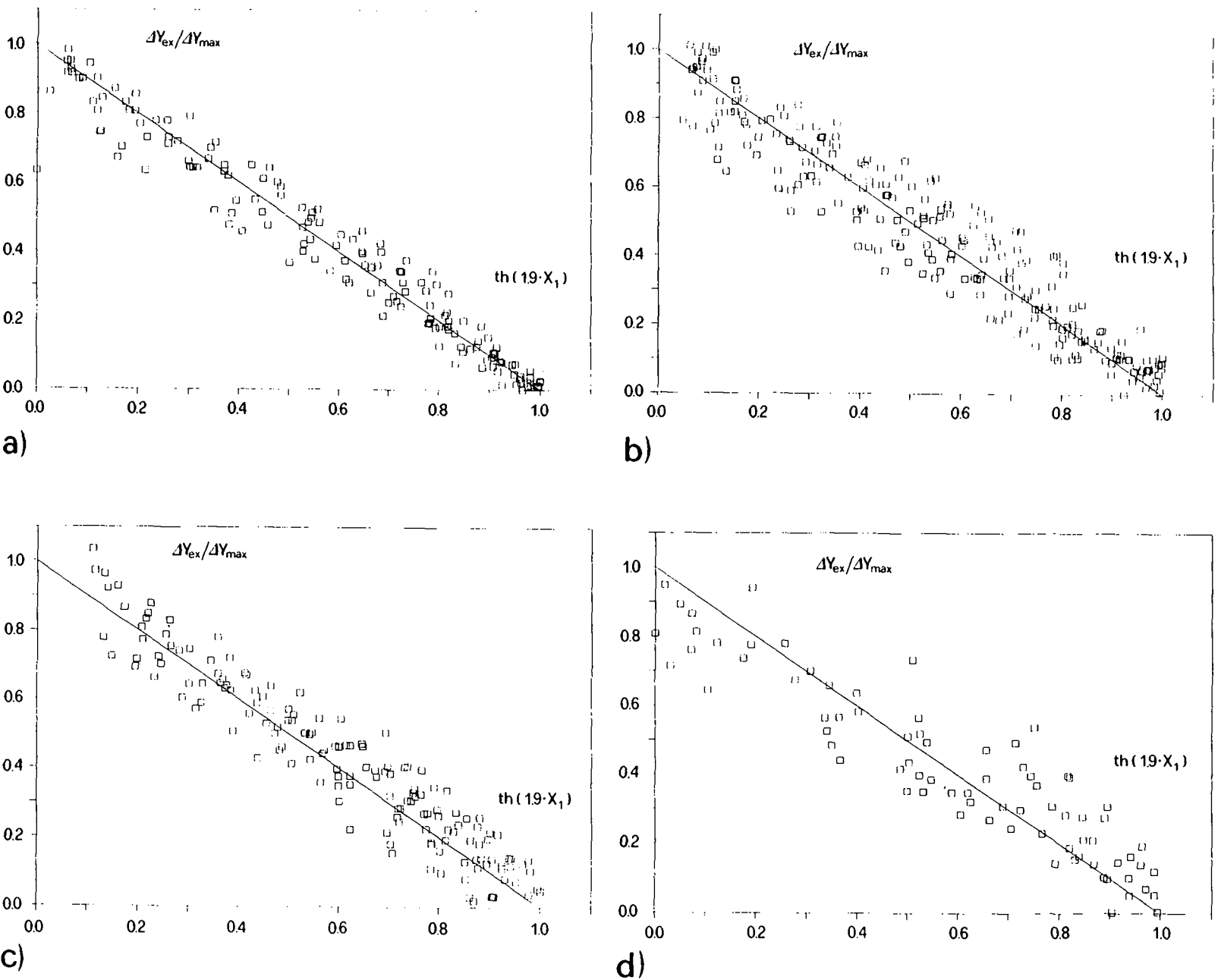


Fig. 5.10 : $\Delta Y_{ex}/\Delta Y_{max}$ as a function of $th(19 \cdot X_1)$. (□) experimental data. (—) Eq. (5.23). a) B=5 series 1.1 ; b) B=3 series 1.2; c) B=1.5 series 1.5 and d) B=1.4 series 1.5.

Fig. 5.10 shows the experimental results obtained for the other expansion ratios B . Herein, the scalings used for the plots have been modified. ΔY_{ex} was normalized by the corresponding value of ΔY_{max} , whereas X_1 was replaced by the term $\text{th}(1.9X_1)$. These scalings lead to a linear relation.

It could be noted that the ratio

$$\frac{\Delta Y_{\text{ex}}}{\Delta Y_{\text{max}}} = \text{th}(\bar{C}X_1) \quad (5.25)$$

is independent of the expansion ratio B . $\bar{C}=1.9$ remains therefore constant for any expansion ratio. Fig. 5.10 shows that the scatter of measurements is larger for small than for large B . It should be remembered that ΔY becomes small for channels with small B (for $B=1.5$, as an example, the result is $0 < \Delta Y < 0.18$). Furthermore, the absolute error remains approximately constant since ΔY_{max} decreases with B . Considering an average deviation of $\pm 0.13 \Delta Y / \Delta Y_{\text{max}}$ leads to an absolute deviation of $\pm 0.03 \Delta Y_{\text{ex}}$ for $B=1.5$.

Fig. 5.10 confirms also that $\Delta Y(X_1=0) = 1 - 1/B^{0.5}$ for any expansion ratio since all data tend asymptotically to $\Delta Y / \Delta Y_{\text{max}} = 1$.

Introducing Eq. (5.23) and Eq. (5.24) into Eq. (5.15) yields finally

$$Y = (Y^* - 1) \cdot \left[\frac{1}{\sqrt{B}} + \left(1 - \frac{1}{\sqrt{B}} \right) \cdot \text{th}(1.9X_1) \right] + 1 \quad (5.26)_1$$

which could also be written as

$$\psi = \frac{Y^* - Y}{Y^* - 1} = \left(1 - \frac{1}{\sqrt{B}} \right) \cdot [1 - \text{th}(1.9X_1)] \quad (5.26)_2$$

The relation for the sequent depths ratio Y may be expressed by a parameter ψ including the approaching Froude number only. ψ depends on the expansion ratio B and the position parameter X_1 , as given in Eq. (5.26)₂.

5.5.5 Discussion of results

It seems useful to outline some of the characteristics of Eq. (5.26). Consider first the limit conditions.

1. For $B=1$, Eq. (5.26) becomes $(Y^* - Y)/(Y^* - 1) = 0 \Rightarrow Y = Y^*$.
2. For $B \neq 1$, two limit conditions have to be considered
 - a. For $X_1 \geq 1.3 \Rightarrow \text{th}(1.9 \cdot X_1) \geq 0.985 \cong 1$, leading to $Y = Y^*$;
 - b. For $X_1 = 0 \Rightarrow \text{th}(1.9 X_1) = 0$ leading to

$$Y(X_1=0) = (Y^* - 1) \cdot \frac{1}{\sqrt{B}} + 1. \tag{5.27}$$

Eq. (5.26) satisfies all limit conditions considered in paragraph 5.5.4. Bélanger's equation could be derived from Eq. (5.26) for a prismatic channel geometry ($B=1$) as well as for jumps located entirely upstream from the expansion section ($X_1 \geq 1.3$).

The effect of each parameter F_1 , B , X_1 on Y could easily be discussed if Eq. (5.26)₂ is rewritten as

$$Y = f_1(F_1) \cdot [f_2(B) \cdot f_3(X_1)] \tag{5.28}$$

in which $f(i)$ is a function of the parameter i . Eq. (5.26) may be split into several functions of which each is including one independent parameter only. The effect of F_1 is thus clearly separated from the effect of the expansion ratio B , and of the toe position parameter X_1 .

The sequent depths ratio Y in sudden expansions may be represented as a product of effects of approaching Froude number F_1 , expansion ratio B and position parameter X_1

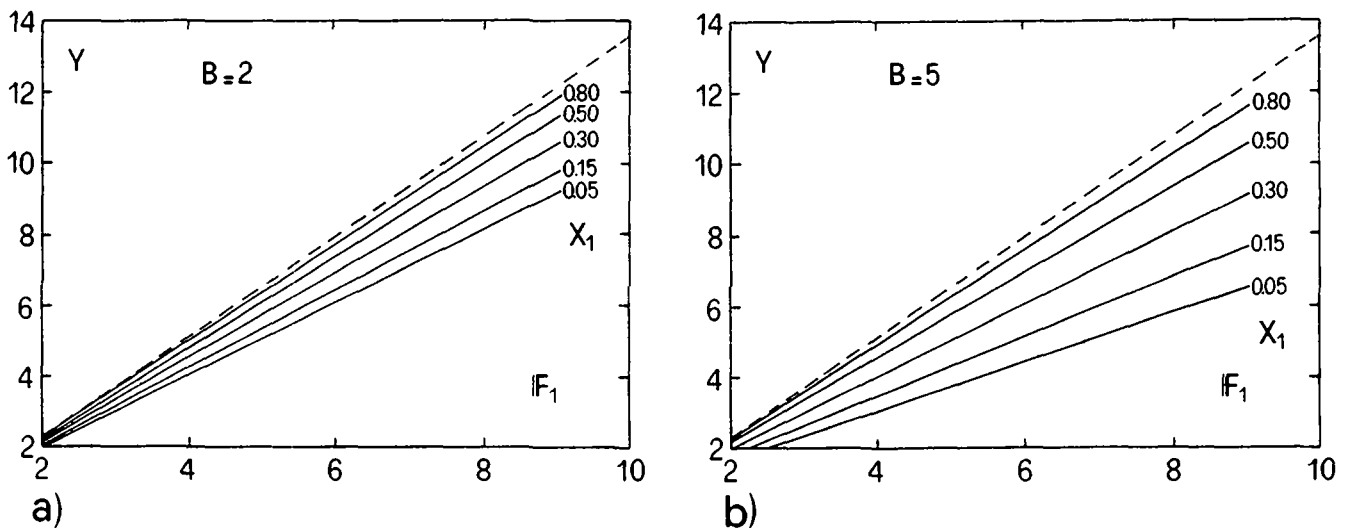


Fig. 5.11 : Sequent depths ratio Y according to Eq. (5.26) for a) $B=2$ and b) $B=5$. (—) Sequent depths ratio according to Eq. (5.1).

Fig. 5.11 shows the sequent depth ratio according to Eq. (5.26) for two expansion ratios B and five values of the position parameter X_1 . The dotted line indicates the sequent depth ratio according to Eq. (5.1).

In many cases, the tailwater level is fixed by the downstream channel or river characteristics. Once the inflow conditions h_1 and F_1 are defined, the value

$$\psi = \frac{Y^* - Y}{Y^* - 1}, \quad 0 < \psi < 1 \quad (5.29)$$

corresponding to the left hand side of Eq. (5.26)₂ could be evaluated. In Fig. 5.12 ψ is plotted against X_1 for several expansion ratios B . Fig. 5.12 outlines the effect of the expansion ratio on the jump position. Considering a constant value of ψ (constant up- and downstream flow depths and F_1) shows that the position X_1 depends exclusively on the expansion ratio B . Only for the degenerated case $B=1$ (prismatic channel) ψ is independent of the toe position X_1 (horizontal axis) since friction forces have been neglected.

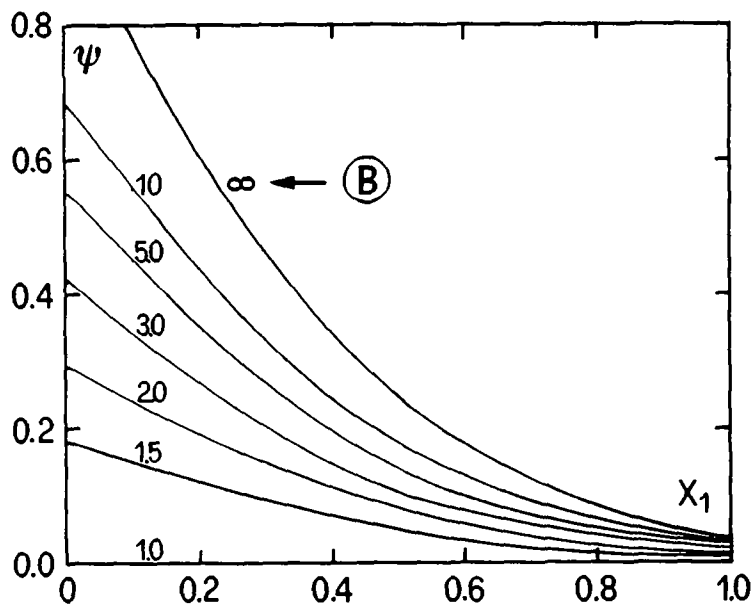


Fig. 5.12 : ψ as a function of X_1 for $1 \leq B < \infty$ according to Eq. (5.26).

Furthermore, the slope of the relation $\psi(X_1)$ for any value of B is a measure of the sensitivity of toe position on tailwater variations. Therefore, for a given increase in the tailwater level, the toe displacement decreases with the expansion ratio B and increases with X_1 . The numerical example presented in paragraph 5.9 shows how Fig. 5.12 could be used to determine rapidly the overall expansion dimensions. Although if in Fig. 5.12 expansion ratios $1 < B < \infty$ were considered, the experimental data used to develop Eq. (5.26) are included in the domains

- $1.5 \leq B \leq 5$,
- $2.5 \leq F_1 \leq 10.6$, and
- $0.0 \leq X_1 \leq 2.6$.

The ranges of application of Eq. (5.26), for which a satisfactory prediction of the sequent depths ratio should be expected may be involved in

- $1 \leq B \leq 10$,
- $2.5 \leq F_1 \leq 12$, and
- $X_1 \geq 0$

It should be outlined that the application domains of Eq. (5.26) provide a satisfactory agreement between predictions and measurements but do not account for the symmetry of jump. In paragraph 5.8, Fig. 5.12 will be subdivided into 3 domains depending on the symmetry characteristics.

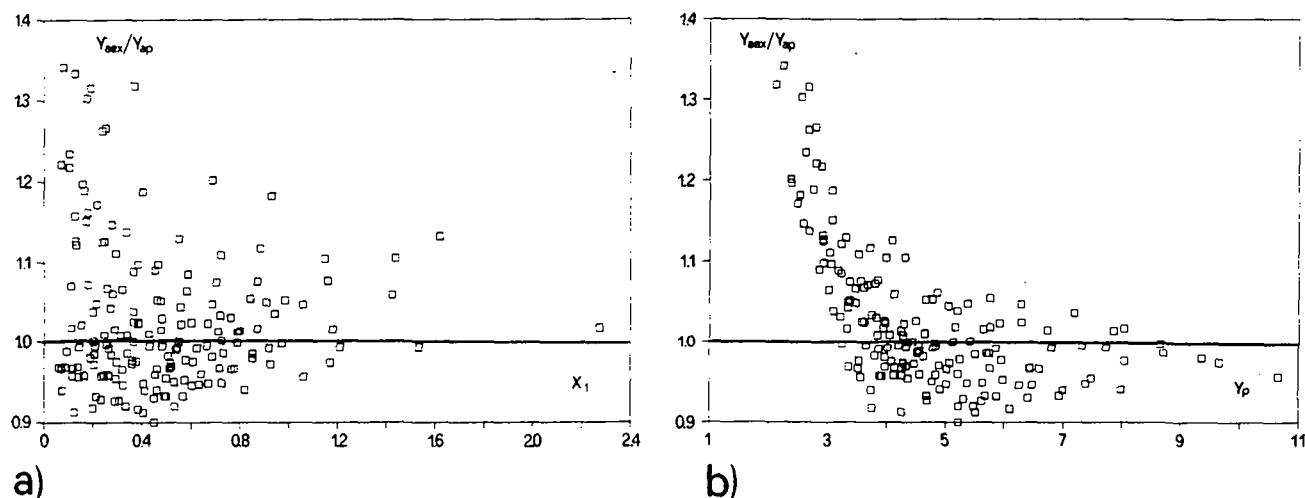


Fig. 5.13 : Average flow depths along the expansion side walls for series 1.3. a) Y_{aex}/Y_{ap} as a function of X_1 and b) Y_{aex}/Y_{ap} as a function of Y_p .

Once the sequent depths ratio established with Eq. (5.26), Y could be introduced in Eq. (5.4) to yield

$$Y_a^2 = \left[Y^2 - \frac{1}{B} \cdot \left(1 + 2F_1^2 - \frac{F_1^2}{YB} \right) \right] \cdot \left(1 - \frac{1}{B} \right)^{-1} . \quad (5.30)$$

Fig. 5.13 shows the ratio Y_{aex}/Y_{ap} as a function of X_1 (Fig. 5.13a) and as a function of Y_p (Fig. 5.13b) for series 1.3. These figures indicate that the agreement of the model

with the experimental data becomes (again) poor for small Y_p . Small Y_p result from small inflowing Froude numbers F_1 and small values of X_1 as indicated by Eq. (5.26). However, for $Y > 4$ the deviation becomes smaller than $\pm 10\%$. The flow depth h_a and its effect on the flow asymmetry will be discussed in paragraph 5.8.

5.5.6 Energy dissipation

The efficiency of hydraulic jumps in sudden expanding channels may be defined as the ratio between the difference of approaching H_1 and downstream H_2 energy heads relative to H_1 , that is

$$\eta = \frac{H_1 - H_2}{H_1} = 1 - \frac{Y + \frac{F_1^2}{2B^2Y^2}}{1 + \frac{F_1^2}{2}} \quad (5.31)$$

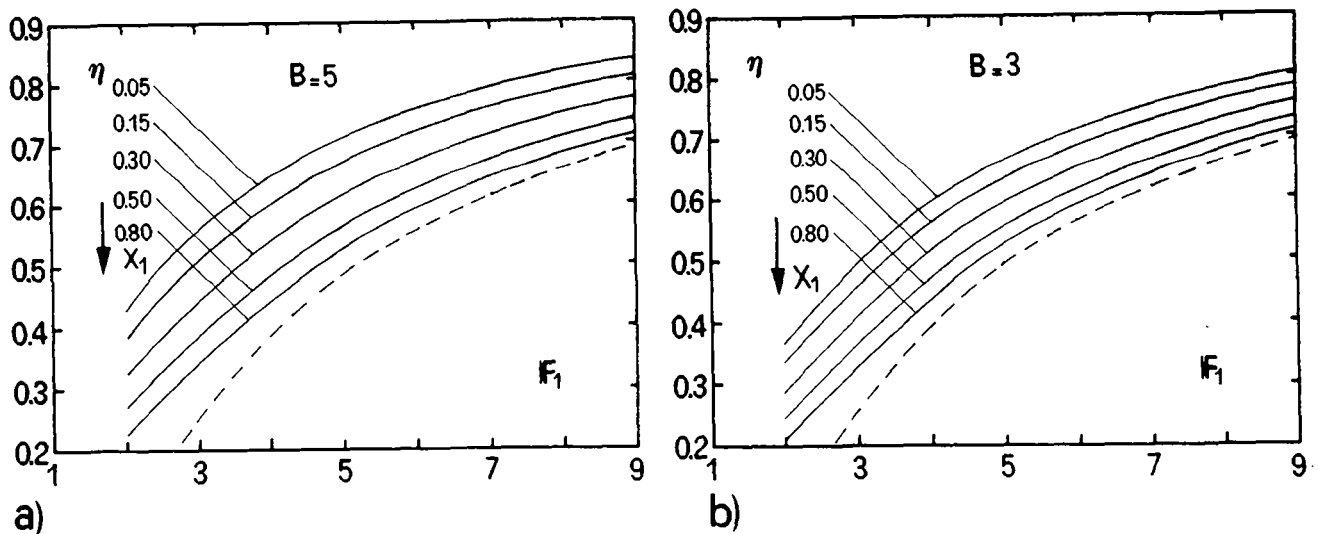


Fig. 5.14 : Efficiency η as a function of F_1 , X_1 , and B . (---) efficiency for $B=1$ according to Eq. (5.1). a) $B=5$, b) $B=3$.

Fig. 5.14 shows the efficiency obtained for two expansion ratios B and different toe locations X_1 when introducing Eq. (5.26) into Eq. (5.31). The dotted line indicates the energy dissipation according to Bélanger's Eq. (5.1).

It is noted that in the domain $F_1 \leq 6$, a significant increase in the energy dissipation is obtained when compared to the classical jump. However, it should be remembered that the jump characteristics become poor for small values of X_1 , due to the flow

asymmetry. Therefore, the relative increase in η is partly reduced by unsatisfactory action of the jump for $B > 2$ as compared to prismatic channels.

The efficiency of jump may significantly be increased by both larger expansion ratio B and small toe position parameter X_1 . Such jumps do not satisfy criteria regarding symmetry and compactness of jump, however.

5.5.7 Volume and efficiency of jump

Besides the efficiency of jump, a further quantity to be considered is the required volume needed to perform the energy dissipation. In a prismatic, rectangular channel, the volume of jump V_j^* could be expressed as

$$V_j^* = h_2^* \cdot b \cdot L_j^* \quad (5.32)$$

with L_j^* according to Eq. (5.5). Rather than the «volume of jump» Eq. (5.32) is an approximation for the volume to be excavated by assuming a horizontal land surface of the same elevation as the tailwater level.

For sudden expanding channels with vertical side walls, the corresponding volume of excavation may be approximated as

$$V_j = h_2 [b_1 x_1 + b_2 x_j] \quad (5.33)$$

when the height of jump is admitted as h_2 (see Fig. 5.2). In order to simplify the estimation of the excavation volume, it will be assumed that the length of the jump is independent from the expansion ratio B and the toe position X_1 . Therefore, inserting Eq. (5.3) in Eq. (5.33) with $L_j = L_j^* = x_1 + x_j$ (Fig. 5.2) leads to

$$V_j = h_2 [b_1 \cdot X_1 \cdot L_r^* + b_2 (L_j^* - X_1 L_r^*)] \quad (5.34)$$

In paragraph 5.7, the effect of X_1 and B on the jump length L_j will be discussed. Therein, it will be shown that the assumption $L_j = L_j^*$ tends to underestimate the jump length for small values of X_1 (typically $X_1 < 0.2$). However, the accuracy of this simplified approach is considered sufficient for a preliminary evaluation of the effect of B on the required excavation volume.

The non-dimensional volume of the classical jump is

$$\bar{V}_j^* = \frac{V_j^*}{bh_1^2} = Y^* \lambda_j^* , \quad (5.35)$$

and for sudden expanding channels

$$\bar{V}_j = \frac{V_j}{b_1 h_1^2} = Y \left\{ X_1 \lambda_r^* + B (\lambda_j^* - X_1 \lambda_r^*) \right\} \quad \text{provided } 0 < X_1 < 1.3 \quad (5.36)$$

in which λ_j^* may be expressed according to Eq. (5.5) and λ_r^* according to Eq. (5.4). Fig. 5.15 shows the ratio $\bar{V}_j / \bar{V}_j^* = V_j / V_j^*$ as a function of F_1 for an expansion ratio of $B=3$ and six values of X_1 . According to Fig. 5.15, the function \bar{V}_j / \bar{V}_j^* could be considered as practically independent from the inflowing Froude number provided $F_1 \geq 4$.

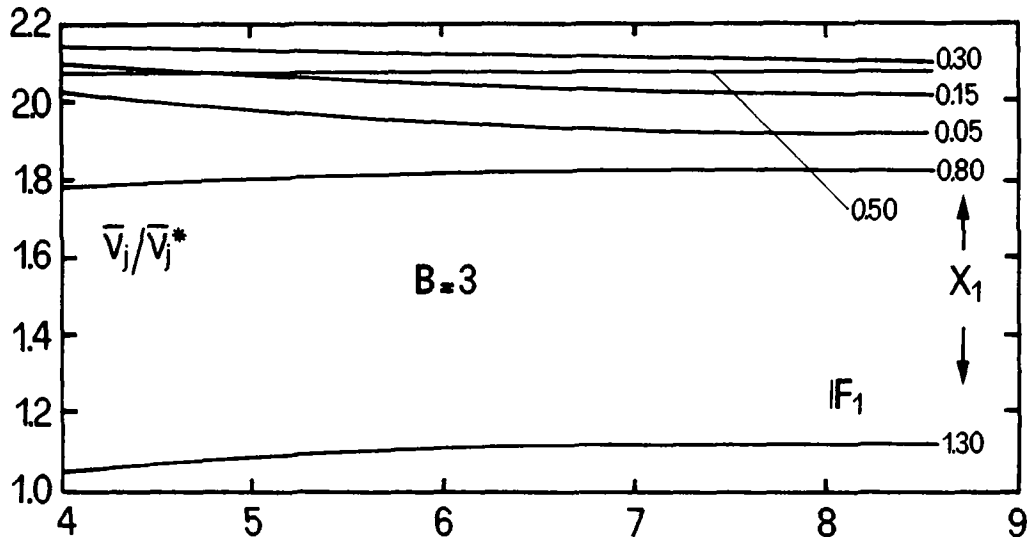


Fig. 5.15 : Ratio \bar{V}_j / \bar{V}_j^* as function of F_1 for $B=3$ and six values of the toe position parameter X_1 .

Fig. 5.16 shows \bar{V}_j / \bar{V}_j^* as function of the position parameter X_1 for different values of B .

For identical inflow conditions, the volume required for sudden expanding channels is always larger than for the prismatic channel. Since Eq. (5.36) tends to underestimate the jump length in the domain $X_1 < 0.2$ (paragraph 5.7), the ratio \bar{V}_j / \bar{V}_j^* may be assumed as practically independent of X_1 for $X_1 < 0.6$. Then the volume of jump required for sudden expanding channels may be approximated as

$$V_j \cong 0.5(1+B)V_j^* \quad \text{provided } 0 < X_1 < 0.6 . \quad (5.37)$$

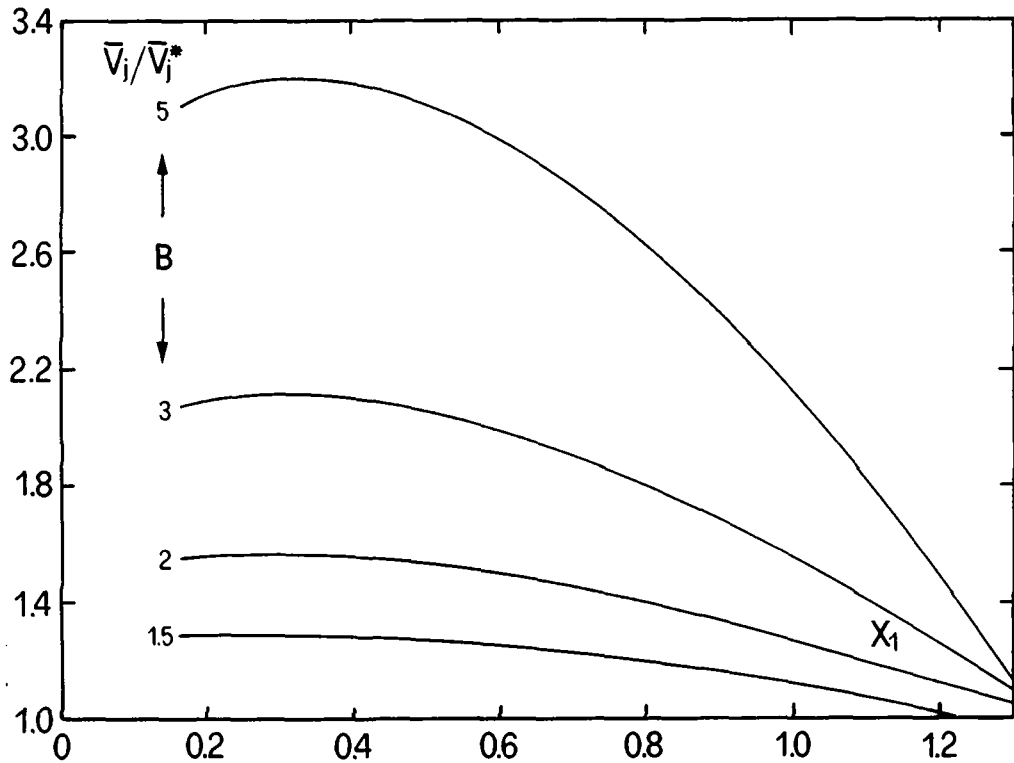


Fig. 5.16 : \bar{V}_j/\bar{V}_j^* as function of the toe position parameter X_1 for four expansion ratios B and $F_1=5$.

The efficiency of jump per unit volume may be defined as

$$\eta_v = \frac{\eta}{\bar{V}_j} \quad (5.38)$$

in which η is the efficiency according to Eq. (5.31) and \bar{V}_j the non-dimensional jump volume. Fig. 5.17 shows the ratio η_v/η_v^* as a function of X_1 for four values of B and $F_1=5$. Herein, $\eta_v^* = \eta/\bar{V}_j^*$ is defined as the efficiency per unit volume in prismatic rectangular channels. Note that η_v/η_v^* could not be considered as independent of F_1 .

As shown in Fig. 5.17, the efficiency per unit volume η_v is always smaller in sudden expanding than in prismatic channels. The additional volume required for sudden expanding channel could be compensated only partially with a more efficient jump, therefore.

Both the required volume of jump, and the dissipation per unit volume of jump are less favorable in expanding dissipators than for the classical jump.

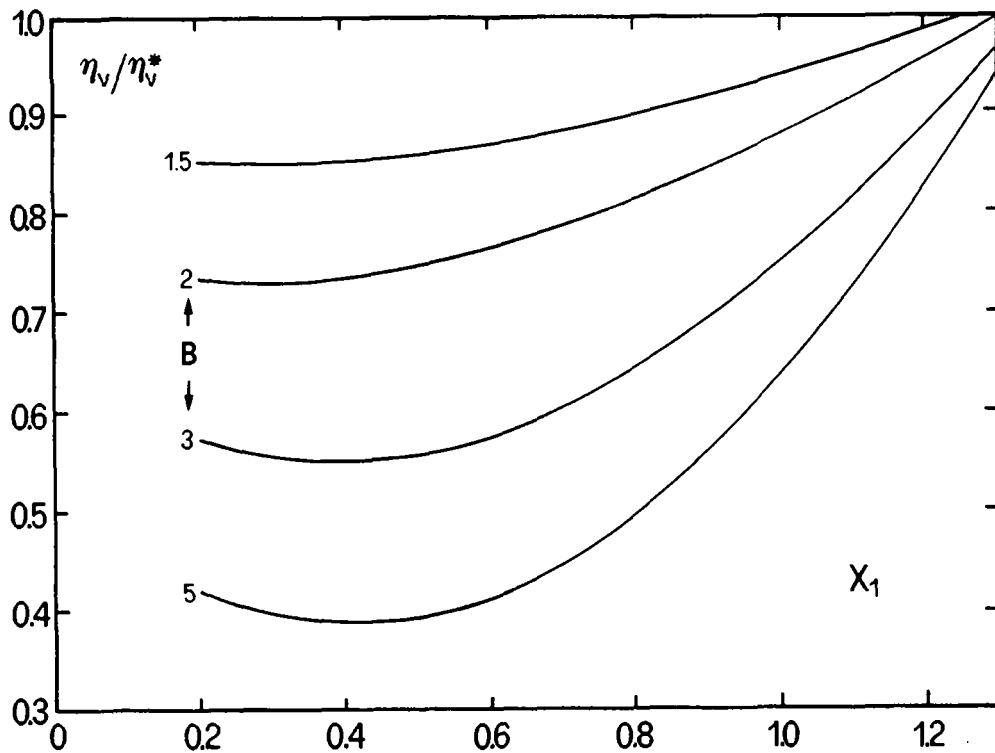


Fig. 5.17 : η_v/η_v^* as a function of X_1 for four expansion ratios B and an inflow Froude number $F_1=5$.

5.6 COMPARISON WITH EXPERIMENTAL RESULTS

5.6.1 Introduction

The computational model developed in paragraph 5.5 will now be compared to investigations described in chapter 3. Particular attention is paid to the results obtained by Unny, since no other investigation considered the toe position.

Despite the lack of sufficient informations on the toe position, the investigation of Herbrand (1971), and Sethuraman and Padmanabhan (1967) will also be considered. Finally, the experimental data collected in channels LCH1 and LCH2 will be presented and discussed.

Several computational models developed for S-jumps will be compared to Eq. (5.27). A detailed investigation of existing computational models for sudden expansions was also presented by Herbrand (1971).

5.6.2 Computational models

Fig. 5.18 shows a comparison of the relations proposed by Herbrand (1971) and Unny (1963) with Eq. (5.27) for the S-jump ($X_1=0$) and an expansion ratio $B=2$.

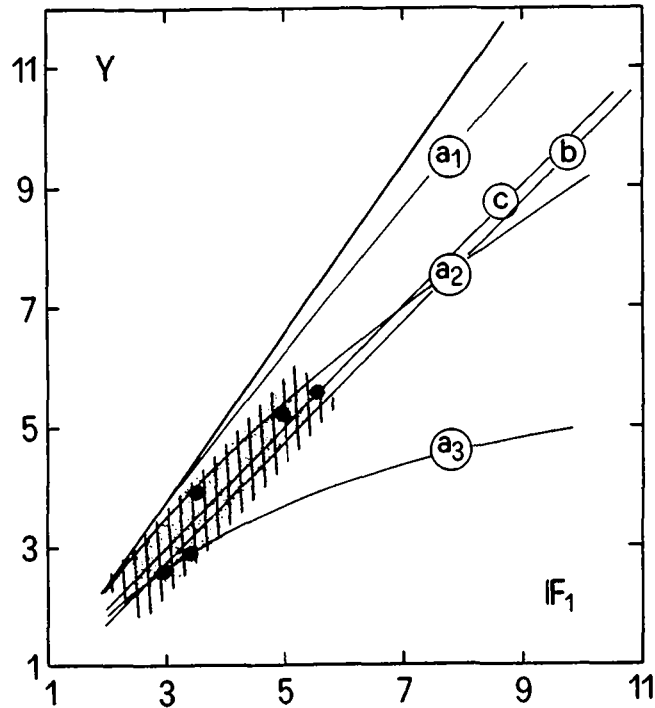


Fig. 5.18 : Comparison of sequent depths relations for $X_1 \cong 0$ and an expansion ratio $B=2$. a) Unny : (a₁) $\omega_1=0.02$; (a₂) $\omega_1=0.06$; (a₃) $\omega_1=0.15$. (b) Herbrand ; (c) Eq. (5.27) ; (—) Bélanger. (●) Experiments of Unny; (⊗) Unny's experimental domain.

It could be noted that Eq. (5.27) is similar to the proposition of Herbrand, but differs considerably of Unny's equation. This deviation is due to Unny's parameter $\omega_1=h_1/b_1$. In Fig. 5.18 Unny's experimental domain is also indicated. His experiments were limited to low values of F_1 and to large values of ω_1 .

5.6.3 Unny's experimental investigation

Unny's analytical approach accounts for S-jumps (paragraph 3.2.1). The data collected for T-jumps were not analyzed, therefore. Fig. 5.19 shows all experimental data published by Unny and the comparison with Eq. (5.26).

The scatter of data seems mainly due to some deviations of the measurement of Y rather than the toe position x_1 . This fact is revealed by jumps located entirely in the upstream channel ($X_1 > 1.3$). Y_{ex} should then be identical or slightly smaller than Y^* as discussed in § 5.5.4. However, the scatter of Y_{ex} for this flow condition is significant and indicates that the accuracy of the measurement technique was insufficient.

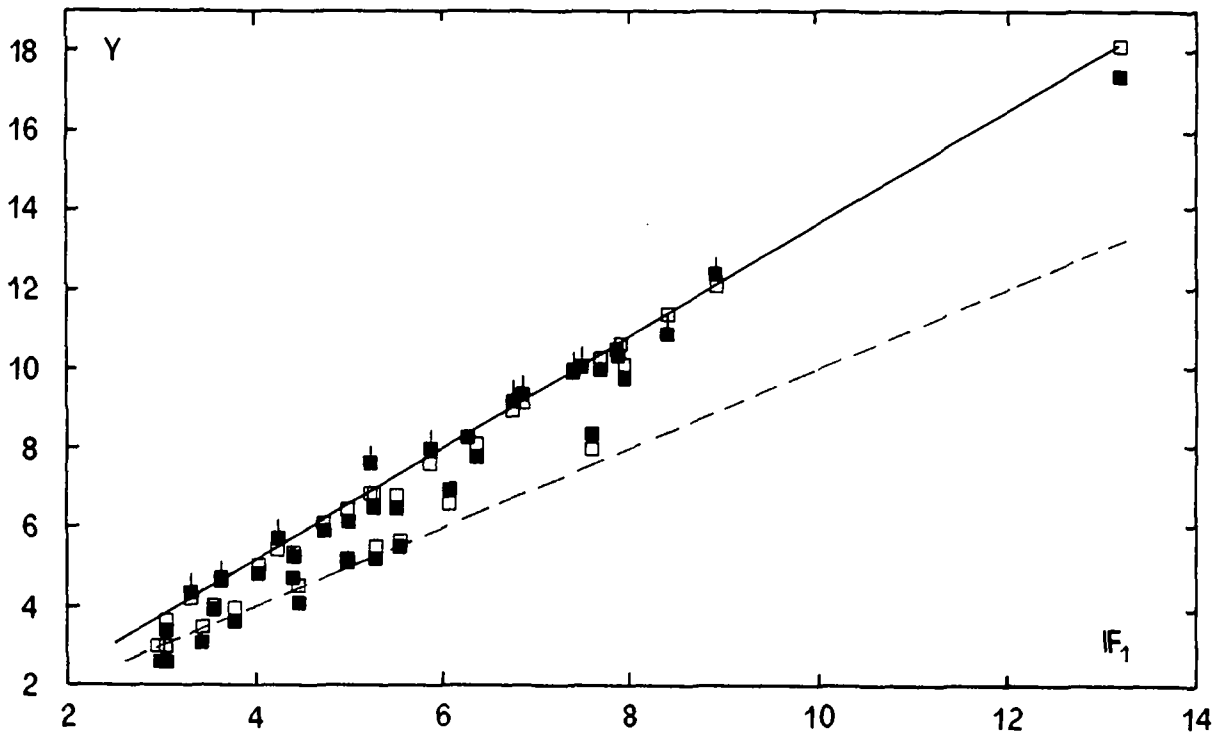


Fig. 5.19 : Experimental data of Unny (1963) ($B=2$) and comparison with Eq. (5.26). (■) Unny's data for $X_1 < 1.3$; (▮) Unny's data for $X_1 > 1.3$; (□) Computed with Eq. (5.26) (—) Sequent depths according to Bélanger. (---) Eq. (5.27).

Despite there exist significant deviations among the analytical approaches for S-jumps, the measurements of Unny are in fair general agreement with Eq. (5.26) because Eq. (5.26) accounts for the toe position relative to the expansion.

Remember that Unny considered all jumps for which $x_1 < 6.0\text{cm}$ as "S-jumps". Analyzing his experimental data shows that several runs were performed with $h_1 < 1.0\text{cm}$. Jumps with $x_1 \cong 6\text{cm}$ and small inflow depths differ considerably from the definition of S-jumps since they involve X_1 values deviating considerably from 0.

5.6.4 Herbrand's experimental investigation.

The experimental investigation of Herbrand was limited to S-jumps (paragraph 3.2.1), yet without indication of the toe position. Based on the analysis of his experimental data it could be assumed that the toe was located shortly upstream from the expansion section.

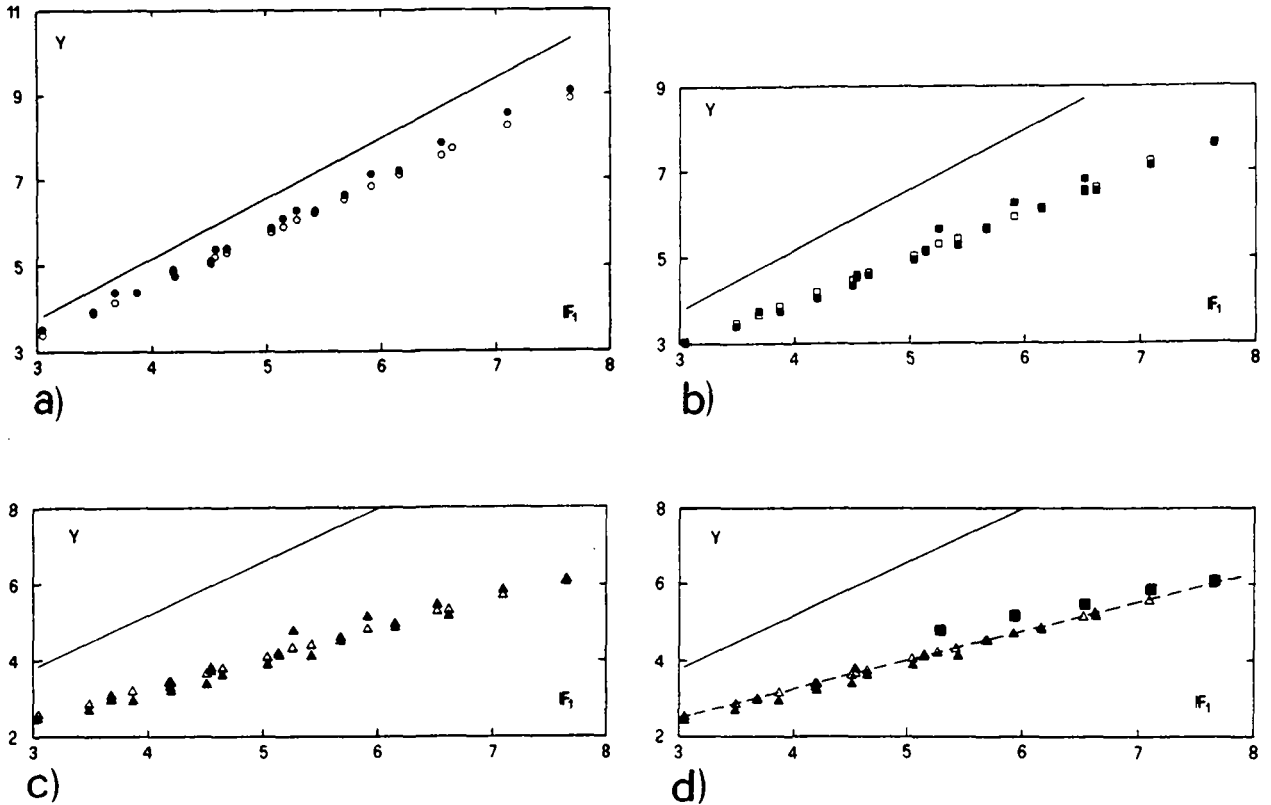


Fig. 5.20 : Comparison of Herbrand's experiments (full signs) with Eq. (5.26) (open signs). a) $B=1.5$ with $x_1=2\text{cm}$; b) $B=2.0$ with $x_1=2\text{cm}$; c) $B=3.47$ with $x_1=2\text{cm}$; and d) $B=3.47$ with $x_1=0$. (---) Eq. (5.27). (—) Sequent depths according to Eq. (5.1).

As his upstream channel was 16cm wide, an average toe position of $x_1=2.0\text{cm}$ could be assumed. In Fig. 5.20 Herbrand's data are compared with Eqs. (5.26) and 5.27). With some few exceptions, the experimental data agree reasonably well with the predictions. Significant deviations are observed for low inflow depths ($h_1 < 2.0\text{cm}$) and low inflow Froude numbers. Such flow conditions led to weak jumps for which an error in x_1 modifies considerably the value of X_1 .

Furthermore, as shown in Fig. 5.20d), the results of Eq. (5.27) are similar to those of Eq. (5.26) if $x_1=0.02\text{m}$. Therefore, the scatter of Herbrand's data should mainly be attributed to variations of the toe position. Indeed, as indicated by Herbrand himself, "the toe was located *approximately* at the expansion section". No sufficient attention

was paid to keep this position as constant as possible, or to retain x_1 as a basic experimental quantity for further analysis.

5.6.5 Experiments of Sethuraman and Padmanabhan

The purpose of the experimental study carried out by Sethuraman and Padmanabhan (1967) was to investigate the effect of an abrupt drop (step) on spatial hydraulic jumps. A few experiments, conducted in a horizontal channel (without step) will be presented in this paragraph.

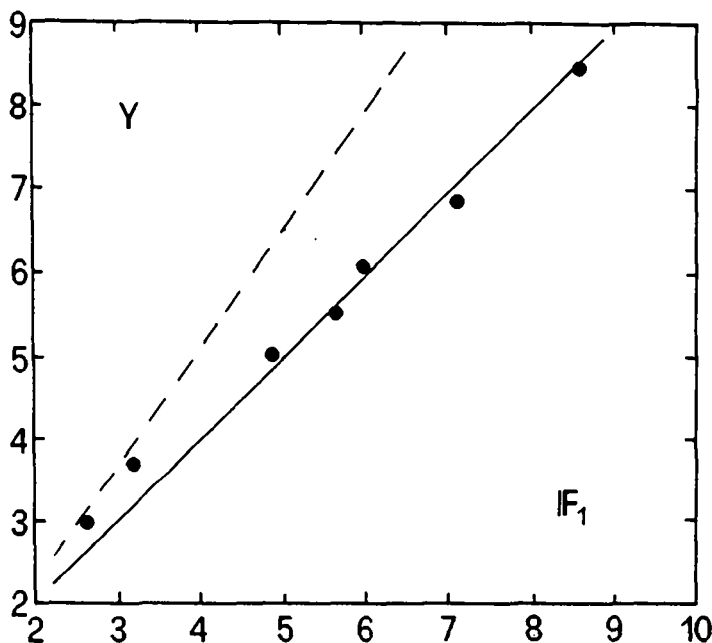


Fig. 5.21 : Comparison of the experiments by Sethuraman and Padmanabhan with (—) Eq. (5.27). $B=2$, $X_1=0$. (---) sequent depth ratio according to Bélanger's Eq. (5.1).

The experiments were limited to sudden expansions with an expansion ratio of $B=2$ (one side expansion). The rectangular inflowing channel was 30cm wide, whereas the width of the tailwater channel downstream from the expansion section attained 60cm. According to Sethuraman and Padmanabhan, the "tailwater is adjusted so as to form the jump at the expansion". As observed for other investigations, no record of the toe position relative to the expansion was retained. Since no indication of the inflowing depths is available, the estimation of the toe position parameter X_1 became difficult. Based on the figures and photographs published by the authors, it seemed reasonable to assume $X_1 \cong 0$. In Fig. 5.21, the experimental data of Sethuraman and Padmanabhan

are compared to Eq. (5.27). Except for very low inflowing Froude numbers, Fig. 5.21 shows a fair agreement between the predicted and the measured values.

5.6.6 Comments on present experiments

As outlined in previous paragraphs, two independent phenomena lead to deviations between the computational model and the experimental data. The first is related to frictional effects (paragraph 5.4.2) which become significant for low values of X_1 . Furthermore, as for classical jumps, the frictional force increases both with increasing inflow Froude number and decreasing inflow depth. The measured sequent depths ratio Y_{ex} is smaller than the ratio according to a conventional momentum approach, therefore.

The second phenomenon is related to the experimental determination of X_1 . For jumps with small h_1 , the toe fluctuations lead to significant scatter in X_1 . Since Eq. (5.26) includes X_1 , the error is transferred to the comparison between Y_{ex} and Y_p .

Fig. 5.22a) compares the experimental data for an expansion ratio $B=5$ (series 1.1) with the prediction according to Eq. (5.26). As indicated in this figure, the scatter of the ratio Y_{ex}/Y_p becomes significant for low values of X_1 (typically $X_1 < 0.3$). As previously discussed, this poor agreement may mainly be attributed to the experimental error involved in the measurement of small values of X_1 .

In order to illustrate the influence of the frictional effects on the sequent depths, in Fig. 5.22b) the measured values Y_{ex} are compared to Y_m according to Eq. (5.8). As indicated in paragraph 5.4, Eq (5.8) involves no frictional forces. Deviations between Y_m and Y_{ex} may therefore be attributed to frictional effects as well as measurement errors. As outlined in this figure, the difference between Y_{ex} and Y_m becomes significant only for $X_1 < 0.3$. As previously mentioned, frictional effects may therefore be neglected provided $X_1 > 0.2$.

The agreement of the present model with observations reported in the literature is fair provided the toe position is accounted for and the effect of wall friction is small.

Since the computational model does not account for frictional forces, some deviations between predictions and the prototype flow depths may occur. Frictional forces are not included in the similitude law according to Froude. The result is a scale effect between scale models and prototypes of stilling basins.

Investigations conducted by Hager and Bremen (1989) in smooth prismatic rectangular channels revealed that the reduction of the sequent depths ratio due to

friction is usually smaller than 5% if the unit discharge Q/b_1 is larger than $0.1\text{m}^2\text{s}^{-1}$ and $F_1 < 12$. However, in case of large expansion ratios ($B > 3$) and small values of X_1 ($X_1 < 0.2$), this reduction may be larger. The increased air entrainment observed for prototypes compared to scale models, does not influence the sequent depth ratio.

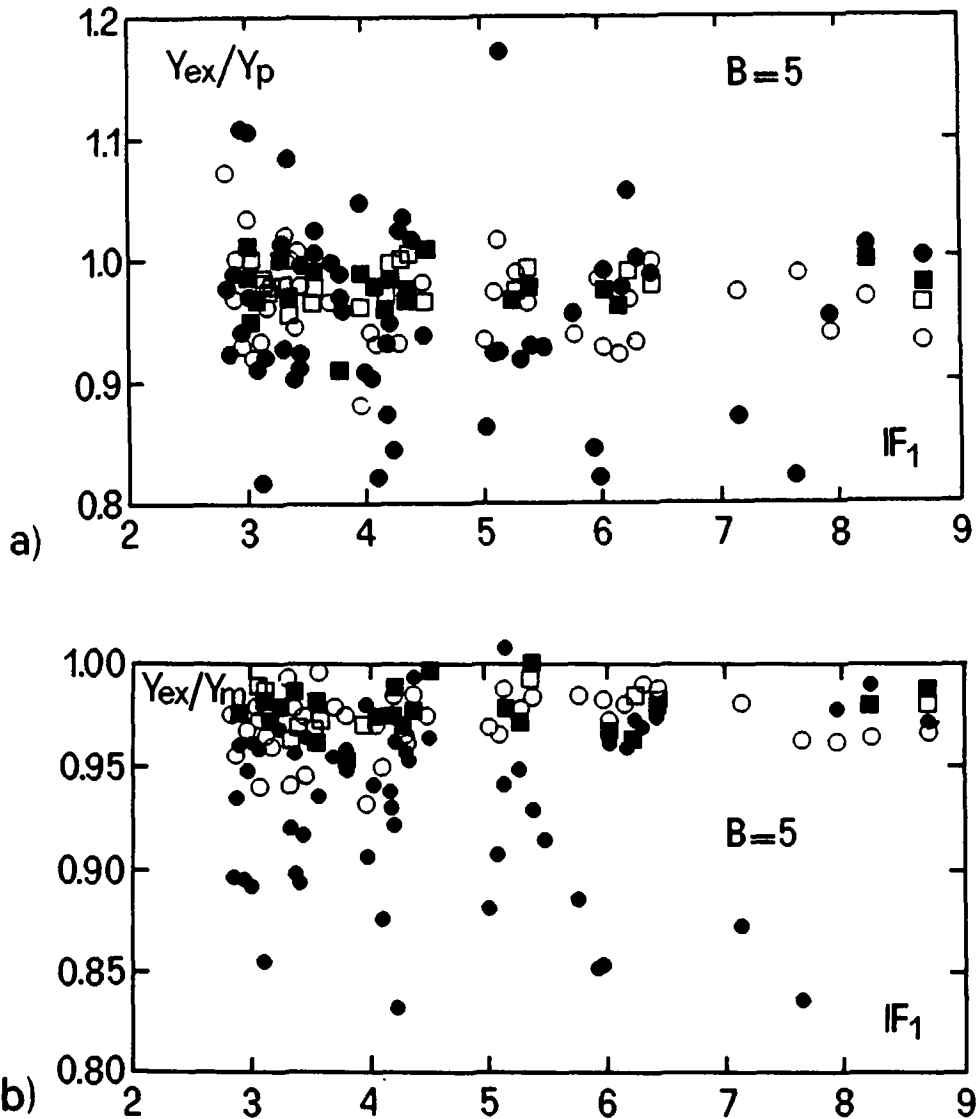


Fig. 5.22 : Effect of friction and experimental errors for series 1.1.

- a) Ratio Y_{ex}/Y_p (Y_p according to Eq. (5.26) as function of F_1 for various domains of X_1 . b) Ratio Y_{ex}/Y_m (Y_m according to Eq. (5.4) as function of F_1 for various domains of X_1 . (\square) $X_1 > 1.0$; (\blacksquare) $0.6 < X_1 \leq 1.0$; (\circ) $0.3 < X_1 \leq 0.6$; (\bullet) $X_1 \leq 0.3$.

Since the air density is only a small fraction of the water density the momentum contribution of the entrained air remains small.

The domain of application of the present model equations is limited to expansion ratios $B \leq 10$, Froude numbers $F_1 < 12$, toe positions $X_1 > 0.05$ and inflow depths larger than 20mm.

5.7 LENGTH OF TRANSITIONAL JUMP

5.7.1 Introduction

The definition of the jump end section adopted for the present experimental investigation was given in paragraph 5.2. The position of this section is defined by the coordinate x_j with the origin at the channel expansion section (Fig. 5.2). The experimental jump length $L_{j,ex}$ is then obtained by adding x_j to x_1 .

The main difficulties encountered in the experimental evaluation of $L_{j,ex}$ may be attributed to

- the jump asymmetry,
- the toe fluctuations,
- the turbulent and pulsating flow phenomena, and
- tailwater wave action.

In order to reduce the scatter of the experimental data, the jump end section was measured for each flow condition by two approaches. To visualize the jump end section a point gauge carried by a trolley (chapter 4) turned out to be a simple but effective means.

The first measure was performed with the trolley located downstream from the jump end section. From this position the point gauge was shifted upstream until the eye indicated the time-averaged end section. The second measure was performed with the trolley's initial position upstream from the jump end. The average value x_j of the two observations was then retained. The same measurement technique was adopted to evaluate the average toe position x_1 . Yet, the data scattered considerably, especially for small tailwater levels and pronounced asymmetric flow.

In order to normalize the experimental data, an appropriate scaling length was sought. Since reference was made to the prismatic channel geometry for the other non-dimensional parameters (X_1, ψ), the jump length L_j in sudden expanding channels was also normalized by the jump length L_j^* . The jump length in prismatic rectangular channel L_j^* was defined in paragraph 5.2 and may be expressed by Eq. (5.5).

5.7.2 Experimental investigation

Qualitative observations of the jump characteristics (Fig. 5.3) in sudden expansions reveal an effect of X_1 on the jump length. Furthermore one could observe a reduction of the jump length for overall symmetric flow conditions. The length of jump thus increases with the degree of asymmetry, that is with increasing B and decreasing X_1 .

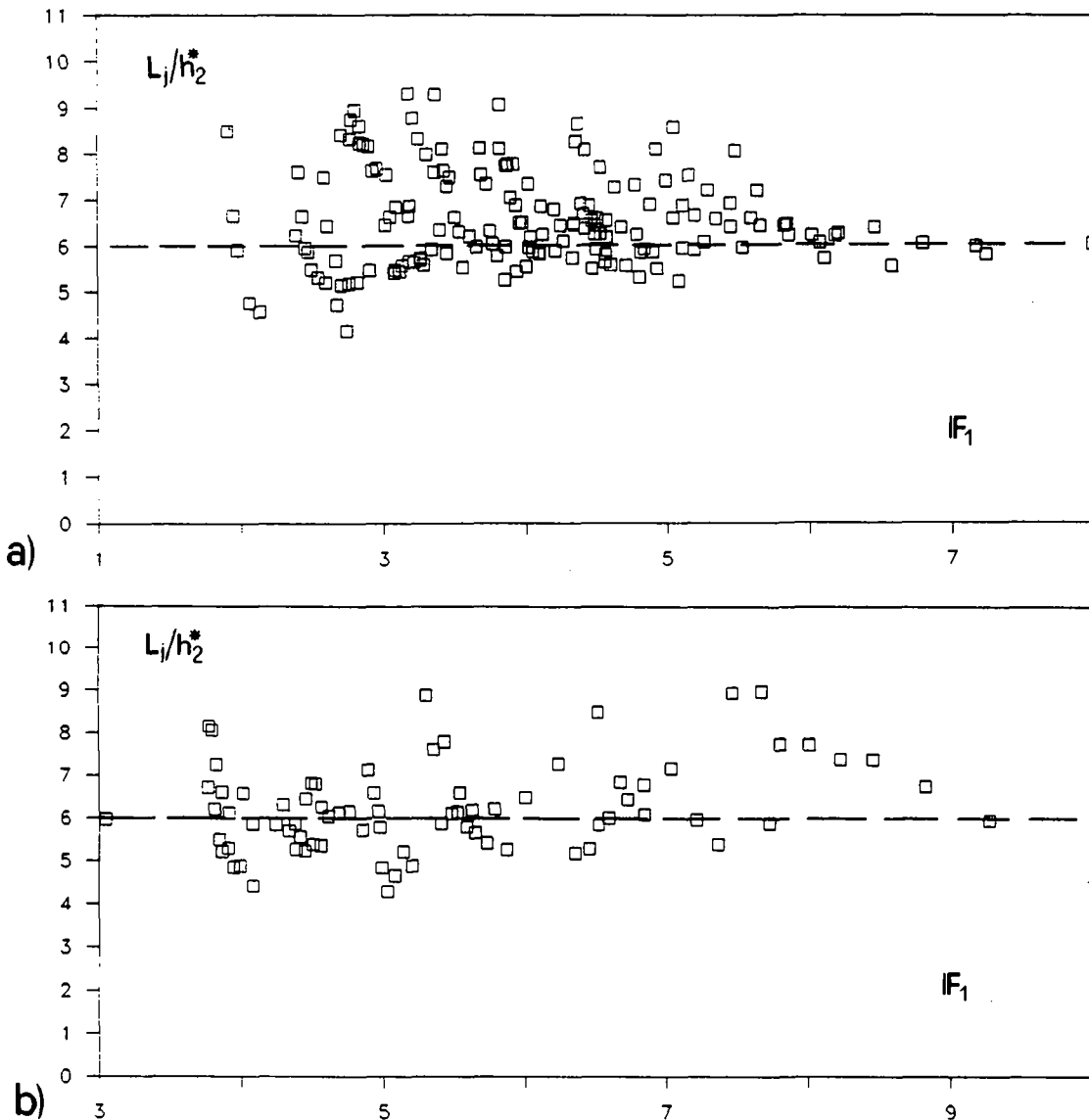


Fig. 5.23 : Relative length of hydraulic jump L_j/h_2^* versus F_1 .

a) $B=3$ (series 1.3) and b) $B=1.5$ (series 1.5). (---) $L_j/h_2^*=6$ Peterka 1983).

For prismatic channels, the ratio L_j/h_2^* depends on F_1 only if $F_1 < 4$ and is constant at $L_j/h_2^*=6$ otherwise (Peterka, 1983). A similar behaviour could be observed for sudden expansions. In Fig. 5.23 the ratio $L_{j,ex}/h_2^*$ is plotted against F_1 for the

expansion ratio $B=3$ (Series 1.3) and $B=1.5$ (Series 1.5) from where no significant effect of F_1 on the length of jump is seen.

Fig. 5.24 relates to the same data as Fig. 5.23. It outlines the significant increase in the length of jump for small values of X_1 . Furthermore, when considering identical values of X_1 , the jump length increases with B provided $X_1 < 0.5$.

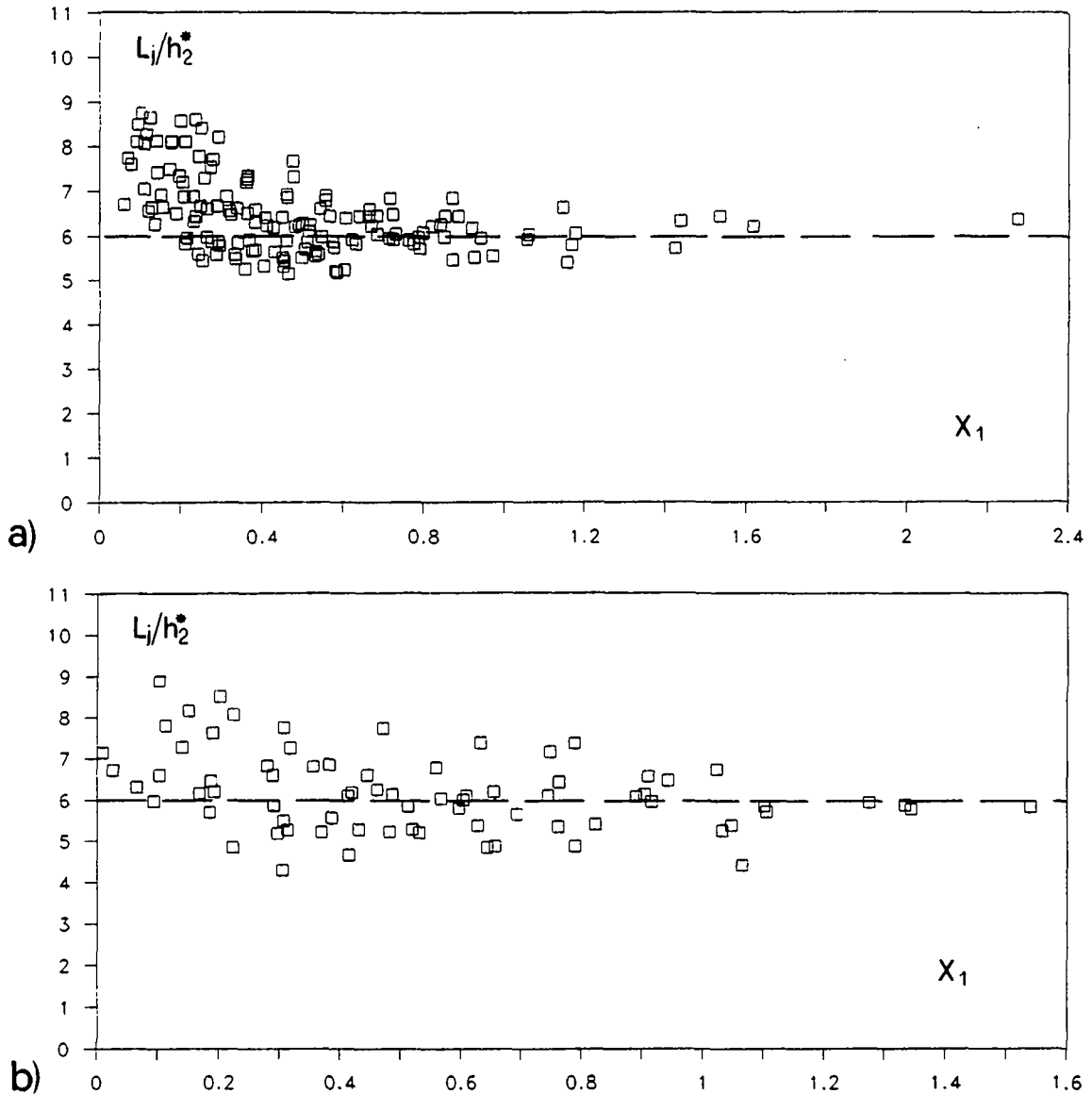


Fig. 5.24 : Relative length of hydraulic jump L_j/h_2^* versus X_1 . a) $B=3$ (series 1.5) and b) $B=1.5$ (series 1.3). (---) $L_j^*/h_2=6$ (Peterka 1983).

Beyond a limit value of X_1 , which depends on the expansion ratio B , the jump length becomes nearly equivalent to the jump length observed in prismatic channels. Despite

a significant scatter of the data in the domain of small X_1 , the ratio L_j/L_j^* increases as X_1 decreases. For $X_1 \rightarrow 0$ deviations up to 50 % were recorded. As discussed in paragraph 5.4 in connection with the sequent depths ratio, frictional effects are then the main reason of the data scatter. To exclude scale effects from the computational model, frictional forces will not be included in the computations, however.

5.7.3 Computational model

Fig. 5.25 shows the ratio L_j/L_j^* as a function of X_1 for the expansion ratio $B=3$. The analysis of the experimental data shows no systematic influence of the inflowing Froude number. Therefore, to predict the jump length in sudden expansions, the expansion ratio B and the toe position parameter X_1 should only be considered.

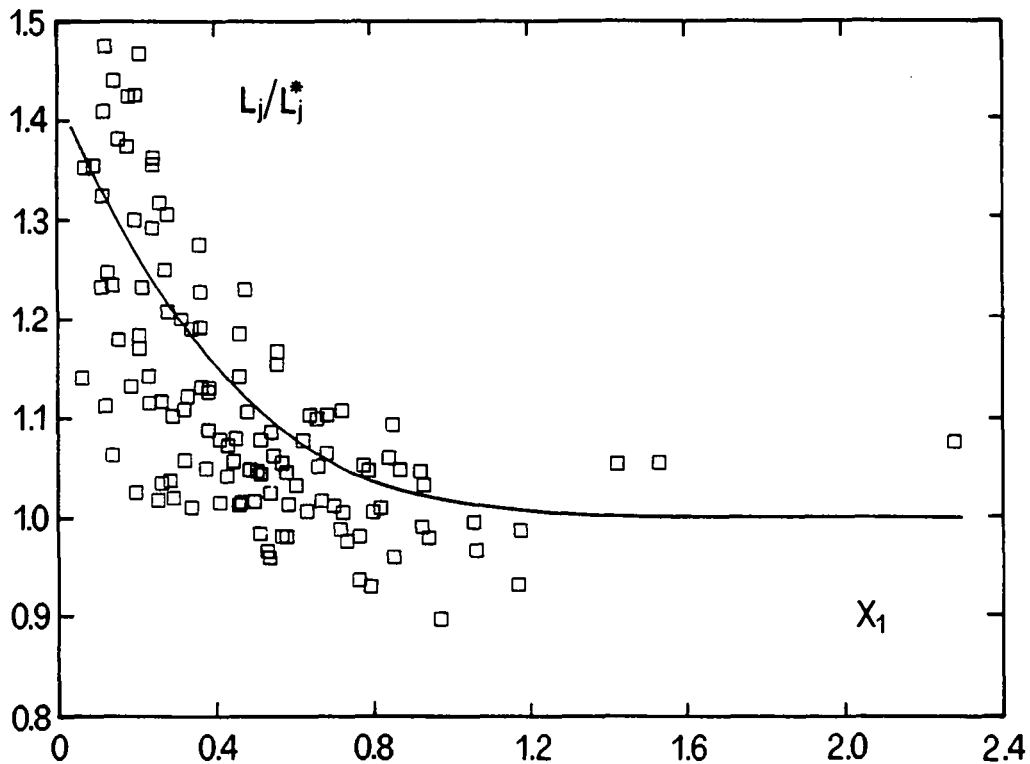


Fig. 5.25 : L_j/L_j^* as function of the toe position parameter X_1 for $B=3$.
(—) Prediction according to Eq. (5.38).

Two limit conditions should be satisfied by the computational model. First, for $B=1$, the condition $L_j=L_j^*$ must be satisfied for any value of X_1 . Second, for $X_1 \geq 1.3$ the identity $L_j \cong L_j^*$ holds for any expansion ratio B . Based on these conditions and on the data collected, the analogy to the sequent depth ratio was observed. Indeed, the length of hydraulic jumps in sudden expansions may be expressed as

$$\frac{L_j}{L_j^*} = 1 + \left(1 - \frac{1}{\sqrt{B}}\right) \cdot [1 - \text{th}(1.9X_1)] \quad (5.39)_1$$

or equally

$$\frac{L_j}{L_j^*} = 1 + \psi \quad (5.39)_2$$

in which L_j^* is the jump length in prismatic channels according to Eq. (5.5). Since, for small values of X_1 , the bottom friction influences the jump pattern, Eq. (5.39) should not be used in the domain $X_1 < 0.1$. Due to the significant friction forces involved in this domain, scale effect would be introduced when transforming the present model results to prototype structures.

The length of jump in a sudden expansion is larger, or at least equal to the length in the prismatic channel. Both length of jump and sequent depth ratio are governed by the same functional expression ψ according to Eq. (5.26).

The numerical example in paragraph 5.9 shows an application of Eq. (5.39).

5.8 SYMMETRY OF JUMP

Hydraulic jumps located in sudden expansions are characterized by an asymmetric flow, as shown in Fig. 5.3. The purpose of this paragraph is not to investigate in detail the origin of the asymmetry but to present a criterion for the estimation of the asymmetry of jump.

A strictly symmetric flow occurred only during a short time until a small perturbation shifted the main flow along the right or left channel side walls. For a wide range of X_1 , the asymmetric flow is then stable without any transverse oscillation. As X_1 approaches 1, the jump is characterized by frequent oscillations of the main stream. For $X_1 > 1.2-1.3$, that is if the jump is entirely in the approaching channel portion, it becomes overall symmetric and free of oscillations.

A qualitative evaluation of the jump asymmetry seems to be difficult. However, asymmetric jumps are characterized by different flow depths along the right and the left expansion side walls. The measurement of this difference in flow depth seems to be the most effective means to analyse the jump asymmetry.

Let the parameter of jump asymmetry ΔY_a be defined as

$$\Delta Y_a = 2 \left[\frac{h_{a,\max} - h_{a,\min}}{h_{a,\max} + h_{a,\min}} \right] \quad (5.40)$$

in which $h_{a,\max}$ and $h_{a,\min}$ are, respectively, the maximum and minimum depths measured along each expansion side wall.

For symmetric channel geometries (series 1.3 and series 1.6) the flow depths of the lateral eddies were recorded at two points of each channel side (Fig. 5.2). For ΔY_a smaller than 3% the jump may be considered practically symmetric. This limit accounts for the difficulty of depth recording during wave generation.

Fig. 5.26 shows a fair agreement between the measurements in channels LCH1 and LCH2 despite the difficulties of measurement. Considering the previous limit condition for symmetric flow, Fig. 5.26 indicates that the flow is asymmetric for $X_1 < 0.7$. In other words, only if 70% of the jump are located upstream from the expansion section symmetric jumps could be expected. ΔY_a increases then rapidly with decreasing X_1 and attains nearly $\Delta Y_a = 50\%$ for $X_1 \approx 0$.

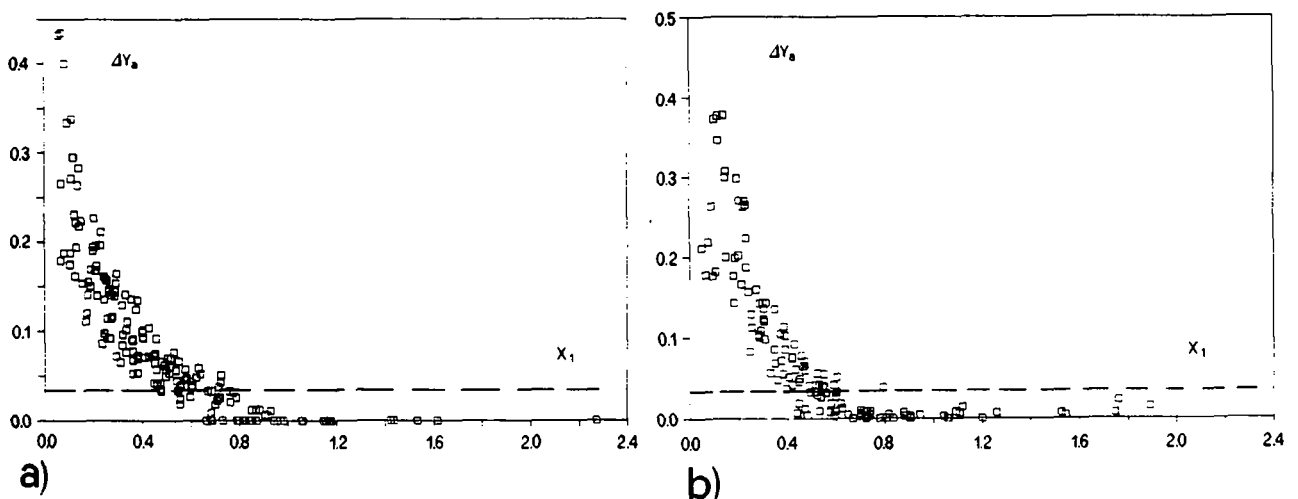


Fig. 5.26 : Parameter of jump asymmetry ΔY_a as a function of X_1 for a) Series 1.3 (LCH1) and b) series 1.6 (LCH2) (See Table 5.1)
(---) $\Delta Y_a = 3\%$.

As indicated in Fig. 5.26, the limit position for which symmetric flow prevail depends only on the channel expansion ratio B . Therefore, to establish the limit position for different expansion ratios, only a few experiments are needed for each channel geometry. Based on some additional experiments conducted for $B=1.5$ and $B=2$ (symmetric geometries) the limit for the appearance of symmetric flow could be

established. Fig. 5.27 shows the connection of these points as a dashed curve. Below this curve the flow is always symmetric (domain ①). This domain may be expressed as

$$\psi = (1/8)[1-(2/3) X_1] \quad (5.41)$$

or equally

$$B_{1/2} = \left[\frac{1}{1 - \frac{(1/8)[1-(2/3) X_1]}{1-\text{th}(1.9 X_1)}} \right]^2 \text{ provided } 0 \leq X_1 \leq 1. \quad (5.42)$$

It is interesting to note that the three points measured and the point $\psi(X_1=1)=0.043$ for $B \rightarrow \infty$ which delimitate domain ① define a straight. For $B \leq B_{1/2}$ the hydraulic jump in the channel expansion is symmetric. Table 5.2 indicates the limit toe positions $X_{1/2}$ as function of B for which symmetric jumps prevail.

If $B > B_{1/2}$ the hydraulic jump is asymmetric. In order to evaluate the "degree" of flow asymmetry a second domain ③ was defined. This domain, for which $\Delta Y_a > 0.2$, includes strongly asymmetric jumps, involving a small lateral expansion of the inflowing stream and significant tailwater wave action. For both expansion ratios $B=3$ and $B=2$ investigated the condition $\Delta Y_a > 0.2$ was satisfied approximately for $\psi > 0.28$ which may also be expressed as

$$B_{2/3} = \left[\frac{1}{1 - \frac{0.28}{1-\text{th}(1.9 X_1)}} \right]^2. \quad (5.43)$$

For $B_{1/2} < B < B_{2/3}$, the hydraulic jump is included in domain ② indicated in Fig. (5.27). In this domain, the hydraulic jump is asymmetric, but its overall patterns are improved in comparison to jumps of the domain ③. An example of an hydraulic jump of domain ② is shown in Fig. 5.5b).

In Table 5.2 the limit toe positions for the three flow domains considered are indicated for various expansions ratios B .

The symmetry of jump depends mainly on the expansion ratio B and the toe position X_1 . No discernible effect of F_1 may be evaluated. Eq. (5.42) and (5.43) may be used to estimate the "degree" of jump asymmetry.

Table 5.2 : Limit toe positions for various expansion ratios B according to Eq. (5.42) and Eq. (5.43).

Expansion ratio B	1.5	2	3	5	10
① symmetric	$X_1 > 0.24$	$X_1 > 0.46$	$X_1 > 0.62$	$X_1 > 0.74$	$X_1 > 0.84$
② slightly asymmetric	$X_1 < 0.24$	$0.03X_1 < 0.46$	$0.19 < X_1 < 0.62$	$0.28X_1 < 0.74$	$0.362X_1 < 0.84$
③ strongly asymmetric	$X_1 < 0$	$X_1 < 0.03$	$X_1 < 0.19$	$X_1 < 0.28$	$X_1 < 0.36$

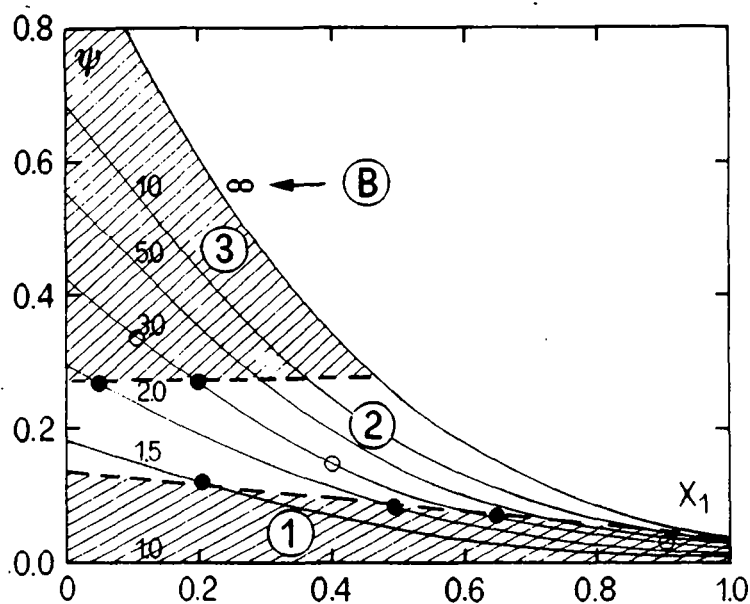


Fig. 5.27 : Jump asymmetry in sudden expansion. Domain of ① symmetric flow, ③ strong asymmetric flow and ② limited asymmetric flow for sudden expansions. (•) Observational points (---) Eq. (5.41). (○) toe positions according to Fig. 5.5.

Based on the considerations regarding the energy dissipation (paragraph 5.5.6), efficient jumps in non-prismatic channels should have values X_1 as small as possible. However, such flows lead to asymmetric jumps, except for small expansion ratios.

For the design of non-prismatic stilling basins, the asymmetric flow pattern cannot be considered effective in terms of length of jump. Therefore the non-prismatic channel geometry as considered in this chapter must normally be excluded as effective energy dissipator. Particular attention must be paid to other effective devices by which the overall flow symmetry is significantly improved. Chapters 7 and 8 contain such propositions.

Based on considerations including energy dissipation, length of jump and asymmetry, the hydraulic jump in an expanding channel without appurtenances cannot be regarded as overall effective.

5.9 Numerical example

The purpose of this example is to show how the results and the computational model developed in this chapter may be used to predict the jump characteristics in sudden expansions. The same example presented hereafter will be reconsidered in the next chapter.

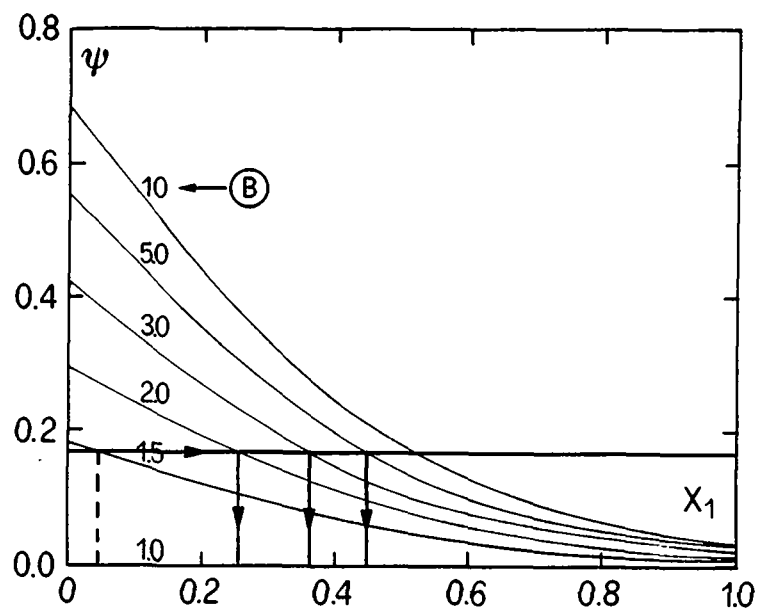


Fig. 5.28 : Numerical example : values of X_1 for $\psi=0.17$ at expansion ratios $B=2, 3$ and 5 according to Fig. 5.12.

Consider an approaching channel 10 m wide with an approaching flow depth $h_1=1.2$ m and an inflow velocity $V_1=25$ m/s. The tailwater is $h_2=10.0$ m. Calculate

the influence of the expansion ratio B on the toe position X_1 , as well as on the required stilling basin volume.

The inflowing Froude number is $F_1=25/(9.81 \cdot 1.2)^{0.5}=7.29$. The sequent depths ratio according to Bélanger (Eq. 5.1) is $Y^*=0.5[(1+8 \cdot (7.29)^2)^{0.5}-1]=9.82$. The required tailwater level for a hydraulic jump in a prismatic rectangular channel thus amounts to $h_2^*=9.82 \cdot 1.2=11.8$ m. h_2^* exceeds by 1.8 m the tailwater level required.

The difference in tailwater may be overcome by a non-prismatic stilling basin. Since the inflow conditions F_1 and h_1 as well as the tailwater level are defined, ψ becomes $\psi=(1-8.33/9.82)/(1-1/9.82)=0.17$. It should be outlined that ψ is independent from X_1 and B . In Fig. 5.28, the toe positions X_1 corresponding to the expansion ratios $B=2, 3$ and 5 for $\psi=0.17$ are indicated. Fig. 5.28 shows clearly the effect of the expansion ratio B on the jump characteristics when a constant sequent depths ratio is considered. For an expansion of $B=2$, the toe would be located at $X_1=0.25$ whereas for the same sequent depths ratio and identical inflow conditions, the toe position parameter becomes $X_1=0.45$ if $B=5$.

Table 5.3 shows the main characteristics of the jumps for different expansion ratios B . Therein, the jump length L_j was computed with Eq. (5.39) and the required volume was estimated with Eq. (5.37).

Table 5.3 : Main characteristics of hydraulic jumps in sudden expansions for different expansion ratios B and identical inflow conditions F_1 , h_1 and tailwater level $h_2=10.0$ m.

Expansion Ratio	Y	$x_1=X_1 \cdot L_r^*$	L_j	V_j
[-]	[-]	[m]	[m]	[m ³]
B=1	9.82	---	73.5	8'660
B=2	8.33	12.70	86.0	12'990
B=3	8.33	18.30	86.0	17'320
B=5	8.33	22.80	86.0	25'980

As shown in Table 5.3 the required volume of stilling basin increases rapidly when large expansion ratios are considered. In order to select one stilling basin geometry, an additional condition on X_1 becomes necessary. Therefore, in the forthcoming chapters, particular attention will be paid to devices improving the flow pattern for

low values of X_1 . Small values of X_1 (typically $X_1 < 0.4$) could be considered for the design of sudden expanding basins only if symmetrical flow may be generated. Fig. 5.29 shows the three geometries considered in the numerical example with the respective jump position relative to the expansion section.

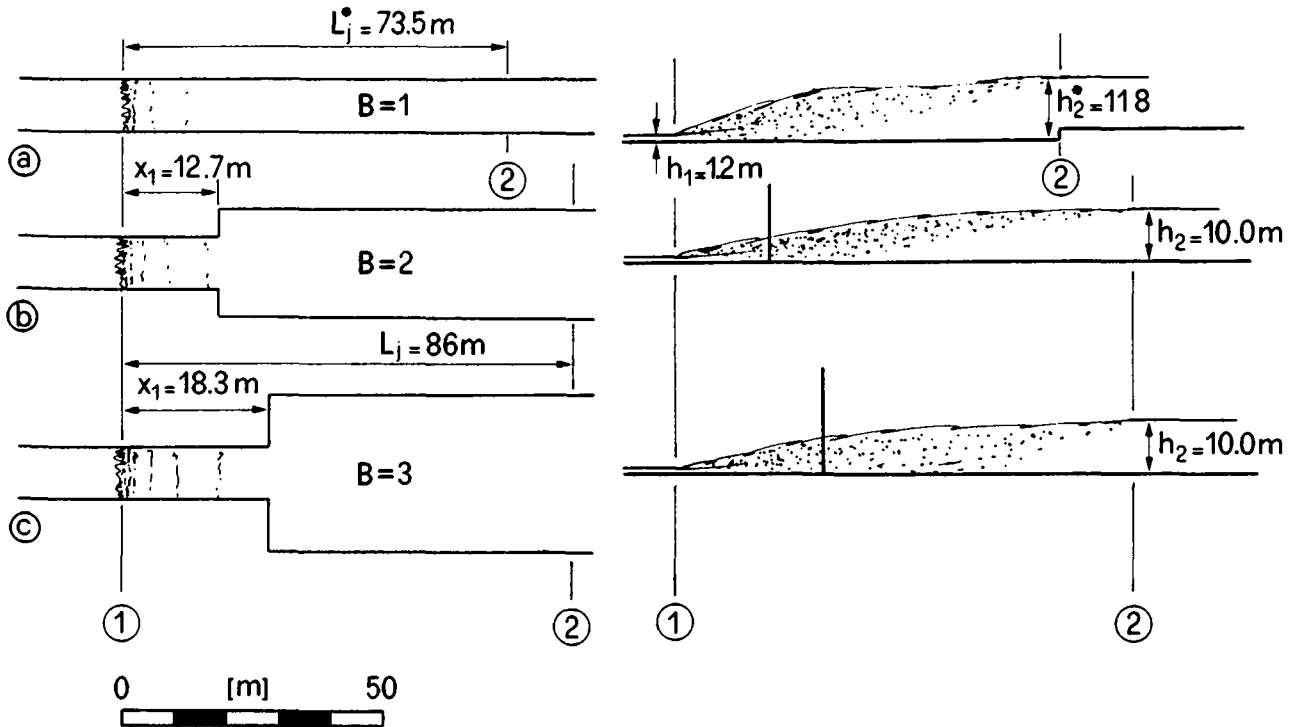


Fig. 5.29 : Numerical example : comparison of three channel geometries with the respective jump locations relative to the expansion section. ① jump toe, ② jump end section. a) prismatic channel; b) sudden expansion $B=2$; c) sudden expansion $B=3$. $h_1=1.2\text{ m}$, $h_2=10.0\text{ m}$, $h_2^*=11.8\text{ m}$, $L_j=86.0\text{ m}$, $L_j^*=73.5\text{ m}$.

5.10 CONCLUSIONS

The flow pattern of hydraulic jumps in sudden horizontal expansions depends on the expansion ratio B , the toe position X_1 relative to the expansion section as well as on the inflow conditions F_1 and h_1 .

A conventional momentum approach can successfully be applied to sudden expansions provided wall friction may be neglected. In order to predict the sequent depths ratio and the average flow depth along the expansion side walls an additional equation was established. It is essentially based on experiments conducted in six different channel geometries and involves some 1200 experimental runs. A comparison of the

computational model developed with the experimental investigations of Unny, Herbrand and Sethuraman and Padmanabhan shows a fair agreement. Deviations between the measured and the predicted values may be attributed mainly to the neglect of frictional forces as well as to experimental inaccuracies.

The equations were then used to predict the rate of energy dissipation, the required volume of jump, and the energy dissipation per unit volume. Despite the increase in efficiency, the energy dissipation per unit volume is always smaller in sudden expanding channels than in the prismatic channel. A simplified equation for the required volume in sudden expanding channels with vertical side walls was also established. Based on the experimental data an equation for the jump length in sudden expanding channels was presented. Except for relatively small values of toe position (typically $X_1 < 0.4$) the lengths of jumps in sudden expansions and prismatic channels are comparable.

The phenomenon of asymmetry presented in chapter 2 was investigated quantitatively in paragraph 5.8. Therein the difference of flow depths along the right and left expansion side walls may be used as a degree of the jump asymmetry. Based on this approach asymmetric flow may be attributed to a wide range of toe positions X_1 . The limit value of toe position parameter X_1 for symmetric flow to appear depends essentially on the expansion ratio B .

Finally, the computational procedure was presented in a numerical example. The effect of the expansion ratio on the sequent depths, the jump position and on the required volume of stilling basin were discussed.

6. EFFECT OF NEGATIVE STEP

6.1 INTRODUCTION

In chapter 5 sudden expansions in a channel with vertical side walls and a horizontal bottom were investigated. Therein, the channel geometry could be described entirely by the expansion ratio B . The flow pattern observed for such geometries depends on the inflow conditions F_1 , h_1 , on the toe position relative to the expansion X_1 , and on the expansion ratio B . However, over a wide range of toe positions X_1 and expansion ratios B , the flow is asymmetric.

In order to avoid or reduce this flow asymmetry, the effect of a negative step located at the expansion section will be investigated in this chapter. The step might correspond to a device improving the flow pattern since the cavity below the inflowing jet connects the eddy currents in the corners of the expansion. Based on the results of chapter 5, the asymmetry of the jump was found to be closely related to a difference of flow depth between these two eddies. The presence of an abrupt step at the expansion section could thus greatly improve the performance of the jump. With exception of the investigation of Sethuraman and Padmanabhan (1967), and considerations of Rouse et al. (1951) no systematic investigation on such geometry seems to have been published.

The purpose of this chapter is to develop a computational model for the jump in an abruptly expanding channel with the step on one hand, and to investigate its performance as regards the jump symmetry on the other hand.

After a short description of the experimental investigation in paragraph 6.2, the applicability of a conventional momentum approach is verified by the experimental data. In paragraph 6.3 the sequent depth relation established in chapter 5 is modified to include the step. The discrepancy between predicted and experimental values is analyzed.

The equation for the jump length L_j developed in paragraph 5.7 is compared to the experimental results obtained for sudden expansions with a negative step in paragraph 6.5. Finally, the jump symmetry is considered qualitatively in paragraph 6.6, and compared to the flow pattern as observed in the preceding chapter.

In paragraph 6.7, a numerical example shows how the computational model can be used to predict the main jump characteristics. Since the same data are used as in paragraph 5.9, the effects of a negative step on the jump pattern are outlined.

6.2 DESCRIPTION OF EXPERIMENTS

The experiments were carried out in the installation LCH1 which was extensively described in paragraphs 4.2 and 4.3. The main characteristics of three series of experiments to be presented in Table 6.1. Two asymmetric and one symmetric channel were investigated. Furthermore, the downstream channel width b_2 (column 2), the expansion ratio B (column 3) as well as the domains of F_1 and $N=s/h_1$ (columns 4 and 5) are indicated.

All experiments were carried out with a vertical step ($s=2.5\text{cm}$), located at the expansion section. For each series, four to five different inflow depths h_1 , and an average of ten different toe locations relative to the expansion section were selected. The number of runs conducted for each series is indicated in column 6.

Due to frictional effects on the inflowing depth h_1 , it was impossible to keep F_1 and N constant for one gate opening and different toe positions (paragraph 4.7). Fig. 6.1 shows the relevant notation and the quantities measured. The measurement techniques and the expected deviations were described in detail in paragraph 5.2. The experimental data are listed in Appendix 3. Except for the parameters related to the step, the notation is identical to that of Appendix 2.

The reference level considered for depth measurement is identical to the channel bottom. At the expansion section the channel bottom downstream from the expansion has been considered as reference level. This choice allows use of the same non-dimensional parameters as in chapter 5.

Table 6.1 : Sudden expansion with negative steps. Overall characteristics of experiments.

Series	b_2	B	shape	F_1		$N=s/h_1$		No of runs
				from	to	from	to	
2.1	0.5	1.5	asym.	3.20	8.43	0.61	1.64	105
2.2	0.5	2	asym.	2.68	8.12	0.59	1.61	112
2.3	0.5	3	sym.	2.05	7.37	0.49	1.66	129

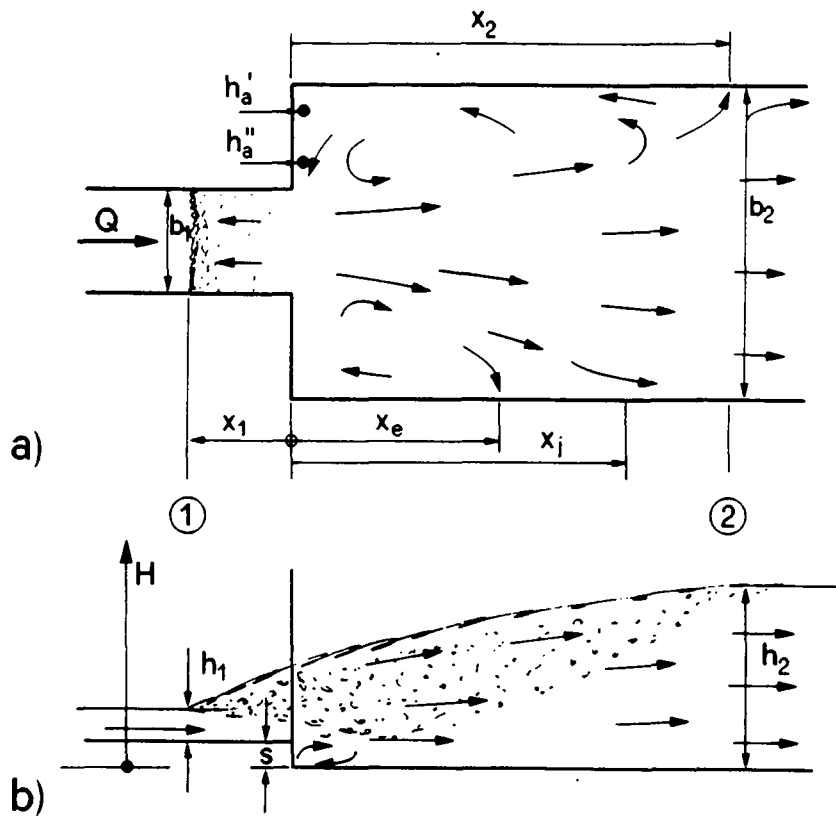


Fig. 6.1 : Notation and quantities measured for sudden expansion with negative step. a) plan view; b) axial section, with arrows indicating surface stream.

6.3 CONVENTIONAL MOMENTUM APPROACH

In chapter 5 it was verified that the assumptions involved in a conventional momentum approach could be adopted for hydraulic jumps in sudden expansions if the sequent depth h_2 is measured at the downstream end of the longer lateral eddy (Fig. 5.2). In the case of significant asymmetric flow, the distance between the toe and the end sections becomes large, and leads to an increase of the frictional forces involved. As concluded in chapter 5, a conventional momentum approach is in fair agreement with the experiments provided $X_1 > 0.2$.

For sudden expansions with negative steps, the streamwise pressure force component on the step face has to be included in the momentum approach. The momentum approach is based on the following assumptions (Fig. 6.2) :

1. hydrostatic pressure distribution.
2. horizontal channel bottom.
3. pressure on step face equivalent to the flow depth h_a along the expansion side walls.
4. frictional forces are neglected.

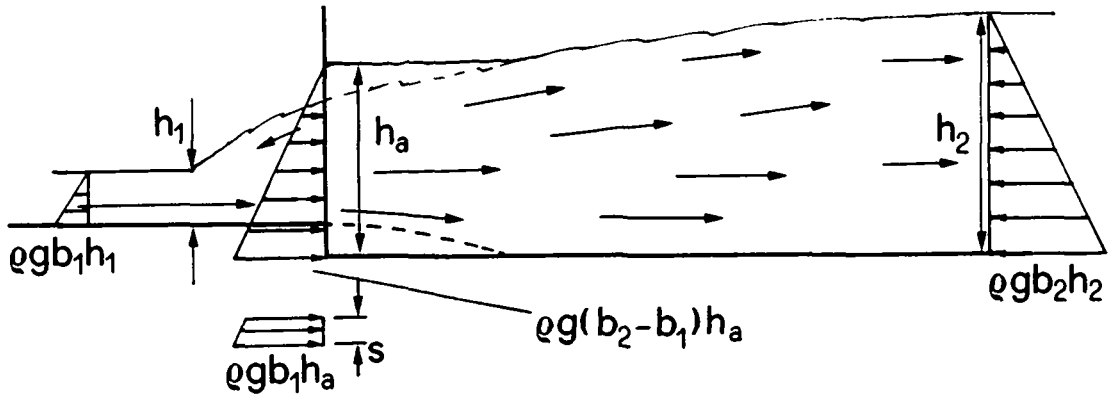


Fig. 6.2 : Conventional momentum approach applied to a sudden expansion with negative step. Pressure distribution considered.

Then the momentum equation for a rectangular channel section may be expressed as

$$\frac{b_1 h_1^2}{2} + (b_2 - b_1) \frac{h_a^2}{2} + s b_1 \left(h_a - \frac{s}{2} \right) + \frac{Q^2}{g b_1 h_1} = \frac{b_2 h_2^2}{2} + \frac{Q^2}{g b_2 h_2} \quad (6.1)$$

Using the continuity equation and introducing the usual parameters

$$Y_N = h_2/h_1 \quad , \quad Y_a = h_a/h_1 \quad , \quad B = b_2/b_1 \quad ,$$

$$F_1^2 = \frac{V_1^2}{g h_1} \quad \text{and} \quad N = s/h_1 \quad (6.2)$$

yields

$$1 + (B-1) Y_a^2 + N (2Y_a - N) + 2F_1^2 = B Y_N^2 + \frac{2F_1^2}{B Y_N} \quad (6.3)$$

Note that Y was modified to Y_s to indicate the presence of the step. Eq. (6.3) could also be written as

$$Y_N^3 - \frac{Y_N}{B} \left[1 - Y_a^2 + B Y_a^2 + 2F_1^2 + N (2Y_a - N) \right] + \frac{2F_1^2}{B^2} = 0 \quad (6.4)$$

on the overall jump characteristics is documented. Therein the inflow conditions as well as X_1 and B were kept constant. To keep X_1 constant in both channel configurations, the tailwater level in Fig. 6.4b) (with step) is higher than the level without step.

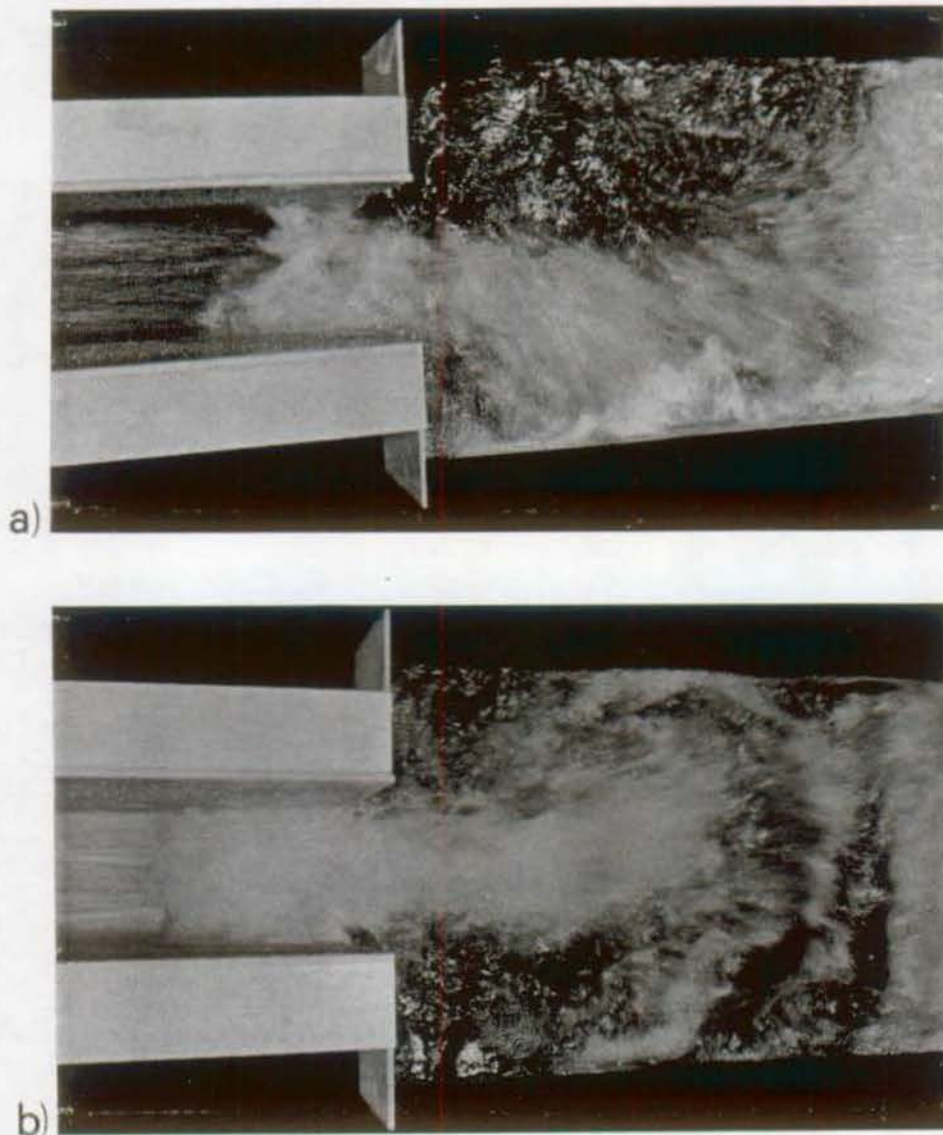


Fig. 6.4 : Effect of a negative step on the overall jump symmetry. $B=3$, $h_1=2.5\text{cm}$, $X_1 = 0.23$, $F_1=5.01$. a) Without step and b) negative step located at the expansion section, $s=2.5\text{cm}$.

The negative step thus improves the jump symmetry by reducing the length of the longer lateral eddy. It should be outlined that a symmetric jump could only be obtained by increasing X_1 , however. The limit value of X_1 for which symmetric jumps occur seems to depend both on N and B . A more detailed analysis of the jump symmetry will be presented in paragraph 6.7.

Eq. (6.4) indicates that the effect of the negative step on the sequent depth ratio Y_N depends on Y_a and on the step parameter N . Therefore, since the step position relative to the expansion remains unchanged, only one additional parameter is needed as compared to Eq. (5.8).

Using the same approach as presented in paragraph 5.4, Eq. (6.4) could be solved for Y_N once the terms B , F_1 , Y_a and N are determined experimentally. The sequent depths ratio obtained by this approach will be indexed with "m", whereas the experimental value will be indexed with "ex". Both values are listed in Appendix 3.

Fig. 6.3 shows the ratio Y_{ex}/Y_m as a function of X_1 for series 2.1 and series 2.3, thereby considering three different domains of N . A fair overall agreement between the measured and the computed sequent depths ratios is noted, especially in the domain of small X_1 (typically $X_1 < 0.2$), where the agreement is better than for horizontal channels. Fig. 6.3 indicates for $X_1=0$ a maximum deviation of some 5% between the measurements and the predictions, whereas deviations up to 20% were recorded for the same expansion ratio with $N=0$.

To explain the improved agreement, two phenomena must be considered. First, for the same inflow conditions and toe position, the expansion with a negative step needs more tailwater. Therefore, the frictional forces, which depend strongly on the flow velocity are reduced.

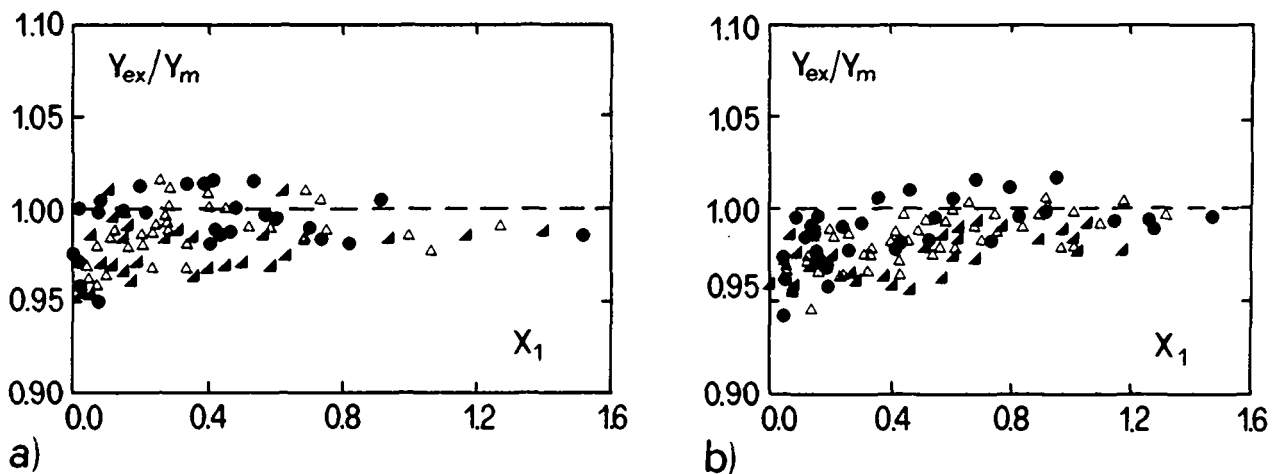


Fig. 6.3 : Sequent depths ratio, Y_{ex}/Y_m as function of X_1 . a) Series 2.1 (▲) $0.61 < N < 0.79$; (△) $0.8 < N < 1.09$ and (●) $1.10 < N < 1.64$; b) Series 2.3 (▲) $0.49 < N < 0.77$; (△) $0.78 < N < 1.05$ and (●) $1.06 < N < 1.66$.

The second reason should be attributed to a reduced length of the lateral eddies observed for expansions with a negative step. In Fig. 6.4 the effect of a negative step

Based on Fig.6.4 a conventional momentum approach may be used to investigate hydraulic jumps in sudden expansions with negative steps. Therein the pressure on the step face could be assumed equivalent to the average flow depth along the expansion side walls.

6.4 SEQUENT DEPTHS

6.4.1 Introduction

In chapter 5, the sequent depths ratio Y and the average flow depth Y_a along the expansion side walls could be approximated by

$$\frac{Y^* - Y}{Y^* - 1} = \left(1 - \frac{1}{\sqrt{B}}\right) \cdot [1 - \text{th}(1.9X_1)] \quad , \quad (6.5)$$

$$Y^3 - \frac{Y}{B} (1 - Y_a^2 + BY_a^2 + 2F_1^2) + \frac{2F_1^2}{B^2} = 0 \quad . \quad (6.6)$$

Eq. (6.6) results from a conventional momentum approach in analogy to Eq. (6.4), whereas Eq. (6.5) accounts for the toe location relative to the expansion section. Therein, the constant $C=1.9$ was established experimentally. The right side of Eq. (6.5) accounts for the effects of channel expansion B and toe location X_1 . For a prismatic horizontal channel, Y^* corresponds to the Bélanger's relation (Eq. 5.1).

To include the step parameter in Eq. (6.5) a modified expression of the type

$$Y_N = Y_N(F_1, X_1, B, N) \quad (6.7)$$

where subscript "s" refers to the step should be developed. Since Eq. (6.7) involves four independent parameters, an explicit formulation of this equation would require an extensive experimental investigation. In order to limit the extent of this investigation some conclusions of chapter 5 will be reconsidered hereafter.

As shown in paragraph 5.5, Eq. (6.5) may be written as a product of functions, each one accounting for one independent parameter. Based on this observation, it could be assumed that the explicit formulation of Eq. (6.7) will present the same characteristics. The right side of Eq. (6.5), which accounts for the expansion ratio B and the toe position X_1 may therefore be independent from the step parameter N . The term Y^* on the left side of Eq. (6.5) accounts for the effect of the inflowing Froude

number when prismatic channels are considered. For sudden expansions with a negative step, Y^* should therefore be replaced by the sequent depths ratio in channels without any expansion but with a negative step. This sequent depth relation will be developed in the next paragraph. In paragraph 6.4.3, the resulting equation is introduced in Eq. (6.5) and solved for Y according to Eq. (6.7). The resulting sequent depths ratio will then be compared to the experimental investigation.

6.4.2 Sequent depth ratio in a prismatic channel with a negative step

In this paragraph a sequent depths relation for a rectangular channel of constant width will be developed by accounting for the toe location relative to the step section. This procedure greatly simplifies the general approach of determining an equation of type (6.7).

Hydraulic jumps at abrupt drops recently received considerable interest (Kawagoshi and Hager 1990). However, instead of analysing the relation Y_N^* (F_1 , X_1 , N), a number of flow types such as the A-jump, the B-jump or the wave-type flow were distinguished. Herein, a different procedure will be considered in order to account for the continuous variation of X_1 in the domain $0 \leq X_1 \leq 1$.

Two limit positions will first be considered. Fig. 6.5a) shows the flow configuration for the minimum tailwater. Therein, the toe of the jump is located at the step section (B-jump). Assuming a pressure head h_1+s at the step section (reference level downstream from the expansion), Eq. (6.4) simplifies for $B=1$ (Y_N^* instead of Y_N) to

$$Y_N^{*3} - Y_N^* \left[1 + 2F_1^2 + N(2 + N) \right] + 2F_1^2 = 0 \quad \text{for } X_1 = 0 \quad . \quad (6.8)$$

The second limit position as shown in Fig. 6.5b) corresponds to a surface roller located entirely upstream from the step ($X_1=1$). It will be assumed that the flow depth attains the tailwater level h_2 at the downstream end of the surface roller. Furthermore, if the flow depth remains unchanged across the step section, Eq. (6.4) becomes for $B=1$

$$Y_N^{*3} - Y_N^* \left[1 + 2F_1^2 + N(2Y_N^* - N) \right] + 2F_1^2 = 0 \quad \text{for } X_1 = 1 \quad . \quad (6.9)$$

For toe positions ranging between $0 < X_1 < 1$, the flow depth on the step face is included in the domain h_1+s ($X_1=0$) and h_{2s}^* ($X_1=1$). Assuming a linear increase of pressure head on the step between $X_1=0$ and $X_1=1$ thus yields

$$\frac{p_s}{\rho g h_1} = \left[(1-X_1) \cdot (h_1+s) + X_1 h_{2s}^* \right] \cdot \frac{1}{h_1} \quad (6.10)$$

where p_s is the pressure on the step face. Introducing Eq. (6.10) in Eq. (6.4) with $B=1$ and $p_s/(\rho g h_1)=Y_a$ leads to

$$Y_N^{*3} - Y_N^* \left\{ 1+2F_1^2+2N \left[Y_N^* X_1 - N X_1 - X_1 + 1 + (1/2)N \right] \right\} + 2F_1^2 = 0 \quad (6.11)$$

provided $0 \leq X_1 \leq 1$.

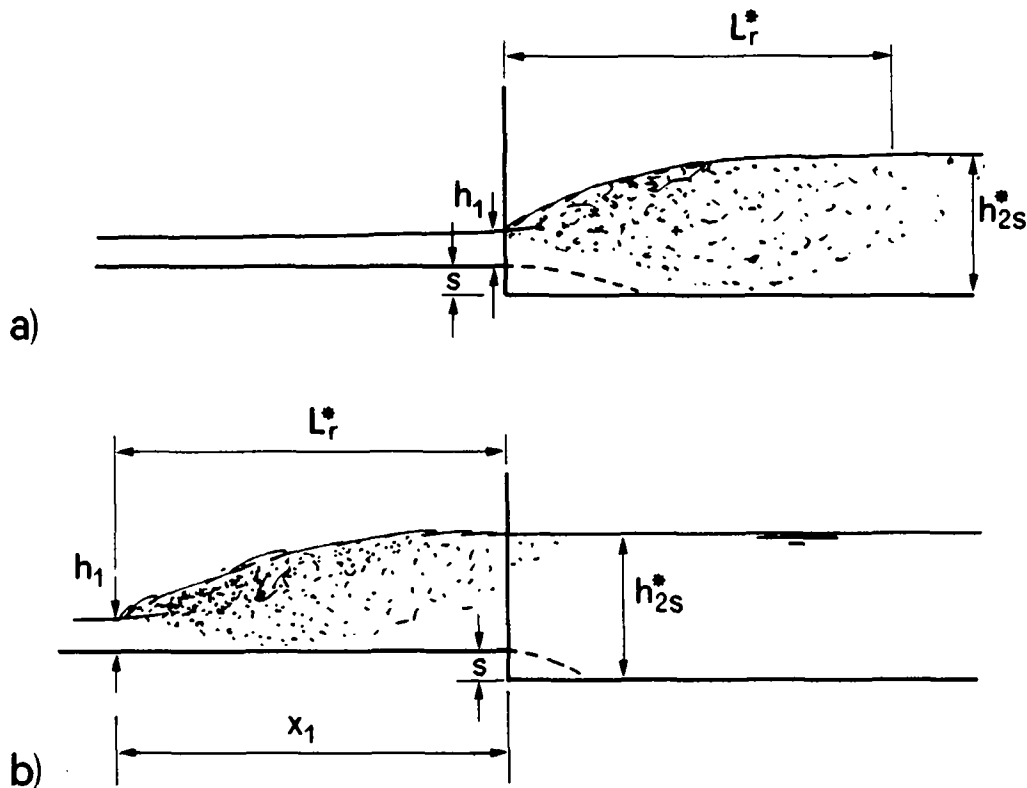


Fig. 6.5 : Limit flow configurations considered : a) toe located at the step section ($X_1=0$), and b) entire surface roller of length L_r^* located upstream from the step ($X_1=1$).

A linear pressure increase as previously assumed involves the assumption that the free surface profile of the jump could be approximated by a linear relation and that the pressure distribution is hydrostatic. Detailed investigations of these features were conducted by Rajaratnam (1962), Gupta (1965), Rajaratnam and Subramanya (1968) and Sarma and Newnham (1973). Therein, the effect of the inflowing Froude number, and the air entrainment on the jump profile was analysed. For high values of

F_1 , the surface profile tends to become linear, whereas for small values of F_1 the convexity of the profile is more pronounced.

Eq. (6.11) ignores the wave-type phenomena observed for hydraulic jumps at a negative step (Moore and Morgan 1959, Ohtsu and Yasuda 1988, Kawagoshi and Hager 1990). These phenomena modify the jump profile and the pressure on the step face. However, for negative steps in sudden expansions, the wave-type phenomena was not observed, as will be discussed in 6.4.3. Eq. (6.11) may therefore be used for any inflow conditions and any value of N provided sudden expanding channels are considered.

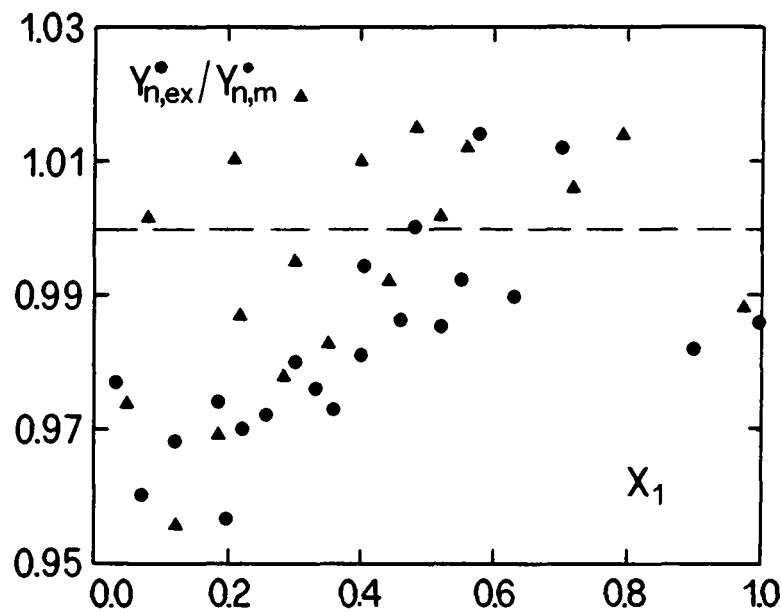


Fig. 6.6 : Sequent depth ratio Y_N^* in prismatic rectangular channel with negative step. Comparison of Eq. (6.11) with experiments.
 (●) $0.93 < N < 1.00$ and (▲) $1.70 < N < 1.88$.

To verify Eq. (6.11), a series of sequent depth measurements were conducted in channel LCH1 equipped with a 2.5cm high negative step. Two domains of N and inflowing Froude numbers F_1 ranging from 4.44 to 8.68 were considered. In Fig. 6.6, $Y_{N,ex}^*$ refers to the experimentally determined sequent depths ratio, whereas $Y_{N,m}^*$ refers to values according to Eq. (6.11).

According to Fig. 6.6, the deviations between the measurements and the predictions are confined to $\pm 3\%$. For jumps with the toe located in the vicinity of the step, Eq.(6.11) tends to overestimate the sequent depths ratio. Note that jumps with a standing wave pattern were excluded from this analysis, as previously discussed.

Despite these restrictive assumptions, the accuracy of Eq. (6.11) was considered sufficient for the purpose of this investigation.

Based on a pressure head on the step face which varies linearly with the toe position X_1 , Eq. (6.11) is shown to describe the sequent depth ratio Y_N^ in the prismatic channel with a negative step of height N as a function of the approaching Froude number F_1 .*

6.4.3 Sequent depth in sudden expansion with negative step

Presently, two channel geometries have been considered namely; firstly the case with a horizontal channel bottom ($N=0$) and secondly the case with constant channel width ($B=1$). In this paragraph, generalisation to a formula of the type of Eq. (6.7) will be made. As previously mentioned these limit conditions were considered by splitting the five parameter equation. The experimental investigation will be compared to the predictions according to this approach in order to check the substitution of Y^* (without step) by Y_N^* (with step).

After the inflow conditions (F_1, h_1), the toe position X_1 , and the step height s are defined, Eq. (6.11) could be solved for Y_N^* . Introducing Y_N^* (in which $Y_N^* \rightarrow Y^*$) and the expansion ratio B considered in Eq. (6.5) leads to a computational value of Y_N . Also, the average flow depth along the expansion side walls Y_a is obtained from Eq. (6.6) since Y_N, B, F_1 and N are known. The efficiency of a hydraulic jump formed in channels with a negative step may be expressed as

$$\eta_s = \frac{H_1 - H_2}{H_1} = 1 - \frac{Y_N + \frac{F_1^2}{2B^2Y_N^2}}{1 + N + \frac{F_1^2}{2}} \quad (6.12)$$

Therein, the origin of the energy head corresponds to the bottom elevation of the tailwater channel (Fig. 6.1). In Fig. 6.7 the sequent depths ratio Y_N as well as the energy dissipation ratio η_s according to Eq. (6.12) are shown for three expansion ratios B , and five values of X_1 . The dotted line refers to Bélanger's relation (Eq. (5.1)). According to the notation used in Fig. 6.1, the sequent depths ratio in channels with a negative step is larger than for channels with a horizontal channel bottom for identical values of X_1, F_1 and B . As regards the efficiency, no systematic difference may be observed between Figs. 5.14 and 6.7.

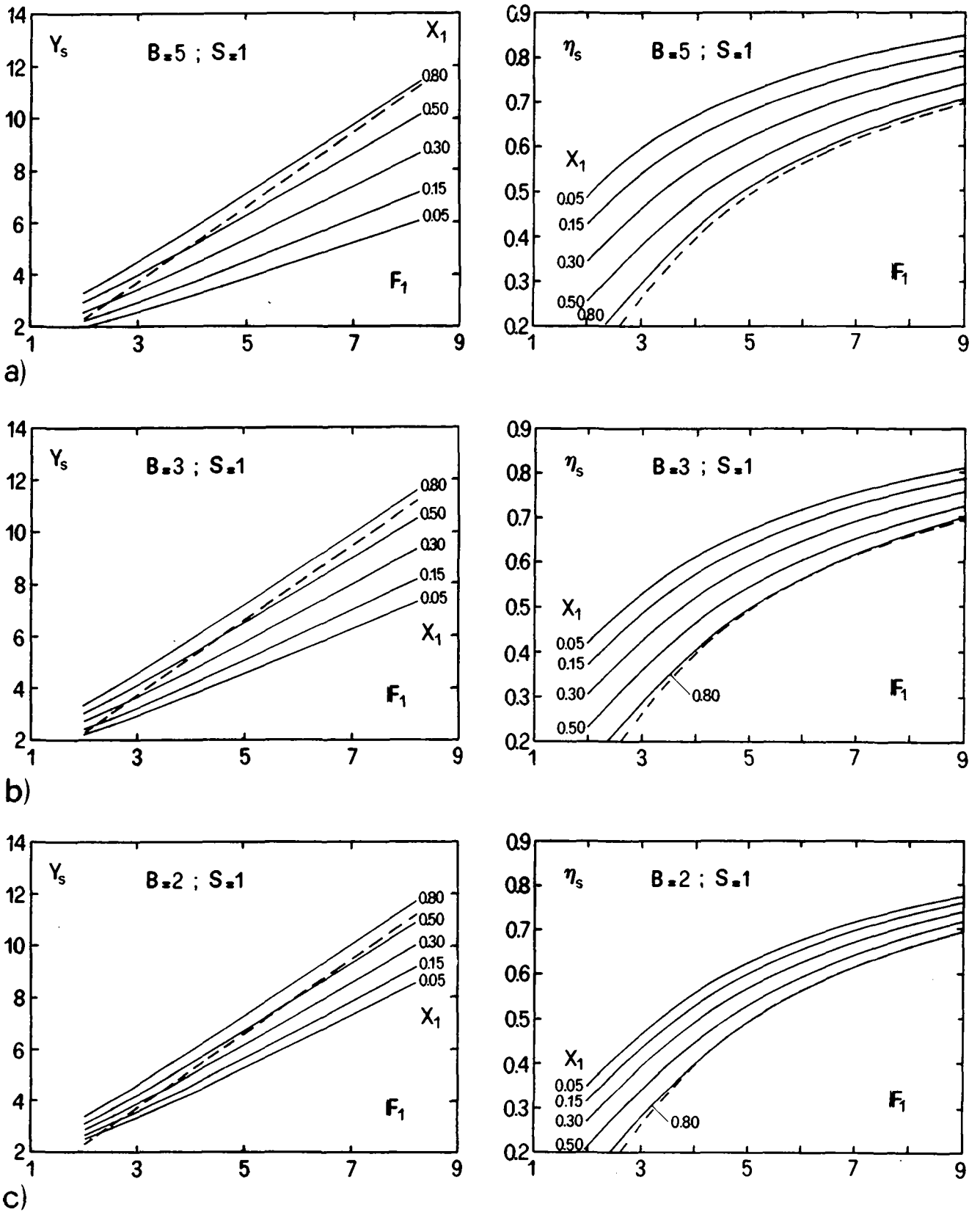


Fig. 6.7 : Sequent depths ratio and energy dissipation ratio according to Eq. (6.5), Eq. (6.11) and Eq. (6.12). a) $B=5, N=1$, b) $B=3, N=1$, c) $B=2, N=1$. (---) sequent depths ratio and energy dissipation ratio according to Bélanger's equation.

The comparison of the computational model with the experiments is shown in Fig. 6.8. Therein, the predicted values Y_p are compared to some experimental data Y_{ex} of series 2.2 and 2.3.

In Fig. 6.8.a) the data of series 2.3 with $0.49 < N < 0.65$ are compared to the prediction and a fair agreement is noted. For a better visualization, the ratio Y_{ex}/Y_p was plotted for all the data of series 2.2 in Fig.6.8b). For $X_1 < 0.5$ the predicted values are generally smaller than the observations and vice versa for $X_1 > 0.5$. Thus, an additional effect of X_1 on Y_N might exist. A reevaluation of the constant $C=1.9$ in Eq.(6.5) would possibly reduce this influence. However, for $X_1=0$, the value of C has no effect on Y_p . Given that typical deviations are less than 5%, no further modifications to Eqs. (6.5) and (6.11) were applied.

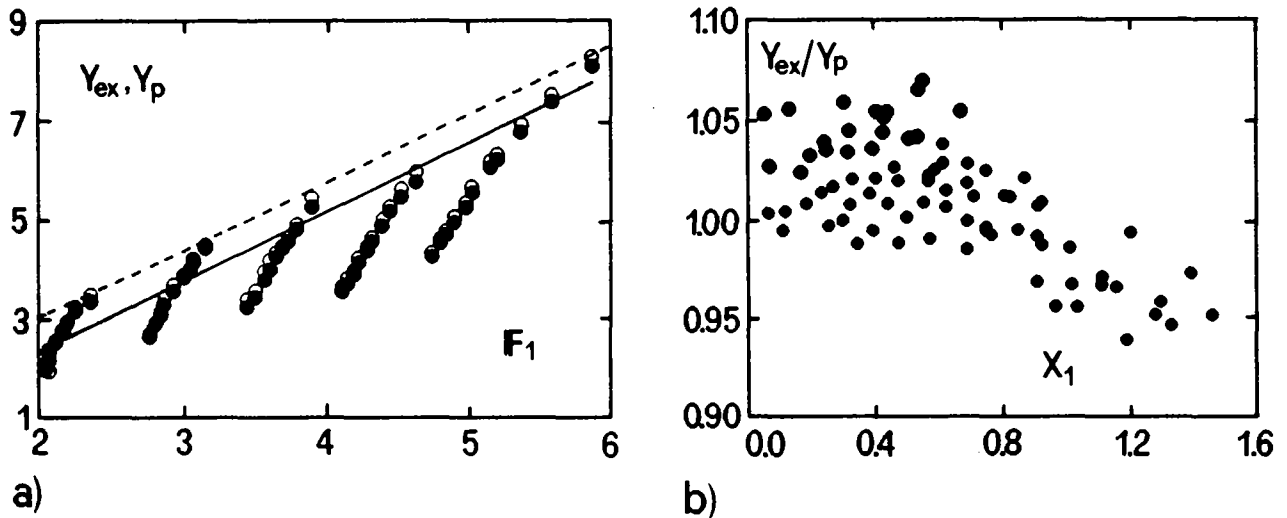


Fig. 6.8 : Sequent depths ratio in sudden expansions with negative steps. Comparison of Eq. (6.5) with the experimental data. a) Series 2.3 for $0.492 < N < 0.65$ (●) experiments, (○) predictions and (—) Bélanger's equation.(- -) Eq.(6.9) for $N=0.5$ and $X_1=1$, b) Series 2.2 .

The maximum deviation of the three series investigated is $\pm 6\%$. Despite several assumptions involved by the present approach, the agreement between the predictions and the experiments is satisfactory, therefore. Recall that in both Eq. (6.5) and Eq. (6.11) the following assumptions apply:

1. all frictional forces are neglected,
2. the pressure distribution is assumed hydrostatic,
3. the surface profile of the jump is linear, and
4. the jump length L_j is independent of the relative step height N .

Furthermore, the deviations may partly be attributed to the measurement technique used. Consider, for example, an inflow depth of 2.0cm and an inflow Froude number $F_1=5.0$. A deviation of ± 2 mm in the tailwater depth leads to an average deviation of $\pm 3.0\%$ in Y_{ex} .

Finally, it seems important to outline that the presence of a negative step modifies only the left hand side of Eq. (6.5). In figure 5.12, the parameter ψ could be replaced by the new function

$$\psi_N = \frac{Y_N^* - Y_N}{Y_N^* - 1} \quad (6.13)$$

which accounts in addition for the step parameter N . ψ_s is contained in the range $0 < \psi_N < 1$. Compared to Y^* , which is independent of X_1 , Y_N^* depends both on the toe location X_1 and on the step height N . Therefore, depending on the parameter configuration, Fig. 5.12 must be used iteratively.

The influence of a step on the sequent depths ratio will be illustrated in the numerical example of paragraph 6.7.

The effect of a negative step at the expansion section can be accounted for by defining a modified sequent depths ratio parameter ψ_N according to Eq. (6.13) instead of ψ according to Eq. (5.26).

6.5 JUMP LENGTH

The jump end section was defined according to paragraph 5.2 and may be located upstream from the end section of the longer lateral eddy.

In Fig. 6.9 a) the normalised jump length L_j/h_2^* for series 2.1 is shown as a function of X_1 . The domains of N considered are indicated in Fig. 6.3. Fig. 6.9 b) and c) show the ratio $L_{j,ex}/L_{j,p}$ as a function of X_1 for series 2.3. Therein, $L_{j,p}$ is the predicted jump length according to Eq. (5.39)₁. As observed in paragraph 5.7.2, the scatter involved by the length measurements is significant, especially for small values of X_1 . Fig. 6.9 b) shows that deviations up to 20% from the average value may occur for $X_1 < 0.5$.

As shown in Fig. 6.9, no systematic effect of the step height on the jump length may be observed. Since no systematic trend has been found between the inflowing Froude number and the ratio $L_{j,ex}/L_{j,p}$, Eq. (5.39)₁ gives a reasonable approximation for the value of L_j . The jump length L_j is therefore independent from the step height N .

The presence of a negative step located at the expansion section has no discernible effect on the length of jump.

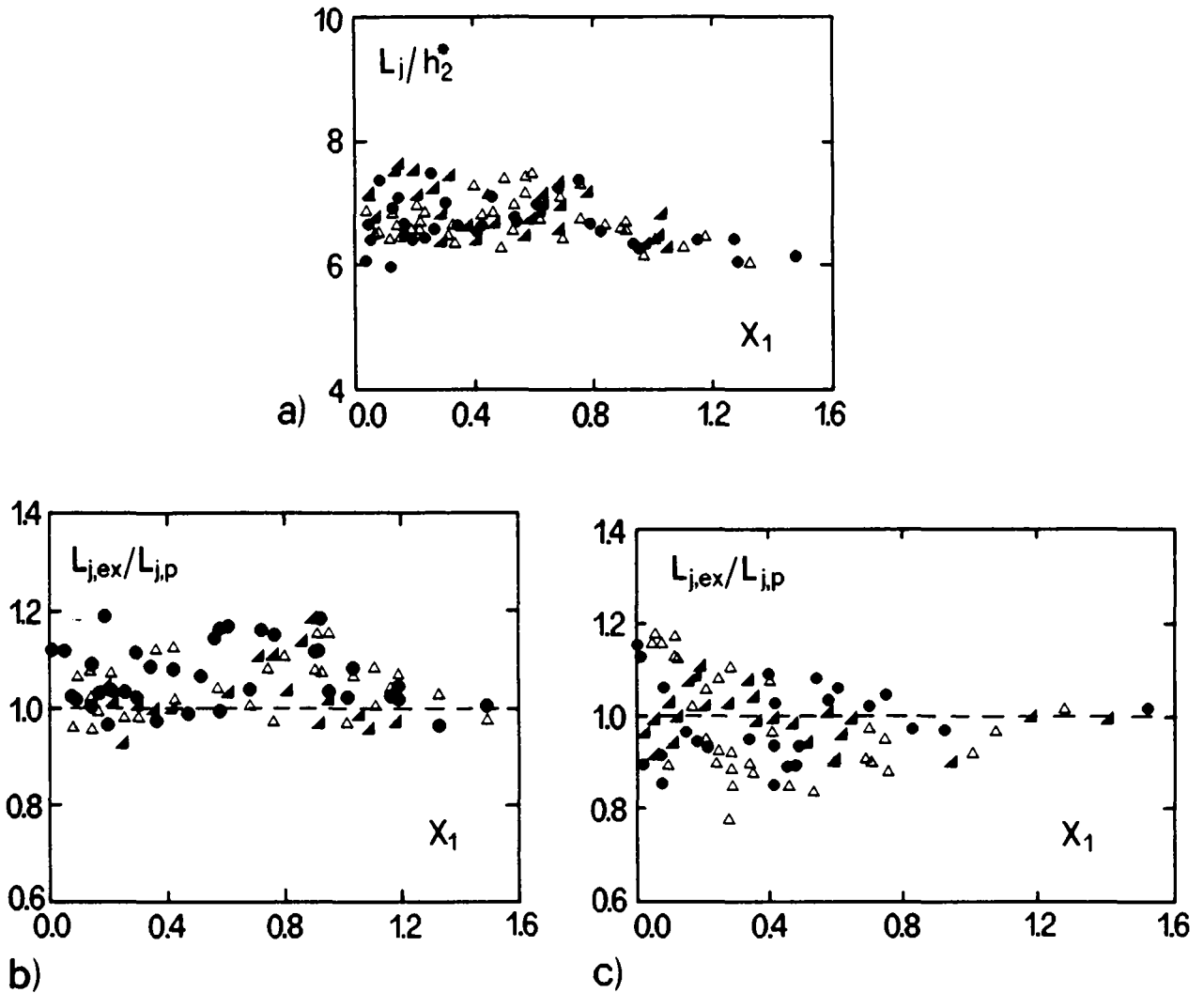


Fig. 6.9 : Jump length. Comparison of the experimental data with Eq. (5.39). a) Relative length L_j/h_2^* as a function of X_1 for Series 2.1; $L_{j,ex}/L_{j,p}$ as a function of X_1 for b) Series 2.2 and c) Series 2.3. (\blacktriangle) $0.49 < N < 0.65$ (\triangle) $0.93 < N < 1.00$ and (\bullet) $1.70 < N < 1.88$.

6.6 JUMP SYMMETRY

As indicated in paragraph 5.8, the jump asymmetry could be estimated quantitatively by measuring the difference of the flow depths h_a between the right and the left channel sides. Due to the wave generation and the measurement technique used, the

hydraulic jump could be considered as symmetric if the depths difference Δh_a between the two sides is smaller than 3%. As mentioned in paragraph 5.8 this limit is only based on visual observations. The experimental investigation described in chapter 5 showed that Δh_a increases with B and decreases with X_1 . The most unfavorable flow condition should be expected for large expansion ratios (typically $B > 3$) and small values of X_1 , therefore. As shown in Fig. 5.27, the limit toe position for which symmetrical flow prevails depends on B , whereas F_1 seems not to influence significantly Δh_a .

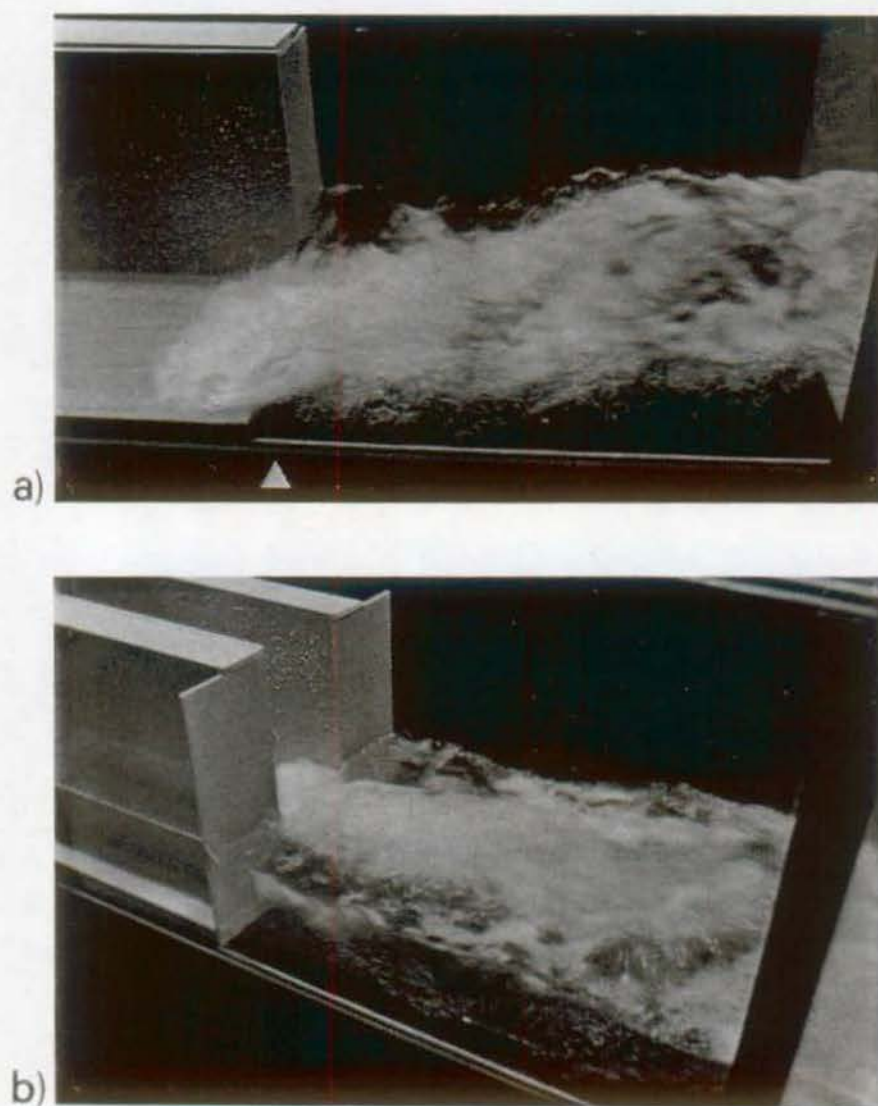


Fig. 6.10 : Effect of negative step located at the expansion section. a) separation zone formed downstream from a negative step. Series 2.1 with $X_1=0.12$, $F_1=3.03$ and $N=1$, b) Overall flow pattern. Series 2.3 with $X_1=0.15$, $F_1=4.15$ and $N=1$.

As described in paragraph 5.8, an asymmetric flow is closely linked to a differential pressure Δh_a acting on the inflowing jet. To improve the jump characteristics, a reduction of Δh_a should reduce the curvature of the main stream. The approaching flow separates from the channel bottom downstream from the step and forms a separation zone (Figs. 6.1b) and 6.10a). The dimensions of the jump depend on the characteristics of the inflowing jet as well as on the step height. The separation zone below the main stream provides a connection between the two lateral eddies allowing a reduction of Δh_a . Therefore, the abrupt expansion with a drop could improve the flow symmetry, as was already suggested in the introduction to this chapter.

Despite an improvement of the overall jump pattern, symmetrical and steady flows were difficult to obtain especially for small values of X_1 . The main flow then still oscillated from one channel side to the other. These oscillations modified continuously the flow depth along the expansion side walls. The oscillations frequency was variable and ranged typically from 1-2 to 10-15 oscillations per minute. Low frequencies were observed for small values of X_1 . An increase of X_1 was accompanied by an increase of the frequency until the jump became stable and permanently symmetric.

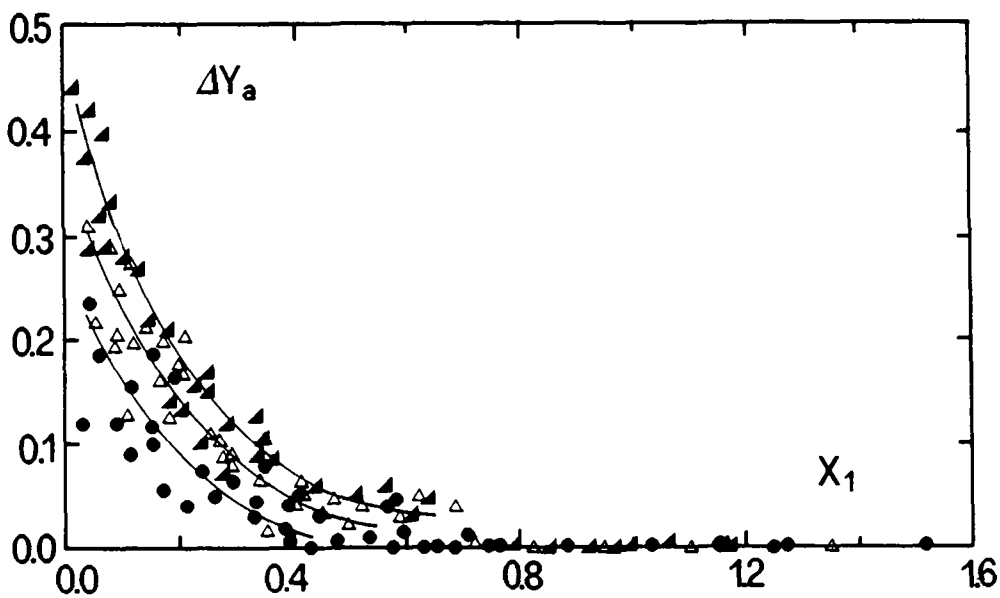


Fig. 6.11 : Asymmetry parameter ΔY_a for series 2.3 and different values of N . (\blacktriangle) $0.49 < N < 0.77$; (\triangle) $0.78 < N < 1.05$ and (\bullet) $1.06 < N < 1.66$. (—) Average experimental curves.

To record the flow depths h_a along the expansion side walls, both the lowest and the highest levels occurring during a period of 2-3 minutes were observed for series 2.3. When the minimum level configuration occurred along one side, the maximum was

attained at the opposite side. The maximum $h_{a,max}$ and minimum $h_{a,min}$ levels were recorded and the difference divided by the average flow depth in analogy to Eq. (5.40). The data collected is shown in Fig. 6.11 for three domains of N and an expansion ratio of $B=3$.

Fig. 6.11 shows $\Delta Y_a = \Delta h_a / h_1$ as a function of X_1 for various relative step heights N and F_1 . It is seen that ΔY_a is practically zero for $X_1 > 0.7$ for any value of N . The data for smaller X_1 are grouped along the lines also plotted in Fig. 6.11 and thus indicate a definite effect of N on ΔY_a .

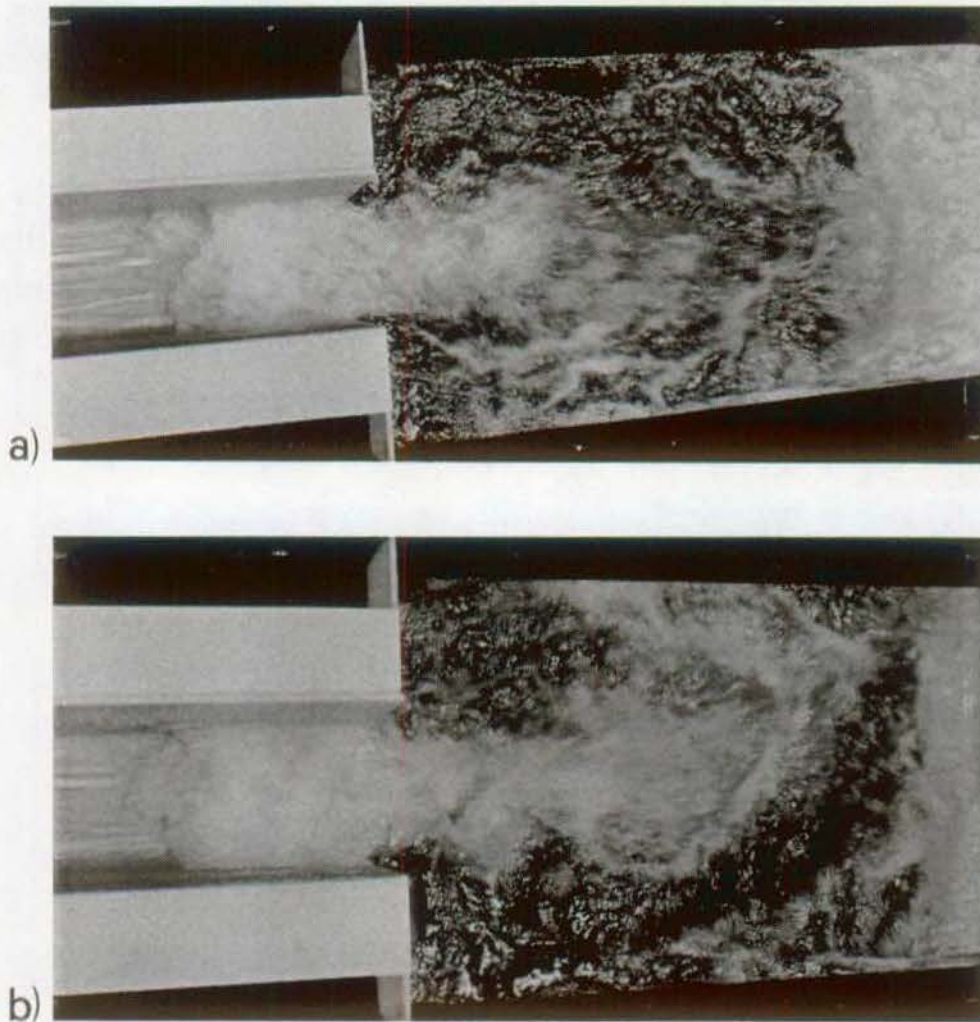


Fig. 6.12 : Effect of the relative step height N on jump symmetry for $B=3$. a) $h_1=1.7\text{cm}$, $F_1=6.05$, $N=1.47$ and $X_1=0.2$. b) $h_1=4.1\text{cm}$, $F_1=3.51$, $N=0.61$ and $X_1=0.18$.

Considering a limit deviation $\Delta Y_a=3\%$ for symmetric flow to occur, the corresponding minimum toe position is in the domain $0.4 < X_1 < 0.6$. Compared to the channel configuration without step (Fig. 5.26), a slight reduction of this position is

obtained, therefore. A closer observation of the data plotted in Fig. 6.11 reveals that the curve $\Delta Y_a(X_1)$ for $0.49 < N < 0.77$ is comparable to the curve for $N=0$ as plotted in Fig. 5.20. The effect of the step thus remains limited when small steps ($N < 1$) are considered. For $1.06 < N < 1.66$ the reduction of ΔY_a is significant and attains the limit value of 3% at about $X_1=0.4$.

The effect of N on the jump pattern is qualitatively reproduced in Fig. 6.12. Therein, two jumps with approximately the same relative toe position X_1 but different inflow depths h_1 are compared. The jump with $N=1.47$ (Fig. 6.12a) seems to be more symmetric than with $N=0.61$ (Fig. 6.12b). Therefore, negative steps located at the expansion section introduce a favorable effect on the overall flow pattern, yet not sufficient to produce symmetric and stable jumps over a wide range of X_1 . Therefore, negative steps should be considered only in addition to other stabilizing devices such as sills or blocks.

The effect of a negative step located at the expansion section is only modest as regards the improvement of jump symmetry.

6.7 NUMERICAL EXAMPLE

In order to illustrate the effect of a negative step on the jump characteristics, the numerical example of paragraph 5.9 will be reconsidered. Therein, the inflowing stream was characterized by $b_1=10.0\text{m}$, $h_1=1.2\text{m}$ and $V_1=25\text{m/s}$, whereas the tailwater level amounted to $h_2=10.0\text{m}$. Estimate the toe position X_1 by considering a negative step of height $N=1$ ($s=1.2\text{m}$) and compare the results with the positions obtained without the step (§ 5.9).

In the present case, ψ_s depends not only on F_1 , h_1 and h_2 but also on X_1 and N . Therefore, an iterative solution procedure of Eq. (6.5) and (6.11) must be used to compute the toe position X_1 . Since X_1 is contained in both equations, the procedure selected was to calculate Y for one given value of X_1 and to compare the result with the imposed ratio $Y=10.0\text{m}/1.2\text{m}=8.33$. The position parameter X_1 was then adjusted until the solution of Eq. (6.5) was in perfect agreement with the given sequent depths ratio. Table 6.2 shows the final toe positions obtained. The solution without the step was used to initiate the computation. The results obtained in Table 6.2 were verified approximately with Fig. 6.7.

As indicated in Table 6.2, the influence of the step ($N=1$) on the toe position is limited for the inflow Froude number $F_1=7.29$ considered. As expected, the channel with a negative step requires a higher tailwater level compared to the horizontal floor geometry for identical inflow conditions, F_1 , h_1 and X_1 . In Fig. 6.13 the computational results are illustrated for an expansion ratio of $B=3$. For identical tailwater conditions (reference level in the tailwater channel) and identical inflow conditions the front of the jump is located 3m further downstream compared to a horizontal channel floor.

Table 6.2 : Effect of the step height on the toe position X_1 .

Geometry	Without step (§ 5.9)			With step $N=1$		
	ψ [-]	X_1 [-]	x_1 [m]	ψ_s [-]	X_1 [-]	x_1 [-]
B=2	0.17	0.25	12.7	0.197	0.177	9.0
B=3	0.17	0.36	18.3	0.207	0.297	15.0
B=5	0.17	0.45	22.8	0.212	0.378	19.2

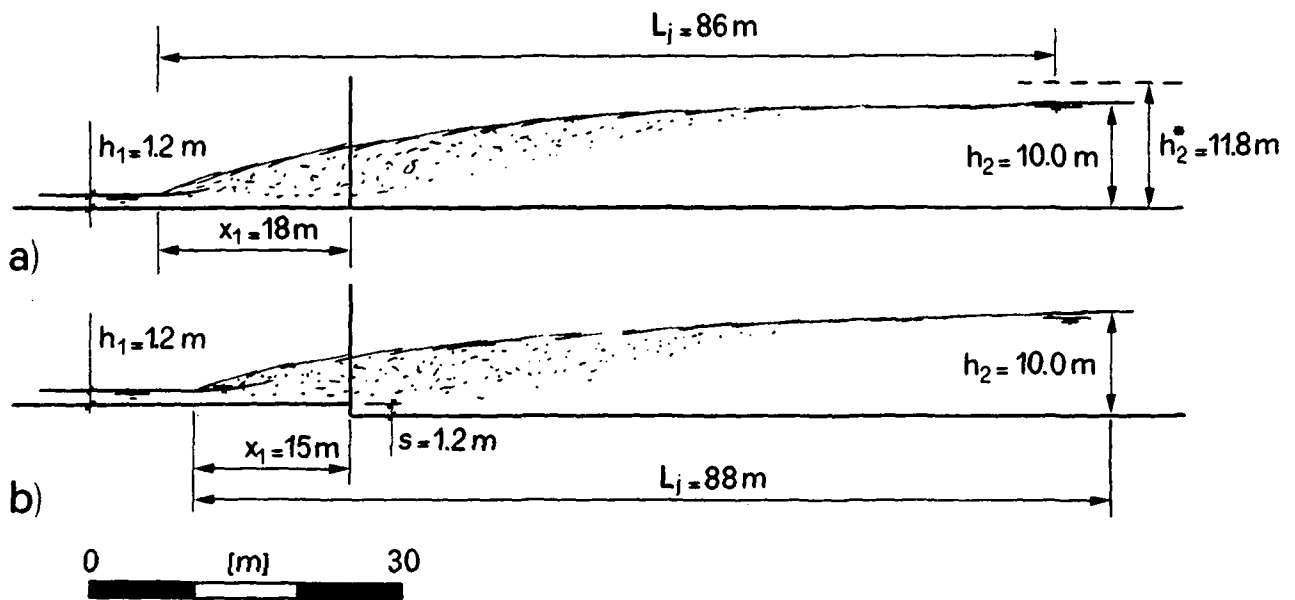


Fig. 6.13 : Effect of a negative step on the toe position for $B=3$. Inflow conditions $h_1=1.2\text{m}$, $b_1=10.0\text{m}$, $F_1=7.29$. Tailwater level $h_2=10.0\text{m}$. a) without step and b) with step ($N=1$).

In the present approach the length of jump does not depend on N , hence it may be estimated with Eq. (5.38)₁ or (5.38)₂. Since the toe position parameter X_1 is smaller

with a step, the jump length is slightly increased compared to the horizontal channel bottom. The required volume of stilling basins is nearly identical for both geometries, therefore.

6.8 CONCLUSIONS

In the present chapter, the effect of an abrupt negative step located at the expansion section on the jump pattern was analysed. The sequent depths ratio Y_N may be expressed as $Y_N = Y_N(F_1, X_1, N, B)$ and thus contains the relative height of step N as an additional parameter when compared to chapter 5. Based on a conventional momentum approach and on the experimental investigation, the computational model was shown to allow the prediction of both the sequent depths ratio Y_N according to both Eq. (6.5) and Eq. (6.11), and the average flow depth Y_a along the expansion side walls according to Eq. (6.6). To determine these quantities, the inflow conditions F_1 and h_1 , the toe position X_1 and the channel geometry B must be defined. Despite several simplifications the computational model was shown to be in fair agreement with the experimental data. For small X_1 the agreement is even better than for channels without steps.

The jump length L_j may be predicted with Eq. (5.39). The step thus has no discernable effect on the length of jump. The jump asymmetry could not be eliminated by the negative step. Oscillations of the main stream were observed for a wide range of X_1 and stable jumps occurred only for $X_1 > 0.5$ ($B=3$). For an expansion ratio of $B=3$, negative steps lead to an unsatisfactory performance of the stilling basin. The effect of other stabilizing means on hydraulic jumps in expansions will be analysed in the following chapter.

7. EFFECT OF DEFLECTORS, BLOCKS AND SILLS

7.1 INTRODUCTION

For design purposes, stilling basins should satisfy the following requirements :

1. low sequent depth combined with high energy dissipation,
2. stability under variable approach and downstream conditions,
3. compact basin,
4. safety against cavitation erosion,
5. acceptable flow conditions downstream from the basin as regards wave action, scour, bank erosion and environmental aspects.

As outlined in chapters 2, 5 and 6, hydraulic jumps in nonprismatic channels may be characterized by an asymmetric flow combined with a significant wave action. The above listed requirements for dissipating structures are therefore only partially satisfied. Hydraulic jumps as described in chapter 5 provide a relatively high energy dissipation. However, the jump is too long and the flow conditions downstream from the jump are unfavorable due to the significant backward flow. The purpose of the present chapter is to investigate whether sudden expansions with devices such as deflectors, blocks and sills are able to meet the requirements of efficient dissipators.

The performance of nonprismatic basins is closely linked to the symmetric flow downstream from the expansion. As outlined in chapter 2, gradual expansions with expansion angles larger than $2\phi=20^\circ$ (Fig. 2.8) generate asymmetrical phenomena such as those observed in sudden expansions, provided $F_1 > 3$. This is in agreement with pressurized expansions as shown by Rouse (1951) or Hager (1990). Therefore, the expansion angle has no effect on the jump pattern beyond a limiting angle which depends mainly on the inflow Froude number.

In chapter 6, the effect of negative steps located at the channel expansion was investigated quantitatively. From the point of view of flow symmetry, a limited improvement could only be observed for $N > 1$.

In this chapter other means will be analysed by which the jump characteristics improve significantly. The appurtenances to be considered include blocks, sills and deflectors. Based on observations in prismatic stilling basins (Bretz, 1987), the effect of such devices depends on the geometry, the position relative to the toe and on the inflow conditions. Besides the jump symmetry, attention will also be paid to the downstream flow conditions. A favorable velocity distribution is characterized by

high velocity concentrations away from the channel walls downstream from the basin, such that scour is inhibited.

In paragraph 7.2 the effect of bottom deflectors located at different positions relative to the expansion section is investigated. Paragraph 7.3 accounts for different types of sills. Photographs illustrate the difference between the flow characteristics with and without the sill. Different sill positions and dimensions are compared and suggestions for further consideration are offered.

Paragraph 7.4 deals with the effect of blocks on the jump symmetry. Since blocks involve a number of geometric parameters, this investigation was limited to one shape of blocks. Finally, in paragraph 7.5, the appurtenances investigated will be compared and discussed. Based on the conclusions of chapter 7, a more detailed investigation on the favored appurtenance will be presented in chapter 8. All experiments discussed in this chapter were carried out in installation LCH 1 by keeping the expansion ratio $B=3$ constant. Only a second series of runs on the effect of blocks was conducted in installation LCH2, also with an expansion ratio of $B=3$.

7.2 DEFLECTORS

Fig. 7.1a) refers to the channel and deflector geometry considered in this paragraph. Fig. 7.1c) shows on the left side the expansion section including the deflector fixed on the floor, and the gravel used to estimate the extent of erodible zones on the right side. Fig. 7.1b) shows the PVC element installed in the channel. A large-sized gravel of diameter 10-15mm and a small gravel depth was selected to avoid an influence of the channel bed shape on the jump characteristics. A more detailed investigation on bed erosion will be presented in paragraph 8.

A deflector located at the channel expansion may increase significantly the size of the separation between the main stream and the channel floor. The connection surface between the two lateral eddies is therefore increased and may be sufficient to insure a uniform pressure on the two sides on the inflowing jet.

Preliminary experiments with deflectors showed that an adequate effect may only be obtained if the deflector angle α was sufficiently large. Therefore, an angle of $\alpha=9.46^\circ$ was selected since experiments with smaller angles led to asymmetric flow for the expansion ratio $B=3$.

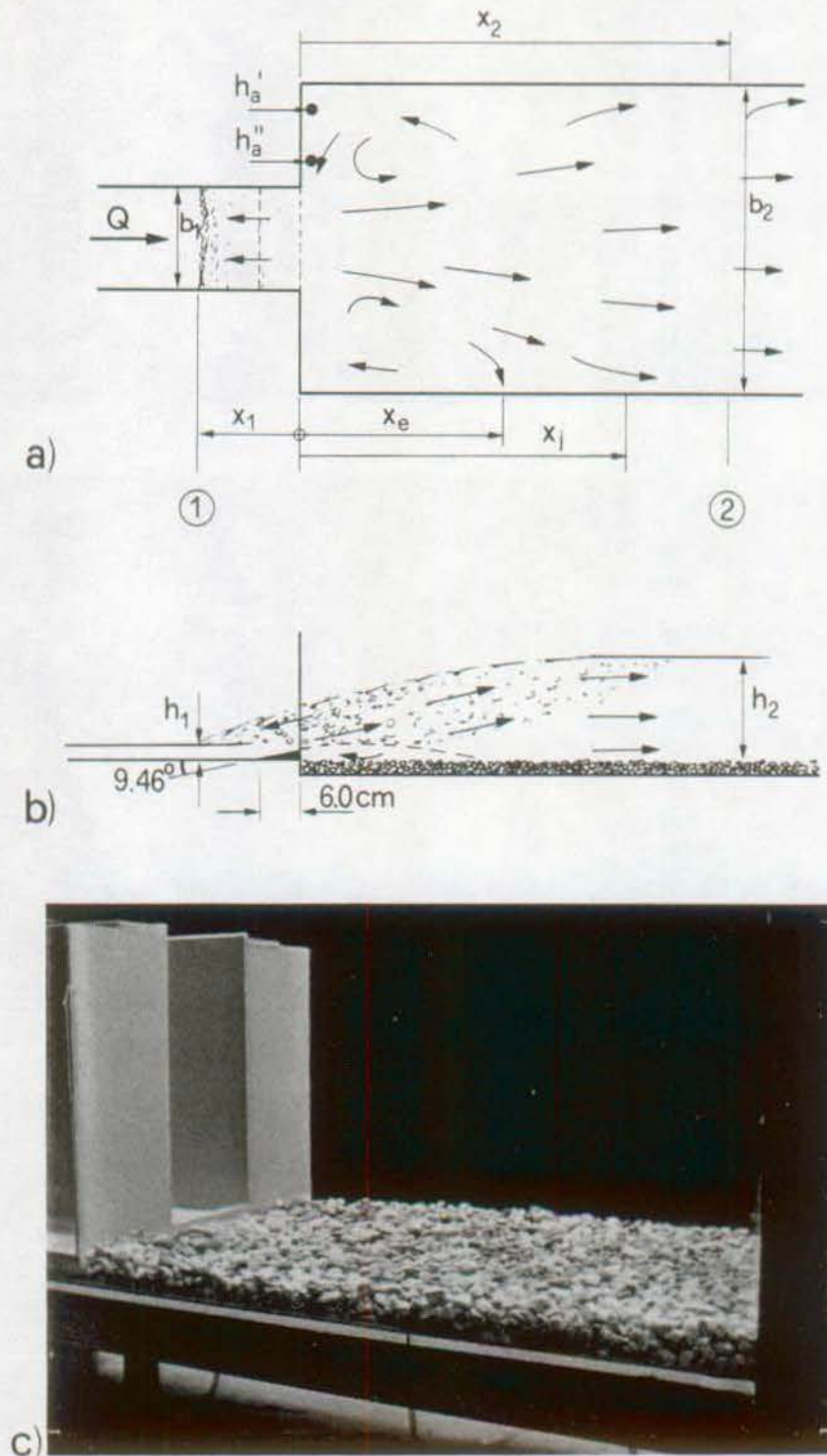


Fig. 7.1 : Channel geometry investigated. a) plan view, b) axial view, c) photograph of the PVC elements and the mobile bed without flow.

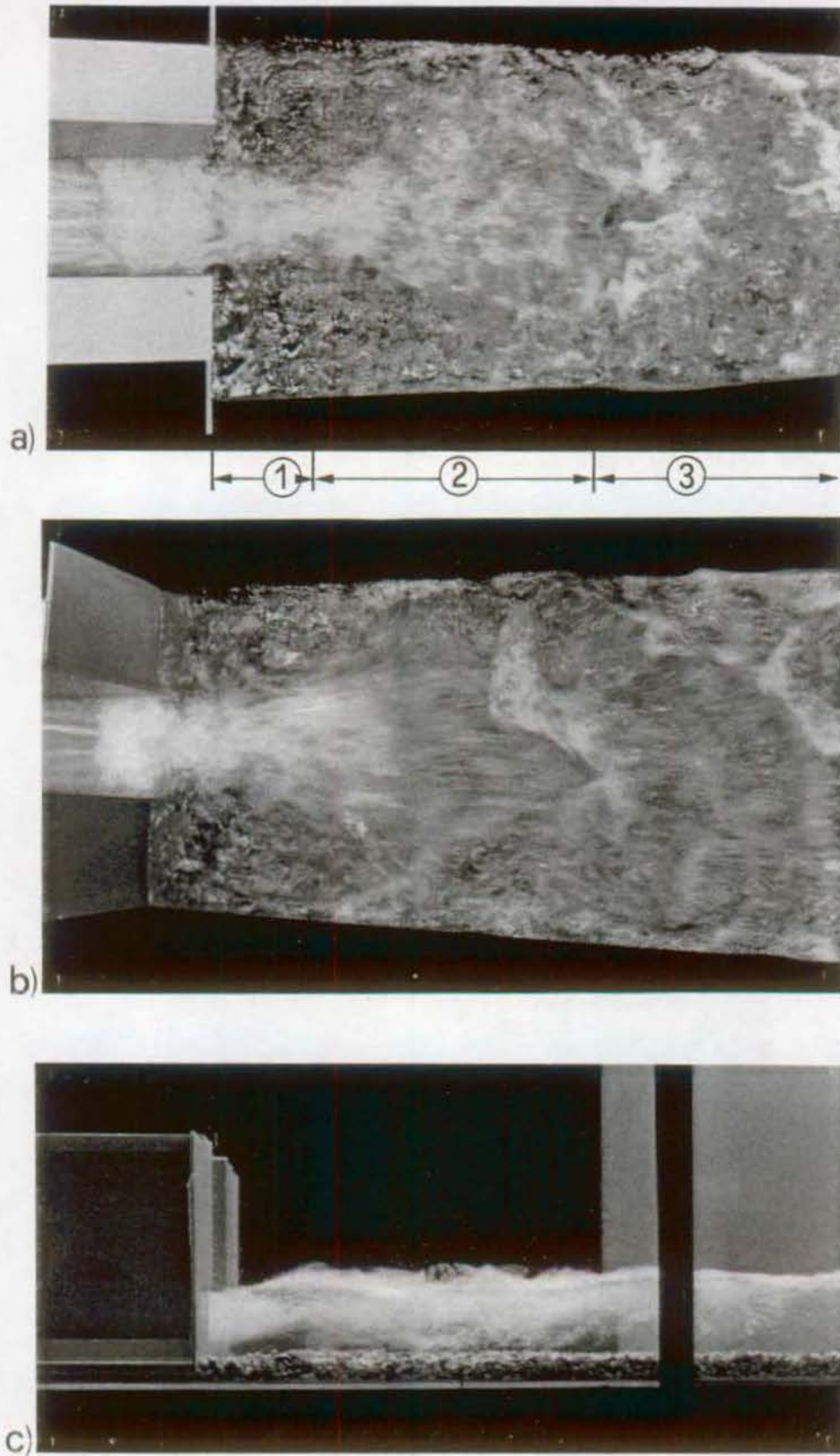


Fig. 7.2 : Effect of a deflector on the jump for $X_1=0.14$. a) plan view; b) downstream view and c) side view.(see text for explanation of domains ① to ③).

dissipation phenomena. As a result, the deflector was not further considered as an improving device for expanding dissipators.

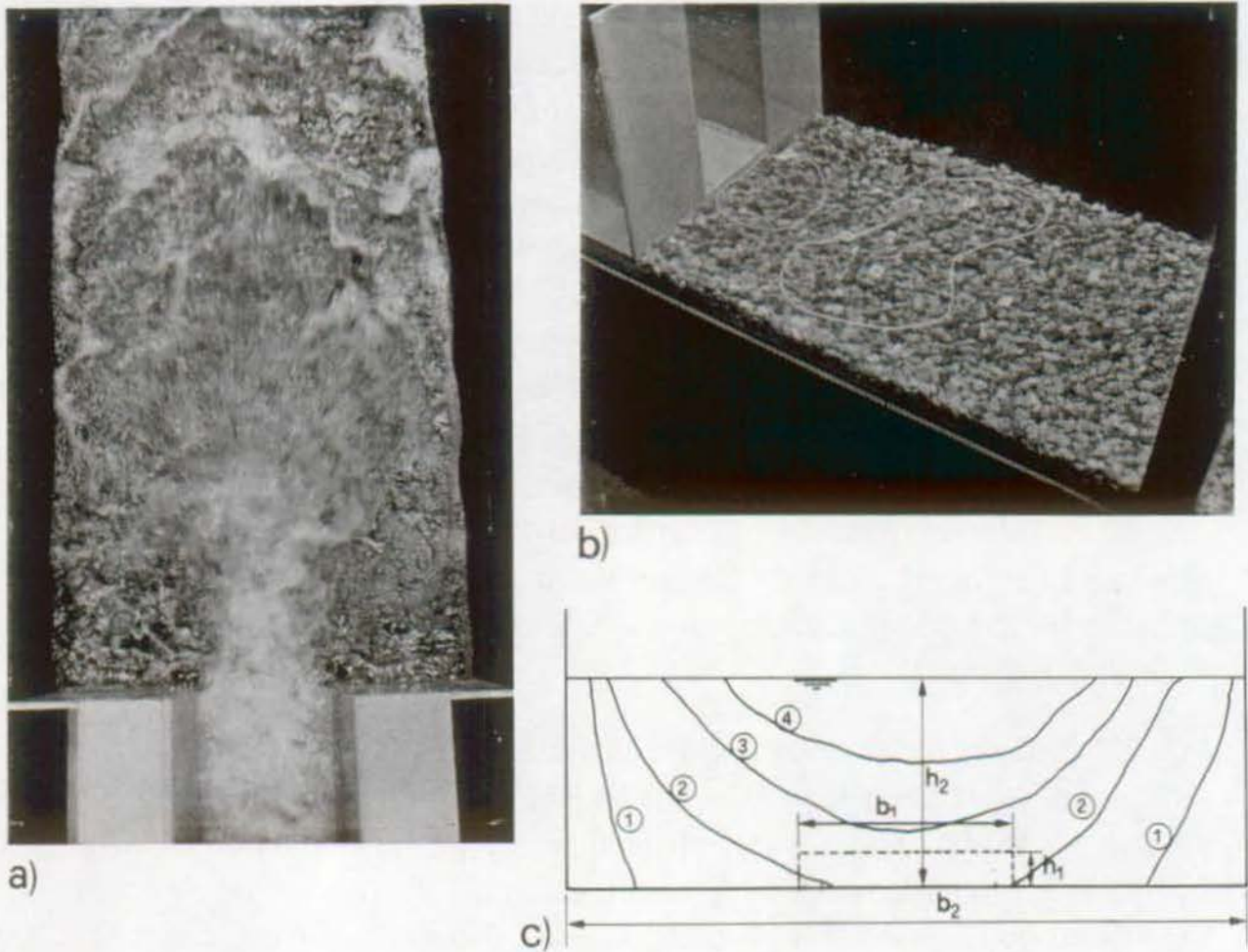


Fig. 7.3 : a) Effect of deflector on flow pattern for $X_1=0.31$. b) Gravel bed erosion after 10 minutes operation. c) Velocity distribution in the tailwater channel. ① $V \approx 0.1$ m/s; ② $V \approx 0.2$ m/s; ③ $V \approx 0.3$ m/s; ④ $V \approx 0.4$ m/s.

Further experiments were conducted with the same deflector when fixed on a negative step located at the expansion section instead of the arrangement according to Fig. 7.1. Yet, no significant flow improvement was noted. For deflectors located downstream from the expansion section, symmetrical flow conditions were difficult to obtain.

A deflector is unable to expand the inflow over a limited reach of tailwater channel. Expanding dissipators with deflectors become too long.

Fig. 7.2 shows a typical flow configuration for $X_1=0.14$, $F_1=5.9$, $h_1=2.5\text{cm}$, and $V_1=2.92\text{ m/s}$ which results in $Y^*=7.84$ and $h_2^*=19.7\text{cm}$. The tailwater depth measured amounted to approximately $h_2=15.0\text{cm}$ from the average gravel bed level (Fig. 7.2c). An overall symmetric flow with high velocities located at the center of the channel was observed. The hydraulic jump may be subdivided into three main domains. In the first domain, located directly downstream from the expansion, the inflowing jet is subjected to the lateral pressure of the side eddies. The width of the inflowing jet is thereby slightly reduced (Fig. 7.2a). The flow located in the lateral expansions is stagnant without much participation in the dissipation phenomena. Where the main stream attains the flow surface domain ② starts. From there, the jet expands gradually until the high velocity stream occupies the entire channel width. The main part of the energy dissipation occurs at the downstream end of this second domain. The third domain ③ is characterized by a plunging zone well observed in Fig. 7.2c). It occupies the entire channel width and seems to be less concentrated than for prismatic channels, therefore. Downstream from this third domain, the flow is uniformly distributed across the channel width and air detrains. The deflection of the main stream and the subsequent plunging current create a significant backward flow under the deflector.

Fig. 7.3a) shows the flow pattern for the inflow conditions of Fig. 7.2 but when increasing the toe position to $X_1=0.31$. Except for a reduction of the jet contraction domain (① in Fig. 7.2), the overall jump characteristics remain unchanged. Fig. 7.3b) gives a qualitative picture of the domains of erosion and sedimentation. Significant bed erosion was recorded directly downstream from the deflector. A second, less pronounced domain of erosion could be observed in the plunging region. Upstream from the plunging zone, in the central part of the channel, a limited zone of deposition is indicated in Fig. 7.3b). Fig. 7.3c) shows the velocity distribution measured in the tailwater channel. The location of the jump end section was fixed according to the definition used in chapter 5. A high velocity stream is seen to be concentrated in the center of the channel near to the flow surface. Since the velocity measurements were performed with a propeller meter (chapter 4), backward flow could not be excluded for $V<0.1\text{ m/s}$.

Based on these observations, the effect of a deflector located at the expansion section is similar to observations made in prismatic channels (Peterka 1983). Such jumps are characterized by a significant length as well as by a plunging phenomena involving an additional energy dissipation. The expansion of the main stream from b_1 to b_2 requires a significant length, especially for small values of X_1 . To reduce the jump length, particular attention should be paid to rapid expansion of the inflowing jet. Furthermore, the flow in the lateral expansions should better participate in the

of the lateral eddy domain. Based on these unfavorable observations, following investigations were limited to sills located downstream from the expansion section. Fig. 7.4 shows the domain of investigated sill heights S and sill positions x_s/h_2 .

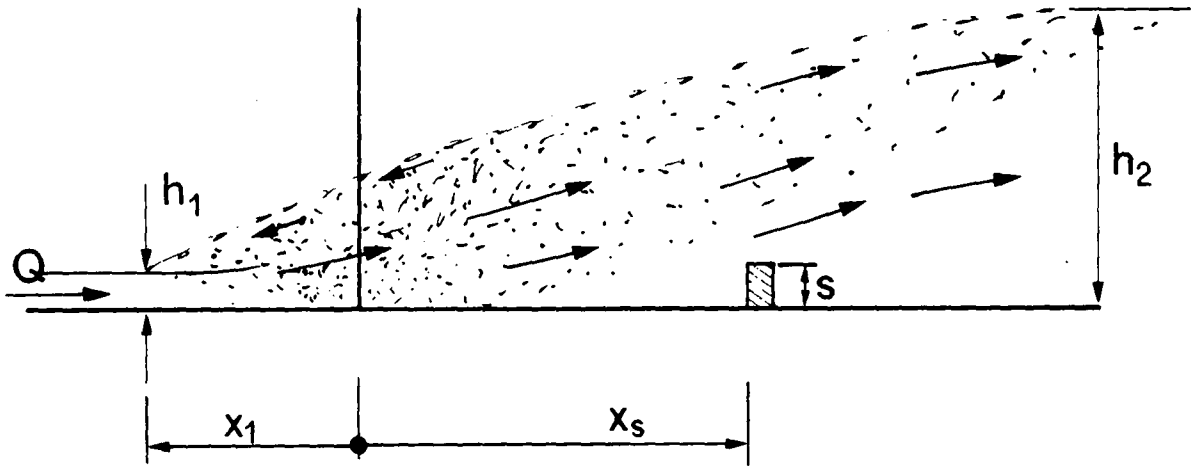


Fig. 7.4 : Notation for sudden expansion with sill. Domain of investigated sill heights $0.5 < S = s/h_1 < 2$ and sill positions $0.5 < x_s/h_2 < 3$.

Effect of sill position

In the first run, a sill of height $S=1$ was investigated for different sill positions x_s relative to the channel expansion. Fig. 7.5 shows the jump characteristics for the sill located at a distance h_2 downstream from the expansion section.

Comparing Fig. 7.5a) with Fig. 7.2a) a significant improvement of the overall flow patterns can be observed. The contraction of the inflowing jet as observed with deflectors disappears at the presence of a sill. Also, the expansion of the main stream is almost radial, and completed a short distance downstream from the sill and seems to be more pronounced than with the step. The flow in the lateral side eddies is much more turbulent than reported in paragraph 7.2.

According to the length definition based on the air detrainment, Fig. 7.5c) shows a jump with a reduction of about 15% of the length as compared to Fig. 7.2c). The plunging zone downstream from the wave is well distributed (Fig. 7.5b) and less pronounced than with the negative step. The radial expansion of the inflow jet obtained with the sill is higher as with the deflector. Based on this first impression, the flow pattern is significantly improved using a sill of height $S=1$, therefore.

The effect of the sill position for otherwise constant hydraulic conditions is demonstrated in Fig. 7.6. In Fig. 7.6a) the same position as in Fig. 7.5 is considered.

7.3 SILLS

7.3.1 Introduction

The effect of sills on the flow pattern in prismatic channels was investigated extensively in the past by Rand (1957), (1965), (1966), (1967), McCorquodale and Regts (1968), Rajaratnam (1971) and Bretz (1987). Based on these investigations, the sequent depths ratio Y_s^* may be expressed as

$$Y_s^* = Y_s^*(F_1, S, K_1) \quad (7.1)$$

where $S=s/h_1$ and K_1 is a position parameter accounting for the distance between the sill and the jump toe. In prismatic channels, the main effect of continuous sills is to stabilize the toe position for various tailwater levels. However, the contribution of the sill has a relatively small influence on the energy dissipation (Bretz, 1987). In case of nonprismatic geometries, the requirements for the sill are different. In order to reduce the length of jump as much as possible, the sill should provide symmetric flow for a wide range of tailwater levels.

In paragraph 5.6 it was quantitatively shown that the effect of the inflowing Froude number on the flow symmetry is of second order compared to the effect of the toe position. Furthermore, it has also been outlined that the asymmetry increases with a reduction of X_1 . Therefore, if the flow is symmetric for a given value of X_1 , it will also remain symmetric for larger values of X_1 .

Based on these considerations, the parameters investigated qualitatively were limited to the sill height s and to the influence of the sill position X_s relative to the expansion section. Furthermore, the experiments were conducted with small values of X_1 (typically $X_1 < 0.2$) and considering only one expansion ratio B .

7.3.2 Experiments

Fig. 7.4 shows a schematic plot of a sill-controlled hydraulic jump in an abrupt expansion. The location of the sill relative to the expansion section is x_s and the toe position is x_1 . The height of sill s will be also normalised by the inflow depth h_1 , as previously discussed. Note that x_s is positive in the direction of flow.

Preliminary runs were conducted with a sill located at the expansion section of height $S=s/h_1=1$. The effect of the sill is an upward deflection of flow and the formation of a wave at the rear sill side. The top of the wave was significantly higher than the tailwater level. The downstream plunging stream hit the channel bottom on a large surface and produced an significant scour. Also, there was only a small participation

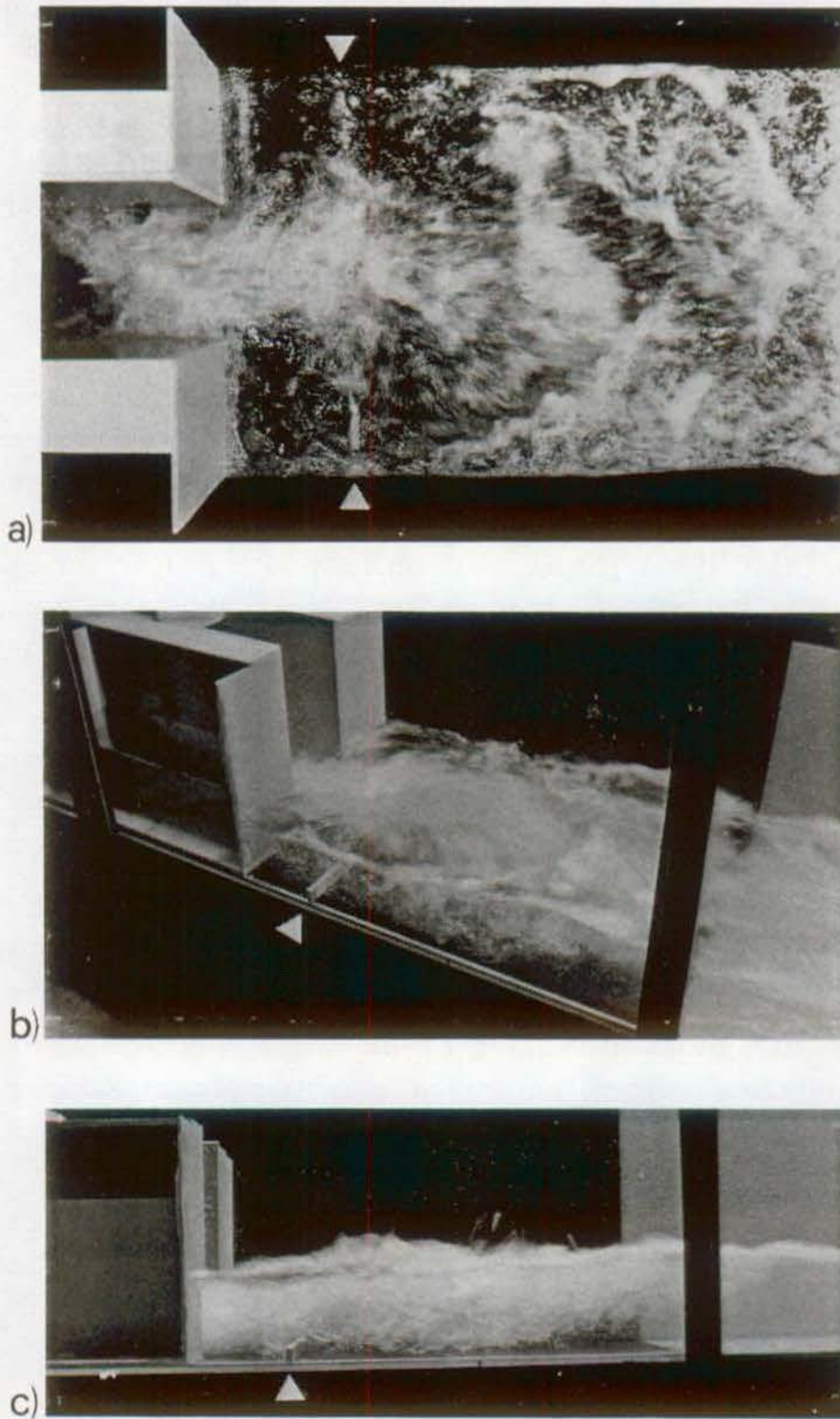


Fig. 7.5 : Effect of a sill of height $S=1$ located at $x_s/h_2=1$ downstream from the expansion section. $F_1=5.9$, $h_1=2.5\text{cm}$, $V_1=2.92\text{ m/s}$, $X_1=0.12$ and $h_2=14.8\text{cm}$. (\blacktriangle) Position of sill.

Fig. 7.6b) shows the flow pattern when the sill is located $1.5 \times h_2$ downstream from the expansion, whereas in Fig. 7.6c) the distance between the expansion and the sill amounts to $2.0 \times h_2$. The sequent depths ratios for the three flow configurations remain unchanged at $h_2=14.8\text{cm}$.

Fig. 7.6 outlines the sensitivity of jump symmetry on the sill position. A relative small displacement of the sill modifies considerably the jump symmetry. The flow pattern observed in Fig. 7.6c) is similar to the jump in an expansion without appurtenances (chap. 5). To produce a significant effect on the jump, the position x_s/h_2 of the sill is limited. On the other hand, for $x_s/h_2=0$ (sill located at the expansion section) the flow is mainly deflected upward combined with a poor jet expansion.

As indicated in Eq. (7.1), the sequent depths ratio in a prismatic channel depends on the inflow Froude number F_1 , the relative sill height S and a sill position parameter. For abruptly expanding channels, the limit position x_{sL} for which symmetric flow prevails seems to depend on F_1 , S , B and X_1 . The effect of sill shape can be neglected according to Bretz (1987). The most unfavorable flow conditions correspond to large expansion ratios and small values of X_1 . Thus, as was verified experimentally for a symmetric jump with a small value of X_1 , its flow symmetry is maintained at increasing values of X_1 provided B remains constant.

It should be noted that the position of the sill was normalised to h_2 in order to account for the length of jump. In chapter 8, another normalising quantity will be used to account for the effect of relative sill position.

Effect of sill height

In the second run, the experiments of the first series were repeated by considering a sill of height $S=2$. Fig. 7.7 shows the effect of sill position on the jump flow for three different locations. As observed in Fig. 7.6, the sill may influence positively the jump symmetry if located sufficiently near to the expansion section. A closer comparison between Fig. 7.6 and Fig. 7.7 shows a significant difference of the flow in the lateral eddies. Increasing the sill height to $S=2$ leads to a more pronounced vorticity in the lateral eddies. This phenomenon is clearly observed when comparing Fig. 7.6a) with Fig. 7.7a) in which the sill positions are identical. In Fig. 7.7b) the air entrainment of the lateral eddies is still significant, whereas in Fig.7.7c) the lateral eddies could be easily distinguished from the main stream.

Fig. 7.8 shows the flow conditions for $x_s = 2 \times h_2$. In order to estimate the effect of the plunging stream on the channel floor, an erodible channel bed was installed in the plunging jet zone.

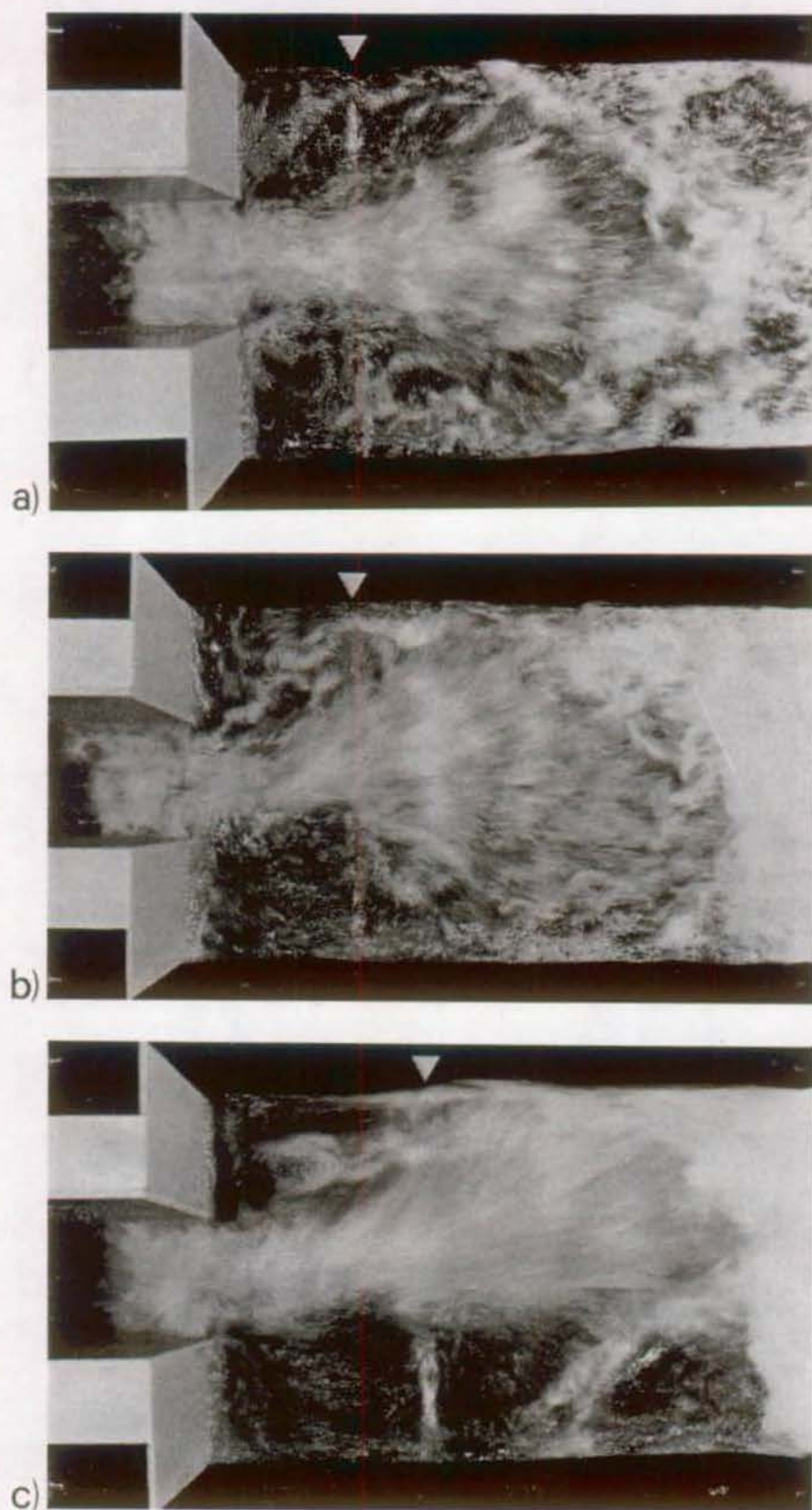


Fig. 7.6 : Effect of sill position on jump symmetry with $S=1$. All other flow characteristics as in Fig. 7.5. a) $x_s/h_2 \cong 1.0$, b) $x_s/h_2 \cong 1.5$, c) $x_s/h_2 \cong 2.0$. (\blacktriangle) Position of sill.

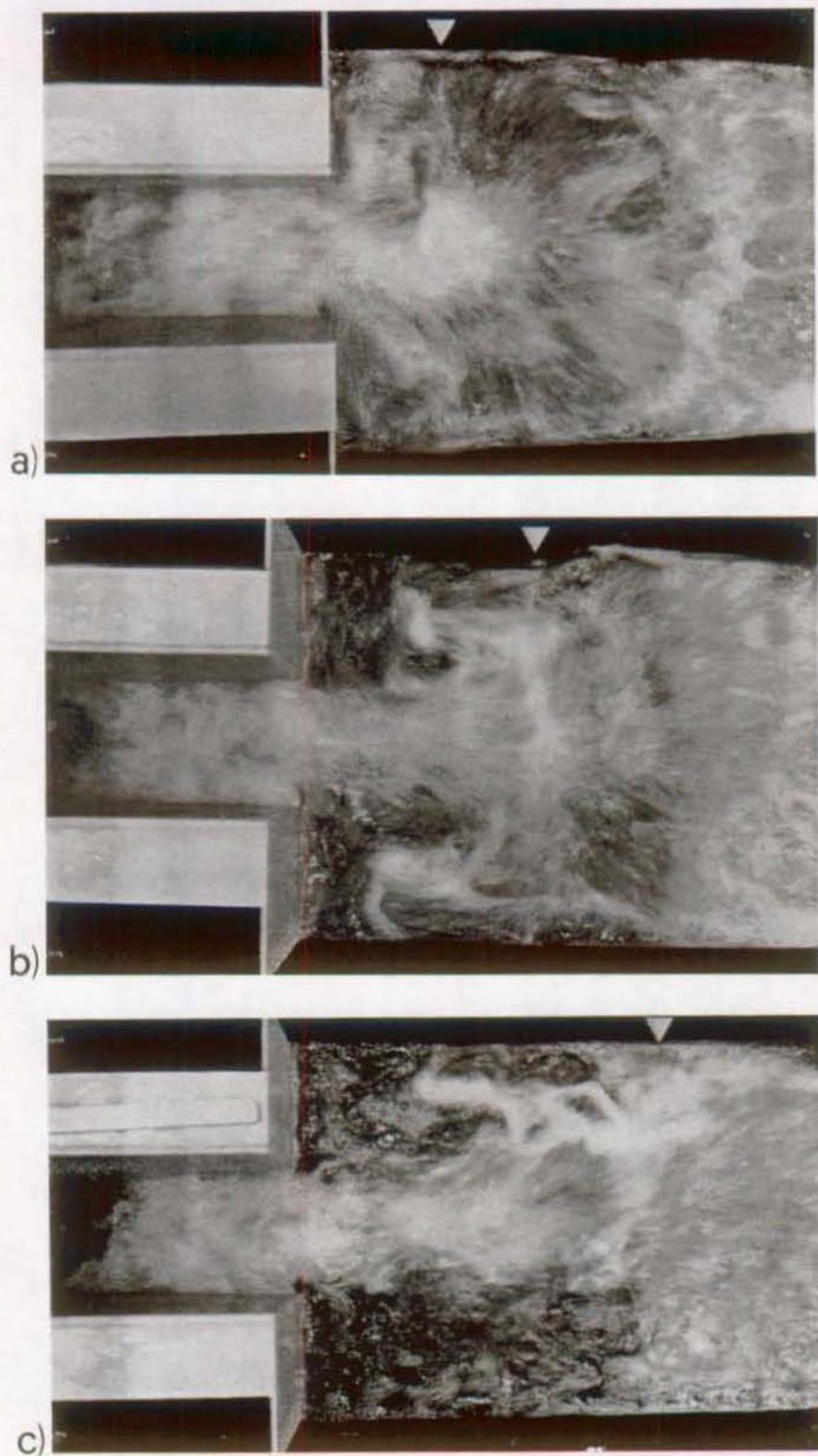


Fig. 7.7 : Effect of the sill position (\blacktriangle) on the flow symmetry. Hydraulic conditions : $F_1=5.95$, $h_1=2.45\text{cm}$, $V_1=2.96\text{ m/s}$, $0.18 < X_1 < 0.22$, $h_2=15.6\text{cm}$. a) $x_s/h_2=1$; b) $x_s/h_2=2$; c) $x_s/h_2=3$.

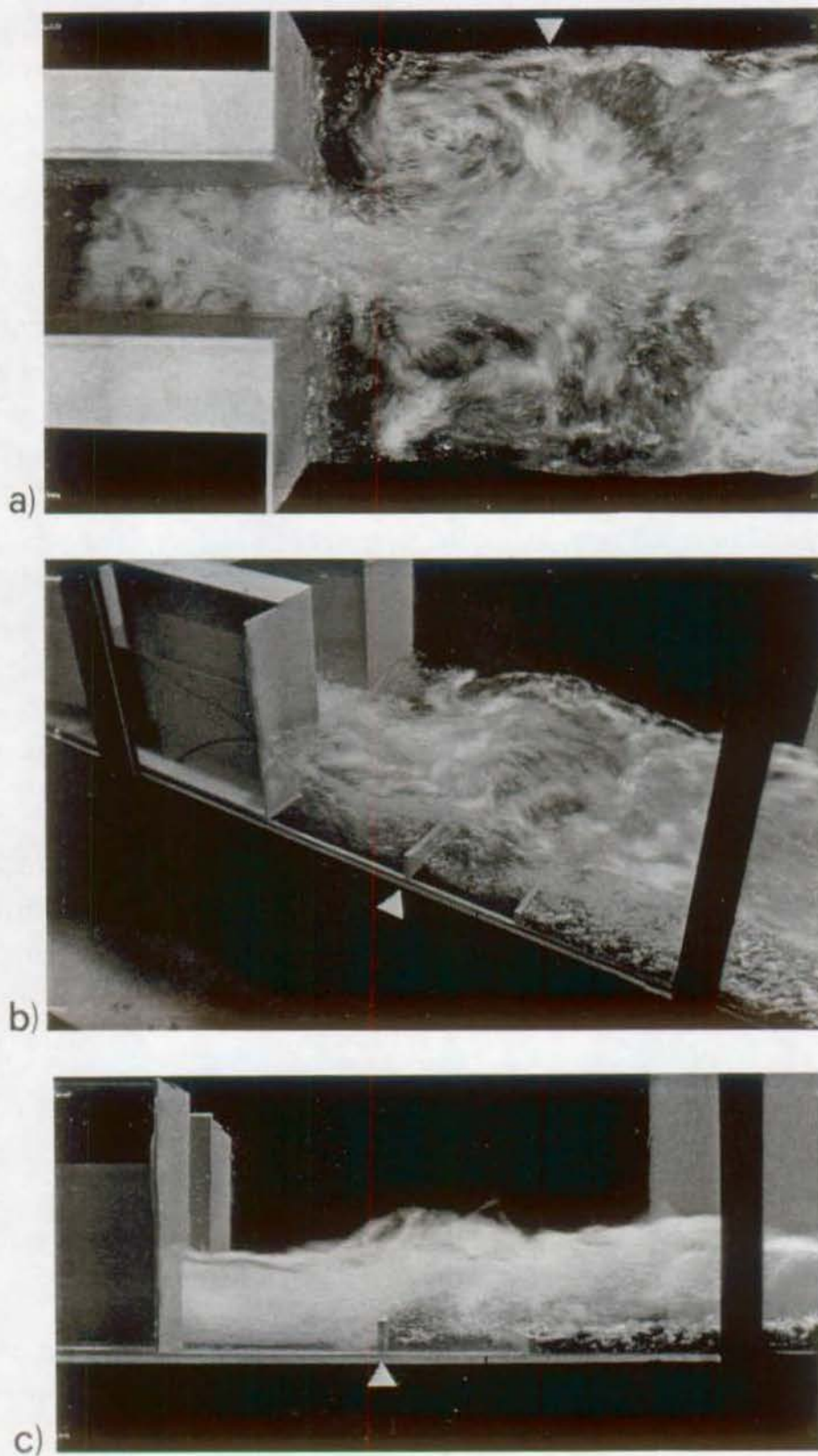


Fig. 7.8 : Effect of a sill of height $S=2$ located at $x_s=2 \times h_2$ downstream from the expansion section. Hydraulic conditions identical to Fig. 7.7. (\blacktriangle) Position of sill.

Comparing Fig. 7.8 to Fig. 7.5 where $S=1$ shows an improved lateral expansion of the main stream for $S=2$. In Fig. 7.8b) the standing wave generated by the sill is well distributed across the channel width and short in length. Due to the increased flow "activity" in the lateral eddies, the flow depths along the expansion side walls decrease, and thereby improve the expansion of the main stream. As a result, no erosion on the channel floor could be observed after 15 minutes of operation.

Effect of transverse sill extent

For sills located relatively near to the channel expansion as previously considered, the width of the main stream section occupies only the approaching channel width. In the lateral channel zones, backward flow prevails. Therefore, the effect of the transverse sill extent on the jump was investigated. Fig. 7.9 shows the sill geometry considered as well as the resulting flow configurations for two different sill locations. In Fig. 7.9b) the sill position is $x_s=0.5 \times h_2$, whereas in Fig. 7.9c) the distance between the expansion section and the sill is $x_s=1 \times h_2$. A comparison between Figs. 7.7b) and Fig. 7.9c) indicates a practically unchanged flow pattern. Therefore, the difference between a sill slightly larger than the width of the upstream channel and a sill across the entire downstream channel is negligible. Thus, to improve the flow pattern in sudden expanding channels, devices fixed on the channel bottom may be effective only in the zone in front of the inflowing stream.

To reduce the wave-height formed at the rear side of the sill and to investigate the effect of the plunging zone on the channel bed, some additional experiments were conducted by considering both negative steps and sills. It was expected to combine the positive influence of both devices on the jump symmetry. The investigation considered a negative step of height $N=1$ located at the expansion section and a sill of height $S=2$ located at different positions.

The improvements expected for the flow characteristics were not attained. Over a wide range of X_1 and several sill positions, the flow was asymmetric and frequent oscillations of the main stream prevailed. Based on these preliminary observations, the combination of negative step and sill was not further considered.

The sill positioned in an expanding dissipator may definitely improve the flow pattern. Its effect depends significantly on the position, the height and the lateral extent of the sill.

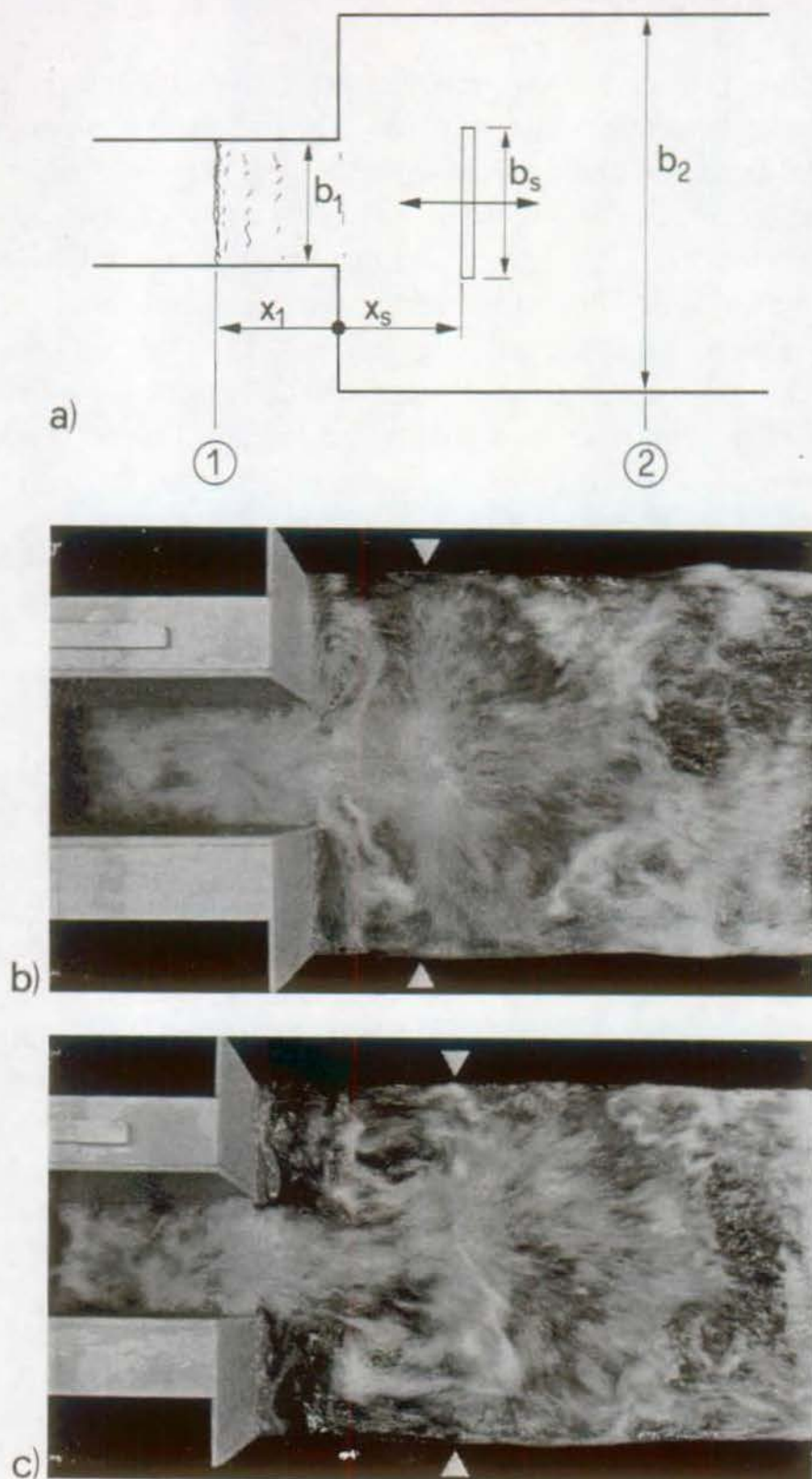


Fig. 7.9 : Effect of sill width on the jump symmetry for $S=2$. Hydraulic conditions identical to Fig. 7.7. a) Sill geometry, $b_s=20.0\text{cm}$, $b_1=16.5\text{cm}$ and $B=b_2/b_1=3$. $0.5 < x_s/h_2 < 2$. Sill located at b) $0.5 \times h_2$ and c) $1 \times h_2$. (\blacktriangle) Position of sill.

7.3.3 Conclusions

The observations presented in the preceding paragraph show that a significant flow modification may be obtained by continuous sills. The effect of the sill is a rapid and efficient radial expansion of the inflowing stream. The two lateral eddies are involved in the dissipation phenomena, instead of corresponding to stagnant water zones. The standing wave formed on the sill is well distributed across the tailwater channel width. As indicated by the experiments, the sill width could be limited to approximately the width of the inflowing channel. The plunging zone downstream from the standing wave has a radial shape without any flow concentration at the channel axis. The favourable flow distribution led to a limited depth of plunging stream as was verified by the qualitative measurements of bed erosion .

For an optimization of the expansion design, particular attention should be paid to the sill height as well as to the sill position relative to the expansion section. The final design recommendation shall be discussed in chapter 8.

7.4 Baffle piers

Based on the satisfactory flow pattern obtained with continuous sills, similar results were expected with dentated sills or baffle piers. For the design of stilling basins, baffle piers are usually preferred to continuous sills. Besides the additional energy dissipation, this type of appurtenance resulted in a reduced basin length, compared to the length without baffle piers (Peterka 1983). A dentated sill has a further advantage in that the high velocity stream is less deviated away from the channel bottom. As a result, the formation of standing waves is greatly inhibited, and plunging does not occur as strongly as with deflecting sills.

The first series was carried out with 5cm cubic blocs. The sharp-edged blocks had a spacing of 5cm (50 % of obstruction) and were fixed on the channel bottom using a 0.5cm high PVC plate. The flow pattern observed for this block configuration and inflow conditions identical to Fig. 7.8 are shown in Fig. 7.10.

The standing wave formed at the rear of the continuous sill (Fig. 7.8 b and c) is strongly reduced using baffle piers. For this type of appurtenance, the flow depth is uniformly distributed in the tailwater channel. However, as outlined in Fig. 7.10a), the hydraulic jump is clearly asymmetric with significant stagnant zones downstream from the expansion section. Compared to the flow pattern without any appurtenance only a slight improvement of flow may be obtained.

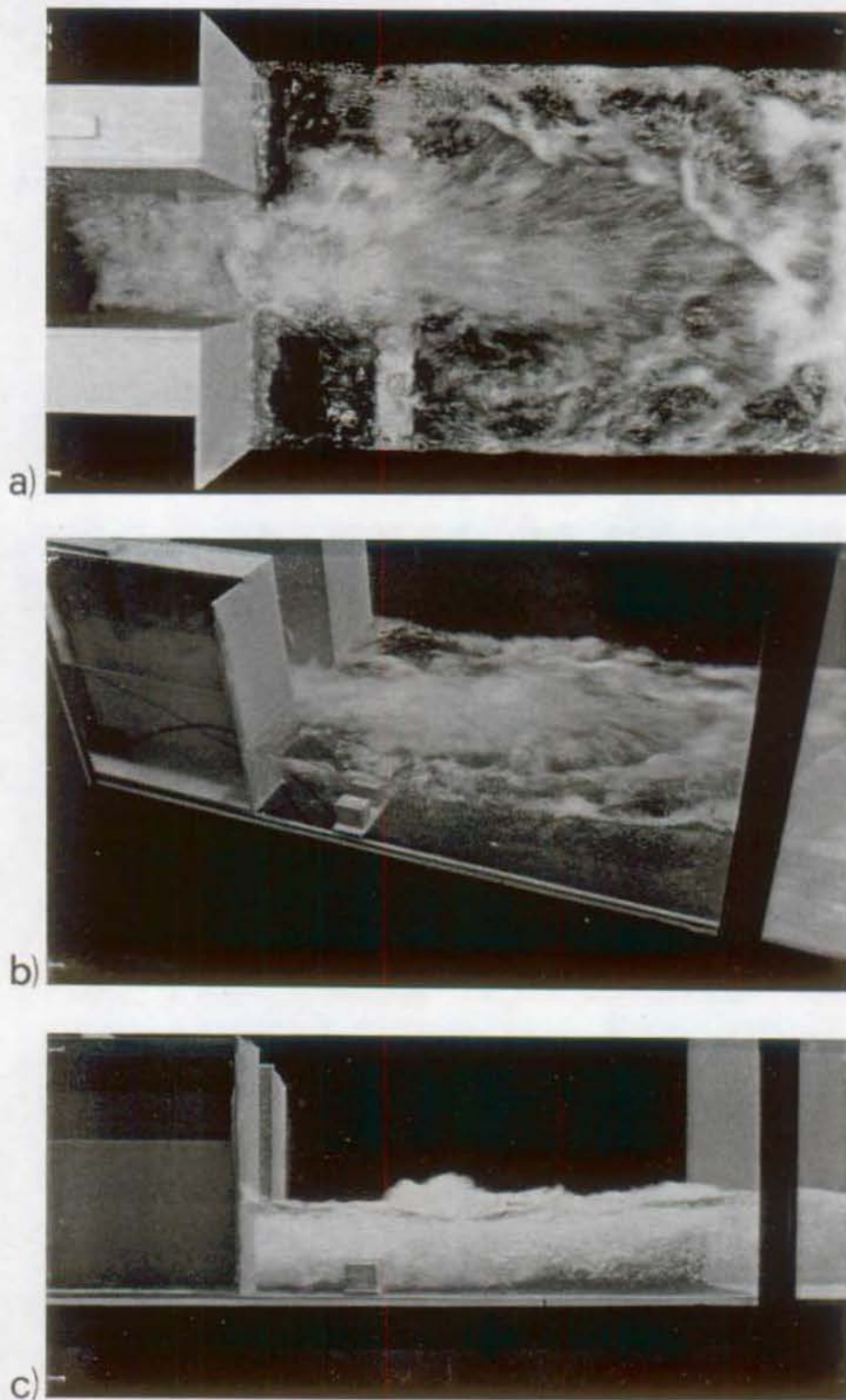


Fig. 7.10 : Overall flow pattern observed with baffle piers located at $x_s=1x_{h2}$ downstream from the expansion section. Hydraulic conditions identical to Fig. 7.8. For details see text.

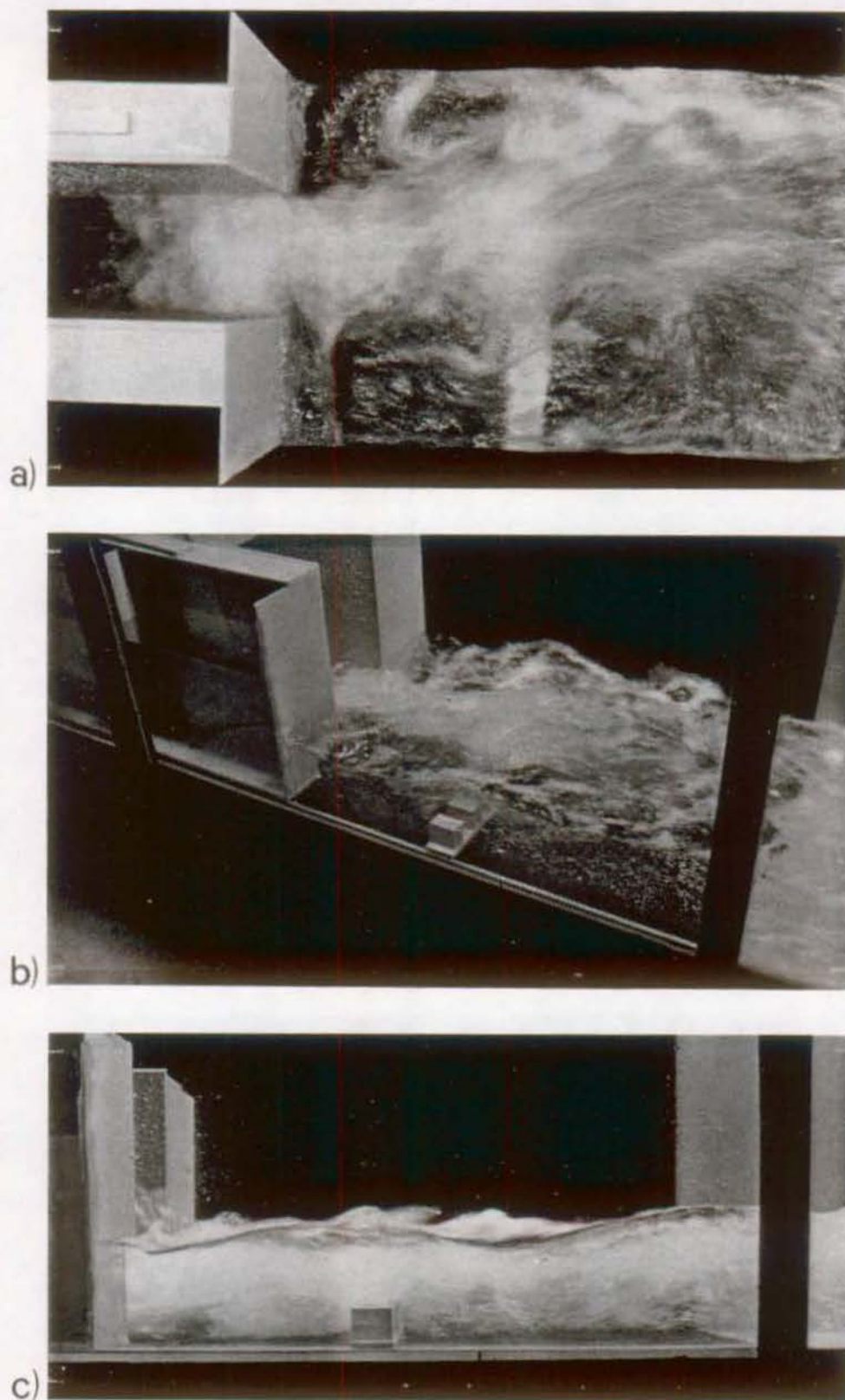


Fig. 7.11 : Overall flow pattern observed with baffle piers located at $x_s=2xh_2$ downstream from the expansion section. Hydraulic conditions identical to Fig. 7.8. For details see text.

To investigate the effect of position of the baffle piers on the flow symmetry, different pier locations were investigated experimentally. Fig. 7.11 shows the flow observed with cubic baffle piers located at $x_s=2xh_2$. It is seen that the appurtenances have practically no effect on the flow.

It is important to note that the total surface of baffle piers facing the inflowing stream is approximately $5(5\text{cm} \times 5\text{cm})=125\text{cm}^2$. In the preceding paragraph, symmetric flow conditions were obtained with a 20cm wide and 5cm high sill located at the same position as the baffle piers in Fig. 7.11. Therefore, for identical flow conditions and identical position of the appurtenances, a continuous sill slightly larger than the inflowing channel leads to flow conditions significantly better than baffle piers.

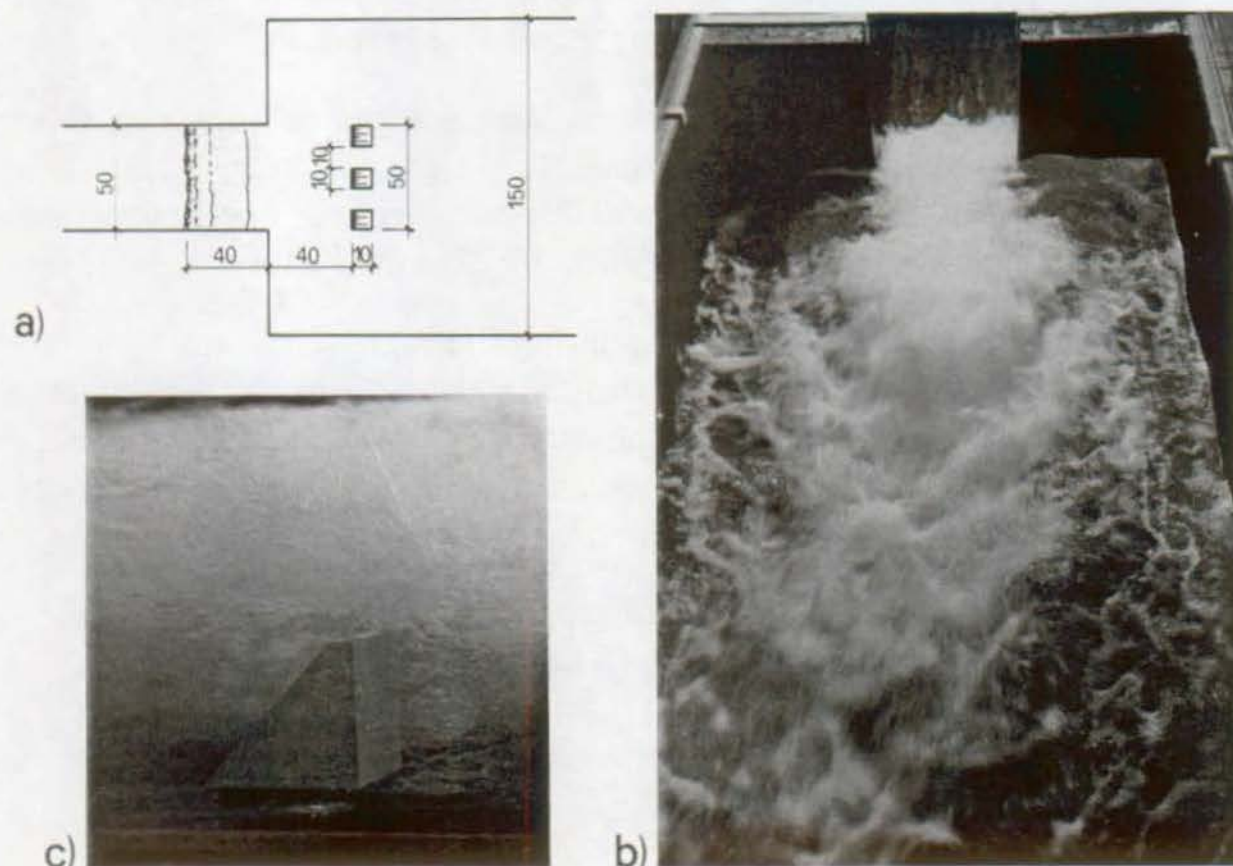


Fig. 7.12 : Flow features observed with standard USBR baffle piers in channel LCH2. a) positions and dimensions of baffle piers. b) downstream view of the jump. c) detailed view of one baffle pier. Hydraulic conditions : $h_1=5.0\text{cm}$, $F_1=8.94$, $Q=156,6$ l/s, $X_1=0.15$, $h_2=41.3\text{cm}$.

Despite the unsatisfactory results obtained with baffle piers, a further series of experiments was performed with this type of appurtenance. The purpose of the additional series was to investigate the behaviour of baffle piers designed according to the USBR standard. In order to provide sufficient dimensions of the USBR baffle piers, the experiments were performed in installation LCH2.

Based on prior observations the baffle blocks were limited to the central part of the tailwater channel, in front of the inflowing stream. The position and dimensions of the blocks are shown in Fig. 7.12a).

For an inflow depth of $h_1=5.0\text{cm}$ and a total head of $H=2.0\text{ m}$ an inflowing Froude number of $F_1=8.94$ was obtained. According to Basco (1971), the optimum efficiency for such flow conditions may be performed with baffle piers of $S=s/h_1\cong 2$ located at approximately $1.7h_2^*$ ($h_2^*\cong 60\text{cm}$) from the toe of the jump.

Following these recommendations the non-prismatic channel geometry, was fitted with three blocks, each 10cm wide and 10cm high, 40cm downstream from the expansion section on the channel bottom. The tailwater level was set to obtain a toe position approximately 40cm upstream from the expansion section ($X_1=0.15$).

Despite a limited expansion of the inflowing stream, the flow was asymmetric as shown in Fig. 7.12b). In the tailwater channel, a high velocity flow was concentrated along one channel side, whereas at the opposite side, backward flow prevailed as described in chapter 5. Based on this additional experiment, the inefficiency of baffle piers to improve the flow pattern was demonstrated.

Baffle piers located in expanding dissipators are unable to improve symmetry and expansion of flow, and therefore were not further considered.

7.5 Conclusions

Hydraulic jumps in sudden expansions without any appurtenance are usually characterized by strongly asymmetric flow. Non-prismatic stilling basins must be equipped with elements by which the performance of the dissipating structure is improved. For inflowing Froude numbers larger than 3, a definite improvement may be obtained by selected appurtenances as was discussed in this chapter.

In order to reduce the jump length and to improve the velocity distribution, a sill located downstream from the expansion section seems to be an effective device. Experimental observations described in paragraph 7.3 indicated an optimum height S

between $1 < S = s/h_1 < 2$. The optimum spacing of the sill from the expansion section seems to be included between $1xh_2$ and $2xh_2$. In chapter 8, both sill height S and sill position x_s will be optimised for a definite design.

Experiments conducted with baffle piers led to unsatisfactory flow conditions. As described in paragraph 7.4, baffle blocks designed according to the USBR standard led to asymmetric flow with a limited expansion on the inflowing jet. It seems, therefore, that baffle piers are ineffective to improve the flow pattern in channel expansions.

8. SUDDEN EXPANSION WITH CENTRAL SILL

8.1 INTRODUCTION

According to chapter 7, a continuous central sill in sudden expansions has proven effective in terms of jump symmetry and jump length. The sill, which is located shortly downstream from the expansion section, should be slightly wider than the inflowing channel width. Compared to baffle piers, deflectors or negative steps, a sill leads to compact and highly efficient jumps. In addition to significant dissipative contribution of the lateral eddies, the velocity is uniformly distributed in the tailwater channel.

The purpose of this chapter is to investigate sill-controlled hydraulic jumps in a sudden expansion. Particular attention will be paid to the optimization of the sill position relative to the expansion section, and the sill height. Based on an experimental investigation, design recommendations will then be developed.

Paragraph 8.2 aims at describing the criteria used to estimate the performance of this type of stilling basin, whereas in paragraph 8.3 the experimental program is presented. In paragraphs 8.4 and 8.5 the effects of the central sill on the sequent depths ratio and on the jump length are discussed. In order to ensure an optimal performance of the dissipator design recommendations for the central sill are presented in paragraph 8.6. For a better visualization of the flow improvement obtained with a sill, experiments conducted with an erodible channel floor will be presented in paragraph 8.7. Cavitation aspects to be considered in relation with appurtenances fixed on the floor of stilling basins will be discussed in paragraph 8.8. Finally, in paragraph 8.9, a numerical example illustrates a preliminary design procedure for sudden expanding stilling basins provided with a central sill.

8.2 STILLING BASIN PERFORMANCE

As described in paragraph 7.1 the performance of a stilling basin involves several requirements. For the optimization of the sill geometry including sill position x_s and sill height s , these requirements will be evaluated by the experimental investigation. In the present paragraph the flow pattern will be described.

As regards the **jump symmetry**, three flow categories may be defined. The first category is characterized by «stable asymmetric flow» which occurs typically for small values of X_1 and basins without appurtenances. The second category includes jumps characterized by frequent lateral oscillations of the main stream. This flow pattern was typically observed in sudden expansions with negative steps (chapter 6). The third category includes symmetric jumps free of oscillations. From the point of view of design, the third type must evidently be strived for. Although the jump should be symmetric, some other jump characteristics must also be taken into account.

The second qualitative flow feature to be evaluated is the **wave formation** in the tailwater channel. In case of prismatic stilling basins, the wave formation is significant for inflow Froude numbers ranging between 2.5 and 4.5 (Peterka, 1983). In order to reduce the wave height Peterka proposed blocks, located on the sloping floor shortly upstream from the stilling basin. As shown in chapter 7, the waves formed at the rear of the continuous sill usually generate relatively high tailwater waves. As for the jump symmetry, the tailwater wave formation will be described by three categories, as is indicated in Table 8.1.

Table 8.1 : Qualitative flow patterns considered for the evaluation of the stilling basin performance.

Characteristic	Category I	Category II	Category III
Symmetry of jump	stable asymmetric	oscillating flow	symmetric
Tailwater waves	large, with spray	no spray formation	small
Vorticity of lateral eddies	nearly stagnant flow	small without air entrainment	significant, with air entrainment
Tailwater velocity distribution	highly nonuniform, with nearly stagnant flow zones	nonuniform but without stagnant zones	nearly uniform

Hydraulic jumps in sudden expansions are characterized by two lateral eddies located downstream from the expansion section. The characteristics and the **intensity of vorticity** of these eddies will also be evaluated by the experimental investigation. Nearly stagnant flow in the lateral eddies was typically observed with a deflector located at the expansion section (paragraph 7.2). The side deflection of the inflowing

stream due to the sill increases the «vorticity» of the lateral eddies, especially for $S > 1$ (paragraph 7.3). An increased participation of the lateral eddies in the dissipation phenomena facilitates a rapid expansion of the inflowing stream. Table 8.1 shows the descriptions adopted for each category. As will be seen, an intense vorticity in the lateral eddies may lead to a highly effective energy dissipation.

Finally, the **velocity distribution** at the jump end section will be considered. As shown in chapter 7, deflectors lead to high velocities in the central zone of channel near to the flow surface, whereas a more uniform distribution is obtained with sills. Distinction is made between highly nonuniform, nonuniform and nearly uniform tailwater velocity distributions.

The purpose of the experimental investigation presented in this chapter is to optimize the sill position and the sill height. Therefore, in addition to quantitative measurements (paragraph 8.3) the four items of Table 8.1 will be evaluated for each run. Hydraulic jumps for which the third category of each characteristic of Table 8.1 was recorded will then be used to optimize the sill geometry.

8.3 EXPERIMENTAL INVESTIGATION

In addition to the criteria described in Table 8.1, quantitative measurements were also performed. The parameters measured for each flow configuration are shown in Fig. 8.1 and the experimental data are collected in Appendix 3.

The standing wave formed at the rear side of sill may be characterized by its maximum height h_w and its downstream extremity, the so-called plunging point x_w . Due to the significant pulsations and spray formation an accurate measurement of these quantities was difficult, however. All observations were repeated at least once, therefore. As regards the maximum wave height h_w the point gauge was set such that it was submerged for approximately the half measuring time by the flow.

The downstream extent of the standing wave x_w was measured on the channel axis (Fig. 8.1a). x_w corresponds to the position where the plunging stream is submerged by the tailwater, as shown in Fig. 8.1b). For high tailwater levels (or large values of X_1) the main stream does not plunge and thus remains on the surface.

The tailwater level h_2 and the location of the jump end section x_j were recorded to evaluate the effect of sill on the sequent depths ratio and the jump length.

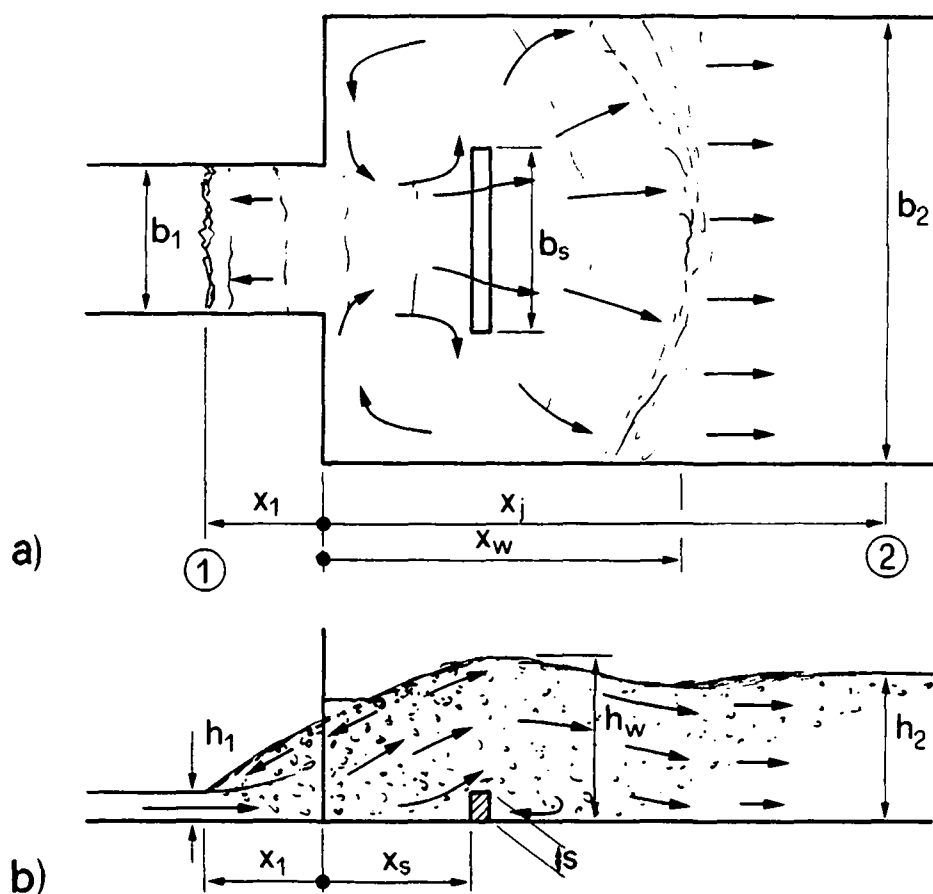


Fig. 8.1 : Quantities measured and notation used for jumps in sudden expansion with central sill. a) Plan view, b) axial view.

As was shown in paragraph 5.7, the asymmetry of jump seems to depend on the expansion ratio B , and on the non-dimensional toe position X_1 , but not on the inflowing Froude number. In order to reduce the number of parameters, the toe

Table 8.2 : Domains of B , S , F_1 , x_s and h_1 considered in the experimental investigation.

Series	b_2 [m]	B [-]	shape	F_1 [-]	S [-]		x_s [cm]		h_1 [cm]		X_1 [-]	No. of runs
					from	to	from	to	from	to		
3.1	1.5	3	sym	3, 5, 7, 9	0.6	3	20	80	2.5	7.5	0.2	78
3.2	1.0	2	sym	3, 5, 7, 9	0.6	3	20	80	2.5	7.5	0.2	75
3.3	0.75	1.5	sym	3, 5, 7, 9	0.6	3	20	80	2.5	7.5	0.2	60

position parameter X_1 was kept constant at $X_1=0.2$ for all series. Based on preliminary experiments, this toe position was found to yield symmetric flow with relatively low sills (less than $2S$). For channel expansions without appurtenances, the value of $X_1=0.2$ leads to pronounced asymmetric jumps involving significant backward flow along one channel side wall (chapter 5).

Depending on the inflow conditions h_1 and F_1 , the tailwater level was adjusted until the toe position corresponded to $X_1=0.2$. Table 8.2 shows the domains of B, S, F_1, x_s and h_1 analyzed in the three series. For each expansion ratio investigated, about 70 runs were performed. All experiments were conducted in channel LCH2.

8.4 SEQUENT DEPTHS RATIO

In this paragraph, the effect of the sill on the sequent depths ratio will be discussed. Fig. 8.2 shows the ratio Y_{ex}/Y_p as a function of S for series 3.1 and 3.2. Therein the sill position x_s varied between $20\text{cm} \leq x_s \leq 80\text{cm}$, whereas the toe position parameter X_1 was kept constant at $X_1=0.2$, as previously discussed. The predicted sequent depths ratio Y_p was computed according to Eq. (5.26) thereby neglecting the presence of the sill.

As shown in Fig. 8.2, the ratio Y_{ex}/Y_p is confined to $0.93 \leq Y_{ex}/Y_p < 1$ for an investigated sill domain of $0.7 \leq S \leq 3$ and four inflow Froude numbers (Table 8.1). An average reduction of the sequent depths ratio of 4 to 5% may therefore be attributed to the presence of sill. Due to this small reduction, it becomes difficult to split the separate effects of channel expansion, Froude number and sill on Y_{ex}/Y_p . Based on Fig. 8.2, no systematic influence of the sill parameter S and of the inflow Froude number could be distinguished. It should be outlined that the effect of the sill on Y is almost of the order of usual scatter of the experimental data.

The influence of a sill on the sequent depths ratio remains small provided $X_1 \geq 0.2$. Eq. (5.26) may be used to predict the sequent depth ratio in sudden expansions with a central sill, therefore. The computed tailwater level will exceed the measured value only by a few percents .

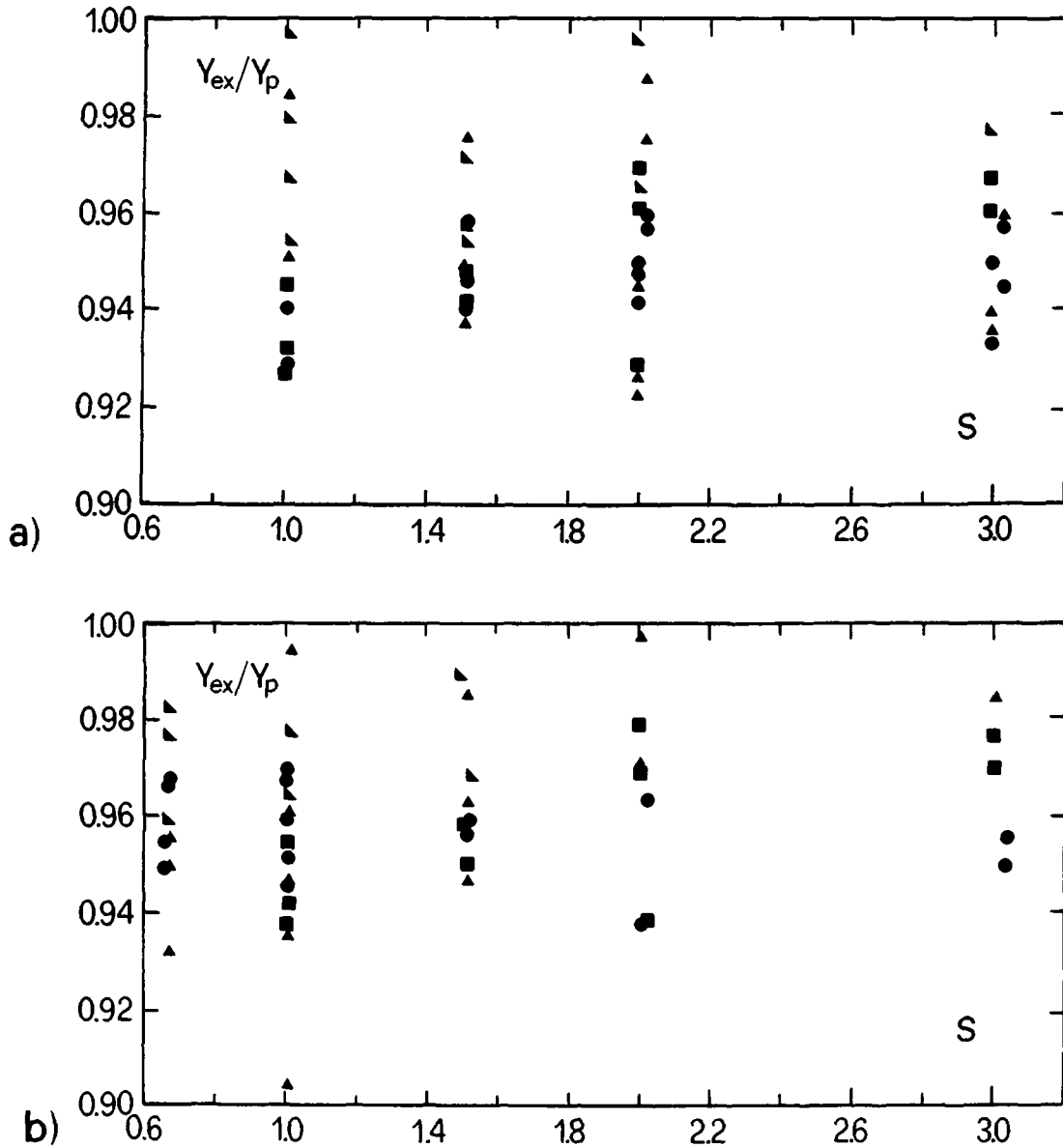


Fig. 8.2 : Y_{ex}/Y_p as function of S for different inflow Froude numbers. (\blacktriangledown) $F_1=3$; (\blacktriangle) $F_1=5$; (\bullet) $F_1=7$; (\blacksquare) $F_1=9$. a) Series 3.2 and b) series 3.1.

8.5 JUMP LENGTH WITH CENTRAL SILL

Based on the experimental data of the three series investigated, the effect of a central sill on the jump length will be evaluated hereafter. The jump end section was measured according to the definition in paragraph 5.2.

In Fig. 8.3 the ratio $L_{j,ex}/L_{j,p}$ is shown as a function of the inflow Froude number F_1 . Therein, the predicted jump length $L_{j,p}$ was computed according to Eq. (5.39)₁. Despite a scatter of approximately $\pm 10\%$ the influence of F_1 on the ratio $L_{j,ex}/L_{j,p}$ is definitely outlined. However, no systematic effect of the sill height and of the sill position on the jump length could be determined. A more extensive experimental investigation would be necessary for a better evaluation of their influences.

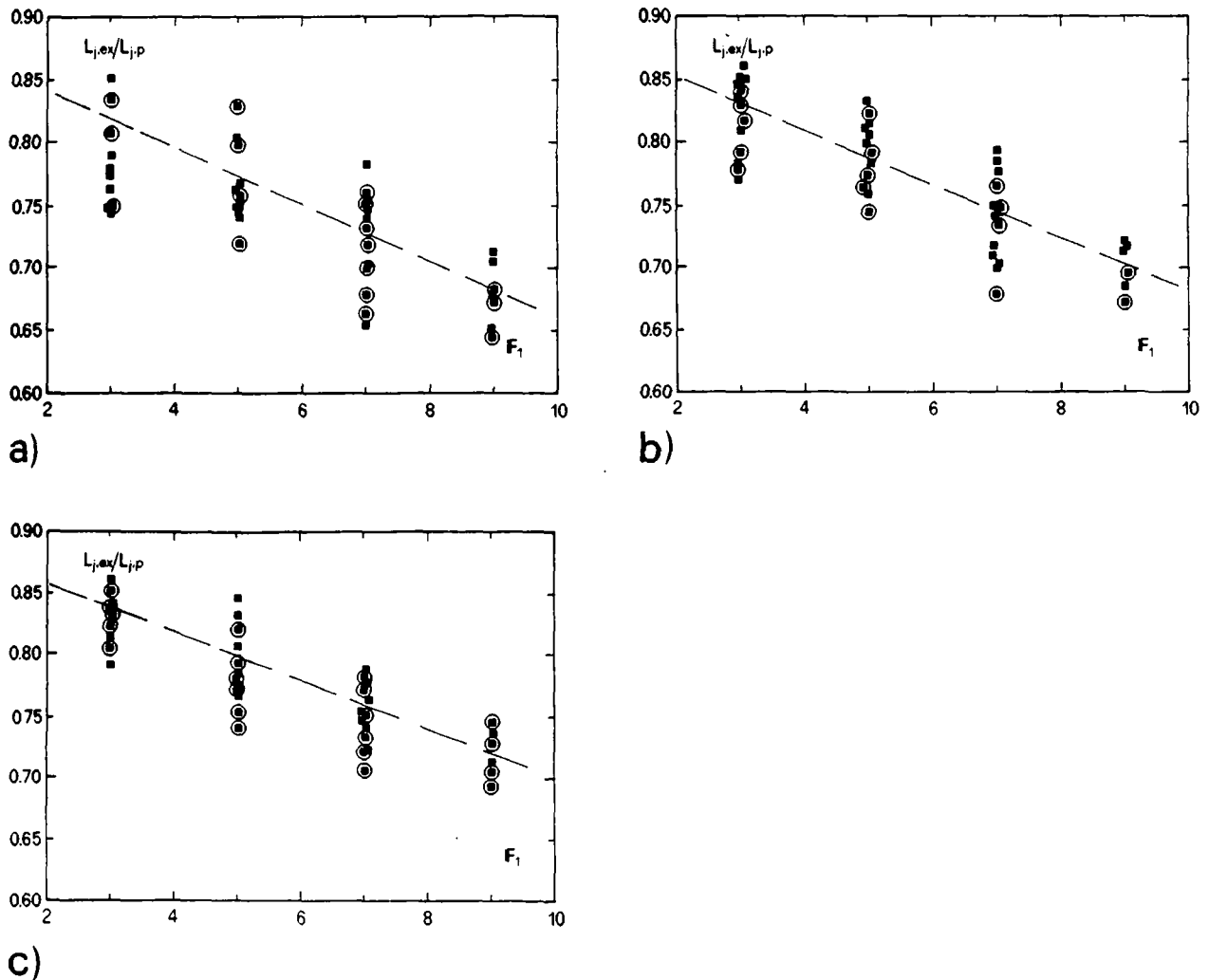


Fig. 8.3 : $L_{j,ex}/L_{j,p}$ as a function of the inflow Froude number F_1 for the expansion ratio a) $B=3$, b) $B=2$, and c) $B=1.5$ for (■) asymmetric jumps and (●) symmetric jumps. (---) Eq. (8.1).

Furthermore, as shown in Fig. 8.3, no effect of the expansion ratio B on the measured jump length may be observed. Based on this preliminary investigation, the jump length in sudden expansions with a central sill may be approximated as

$$L_{j,s} = L_j^* (1+\psi) \cdot (0.9-0.02F_1) \quad (8.1)$$

provided $0.6 < S < 3$, $X_s < 0.5$ and $2 < F_1 < 10$.

The length L_j^* of a classical jump is obtained with Eq. (5.5), whereas the function ψ depends on B and X_1 as given in Eq. (5.26)₂.

Compared to a sudden expanding channel without appurtenances, the presence of a central sill reduces the length of jump by approximately 20%, depending on the approaching Froude number F_1 .

8.6 JUMP SYMMETRY

8.6.1 Effect of sill position

Preliminary experiments in chapter 7 with sills seemed to indicate that the symmetry of hydraulic jumps in a sudden expansion depends on the expansion ratio B , the toe position X_1 and the sill geometry. The purpose of the present paragraph is to determine the parameters involved in the symmetry phenomenon. First a non-dimensional sill position parameter is defined to verify the assumptions of chapter 7. Then, the height of sill will be analysed for an optimum dissipator performance. The non-dimensional sill position X_s will be defined as

$$X_s = \frac{x_s}{L_r^*} \quad (8.2)$$

in accordance with parameters such as $X_1 = x_1/L_r^*$. x_s is the distance between the expansion section and the front face of sill (Fig. 8.1) and L_r^* is the roller length of a classical jump according to Eq. (5.4).

Fig. 8.4 shows the flow pattern of two jumps with identical parameters X_1 , F_1 , X_s , S and B . The inflowing depth in Fig. 8.4a) is $h_1 = 2.5\text{cm}$ and thus $L_r^* = 1.01\text{m}$ whereas an inflow depth of $h_1 = 7.5\text{cm}$ ($L_r^* = 3.03\text{m}$) is considered in Fig. 8.4b). In order to keep X_s constant the sill is located at $x_s = 20\text{cm}$ (Fig. 8.4a) whereas $x_s = 60\text{cm}$ in Fig. 8.4b). According to the conclusions of chapter 7 and the present assumptions, the flow pattern should then be similar in both figures.

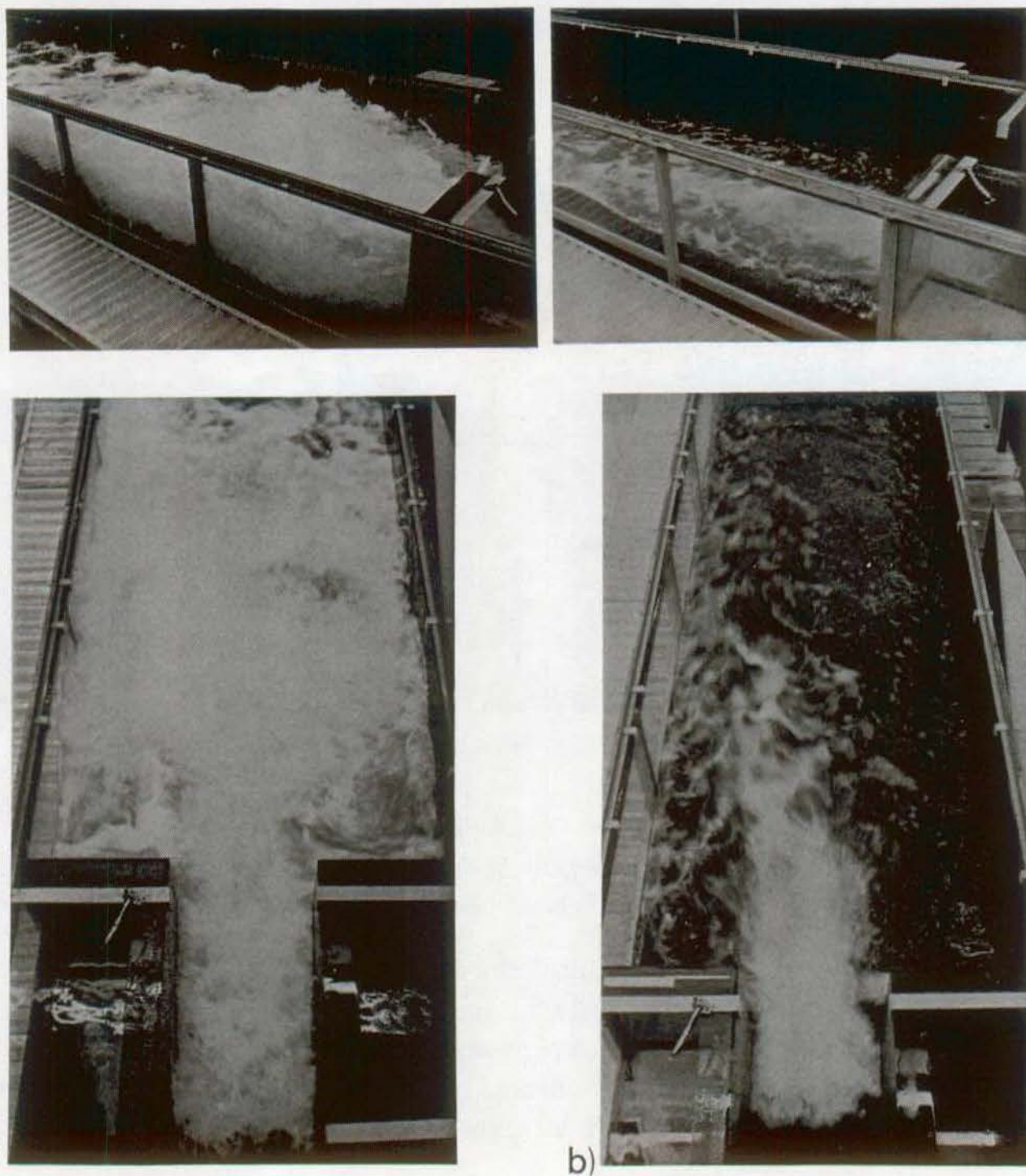


Fig. 8.4 : Flow pattern for identical parameters $F_1=7.0$, $X_1=0.2$, $X_s=0.2$, $S=1$, and $B=3$ but different inflow depths h_1 . a) $h_1=7.5\text{cm}$, $L_r^*=303\text{cm}$, b) $h_1=2.5\text{cm}$, $L_r^*=101\text{cm}$.

As shown in Fig. 8.4, the flow characteristics differ considerably, however. In Fig. 8.4a) the expansion of flow is poor with nearly stagnant flow in the lateral eddies. Thus, the jump becomes slightly asymmetric especially in the downstream, portion.

The jump shown in Fig. 8.4b) is symmetrical with a satisfactory expansion of the inflowing stream. The «vorticity» of the lateral eddies is clearly outlined by the motion of air bubble. Furthermore, the standing wave formed on the rear side of the sill is seen in Fig. 8.4b) but nearly non-existent in Fig. 8.4a). The jump in Fig. 8.4b) is thus much more forced than in Fig. 8.4a).

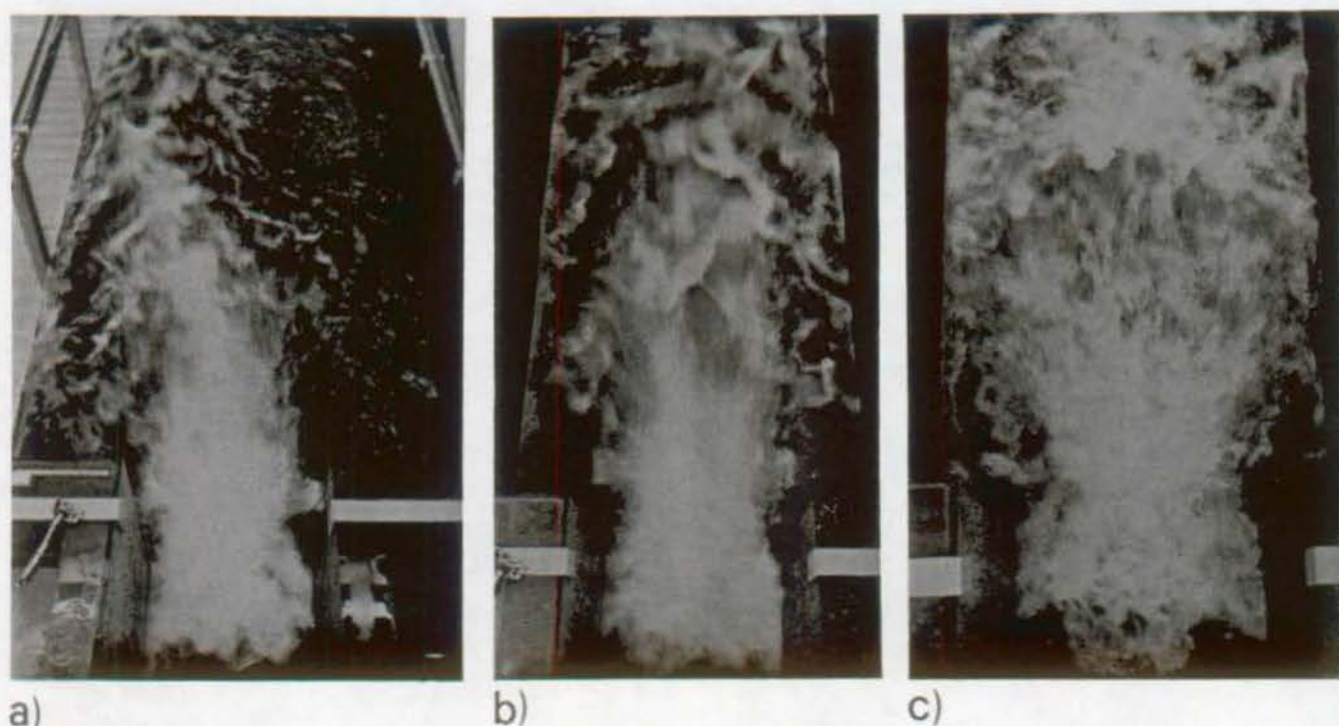


Fig. 8.5 : Flow pattern as a function of expansion ratio B for otherwise constant parameters $h_1=2.5\text{cm}$, $X_1=0.2$, $X_s=0.2$, $F_1=7.0$, $S=1$. a) $B=3$, b) $B=2$, c) $B=1.5$.

Based on these and further observations, the parameters X_1 , F_1 , S , X_s and B seem not to be sufficient in describing the symmetry of sill-controlled jumps in sudden expansions. Since the effects of the parameters F_1 and S were verified in prismatic channel geometries (Karki (1976), Bretz (1987)), particular attention will be paid to parameters accounting for the channel expansion.

Fig. 8.5 shows flows in channels with various expansion ratios B but otherwise unchanged parameters. In order to keep the position X_1 constant, the tailwater level was adjusted for each expansion geometry. For the particular case investigated, the expansion of the inflowing stream is seen to become satisfactory if $B \leq 2$. Accordingly, the previously mentioned parameters do not suffice to characterize the jump in an expanding channel, as its performance varies significantly with B . It should be

observed (chapter 7) that stagnant flow in the lateral eddies leads usually to poor jet expansions as shown in Fig. 8.5a). A participation of the lateral eddies in the dissipation is therefore necessary to obtain suitable jump pattern as outlined in Fig. 8.5c).

Following the observations outlined in Figs. 8.4 and 8.5, additional laboratory tests were performed in order to establish the conditions for which a satisfactory jet expansion occurs. These revealed that the flow pattern in the lateral eddies depends mainly on the ratio of length to width of corner geometry, that is on the ratio (Fig. 8.1)

$$X_p = \frac{X_s}{\left(\frac{b_2 - b_1}{2}\right)} = 2 \frac{X_s}{b_1} \cdot \frac{1}{B-1} \quad (8.3)$$

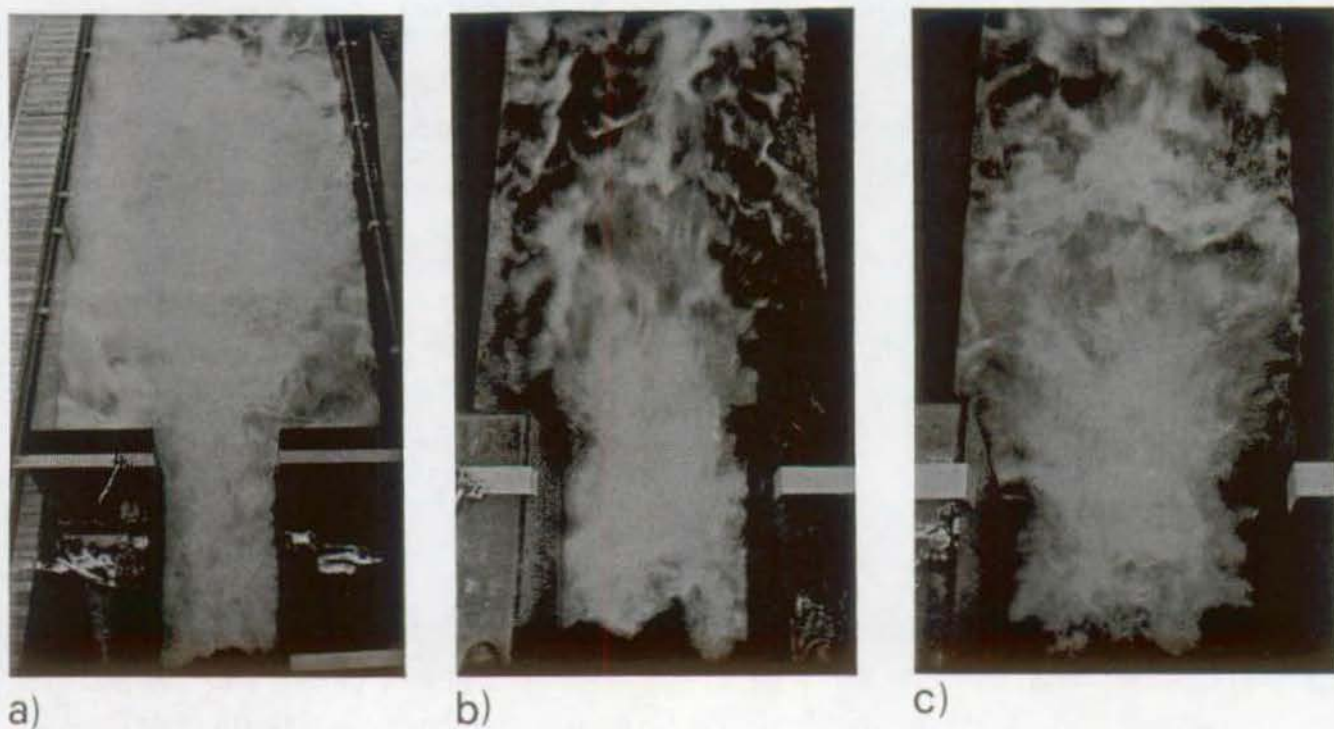


Fig. 8.6 : Experiments with constant values of $X_1=0.2$, $S=1$, $F_1=7.0$, $X_s=0.2$ and $X_p \cong 1$, but different expansion ratios B and inflow depths h_1 . a) $h_1=7.5\text{cm}$, $X_p=1.0$, $B=3$; b) $h_1=2.5\text{cm}$, $X_p=0.8$, $B=2$; and c) $h_1=2.5\text{cm}$, $X_p=1.2$, $B=1.5$.

The experiments conducted in channel LCH2 indicated that for otherwise constant parameters X_1 , S , F_1 and X_s , the best flow conditions were obtained for $X_p \geq 0.8$. For

smaller values of X_p , it became impossible to produce a symmetric jump. Fig. 8.6 shows three jumps for which X_1 , S , F_1 , X_s and X_p were nearly constant but where the expansion ratios B varied. In order to keep these parameters as constant as possible, the inflow conditions were adapted to the expansion ratios B .

The three jumps shown in Fig. 8.6 reveal similar flow patterns despite of a notable difference in size. It should be noted that $X_p=0.8$ in Fig. 8.6b) corresponds to the minimum value required for symmetric flow. For otherwise identical flow conditions the value of sill position parameter was $X_p=1.2$ in Fig. 8.6c). For the investigation of the jump symmetry, the expansion ratio parameter B may therefore be substituted with the ratio X_p accounting for both the sill position x_s and the channel expansion ratio B .

The symmetry of jump is thus described with the new parameter X_p , that is the combined effect of x_s/b_1 and B , in addition to X_s according to Eq. (8.2). Note that in Fig. 8.5a) an asymmetric jump prevails since $X_p=0.4$ only.

The effect of the parameter X_s on the jump symmetry was described in the preceding chapter. In Fig. 7.6, different sill locations were considered for otherwise constant inflow conditions, and sill height

The symmetry of the sill-controlled jump depends on the corner length to width ratio X_p as given in Eq. (8.3), on the non-dimensional sill position parameter X_s and on the non-dimensional sill height. The performance of corner vorticity may be regarded sufficient provided $X_p \geq 0.8$.

8.6.2 Effect of the sill height

Based on the observations in the preceding paragraph, five parameters (X_1 , S , F_1 , X_s , X_p) must be considered for the analysis of symmetric flow in sudden expansions. The experimental investigation required to perform this analysis would be quite extensive. As previously indicated, the toe position parameter X_1 was therefore kept constant at $X_1=0.2$ during all runs.

In what follows the optimum height of sill S_{opt} will be determined for different sill positions X_s . In Fig. 8.7, the parameter $X_s=x_s/L_r^*$ is shown as a function of the non-dimensional sill height S for hydraulic jumps which satisfied all conditions in category III (Table 8.1). In addition to the requirement of jump symmetry, the vorticity of lateral eddies, a uniform tailwater velocity distribution and the tailwater wave generation were thus also acceptable.

As regards the tailwater wave action category III was difficult to satisfy for inflow depths $h_1 > 5.0\text{cm}$ in conjunction with inflow Froude numbers $F_1 > 5$. For the data shown in Fig. 8.7, the wave criterion was satisfied only partially, therefore. Fig. 8.7 includes the experiments for the three channel geometries (Table 8.2) with inflow depths h_1 ranging from 2.5cm to 7.5cm and sill position parameters $0.8 < X_p < 1.2$.

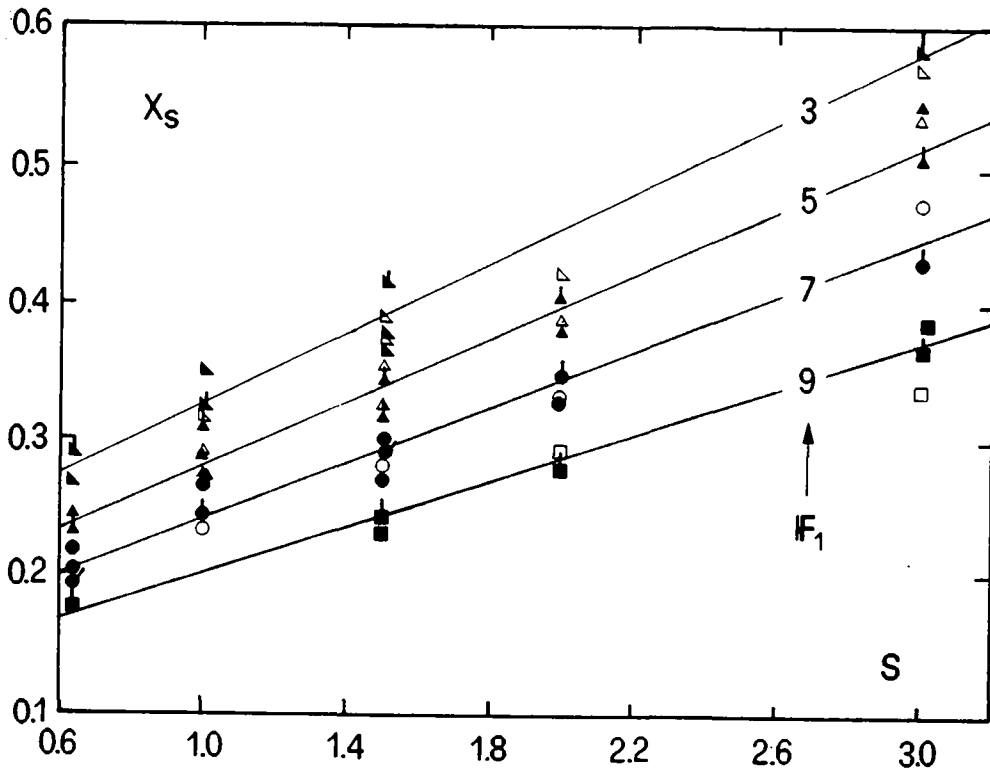


Fig. 8.7 : Sill position parameter X_s as function of non-dimensional sill height S_{opt} for optimal flow conditions (category III in Table 8.1). Domains of experiments $1.5 \leq B \leq 3$; $0.8 \leq X_p \leq 1.2$; $3 \leq F_1 \leq 9$, $X_1 = 0.2$. (\blacktriangledown) $F_1 = 3$, (\blacktriangle) $F_1 = 5$, (\bullet) $F_1 = 7$, (\blacksquare) $F_1 = 9$. (\bullet) $B = 3$, (\circ) $B = 2$, (\bullet) $B = 1.5$. (—) prediction according to Eq. (8.4).

As shown in Fig. 8.7, the inflow Froude number F_1 influences significantly the optimum sill height S_{opt} for a given sill position X_s . Furthermore, the choice of the parameter X_p instead of B seems to be successful since no additional effects of B on X_s could be observed. Based on the experimental data, the non-dimensional optimal sill height S_{opt} may be expressed only as a function of the sill position X_s and the Froude number F_1 .

It may be approximated as (Fig. 8.7)

$$S_{opt} = \frac{X_s + 0.0116F_1 - 0.225}{0.155 - 0.008 F_1} \quad (8.4)$$

The application domain of Eq. (8.4) is limited as follows :

- $1 < B \leq 5$,
- $3 \leq F_1 \leq 10$,
- $X_p \geq 0.8, X_1 \geq 0.2$,
- $0.2 \leq X_s \leq 0.5$, and
- $0.6 \leq S \leq 3$.

The numerical example presented in paragraph 8.9 will illustrate an application of Eq. (8.4).

Based on Eq. (8.4) and its limits of application, a central sill is not an optimum solution for any expansion ratio B and any inflow and outflow conditions. As outlined in the numerical example, large expansion ratios and small jumps (small inflow depths and small inflow Froude numbers) require too large sills to perform a symmetric jump.

As outlined in chapter 7, the width b_s (Fig. 8.1) of the central sill has no discernable effect on the overall jump pattern provided b_s is larger than the inflow channel width b_1 . A satisfactory performance of the dissipator was obtained when the width of sill was at least equal to b_1 plus 25% of the expansion width ($b_2 - b_1$), that is

$$b_s = b_1 \left(1 + \frac{1}{4}(B-1) \right) \quad (8.5)$$

Equation (8.5) was obtained during additional runs in channel LCH1, with an expansion ratio $B=5$. Based on the observations with expansions $B \leq 3$, a 10% increase of b_s relative to b_1 was originally considered sufficient. Yet, the experiments with $B=5$ clearly indicated that the deflective action of central sill was insufficient. Only when the sill was designed according to Eq. (8.5) symmetric jumps occurred, as previously observed in LCH2 for $B \leq 3$. The sill width b_s according to Eq. (8.5) was then reconsidered in channel LCH2 for $B \leq 3$, and no effect of b_s/b_1 could be observed. Therefore, Eq. (8.5) should be considered as a minimum; however, the central sill should not be designed over the entire downstream channel ($b_s=b_2$) since debris might remain in the corners otherwise.

The first experiment was conducted in a sudden expansion of ratio $B=3$ without appurtenances. In order to increase the bed erosion downstream from the end sill, a reduction of the non-dimensional toe position parameter from $X_1=0.2$ to $X_1=0.15$ became necessary. The erosion of the channel floor after 15 min. of operation is shown in Fig. 8.9b) whereas Fig. 8.9a) shows the stilling basin in operation.

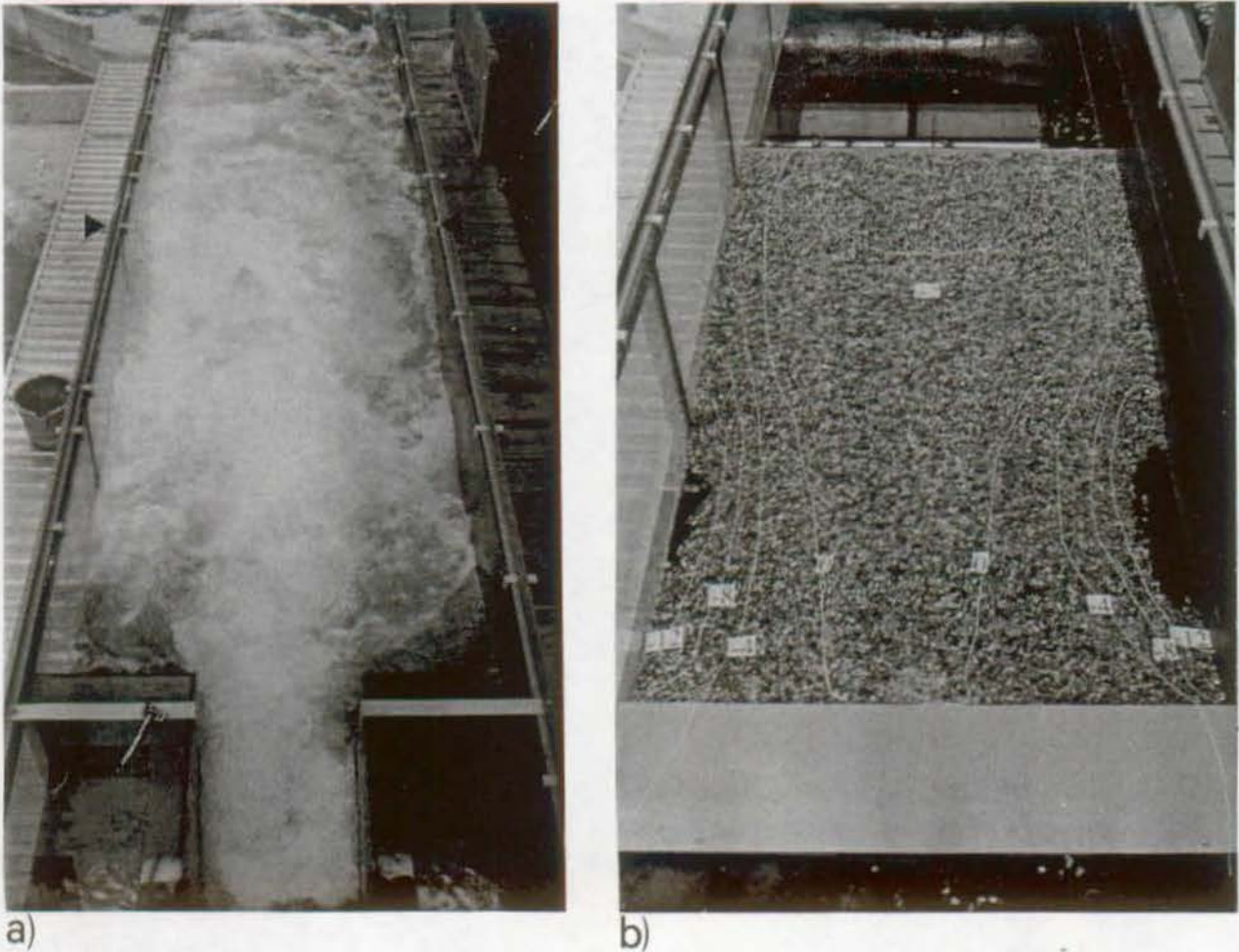


Fig. 8.9 : Flow pattern and bed erosion after 15 min. of operation without central baffle sill. $h_1=8.0\text{cm}$, $h_2=55\text{cm}$, $F_1=7.0$, $L_r^*=323\text{cm}$, $L_j^*=470\text{cm}$, $X_1=0.15$, $B=3$. a) Overall jump pattern; b) bed erosion downstream from end sill. (\blacktriangle) Position of end sill.

Compared to the experiments conducted in chapter 5, the end sill is seen to improve the overall jump pattern. Instead of a stable asymmetric jump, the main stream now oscillates from one channel side to the other at a period of approximately 20 seconds. Fig 8.9a) shows the hydraulic jump formed with the main stream along the left channel side. As shown in this photograph, nearly stagnant flow prevails in the lateral

8.7 EXPERIMENTS WITH ERODIBLE CHANNEL BED

8.7.1 Stilling basin without baffle elements

For a better visualization of the flow improvement obtained with a central sill, additional experiments were performed in channel LCH2. A 1:2 sloping end sill (Fig. 8.8b) was fixed on the channel floor. Downstream from the end sill, the channel floor was covered with a 15cm gravel layer of grain average diameter $\sim 1.0\text{cm}$, as shown in Fig. 8.8a). The distance between the end sill and the toe position corresponds to approximately 80% of L_r^* . The end sill and the inflow conditions considered for the experiments are also indicated. The height of the end sill was designed according to the recommendation of USBR Basin III (Peterka, 1983). For an inflow depth $h_1=8.0\text{cm}$ and an inflow Froude number $F_1=7.0$, the height of the end sill becomes $h_{e,s} \approx 1.45 \cdot 8 \approx 12\text{cm}$. For the experiments a slightly higher end sill ($h_{e,s}=15\text{cm}$) was finally selected.

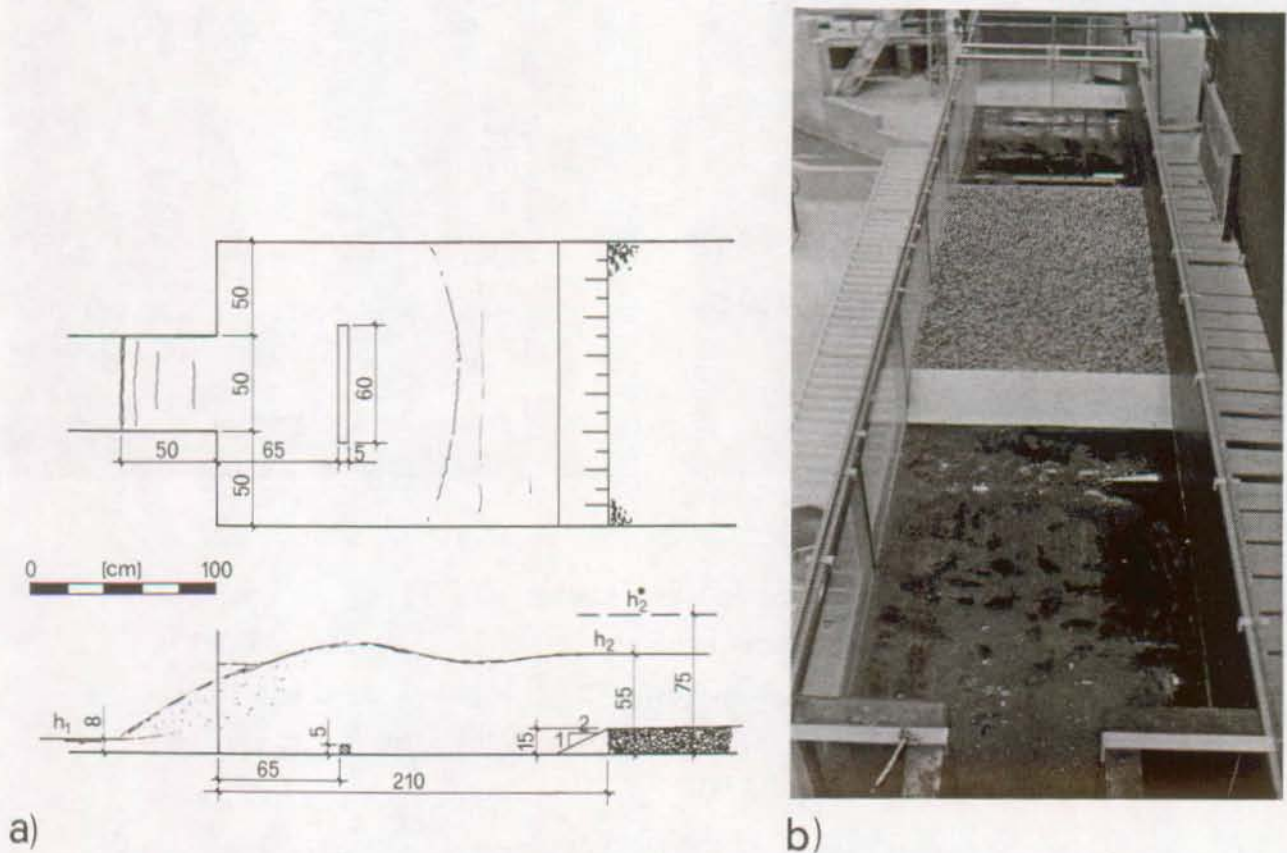


Fig. 8.8 : Erodible channel floor downstream from end sill, $h_1=8.0\text{cm}$, $F_1=7.0$, $S=0.62$, $h_2 \approx 55\text{cm}$, $h_2^* = 75\text{cm}$, $L_r^* = 323\text{cm}$. a) Overall dimension of experimental channel (case with sill and sudden expansion), b) photograph of the end sill and the erodible bed prior to experiment.

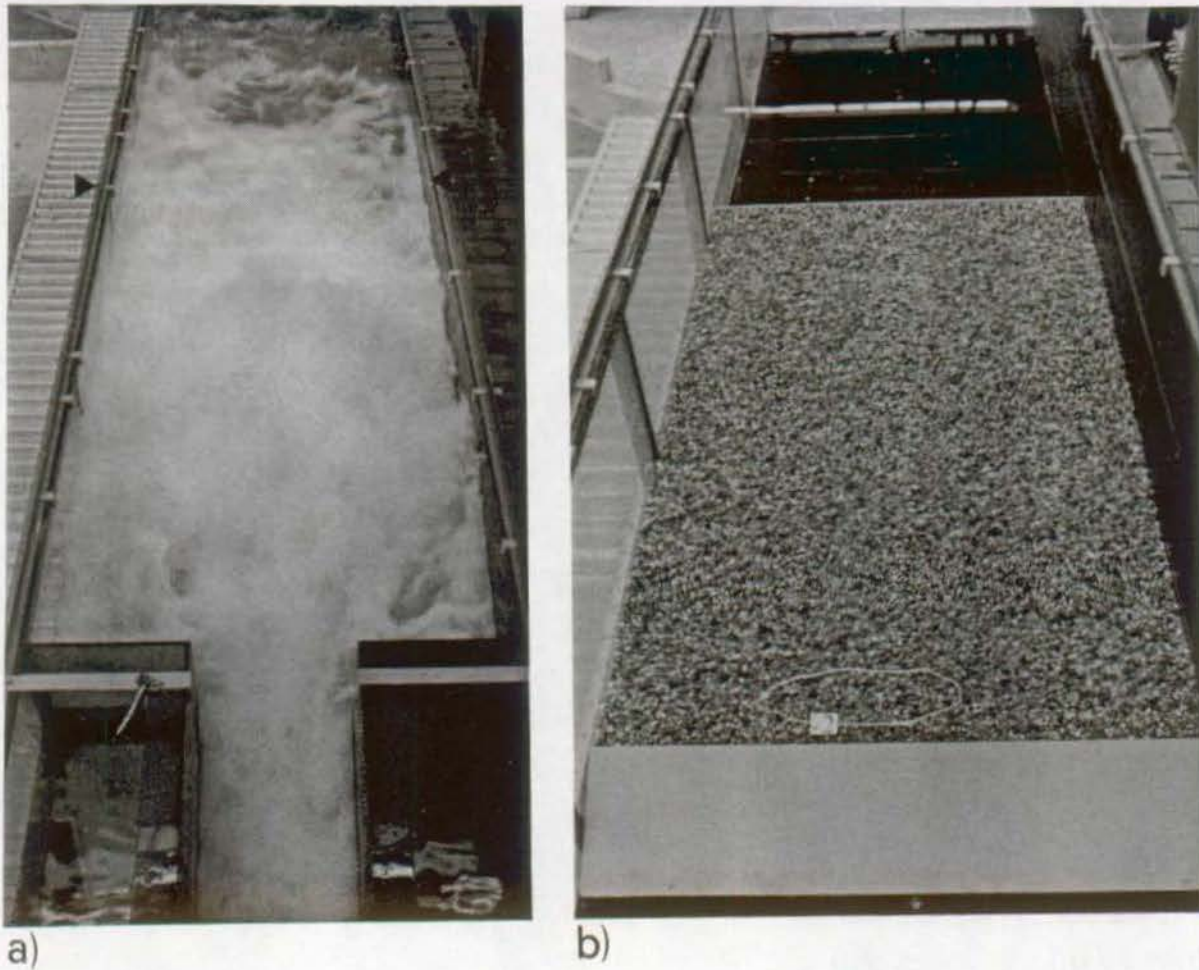


Fig. 8.10 : Flow pattern and bed erosion after 15 min. of operation with central sill. $h_1=8.0\text{cm}$, $h_2=55\text{cm}$, $F_1=7.0$, $X_1=0.18$, $B=3$, $X_s=0.2$, $X_p=1.3$. a) Overall jump pattern, b) bed erosion downstream from end sill. (\blacktriangle) Position of end sill.

8.7.3 Gradual expansion with central sill

Finally, a third run was performed in which a gradual linear expansion of $2\phi=90^\circ$ was considered instead of the sudden expansion. Therein the inflow and tailwater conditions, and the sill geometry were identical to those labelled in Fig. 8.10. The purpose of this run was to evaluate the effect of the gradual expansion geometry both on the jump pattern and the bed erosion downstream from the end sill.

Fig. 8.11 shows the overall jump characteristics and the shape of the erodible channel floor after 30 min. of operation. It seems important to state that the difference in the toe position between the sudden and the gradual linear expansions is approximately 10cm for the configurations selected, which corresponds to only 3% of L_r^* . As

eddies. Due to the oscillations of the high velocity jet from one channel side to the other, the final bed erosion shown in Fig. 8.9b) is nearly symmetric. Note the gravel accumulation in the central part of the channel combined with serious scour at the wall regions beyond the end sill, as shown in the figure 8.9b). These observations outline the existence of a highly nonuniform velocity distribution downstream from the end sill, as already discussed in chapter 5.

In addition to poor symmetry, serious tailwater wave action and a long basin, the hydraulic jump in expanding channels without baffle elements involves significant scour, and thus is unacceptable as an energy dissipator.

8.7.2 Stilling basin with central sill

The second run was carried out with the same channel geometry and identical inflow conditions as in Fig. 8.9 but with a central baffle sill of height $s=5.0\text{cm}$ ($S=0.62$) additionally. A sill position of $x_s=65\text{cm}$ was selected for which $X_s=0.2$ and $X_p=1.3$ in order to obtain an optimum flow configuration according to Fig. 8.7. Due to Eq. (8.4), a slightly reduced optimum sill height $S_{\text{opt}}=0.57$ would be needed. The overall flow pattern is shown in Fig. 8.10a), whereas Fig. 8.10b) shows the bed erosion again after 15 min. of operation.

Compared to Fig. 8.9, the jump characteristics are significantly improved with the central sill. In addition to a length reduction of 27% (Fig. 8.3a) and a better participation of the lateral eddies, the bed erosion is significantly reduced. In Fig. 8.10b) the maximum erosion depths occurred shortly downstream from the end sill and attained only -2.5cm below the end sill level, whereas in Fig. 8.9b) an erosion depth of -15cm was attained on both channel sides.

Due to the presence of the central sill, a slight increase in the toe position from $X_1=0.15$ to $X_1=0.18$ was observed, as the tailwater depth h_2 was identical in both cases. This must be attributed to the momentum contribution of the central sill as described in 8.4.

The improvement of the erosion pattern obtained with the central sill of optimal height is significant in comparison to the sudden expansion without baffle appurtenances. The length of basin may thus be reduced.

outlined in Fig. 8.11 no discernable effect on the jump may be observed when replacing the sudden expansion with a gradual linear expansion of considerable expansion angle ($2\phi=90^\circ$). As regards the bed erosion downstream from the end sill, nearly identical erosion depths were recorded in Figs. 8.11b) and 8.10b).

The influence of expansion angle on the jump pattern was not investigated systematically in the present study, however. Therefore the observations discussed in this paragraph should be verified for other expansion ratios B , and other inflow and tailwater conditions.

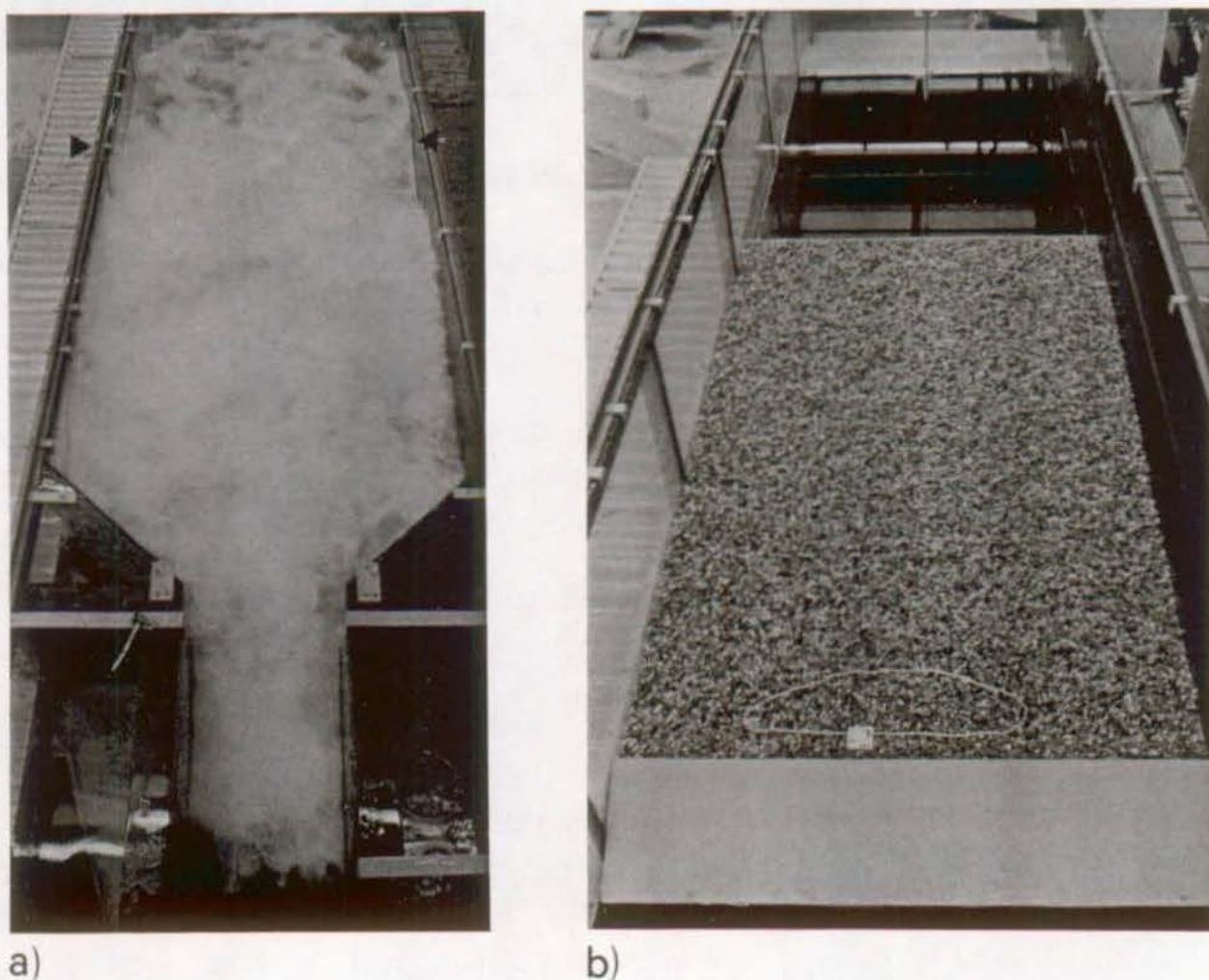


Fig. 8.11 : Flow pattern and bed erosion for gradual linear expansion with central sill. $\phi=45^\circ$, $h_1=8.0\text{cm}$, $h_2=55\text{cm}$ $F_1=7.0$, $X_1=0.14$, $B=3$, $X_s=0.2$, $X_p=1.3$. a) Overall view of the jump; b) bed erosion after 30 min of operation.(\blacktriangle) Position of end sill.

Hydraulic jumps in gradual and abruptly expanding channels behave similarly if the expansion angle is large and a minimum Froude number is exceeded. Based on the preliminary analysis, a limit expansion angle of $2\times 30^\circ$, and a limit inflow Froude number $F_1=3$ should be considered.

8.7.4 Basin length and dissipator volume

The length L_B of a dissipator has to be designed in order to avoid or at least limit the extent of bed erosion in the tailwater channel. Since site-specific conditions have to be accounted for, model tests are strongly recommended for the final design. However, the experiments conducted with the erodible channel floor allow a preliminary evaluation of the required length of dissipator.

Experiments definitely indicated that the end sill is effective in deviating the high-velocity concentrations away from the channel floor. Based on the scour patterns as observed during the experimental study, it was found that the length of basin could be set equal to the length of roller for the classical jump, that is

$$L_B = L_r^* = h_1(6.29 \cdot F_1 - 3.59) \cong 4.5 h_2^* \quad . \quad (8.6)$$

Eq. (8.6) may be used for a preliminary evaluation of the stilling basin length provided an end sill according to USBR Basin III (Peterka, 1983) is placed at the end of the dissipator.

The length of the basin L_B should be equal to the jump length $L_{j,s}^*$ (Eq. 8.1) for stilling basins without an end sill. Both recommendations are essentially based on the presence of the central baffle sill according to paragraphs 8.6.1 and 8.6.2.

Based on Eqs. (5.34) and (8.1) the "jump volume" becomes

$$V_{j,s} = h_2 [b_1 \cdot x_1 L_r^* + b_2 (L_{j,s} - x_1 L_r^*)] \quad . \quad (8.7)$$

where $L_{j,s}$ may be evaluated with Eq. (8.1). In order to compare the volume of the proposed dissipator with USBR dissipators, the number of parameters of Eq. (8.7) should be reduced. For a maximum value of $\psi=0.3$ and an average inflow Froude number of $F_1=6$, the jump length $L_{j,s}$ may be approximated to $L_{j,s} \cong L_j^*$ according to Eq. (8.1). Based on the approach presented in paragraph 5.5.7 for a preliminary evaluation Eq. (8.7) thus reduces to

$$V_{j,s} \cong 0.5 (1 + B) V_j^* \quad (8.8)$$

where V_j^* is the volume of the dissipator USBR Basin I. In the numerical example (§ 8.9) Eqs. (8.7) and (8.8) are compared.

For a dissipator with an optimum central sill and an end sill according to USBR Basin III, the dissipator volume may be approximated as

$$V_{B,s} \cong 0.5 (1 + B) V_{B,II}^* \quad (8.9)$$

where $V_{B,II}^* = b_1 h_2 L_r^*$. $V_{B,II}^*$ corresponds approximately to the dissipator volume for the USBR Basin II.

For a sudden expanding dissipator provided with an optimal central sill and an end sill according to USBR Basin III, the stilling basin length may be reduced to $L_B \cong 4.5 h_2^$. The dissipator volume may be evaluated with Eq.(8.9).*

8.8 CAVITATION ASPECTS

The application domains of baffle piers, sills and other appurtenances placed on the floor of stilling basins are limited by the risk of cavitation erosion. Cavitation includes the formation, movement and subsequent collapse of vapor cavities in a liquid of usual temperature due to pressure reduction. In water, this occurs when the local pressure attains approximately -10m of water column below the atmosphere. When the air bubbles are carried to regions where the pressure increases, the bubbles collapse, thereby causing high and rapidly fluctuating shock radiation. The cavitation potential differs widely, depending on the size and the shape of the appurtenance on the one hand, and on the local pressure and velocity distributions on the other hand (Ball, 1963, 1976).

The satisfactory performance of the dissipator presented in this chapter is essentially based on the presence of a central baffle sill. Without it the pattern of the hydraulic jumps in sudden expansions becomes poor as shown in Fig. 8.9a). The domain of application of the stilling basin proposed is therefore mainly limited by the risk of cavitation erosion for the central sill.

No laboratory test could be carried out to establish the critical conditions for which cavitation damages appear on the sill. To limit the application domain of the dissipator proposed, reference will be made to the recommendations of Peterka (1983) for the use of baffle piers in stilling basins.

The present basin may be compared to the USBR Basins II or III. Peterka (1983) considered upper limits of discharge per unit width, typically ranging from $20\text{m}^3\text{s}^{-1}$ to $60\text{m}^3\text{s}^{-1}$ per meter width. Such restrictions are related to the formation of macroturbulence, and its erosive action beyond the end of basin. Although such

prototype results are not yet available for the present structure, the discharge per unit width should be limited to 20 to 30m²s⁻¹.

For sudden expanding stilling basins with a central sill, the velocity of the inflow stream should not exceed values of the order of 20m/s and the discharge per unit width should be limited to 20 to 30m²s⁻¹.

For projects involving a risk of damages due to cavitation erosion, a detailed analysis of the dissipator should be performed.

Based on these criteria, the application of the proposed stilling basin will be limited to relatively small structures.

8.9 Numerical example

In order to illustrate the design procedure for an optimum performance of the sudden expanding stilling basin as proposed herein a numerical example will now be presented. The examples of chapters 5 and 7 will not be reconsidered since the inflow velocity exceeded the limit value of 20 to 25m/s indicated in the preceding paragraph.

Consider an approaching channel 5m wide with a flow depth of $h_1=0.5$ m, and an inflow velocity of $V_1=15$ m/s. A backwater curve calculation of the flow in the tailwater channel indicated a corresponding downstream level of $h_2=3.0$ m. Compute the main dimensions of the sudden expanding stilling basins for expansion ratios $B=2$, 3 and 5.

The inflowing Froude number is $F_1=15/(9.81 \cdot 0.5)^{0.5}=6.8$. The sequent depths ratio for the classical jump is $Y^*=0.5[(1+8(6.8)^2)^{0.5}-1]=9.1$ according to Eq. (5.1). The sequent depth according to Bélanger becomes thus $h_2^*=4.55$ m whereas the corresponding roller length attains $L_r^*=(6.29 \cdot 6.8 - 3.59) \cdot 0.5=19.6$ m \cong 20m from Eq. (5.3). An excavation of approximately 1.5m below the river bed would therefore be required for a prismatic rectangular stilling basin without appurtenances.

The toe position X_1 for the three expansion ratios considered may be evaluated with Fig. 5.12. Based on the previous observations, optimum flow conditions in sudden expansions with a central sill occur if $X_p \geq 0.8$. In order to obtain the non-dimensional sill position parameter $X_s=x_s/L_r^*$, x_s may be evaluated with Eq. (8.3) in which X_p is assumed equal to 1. In Table 8.3 the main results for each expansion ratio are summarized. Therein, the value of X_s obtained for $B=2$ is fixed to $X_s=0.2$ ($X_p=1.6$) since the value obtained with $X_p=1$ exceeds the application domain indicated in paragraph 8.6.

The optimum sill height may be predicted with Eq. (8.4) or Fig. 8.7 both as a function of F_1 and X_s whereas Eq. (8.5) may be used to evaluate the sill with b_s . A preliminary evaluation of the jump volume may be obtained with Eq. (8.7). Both quantities $L_{j,s}$ and $V_{j,s}$ are given in Table 8.3 for the considered geometries.

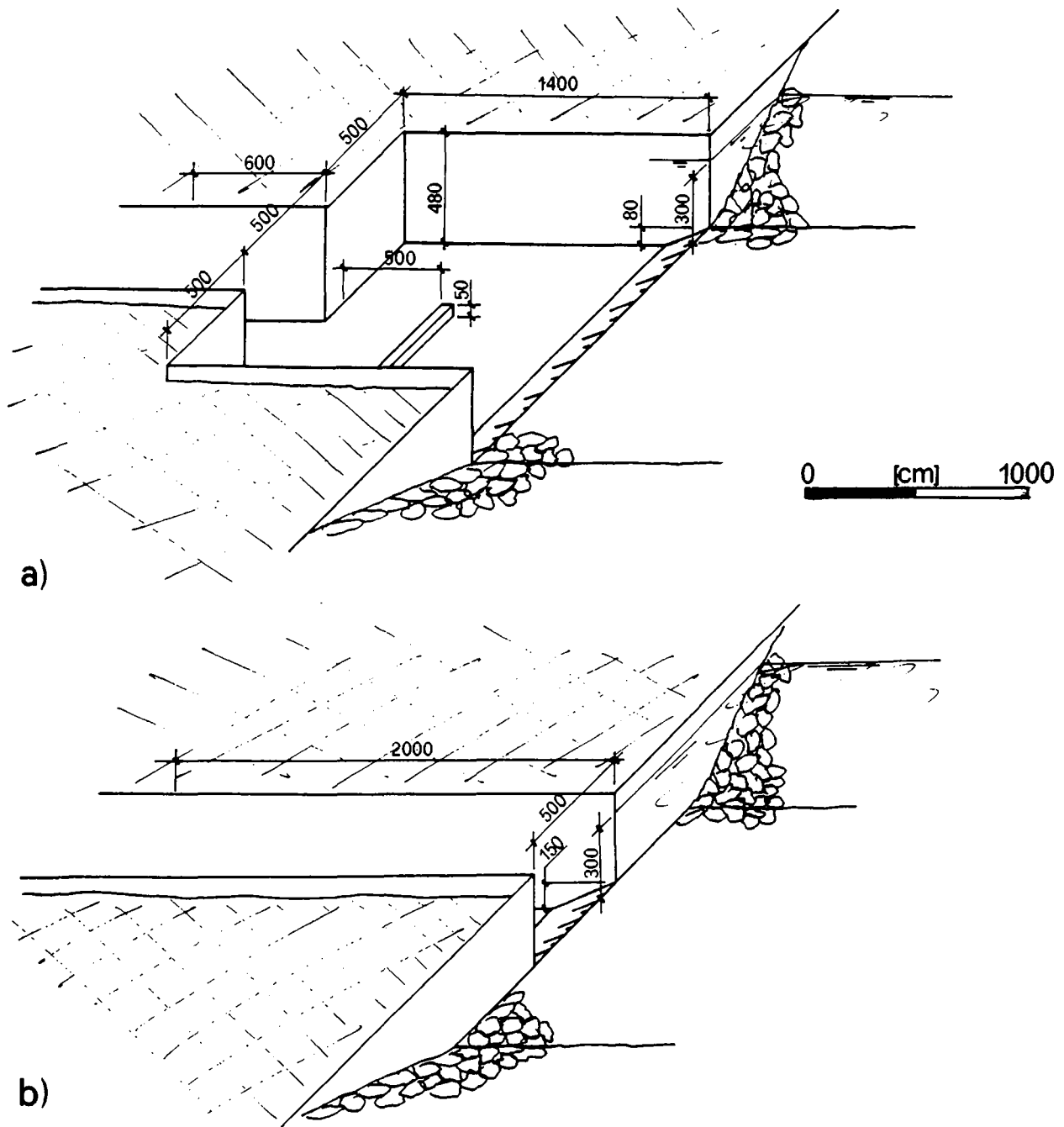


Fig. 8.12 : Numerical example. Schematic view of stilling basins for an expansion ratio a) $B=3$ and b) $B=1$ (hydraulic jump in prismatic channel geometry, and transition to the tailwater channel in entirely subcritical domain of flow) for identical tailwater channel geometry.

Note that the jump volume based on Eq. (8.8) differ by less than 5% from the values indicated in Table (8.3) namely for $B=2$, $V_{j,s}=1.5 \cdot 6.37=955\text{m}^3$; for $B=3$, $V_{j,s}=1274\text{m}^3$ and for $B=5$ $V_{j,s}=1911\text{m}^3$.

In this example a constant value $\psi=0.2$ is used for the three expansion ratios considered. However, according to the limits of domain 2 shown in Fig. 5.27 slightly larger values of ψ may be selected. Especially for the expansion ratio $B=5$ for which $X_1=0.4$ an increase in ψ would lead to a reduction of X_1 .

As shown in Table 8.3, the non-dimensional sill height S increases significantly with the expansion ratio B .

Table 8.3 : Numerical example. Main characteristics of sudden expanding stilling basin with central sill.

Expansion ratio B	Y [-]	X_1 [-]	x_s [m]	X_s [-]	S [-]	$L_{j,s}$ [m]	$V_{j,s}$ [m ³]
1	9.1	-	-	-	-	28.3	637
2	7.5	0.2	2.5	(0.125) 0.2	(0.53) 0.6	26.0	912
3	7.5	0.3	5	0.25	1	26.0	1254
5	7.5	0.4	7.5	0.375	2.2	26.0	1862

In Fig. 8.12 the main dimensions of the stilling basins obtained for $B=3$ and $B=1$ (prismatic geometry) are illustrated by assuming an identical geometry of the tailwater channel.

It should be noted that for $B=1$, the floor of the stilling basin is 1.5m below the tailwater bed, instead of 0.8m for the sudden expanding basin ($0.8/0.5=1.6$). For both geometries the length of stilling basin is assumed equal to $L_r^*=20.0\text{m}$ according to Eq. (8.6). The toe position for $B=3$ is located at $x_1=0.3 \cdot 20.0\text{m}=6.0\text{m}$ upstream from the expansion section (Fig. 8.12a).

8.10 CONCLUSIONS

The performance of the sudden expanding stilling basin was investigated in the present chapter by optimizing position and height of the the central baffle sill. Four criteria, namely jump symmetry, tailwater wave action, vorticity of the lateral eddies and tailwater velocity distribution were used for the optimisation procedure.

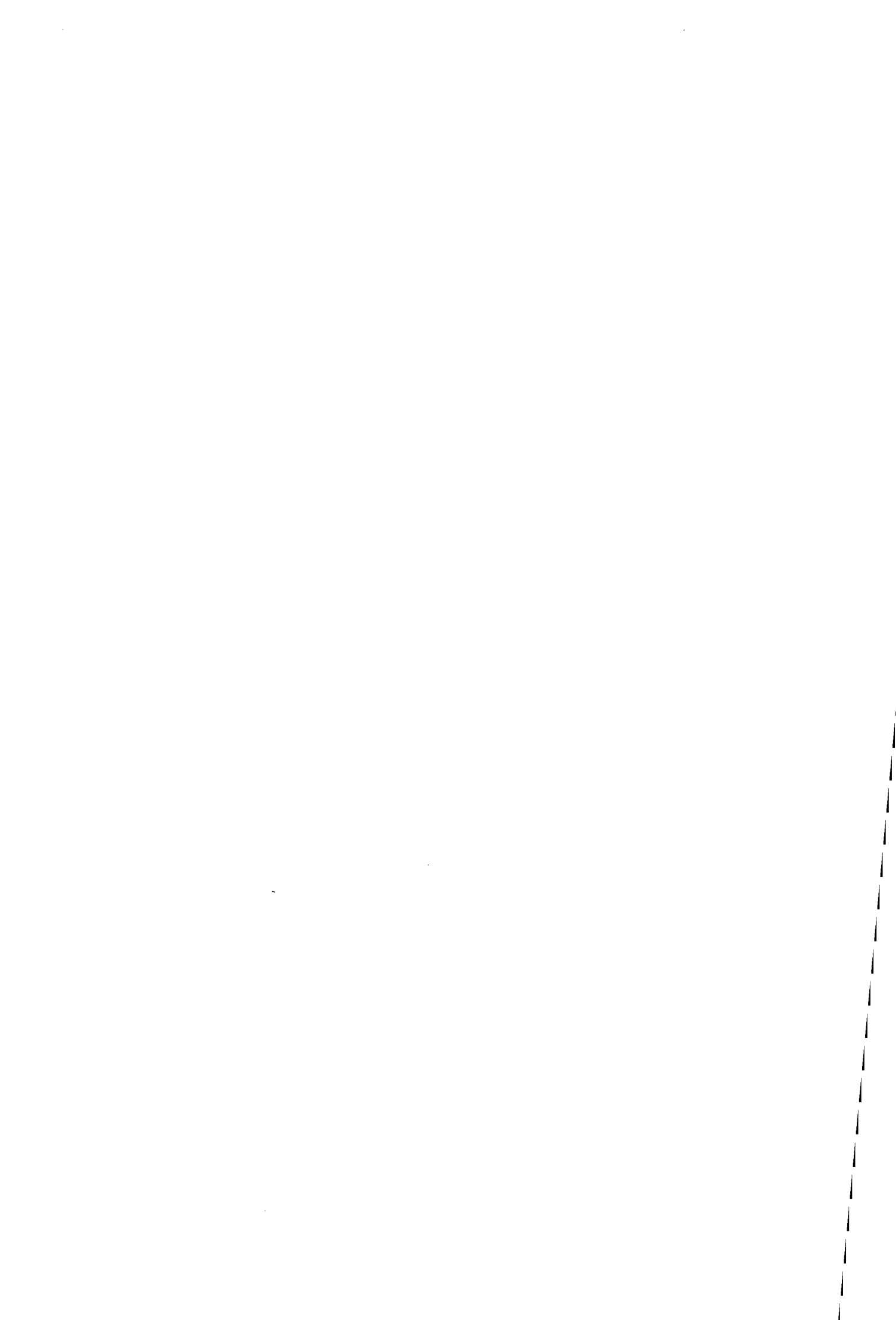
According to the design procedure proposed, the non-dimensional, optimal sill height S_{opt} depends on both the expansion ratio B and the inflow Froude number F_1 . The optimum non-dimensional sill position X_s , in turn, depends on both the expansion ratio B and the width of the inflow stream b_1 . Due to the limited experimental investigation of 213 runs only, the toe position parameter X_1 was kept constant at $X_1=0.2$ for all runs . Since for a given expansion ratio B the flow asymmetry decreases as X_1 increases (chapter 5), the design recommendations are also applicable to larger values of X_1 .

The experimental investigation revealed that the effect of sill on the sequent depths ratio remains generally small. Eq. (5.26) as developed for sudden expansions without appurtenances may therefore be used for stilling basins with a central sill. The corresponding length of jump may be computed with Eq. (8.1). Typically, a reduction of some 20% relative to the jump length in a basin without sill is obtained.

Selected experiments with an erodible channel bed downstream from the end sill confirmed the flow improvements obtained with the central sill. Also, a gradual linear expansion of $2\phi=90^\circ$ showed no substantial departure from the jump pattern and the bed erosion downstream from the end sill. Additional laboratory tests must be performed to verify these observations for other expansion geometries (expansion ratio B and expansion angles ϕ) and other inflow conditions.

The application domain of the proposed dissipator is mainly limited by cavitation aspects. Based on similar experiments, an upper approaching velocity of some 20 to 25ms^{-1} should not be exceeded.

The numerical example at the end of the chapter illustrates the procedure proposed for the design of an optimum dissipator. Therein, the effects of the expansion ratio B on the sill height and its position are outlined.



9. CONCLUSIONS

9.1 PRELIMINARY REMARKS

The present research project deals with hydraulic jumps in expanding channels. An extensive experimental investigation was carried out at the "Laboratoire de Constructions Hydrauliques" of the "Ecole Polytechnique Fédérale de Lausanne (EPFL)" to improve and widen the knowledge on the behavior of this type of hydraulic jump. The attempt was even made to introduce a new dissipator for expanding channels.

The purpose of the present investigation was dual. First, a computational model allowing an estimation of the main jump characteristics should be offered. This model may be used to evaluate the sequent depths ratio, the jump position relative to the expansion section, the jump length and its symmetry pattern. The second purpose of the present investigation was to introduce an economic and efficient device by which the performance of jump in expanding channels may be improved. Therein, particular attention was paid to the reduction of the flow asymmetry which is typical for all jumps in expanding channels with a horizontal floor. The analysis of published investigations in this domain of hydraulic jumps indicates that the phenomenon of asymmetric jump, and its elimination was yet not investigated systematically. The development of the computational model is based on theoretical means and extensive experimental tests. Paragraph 9.2 focuses the relevant patterns of hydraulic jumps in expanding channels. The computational procedure recommended for the evaluation of the main jump patterns is summarized in paragraphs 9.3.2 to 9.3.4. Therein, the basic equations used for the evaluation of the sequent depths ratio, the jump length and the jump symmetry are presented. Applications of the present approach are presented in examples as discussed in chapters 5, 6, and 8.

The highlight of this study is the introduction of a new type of dissipator of which the main element is a central sill. Recommendations for the optimal design of the central sill in order to obtain symmetric and compact jumps are reported in paragraph 9.3.5. Therein, the application domains of sill-controlled jumps in expansions are presented. The central sill on the floor of the non-prismatic stilling basin is of particular interest for the design engineer since its presence significantly improves the jump pattern.

Final remarks on this research project and some suggestions for future investigations are presented in paragraph 9.4.

9.2 JUMP PATTERNS IN EXPANDING CHANNELS

The essential features of hydraulic jumps in expanding channels may be summarized as follows.

1. The jump pattern of hydraulic jumps in expanding channels may differ significantly from the characteristics observed in prismatic channels. Depending on the jump location and the channel geometry considered, surface roller and symmetric flow do not appear in expanding channels.
2. The performance of jump in expanding channels depends significantly on the tailwater. Based on a preliminary analysis in chapter 2, low tailwater leads to R- and S-jumps of which the general requirements for energy dissipation are poor. This project thus considered mainly T-jumps, for which the toe is located upstream from the expansion section.
3. The position of the jump relative to the channel expansion influences its overall characteristics. A small variation of the inflow or tailwater conditions may produce an abrupt modification of the internal structure of jump. Depending on the toe position, the jump may be similar to a classical jump or contain more similarity to surface jets.
4. The expansion angle of the side walls has only a small effect on the overall jump pattern provided a limit inflow Froude number of typically $F_1=3$ is exceeded and small expansion angles typically below 30° degrees are excluded. As the maximum effect of non-prismatic channel geometry occurs in the $2\times 90^\circ$ expansion, the so-called abrupt expansion received outstanding attention in the present study.
5. In addition to the sequent depths ratio and the jump length, a computational model for hydraulic jumps in expanding channels should also include an evaluation of flow asymmetry.
6. For large expansion ratios (typically $b_2/b_1 \geq 2$) the hydraulic jump is significantly improved with a central baffle sill. Bed deflectors or adversely sloping stilling basin floors may be effective for small expansion ratios (typically $b_2/b_1 < 2$) only. Baffle piers, chute blocks or other appurtenances placed on the floor of the dissipator were found ineffective.

These fundamental aspects of jumps in expanding channels should be considered for the design of non-prismatic stilling basins.

9.3 PREDICTION OF MAIN JUMP PATTERNS IN SUDDEN EXPANSIONS

9.3.1 Introduction

As outlined in the preceding paragraph, hydraulic jumps in channel expansions may appear under widely variable appearance depending on the jump position and the channel geometry considered. In the present paragraph, the computational model used to evaluate the main jump features will be presented. This model, which was initially developed for sudden expansions with a horizontal channel floor was then adapted to include the effects of either a negative step or a central baffle sill. In addition to the sequent depths ratio also the jump length and its symmetry patterns may be evaluated.

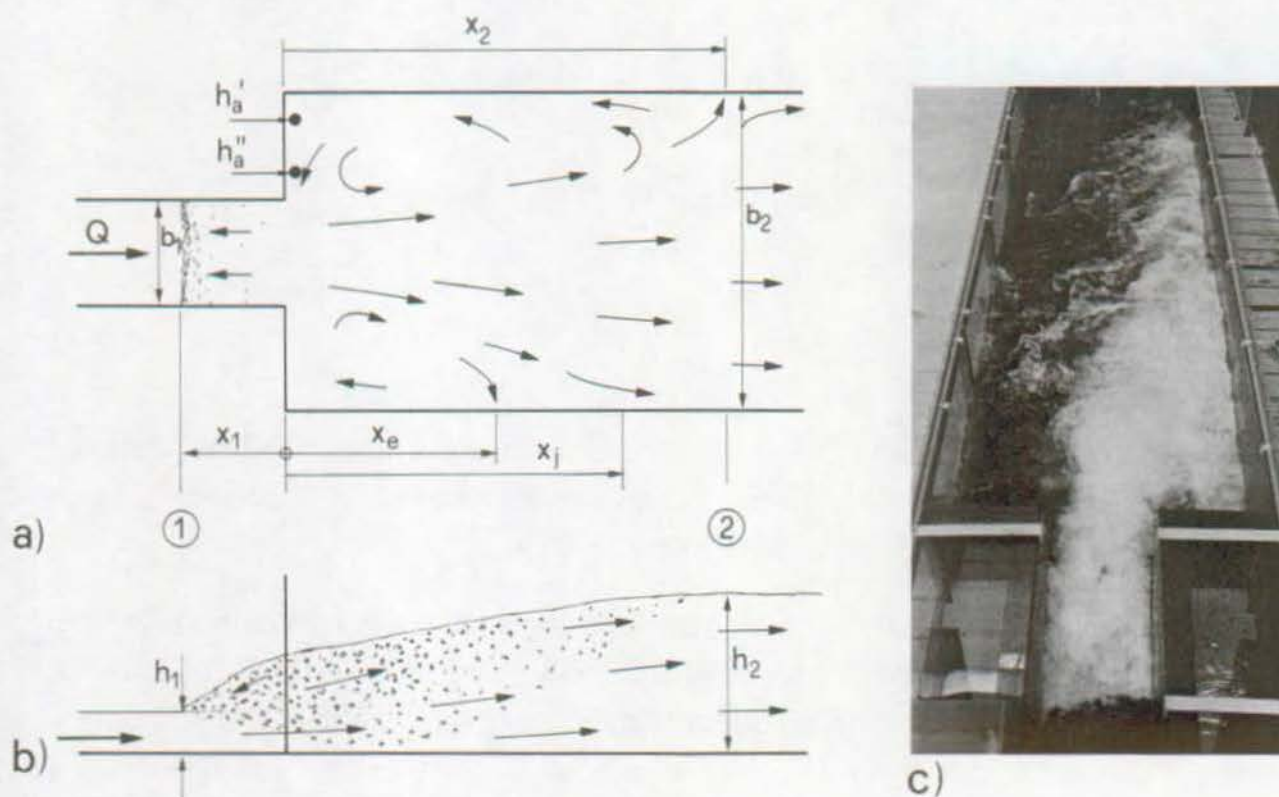


Fig. 9.1 : Hydraulic jump in sudden expansion. Notation a) plan view and b) axial view, c) photograph of T-jump.

The central baffle sill has proven effective to avoid the jump asymmetry and to reduce significantly the length of jump. The final part of the present paragraph deals with the prediction of the optimum sill height and position for a satisfactory performance of the stilling basin.

Figs. 9.1a) and b) show the notation used for the stilling basin without appurtenances, whereas Fig. 9.1c) outlines the flow asymmetry of a hydraulic jump in a sudden expansion. Clearly, such flow is unacceptable in a stilling basin. Yet, this basic configuration must be considered first to proceed later to more complex basin geometry.

9.3.2 Prediction of sequent depths ratio

For sudden expansions with a **horizontal channel floor**, the sequent depths ratio $Y=h_2/h_1$ depends on the inflow Froude number $F_1=Q/(gb_1^2h_1^3)^{1/2}$, the non-dimensional front position relative to the expansion section $X_1=x_1/L_r^*$ and on the expansion ratio $B=b_2/b_1$. The relation between these non-dimensional parameters is

$$\psi = \frac{Y^* - Y}{Y^* - 1} = \left(1 - \frac{1}{\sqrt{B}}\right) \cdot [1 - \text{th}(1.9X_1)] \quad . \quad (9.1)$$

where $\text{th}(i)=[\exp(i) - \exp(-i)]/[\exp(i) + \exp(-i)]$, and

$$X_1 = \frac{x_1}{L_r^*} \quad \text{in which} \quad \frac{L_r^*}{h_1} = (6.29F_1 - 3.59) \quad . \quad (9.2)$$

$Y^*=h_2^*/h_1$ is the sequent depths ratio for a so-called classical jump (further quantities referring to it are marked with a star) according to Bélanger's equation (5.1). A graphical representation of Eq. (9.1) is given in Fig. 9.2.

Eq. (9.1) may be used to predict the sequent depth ratio Y or the toe position X_1 for a given expansion ratio B , provided $1 \leq B \leq 10$, $2.5 \leq F_1 \leq 12$ and $X_1 \geq 0.05$. It should be noted that, for given inflow and tailwater conditions (h_1 , F_1 and h_2), the function ψ may be evaluated according to Eq. (9.1). If ψ is larger than $\psi(X_1=0)=1-1/\sqrt{B}$ for a given expansion ratio B , the toe is located downstream from the channel expansion section, and the jump characteristics may not be predicted with the present model. Highly asymmetric jumps even worse than shown in Fig. 9.1c) for a T-jump then result, which should be avoided (chapter 2).

For sudden expanding channels with a **negative step** of height $N=s/h_1$ located at the expansion section, Eq (9.1) may also be used to evaluate the sequent depths ratio, provided its left hand side is replaced by the expression

$$\psi_N = \frac{Y_N^* - Y_N}{Y_N^* - 1} \quad (9.3)$$

where the unknown $Y_N^* = h_N^*/h_1$ depends on F_1 , X_1 and N as (for notation see Fig. 6.1)

$$Y_N^{*3} - Y_N^* \left\{ 1 + 2F_1^2 + 2N \left[Y_N^* X_1 - N X_1 - X_1 + 1 + (1/2)N \right] \right\} + 2F_1^2 = 0 \quad (9.4)$$

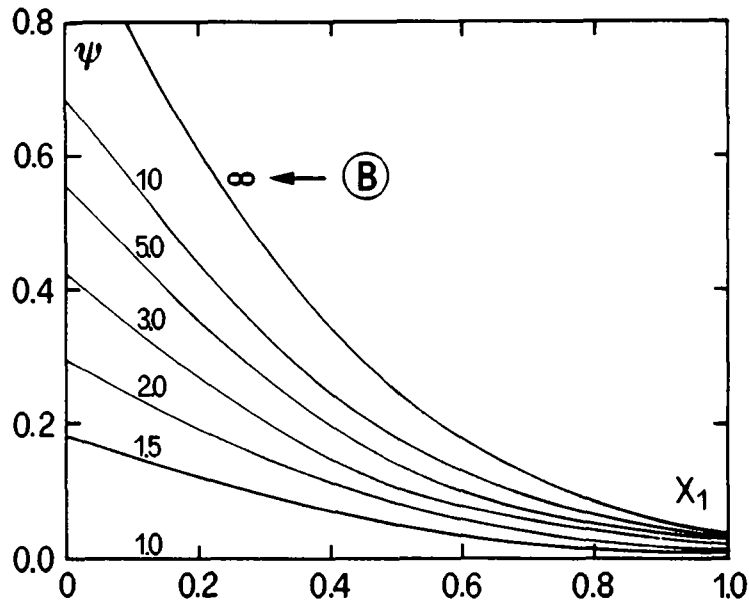


Fig. 9.2 : Prediction of the sequent depths ratio in sudden expansions according to Eq. (9.1). ψ as function of X_1 for different expansion ratios B .

The experimental investigation presented in chapter 8 shows that a **central sill** of optimal height as considered in paragraph 9.3.5 has only a small effect on the sequent depths ratio. Eq. (9.1) may therefore be used for a preliminary evaluation of either the sequent depths ratio or the front position X_1 , provided the application domains according to paragraph 9.3.5 are respected.

The average flow depth $h_a = Y_a \cdot h_1$ along the expansion side walls is given by

$$Y_a^2 = \left[Y^2 - \frac{1}{B} \cdot \left(1 + 2F_1^2 - \frac{F_1^2}{YB} \right) \right] \cdot \left(1 - \frac{1}{B} \right)^{-1} \quad (9.5)$$

according to a conventional momentum approach.

9.3.3 Prediction of jump length

For sudden expansions with a **horizontal channel floor**, the jump length L_j as defined in paragraph 5.2 depends on the inflow Froude number F_1 , the non-dimensional front position X_1 , the expansion ratio B and the inflow depth h_1 . L_j may be evaluated as

$$L_j = \left\{ 1 + \left(1 - \frac{1}{\sqrt{B}} \right) \cdot [1 - \text{th}(1.9 X_1)] \right\} \cdot L_j^* \quad (9.6)_1$$

which may also be written as

$$L_j = L_j^* (1 + \psi) \quad (9.6)_2$$

where L_j^* is the length of the classical jump. Based on the experimental investigation conducted by Peterka (1983), L_j^* may be estimated by the relation

$$L_j^* = h_1 \cdot 220 \text{th} \left(\frac{F_1 - 1}{22} \right) \quad (9.7)$$

In comparison to the jump length in prismatic channels, sudden expansions involve longer jumps provided identical inflow conditions are considered (Eq. (9.6)). This increase is related to the asymmetry phenomenon observed in expanding channel.

Since no significant improvement of the jump symmetry is obtained with a **negative step** located at the expansion section, the modified Eq. (9.6)₂

$$L_{j,N} = L_j^* (1 + \psi_N) \quad (9.8)$$

applies to this jump length.

A notable reduction of the jump length may be obtained with a central sill of optimal height as described in paragraph 9.3.5. The length of jump then is

$$L_{j,s} = L_j^* (1 + \psi) (0.9 - 0.02 F_1) \quad (9.9)$$

and thus depends in addition on F_1 . Note the reduction of $L_{j,s}$ as compared to Eq. (9.6)₂ due to the presence of sill.

For the evaluation of the stilling basin length, two distinct aspects may be discussed. The prediction of the dissipator length should account for the length of hydraulic

jump as given in Eqs.(9.6), (9.8) and (9.9) on the one hand, and for the characteristics of the bottom material in the tailwater channel on the other hand. The length of dissipator must avoid or at least limit the extent of scour downstream from the stilling basin. Since the scour pattern depends mainly on site-specific conditions, model tests are strongly recommended for the final design. The following propositions for the stilling basin length should be used for a preliminary evaluation only and the length of basin may be reduced if favourable site-conditions prevail.

Without appurtenances on the channel floor, the flow asymmetry leads to high velocity concentrations near one side wall (Fig. 9.1c). The channel portion to be protected against bed scour should therefore be at least equal to L_j according to Eq. (9.6) or Eq. (9.8). The presence of sill greatly improves the overall flow pattern, the sill-controlled basin should be preferred to the basin without sill.

For a sill-controlled dissipator with an optimised sill geometry (§ 9.3.5) the maximum length of stilling basin is $L_B=L_{j,s}$ where $L_{j,s}$ is computed according to Eq. (9.9). If an end sill according to the comparable USBR Basin III is provided, the length of the dissipator may be reduced to even $L_B=L_r^* \cong 4.5 h_2^*$.

9.3.4 Evaluation of the jump symmetry

For a sudden expansion with a horizontal channel floor the symmetry of jump depends mainly on the non-dimensional toe position X_1 and the expansion ratio B . Without appurtenances the hydraulic jump in a sudden expansion is symmetric provided $B < B_{1/2}$ where

$$B_{1/2} = \left[\frac{1}{1 - \frac{1/8 [1 - (2/3) X_1]}{1 - \text{th}(1.9X_1)}} \right]^2, \quad 0 < X_1 < 1 \quad (9.10)$$

According to Eq. (9.10) a symmetric hydraulic jump may be located entirely downstream from the expansion section ($X_1=0$) for an expansion ratio $B \leq 1.3$. In practice, this value of B is too small to be of design relevance.

If $B > B_{1/2}$ the hydraulic jump is asymmetric. The degree of jump asymmetry may be evaluated by the parameter

$$B_{2/3} = \left[\frac{1}{1 - \frac{0.28}{(1 - \text{th}(1.9X_1))}} \right]^2 \quad (9.11)$$

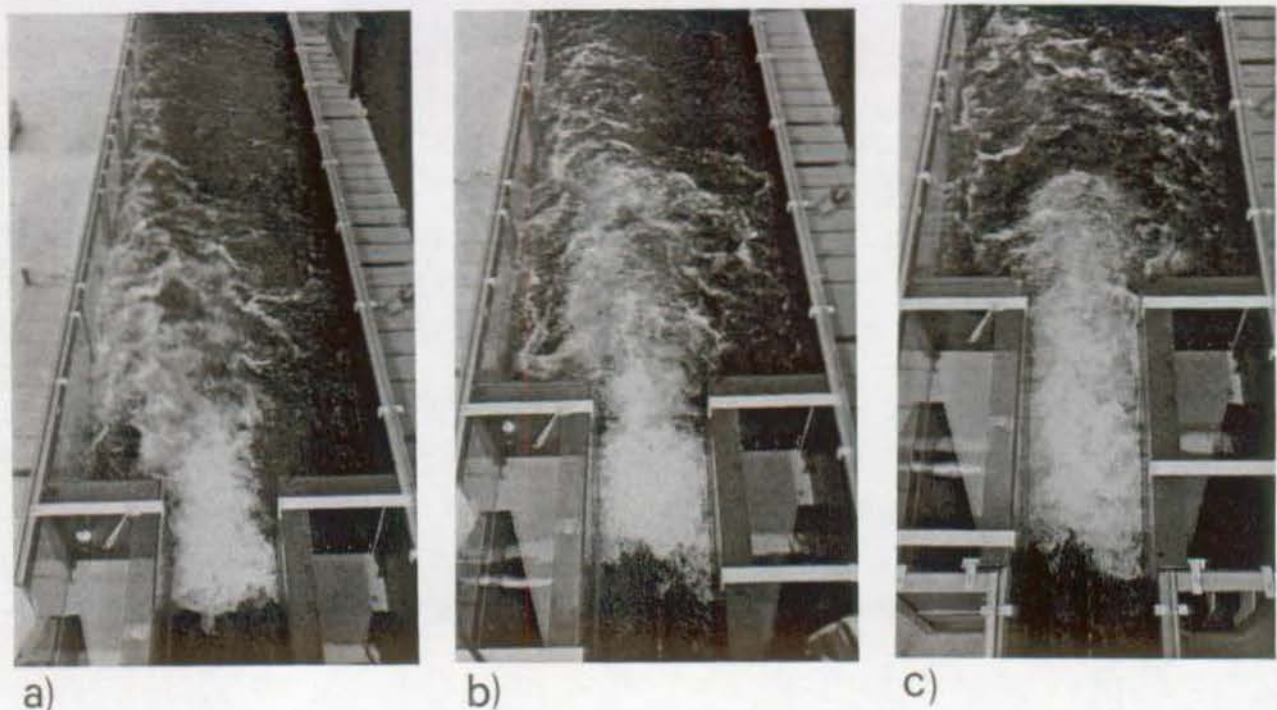


Fig. 9.3 : Prediction of jump symmetry in sudden expansion. a) strong asymmetric jump ($\psi=0.35$), b) slightly symmetric jump ($\psi=0.17$) and c) symmetric jump ($\psi=0.04$).

If the expansion ratio B is smaller than $B_{2/3}$, then the jump may be considered slightly asymmetric (Fig. 9.3b), whereas strongly asymmetric flow (Fig. 9.3a) prevails if $B > B_{2/3}$. The hydraulic jump shown in Fig. 9.3c) may be assumed as symmetric since $B < B_{1/2}$. Note that the condition $B \leq B_{2/3}$ may also be expressed as $\psi \leq 0.28$.

9.3.5 Prediction of sill geometry

In order to insure a satisfactory performance of sudden expanding dissipators, a central sill has proven to be effective (Fig. 9.4a). The optimal design of sill leads to symmetric jumps with a considerable participation of the lateral eddies in the energy dissipation process, and nearly uniform tailwater velocity distribution. Also, the length of stilling basin is comparable to the length of roller in a classical jump, and tailwater wave action is limited.

The optimal sill geometry depends mainly on the inflow Froude number F_1 , the expansion ratio B , the inflow depth h_1 and the width b_1 of the inflow channel. The optimal sill position x_s (Fig. 9.4a) satisfies the relation

$$x_s = \frac{1}{2} C_s (b_2 - b_1). \quad (9.11)$$

C_s should normally be larger than 1, but can be exceptionally reduced to $C_s=0.8$. In addition to Eq. (9.11), the position of sill must also be included in the domain $0.2 \leq x_s/L_r^* \leq 0.5$, that is the position of sill should be in the first portion of length of surface roller in a classical jump. If the sill is located too close to the toe of jump, the deflection of inflow jet is too large, and spray and pulsating flow occurred. If the sill is too far away from the toe of jump, its action is insufficient, however.

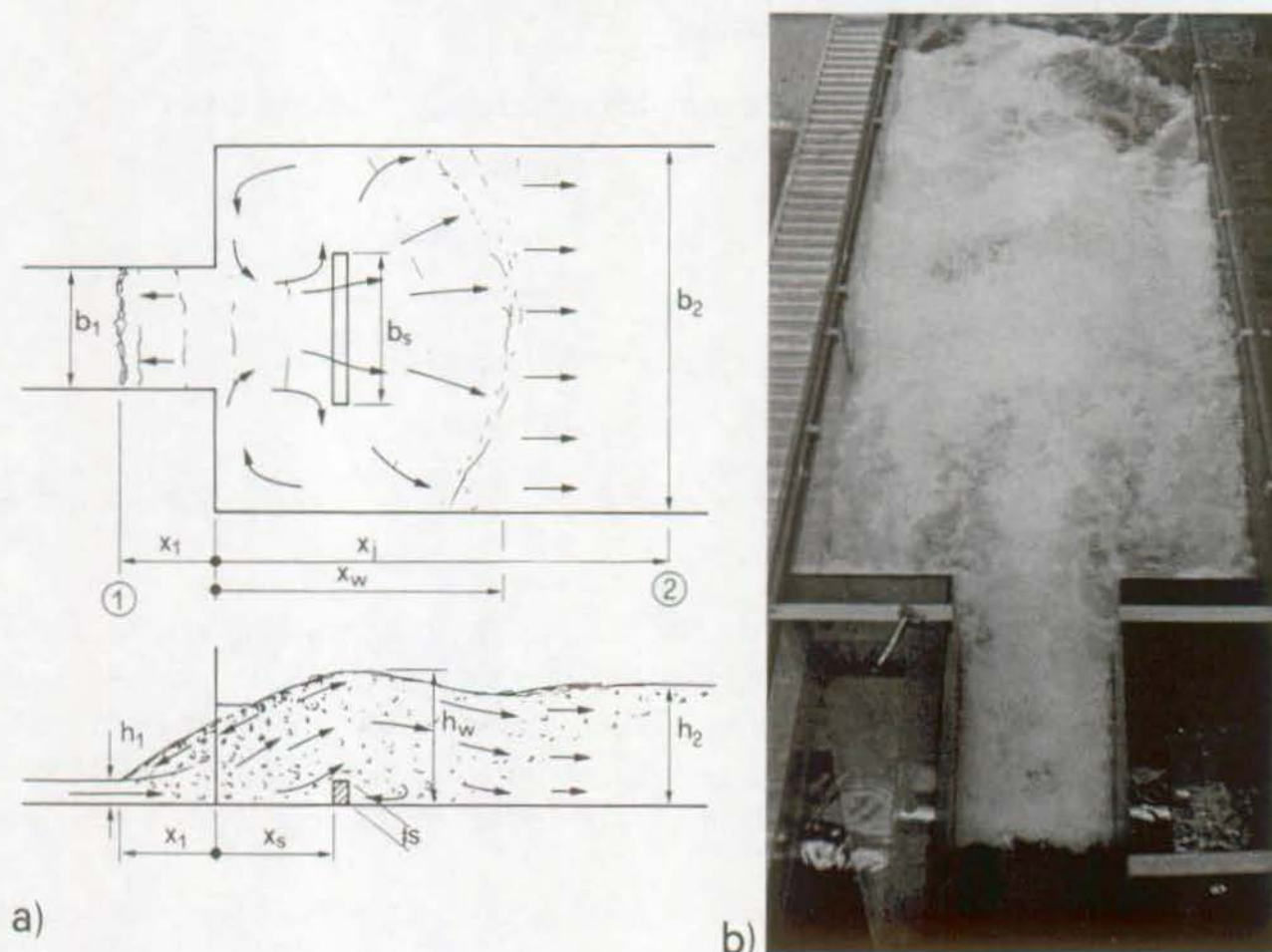


Fig. 9.4 : Notation and overall flow pattern for sill-controlled jumps in sudden expansion. a) Notation, b) overall jump pattern.

The design of sill is based on the toe position $X_1=0.2$. This was considered as the optimal toe position for yielding typical forced jumps. Since the flow asymmetry decreases with increasing X_1 , the proposed sill design will also lead to symmetric jump for $X_1 > 0.20$. The optimal sill height $s_{opt} = S_{opt} \cdot h_1$ may be expressed in terms of F_1 and X_s as

$$S_{opt} = \frac{X_s + 0.0116 F_1 - 0.225}{0.155 - 0.008 F_1} \quad (9.12)$$

where $X_s = x_s/L_r^*$ is the non-dimensional sill position as previously considered. The design must be based on the discharge by which the minimum value in X_1 occurs.

Increasing X_1 corresponds to a gain of safety factor. The width b_s of the central sill should be at least

$$b_s = b_1 \left(1 + \frac{1}{4} (B-1) \right) \quad . \quad (9.13)$$

This width accounts for a sufficient action of corner vortices and the resulting spreading of jet in the tailwater channel.

The **application domains** of sill-controlled sudden expansions are thus (Fig. 9.4a)

- $1 < B \leq 5$, width ratio
- $2 \leq F_1 \leq 10$, Froude number
- $X_1 \geq 0.2$, toe position
- $0.2 \leq X_s \leq 0.5$, and sill location
- $0.6 \leq S \leq 3$. sill height

The length of sill-controlled hydraulic jump, and recommendations for the length of stilling basin were given in paragraph 9.3.3.

In addition to limitations of the computational model, the approaching velocity should not exceed 20 to 25 m/s to avoid effects of cavitation on the central sill. Also, the discharge per unit width should be limited, based on the prototype experiences obtained with USBR basins II and III, to approximately 20 to 30 m²/s. Based on these limitations the proposed stilling basin may therefore only be suggested for relatively small structures.

9.4 CONCLUSIVE REMARKS

In the present research project, the main flow patterns of S- and T-jumps in sudden expansions were investigated both by theoretical and experimental means. The purpose of the research was not only to develop a computational model accounting for the channel expansion, but also to illustrate the significant differences which may exist between hydraulic jumps in prismatic and expanding channels. Of primary concern was the formation of asymmetric flow and its removal. Without additional appurtenances, the expanding channel was found to be an ineffective dissipator. The improvement of the jump obtained with a central baffle sill and an end sill may be useful for the design of relatively small dissipators.

Hydraulic jumps in gradual expansions were not investigated in detail in the present research project. If small expansion angle and small inflow Froude numbers are excluded, the general behavior of gradual expansions was found analogous as in sudden expansions. However, additional investigations would be required to define limit conditions for which the influence of the expansion angle may be neglected. The asymmetry phenomenon in expanding channels involving small expansion angles depends on the inflow conditions, the expansion angle, the expansion ratio and on the jump position relative to the channel expansion. Compared to sudden expansions, one additional parameter such as the expansion angle should therefore be included in such an investigation. A research project generalising the present results by including also gradually expanding stilling basin would be certainly worthwhile.

APPENDICES

APPENDIX 1 : MEASUREMENTS OF CHAPTER 5

APPENDIX 2 : MEASUREMENTS OF CHAPTER 6

APPENDIX 3 : MEASUREMENTS OF CHAPTER 8

APPENDIX 1

MEASUREMENTS OF CHAPTER 5

Appendix 1 includes the data of the experimental investigation presented in chapter 5. These tests were performed in sudden expanding channels with a horizontal floor free of appurtenances. Table 1.1 indicates the main characteristics of the investigated geometries whereas the relevant notation is given in Fig. 1.1.

Table 1.1 : Sudden expanding channels: Overall characteristics of experiments.

Series 1	b ₂ [m] 2	B [-] 3	channel shape 4	F ₁		ω ₁ =h ₁ /b ₁		No of runs 7
				from 5	to	from 6	to	
1.1	0.50	5	asym	2.65	8.12	0.13	0.61	238
1.2	0.50	3	asym	2.62	8.15	0.076	0.38	240
1.3	0.50	3	sym	2.63	8.05	0.073	0.37	221
1.4	0.50	2	asym	2.67	8.18	0.052	0.24	236
1.5	0.50	1.5	asym	2.65	8.13	0.036	0.19	108
1.6	1.50	3	sym	2.99	10.60	0.044	0.12	172

In addition to the symbols indicated in Fig. 1.1, the following non-dimensional terms are used :

$Y = h_2/h_1$: experimental sequent depths ratio

$Y_m = h_{2,m}/h_1$: sequent depths ratio according to Eq. (5.8)

$Y^* = h_2^*/h_1$: sequent depths ratio according to Eq. (5.1)

$Y_p = h_{2,p}/h_1$: predicted sequent depths ratio Eq. (5.26)

$X_1 = x_1/L_r^*$: non-dimensional toe position Eq. (5.3)

$X_e = x_e/L_r^*$: non-dimensional length of the smaller lateral eddy

$X_2 = x_2/L_r^*$: non-dimensional length of the longer lateral eddy.

L_r^* : surface roller length in prismatic channel Eq. (5.4).

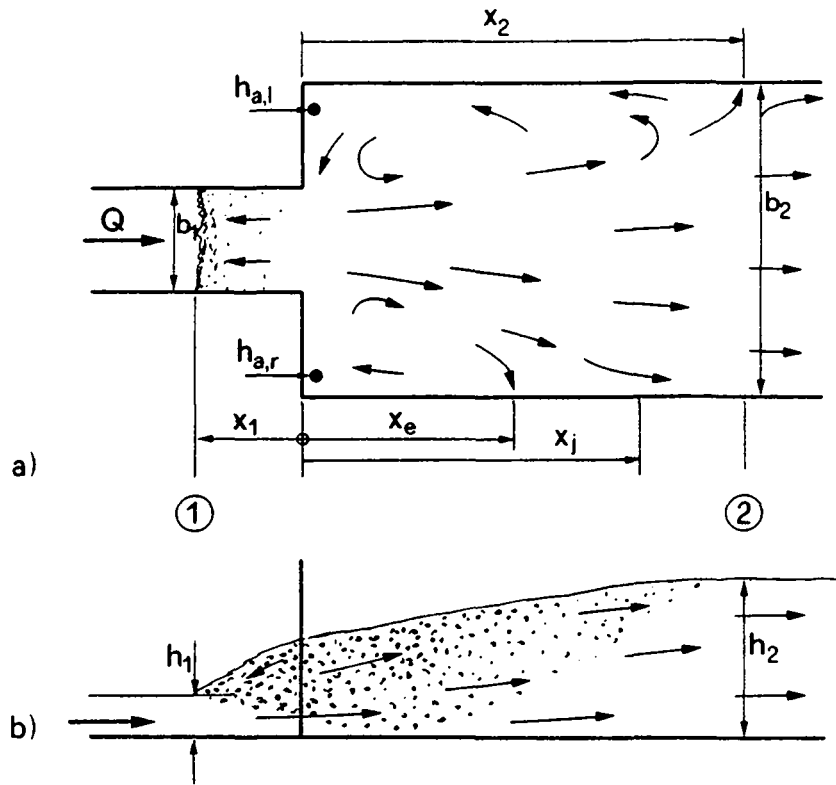


Fig. 1.1 : Relevant notation of sudden expansions investigated in chapter 5.
a) Plan view; b) axial view.

Q	h _a	H ₁	h ₁	F ₁	x ₂	x ₁	h ₂	Y	Y*	Y _m	X ₁	Y _p	
[l/s]	[cm]	[cm]	[mm]	[-]	[cm]	[cm]	[cm]	[-]	[-]	[-]	[-]	[-]	
1 A	18,1	11,0	52,4	60,6	3,91	450	4,0	15,1	2,49	5,05	2,92	0,0314	2,94
2 A	18,1	11,2	52,6	60,5	3,92	415	7,0	15,2	2,51	5,07	2,94	0,0549	3,05
3 A	18,1	12,3	52,6	60,5	3,93	427	8,0	15,4	2,55	5,07	3,04	0,0627	3,09
4 A	18,1	14,9	53,4	59,9	3,98	301	21,0	17,5	2,92	5,15	3,33	0,1635	3,54
5 A	18,1	16,6	53,7	59,8	3,99	273	25,0	18,0	3,01	5,17	3,52	0,1942	3,68
6 A	18,1	18,2	54,2	59,4	4,03	226	34,0	20,6	3,47	5,22	3,72	0,2629	3,97
7 A	18,1	20,6	54,6	59,2	4,06	178	40,0	22,4	3,79	5,26	4,02	0,3083	4,14
8 A	18,1	23,3	55,4	58,6	4,11	124	53,0	24,2	4,13	5,34	4,39	0,4058	4,49
9 A	18,1	23,8	56,2	58,1	4,16	128	65,0	24,4	4,20	5,41	4,50	0,4946	4,76
1 B	16,1	10,9	43,0	60,4	3,50	426	4,0	14,7	2,43	4,47	2,71	0,0360	2,68
2 B	16,1	13,7	43,5	60,0	3,54	344	14,0	17,1	2,85	4,52	3,01	0,1252	3,03
3 B	16,1	16,4	43,9	59,6	3,57	264	23,0	19,2	3,22	4,57	3,32	0,2046	3,33
4 B	16,1	19,0	44,6	59,0	3,62	210	36,0	21,2	3,59	4,64	3,67	0,3179	3,72
5 B	16,1	20,5	45,1	58,6	3,66	194	46,0	21,9	3,74	4,70	3,88	0,4039	3,97
6 B	16,1	21,5	45,6	58,2	3,70	169	55,0	22,7	3,90	4,75	4,04	0,4805	4,17
7 B	16,1	22,1	45,9	58,0	3,72	167	61,0	23,2	4,00	4,78	4,13	0,5312	4,29
8 B	16,1	22,7	46,4	57,6	3,76	160	70,0	23,3	4,04	4,83	4,24	0,6065	4,45
1 C	14,0	9,9	34,5	59,7	3,09	469	3,0	13,3	2,23	3,90	2,43	0,0317	2,39
2 C	14,0	11,7	34,6	59,6	3,10	396	6,0	14,9	2,50	3,92	2,61	0,0632	2,50
3 C	14,0	12,9	34,8	59,4	3,12	350	11,0	15,8	2,66	3,94	2,75	0,1155	2,67
4 C	14,0	14,2	35,0	59,2	3,14	311	16,0	16,6	2,81	3,97	2,91	0,1675	2,83
5 C	14,0	15,6	35,2	58,9	3,16	255	21,0	17,7	3,00	3,99	3,09	0,2191	2,99
6 C	14,0	17,4	35,6	58,5	3,19	235	30,0	18,8	3,21	4,04	3,33	0,3112	3,25
7 C	14,0	18,4	36,1	58,0	3,23	253	41,0	19,8	3,41	4,09	3,49	0,4224	3,52
8 C	14,0	19,4	36,4	57,7	3,25	212	48,0	20,5	3,55	4,13	3,64	0,4924	3,67
9 C	14,0	20,3	36,8	57,3	3,30	202	59,0	21,3	3,72	4,19	3,79	0,6011	3,86
10C	14,0	20,7	37,1	57,0	3,32	182	65,0	21,4	3,76	4,22	3,86	0,6598	3,95
1 D	12,0	9,6	26,9	59,8	2,65	410	1,0	12,1	2,02	3,28	2,19	0,0128	2,05
2 D	12,0	12,3	27,2	59,4	2,67	312	9,0	14,2	2,39	3,31	2,50	0,1145	2,31
3 D	12,0	14,3	27,4	59,0	2,70	274	18,0	15,6	2,65	3,36	2,76	0,2276	2,58
4 D	12,0	15,3	27,6	58,7	2,72	249	23,0	16,4	2,79	3,38	2,90	0,2897	2,72
5 D	12,0	15,6	27,7	58,5	2,74	218	28,0	16,8	2,87	3,40	2,95	0,3514	2,85
6 D	12,0	16,6	28,1	58,0	2,77	240	38,0	17,4	3,00	3,45	3,10	0,4734	3,07
7 D	12,0	17,5	28,3	57,6	2,80	226	46,0	18,1	3,14	3,49	3,24	0,5698	3,21
8 D	12,0	17,7	28,5	57,4	2,82	224	51,0	18,4	3,21	3,51	3,28	0,6294	3,28
9 D	12,0	18,2	28,7	57,1	2,84	210	58,0	18,7	3,28	3,55	3,37	0,7122	3,37
10D	12,0	18,8	29,1	56,5	2,88	200	70,0	19,2	3,40	3,61	3,49	0,8522	3,50
1 E	13,0	8,8	56,1	41,1	5,03	407	4,0	14,2	3,45	6,63	3,67	0,0347	3,72
2 E	13,0	11,2	56,8	40,8	5,08	315	12,0	15,4	3,77	6,70	4,00	0,1036	4,16
3 E	13,0	12,9	57,1	40,7	5,11	277	16,0	17,0	4,18	6,74	4,26	0,1378	4,38
4 E	13,0	14,6	57,7	40,5	5,15	244	22,0	17,5	4,32	6,79	4,55	0,1888	4,69
5 E	13,0	15,6	58,2	40,3	5,18	217	28,0	18,4	4,57	6,85	4,74	0,2394	4,99
6 E	13,0	16,6	58,5	40,2	5,21	211	32,0	19,2	4,78	6,89	4,93	0,2730	5,18
7 E	13,0	18,2	59,2	39,9	5,26	204	39,0	20,6	5,16	6,95	5,24	0,3314	5,50
8 E	13,0	19,4	60,0	39,6	5,32	195	48,0	21,4	5,40	7,04	5,50	0,4057	5,86
9 E	13,0	20,1	60,3	39,5	5,35	182	52,0	22,1	5,60	7,08	5,65	0,4385	6,01
10E	13,0	21,7	61,8	39,0	5,45	170	67,0	23,4	6,00	7,22	6,04	0,5602	6,49
1 F	12,0	9,5	49,5	40,6	4,73	347	-5,0	13,5	3,33	6,21	3,61	0,0470	3,59

	Q	h_a	H_1	h_1	F_1	x_2	x_1	h_2	Y	Y^*	Y_m	X_1	Y_p
	[l/s]	[cm]	[cm]	[mm]	[-]	[cm]	[cm]	[cm]	[-]	[-]	[-]	[-]	[-]
2 F	12,0	11,5	50,0	40,4	4,77	309	11,0	13,8	3,42	6,27	3,91	0,1031	3,92
3 F	12,0	13,2	50,4	40,2	4,80	242	16,0	16,2	4,03	6,31	4,20	0,1495	4,19
4 F	12,0	14,5	50,8	40,0	4,84	218	22,0	17,1	4,28	6,36	4,43	0,2049	4,50
5 F	12,0	16,1	51,4	39,7	4,89	194	30,0	18,2	4,58	6,43	4,74	0,2780	4,88
6 F	12,0	17,0	51,8	39,5	4,92	190	35,0	18,9	4,78	6,48	4,93	0,3234	5,11
7 F	12,0	18,1	52,2	39,4	4,95	187	40,0	19,7	5,00	6,52	5,15	0,3685	5,31
8 F	12,0	19,0	52,9	39,1	5,01	165	48,0	20,4	5,22	6,60	5,36	0,4400	5,62
9 F	12,0	20,0	53,3	38,9	5,04	177	53,0	21,4	5,50	6,64	5,58	0,4844	5,79
10F	12,0	20,7	54,1	38,6	5,10	155	63,0	21,8	5,65	6,74	5,77	0,5723	6,09
1 G	10,0	9,4	35,5	40,7	3,93	355	5,0	12,4	3,05	5,08	3,20	0,0582	3,07
2 G	10,0	11,2	35,9	40,4	3,97	295	12,0	13,6	3,36	5,13	3,50	0,1389	3,44
3 G	10,0	12,2	36,0	40,3	3,98	257	15,0	14,7	3,65	5,16	3,68	0,1733	3,59
4 G	10,0	14,0	36,4	40,1	4,02	244	22,0	16,0	3,99	5,21	4,01	0,2529	3,92
5 G	10,0	15,1	36,7	39,8	4,05	218	28,0	16,7	4,19	5,26	4,24	0,3206	4,18
6 G	10,0	16,1	37,2	39,6	4,10	203	36,0	17,2	4,35	5,32	4,46	0,4100	4,49
7 G	10,0	16,8	37,6	39,3	4,14	179	43,0	17,9	4,55	5,38	4,62	0,4874	4,72
8 G	10,0	17,7	38,0	39,1	4,17	160	49,0	18,6	4,76	5,42	4,83	0,5531	4,89
9 G	10,0	18,1	38,2	38,9	4,20	150	53,0	19,1	4,90	5,46	4,92	0,5966	4,99
10G	10,0	19,1	39,2	38,4	4,29	136	69,0	20,0	5,21	5,59	5,21	0,7683	5,33
1 H	8,1	9,3	24,8	40,6	3,19	310	6,0	10,3	2,54	4,04	2,86	0,0896	2,64
2 H	8,1	11,2	25,0	40,3	3,23	269	13,0	12,1	3,00	4,09	3,20	0,1930	2,98
3 H	8,1	12,4	25,3	40,0	3,26	226	21,0	13,2	3,30	4,14	3,45	0,3098	3,32
4 H	8,1	13,3	25,5	39,8	3,29	198	26,0	13,7	3,44	4,18	3,63	0,3820	3,51
5 H	8,1	14,0	25,8	39,5	3,32	172	33,0	14,6	3,69	4,23	3,80	0,4821	3,73
6 H	8,1	14,6	26,1	39,3	3,36	161	40,0	15,1	3,85	4,27	3,94	0,5811	3,92
7 H	8,1	15,2	26,3	39,1	3,38	154	45,0	15,4	3,94	4,31	4,08	0,6511	4,03
8 H	8,1	15,1	26,5	38,9	3,41	130	50,0	15,6	4,01	4,35	4,09	0,7205	4,12
9 H	8,1	15,6	26,7	38,7	3,43	126	55,0	15,7	4,06	4,38	4,21	0,7894	4,20
10H	8,1	16,3	27,4	38,0	3,53	103	73,0	16,3	4,29	4,51	4,44	1,0329	4,44
1 I	7,1	6,4	49,4	23,6	6,31	422	3,0	9,9	4,19	8,44	4,62	0,0352	4,60
2 I	7,1	8,2	50,0	23,5	6,37	303	8,0	11,1	4,73	8,52	5,06	0,0934	5,09
3 I	7,1	9,9	50,4	23,3	6,42	248	12,0	12,4	5,31	8,59	5,52	0,1397	5,48
4 I	7,1	10,9	50,9	23,2	6,47	210	16,0	12,7	5,47	8,66	5,83	0,1857	5,86
5 I	7,1	11,8	51,6	23,1	6,54	186	22,0	13,6	5,90	8,76	6,14	0,2541	6,40
6 I	7,1	13,5	52,4	22,9	6,62	168	28,0	14,9	6,51	8,87	6,71	0,3218	6,89
7 I	7,1	14,4	53,1	22,7	6,69	142	34,0	15,5	6,83	8,98	7,06	0,3888	7,34
8 I	7,1	15,5	53,6	22,6	6,74	133	38,0	16,0	7,08	9,05	7,45	0,4331	7,61
9 I	7,1	16,6	54,9	22,3	6,88	109	48,0	17,1	7,67	9,24	7,93	0,5427	8,21
10I	7,1	18,2	57,4	21,8	7,12	90	66,0	18,4	8,45	9,58	8,71	0,7351	9,04
1 J	6,2	7,1	38,0	23,7	5,48	326	5,0	9,2	3,88	7,27	4,34	0,0683	4,25
2 J	6,2	9,6	38,6	23,5	5,56	232	12,0	11,4	4,85	7,37	5,04	0,1629	4,91
3 J	6,2	11,0	39,1	23,3	5,62	198	18,0	12,5	5,36	7,46	5,50	0,2431	5,43
4 J	6,2	12,0	39,6	23,2	5,68	187	23,0	13,3	5,74	7,54	5,84	0,3093	5,84
5 J	6,2	13,2	40,1	23,0	5,73	167	28,0	13,9	6,04	7,62	6,25	0,3749	6,20
6 J	6,2	14,4	40,8	22,8	5,81	144	35,0	15,0	6,58	7,73	6,73	0,4658	6,65
7 J	6,2	15,2	41,5	22,6	5,89	108	42,0	15,3	6,78	7,85	7,07	0,5555	7,03
8 J	6,2	15,5	41,9	22,5	5,94	99	46,0	15,7	6,99	7,92	7,21	0,6063	7,22
9 J	6,2	16,6	43,6	22,0	6,14	91	62,0	16,6	7,55	8,19	7,78	0,8057	7,84
10J	6,2	17,1	44,8	21,7	6,28	52	73,0	17,0	7,85	8,39	8,09	0,9394	8,17

Q	h _a	H ₁	h ₁	F ₁	x ₂	x ₁	h ₂	Y	Y*	Y _m	X ₁	Y _p	
[1/s]	[cm]	[cm]	[mm]	[-]	[cm]	[cm]	[cm]	[-]	[-]	[-]	[-]	[-]	
1 K	5,2	7,2	27,5	23,6	4,62	287	4,0	8,4	3,55	6,05	3,96	0,0665	3,61
2 K	5,2	9,6	28,1	23,3	4,70	221	13,0	10,8	4,63	6,17	4,71	0,2143	4,41
3 K	5,2	10,9	28,6	23,1	4,77	190	20,0	11,7	5,06	6,27	5,17	0,3274	4,96
4 K	5,2	12,1	29,2	22,9	4,85	157	28,0	12,5	5,47	6,38	5,63	0,4548	5,48
5 K	5,2	12,7	29,6	22,7	4,91	118	34,0	12,9	5,69	6,46	5,88	0,5491	5,80
6 K	5,2	13,5	30,1	22,5	4,98	97	41,0	13,7	6,10	6,57	6,22	0,6576	6,10
7 K	5,2	13,8	30,7	22,2	5,06	90	48,0	13,9	6,25	6,67	6,40	0,7647	6,35
8 K	5,2	13,9	31,1	22,1	5,11	82	53,0	14,0	6,34	6,75	6,48	0,8402	6,50
9 K	5,2	14,5	32,0	21,7	5,25	63	65,0	14,4	6,64	6,94	6,83	1,0184	6,80
10K	5,2	14,7	32,8	21,4	5,35	55	74,0	14,9	6,96	7,08	7,00	1,1492	7,00
1 L	4,2	6,5	18,9	23,6	3,74	297	4,0	7,8	3,31	4,82	3,40	0,0850	3,04
2 L	4,2	8,0	19,1	23,4	3,79	274	10,0	8,8	3,77	4,89	3,86	0,2112	3,56
3 L	4,2	9,1	19,5	23,1	3,86	345	18,0	9,5	4,11	4,98	4,28	0,3767	4,13
4 L	4,2	10,5	20,0	22,8	3,95	187	28,0	10,6	4,66	5,10	4,82	0,5795	4,65
5 L	4,2	11,0	20,4	22,5	4,02	146	36,0	11,2	4,98	5,20	5,05	0,7384	4,94
6 L	4,2	11,4	20,7	22,3	4,07	127	42,0	11,4	5,12	5,28	5,25	0,8557	5,10
7 L	4,2	11,7	21,1	22,0	4,14	100	49,0	11,5	5,22	5,37	5,41	0,9905	5,26
8 L	4,2	11,7	21,3	21,9	4,18	72	53,0	11,7	5,34	5,43	5,45	1,0665	5,34
9 L	4,2	11,8	21,7	21,6	4,25	64	61,0	11,9	5,50	5,54	5,56	1,2165	5,49
10L	4,2	12,0	22,3	21,3	4,34	61	70,0	12,1	5,67	5,66	5,72	1,3818	5,64
1 M	3,3	6,4	12,0	24,4	2,80	273	6,0	6,9	2,83	3,48	2,94	0,1758	2,55
2 M	3,3	7,1	12,1	24,2	2,83	258	11,0	7,5	3,10	3,53	3,18	0,3201	2,89
3 M	3,3	8,0	12,4	23,8	2,91	239	22,0	8,1	3,41	3,64	3,53	0,6304	3,40
4 M	3,3	8,1	12,6	23,5	2,95	254	28,0	8,3	3,53	3,70	3,60	0,7956	3,56
5 M	3,3	8,4	12,8	23,3	3,00	257	35,0	8,7	3,74	3,77	3,75	0,9848	3,70
6 M	3,3	8,5	12,9	23,2	3,02	254	38,0	8,7	3,76	3,80	3,80	1,0647	3,75
7 M	3,3	8,5	13,1	22,9	3,07	232	44,0	8,7	3,79	3,87	3,84	1,2226	3,83
8 M	3,3	8,6	13,4	22,6	3,14	221	53,0	8,7	3,85	3,96	3,92	1,4544	3,95
9 M	3,3	8,7	13,7	22,2	3,21	207	62,0	8,8	3,96	4,06	4,04	1,6803	4,06
10M	3,3	8,8	14,2	21,7	3,34	199	78,0	8,8	4,06	4,25	4,20	2,0679	4,25
1 N	3,2	4,0	23,1	15,7	5,24	415	2,0	5,2	3,31	6,93	3,98	0,0433	3,92
2 N	3,2	5,2	23,4	15,6	5,29	317	5,0	6,3	4,03	6,99	4,44	0,1079	4,35
3 N	3,2	6,7	24,0	15,4	5,41	248	13,0	7,6	4,94	7,17	5,16	0,2776	5,41
4 N	3,2	8,0	24,4	15,3	5,47	222	17,0	8,7	5,70	7,26	5,81	0,3611	5,86
5 N	3,2	9,5	24,7	15,1	5,54	237	21,0	9,8	6,47	7,35	6,60	0,4437	6,25
6 N	3,2	10,3	25,8	14,8	5,74	212	33,0	10,5	7,10	7,64	7,20	0,6862	7,13
7 N	3,2	11,0	27,2	14,4	6,00	222	47,0	11,0	7,66	7,99	7,82	0,9589	7,80
8 N	3,2	11,4	28,4	14,0	6,21	217	58,0	11,4	8,12	8,29	8,25	1,1655	8,20
9 N	3,2	11,5	29,6	13,7	6,41	202	68,0	11,5	8,37	8,58	8,50	1,3476	8,53
1 O	4,1	3,6	38,1	15,5	6,88	414	2,0	5,4	3,49	9,24	4,76	0,0326	4,96
2 O	4,1	5,3	38,5	15,4	6,93	372	5,0	7,2	4,68	9,32	5,31	0,0812	5,42
3 O	4,1	6,1	38,6	15,4	6,95	326	6,0	7,9	5,15	9,35	5,61	0,0974	5,57
4 O	4,1	8,3	39,6	15,2	7,09	214	13,0	9,3	6,14	9,54	6,61	0,2092	6,60
5 O	4,1	9,8	40,7	14,9	7,25	186	21,0	10,6	7,10	9,76	7,42	0,3349	7,64
6 O	4,1	11,6	41,7	14,7	7,39	176	28,0	12,0	8,14	9,96	8,43	0,4428	8,41
7 O	4,1	12,8	43,4	14,4	7,63	147	39,0	13,1	9,08	10,30	9,27	0,6087	9,37
8 O	4,1	13,9	45,6	14,1	7,92	142	52,0	14,1	10,02	10,72	10,14	0,7990	10,23
9 O	4,1	14,4	47,7	13,7	8,21	182	64,0	14,5	10,56	11,13	10,71	0,9690	10,85

Q	h_a	H_1	h_1	F_1	x_2	x_1	h_2	Y	Y^*	Y_m	X_1	Y_p	
[l/s]	[cm]	[cm]	[mm]	[-]	[cm]	[cm]	[cm]	[-]	[-]	[-]	[-]	[-]	
100	4,1	14,9	51,2	13,2	8,68	172	82,0	14,9	11,26	11,79	11,45	1,2139	11,67
1 P	2,3	3,9	11,7	16,5	3,49	357	2,0	4,5	2,72	4,46	3,03	0,0659	2,78
2 P	2,3	4,4	11,8	16,4	3,52	286	5,0	5,2	3,16	4,50	3,25	0,1639	3,15
3 P	2,3	5,2	11,9	16,3	3,55	247	8,0	5,8	3,55	4,55	3,62	0,2610	3,49
4 P	2,3	6,1	12,1	16,2	3,61	242	13,0	6,5	4,02	4,63	4,07	0,4207	3,95
5 P	2,3	6,6	12,4	16,0	3,68	232	19,0	6,8	4,26	4,73	4,36	0,6087	4,36
6 P	2,3	7,2	12,7	15,7	3,76	224	26,0	7,3	4,64	4,85	4,73	0,8234	4,67
7 P	2,3	7,4	13,3	15,3	3,93	237	39,0	7,4	4,84	5,08	4,99	1,2086	5,03
8 P	2,3	7,7	14,1	14,7	4,15	212	55,0	7,7	5,23	5,39	5,35	1,6591	5,38
9 P	2,3	7,9	15,4	14,0	4,46	227	76,0	7,9	5,63	5,83	5,77	2,2121	5,83
1 Q	2,0	3,8	8,7	17,3	2,84	402	0,0	4,1	2,37	3,55	2,65	0,0000	2,14
2 Q	2,0	4,6	8,8	17,1	2,88	287	4,0	5,2	3,03	3,60	3,01	0,1610	2,59
3 Q	2,0	5,4	9,1	16,8	2,97	202	14,0	5,7	3,40	3,73	3,44	0,5529	3,40
4 Q	2,0	5,7	9,3	16,5	3,04	212	21,0	5,9	3,57	3,83	3,64	0,8184	3,70
5 Q	2,0	6,1	9,5	16,3	3,10	197	27,0	6,2	3,81	3,92	3,88	1,0404	3,86
6 Q	2,0	6,3	10,0	15,7	3,28	212	43,0	6,4	4,08	4,17	4,15	1,6074	4,16
7 Q	2,0	6,6	10,8	14,9	3,53	232	64,0	6,6	4,42	4,52	4,54	2,2987	4,52

	Q	h _a	H ₁	h ₁	F ₁	x ₂	x ₁	h ₂	Y	Y*	Y _m	X ₁	Y _p
	[l/s]	[cm]	[cm]	[mm]	[-]	[cm]	[cm]	[cm]	[-]	[-]	[-]	[-]	[-]
1 A	31,7	10,80	55,3	62,4	3,96	451	6,0	18,80	3,01	5,13	3,43	0,0450	3,53
2 A	31,7	13,90	55,4	62,4	3,97	381	8,0	21,10	3,39	5,14	3,63	0,0600	3,59
3 A	31,7	16,30	55,9	62,0	4,01	338	20,0	22,90	3,70	5,19	3,84	0,1493	3,91
4 A	31,7	17,80	56,2	61,8	4,02	293	26,0	23,50	3,81	5,21	3,97	0,1937	4,06
5 A	31,7	19,90	56,8	61,4	4,06	249	38,0	24,80	4,04	5,27	4,18	0,2818	4,35
6 A	31,7	21,30	57,1	61,2	4,08	211	44,0	25,40	4,15	5,29	4,32	0,3255	4,48
7 A	31,7	23,20	57,7	60,8	4,12	157	56,0	26,80	4,41	5,35	4,53	0,4124	4,71
8 A	31,7	23,80	58,1	60,6	4,15	151	65,0	27,30	4,51	5,39	4,61	0,4770	4,87
9 A	31,7	25,20	58,7	60,2	4,18	151	76,0	28,20	4,68	5,44	4,78	0,5554	5,03
1 B	29,8	11,70	49,6	62,3	3,73	433	5,0	18,80	3,02	4,80	3,32	0,0404	3,32
2 B	29,8	14,70	49,8	62,1	3,75	353	10,0	20,80	3,35	4,82	3,54	0,0806	3,45
3 B	29,8	17,30	50,4	61,6	3,79	301	24,0	22,50	3,65	4,88	3,78	0,1924	3,81
4 B	29,8	18,50	50,6	61,5	3,80	273	29,0	23,20	3,78	4,90	3,90	0,2320	3,94
5 B	29,8	20,10	51,1	61,1	3,84	235	40,0	23,90	3,91	4,95	4,07	0,3186	4,18
6 B	29,8	21,30	51,5	60,8	3,86	220	49,0	24,70	4,06	4,99	4,20	0,3889	4,36
7 B	29,8	22,50	51,9	60,5	3,89	183	59,0	25,50	4,22	5,03	4,35	0,4664	4,54
8 B	29,8	24,30	52,6	60,0	3,94	154	74,0	26,60	4,43	5,10	4,57	0,5814	4,75
1 C	26,9	12,30	41,7	62,2	3,38	345	5,0	18,30	2,94	4,30	3,12	0,0455	3,03
2 C	26,9	14,00	41,9	62,1	3,39	350	9,0	19,10	3,08	4,32	3,26	0,0817	3,13
3 C	26,9	14,80	42,0	62,0	3,40	367	12,0	19,90	3,21	4,33	3,33	0,1089	3,21
4 C	26,9	16,10	42,2	61,8	3,41	347	17,0	20,60	3,34	4,35	3,45	0,1539	3,34
5 C	26,9	16,70	42,2	61,8	3,42	311	19,0	21,05	3,41	4,36	3,50	0,1718	3,39
6 C	26,9	17,20	42,4	61,6	3,43	306	23,0	21,40	3,48	4,37	3,55	0,2076	3,48
7 C	26,9	18,10	42,5	61,5	3,44	279	26,0	21,50	3,50	4,39	3,64	0,2344	3,55
8 C	26,9	19,20	42,7	61,3	3,45	277	32,0	22,30	3,64	4,41	3,76	0,2878	3,69
9 C	26,9	19,80	42,9	61,2	3,47	259	37,0	22,50	3,68	4,43	3,83	0,3320	3,79
10C	26,9	21,10	43,3	60,8	3,50	241	49,0	23,60	3,89	4,48	3,98	0,4374	4,01
11C	26,9	22,20	43,8	60,3	3,54	207	62,0	24,50	4,06	4,53	4,13	0,5503	4,20
1 D	24,0	12,90	34,6	61,9	3,03	317	6,0	17,60	2,84	3,81	2,94	0,0626	2,77
2 D	24,0	14,20	34,7	61,8	3,04	276	9,0	18,30	2,96	3,82	3,06	0,0938	2,84
3 D	24,0	15,60	34,9	61,6	3,05	276	15,0	19,00	3,09	3,85	3,19	0,1559	2,99
4 D	24,0	14,50	35,0	61,4	3,07	256	21,0	19,80	3,23	3,87	3,11	0,2176	3,13
5 D	24,0	17,60	35,2	61,2	3,08	233	26,0	20,50	3,35	3,89	3,40	0,2688	3,24
6 D	24,0	18,80	35,4	61,0	3,10	207	34,0	20,80	3,41	3,92	3,53	0,3502	3,40
7 D	24,0	20,00	35,7	60,6	3,13	211	44,0	21,80	3,60	3,95	3,68	0,4510	3,57
8 D	24,0	20,60	36,0	60,3	3,16	190	54,0	22,40	3,72	3,99	3,77	0,5509	3,72
9 D	24,0	21,30	36,3	60,0	3,18	180	62,0	22,70	3,79	4,02	3,86	0,6301	3,81
1 E	20,9	11,30	27,8	62,0	2,64	333	2,0	15,50	2,50	3,26	2,57	0,0248	2,35
2 E	20,9	12,90	27,8	61,9	2,64	308	5,0	16,20	2,62	3,27	2,71	0,0619	2,43
3 E	20,9	14,50	28,0	61,6	2,66	254	12,0	17,40	2,83	3,30	2,86	0,1481	2,59
4 E	20,9	15,50	28,1	61,4	2,68	241	19,0	17,80	2,90	3,32	2,97	0,2335	2,75
5 E	20,9	16,40	28,3	61,1	2,69	233	25,0	18,30	3,00	3,34	3,07	0,3063	2,87
6 E	20,9	17,60	28,4	61,0	2,70	222	29,0	19,35	3,18	3,36	3,20	0,3545	2,95
7 E	20,9	18,30	28,7	60,5	2,74	191	42,0	19,70	3,26	3,40	3,30	0,5098	3,15
8 E	20,9	18,80	28,9	60,1	2,76	191	52,0	20,00	3,33	3,44	3,38	0,6277	3,26
9 E	20,9	19,10	29,2	59,7	2,79	161	64,0	20,40	3,42	3,48	3,44	0,7676	3,37
1 F	25,8	11,30	55,1	50,2	4,47	397	5,0	19,10	3,81	5,84	3,99	0,0406	3,95
2 F	25,8	12,00	55,2	50,1	4,48	355	7,0	19,10	3,82	5,85	4,05	0,0569	4,02

	Q	h_a	H_1	h_1	F_1	x_2	x_1	h_2	Y	Y^*	Y_m	X_1	Y_p
	[l/s]	[cm]	[cm]	[mm]	[-]	[cm]	[cm]	[cm]	[-]	[-]	[-]	[-]	[-]
3 F	25,8	13,90	55,4	50,0	4,49	316	11,0	20,50	4,11	5,87	4,23	0,0892	4,16
4 F	25,8	15,10	55,7	49,9	4,51	307	16,0	20,80	4,18	5,90	4,36	0,1295	4,33
5 F	25,8	15,90	56,0	49,7	4,53	276	21,0	21,40	4,31	5,93	4,45	0,1696	4,49
6 F	25,8	16,90	56,2	49,6	4,54	269	24,0	22,00	4,44	5,94	4,57	0,1935	4,59
7 F	25,8	18,00	56,6	49,4	4,57	251	31,0	22,70	4,60	5,98	4,71	0,2492	4,81
8 F	25,8	19,00	56,8	49,3	4,58	228	34,0	23,00	4,67	6,00	4,83	0,2730	4,90
9 F	25,8	20,35	57,3	49,1	4,62	221	43,0	23,90	4,87	6,05	5,01	0,3440	5,15
10F	25,8	21,20	57,7	48,9	4,65	192	50,0	24,20	4,96	6,09	5,14	0,3988	5,32
11F	25,8	22,60	58,2	48,6	4,69	183	59,0	25,40	5,23	6,15	5,34	0,4688	5,52
1 G	24,0	11,90	47,7	50,6	4,10	337	5,0	18,00	3,56	5,33	3,78	0,0445	3,65
2 G	24,0	12,90	47,9	50,5	4,12	325	9,0	18,50	3,67	5,35	3,88	0,0799	3,79
3 G	24,0	14,80	48,2	50,2	4,15	299	17,0	19,80	3,95	5,39	4,08	0,1504	4,05
4 G	24,0	15,90	48,4	50,1	4,16	274	20,0	20,10	4,01	5,40	4,20	0,1767	4,15
5 G	24,0	17,00	48,7	50,0	4,18	257	26,0	20,90	4,19	5,44	4,34	0,2291	4,33
6 G	24,0	17,90	48,9	49,8	4,20	234	30,0	21,80	4,38	5,46	4,45	0,2639	4,45
7 G	24,0	19,10	49,3	49,6	4,23	210	38,0	22,20	4,48	5,50	4,61	0,3330	4,66
8 G	24,0	19,80	49,5	49,5	4,24	219	42,0	23,00	4,65	5,52	4,71	0,3674	4,76
9 G	24,0	20,60	49,8	49,3	4,27	211	48,0	23,30	4,73	5,55	4,83	0,4188	4,90
10G	24,0	21,40	50,2	49,1	4,29	191	55,0	23,80	4,85	5,59	4,95	0,4784	5,05
1 H	22,1	11,00	41,1	50,8	3,77	370	5,0	16,50	3,21	4,85	3,46	0,0490	3,38
2 H	22,1	13,70	41,3	50,6	3,78	313	9,0	18,20	3,55	4,87	3,72	0,0880	3,51
3 H	22,1	15,10	41,7	50,4	3,81	311	18,0	18,80	3,68	4,92	3,89	0,1752	3,79
4 H	22,1	16,60	42,0	50,1	3,84	270	25,0	20,00	3,94	4,95	4,07	0,2425	4,00
5 H	22,1	17,30	42,3	49,9	3,86	244	32,0	20,40	4,03	4,99	4,17	0,3094	4,19
6 H	22,1	18,00	42,4	49,8	3,88	240	36,0	20,80	4,12	5,01	4,26	0,3475	4,29
7 H	22,1	19,10	42,7	49,6	3,90	195	43,0	21,40	4,26	5,04	4,41	0,4137	4,46
8 H	22,1	19,80	43,4	49,1	3,96	207	59,0	22,00	4,42	5,12	4,55	0,5633	4,76
9 H	22,1	20,60	43,5	49,0	3,97	195	61,0	22,50	4,52	5,14	4,66	0,5819	4,79
1 I	19,1	11,80	32,4	50,3	3,30	305	3,0	15,80	3,14	4,19	3,24	0,0348	2,93
2 I	19,1	12,70	32,6	50,1	3,32	313	9,0	16,40	3,28	4,22	3,35	0,1039	3,12
3 I	19,1	13,95	32,7	50,0	3,33	288	13,0	17,00	3,40	4,24	3,50	0,1498	3,25
4 I	19,1	14,50	32,8	49,9	3,34	281	17,0	17,40	3,49	4,25	3,57	0,1955	3,37
5 I	19,1	15,70	33,1	49,6	3,37	248	24,0	18,30	3,69	4,29	3,73	0,2750	3,56
6 I	19,1	16,40	33,2	49,5	3,38	221	28,0	18,60	3,76	4,30	3,82	0,3201	3,67
7 I	19,1	17,15	33,4	49,3	3,40	225	34,0	19,00	3,86	4,33	3,93	0,3875	3,81
8 I	19,1	18,50	33,9	48,8	3,45	207	49,0	20,10	4,12	4,40	4,15	0,5541	4,09
9 I	19,1	19,00	34,1	48,7	3,47	167	54,0	20,30	4,17	4,43	4,23	0,6090	4,17
10I	19,1	19,80	34,8	48,0	3,53	172	74,0	20,90	4,35	4,52	4,40	0,8260	4,40
1 J	16,3	11,50	24,5	51,1	2,75	199	5,0	14,10	2,76	3,43	2,86	0,0713	2,54
2 J	16,3	13,40	24,8	50,6	2,79	269	18,0	15,70	3,11	3,48	3,11	0,2546	2,90
3 J	16,3	14,10	24,9	50,4	2,81	265	23,0	15,85	3,15	3,50	3,20	0,3243	3,02
4 J	16,3	15,00	25,1	50,1	2,83	249	32,0	16,45	3,28	3,54	3,34	0,4487	3,21
5 J	16,3	15,90	25,3	49,8	2,86	203	41,0	17,00	3,42	3,57	3,47	0,5718	3,35
6 J	16,3	16,45	25,6	49,5	2,89	213	51,0	18,00	3,64	3,62	3,57	0,7070	3,48
7 J	16,3	17,20	26,3	48,5	2,98	205	79,0	18,00	3,71	3,74	3,75	1,0768	3,70
1 K	19,9	11,00	56,4	37,7	5,28	343	4,0	17,30	4,59	6,99	4,83	0,0358	4,63
2 K	19,9	12,20	56,8	37,6	5,31	291	9,0	18,25	4,86	7,03	5,00	0,0803	4,87
3 K	19,9	13,70	57,3	37,4	5,35	263	15,0	18,70	5,00	7,08	5,21	0,1334	5,15

	Q	h _a	H ₁	h ₁	F ₁	x ₂	x ₁	h ₂	Y	Y*	Y _m	X ₁	Y _p
	[1/s]	[cm]	[cm]	[mm]	[-]	[cm]	[cm]	[cm]	[-]	[-]	[-]	[-]	[-]
4 K	19,9	15,00	57,5	37,3	5,37	255	19,0	19,70	5,29	7,11	5,40	0,1686	5,33
5 K	19,9	16,20	58,3	37,0	5,43	247	29,0	20,70	5,59	7,19	5,62	0,2561	5,76
6 K	19,9	17,10	58,6	36,9	5,45	231	33,0	20,80	5,64	7,23	5,77	0,2909	5,92
7 K	19,9	18,30	59,1	36,8	5,49	211	39,0	21,45	5,84	7,28	5,99	0,3428	6,15
8 K	19,9	19,00	59,5	36,6	5,52	216	44,0	22,00	6,01	7,32	6,12	0,3858	6,32
9 K	19,9	19,80	59,9	36,5	5,55	191	49,0	22,50	6,17	7,36	6,28	0,4286	6,48
10K	19,9	21,00	60,4	36,3	5,59	166	56,0	23,10	6,36	7,42	6,51	0,4881	6,69
1 L	17,9	10,40	46,9	37,5	4,80	316	5,0	15,70	4,20	6,31	4,44	0,0502	4,28
2 L	17,9	11,95	47,2	37,4	4,82	301	9,0	17,00	4,56	6,34	4,64	0,0901	4,46
3 L	17,9	13,00	47,5	37,2	4,85	258	14,0	17,50	4,71	6,37	4,80	0,1398	4,69
4 L	17,9	14,10	47,8	37,1	4,87	264	19,0	17,85	4,82	6,41	4,98	0,1892	4,91
5 L	17,9	15,10	48,2	36,9	4,91	249	26,0	18,90	5,13	6,47	5,16	0,2580	5,21
6 L	17,9	16,10	48,5	36,8	4,94	235	31,0	19,45	5,30	6,51	5,33	0,3068	5,40
7 L	17,9	16,80	48,7	36,7	4,96	229	34,0	20,10	5,49	6,53	5,45	0,3359	5,51
8 L	17,9	18,20	49,2	36,5	5,00	196	41,0	20,60	5,65	6,58	5,71	0,4036	5,75
9 L	17,9	19,20	49,9	36,2	5,06	187	52,0	21,50	5,95	6,67	5,94	0,5090	6,07
10L	17,9	20,55	50,9	35,8	5,14	169	66,0	22,00	6,15	6,79	6,24	0,6413	6,40
1 M	16,1	9,90	37,9	37,9	4,24	345	3,0	14,10	3,72	5,52	3,99	0,0342	3,74
2 M	16,1	11,30	38,1	37,8	4,26	318	7,0	15,00	3,97	5,55	4,18	0,0797	3,92
3 M	16,1	11,90	38,3	37,7	4,28	311	11,0	15,50	4,12	5,58	4,28	0,1250	4,09
4 M	16,1	13,10	38,5	37,6	4,30	276	14,0	16,10	4,29	5,60	4,45	0,1588	4,23
5 M	16,1	14,10	38,8	37,4	4,33	263	20,0	16,70	4,47	5,64	4,63	0,2262	4,47
6 M	16,1	14,70	39,0	37,3	4,35	252	24,0	17,40	4,67	5,67	4,73	0,2708	4,63
7 M	16,1	15,90	39,3	37,1	4,38	231	31,0	18,30	4,94	5,72	4,95	0,3484	4,88
8 M	16,1	16,50	39,6	37,0	4,40	211	35,0	18,75	5,07	5,75	5,07	0,3925	5,01
9 M	16,1	17,40	40,0	36,7	4,45	197	44,0	19,20	5,23	5,81	5,26	0,4910	5,27
10M	16,1	18,20	40,6	36,4	4,51	177	55,0	19,90	5,47	5,89	5,45	0,6099	5,52
11M	16,1	19,10	40,8	36,3	4,53	176	59,0	20,30	5,59	5,92	5,63	0,6529	5,60
1 N	14,4	9,10	30,2	38,5	3,70	373	3,0	12,50	3,25	4,76	3,51	0,0396	3,29
2 N	14,4	10,80	30,4	38,4	3,72	308	7,0	13,55	3,53	4,78	3,74	0,0921	3,46
3 N	14,4	12,30	30,6	38,2	3,74	299	13,0	14,60	3,82	4,82	3,98	0,1704	3,71
4 N	14,4	13,20	30,8	38,0	3,77	265	19,0	15,30	4,03	4,85	4,13	0,2482	3,94
5 N	14,4	14,20	31,0	37,9	3,79	235	24,0	15,80	4,17	4,89	4,31	0,3125	4,12
6 N	14,4	15,10	31,5	37,6	3,84	239	35,0	16,35	4,36	4,96	4,50	0,4528	4,45
7 N	14,4	15,70	31,7	37,4	3,86	189	40,0	17,10	4,57	4,99	4,62	0,5159	4,57
8 N	14,4	16,20	31,9	37,3	3,89	185	45,0	17,50	4,70	5,02	4,72	0,5786	4,68
9 N	14,4	17,10	32,4	36,9	3,95	171	58,0	18,20	4,94	5,11	4,94	0,7400	4,91
10N	14,4	17,80	33,1	36,5	4,02	152	72,0	18,70	5,13	5,20	5,13	0,9109	5,09
1 O	12,1	9,60	23,0	37,8	3,19	338	3,0	12,00	3,17	4,04	3,27	0,0481	2,87
2 O	12,1	10,60	23,2	37,7	3,21	297	8,0	12,40	3,29	4,06	3,44	0,1280	3,08
3 O	12,1	12,10	23,5	37,4	3,25	325	18,0	13,50	3,62	4,12	3,71	0,2859	3,46
4 O	12,1	12,90	23,8	37,1	3,29	251	28,0	13,80	3,73	4,18	3,87	0,4417	3,76
5 O	12,1	13,50	24,1	36,7	3,34	221	39,0	14,30	3,90	4,24	4,02	0,6106	4,00
6 O	12,1	14,20	24,3	36,5	3,37	206	46,0	14,70	4,03	4,29	4,17	0,7167	4,12
7 O	12,1	14,80	24,7	36,2	3,41	201	57,0	15,20	4,21	4,35	4,32	0,8814	4,26
8 O	12,1	15,10	25,0	35,9	3,45	201	66,0	15,45	4,31	4,41	4,42	1,0142	4,35
9 O	12,1	15,30	25,3	35,6	3,49	206	74,0	15,50	4,35	4,46	4,49	1,1310	4,42
1 P	10,0	7,30	17,1	37,6	2,66	437	2,0	9,20	2,45	3,30	2,64	0,0404	2,40

	Q	h _a	H ₁	h ₁	F ₁	x ₂	x ₁	h ₂	Y	Y*	Y _m	X ₁	Y _p
	[l/s]	[cm]	[cm]	[mm]	[-]	[cm]	[cm]	[cm]	[-]	[-]	[-]	[-]	[-]
2 P	10,0	8,30	19,3	34,8	2,99	345	3,0	10,10	2,69	3,76	2,97	0,0567	2,72
3 P	10,0	9,30	17,2	37,4	2,69	301	7,0	10,50	2,81	3,33	2,95	0,1408	2,60
4 P	10,0	9,80	17,3	37,2	2,70	266	11,0	10,90	2,93	3,35	3,05	0,2205	2,75
5 P	10,0	10,70	17,5	36,9	2,73	241	20,0	11,30	3,06	3,40	3,22	0,3979	3,03
6 P	10,0	11,60	17,9	36,4	2,79	231	36,0	12,10	3,32	3,48	3,44	0,7070	3,35
7 P	10,0	12,20	18,2	35,9	2,85	216	51,0	12,60	3,51	3,57	3,60	0,9895	3,52
8 P	10,0	12,50	18,5	35,4	2,91	211	65,0	12,80	3,61	3,64	3,71	1,2469	3,63
9 P	10,0	12,70	18,9	34,9	2,97	206	81,0	13,00	3,72	3,74	3,81	1,5341	3,73
1 Q	12,9	8,30	55,5	24,5	6,58	410	3,0	13,40	5,48	8,83	5,94	0,0324	5,72
2 Q	12,9	10,00	55,9	24,4	6,62	306	7,0	15,00	6,16	8,88	6,27	0,0754	6,03
3 Q	12,9	11,10	56,3	24,3	6,66	262	11,0	15,20	6,26	8,94	6,51	0,1182	6,33
4 Q	12,9	12,40	57,0	24,1	6,73	249	17,0	15,80	6,55	9,02	6,83	0,1820	6,76
5 Q	12,9	13,30	57,4	24,0	6,77	243	21,0	16,30	6,79	9,08	7,06	0,2243	7,04
6 Q	12,9	14,10	57,7	23,9	6,80	221	24,0	17,10	7,14	9,13	7,27	0,2558	7,24
7 Q	12,9	15,00	58,3	23,8	6,85	196	29,0	17,70	7,43	9,20	7,53	0,3081	7,56
8 Q	12,9	16,00	59,0	23,7	6,91	195	35,0	18,30	7,73	9,29	7,83	0,3704	7,92
9 Q	12,9	17,40	59,9	23,5	7,00	176	43,0	19,30	8,22	9,41	8,26	0,4527	8,34
10Q	12,9	18,70	61,1	23,2	7,11	168	53,0	20,15	8,67	9,57	8,71	0,5543	8,79
1 R	12,1	9,90	48,6	24,4	6,14	282	5,0	14,20	5,81	8,20	5,92	0,0584	5,50
2 R	12,1	11,00	49,2	24,3	6,21	268	12,0	14,60	6,02	8,30	6,19	0,1394	6,01
3 R	12,1	12,00	49,6	24,2	6,25	237	16,0	15,25	6,31	8,35	6,44	0,1854	6,30
4 R	12,1	13,40	50,6	23,9	6,35	213	26,0	16,55	6,92	8,49	6,84	0,2992	6,95
5 R	12,1	13,80	50,8	23,9	6,37	212	28,0	16,50	6,91	8,52	6,95	0,3218	7,08
6 R	12,1	15,00	51,2	23,8	6,41	201	32,0	17,10	7,20	8,58	7,28	0,3667	7,30
7 R	12,1	16,30	52,1	23,5	6,50	183	41,0	18,10	7,69	8,71	7,70	0,4670	7,76
8 R	12,1	17,10	52,7	23,4	6,56	179	47,0	18,60	7,95	8,79	7,97	0,5332	8,03
9 R	12,1	18,10	53,9	23,1	6,68	146	58,0	19,45	8,41	8,96	8,35	0,6530	8,44
10R	12,1	18,80	55,8	22,7	6,87	147	75,0	19,70	8,68	9,22	8,74	0,8346	8,95
1 S	11,2	8,80	41,5	24,7	5,63	336	5,0	12,70	5,15	7,47	5,35	0,0637	5,07
2 S	11,2	11,10	41,9	24,5	5,67	269	10,0	14,10	5,75	7,53	5,85	0,1270	5,43
3 S	11,2	12,50	42,5	24,3	5,74	245	18,0	14,95	6,14	7,63	6,22	0,2274	5,97
4 S	11,2	14,00	43,1	24,2	5,81	220	25,0	15,85	6,56	7,72	6,64	0,3143	6,40
5 S	11,2	14,80	43,7	24,0	5,87	193	32,0	16,35	6,82	7,82	6,90	0,4003	6,79
6 S	11,2	15,40	44,3	23,8	5,94	174	39,0	16,90	7,10	7,91	7,12	0,4855	7,11
7 S	11,2	16,50	45,1	23,6	6,02	162	48,0	17,55	7,45	8,03	7,49	0,5937	7,47
8 S	11,2	17,00	45,8	23,4	6,10	172	56,0	18,10	7,75	8,14	7,70	0,6887	7,74
9 S	11,2	17,40	46,8	23,1	6,20	147	66,0	18,30	7,92	8,29	7,92	0,8059	8,01
10S	11,2	17,90	48,0	22,8	6,34	106	79,0	18,70	8,21	8,48	8,19	0,9557	8,32
1 T	9,4	8,90	29,0	25,1	4,60	197	4,0	11,30	4,50	6,02	4,67	0,0629	4,15
2 T	9,4	9,90	29,3	25,0	4,63	176	9,0	12,00	4,80	6,07	4,91	0,1410	4,49
3 T	9,4	11,10	29,6	24,8	4,67	261	14,0	12,50	5,03	6,12	5,22	0,2185	4,81
4 T	9,4	12,20	30,2	24,6	4,75	228	24,0	13,50	5,49	6,23	5,56	0,3717	5,37
5 T	9,4	13,00	30,7	24,3	4,82	236	33,0	14,05	5,78	6,33	5,83	0,5075	5,76
6 T	9,4	13,85	31,2	24,1	4,89	189	42,0	14,65	6,08	6,44	6,12	0,6414	6,07
7 T	9,4	14,50	32,0	23,8	4,99	163	54,0	15,05	6,33	6,58	6,40	0,8170	6,38
8 T	9,4	14,90	33,2	23,3	5,16	151	73,0	15,45	6,64	6,81	6,67	1,0881	6,73
1 U	7,1	7,70	18,2	24,6	3,58	318	3,0	9,30	3,79	4,59	3,83	0,0645	3,26
2 U	7,1	9,60	18,6	24,2	3,66	243	15,0	10,45	4,32	4,70	4,36	0,3190	3,98

	Q	h _a	H ₁	h ₁	F ₁	x ₂	x ₁	h ₂	Y	Y*	Y _m	X ₁	Y _p
	[l/s]	[cm]	[cm]	[mm]	[-]	[cm]	[cm]	[cm]	[-]	[-]	[-]	[-]	[-]
3 U	7,1	10,10	18,9	24,0	3,72	229	24,0	10,60	4,43	4,78	4,55	0,5061	4,38
4 U	7,1	10,70	19,1	23,8	3,75	261	29,0	11,10	4,66	4,83	4,75	0,6087	4,54
5 U	7,1	11,20	19,6	23,5	3,84	205	41,0	11,60	4,95	4,95	4,97	0,8508	4,82
6 U	7,1	11,30	20,0	23,2	3,91	178	51,0	11,80	5,09	5,05	5,07	1,0483	4,99
7 U	7,1	11,50	20,6	22,8	4,01	168	64,0	11,95	5,24	5,19	5,23	1,2994	5,17
8 U	7,1	11,70	21,5	22,2	4,16	171	84,0	12,10	5,45	5,41	5,45	1,6733	5,41
1 V	7,0	6,90	46,1	14,4	7,88	406	3,0	10,00	6,94	10,65	7,43	0,0453	6,92
2 V	7,0	8,30	46,7	14,3	7,96	255	7,0	11,00	7,69	10,76	7,95	0,1053	7,45
3 V	7,0	9,50	47,3	14,2	8,04	227	11,0	11,70	8,23	10,88	8,46	0,1648	7,97
4 V	7,0	10,30	48,0	14,1	8,12	233	15,0	12,30	8,72	11,00	8,84	0,2238	8,47
5 V	7,0	10,80	48,6	14,0	8,21	206	19,0	12,75	9,10	11,12	9,12	0,2822	8,94
6 V	7,0	12,50	49,9	13,8	8,38	228	27,0	13,95	10,09	11,36	10,01	0,3977	9,78
7 V	7,0	13,40	50,9	13,7	8,51	178	33,0	14,65	10,71	11,55	10,54	0,4829	10,33
8 V	7,0	14,20	52,2	13,5	8,67	156	40,0	14,90	11,03	11,78	11,08	0,5810	10,88
9 V	7,0	15,10	55,2	13,1	9,06	131	56,0	15,50	11,82	12,33	11,91	0,7991	11,89
10V	7,0	15,60	60,3	12,5	9,70	128	80,0	16,10	12,85	13,23	12,84	1,1110	13,09
1 W	6,0	7,10	34,7	14,4	6,81	330	3,0	9,35	6,50	9,14	6,78	0,0532	6,04
2 W	6,0	8,80	35,6	14,2	6,93	233	10,0	10,60	7,46	9,31	7,52	0,1759	6,93
3 W	6,0	9,80	36,0	14,1	7,00	229	14,0	11,20	7,94	9,42	7,99	0,2451	7,41
4 W	6,0	10,90	36,8	14,0	7,12	183	20,0	11,90	8,52	9,58	8,57	0,3478	8,05
5 W	6,0	11,60	37,4	13,8	7,22	180	25,0	12,35	8,93	9,72	8,98	0,4323	8,52
6 W	6,0	12,60	38,4	13,6	7,38	149	33,0	13,05	9,57	9,94	9,61	0,5654	9,16
7 W	6,0	13,10	41,3	13,1	7,80	106	53,0	13,30	10,13	10,55	10,29	0,8871	10,28
8 W	6,0	13,30	43,3	12,8	8,11	82	66,0	13,50	10,55	10,97	10,71	1,0876	10,85
9 W	6,0	13,70	45,4	12,5	8,40	67	78,0	13,80	11,04	11,39	11,23	1,2667	11,33
1 X	5,1	8,00	25,4	14,5	5,76	245	5,0	9,50	6,57	7,66	6,46	0,1059	5,41
2 X	5,1	9,10	26,2	14,2	5,90	221	14,0	10,05	7,06	7,86	7,05	0,2932	6,43
3 X	5,1	9,90	26,8	14,1	6,00	173	20,0	10,35	7,35	8,00	7,50	0,4159	7,00
4 X	5,1	10,40	27,4	13,9	6,12	126	27,0	10,90	7,85	8,17	7,85	0,5566	7,52
5 X	5,1	10,70	28,5	13,6	6,32	108	38,0	11,10	8,16	8,45	8,19	0,7727	8,14
6 X	5,1	11,10	29,3	13,4	6,47	96	46,0	11,30	8,44	8,66	8,54	0,9260	8,48
7 X	5,1	11,30	30,3	13,2	6,64	84	55,0	11,40	8,67	8,91	8,82	1,0945	8,81
8 X	5,1	11,60	31,9	12,8	6,91	92	68,0	11,70	9,13	9,29	9,26	1,3306	9,25
1 Y	4,3	7,10	17,0	15,2	4,50	323	3,0	8,00	5,26	5,89	5,24	0,0797	4,13
2 Y	4,3	7,80	17,4	15,0	4,62	241	12,0	8,25	5,51	6,05	5,64	0,3150	5,06
3 Y	4,3	8,10	17,8	14,8	4,70	249	18,0	8,55	5,78	6,16	5,84	0,4687	5,53
4 Y	4,3	8,40	18,2	14,6	4,78	211	24,0	8,80	6,01	6,27	6,06	0,6200	5,89
5 Y	4,3	8,70	18,5	14,5	4,86	212	30,0	8,80	6,08	6,39	6,27	0,7687	6,16
6 Y	4,3	9,10	19,8	13,9	5,14	213	49,0	9,10	6,53	6,79	6,75	1,2234	6,74
7 Y	4,3	9,30	20,5	13,7	5,28	211	58,0	9,35	6,84	6,99	6,99	1,4301	6,97
8 Y	4,3	9,40	21,5	13,3	5,50	214	71,0	9,40	7,06	7,30	7,27	1,7190	7,29
1 Z	3,3	4,90	10,0	15,8	3,27	346	2,0	5,50	3,49	4,15	3,64	0,0746	3,01
2 Z	3,3	5,60	10,2	15,6	3,34	309	9,0	5,85	3,76	4,25	3,97	0,3322	3,64
3 Z	3,3	6,20	10,6	15,2	3,45	283	20,0	6,30	4,14	4,41	4,33	0,7251	4,24
4 Z	3,3	6,40	10,9	15,0	3,54	251	28,0	6,35	4,24	4,53	4,50	1,0020	4,47
5 Z	3,3	6,60	11,4	14,5	3,70	212	42,0	6,70	4,61	4,75	4,75	1,4689	4,74
6 Z	3,3	6,80	11,7	14,3	3,80	198	50,0	6,80	4,76	4,89	4,94	1,7256	4,89
7 Z	3,3	6,90	11,9	14,2	3,85	209	54,0	6,80	4,80	4,96	5,04	1,8513	4,96

Q	h_a	H_1	h_1	F_1	x_2	x_1	h_2	Y	Y^*	Y_m	X_1	Y_p	
[l/s]	[cm]	[cm]	[mm]	[-]	[cm]	[cm]	[cm]	[-]	[-]	[-]	[-]	[-]	
8 Z	3,3	7,00	13,0	13,4	4,18	187	79,0	7,00	5,23	5,44	5,43	2,5973	5,44

	Q	$h_{a,l}$	$h_{a,r}$	H_1	h_1	F_1	x_e	x_2	x_1	x_j	h_2	Y	Y*	Y_m	X_1	Y_p
	[1/s]	[cm]	[cm]	[cm]	[mm]	[-]	[cm]	[cm]	[cm]	[cm]	[cm]	[-]	[-]	[-]	[-]	[-]
1 A	26,9	11,40	5,85	51,1	54,80	4,08	57	369	7,0		18,7	3,41	5,29	3,47	0,0579	3,68
2 A	26,9	13,30	8,50	51,3	54,67	4,10	44	319	9,0		19,9	3,63	5,31	3,63	0,0742	3,74
3 A	26,9	14,80	11,00	51,8	54,34	4,13	42	249	14,0		20,8	3,83	5,37	3,81	0,1150	3,92
4 A	26,9	16,60	13,00	52,5	53,95	4,18	41	229	20,0		21,8	4,03	5,43	4,00	0,1634	4,12
5 A	26,9	14,70	18,20	53,0	53,62	4,22	49	184	25,0		22,7	4,23	5,48	4,19	0,2033	4,28
6 A	26,9	17,10	20,20	54,5	52,77	4,32	44	129	38,0		23,3	4,42	5,63	4,49	0,3054	4,69
7 A	26,9	21,00	18,10	55,4	52,25	4,38	42	104	46,0		24,2	4,63	5,72	4,64	0,3671	4,92
8 A	26,9	21,70	20,80	56,7	51,54	4,47	35	84	57,0	109	24,8	4,81	5,85	4,91	0,4504	5,22
9 A	26,9	24,20	22,00	58,1	50,82	4,57	34	89	68,0	104	26,15	5,15	5,98	5,21	0,5319	5,49
1 B	24,0	8,40	12,60	41,8	54,82	3,64	47	344	9,0	257	17,7	3,23	4,67	3,27	0,0851	3,37
2 B	24,0	10,60	14,10	42,3	54,41	3,68	41	304	15,0	194	18,6	3,42	4,73	3,45	0,1410	3,56
3 B	24,0	11,70	15,30	42,8	54,00	3,72	39	284	21,0	169	19,1	3,54	4,79	3,59	0,1962	3,75
4 B	24,0	13,50	16,70	43,1	53,73	3,75	41	229	25,0	139	20,1	3,74	4,83	3,76	0,2327	3,88
5 B	24,0	15,60	18,40	43,8	53,26	3,80	37	159	32,0	119	21,2	3,98	4,90	4,00	0,2958	4,09
6 B	24,0	17,10	19,60	44,4	52,78	3,85	36	119	39,0	99	22,1	4,19	4,97	4,18	0,3581	4,28
7 B	24,0	19,10	20,60	45,5	52,04	3,93	34	109	50,0	94	22,8	4,38	5,09	4,43	0,4542	4,56
8 B	24,0	20,00	21,60	46,4	51,43	4,00	33	109	59,0	89	23,7	4,61	5,18	4,60	0,5312	4,77
9 B	24,0	21,30	22,60	47,6	50,62	4,10	37	109	71,0	86	24,4	4,82	5,32	4,83	0,6318	5,01
1 C	20,1	10,40	13,00	31,0	54,90	3,05	46	299	11,0	129	16,3	2,97	3,84	2,98	0,1286	2,93
2 C	20,1	11,40	13,80	31,4	54,46	3,08	43	279	17,0	99	16,7	3,07	3,89	3,10	0,1974	3,11
3 C	20,1	12,30	14,40	31,7	54,10	3,12	39	249	22,0	94	17,2	3,18	3,93	3,20	0,2540	3,25
4 C	20,1	13,30	15,30	31,9	53,88	3,13	37	219	25,0	94	17,7	3,29	3,96	3,31	0,2877	3,33
5 C	20,1	14,30	16,20	32,4	53,30	3,19	37	199	33,0	89	18,3	3,43	4,03	3,46	0,3763	3,54
6 C	20,1	15,50	17,20	32,7	52,94	3,22	35	174	38,0	84	19,0	3,59	4,08	3,60	0,4309	3,65
7 C	20,1	16,50	17,70	33,2	52,43	3,27	34	139	45,0	79	19,6	3,74	4,15	3,73	0,5063	3,81
8 C	20,1	17,10	18,10	33,4	52,21	3,29	34	114	48,0	74	19,9	3,81	4,17	3,81	0,5382	3,87
9 C	20,1	18,90	18,00	34,0	51,64	3,34	34	109	56,0	74	20,4	3,95	4,25	3,96	0,6223	4,01
10C	20,1	18,80	19,40	35,1	50,56	3,45	33	104	71,0	59	20,7	4,09	4,40	4,14	0,7758	4,26
11C	20,1	20,40	19,60	36,3	49,50	3,56	32	104	86,0	39	21,5	4,34	4,56	4,37	0,9240	4,47
1 D	16,1	8,70	10,50	21,6	55,39	2,41	51	329	5,0	119	13,0	2,35	2,94	2,39	0,0781	2,24
2 D	16,1	9,60	11,20	21,8	54,98	2,44	44	289	10,0	99	13,6	2,47	2,98	2,48	0,1550	2,38
3 D	16,1	10,60	12,20	22,0	54,65	2,46	42	249	14,0	84	14,1	2,58	3,01	2,60	0,2158	2,49
4 D	16,1	11,50	12,90	22,1	54,33	2,48	39	219	18,0	79	14,4	2,65	3,04	2,71	0,2759	2,59
5 D	16,1	12,50	13,50	22,3	54,01	2,50	39	179	22,0	69	14,9	2,76	3,07	2,81	0,3354	2,69
6 D	16,1	13,40	14,30	22,6	53,36	2,55	37	149	30,0	59	15,7	2,94	3,14	2,95	0,4522	2,86
7 D	16,1	14,30	15,00	23,1	52,64	2,60	34	144	39,0	49	16,1	3,06	3,21	3,09	0,5804	3,02
8 D	16,1	15,50	15,00	23,7	51,60	2,68	32	139	52,0	29	16,5	3,20	3,32	3,24	0,7600	3,22
9 D	16,1	16,20	16,10	24,2	50,73	2,75	31	134	63,0	9	16,6	3,27	3,42	3,42	0,9068	3,35
1 E	23,9	7,80	12,10	51,6	48,16	4,41	57	339	7,0	179	18,3	3,80	5,76	3,88	0,0602	3,97
2 E	23,9	10,10	13,60	52,5	47,71	4,47	51	299	14,0	169	19,3	4,04	5,84	4,09	0,1196	4,25
3 E	23,9	11,50	15,00	52,7	47,59	4,49	47	239	16,0	159	20,2	4,24	5,87	4,24	0,1364	4,33
4 E	23,9	13,80	16,80	53,8	47,01	4,57	39	199	25,0	139	21,0	4,47	5,99	4,51	0,2112	4,68
5 E	23,9	15,40	18,10	54,4	46,75	4,61	36	179	29,0	129	22,0	4,71	6,04	4,70	0,2441	4,83
6 E	23,9	17,10	19,70	55,8	46,05	4,72	35	139	40,0	119	23,0	4,99	6,19	4,99	0,3331	5,22
7 E	23,9	18,80	20,80	57,1	45,47	4,81	35	129	49,0	104	23,9	5,26	6,32	5,24	0,4044	5,52
8 E	23,9	21,40	22,50	58,8	44,71	4,93	34	109	51,0	99	24,8	5,55	6,49	5,63	0,4975	5,88
9 E	23,9	23,40	24,30	60,9	43,82	5,08	34	89	75,0	79	25,8	5,89	6,70	6,04	0,6032	6,26
1 F	21,0	11,20	7,20	40,7	48,24	3,86	51	319	7,0	179	16,2	3,36	4,98	3,42	0,0702	3,52

	Q	$h_{a,l}$	$h_{a,r}$	H_1	h_1	F_1	x_e	x_2	x_1	x_j	h_2	Y	Y^*	Y_m	X_1	Y_p
	[l/s]	[cm]	[cm]	[cm]	[mm]	[-]	[cm]	[cm]	[cm]	[cm]	[cm]	[-]	[-]	[-]	[-]	[-]
2 F	21,0	13,40	10,20	41,1	47,97	3,89	43	284	11,0	159	17,5	3,65	5,03	3,68	0,1098	3,67
3 F	21,0	14,30	12,30	41,9	47,44	3,96	45	229	19,0	139	18,4	3,88	5,12	3,89	0,1880	3,97
4 F	21,0	16,10	13,90	42,7	46,90	4,02	39	189	27,0	119	19,1	4,07	5,21	4,13	0,2650	4,26
5 F	21,0	16,80	14,40	43,0	46,70	4,05	35	169	30,0	114	20,0	4,28	5,25	4,22	0,2935	4,36
6 F	21,0	18,10	16,20	43,5	46,37	4,09	35	139	35,0	109	20,8	4,49	5,31	4,45	0,3405	4,53
7 F	21,0	19,30	17,60	44,9	45,50	4,21	34	119	48,0	99	21,6	4,75	5,48	4,72	0,4606	4,91
8 F	21,0	20,50	19,30	45,6	45,10	4,27	34	94	54,0	99	22,1	4,90	5,56	4,96	0,5148	5,08
9 F	21,0	21,40	20,20	46,4	44,64	4,33	34	79	61,0	84	22,9	5,13	5,65	5,15	0,5772	5,25
10F	21,0	22,20	21,10	48,5	43,52	4,50	34	84	78,0	74	23,3	5,35	5,89	5,44	0,7246	5,64
1 G	18,0	12,40	10,20	31,8	47,80	3,36	53	349	11,0	179	15,8	3,31	4,28	3,29	0,1310	3,23
2 G	18,0	13,80	11,60	32,3	47,30	3,41	47	309	18,0	149	16,4	3,47	4,36	3,49	0,2127	3,48
3 G	18,0	14,80	13,20	32,6	47,02	3,45	45	299	22,0	129	17,1	3,64	4,40	3,67	0,2587	3,61
4 G	18,0	15,50	14,00	33,2	46,53	3,50	45	229	29,0	109	17,8	3,83	4,48	3,81	0,3382	3,84
5 G	18,0	16,30	15,20	33,5	46,25	3,53	43	209	33,0	99	18,3	3,96	4,52	3,96	0,3830	3,96
6 G	18,0	17,20	16,10	34,2	45,62	3,61	39	189	42,0	89	19,1	4,19	4,62	4,15	0,4822	4,20
7 G	18,0	17,80	17,20	34,7	45,20	3,66	37	159	48,0	79	19,3	4,27	4,69	4,31	0,5471	4,35
8 G	18,0	18,70	18,10	35,9	44,30	3,77	36	139	61,0	69	20,1	4,54	4,85	4,54	0,6845	4,63
9 G	18,0	19,20	19,70	36,8	43,61	3,86	35	119	71,0	59	20,7	4,75	4,98	4,78	0,7872	4,82
1 H	15,1	10,50	8,70	23,4	48,26	2,78	49	349	7,0	139	13,1	2,71	3,46	2,74	0,1045	2,62
2 H	15,1	11,20	10,20	23,6	47,95	2,80	48	299	11,0	139	13,5	2,82	3,50	2,88	0,1633	2,76
3 H	15,1	12,10	11,10	23,9	47,57	2,84	46	279	16,0	129	14,0	2,94	3,54	3,02	0,2359	2,92
4 H	15,1	12,90	12,00	24,1	47,27	2,86	42	259	20,0	119	14,8	3,13	3,58	3,14	0,2932	3,04
5 H	15,1	13,60	12,90	24,4	46,89	2,90	39	229	25,0	114	15,2	3,24	3,63	3,27	0,3639	3,18
6 H	15,1	14,40	13,80	24,9	46,29	2,96	37	199	33,0	99	15,8	3,41	3,71	3,44	0,4750	3,39
7 H	15,1	15,00	14,60	25,4	45,62	3,02	35	179	42,0	89	16,3	3,57	3,80	3,59	0,5971	3,58
8 H	15,1	15,90	15,50	26,0	44,94	3,09	35	159	51,0	69	16,9	3,76	3,90	3,78	0,7159	3,75
9 H	15,1	16,30	16,10	26,7	44,05	3,18	34	159	63,0	59	17,3	3,93	4,03	3,95	0,8697	3,94
10H	15,1	17,00	16,80	28,8	41,99	3,42	34	159	91,0	49	17,7	4,22	4,37	4,29	1,2083	4,34
1 I	17,1	11,20	8,00	47,0	35,78	4,92	57	359	9,0	179	16,0	4,47	6,48	4,49	0,0918	4,56
2 I	17,1	12,70	10,20	47,7	35,46	4,99	54	319	14,0	159	17,0	4,79	6,57	4,77	0,1420	4,84
3 I	17,1	14,50	11,90	49,1	34,90	5,11	48	269	23,0	139	17,8	5,10	6,75	5,12	0,2307	5,32
4 I	17,1	15,60	13,50	50,0	34,52	5,20	47	239	29,0	129	18,8	5,45	6,86	5,40	0,2887	5,62
5 I	17,1	17,40	15,20	51,7	33,89	5,34	45	229	39,0	119	19,9	5,87	7,07	5,81	0,3835	6,10
6 I	17,1	18,30	17,00	53,0	33,45	5,45	44	209	46,0	109	20,7	6,19	7,22	6,14	0,4483	6,41
7 I	17,1	18,40	20,30	55,4	32,63	5,65	40	159	59,0	99	21,4	6,56	7,51	6,64	0,5654	6,93
8 I	17,1	20,50	21,20	57,9	31,87	5,86	37	109	71,0	84	22,5	7,06	7,80	7,12	0,6699	7,38
9 I	17,1	22,00	22,00	61,8	30,74	6,18	35	69	89,0	69	23,4	7,61	8,26	7,68	0,8200	8,00
1 J	15,3	7,80	10,50	37,7	35,99	4,36	50	359	10,0	159	14,4	4,00	5,68	4,04	0,1167	4,13
2 J	15,3	9,50	11,90	38,1	35,80	4,39	47	319	13,0	129	15,2	4,25	5,73	4,26	0,1511	4,29
3 J	15,3	10,90	12,90	38,7	35,48	4,45	49	299	18,0	124	16,0	4,51	5,81	4,48	0,2079	4,54
4 J	15,3	12,20	14,10	39,3	35,15	4,51	49	259	23,0	114	16,6	4,72	5,90	4,73	0,2638	4,79
5 J	15,3	13,00	14,80	39,9	34,82	4,58	47	239	28,0	109	17,2	4,94	5,99	4,90	0,3191	5,02
6 J	15,3	14,40	15,80	41,0	34,30	4,68	46	219	36,0	99	17,6	5,13	6,14	5,19	0,4059	5,37
7 J	15,3	15,50	16,50	42,1	33,78	4,79	45	179	44,0	89	18,2	5,39	6,29	5,45	0,4907	5,69
8 J	15,3	17,30	16,40	42,4	33,65	4,82	43	149	46,0	79	18,8	5,59	6,33	5,63	0,5116	5,77
9 J	15,3	17,70	16,90	43,3	33,26	4,90	42	119	52,0	74	19,3	5,80	6,45	5,79	0,5736	5,98
10J	15,3	19,20	18,50	45,5	32,35	5,11	42	89	66,0	64	20,0	6,18	6,75	6,29	0,7142	6,44
11J	15,3	19,40	19,00	46,3	32,02	5,19	41	79	71,0	59	20,4	6,37	6,86	6,44	0,7629	6,60

SERIES : 1.3

A1-15

Q	h _{a,l}	h _{a,r}	H ₁	h ₁	F ₁	x _e	x ₂	x ₁	x _j	h ₂	Y	Y*	Y _m	X ₁	Y _p	
[1/S]	[CM]	[CM]	[CM]	[MM]	[-]	[CM]	[CM]	[CM]	[CM]	[CM]	[-]	[-]	[-]	[-]	[-]	
1 K	13,2	11,10	9,50	29,5	35,58	3,82	55	309	13,0	129	13,7	3,85	4,92	3,84	0,1789	3,80
2 K	13,2	11,80	10,30	29,9	35,24	3,87	53	299	18,0	119	14,1	4,00	5,00	4,00	0,2460	4,04
3 K	13,2	12,60	11,80	30,4	34,90	3,93	49	239	23,0	99	14,7	4,21	5,08	4,24	0,3120	4,27
4 K	13,2	13,40	12,40	30,8	34,63	3,97	46	219	27,0	89	15,0	4,33	5,14	4,39	0,3641	4,44
5 K	13,2	14,40	13,40	31,3	34,29	4,03	43	199	32,0	79	15,5	4,52	5,23	4,62	0,4284	4,64
6 K	13,2	13,80	14,80	32,1	33,81	4,12	43	179	39,0	74	16,1	4,76	5,35	4,77	0,5167	4,89
7 K	13,2	14,80	15,60	33,2	33,13	4,25	41	129	49,0	69	16,8	5,07	5,53	5,06	0,6395	5,22
8 K	13,2	16,10	16,80	34,0	32,66	4,34	37	109	56,0	64	17,3	5,30	5,66	5,39	0,7232	5,42
9 K	13,2	16,80	17,00	35,4	31,91	4,49	35	99	67,0	54	18,0	5,64	5,87	5,63	0,8508	5,72
10K	13,2	17,30	17,40	36,2	31,50	4,58	35	99	73,0	44	18,1	5,75	6,00	5,81	0,9186	5,87
1 L	11,2	8,10	6,20	21,1	36,98	3,06	49	394	4,0	169	10,8	2,92	3,86	2,90	0,0689	2,81
2 L	11,2	8,70	7,30	21,2	36,84	3,08	49	339	6,0	139	11,2	3,04	3,89	3,02	0,1031	2,90
3 L	11,2	9,50	8,50	21,4	36,55	3,12	47	299	10,0	129	11,8	3,23	3,94	3,19	0,1706	3,09
4 L	11,2	10,20	9,30	21,8	36,11	3,18	46	289	16,0	119	12,2	3,38	4,02	3,36	0,2703	3,35
5 L	11,2	11,10	10,20	22,0	35,90	3,21	45	289	19,0	109	12,6	3,51	4,06	3,52	0,3194	3,47
6 L	11,2	11,40	10,60	22,3	35,61	3,24	43	289	23,0	99	13,0	3,65	4,12	3,62	0,3841	3,62
7 L	11,2	12,20	11,80	22,7	35,17	3,30	42	269	29,0	89	13,6	3,87	4,20	3,84	0,4794	3,82
8 L	11,2	12,80	12,30	23,1	34,81	3,36	39	239	34,0	79	14,0	4,02	4,27	3,99	0,5574	3,97
9 L	11,2	13,50	13,20	23,9	34,08	3,46	37	199	44,0	69	14,4	4,23	4,42	4,24	0,7092	4,24
10L	11,2	15,00	15,00	25,5	32,71	3,69	36	149	63,0	54	15,6	4,77	4,74	4,77	0,9832	4,66
1 M	9,2	6,60	7,90	15,6	36,74	2,54	45	339	3,0	169	9,7	2,64	3,13	2,59	0,0658	2,34
2 M	9,2	7,80	8,80	15,8	36,35	2,59	44	299	8,0	79	10,1	2,78	3,19	2,78	0,1737	2,56
3 M	9,2	8,80	9,20	15,9	36,12	2,61	45	259	11,0	64	10,4	2,88	3,23	2,92	0,2374	2,68
4 M	9,2	9,10	9,60	16,2	35,57	2,67	43	229	18,0	49	11,0	3,09	3,31	3,03	0,3830	2,94
5 M	9,2	9,80	10,20	16,4	35,26	2,71	41	219	22,0	39	11,3	3,20	3,36	3,18	0,4644	3,07
6 M	9,2	10,40	10,90	16,7	34,79	2,76	42	209	28,0	34	11,6	3,33	3,44	3,34	0,5841	3,23
7 M	9,2	11,20	11,00	17,1	34,32	2,82	44	199	34,0	29	12,0	3,50	3,52	3,48	0,7007	3,38
8 M	9,2	11,70	11,70	17,6	33,62	2,91	43	179	43,0	24	12,3	3,66	3,64	3,68	0,8704	3,56
9 M	9,2	12,40	12,40	18,6	32,38	3,08	42	139	59,0	9	12,7	3,92	3,88	3,99	1,1564	3,85
10M	9,2	12,70	12,70	19,7	31,14	3,26	45	129	75,0	-1	13,0	4,17	4,14	4,24	1,4233	4,13
1 N	7,2	6,70	7,50	10,7	37,55	1,92	51	279	3,0	69	8,2	2,18	2,26	2,19	0,0944	1,82
2 N	7,2	7,10	7,80	10,8	37,09	1,95	46	209	8,0	49	8,5	2,29	2,31	2,28	0,2482	2,00
3 N	7,2	8,00	7,70	10,9	36,73	1,98	47	169	12,0	39	8,9	2,42	2,35	2,38	0,3681	2,12
4 N	7,2	8,60	8,60	11,2	35,72	2,07	45	179	23,0	19	9,2	2,58	2,46	2,59	0,6846	2,38
5 N	7,2	9,10	9,00	11,5	34,90	2,14	48	189	32,0	9	9,5	2,72	2,57	2,74	0,9294	2,53
6 N	7,2	9,60	9,60	12,5	32,40	2,39	49	179	60,0	-1	9,9	3,06	2,92	3,10	1,6166	2,92
1 O	10,1	6,40	9,00	37,5	23,39	5,48	49	369	3,0	129	12,2	5,22	7,27	5,12	0,1108	5,17
2 O	10,1	8,60	10,80	38,7	22,96	5,63	51	279	15,0	109	13,2	5,75	7,48	5,66	0,2051	5,76
3 O	10,1	10,90	12,00	40,5	22,40	5,84	49	249	24,0	89	14,2	6,34	7,78	6,26	0,3229	6,48
4 O	10,1	12,20	13,10	42,0	21,97	6,02	49	244	31,0	79	15,0	6,83	8,03	6,73	0,4117	7,00
5 O	10,1	13,50	14,30	43,6	21,53	6,20	46	239	38,0	74	15,8	7,34	8,29	7,24	0,4981	7,48
6 O	10,1	15,60	15,00	45,8	20,96	6,46	44	99	47,0	69	16,6	7,92	8,65	7,89	0,6054	8,05
7 O	10,1	16,50	16,50	48,8	20,26	6,80	49	49	58,0	54	17,5	8,64	9,12	8,60	0,7310	8,72
8 O	10,1	17,20	17,20	52,2	19,55	7,17	46	46	69,0	44	18,0	9,20	9,65	9,20	0,8503	9,37
9 O	10,1	18,00	18,00	59,8	18,20	7,98	39	39	90,0	29	18,7	10,28	10,80	10,31	1,0605	10,65
1 P	9,1	7,90	9,60	31,7	23,11	5,05	47	359	13,0	119	11,8	5,11	6,65	5,07	0,1997	5,13
2 P	9,1	9,20	10,60	32,5	22,80	5,15	49	309	18,0	99	12,6	5,53	6,80	5,43	0,2740	5,52
3 P	9,1	10,60	11,60	33,5	22,42	5,28	46	259	24,0	89	13,4	5,98	6,99	5,85	0,3611	5,96

Q	$h_{a,l}$	$h_{a,r}$	H_1	h_1	F_1	x_e	x_2	x_1	x_j	h_2	Y	Y^*	Y_m	X_1	Y_p	
[1/S]	[cm]	[cm]	[cm]	[mm]	[-]	[cm]	[cm]	[cm]	[cm]	[cm]	[-]	[-]	[-]	[-]	[-]	
4 P	9,1	11,80	12,50	34,8	21,98	5,44	49	249	31,0	79	14,0	6,37	7,22	6,28	0,4601	6,43
5 P	9,1	13,60	13,00	35,9	21,59	5,59	44	219	37,0	69	14,7	6,81	7,42	6,74	0,5427	6,81
6 P	9,1	14,30	14,30	37,7	21,01	5,82	42	99	46,0	59	15,5	7,38	7,75	7,26	0,6625	7,32
7 P	9,1	15,40	15,40	40,0	20,36	6,11	44	44	56,0	39	16,4	8,06	8,15	7,89	0,7900	7,86
8 P	9,1	16,10	16,10	43,9	19,37	6,58	42	42	71,0	24	16,6	8,57	8,82	8,61	0,9698	8,65
9 P	9,1	16,60	16,60	49,4	18,18	7,24	34	34	89,0	14	16,8	9,24	9,75	9,46	1,1676	9,66
1 Q	8,1	6,50	8,20	24,8	23,54	4,37	49	349	7,0	109	10,3	4,38	5,70	4,31	0,1245	4,17
2 Q	8,1	7,90	9,10	25,2	23,34	4,42	46	339	10,0	99	10,7	4,58	5,77	4,61	0,1769	4,41
3 Q	8,1	8,90	10,00	25,9	22,96	4,53	46	289	16,0	89	11,4	4,97	5,93	4,94	0,2796	4,86
4 Q	8,1	10,00	10,70	26,5	22,63	4,63	43	269	21,0	79	11,9	5,26	6,07	5,26	0,3633	5,21
5 Q	8,1	11,10	11,50	27,5	22,18	4,77	41	259	28,0	74	12,5	5,64	6,27	5,65	0,4774	5,64
6 Q	8,1	11,90	12,20	28,2	21,85	4,88	42	199	33,0	64	13,1	6,00	6,42	5,97	0,5568	5,93
7 Q	8,1	12,80	12,80	29,3	21,38	5,04	41	79	40,0	54	13,8	6,45	6,65	6,35	0,6649	6,29
8 Q	8,1	13,40	13,40	30,9	20,78	5,26	41	59	49,0	39	14,3	6,88	6,96	6,76	0,7987	6,73
9 Q	8,1	14,30	14,30	32,8	20,11	5,53	39	39	59,0	29	14,8	7,36	7,34	7,32	0,9405	7,19
10Q	8,1	14,90	14,90	36,8	18,88	6,08	39	49	77,0	16	15,1	8,00	8,11	8,09	1,1773	8,04
1 R	7,1	6,80	8,00	19,5	23,55	3,81	45	319	6,0	99	9,6	4,08	4,92	3,98	0,1249	3,65
2 R	7,1	7,80	8,60	20,0	23,15	3,91	45	299	12,0	79	10,0	4,32	5,06	4,26	0,2466	4,09
3 R	7,1	8,40	9,20	20,6	22,75	4,02	41	239	18,0	69	10,6	4,66	5,20	4,51	0,3650	4,49
4 R	7,1	9,70	10,10	21,1	22,41	4,11	39	219	23,0	59	11,2	5,00	5,33	4,89	0,4613	4,79
5 R	7,1	10,40	10,60	21,7	22,08	4,20	39	209	28,0	54	11,6	5,25	5,46	5,15	0,5553	5,05
6 R	7,1	11,20	11,30	22,5	21,60	4,34	38	169	35,0	44	12,1	5,60	5,66	5,50	0,6831	5,39
7 R	7,1	12,00	12,00	23,7	20,98	4,54	39	89	44,0	34	12,6	6,01	5,93	5,93	0,8409	5,77
8 R	7,1	12,60	12,60	25,6	20,07	4,85	35	69	57,0	19	13,1	6,53	6,37	6,44	1,0559	6,29
9 R	7,1	13,20	13,20	31,9	17,75	5,83	39	39	90,0	-1	13,5	7,61	7,76	7,68	1,5331	7,74
1 S	5,1	5,40	6,40	11,0	23,85	2,68	52	329	6,0	69	7,2	3,00	3,32	2,94	0,1895	2,68
2 S	5,1	5,80	6,80	11,1	23,70	2,71	47	309	8,0	59	7,5	3,16	3,36	3,07	0,2513	2,80
3 S	5,1	6,70	7,40	11,3	23,33	2,77	49	274	13,0	54	8,0	3,43	3,45	3,32	0,4025	3,08
4 S	5,1	7,20	7,70	11,5	22,96	2,84	49	239	18,0	49	8,3	3,62	3,55	3,50	0,5495	3,31
5 S	5,1	7,80	8,00	11,9	22,51	2,92	44	199	24,0	39	8,7	3,87	3,67	3,71	0,7202	3,53
6 S	5,1	8,30	8,40	12,2	22,06	3,01	43	159	30,0	24	8,9	4,03	3,79	3,93	0,8847	3,71
7 S	5,1	8,70	8,70	12,9	21,30	3,18	39	139	40,0	17	9,2	4,32	4,02	4,21	1,1454	3,99
8 S	5,1	9,10	9,10	13,8	20,37	3,40	37	149	52,0	4	9,4	4,61	4,33	4,56	1,4361	4,32
9 S	5,1	9,60	9,60	18,4	17,09	4,42	37	139	94,0	-31	9,7	5,67	5,77	5,80	2,2716	5,77

Q	h ₂	H ₁	h ₁	F ₁	x ₂	x ₁	h ₂	Y	Y*	Y _m	X ₁	Y _p	
[1/s]	[cm]	[cm]	[mm]	[-]	[cm]	[cm]	[cm]	[-]	[-]	[-]	[-]	[-]	
1 A	31,7	10,80	55,3	62,4	3,96	451	6,0	18,80	3,01	5,13	3,43	0,0450	3,53
2 A	31,7	13,90	55,4	62,4	3,97	381	8,0	21,10	3,39	5,14	3,63	0,0600	3,59
3 A	31,7	16,30	55,9	62,0	4,01	338	20,0	22,90	3,70	5,19	3,84	0,1493	3,91
4 A	31,7	17,80	56,2	61,8	4,02	293	26,0	23,50	3,81	5,21	3,97	0,1937	4,06
5 A	31,7	19,90	56,8	61,4	4,06	249	38,0	24,80	4,04	5,27	4,18	0,2818	4,35
6 A	31,7	21,30	57,1	61,2	4,08	211	44,0	25,40	4,15	5,29	4,32	0,3255	4,48
7 A	31,7	23,20	57,7	60,8	4,12	157	56,0	26,80	4,41	5,35	4,53	0,4124	4,71
8 A	31,7	23,80	58,1	60,6	4,15	151	65,0	27,30	4,51	5,39	4,61	0,4770	4,87
9 A	31,7	25,20	58,7	60,2	4,18	151	76,0	28,20	4,68	5,44	4,78	0,5554	5,03
1 B	29,8	11,70	49,6	62,3	3,73	433	5,0	18,80	3,02	4,80	3,32	0,0404	3,32
2 B	29,8	14,70	49,8	62,1	3,75	353	10,0	20,80	3,35	4,82	3,54	0,0806	3,45
3 B	29,8	17,30	50,4	61,6	3,79	301	24,0	22,50	3,65	4,88	3,78	0,1924	3,81
4 B	29,8	18,50	50,6	61,5	3,80	273	29,0	23,20	3,78	4,90	3,90	0,2320	3,94
5 B	29,8	20,10	51,1	61,1	3,84	235	40,0	23,90	3,91	4,95	4,07	0,3186	4,18
6 B	29,8	21,30	51,5	60,8	3,86	220	49,0	24,70	4,06	4,99	4,20	0,3889	4,36
7 B	29,8	22,50	51,9	60,5	3,89	183	59,0	25,50	4,22	5,03	4,35	0,4664	4,54
8 B	29,8	24,30	52,6	60,0	3,94	154	74,0	26,60	4,43	5,10	4,57	0,5814	4,75
1 C	26,9	12,30	41,7	62,2	3,38	345	5,0	18,30	2,94	4,30	3,12	0,0455	3,03
2 C	26,9	14,00	41,9	62,1	3,39	350	9,0	19,10	3,08	4,32	3,26	0,0817	3,13
3 C	26,9	14,80	42,0	62,0	3,40	367	12,0	19,90	3,21	4,33	3,33	0,1089	3,21
4 C	26,9	16,10	42,2	61,8	3,41	347	17,0	20,60	3,34	4,35	3,45	0,1539	3,34
5 C	26,9	16,70	42,2	61,8	3,42	311	19,0	21,05	3,41	4,36	3,50	0,1718	3,39
6 C	26,9	17,20	42,4	61,6	3,43	306	23,0	21,40	3,48	4,37	3,55	0,2076	3,48
7 C	26,9	18,10	42,5	61,5	3,44	279	26,0	21,50	3,50	4,39	3,64	0,2344	3,55
8 C	26,9	19,20	42,7	61,3	3,45	277	32,0	22,30	3,64	4,41	3,76	0,2878	3,69
9 C	26,9	19,80	42,9	61,2	3,47	259	37,0	22,50	3,68	4,43	3,83	0,3320	3,79
10C	26,9	21,10	43,3	60,8	3,50	241	49,0	23,60	3,89	4,48	3,98	0,4374	4,01
11C	26,9	22,20	43,8	60,3	3,54	207	62,0	24,50	4,06	4,53	4,13	0,5503	4,20
1 D	24,0	12,90	34,6	61,9	3,03	317	6,0	17,60	2,84	3,81	2,94	0,0626	2,77
2 D	24,0	14,20	34,7	61,8	3,04	276	9,0	18,30	2,96	3,82	3,06	0,0938	2,84
3 D	24,0	15,60	34,9	61,6	3,05	276	15,0	19,00	3,09	3,85	3,19	0,1559	2,99
4 D	24,0	14,50	35,0	61,4	3,07	256	21,0	19,80	3,23	3,87	3,11	0,2176	3,13
5 D	24,0	17,60	35,2	61,2	3,08	233	26,0	20,50	3,35	3,89	3,40	0,2688	3,24
6 D	24,0	18,80	35,4	61,0	3,10	207	34,0	20,80	3,41	3,92	3,53	0,3502	3,40
7 D	24,0	20,00	35,7	60,6	3,13	211	44,0	21,80	3,60	3,95	3,68	0,4510	3,57
8 D	24,0	20,60	36,0	60,3	3,16	190	54,0	22,40	3,72	3,99	3,77	0,5509	3,72
9 D	24,0	21,30	36,3	60,0	3,18	180	62,0	22,70	3,79	4,02	3,86	0,6301	3,81
1 E	20,9	11,30	27,8	62,0	2,64	333	2,0	15,50	2,50	3,26	2,57	0,0248	2,35
2 E	20,9	12,90	27,8	61,9	2,64	308	5,0	16,20	2,62	3,27	2,71	0,0619	2,43
3 E	20,9	14,50	28,0	61,6	2,66	254	12,0	17,40	2,83	3,30	2,86	0,1481	2,59
4 E	20,9	15,50	28,1	61,4	2,68	241	19,0	17,80	2,90	3,32	2,97	0,2335	2,75
5 E	20,9	16,40	28,3	61,1	2,69	233	25,0	18,30	3,00	3,34	3,07	0,3063	2,87
6 E	20,9	17,60	28,4	61,0	2,70	222	29,0	19,35	3,18	3,36	3,20	0,3545	2,95
7 E	20,9	18,30	28,7	60,5	2,74	191	42,0	19,70	3,26	3,40	3,30	0,5098	3,15
8 E	20,9	18,80	28,9	60,1	2,76	191	52,0	20,00	3,33	3,44	3,38	0,6277	3,26
9 E	20,9	19,10	29,2	59,7	2,79	161	64,0	20,40	3,42	3,48	3,44	0,7676	3,37
1 F	25,8	11,30	55,1	50,2	4,47	397	5,0	19,10	3,81	5,84	3,99	0,0406	3,95

	Q	h _a	H ₁	h ₁	F ₁	x ₂	x ₁	h ₂	Y	Y*	Y _m	X ₁	Y _p
	[l/s]	[cm]	[cm]	[mm]	[-]	[cm]	[cm]	[cm]	[-]	[-]	[-]	[-]	[-]
2 F	25,8	12,00	55,2	50,1	4,48	355	7,0	19,10	3,82	5,85	4,05	0,0569	4,02
3 F	25,8	13,90	55,4	50,0	4,49	316	11,0	20,50	4,11	5,87	4,23	0,0892	4,16
4 F	25,8	15,10	55,7	49,9	4,51	307	16,0	20,80	4,18	5,90	4,36	0,1295	4,33
5 F	25,8	15,90	56,0	49,7	4,53	276	21,0	21,40	4,31	5,93	4,45	0,1696	4,49
6 F	25,8	16,90	56,2	49,6	4,54	269	24,0	22,00	4,44	5,94	4,57	0,1935	4,59
7 F	25,8	18,00	56,6	49,4	4,57	251	31,0	22,70	4,60	5,98	4,71	0,2492	4,81
8 F	25,8	19,00	56,8	49,3	4,58	228	34,0	23,00	4,67	6,00	4,83	0,2730	4,90
9 F	25,8	20,35	57,3	49,1	4,62	221	43,0	23,90	4,87	6,05	5,01	0,3440	5,15
10F	25,8	21,20	57,7	48,9	4,65	192	50,0	24,20	4,96	6,09	5,14	0,3988	5,32
11F	25,8	22,60	58,2	48,6	4,69	183	59,0	25,40	5,23	6,15	5,34	0,4688	5,52
1 G	24,0	11,90	47,7	50,6	4,10	337	5,0	18,00	3,56	5,33	3,78	0,0445	3,65
2 G	24,0	12,90	47,9	50,5	4,12	325	9,0	18,50	3,67	5,35	3,88	0,0799	3,79
3 G	24,0	14,80	48,2	50,2	4,15	299	17,0	19,80	3,95	5,39	4,08	0,1504	4,05
4 G	24,0	15,90	48,4	50,1	4,16	274	20,0	20,10	4,01	5,40	4,20	0,1767	4,15
5 G	24,0	17,00	48,7	50,0	4,18	257	26,0	20,90	4,19	5,44	4,34	0,2291	4,33
6 G	24,0	17,90	48,9	49,8	4,20	234	30,0	21,80	4,38	5,46	4,45	0,2639	4,45
7 G	24,0	19,10	49,3	49,6	4,23	210	38,0	22,20	4,48	5,50	4,61	0,3330	4,66
8 G	24,0	19,80	49,5	49,5	4,24	219	42,0	23,00	4,65	5,52	4,71	0,3674	4,76
9 G	24,0	20,60	49,8	49,3	4,27	211	48,0	23,30	4,73	5,55	4,83	0,4188	4,90
10G	24,0	21,40	50,2	49,1	4,29	191	55,0	23,80	4,85	5,59	4,95	0,4784	5,05
1 H	22,1	11,00	41,1	50,8	3,77	370	5,0	16,50	3,21	4,85	3,46	0,0490	3,38
2 H	22,1	13,70	41,3	50,6	3,78	313	9,0	18,20	3,55	4,87	3,72	0,0880	3,51
3 H	22,1	15,10	41,7	50,4	3,81	311	18,0	18,80	3,68	4,92	3,89	0,1752	3,79
4 H	22,1	16,60	42,0	50,1	3,84	270	25,0	20,00	3,94	4,95	4,07	0,2425	4,00
5 H	22,1	17,30	42,3	49,9	3,86	244	32,0	20,40	4,03	4,99	4,17	0,3094	4,19
6 H	22,1	18,00	42,4	49,8	3,88	240	36,0	20,80	4,12	5,01	4,26	0,3475	4,29
7 H	22,1	19,10	42,7	49,6	3,90	195	43,0	21,40	4,26	5,04	4,41	0,4137	4,46
8 H	22,1	19,80	43,4	49,1	3,96	207	59,0	22,00	4,42	5,12	4,55	0,5633	4,76
9 H	22,1	20,60	43,5	49,0	3,97	195	61,0	22,50	4,52	5,14	4,66	0,5819	4,79
1 I	19,1	11,80	32,4	50,3	3,30	305	3,0	15,80	3,14	4,19	3,24	0,0348	2,93
2 I	19,1	12,70	32,6	50,1	3,32	313	9,0	16,40	3,28	4,22	3,35	0,1039	3,12
3 I	19,1	13,95	32,7	50,0	3,33	288	13,0	17,00	3,40	4,24	3,50	0,1498	3,25
4 I	19,1	14,50	32,8	49,9	3,34	281	17,0	17,40	3,49	4,25	3,57	0,1955	3,37
5 I	19,1	15,70	33,1	49,6	3,37	248	24,0	18,30	3,69	4,29	3,73	0,2750	3,56
6 I	19,1	16,40	33,2	49,5	3,38	221	28,0	18,60	3,76	4,30	3,82	0,3201	3,67
7 I	19,1	17,15	33,4	49,3	3,40	225	34,0	19,00	3,86	4,33	3,93	0,3875	3,81
8 I	19,1	18,50	33,9	48,8	3,45	207	49,0	20,10	4,12	4,40	4,15	0,5541	4,09
9 I	19,1	19,00	34,1	48,7	3,47	167	54,0	20,30	4,17	4,43	4,23	0,6090	4,17
10I	19,1	19,80	34,8	48,0	3,53	172	74,0	20,90	4,35	4,52	4,40	0,8260	4,40
1 J	16,3	11,50	24,5	51,1	2,75	199	5,0	14,10	2,76	3,43	2,86	0,0713	2,54
2 J	16,3	13,40	24,8	50,6	2,79	269	18,0	15,70	3,11	3,48	3,11	0,2546	2,90
3 J	16,3	14,10	24,9	50,4	2,81	265	23,0	15,85	3,15	3,50	3,20	0,3243	3,02
4 J	16,3	15,00	25,1	50,1	2,83	249	32,0	16,45	3,28	3,54	3,34	0,4487	3,21
5 J	16,3	15,90	25,3	49,8	2,86	203	41,0	17,00	3,42	3,57	3,47	0,5718	3,35
6 J	16,3	16,45	25,6	49,5	2,89	213	51,0	18,00	3,64	3,62	3,57	0,7070	3,48
7 J	16,3	17,20	26,3	48,5	2,98	205	79,0	18,00	3,71	3,74	3,75	1,0768	3,70
1 K	19,9	11,00	56,4	37,7	5,28	343	4,0	17,30	4,59	6,99	4,83	0,0358	4,63

	Q	h _a	H ₁	h ₁	F ₁	x ₂	x ₁	h ₂	Y	Y*	Y _m	X ₁	Y _p
	[1/s]	[cm]	[cm]	[mm]	[-]	[cm]	[cm]	[cm]	[-]	[-]	[-]	[-]	[-]
2 K	19,9	12,20	56,8	37,6	5,31	291	9,0	18,25	4,86	7,03	5,00	0,0803	4,87
3 K	19,9	13,70	57,3	37,4	5,35	263	15,0	18,70	5,00	7,08	5,21	0,1334	5,15
4 K	19,9	15,00	57,5	37,3	5,37	255	19,0	19,70	5,29	7,11	5,40	0,1686	5,33
5 K	19,9	16,20	58,3	37,0	5,43	247	29,0	20,70	5,59	7,19	5,62	0,2561	5,76
6 K	19,9	17,10	58,6	36,9	5,45	231	33,0	20,80	5,64	7,23	5,77	0,2909	5,92
7 K	19,9	18,30	59,1	36,8	5,49	211	39,0	21,45	5,84	7,28	5,99	0,3428	6,15
8 K	19,9	19,00	59,5	36,6	5,52	216	44,0	22,00	6,01	7,32	6,12	0,3858	6,32
9 K	19,9	19,80	59,9	36,5	5,55	191	49,0	22,50	6,17	7,36	6,28	0,4286	6,48
10K	19,9	21,00	60,4	36,3	5,59	166	56,0	23,10	6,36	7,42	6,51	0,4881	6,69
1 L	17,9	10,40	46,9	37,5	4,80	316	5,0	15,70	4,20	6,31	4,44	0,0502	4,28
2 L	17,9	11,95	47,2	37,4	4,82	301	9,0	17,00	4,56	6,34	4,64	0,0901	4,46
3 L	17,9	13,00	47,5	37,2	4,85	258	14,0	17,50	4,71	6,37	4,80	0,1398	4,69
4 L	17,9	14,10	47,8	37,1	4,87	264	19,0	17,85	4,82	6,41	4,98	0,1892	4,91
5 L	17,9	15,10	48,2	36,9	4,91	249	26,0	18,90	5,13	6,47	5,16	0,2580	5,21
6 L	17,9	16,10	48,5	36,8	4,94	235	31,0	19,45	5,30	6,51	5,33	0,3068	5,40
7 L	17,9	16,80	48,7	36,7	4,96	229	34,0	20,10	5,49	6,53	5,45	0,3359	5,51
8 L	17,9	18,20	49,2	36,5	5,00	196	41,0	20,60	5,65	6,58	5,71	0,4036	5,75
9 L	17,9	19,20	49,9	36,2	5,06	187	52,0	21,50	5,95	6,67	5,94	0,5090	6,07
10L	17,9	20,55	50,9	35,8	5,14	169	66,0	22,00	6,15	6,79	6,24	0,6413	6,40
1 M	16,1	9,90	37,9	37,9	4,24	345	3,0	14,10	3,72	5,52	3,99	0,0342	3,74
2 M	16,1	11,30	38,1	37,8	4,26	318	7,0	15,00	3,97	5,55	4,18	0,0797	3,92
3 M	16,1	11,90	38,3	37,7	4,28	311	11,0	15,50	4,12	5,58	4,28	0,1250	4,09
4 M	16,1	13,10	38,5	37,6	4,30	276	14,0	16,10	4,29	5,60	4,45	0,1588	4,23
5 M	16,1	14,10	38,8	37,4	4,33	263	20,0	16,70	4,47	5,64	4,63	0,2262	4,47
6 M	16,1	14,70	39,0	37,3	4,35	252	24,0	17,40	4,67	5,67	4,73	0,2708	4,63
7 M	16,1	15,90	39,3	37,1	4,38	231	31,0	18,30	4,94	5,72	4,95	0,3484	4,88
8 M	16,1	16,50	39,6	37,0	4,40	211	35,0	18,75	5,07	5,75	5,07	0,3925	5,01
9 M	16,1	17,40	40,0	36,7	4,45	197	44,0	19,20	5,23	5,81	5,26	0,4910	5,27
10M	16,1	18,20	40,6	36,4	4,51	177	55,0	19,90	5,47	5,89	5,45	0,6099	5,52
11M	16,1	19,10	40,8	36,3	4,53	176	59,0	20,30	5,59	5,92	5,63	0,6529	5,60
1 N	14,4	9,10	30,2	38,5	3,70	373	3,0	12,50	3,25	4,76	3,51	0,0396	3,29
2 N	14,4	10,80	30,4	38,4	3,72	308	7,0	13,55	3,53	4,78	3,74	0,0921	3,46
3 N	14,4	12,30	30,6	38,2	3,74	299	13,0	14,60	3,82	4,82	3,98	0,1704	3,71
4 N	14,4	13,20	30,8	38,0	3,77	265	19,0	15,30	4,03	4,85	4,13	0,2482	3,94
5 N	14,4	14,20	31,0	37,9	3,79	235	24,0	15,80	4,17	4,89	4,31	0,3125	4,12
6 N	14,4	15,10	31,5	37,6	3,84	239	35,0	16,35	4,36	4,96	4,50	0,4528	4,45
7 N	14,4	15,70	31,7	37,4	3,86	189	40,0	17,10	4,57	4,99	4,62	0,5159	4,57
8 N	14,4	16,20	31,9	37,3	3,89	185	45,0	17,50	4,70	5,02	4,72	0,5786	4,68
9 N	14,4	17,10	32,4	36,9	3,95	171	58,0	18,20	4,94	5,11	4,94	0,7400	4,91
10N	14,4	17,80	33,1	36,5	4,02	152	72,0	18,70	5,13	5,20	5,13	0,9109	5,09
1 O	12,1	9,60	23,0	37,8	3,19	338	3,0	12,00	3,17	4,04	3,27	0,0481	2,87
2 O	12,1	10,60	23,2	37,7	3,21	297	8,0	12,40	3,29	4,06	3,44	0,1280	3,08
3 O	12,1	12,10	23,5	37,4	3,25	325	18,0	13,50	3,62	4,12	3,71	0,2859	3,46
4 O	12,1	12,90	23,8	37,1	3,29	251	28,0	13,80	3,73	4,18	3,87	0,4417	3,76
5 O	12,1	13,50	24,1	36,7	3,34	221	39,0	14,30	3,90	4,24	4,02	0,6106	4,00
6 O	12,1	14,20	24,3	36,5	3,37	206	46,0	14,70	4,03	4,29	4,17	0,7167	4,12
7 O	12,1	14,80	24,7	36,2	3,41	201	57,0	15,20	4,21	4,35	4,32	0,8814	4,26
8 O	12,1	15,10	25,0	35,9	3,45	201	66,0	15,45	4,31	4,41	4,42	1,0142	4,35

	Q	h_a	H_1	h_1	F_1	x_2	x_1	h_2	Y	Y^*	Y_m	X_1	Y_p
	[1/s]	[cm]	[cm]	[mm]	[-]	[cm]	[cm]	[cm]	[-]	[-]	[-]	[-]	[-]
9 O	12,1	15,30	25,3	35,6	3,49	206	74,0	15,50	4,35	4,46	4,49	1,1310	4,42
1 P	10,0	7,30	17,1	37,6	2,66	437	2,0	9,20	2,45	3,30	2,64	0,0404	2,40
2 P	10,0	8,30	19,3	34,8	2,99	345	3,0	10,10	2,69	3,76	2,97	0,0567	2,72
3 P	10,0	9,30	17,2	37,4	2,69	301	7,0	10,50	2,81	3,33	2,95	0,1408	2,60
4 P	10,0	9,80	17,3	37,2	2,70	266	11,0	10,90	2,93	3,35	3,05	0,2205	2,75
5 P	10,0	10,70	17,5	36,9	2,73	241	20,0	11,30	3,06	3,40	3,22	0,3979	3,03
6 P	10,0	11,60	17,9	36,4	2,79	231	36,0	12,10	3,32	3,48	3,44	0,7070	3,35
7 P	10,0	12,20	18,2	35,9	2,85	216	51,0	12,60	3,51	3,57	3,60	0,9895	3,52
8 P	10,0	12,50	18,5	35,4	2,91	211	65,0	12,80	3,61	3,64	3,71	1,2469	3,63
9 P	10,0	12,70	18,9	34,9	2,97	206	81,0	13,00	3,72	3,74	3,81	1,5341	3,73
1 Q	12,9	8,30	55,5	24,5	6,58	410	3,0	13,40	5,48	8,83	5,94	0,0324	5,72
2 Q	12,9	10,00	55,9	24,4	6,62	306	7,0	15,00	6,16	8,88	6,27	0,0754	6,03
3 Q	12,9	11,10	56,3	24,3	6,66	262	11,0	15,20	6,26	8,94	6,51	0,1182	6,33
4 Q	12,9	12,40	57,0	24,1	6,73	249	17,0	15,80	6,55	9,02	6,83	0,1820	6,76
5 Q	12,9	13,30	57,4	24,0	6,77	243	21,0	16,30	6,79	9,08	7,06	0,2243	7,04
6 Q	12,9	14,10	57,7	23,9	6,80	221	24,0	17,10	7,14	9,13	7,27	0,2558	7,24
7 Q	12,9	15,00	58,3	23,8	6,85	196	29,0	17,70	7,43	9,20	7,53	0,3081	7,56
8 Q	12,9	16,00	59,0	23,7	6,91	195	35,0	18,30	7,73	9,29	7,83	0,3704	7,92
9 Q	12,9	17,40	59,9	23,5	7,00	176	43,0	19,30	8,22	9,41	8,26	0,4527	8,34
10Q	12,9	18,70	61,1	23,2	7,11	168	53,0	20,15	8,67	9,57	8,71	0,5543	8,79
1 R	12,1	9,90	48,6	24,4	6,14	282	5,0	14,20	5,81	8,20	5,92	0,0584	5,50
2 R	12,1	11,00	49,2	24,3	6,21	268	12,0	14,60	6,02	8,30	6,19	0,1394	6,01
3 R	12,1	12,00	49,6	24,2	6,25	237	16,0	15,25	6,31	8,35	6,44	0,1854	6,30
4 R	12,1	13,40	50,6	23,9	6,35	213	26,0	16,55	6,92	8,49	6,84	0,2992	6,95
5 R	12,1	13,80	50,8	23,9	6,37	212	28,0	16,50	6,91	8,52	6,95	0,3218	7,08
6 R	12,1	15,00	51,2	23,8	6,41	201	32,0	17,10	7,20	8,58	7,28	0,3667	7,30
7 R	12,1	16,30	52,1	23,5	6,50	183	41,0	18,10	7,69	8,71	7,70	0,4670	7,76
8 R	12,1	17,10	52,7	23,4	6,56	179	47,0	18,60	7,95	8,79	7,97	0,5332	8,03
9 R	12,1	18,10	53,9	23,1	6,68	146	58,0	19,45	8,41	8,96	8,35	0,6530	8,44
10R	12,1	18,80	55,8	22,7	6,87	147	75,0	19,70	8,68	9,22	8,74	0,8346	8,95
1 S	11,2	8,80	41,5	24,7	5,63	336	5,0	12,70	5,15	7,47	5,35	0,0637	5,07
2 S	11,2	11,10	41,9	24,5	5,67	269	10,0	14,10	5,75	7,53	5,85	0,1270	5,43
3 S	11,2	12,50	42,5	24,3	5,74	245	18,0	14,95	6,14	7,63	6,22	0,2274	5,97
4 S	11,2	14,00	43,1	24,2	5,81	220	25,0	15,85	6,56	7,72	6,64	0,3143	6,40
5 S	11,2	14,80	43,7	24,0	5,87	193	32,0	16,35	6,82	7,82	6,90	0,4003	6,79
6 S	11,2	15,40	44,3	23,8	5,94	174	39,0	16,90	7,10	7,91	7,12	0,4855	7,11
7 S	11,2	16,50	45,1	23,6	6,02	162	48,0	17,55	7,45	8,03	7,49	0,5937	7,47
8 S	11,2	17,00	45,8	23,4	6,10	172	56,0	18,10	7,75	8,14	7,70	0,6887	7,74
9 S	11,2	17,40	46,8	23,1	6,20	147	66,0	18,30	7,92	8,29	7,92	0,8059	8,01
10S	11,2	17,90	48,0	22,8	6,34	106	79,0	18,70	8,21	8,48	8,19	0,9557	8,32
1 T	9,4	8,90	29,0	25,1	4,60	197	4,0	11,30	4,50	6,02	4,67	0,0629	4,15
2 T	9,4	9,90	29,3	25,0	4,63	176	9,0	12,00	4,80	6,07	4,91	0,1410	4,49
3 T	9,4	11,10	29,6	24,8	4,67	261	14,0	12,50	5,03	6,12	5,22	0,2185	4,81
4 T	9,4	12,20	30,2	24,6	4,75	228	24,0	13,50	5,49	6,23	5,56	0,3717	5,37
5 T	9,4	13,00	30,7	24,3	4,82	236	33,0	14,05	5,78	6,33	5,83	0,5075	5,76
6 T	9,4	13,85	31,2	24,1	4,89	189	42,0	14,65	6,08	6,44	6,12	0,6414	6,07
7 T	9,4	14,50	32,0	23,8	4,99	163	54,0	15,05	6,33	6,58	6,40	0,8170	6,38

Q	h _a	H ₁	h ₁	F ₁	x ₂	x ₁	h ₂	Y	Y*	Y _m	X ₁	Y _p	
[1/s]	[cm]	[cm]	[mm]	[-]	[cm]	[cm]	[cm]	[-]	[-]	[-]	[-]	[-]	
8 T	9,4	14,90	33,2	23,3	5,16	151	73,0	15,45	6,64	6,81	6,67	1,0881	6,73
1 U	7,1	7,70	18,2	24,6	3,58	318	3,0	9,30	3,79	4,59	3,83	0,0645	3,26
2 U	7,1	9,60	18,6	24,2	3,66	243	15,0	10,45	4,32	4,70	4,36	0,3190	3,98
3 U	7,1	10,10	18,9	24,0	3,72	229	24,0	10,60	4,43	4,78	4,55	0,5061	4,38
4 U	7,1	10,70	19,1	23,8	3,75	261	29,0	11,10	4,66	4,83	4,75	0,6087	4,54
5 U	7,1	11,20	19,6	23,5	3,84	205	41,0	11,60	4,95	4,95	4,97	0,8508	4,82
6 U	7,1	11,30	20,0	23,2	3,91	178	51,0	11,80	5,09	5,05	5,07	1,0483	4,99
7 U	7,1	11,50	20,6	22,8	4,01	168	64,0	11,95	5,24	5,19	5,23	1,2994	5,17
8 U	7,1	11,70	21,5	22,2	4,16	171	84,0	12,10	5,45	5,41	5,45	1,6733	5,41
1 V	7,0	6,90	46,1	14,4	7,88	406	3,0	10,00	6,94	10,65	7,43	0,0453	6,92
2 V	7,0	8,30	46,7	14,3	7,96	255	7,0	11,00	7,69	10,76	7,95	0,1053	7,45
3 V	7,0	9,50	47,3	14,2	8,04	227	11,0	11,70	8,23	10,88	8,46	0,1648	7,97
4 V	7,0	10,30	48,0	14,1	8,12	233	15,0	12,30	8,72	11,00	8,84	0,2238	8,47
5 V	7,0	10,80	48,6	14,0	8,21	206	19,0	12,75	9,10	11,12	9,12	0,2822	8,94
6 V	7,0	12,50	49,9	13,8	8,38	228	27,0	13,95	10,09	11,36	10,01	0,3977	9,78
7 V	7,0	13,40	50,9	13,7	8,51	178	33,0	14,85	10,71	11,55	10,54	0,4829	10,33
8 V	7,0	14,20	52,2	13,5	8,67	156	40,0	14,90	11,03	11,78	11,08	0,5810	10,88
9 V	7,0	15,10	55,2	13,1	9,06	131	56,0	15,50	11,82	12,33	11,91	0,7991	11,89
10V	7,0	15,60	60,3	12,5	9,70	128	80,0	16,10	12,85	13,23	12,84	1,1110	13,09
1 W	6,0	7,10	34,7	14,4	6,81	330	3,0	9,35	6,50	9,14	6,78	0,0532	6,04
2 W	6,0	8,80	35,6	14,2	6,93	233	10,0	10,60	7,46	9,31	7,52	0,1759	6,93
3 W	6,0	9,80	36,0	14,1	7,00	229	14,0	11,20	7,94	9,42	7,99	0,2451	7,41
4 W	6,0	10,90	36,8	14,0	7,12	183	20,0	11,90	8,52	9,58	8,57	0,3478	8,05
5 W	6,0	11,60	37,4	13,8	7,22	180	25,0	12,35	8,93	9,72	8,98	0,4323	8,52
6 W	6,0	12,60	38,4	13,6	7,38	149	33,0	13,05	9,57	9,94	9,61	0,5654	9,16
7 W	6,0	13,10	41,3	13,1	7,80	106	53,0	13,30	10,13	10,55	10,29	0,8871	10,28
8 W	6,0	13,30	43,3	12,8	8,11	82	66,0	13,50	10,55	10,97	10,71	1,0876	10,85
9 W	6,0	13,70	45,4	12,5	8,40	67	78,0	13,80	11,04	11,39	11,23	1,2667	11,33
1 X	5,1	8,00	25,4	14,5	5,76	245	5,0	9,50	6,57	7,66	6,46	0,1059	5,41
2 X	5,1	9,10	26,2	14,2	5,90	221	14,0	10,05	7,06	7,86	7,05	0,2932	6,43
3 X	5,1	9,90	26,8	14,1	6,00	173	20,0	10,35	7,35	8,00	7,50	0,4159	7,00
4 X	5,1	10,40	27,4	13,9	6,12	126	27,0	10,90	7,85	8,17	7,85	0,5566	7,52
5 X	5,1	10,70	28,5	13,6	6,32	108	38,0	11,10	8,16	8,45	8,19	0,7727	8,14
6 X	5,1	11,10	29,3	13,4	6,47	96	46,0	11,30	8,44	8,66	8,54	0,9260	8,48
7 X	5,1	11,30	30,3	13,2	6,64	84	55,0	11,40	8,67	8,91	8,82	1,0945	8,81
8 X	5,1	11,60	31,9	12,8	6,91	92	68,0	11,70	9,13	9,29	9,26	1,3306	9,25
1 Y	4,3	7,10	17,0	15,2	4,50	323	3,0	8,00	5,26	5,89	5,24	0,0797	4,13
2 Y	4,3	7,80	17,4	15,0	4,62	241	12,0	8,25	5,51	6,05	5,64	0,3150	5,06
3 Y	4,3	8,10	17,8	14,8	4,70	249	18,0	8,55	5,78	6,16	5,84	0,4687	5,53
4 Y	4,3	8,40	18,2	14,6	4,78	211	24,0	8,80	6,01	6,27	6,06	0,6200	5,89
5 Y	4,3	8,70	18,5	14,5	4,86	212	30,0	8,80	6,08	6,39	6,27	0,7687	6,16
6 Y	4,3	9,10	19,8	13,9	5,14	213	49,0	9,10	6,53	6,79	6,75	1,2234	6,74
7 Y	4,3	9,30	20,5	13,7	5,28	211	58,0	9,35	6,84	6,99	6,99	1,4301	6,97
8 Y	4,3	9,40	21,5	13,3	5,50	214	71,0	9,40	7,06	7,30	7,27	1,7190	7,29
1 Z	3,3	4,90	10,0	15,8	3,27	346	2,0	5,50	3,49	4,15	3,64	0,0746	3,01
2 Z	3,3	5,60	10,2	15,6	3,34	309	9,0	5,85	3,76	4,25	3,97	0,3322	3,64

Q	h_a	H_1	h_1	F_1	x_2	x_1	h_2	Y	Y^*	Y_m	X_1	Y_p	
[1/s]	[cm]	[cm]	[mm]	[-]	[cm]	[cm]	[cm]	[-]	[-]	[-]	[-]	[-]	
3 Z	3,3	6,20	10,6	15,2	3,45	283	20,0	6,30	4,14	4,41	4,33	0,7251	4,24
4 Z	3,3	6,40	10,9	15,0	3,54	251	28,0	6,35	4,24	4,53	4,50	1,0020	4,47
5 Z	3,3	6,60	11,4	14,5	3,70	212	42,0	6,70	4,61	4,75	4,75	1,4689	4,74
6 Z	3,3	6,80	11,7	14,3	3,80	198	50,0	6,80	4,76	4,89	4,94	1,7256	4,89
7 Z	3,3	6,90	11,9	14,2	3,85	209	54,0	6,80	4,80	4,96	5,04	1,8513	4,96
8 Z	3,3	7,00	13,0	13,4	4,18	187	79,0	7,00	5,23	5,44	5,43	2,5973	5,44

	Q	h _a	H ₁	h ₁	F ₁	x ₂	x ₁	L _j	h ₂	Y	Y*	Y _m	X ₁	Y _p
	[l/s]	[cm]	[cm]	[mm]	[-]	[cm]	[cm]	[cm]	[cm]	[-]	[-]	[-]	[-]	[-]
1 A	14,0	9,30	42,6	14,8	7,46	282	1,0	133	13,10	8,88	10,07	9,10	0,0156	8,45
2 A	14,0	10,50	44,1	14,5	7,67	227	13,0	135	13,60	9,39	10,36	9,55	0,2008	9,27
3 A	14,0	11,50	45,0	14,3	7,80	127	20,0	117	13,80	9,63	10,54	9,89	0,3069	9,71
4 A	14,0	11,90	46,5	14,1	8,00	97	31,0	118	14,00	9,94	10,83	10,21	0,4707	10,31
5 A	14,0	12,40	48,1	13,8	8,22	77	42,0	114	14,30	10,33	11,13	10,57	0,6308	10,82
6 A	14,0	12,90	49,8	13,6	8,45	72	53,0	115	14,60	10,74	11,45	10,95	0,7872	11,27
7 A	14,0	14,60	52,7	13,2	8,82	67	70,0	107	15,20	11,51	11,98	11,80	1,0218	11,90
8 A	14,0	14,90	56,1	12,8	9,27	47	89,0	96	15,40	12,05	12,61	12,42	1,2735	12,58
1 B	12,0	8,30	31,6	14,8	6,39	277	3,0	120	11,30	7,66	8,55	7,81	0,0555	7,31
2 B	12,0	9,70	32,4	14,6	6,51	207	11,0	108	11,80	8,10	8,72	8,21	0,2019	7,82
3 B	12,0	10,50	33,3	14,3	6,67	157	21,0	88	12,10	8,44	8,95	8,56	0,3816	8,39
4 B	12,0	10,90	34,4	14,1	6,84	127	31,0	88	12,30	8,72	9,18	8,84	0,5574	8,86
5 B	12,0	11,30	35,6	13,9	7,03	107	42,0	94	12,50	9,02	9,45	9,16	0,7464	9,28
6 B	12,0	12,00	36,7	13,6	7,21	97	52,0	79	12,60	9,25	9,71	9,54	0,9143	9,61
7 B	12,0	12,50	37,7	13,4	7,36	87	60,0	72	12,90	9,60	9,92	9,84	1,0458	9,86
8 B	12,0	13,00	40,1	13,0	7,72	77	78,0	80	13,30	10,22	10,43	10,41	1,3328	10,41
1 C	10,0	8,10	23,0	14,6	5,43	237	5,0	82	9,80	6,70	7,19	6,80	0,1120	6,29
2 C	10,0	8,60	23,5	14,4	5,53	187	13,0	70	10,00	6,93	7,34	7,03	0,2885	6,76
3 C	10,0	8,90	24,0	14,3	5,62	137	19,0	66	10,20	7,14	7,46	7,20	0,4189	7,06
4 C	10,0	9,20	24,8	14,0	5,78	137	30,0	67	10,30	7,35	7,69	7,46	0,6531	7,50
5 C	10,0	9,70	26,0	13,7	6,00	127	44,0	71	10,50	7,68	8,00	7,83	0,9424	7,93
1 D	28,0	11,10	53,1	26,6	6,16	247	4,0	201	19,00	7,14	8,22	7,24	0,0428	7,00
2 D	28,0	13,70	53,8	26,4	6,23	147	13,0	160	19,20	7,27	8,32	7,53	0,1384	7,32
3 D	28,0	15,40	55,1	26,1	6,34	87	28,0	115	19,50	7,48	8,48	7,83	0,2956	7,81
4 D	28,0	16,50	56,2	25,8	6,45	77	41,0	118	19,90	7,71	8,63	8,07	0,4298	8,17
5 D	28,0	17,80	56,9	25,6	6,51	77	49,0	131	20,40	7,96	8,72	8,29	0,5115	8,37
6 D	28,0	18,80	57,7	25,4	6,59	87	58,0	135	21,00	8,26	8,83	8,50	0,6025	8,57
7 D	28,0	19,80	59,2	25,1	6,72	72	74,0	146	21,50	8,57	9,02	8,78	0,7619	8,87
8 D	28,0	20,10	60,5	24,8	6,84	47	87,0	139	21,80	8,79	9,18	8,96	0,8894	9,09
1 E	23,9	11,20	39,5	26,6	5,27	237	3,0	180	16,00	6,02	6,96	6,30	0,0382	5,95
2 E	23,9	12,00	39,8	26,5	5,30	187	8,0	165	16,30	6,15	7,01	6,41	0,1015	6,12
3 E	23,9	13,10	40,3	26,3	5,35	147	15,0	142	16,70	6,34	7,08	6,57	0,1896	6,35
4 E	23,9	14,40	40,8	26,1	5,40	87	23,0	110	17,20	6,58	7,16	6,77	0,2894	6,59
5 E	23,9	14,90	41,4	25,9	5,47	82	33,0	115	17,40	6,71	7,26	6,91	0,4128	6,86
6 E	23,9	15,30	41,8	25,8	5,52	82	39,0	116	17,60	6,83	7,32	7,01	0,4861	7,00
7 E	23,9	16,20	42,4	25,6	5,58	87	48,0	110	18,10	7,08	7,41	7,19	0,5952	7,19
8 E	23,9	16,70	43,0	25,4	5,64	87	56,0	108	18,40	7,24	7,49	7,32	0,6911	7,33
9 E	23,9	17,10	43,7	25,2	5,72	102	67,0	104	18,70	7,43	7,61	7,47	0,8214	7,51
10E	23,9	17,7	45,1	24,8	5,87	87	85,0	102	18,90	7,64	7,81	7,72	1,0310	7,76
1 F	19,9	10,30	28,4	26,6	4,40	257	3,0	150	13,90	5,23	5,74	5,31	0,0469	4,95
2 F	19,9	11,30	28,7	26,4	4,45	207	12,0	99	14,10	5,35	5,82	5,48	0,1865	5,23
3 F	19,9	11,90	29,0	26,2	4,49	187	18,0	105	14,40	5,49	5,87	5,58	0,2787	5,41
4 F	19,9	12,50	29,2	26,1	4,52	157	23,0	105	14,60	5,60	5,91	5,69	0,3549	5,54
5 F	19,9	13,00	29,6	25,9	4,56	137	30,0	97	14,90	5,75	5,97	5,80	0,4608	5,70
6 F	19,9	13,40	29,9	25,8	4,61	117	37,0	94	15,20	5,90	6,03	5,90	0,5658	5,84
7 F	19,9	14,10	30,5	25,5	4,68	102	49,0	96	15,40	6,04	6,14	6,08	0,7434	6,04
8 F	19,9	14,60	31,0	25,2	4,76	82	60,0	97	15,50	6,15	6,24	6,23	0,9037	6,18
9 F	19,9	15,00	31,8	24,9	4,85	57	74,0	91	15,70	6,31	6,38	6,39	1,1043	6,35

	Q	h_a	H_1	h_1	F_1	x_2	x_1	L_j	h_2	Y	Y^*	Y_m	X_1	Y_p
	[1/s]	[cm]	[cm]	[mm]	[-]	[cm]	[cm]	[cm]	[cm]	[-]	[-]	[-]	[-]	[-]
10F	19,9	15,40	32,7	24,5	4,97	42	91,0	93	15,90	6,49	6,55	6,59	1,3427	6,53
1 G	17,0	8,60	21,2	26,7	3,73	277	0,0	207	11,30	4,24	4,80	4,47	0,0000	4,11
2 G	17,0	8,90	21,3	26,6	3,74	237	2,0	139	11,40	4,28	4,82	4,51	0,0377	4,17
3 G	17,0	9,30	21,5	26,5	3,78	207	8,0	105	11,60	4,38	4,86	4,59	0,1500	4,35
4 G	17,0	9,60	21,6	26,4	3,80	197	12,0	104	11,80	4,48	4,89	4,64	0,2243	4,47
5 G	17,0	10,20	21,8	26,2	3,82	177	17,0	94	12,00	4,57	4,93	4,74	0,3166	4,60
6 G	17,0	11,00	22,0	26,1	3,86	157	24,0	86	12,40	4,76	4,99	4,88	0,4447	4,76
7 G	17,0	11,50	22,4	25,8	3,91	137	33,0	80	12,70	4,92	5,06	5,00	0,6075	4,92
8 G	17,0	12,10	23,0	25,4	4,01	127	50,0	87	13,10	5,16	5,20	5,19	0,9091	5,15
9 G	17,0	12,50	23,4	25,1	4,08	107	61,0	78	13,30	5,29	5,29	5,32	1,1002	5,26
10G	17,0	13,00	24,4	24,5	4,24	67	87,0	79	13,50	5,51	5,51	5,58	1,5395	5,51
1 H	26,8	10,90	23,4	41,4	3,05	189	6,0	95	14,30	3,46	3,84	3,62	0,0930	3,41
2 H	26,8	12,15	23,5	41,2	3,07	118	14,0	65	15,20	3,69	3,87	3,73	0,2161	3,55
3 H	26,8	13,30	23,7	41,0	3,09	117	21,0	56	15,15	3,70	3,90	3,84	0,3230	3,66
4 H	26,8	13,80	24,0	40,7	3,13	110	33,0	55	15,20	3,74	3,95	3,92	0,5043	3,81
5 H	26,8	14,00	24,1	40,5	3,15	99	40,0	59	15,25	3,77	3,98	3,96	0,6090	3,88
6 H	26,8	14,50	24,3	40,3	3,17	93	46,0	54	15,85	3,93	4,01	4,02	0,6981	3,94
7 H	26,8	15,2	24,6	39,9	3,21	67	61,0	48	15,90	3,98	4,07	4,13	0,9183	4,04
8 H	26,8	15,5	24,9	39,6	3,26	82	74,0	50	16,20	4,09	4,13	4,20	1,1064	4,11
1 I	29,9	12,40	31,3	38,6	3,77	197	2,0	126	16,30	4,22	4,85	4,50	0,0257	4,18
2 I	29,9	13,95	31,7	38,3	3,81	157	15,0	117	17,50	4,57	4,92	4,66	0,1919	4,45
3 I	29,9	15,25	32,0	38,1	3,85	113	24,0	104	17,80	4,67	4,96	4,79	0,3057	4,61
4 I	29,9	15,40	32,2	38,0	3,86	109	29,0	99	18,15	4,78	4,99	4,83	0,3685	4,70
5 I	29,9	16,80	32,6	37,7	3,91	89	41,0	101	18,00	4,77	5,05	4,99	0,5180	4,87
6 I	29,9	17,30	32,9	37,5	3,95	85	51,0	93	18,65	4,98	5,10	5,08	0,6412	4,98
7 I	29,9	18,00	33,3	37,2	3,99	78	63,0	94	19,20	5,17	5,17	5,20	0,7875	5,09
8 I	29,9	18,10	34,2	36,6	4,08	51	86,0	86	19,60	5,35	5,29	5,31	1,0632	5,27
1 J	35,0	13,50	40,2	39,3	4,29	179	6,0	139	19,40	4,93	5,59	5,09	0,0651	4,85
2 J	35,0	15,95	40,6	39,1	4,33	137	17,0	126	20,20	5,17	5,65	5,30	0,1837	5,08
3 J	35,0	16,95	41,0	38,9	4,37	129	27,0	130	20,70	5,33	5,70	5,42	0,2905	5,27
4 J	35,0	17,15	41,1	38,8	4,38	127	29,0	117	21,00	5,41	5,72	5,44	0,3118	5,31
5 J	35,0	18,05	41,4	38,6	4,41	99	36,0	124	21,15	5,47	5,75	5,54	0,3859	5,43
6 J	35,0	18,95	41,8	38,4	4,44	102	45,0	117	21,30	5,54	5,80	5,66	0,4804	5,56
7 J	35,0	19,60	42,4	38,1	4,50	89	59,0	121	21,90	5,75	5,88	5,78	0,6261	5,73
8 J	35,0	20,5	43,0	37,8	4,55	76	72,0	121	22,20	5,87	5,96	5,92	0,7597	5,86
1 K	40,0	12,20	51,0	39,4	4,89	275	1,0	181	21,60	5,48	6,43	5,65	0,0093	5,45
2 K	40,0	14,25	51,5	39,2	4,93	212	11,0	168	21,70	5,54	6,49	5,81	0,1024	5,68
3 K	40,0	16,40	51,9	39,0	4,96	198	18,0	157	22,70	5,82	6,53	5,97	0,1672	5,83
4 K	40,0	17,60	52,2	38,9	4,99	109	24,0	124	23,00	5,92	6,57	6,08	0,2223	5,95
5 K	40,0	19,20	52,7	38,7	5,02	98	33,0	110	23,35	6,04	6,62	6,24	0,3046	6,13
6 K	40,0	20,70	53,3	38,4	5,08	109	45,0	120	24,15	6,29	6,70	6,41	0,4134	6,34
7 K	40,0	21,80	54,0	38,1	5,13	105	58,0	135	24,90	6,53	6,78	6,57	0,5301	6,53
8 K	40,0	22,90	54,8	37,8	5,20	93	72,0	127	25,10	6,64	6,87	6,73	0,6543	6,70

SERIES : 1.6

A1 - 25

	Q	h _{a,l}	h _{e,r}	H ₁	h ₁	F ₁	x _e	x ₂	x ₁	h ₂	Y	Y*	Y _m	X ₁	Y _p
	[1/s]	[cm]	[cm]	[cm]	[mm]	[-]	[m]	[m]	[cm]	[cm]	[-]	[-]	[-]	[-]	[-]
1 A	32,8	8,25	6,90	23,6	32,86	3,52		1,90	4,0	9,2	2,78	4,50	3,36	0,066	3,20
2 A	32,8	11,30	10,40	23,9	32,62	3,56		1,25	15,0	11,5	3,53	4,55	4,01	0,245	3,70
3 A	32,8	12,00	11,40	24,1	32,39	3,59		1,37	25,0	12,7	3,92	4,60	4,17	0,406	4,07
4 A	32,8	12,80	12,30	24,4	32,19	3,63		1,62	34,0	13,4	4,16	4,65	4,35	0,549	4,31
5 A	32,8	13,80	13,70	25,0	31,72	3,71		1,67	55,0	14,1	4,45	4,77	4,63	0,879	4,66
6 A	32,8	14,30	14,20	25,4	31,38	3,77	5,40	1,62	70,0	14,7	4,69	4,85	4,79	1,109	4,80
7 A	32,8	14,40	14,30	25,7	31,16	3,81	4,30	1,55	80,0	14,8	4,76	4,91	4,86	1,261	4,88
8 A	32,8	14,80	14,70	26,7	30,42	3,95	4,50	1,70	113,0	15,1	4,98	5,11	5,08	1,749	5,10
1 B	48,2	6,70	11,50	47,0	32,93	5,15	1,32		9,0	12,5	3,80	6,81	4,68	0,095	4,79
2 B	48,2	8,60	12,20	47,1	32,89	5,16	1,42		11,0	13,1	3,98	6,82	4,85	0,116	4,89
3 B	48,2	10,80	13,20	47,3	32,83	5,18	1,40		14,0	14,1	4,29	6,84	5,09	0,147	5,04
4 B	48,2	12,40	14,80	47,4	32,77	5,19	1,30		17,0	15,2	4,64	6,86	5,35	0,178	5,19
5 B	48,2	13,80	15,70	47,8	32,63	5,22	1,44		24,0	16,1	4,93	6,91	5,57	0,251	5,52
6 B	48,2	14,80	16,50	48,0	32,55	5,24	1,38		28,0	16,8	5,16	6,93	5,74	0,293	5,69
7 B	48,2	16,10	17,30	48,4	32,39	5,28	1,41		36,0	18,0	5,56	6,99	5,97	0,375	6,01
8 B	48,2	17,20	18,00	48,8	32,25	5,32	1,44		43,0	19,0	5,88	7,04	6,17	0,446	6,25
9 B	48,2	18,30	18,90	49,4	32,03	5,37	1,42		54,0	19,8	6,17	7,11	6,41	0,558	6,56
10B	48,2	20,10	20,20	50,4	31,67	5,46	1,40	4,80	72,0	21,0	6,63	7,24	6,80	0,738	6,94
1 C	67,5	8,60	15,40	78,2	35,28	6,51	1,45		11,0	16,6	4,71	8,72	5,89	0,083	5,97
2 C	67,5	11,40	16,70	78,8	35,14	6,54	1,46		18,0	18,1	5,15	8,77	6,16	0,136	6,32
3 C	67,5	14,20	18,50	79,6	34,94	6,60	1,35		29,0	20,2	5,78	8,85	6,52	0,219	6,84
4 C	67,5	17,60	20,30	80,4	34,77	6,65	1,35		38,0	22,3	6,41	8,92	6,94	0,286	7,23
5 C	67,5	20,10	21,90	81,0	34,62	6,69	1,32		46,0	23,5	6,78	8,98	7,30	0,345	7,55
6 C	67,5	21,70	23,40	81,8	34,43	6,75	1,25		56,0	25,5	7,42	9,06	7,61	0,418	7,90
7 C	67,5	23,80	24,80	83,0	34,19	6,82	1,34		69,0	26,8	7,83	9,16	7,98	0,513	8,30
8 C	67,5	25,50	25,60	83,9	33,98	6,88	1,30	3,70	80,0	28,0	8,24	9,25	8,27	0,593	8,58
9 C	67,5	27,30	27,30	85,5	33,64	6,99	1,20	1,20	98,0	29,4	8,73	9,39	8,69	0,722	8,96
10C	67,5	28,40	28,40	87,9	33,16	7,14	1,00	1,00	124,0	30,0	9,04	9,61	9,05	0,905	9,39
1 D	89,7	12,80	19,90	121,9	37,27	7,96	1,46		26,0	22,8	6,12	10,77	7,31	0,150	7,79
2 D	89,7	18,30	22,90	123,4	37,02	8,04	1,40		40,0	25,6	6,92	10,89	7,89	0,230	8,42
3 D	89,7	23,40	26,80	125,9	36,64	8,17	1,45		61,0	29,7	8,11	11,06	8,62	0,348	9,27
4 D	89,7	27,00	28,70	127,7	36,38	8,26	1,40		76,0	31,8	8,74	11,19	9,12	0,432	9,79
5 D	89,7	31,10	31,40	129,8	36,05	8,37	1,40	1,40	94,0	34,7	9,63	11,35	9,77	0,531	10,32
6 D	89,7	33,70	33,70	133,0	35,61	8,53	1,10	1,10	119,0	36,9	10,36	11,57	10,34	0,668	10,91
7 D	89,7	36,20	36,20	137,0	35,06	8,73	1,00	1,00	150,0	38,3	10,93	11,85	10,98	0,834	11,48
8 D	89,7	38,00	38,00	143,1	34,27	9,03			194,0	39,9	11,63	12,28	11,62	1,064	12,11
1 E	106,1	19,20	6,60	159,8	38,37	9,02		1,80	22,0	24,3	6,33	12,26	7,73	0,108	8,46
2 E	106,1	25,20	19,30	163,3	37,93	9,17		1,70	47,0	29,8	7,86	12,48	8,79	0,229	9,61
3 E	106,1	28,20	25,00	165,7	37,66	9,27		1,50	63,0	32,7	8,68	12,62	9,43	0,306	10,28
4 E	106,1	31,60	28,20	168,2	37,36	9,38		1,70	80,0	35,7	9,56	12,78	9,99	0,386	10,91
5 E	106,1	33,30	30,80	170,5	37,10	9,48		1,90	95,0	37,2	10,02	12,92	10,39	0,457	11,41
6 E	106,1	34,30	33,20	171,7	36,96	9,53		1,70	103,0	39,3	10,64	12,99	10,70	0,494	11,65
7 E	106,1	38,10	37,40	176,0	36,50	9,72	2,30	1,70	130,0	41,1	11,26	13,25	11,52	0,619	12,35
8 E	106,1	39,50	39,10	179,0	36,19	9,84	1,40	1,40	148,0	42,8	11,84	13,43	11,90	0,701	12,75
9 E	106,1	41,60	41,40	183,3	35,74	10,03	1,20	1,20	174,0	44,2	12,37	13,69	12,47	0,818	13,24
1 F	57,9	10,30	7,90	30,7	51,74	3,14		1,90	3,0	11,9	2,30	3,97	2,86	0,036	2,80
2 F	57,9	13,60	11,40	30,8	51,63	3,15		1,70	8,0	14,2	2,75	3,98	3,19	0,095	2,95

	Q	$h_{a,l}$	$h_{e,r}$	H_1	h_1	F_1	x_e	x_2	x_1	h_2	Y	Y*	Y_m	X_1	Y_p
	[1/s]	[cm]	[cm]	[cm]	[mm]	[-]	[m]	[m]	[cm]	[cm]	[-]	[-]	[-]	[-]	[-]
3 F	57,9	15,70	14,20	31,1	51,27	3,18		1,70	24,0	16,5	3,22	4,03	3,48	0,285	3,38
4 F	57,9	17,10	16,10	31,5	50,91	3,22		1,72	40,0	18,2	3,58	4,08	3,70	0,472	3,71
5 F	57,9	18,80	18,10	32,1	50,28	3,28	5,20	1,60	68,0	19,4	3,85	4,16	3,98	0,794	4,04
6 F	57,9	20,00	19,60	33,1	49,25	3,38	2,80	1,70	114,0	20,6	4,18	4,31	4,26	1,309	4,29
7 F	57,9	20,40	20,10	34,4	48,05	3,51	1,40	1,40	168,0	20,9	4,35	4,49	4,45	1,892	4,48
1 G	86,8	18,00	12,30	70,4	48,43	5,20		1,60	16,0	18,6	3,84	6,87	4,86	0,113	4,92
2 G	86,8	20,20	16,50	71,0	48,20	5,24		1,54	28,0	21,7	4,50	6,93	5,21	0,198	5,32
3 G	86,8	22,50	19,90	71,7	47,91	5,29		1,50	43,0	24,5	5,11	6,99	5,56	0,303	5,77
4 G	86,8	24,60	22,80	72,6	47,59	5,34		1,60	60,0	26,9	5,65	7,07	5,90	0,420	6,20
5 G	86,8	26,70	25,60	73,5	47,28	5,39		1,50	76,0	28,6	6,06	7,14	6,25	0,530	6,53
6 G	86,8	28,20	28,30	75,0	46,76	5,48	1,50	2,30	103,0	30,7	6,56	7,27	6,61	0,713	6,94
7 G	86,8	29,20	29,20	75,8	46,49	5,53	1,36	1,36	117,0	31,1	6,69	7,34	6,78	0,807	7,10
8 G	86,8	30,30	30,20	76,5	46,24	5,58	1,25	1,25	130,0	31,9	6,90	7,40	6,97	0,893	7,22
9 G	86,8	31,10	31,10	78,0	45,76	5,66	1,30	1,30	155,0	32,4	7,09	7,52	7,18	1,057	7,43
10G	86,8	31,50	31,50	79,3	45,34	5,74	1,20	1,20	177,0	32,7	7,20	7,64	7,31	1,200	7,58
1 H	115,8	20,70	14,20	114,6	49,93	6,62		1,50	19,0	24,1	4,83	8,88	6,01	0,100	6,17
2 H	115,8	24,40	18,60	116,5	49,50	6,71		1,51	43,0	28,1	5,68	9,01	6,43	0,225	6,98
3 H	115,8	23,90	27,60	117,6	49,25	6,76	1,48		57,0	31,8	6,46	9,08	6,90	0,297	7,41
4 H	115,8	27,90	30,40	119,0	48,92	6,83	1,60		75,0	33,7	6,88	9,17	7,33	0,389	7,89
5 H	115,8	33,20	31,10	120,3	48,65	6,89		1,60	90,0	36,5	7,49	9,25	7,73	0,465	8,24
6 H	115,8	34,90	34,60	122,2	48,25	6,97	2,50	1,30	112,0	37,6	7,79	9,38	8,12	0,576	8,66
7 H	115,8	37,10	37,20	124,3	47,80	7,07	1,50	1,50	137,0	39,9	8,34	9,51	8,52	0,701	9,04
8 H	115,8	38,80	38,80	125,8	47,52	7,14	1,55	1,55	153,0	41,1	8,65	9,61	8,80	0,780	9,25
9 H	115,8	40,30	40,20	128,1	47,05	7,24	1,35	1,35	179,0	42,1	8,95	9,76	9,10	0,906	9,53
1 I	144,7	25,30	15,30	166,2	51,49	7,91		1,40	42,0	31,5	6,12	10,70	7,10	0,177	7,92
2 I	144,7	30,30	22,90	168,6	51,11	8,00		1,30	64,0	35,8	7,01	10,82	7,69	0,268	8,62
3 I	144,7	32,80	33,80	169,7	50,93	8,04		1,50	74,0	38,8	7,62	10,88	8,38	0,309	8,91
4 I	144,7	36,10	34,80	172,0	50,57	8,13		1,60	95,0	43,3	8,55	11,00	8,68	0,395	9,46
5 I	144,7	37,60	36,90	173,5	50,34	8,18		1,30	108,0	44,6	8,86	11,08	8,93	0,448	9,77
6 I	144,7	40,90	38,70	176,4	49,91	8,29		1,30	133,0	45,7	9,16	11,23	9,32	0,549	10,27
7 I	144,7	43,60	41,80	177,6	49,74	8,33	1,40	1,40	143,0	46,9	9,42	11,29	9,70	0,589	10,45
8 I	144,7	45,10	44,90	179,3	49,48	8,40	1,40	1,40	158,0	48,6	9,83	11,38	10,04	0,649	10,70
9 I	144,7	46,70	46,60	181,8	49,13	8,49	1,60	1,60	178,0	50,5	10,27	11,51	10,34	0,728	10,98
1 J	154,4	22,70	29,80	192,7	50,89	8,59	1,60		52,0	37,2	7,31	11,65	8,07	0,203	8,80
2 J	154,4	29,40	32,60	195,3	50,53	8,68	1,60		73,0	42,0	8,32	11,78	8,58	0,283	9,46
3 J	154,4	34,60	34,60	197,2	50,27	8,74	1,70		88,0	43,9	8,73	11,88	9,00	0,340	9,90
4 J	154,4	39,20	37,60	200,0	49,91	8,84	1,50		109,0	46,6	9,33	12,01	9,49	0,420	10,44
5 J	154,4	41,30	41,80	201,8	49,67	8,90	2,30	2,30	123,0	47,9	9,64	12,10	9,90	0,472	10,76
6 J	154,4	44,00	45,80	204,4	49,35	8,99	1,60	1,50	142,0	50,0	10,12	12,22	10,37	0,543	11,15
7 J	154,4	48,10	46,80	206,4	49,09	9,06	1,60	1,60	157,0	51,5	10,49	12,32	10,75	0,599	11,43
8 J	154,4	49,10	49,40	210,4	48,62	9,19	1,60	1,60	185,0	54,4	11,19	12,51	11,11	0,701	11,88
1 K	77,2	10,60	13,10	37,5	62,28	3,17		1,72	5,0	15,1	2,42	4,01	2,95	0,049	2,86
2 K	77,2	13,90	15,90	37,7	62,11	3,18		1,65	13,0	18,2	2,93	4,03	3,20	0,127	3,05
3 K	77,2	16,00	17,90	38,0	61,82	3,21		1,65	26,0	19,4	3,14	4,06	3,40	0,254	3,35
4 K	77,2	18,30	19,20	38,2	61,57	3,23		1,70	37,0	20,7	3,36	4,09	3,58	0,360	3,56
5 K	77,2	20,10	20,70	38,5	61,20	3,26		1,75	54,0	21,8	3,57	4,13	3,77	0,522	3,81
6 K	77,2	22,00	22,20	39,0	60,69	3,30	4,20	1,50	77,0	23,6	3,89	4,19	3,98	0,740	4,04

	Q	$h_{a,l}$	$h_{e,r}$	H_1	h_1	F_1	x_e	x_2	x_1	h_2	Y	Y*	Y_m	X_1	Y_p
	[1/s]	[cm]	[cm]	[cm]	[mm]	[-]	[m]	[m]	[cm]	[cm]	[-]	[-]	[-]	[-]	[-]
7 K	77,2	23,10	23,20	39,5	60,20	3,34	4,40	1,70	99,0	24,4	4,05	4,24	4,12	0,945	4,17
8 K	77,2	23,60	23,80	39,9	59,85	3,37	1,55	2,30	115,0	24,8	4,14	4,29	4,21	1,093	4,24
9 K	77,2	24,30	24,40	41,0	58,76	3,46	1,50	4,10	165,0	25,0	4,25	4,42	4,38	1,545	4,41
1 L	115,8	15,30	20,70	77,8	61,77	4,81		1,60	24,0	24,1	3,90	6,33	4,51	0,146	4,68
2 L	115,8	19,90	23,50	78,3	61,56	4,84		1,50	35,0	27,3	4,43	6,36	4,81	0,212	4,96
3 L	115,8	23,30	25,70	79,0	61,25	4,88		1,35	51,0	28,6	4,68	6,41	5,08	0,307	5,33
4 L	115,8	25,40	27,20	79,3	61,11	4,89		1,50	58,0	30,6	5,01	6,44	5,26	0,349	5,47
5 L	115,8	27,60	29,00	80,0	60,78	4,93		1,60	75,0	32,1	5,29	6,49	5,48	0,450	5,78
6 L	115,8	29,70	30,70	80,5	60,57	4,96		1,65	86,0	33,8	5,58	6,53	5,69	0,514	5,95
7 L	115,8	31,70	32,10	81,4	60,21	5,00	3,10	1,50	105,0	35,2	5,85	6,59	5,90	0,625	6,19
8 L	115,8	33,80	33,50	82,2	59,88	5,05	1,70	1,70	122,0	36,5	6,09	6,65	6,12	0,724	6,37
9 L	115,8	34,90	35,00	83,5	59,36	5,11	1,60	1,60	149,0	37,5	6,32	6,75	6,32	0,879	6,58
10L	115,8	36,20	36,30	84,9	58,80	5,18	1,55	1,55	178,0	38,2	6,50	6,85	6,53	1,043	6,76
1 M	154,4	13,70	23,40	131,6	62,24	6,35		1,70	25,0	28,9	4,64	8,49	5,61	0,111	5,98
2 M	154,4	19,70	26,60	133,0	61,90	6,40		1,75	44,0	33,6	5,43	8,56	5,95	0,194	6,49
3 M	154,4	24,70	29,80	133,5	61,75	6,42		1,80	52,0	35,8	5,80	8,60	6,27	0,229	6,70
4 M	154,4	28,10	32,20	134,8	61,45	6,47		1,65	69,0	37,6	6,12	8,66	6,55	0,303	7,10
5 M	154,4	30,80	34,20	136,0	61,16	6,52		1,70	85,0	39,4	6,45	8,73	6,79	0,372	7,45
6 M	154,4	33,10	36,30	136,9	60,92	6,55	5,40	1,70	98,0	41,4	6,80	8,78	7,02	0,427	7,70
7 M	154,4	38,00	35,40	137,7	60,74	6,58	1,80		108,0	42,5	7,00	8,82	7,23	0,470	7,87
8 M	154,4	40,20	38,00	138,6	60,53	6,62	1,70	4,20	120,0	44,2	7,30	8,87	7,49	0,521	8,07
9 M	154,4	42,80	41,40	140,1	60,19	6,67	1,65	2,90	139,0	46,6	7,74	8,95	7,83	0,601	8,33
10M	154,4	44,60	45,00	142,5	59,65	6,77	1,70	2,30	169,0	48,6	8,15	9,08	8,20	0,727	8,68
1 N	192,9	27,60	15,20	197,6	62,98	7,80		1,80	38,0	35,2	5,59	10,54	6,82	0,133	7,50
2 N	192,9	36,20	23,20	199,8	62,62	7,86		1,70	59,0	43,4	6,93	10,63	7,39	0,205	8,07
3 N	192,9	34,20	34,30	201,8	62,29	7,93		1,70	78,0	47,5	7,62	10,72	7,78	0,271	8,55
4 N	192,9	38,10	37,60	203,6	62,01	7,98		1,60	94,0	49,5	7,99	10,79	8,11	0,325	8,93
5 N	192,9	42,00	41,70	205,8	61,65	8,05		1,70	115,0	51,2	8,30	10,89	8,52	0,397	9,38
6 N	192,9	45,20	44,90	207,3	61,43	8,09	2,30	2,30	128,0	53,8	8,75	10,96	8,84	0,440	9,63
7 N	192,9	48,00	47,80	208,6	61,22	8,13	2,10	2,40	140,0	55,2	9,02	11,01	9,14	0,481	9,84
8 N	192,9	48,30	49,60	210,5	60,93	8,19	2,20	2,20	157,0	55,9	9,18	11,10	9,30	0,537	10,12
9 N	192,9	52,00	52,50	212,6	60,62	8,25	2,10	2,10	175,0	58,4	9,63	11,18	9,68	0,597	10,38
1 O	19,3	4,60	5,20	14,0	25,69	2,99		2,20	3,0	6,0	2,34	3,76	2,83	0,077	2,76
2 O	19,3	4,90	5,50	14,0	25,69	2,99		2,05	3,0	6,3	2,45	3,76	2,89	0,077	2,76
3 O	19,3	5,10	5,80	14,1	25,65	3,00		2,00	5,0	6,4	2,50	3,77	2,94	0,128	2,88
4 O	19,3	5,80	6,30	14,1	25,62	3,00		2,10	6,0	6,8	2,65	3,78	3,07	0,153	2,93
5 O	19,3	6,60	7,00	14,1	25,62	3,00		2,08	6,0	7,3	2,85	3,78	3,23	0,153	2,93
6 O	19,3	6,90	7,30	14,2	25,45	3,03		2,00	13,0	8,1	3,18	3,82	3,32	0,330	3,29
7 O	19,3	7,60	8,00	14,5	25,19	3,08		1,80	24,0	8,6	3,41	3,89	3,53	0,603	3,66
8 O	19,3	8,10	8,40	14,9	24,75	3,16		1,70	42,0	9,0	3,64	4,00	3,72	1,040	3,96
9 O	19,3	8,70	8,90	15,6	23,99	3,32		1,70	73,0	9,3	3,88	4,22	4,00	1,762	4,21
1 P	28,9	7,10	5,70	31,2	24,35	4,86		1,75	5,0	8,8	3,61	6,40	4,42	0,076	4,44
2 P	28,9	8,60	6,60	31,2	24,33	4,87		1,65	6,0	9,8	4,03	6,40	4,64	0,091	4,51
3 P	28,9	9,60	8,00	31,3	24,31	4,88		1,50	7,0	10,5	4,32	6,41	4,88	0,106	4,58
4 P	28,9	10,50	9,10	31,5	24,21	4,91		1,35	12,0	11,2	4,63	6,46	5,12	0,182	4,92
5 P	28,9	11,50	9,80	31,8	24,08	4,94		1,20	18,0	11,9	4,94	6,51	5,35	0,272	5,29
6 P	28,9	12,30	11,10	32,2	23,92	5,00		1,10	26,0	12,7	5,31	6,58	5,65	0,390	5,71

	Q	$h_{a,l}$	$h_{c,r}$	H_1	h_1	F_1	x_e	x_2	x_1	h_2	Y	Y^*	Y_m	X_1	Y_p
	[l/s]	[cm]	[cm]	[cm]	[mm]	[-]	[m]	[m]	[cm]	[cm]	[-]	[-]	[-]	[-]	[-]
7 P	28,9	13,00	12,00	33,5	23,41	5,16		1,00	50,0	13,5	5,77	6,81	6,01	0,740	6,53
8 P	28,9	13,70	12,80	34,6	22,97	5,31		1,20	71,0	14,1	6,14	7,02	6,35	1,037	6,93
9 P	28,9	14,20	14,00	35,0	22,84	5,35		1,40	77,0	14,8	6,48	7,09	6,62	1,120	7,01
10P	28,9	15,00	15,10	36,8	22,20	5,59		1,20	107,0	15,6	7,00	7,41	7,12	1,528	7,40
1 Q	48,2	6,80	12,10	67,6	27,02	6,94		1,30	14,0	13,9	5,14	9,32	6,23	0,129	6,65
2 Q	48,2	10,20	13,90	67,8	26,98	6,95		1,40	16,0	15,1	5,60	9,34	6,65	0,148	6,78
3 Q	48,2	12,70	15,50	68,2	26,90	6,98		1,45	20,0	17,2	6,39	9,38	7,04	0,184	7,03
4 Q	48,2	14,10	16,50	68,7	26,79	7,02		1,50	26,0	18,1	6,76	9,45	7,31	0,239	7,39
5 Q	48,2	15,60	18,00	69,5	26,64	7,08		1,40	34,0	19,2	7,19	9,53	7,67	0,311	7,84
6 Q	48,2	17,60	18,60	70,2	26,49	7,15		1,45	42,0	20,6	7,78	9,62	8,00	0,383	8,24
7 Q	48,2	19,20	20,00	71,4	26,26	7,24		1,60	54,0	21,8	8,32	9,75	8,43	0,490	8,76
8 Q	48,2	21,00	20,60	72,4	26,07	7,32		1,45	64,0	22,8	8,73	9,86	8,78	0,578	9,11
9 Q	48,2	22,20	21,90	74,5	25,68	7,48		1,55	84,0	23,9	9,30	10,09	9,24	0,752	9,68
10Q	48,2	23,40	23,20	77,2	25,20	7,70	1,40	1,40	109,0	24,7	9,81	10,40	9,77	0,965	10,20
11Q	48,2	24,50	24,40	82,6	24,30	8,13	1,30	1,30	155,0	25,5	10,51	11,00	10,51	1,342	10,95
1 R	67,5	15,80	7,90	117,8	28,43	8,99		1,45	20,0	18,8	6,61	12,23	7,97	0,133	8,65
2 R	67,5	17,20	10,10	118,1	28,40	9,01		1,50	22,0	19,4	6,83	12,25	8,23	0,146	8,78
3 R	67,5	20,10	14,80	120,4	28,11	9,15		1,40	38,0	22,7	8,08	12,45	8,93	0,250	9,75
4 R	67,5	22,10	18,80	121,8	27,95	9,23		1,40	47,0	24,6	8,80	12,56	9,53	0,309	10,25
5 R	67,5	23,20	20,70	122,7	27,84	9,28		1,50	53,0	25,9	9,30	12,64	9,86	0,347	10,56
6 R	67,5	24,90	23,30	124,4	27,64	9,38		1,45	64,0	27,2	9,84	12,78	10,38	0,418	11,09
7 R	67,5	26,50	25,50	126,5	27,41	9,50		1,50	77,0	29,5	10,75	12,95	10,89	0,500	11,63
8 R	67,5	28,00	27,40	129,4	27,09	9,67		1,40	95,0	30,8	11,37	13,19	11,43	0,613	12,27
9 R	67,5	29,30	29,00	132,7	26,74	9,86	1,80	1,30	114,0	32,1	12,02	13,45	11,94	0,729	12,83
10R	67,5	31,10	31,10	136,7	26,33	10,09	1,15	1,15	137,0	33,3	12,64	13,78	12,63	0,869	13,40
11R	67,5	33,20	33,20	145,7	25,48	10,60	1,00	1,00	184,0	34,5	13,54	14,50	13,66	1,144	14,35

APPENDIX 2

MEASUREMENTS OF CHAPTER 6

Appendix 2 includes the data of the experimental investigation presented in chapter 6. These tests were performed in sudden expanding channels with a negative step located at the expansion section. The main characteristics of the channel geometries investigated are given in Table 2.1, whereas the relevant notation used is given in Fig.2.1.

Table 2.1 : Sudden expanding channels with negative step: Overall characteristics of experiments.

Series	b ₂ [m]	B [-]	shape	F ₁		N=s/h ₁		No of runs
				from	to	from	to	
2.1	0.50	1.5	asym	3.20	8.43	0.61	1.64	105
2.2	0.50	2	asym	2.68	8.12	0.59	1.61	112
2.3	0.50	3	sym	2.05	7.37	0.49	1.66	129

In addition to the symbols indicated in Fig.2.1, the following non-dimensional terms are used:

- N = s/h₁: non-dimensional sill height
- Y = h₂/h₁: experimental sequent depths ratio
- Y_N^{*} = h_{2,N}^{*}/h₁: sequent depths ratio according to Eq. (6.11)
- Y_m = h_{2,m}/h₁: sequent depths ratio according to Eq. (6.4)
- Y_p = h_{2,p}/h₁: predicted sequent depths ratio Eq. (6.5)
- X₁ = x₁/L_r^{*}: non-dimensional toe position Eq. (5.3)
- X_e = x_e/L_r^{*}: non-dimensional length of the smaller lateral eddy
- X₂ = x₂/L_r^{*}: non-dimensional length of the longer lateral eddy.
- L_r^{*}: surface roller length in prismatic channel Eq. (5.4).
- L_j: measured jump length.

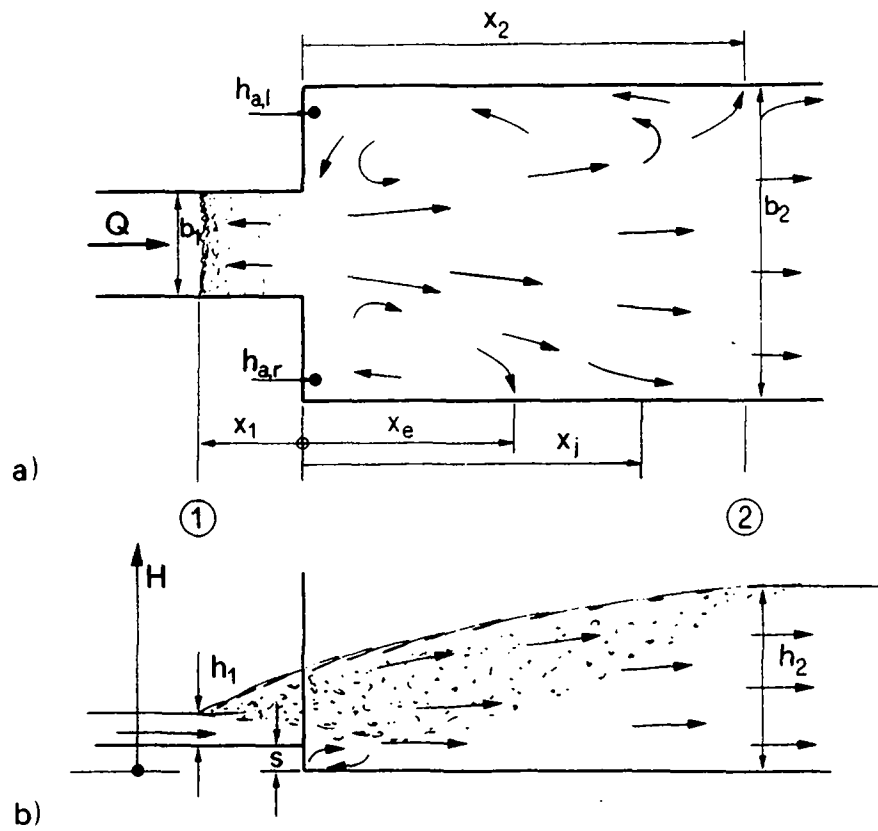


Fig. 2.1 : Relevant notation of sudden expansions with negative step investigated in chapter 6. a) Plan view; b) axial view.

	Q	h _a	H ₁	h ₁	F ₁	N	x ₂	x ₁	L _j	h ₂	Y	Y*	Y _N *	X ₁	Y _p
	[l/s]	[cm]	[cm]	[mm]	[-]	[-]	[m]	[cm]	[cm]	[cm]	[-]	[-]	[-]	[-]	[-]
1A	23,2	12,10	46,0	23,89	6,04	1,05	0,90	5,0	125	17,1	7,16	8,32	7,74	0,0608	7,13
2A	23,2	14,10	46,6	23,74	6,10	1,05	0,76	10,0	115	17,6	7,41	8,46	8,09	0,1210	7,39
3A	23,2	15,60	47,2	23,59	6,16	1,06	0,70	15,0	110	18,2	7,72	8,60	8,39	0,1808	7,66
4A	23,2	16,50	47,8	23,40	6,24	1,07	0,65	21,0	106	18,6	7,95	8,76	8,62	0,2518	7,97
5A	23,2	17,10	48,3	23,28	6,29	1,07	0,60	25,0	105	19,0	8,16	8,88	8,78	0,2987	8,17
6A	23,2	17,60	49,3	23,03	6,39	1,09	0,59	33,0	113	19,6	8,51	9,11	8,99	0,3916	8,56
7A	23,2	18,60	50,2	22,81	6,48	1,10	0,57	40,0	116	20,0	8,77	9,32	9,27	0,4717	8,88
8A	23,2	19,40	51,3	22,53	6,60	1,11	0,54	49,0	125	20,7	9,19	9,59	9,56	0,5733	9,27
9A	23,2	19,90	52,7	22,22	6,74	1,13	0,08	59,0	124	21,2	9,54	9,91	9,82	0,6842	9,68
10A	23,2	20,70	56,7	21,38	7,14	1,17	0,38	86,0	126	21,9	10,24	10,82	10,48	0,9732	10,72
1B	20,1	12,70	35,3	23,85	5,26	1,05	0,99	3,0	118	15,9	6,67	7,23	7,08	0,0427	6,18
2B	20,1	13,90	35,9	23,66	5,32	1,06	0,82	9,0	114	16,2	6,85	7,39	7,35	0,1273	6,49
3B	20,1	15,20	36,6	23,41	5,41	1,07	0,66	17,0	108	16,8	7,18	7,61	7,67	0,2387	6,91
4B	20,1	15,80	37,0	23,24	5,46	1,08	0,64	22,0	109	17,2	7,40	7,75	7,84	0,3074	7,16
5B	20,1	16,10	37,7	23,02	5,54	1,09	-0,15	29,0	112	17,6	7,65	7,95	7,99	0,4026	7,50
6B	20,1	17,10	38,2	22,86	5,60	1,09	0,56	34,0	114	18,0	7,87	8,10	8,24	0,4698	7,72
8B	20,1	17,60	39,3	22,50	5,74	1,11	0,60	45,0	120	18,7	8,31	8,43	8,50	0,6153	8,19
8B	20,1	18,20	40,0	22,28	5,82	1,12	0,58	52,0	197	19,1	8,57	8,65	8,72	0,7063	8,47
9B	20,1	18,40	41,2	21,92	5,97	1,14	0,43	63,0	116	19,4	8,85	9,01	8,94	0,8467	8,89
10B	20,1	18,90	42,8	21,47	6,16	1,16	0,43	77,0	114	19,5	9,08	9,47	9,28	1,0208	9,39
1C	17,1	11,00	26,6	23,63	4,53	1,06	1,98	3,0	93	14,1	5,97	6,26	6,17	0,0509	5,39
2C	17,1	11,60	26,9	23,49	4,57	1,06	1,48	7,0	97	14,4	6,13	6,37	6,32	0,1184	5,60
3C	17,1	12,20	27,0	23,42	4,59	1,07	1,33	9,0	94	14,7	6,28	6,43	6,44	0,1519	5,71
4C	17,1	13,00	27,2	23,32	4,62	1,07	0,88	12,0	92	15,0	6,43	6,51	6,62	0,2019	5,86
5C	17,1	13,80	27,4	23,22	4,65	1,08	0,75	15,0	90	15,4	6,63	6,59	6,80	0,2516	6,02
6C	17,1	14,30	27,8	23,06	4,70	1,08	0,65	20,0	90	15,6	6,77	6,74	6,95	0,3338	6,27
7C	17,1	14,80	28,2	22,85	4,76	1,09	0,55	26,0	91	15,8	6,91	6,91	7,12	0,4312	6,56
8C	17,1	15,10	28,7	22,65	4,83	1,10	0,56	32,0	97	16,1	7,11	7,09	7,26	0,5274	6,82
9C	17,1	15,70	29,4	22,32	4,94	1,12	0,62	42,0	103	16,6	7,44	7,40	7,51	0,6851	7,24
10C	17,1	16,10	30,2	22,01	5,04	1,14	0,64	51,0	96	16,9	7,68	7,69	7,72	0,8240	7,59
11C	17,1	16,60	31,8	21,37	5,27	1,17	0,68	70,0	93	17,2	8,05	8,34	8,12	1,1083	8,30
1D	14,4	10,60	19,7	23,55	3,83	1,06	2,03	6,0	81	12,6	5,35	5,39	5,50	0,1241	4,77
2D	14,4	11,10	19,8	23,48	3,85	1,06	1,70	8,0	81	12,8	5,45	5,45	5,61	0,1651	4,88
3D	14,4	11,40	19,9	23,41	3,87	1,07	1,13	10,0	80	13,1	5,60	5,50	5,69	0,2059	4,98
4D	14,4	12,00	20,1	23,23	3,91	1,08	0,96	15,0	82	13,5	5,81	5,65	5,85	0,3071	5,24
5D	14,4	12,50	20,5	22,98	3,98	1,09	0,83	22,0	81	13,8	6,00	5,85	6,03	0,4468	5,57
6D	14,4	13,00	20,7	22,84	4,01	1,09	0,73	26,0	82	14,0	6,13	5,97	6,17	0,5256	5,75
7D	14,4	13,50	21,1	22,59	4,08	1,11	0,68	33,0	82	14,4	6,37	6,19	6,36	0,6616	6,05
8D	14,4	14,00	21,9	22,09	4,22	1,13	0,73	47,0	77	14,7	6,65	6,65	6,64	0,9270	6,59
9D	14,4	14,50	23,1	21,42	4,42	1,17	0,73	66,0	79	14,9	6,96	7,33	7,01	1,2726	7,31
10D	14,4	15,10	24,9	20,50	4,72	1,22	0,73	92,0	80	15,3	7,46	8,36	7,54	1,7192	8,35
1E	39,5	15,80	47,3	40,82	4,60	0,61	3,68	7,0	157	22,5	5,51	6,20	5,79	0,0676	5,37
2E	39,5	17,60	47,9	40,51	4,65	0,62	2,28	17,0	162	23,4	5,78	6,33	5,99	0,1634	5,64
3E	39,5	18,90	48,4	40,29	4,69	0,62	1,98	24,0	164	23,8	5,91	6,42	6,14	0,2297	5,83
4E	39,5	19,90	48,6	40,17	4,71	0,62	1,78	28,0	163	24,2	6,02	6,47	6,26	0,2675	5,93
5E	39,5	21,50	49,0	39,98	4,75	0,63	1,58	34,0	165	24,8	6,20	6,54	6,44	0,3237	6,08
6E	39,5	22,30	49,4	39,79	4,78	0,63	1,33	40,0	165	25,1	6,31	6,62	6,55	0,3796	6,22
7E	39,5	23,00	49,9	39,61	4,81	0,63	1,03	46,0	161	25,4	6,41	6,70	6,66	0,4351	6,36

	Q	h _a	H ₁	h ₁	F ₁	N	x ₂	x ₁	L _j	h ₂	Y	Y*	Y _N *	X ₁	Y _p
	[1/s]	[cm]	[cm]	[mm]	[-]	[-]	[m]	[cm]	[cm]	[cm]	[-]	[-]	[-]	[-]	[-]
8E	39,5	24,20	50,7	39,24	4,88	0,64	0,98	58,0	170	26,2	6,68	6,86	6,85	0,5450	6,61
9E	39,5	24,80	51,3	38,99	4,93	0,64	0,88	66,0	169	26,6	6,82	6,97	6,97	0,6174	6,77
10E	39,5	25,50	52,4	38,53	5,02	0,65	0,78	81,0	171	27,0	7,01	7,17	7,15	0,7515	7,05
1F	34,6	14,40	37,4	40,76	4,05	0,61	2,98	4,0	61	20,1	4,93	5,43	5,14	0,0449	4,69
2F	34,6	16,40	38,1	40,34	4,11	0,62	2,45	17,0	162	21,0	5,21	5,59	5,38	0,1893	5,04
3F	34,6	18,10	38,3	40,17	4,13	0,62	1,88	22,0	162	21,5	5,35	5,66	5,56	0,2443	5,17
4F	34,6	19,20	38,7	39,98	4,16	0,63	1,68	28,0	161	22,2	5,55	5,73	5,70	0,3098	5,32
5F	34,6	19,70	39,0	39,76	4,20	0,63	1,53	35,0	163	22,6	5,68	5,82	5,79	0,3857	5,49
6F	34,6	20,40	39,4	39,53	4,24	0,63	1,43	42,0	155	22,9	5,79	5,91	5,90	0,4609	5,64
7F	34,6	21,70	40,0	39,21	4,29	0,64	1,30	52,0	157	23,4	5,97	6,05	6,09	0,5672	5,85
8F	34,6	22,50	40,6	38,86	4,35	0,64	1,13	63,0	160	24,0	6,18	6,19	6,25	0,6827	6,06
9F	34,6	23,30	39,8	39,27	4,28	0,64	0,78	50,0	130	24,4	6,21	6,02	6,24	0,5461	5,81
1G	27,0	13,40	24,7	40,45	3,20	0,62	2,48	3,0	103	16,8	4,15	4,29	4,27	0,0449	3,74
2G	27,0	14,10	24,9	40,21	3,22	0,62	1,73	10,0	125	17,3	4,30	4,38	4,38	0,1490	3,93
3G	27,0	15,20	25,2	39,92	3,26	0,63	1,63	18,0	123	17,8	4,46	4,48	4,52	0,2666	4,14
4G	27,0	16,30	25,5	39,61	3,30	0,63	1,38	27,0	121	18,2	4,60	4,60	4,68	0,3973	4,36
5G	27,0	16,70	25,7	39,36	3,33	0,64	1,28	34,0	124	18,5	4,70	4,70	4,76	0,4978	4,52
6G	27,0	17,30	26,0	39,08	3,36	0,64	1,16	42,0	130	19,0	4,86	4,81	4,87	0,6114	4,68
7G	27,0	18,00	26,4	38,73	3,41	0,65	0,98	52,0	125	19,3	4,98	4,95	5,00	0,7515	4,87
8G	27,0	18,60	26,9	38,31	3,47	0,65	0,93	64,0	122	19,6	5,12	5,12	5,14	0,9169	5,07
9G	27,0	19,20	28,0	37,34	3,60	0,67	0,88	92,0	118	19,8	5,30	5,55	5,38	1,2917	5,53
1H	15,2	9,40	35,6	17,73	6,18	1,41	0,88	0,0	120	13,7	7,73	8,56	8,08	0,0000	7,17
2H	15,2	10,80	36,0	17,63	6,23	1,42	0,90	3,0	118	14,4	8,17	8,68	8,42	0,0478	7,39
3H	15,2	11,90	36,7	17,44	6,33	1,43	1,40	9,0	124	15,1	8,66	8,93	8,78	0,1424	7,86
4H	15,2	12,80	37,1	17,34	6,38	1,44	1,08	12,0	122	15,5	8,94	9,06	9,05	0,1892	8,09
5H	15,2	1,70	38,0	17,12	6,51	1,46	0,80	19,0	125	15,8	9,23	9,37	7,25	0,2971	8,61
6H	15,2	14,50	39,1	16,86	6,66	1,48	0,58	27,0	122	16,3	9,67	9,73	9,79	0,4180	9,19
7H	15,2	15,10	41,0	16,44	6,92	1,52	0,53	40,0	131	17,0	10,34	10,36	10,27	0,6094	10,05
8H	15,2	16,10	43,0	16,01	7,19	1,56	0,48	53,0	133	17,6	10,99	11,03	10,88	0,7942	10,86
9H	15,2	16,30	44,6	15,72	7,40	1,59	0,48	62,0	137	17,7	11,26	11,52	11,20	0,9183	11,40
10H	15,2	17,60	47,2	15,26	7,73	1,64	0,48	76,0	134	18,1	11,86	12,33	11,99	1,1051	12,26
1I	16,1	11,70	40,3	17,68	6,60	1,41	1,98	5,0	115	15,1	8,54	9,22	8,95	0,0746	7,92
2I	16,1	13,20	40,8	17,55	6,67	1,42	1,28	9,0	111	15,5	8,83	9,38	9,35	0,1336	8,22
3I	16,1	14,10	41,4	17,42	6,74	1,43	0,61	13,0	106	16,1	9,24	9,55	9,64	0,1921	8,53
4I	16,1	14,90	42,4	17,20	6,87	1,45	0,54	20,0	110	16,5	9,59	9,86	9,99	0,2932	9,05
5I	16,1	15,50	43,7	16,92	7,05	1,48	0,56	29,0	114	17,1	10,11	10,27	10,35	0,4206	9,70
6I	16,1	16,20	45,7	16,53	7,30	1,51	0,48	41,0	122	17,8	10,77	10,85	10,84	0,5861	10,50
7I	16,1	16,90	47,9	16,11	7,58	1,55	0,43	54,0	121	18,1	11,23	11,52	11,38	0,7597	11,31
8I	16,1	17,40	50,0	15,76	7,84	1,59	0,43	65,0	118	18,3	11,61	12,12	11,84	0,9019	11,98
9I	16,1	18,20	52,0	15,43	8,09	1,62	0,43	75,0	115	18,6	12,05	12,69	12,38	1,0274	12,60
10I	16,1	18,50	54,9	15,01	8,43	1,67	0,43	88,0	110	18,9	12,59	13,47	12,91	1,1853	13,41
1J	14,1	12,00	31,5	17,58	5,82	1,42	1,53	8,0	103	14,5	8,25	8,23	8,32	0,1378	7,23
2J	14,1	13,20	32,0	17,45	5,89	1,43	0,63	12,0	97	14,9	8,54	8,39	8,69	0,2057	7,54
3J	14,1	14,00	32,9	17,19	6,02	1,45	0,53	20,0	99	15,2	8,84	8,74	9,05	0,3394	8,12
4J	14,1	14,40	34,6	16,72	6,27	1,49	0,43	34,0	104	15,5	9,27	9,39	9,47	0,5667	9,07
5J	14,1	15,10	36,0	16,36	6,48	1,53	0,43	45,0	105	15,9	9,72	9,94	9,93	0,7394	9,75
6J	14,1	15,60	37,6	15,99	6,71	1,56	0,43	56,0	101	16,5	10,32	10,51	10,35	0,9069	10,40

	Q	h_a	H_1	h_1	F_1	N	x_2	x_1	L_j	h_2	Y	Y^*	Y_N^*	X_1	Y_p
	[1/s]	[cm]	[cm]	[mm]	[-]	[-]	[m]	[cm]	[cm]	[cm]	[-]	[-]	[-]	[-]	[-]
7J	14,1	16,10	38,6	15,76	6,86	1,59	0,43	63,0	93	16,8	10,66	10,90	10,68	1,0107	10,82
8J	14,1	16,50	40,2	15,42	7,08	1,62	0,43	73,0	94	17,0	11,02	11,47	11,09	1,1553	11,42
9J	14,1	16,80	42,3	15,02	7,37	1,66	0,43	85,0	90	17,3	11,52	12,20	11,56	1,3231	12,17
1K	11,0	10,00	19,8	17,61	4,52	1,42	1,98	4,0	72	11,8	6,70	6,44	6,74	0,0913	5,61
2K	11,0	10,40	20,0	17,51	4,56	1,43	1,58	7,0	72	12,0	6,85	6,56	6,89	0,1592	5,84
3K	11,0	11,40	20,3	17,37	4,62	1,44	0,98	11,0	71	12,4	7,14	6,73	7,21	0,2487	6,14
4K	11,0	11,80	20,6	17,20	4,69	1,45	0,58	16,0	66	12,8	7,44	6,96	7,41	0,3592	6,52
5K	11,0	12,20	21,0	17,02	4,76	1,47	0,63	21,0	66	13,1	7,70	7,17	7,61	0,4680	6,82
6K	11,0	12,60	21,8	16,67	4,91	1,50	0,48	31,0	69	13,4	8,04	7,60	7,92	0,6808	7,35
7K	11,0	13,00	22,9	16,21	5,12	1,54	0,43	44,0	69	13,7	8,45	8,19	8,32	0,9478	7,94
8K	11,0	13,40	24,0	15,78	5,33	1,58	0,43	56,0	71	13,8	8,74	8,89	8,72	1,1845	8,73
9K	11,0	13,80	25,7	15,21	5,64	1,64	0,43	72,0	70	14,0	9,20	10,01	9,25	1,4855	9,99

	Q	h_a	H_1	h_1	F_1	N	x_2	x_1	L_j	h_2	Y	Y^*	Y_N^*	X_1	Y_p
	[1/s]	[cm]	[cm]	[mm]	[-]	[-]	[m]	[cm]	[cm]	[cm]	[-]	[-]	[-]	[-]	[-]
1A	23,2	12,10	46,0	23,89	6,04	1,05	0,90	5,0	125	17,1	7,16	8,32	7,74	0,0608	7,13
2A	23,2	14,10	46,6	23,74	6,10	1,05	0,76	10,0	115	17,6	7,41	8,46	8,09	0,1210	7,39
3A	23,2	15,60	47,2	23,59	6,16	1,06	0,70	15,0	110	18,2	7,72	8,60	8,39	0,1808	7,66
4A	23,2	16,50	47,8	23,40	6,24	1,07	0,65	21,0	106	18,6	7,95	8,76	8,62	0,2518	7,97
5A	23,2	17,10	48,3	23,28	6,29	1,07	0,60	25,0	105	19,0	8,16	8,88	8,78	0,2987	8,17
6A	23,2	17,60	49,3	23,03	6,39	1,09	0,59	33,0	113	19,6	8,51	9,11	8,99	0,3916	8,56
7A	23,2	18,60	50,2	22,81	6,48	1,10	0,57	40,0	116	20,0	8,77	9,32	9,27	0,4717	8,88
8A	23,2	19,40	51,3	22,53	6,60	1,11	0,54	49,0	125	20,7	9,19	9,59	9,56	0,5733	9,27
9A	23,2	19,90	52,7	22,22	6,74	1,13	0,08	59,0	124	21,2	9,54	9,91	9,82	0,6842	9,68
10A	23,2	20,70	56,7	21,38	7,14	1,17	0,38	86,0	126	21,9	10,24	10,82	10,48	0,9732	10,72
1B	20,1	12,70	35,3	23,85	5,26	1,05	0,99	3,0	118	15,9	6,67	7,23	7,08	0,0427	6,18
2B	20,1	13,90	35,9	23,66	5,32	1,06	0,82	9,0	114	16,2	6,85	7,39	7,35	0,1273	6,49
3B	20,1	15,20	36,6	23,41	5,41	1,07	0,66	17,0	108	16,8	7,18	7,61	7,67	0,2387	6,91
4B	20,1	15,80	37,0	23,24	5,46	1,08	0,64	22,0	109	17,2	7,40	7,75	7,84	0,3074	7,16
5B	20,1	16,10	37,7	23,02	5,54	1,09	-0,15	29,0	112	17,6	7,65	7,95	7,99	0,4026	7,50
6B	20,1	17,10	38,2	22,86	5,60	1,09	0,56	34,0	114	18,0	7,87	8,10	8,24	0,4698	7,72
8B	20,1	17,60	39,3	22,50	5,74	1,11	0,60	45,0	120	18,7	8,31	8,43	8,50	0,6153	8,19
8B	20,1	18,20	40,0	22,28	5,82	1,12	0,58	52,0	197	19,1	8,57	8,65	8,72	0,7063	8,47
9B	20,1	18,40	41,2	21,92	5,97	1,14	0,43	63,0	116	19,4	8,85	9,01	8,94	0,8467	8,89
10B	20,1	18,90	42,8	21,47	6,16	1,16	0,43	77,0	114	19,5	9,08	9,47	9,28	1,0208	9,39
1C	17,1	11,00	26,6	23,63	4,53	1,06	1,98	3,0	93	14,1	5,97	6,26	6,17	0,0509	5,39
2C	17,1	11,60	26,9	23,49	4,57	1,06	1,48	7,0	97	14,4	6,13	6,37	6,32	0,1184	5,60
3C	17,1	12,20	27,0	23,42	4,59	1,07	1,33	9,0	94	14,7	6,28	6,43	6,44	0,1519	5,71
4C	17,1	13,00	27,2	23,32	4,62	1,07	0,88	12,0	92	15,0	6,43	6,51	6,62	0,2019	5,86
5C	17,1	13,80	27,4	23,22	4,65	1,08	0,75	15,0	90	15,4	6,63	6,59	6,80	0,2516	6,02
6C	17,1	14,30	27,8	23,06	4,70	1,08	0,65	20,0	90	15,6	6,77	6,74	6,95	0,3338	6,27
7C	17,1	14,80	28,2	22,85	4,76	1,09	0,55	26,0	91	15,8	6,91	6,91	7,12	0,4312	6,56
8C	17,1	15,10	28,7	22,65	4,83	1,10	0,56	32,0	97	16,1	7,11	7,09	7,26	0,5274	6,82
9C	17,1	15,70	29,4	22,32	4,94	1,12	0,62	42,0	103	16,6	7,44	7,40	7,51	0,6851	7,24
10C	17,1	16,10	30,2	22,01	5,04	1,14	0,64	51,0	96	16,9	7,68	7,69	7,72	0,8240	7,59
11C	17,1	16,60	31,8	21,37	5,27	1,17	0,68	70,0	93	17,2	8,05	8,34	8,12	1,1083	8,30
1D	14,4	10,60	19,7	23,55	3,83	1,06	2,03	6,0	81	12,6	5,35	5,39	5,50	0,1241	4,77
2D	14,4	11,10	19,8	23,48	3,85	1,06	1,70	8,0	81	12,8	5,45	5,45	5,61	0,1651	4,88
3D	14,4	11,40	19,9	23,41	3,87	1,07	1,13	10,0	80	13,1	5,60	5,50	5,69	0,2059	4,98
4D	14,4	12,00	20,1	23,23	3,91	1,08	0,96	15,0	82	13,5	5,81	5,65	5,85	0,3071	5,24
5D	14,4	12,50	20,5	22,98	3,98	1,09	0,83	22,0	81	13,8	6,00	5,85	6,03	0,4468	5,57
6D	14,4	13,00	20,7	22,84	4,01	1,09	0,73	26,0	82	14,0	6,13	5,97	6,17	0,5256	5,75
7D	14,4	13,50	21,1	22,59	4,08	1,11	0,68	33,0	82	14,4	6,37	6,19	6,36	0,6616	6,05
8D	14,4	14,00	21,9	22,09	4,22	1,13	0,73	47,0	77	14,7	6,65	6,65	6,64	0,9270	6,59
9D	14,4	14,50	23,1	21,42	4,42	1,17	0,73	66,0	79	14,9	6,96	7,33	7,01	1,2726	7,31
10D	14,4	15,10	24,9	20,50	4,72	1,22	0,73	92,0	80	15,3	7,46	8,36	7,54	1,7192	8,35
1E	39,5	15,80	47,3	40,82	4,60	0,61	3,68	7,0	157	22,5	5,51	6,20	5,79	0,0676	5,37
2E	39,5	17,60	47,9	40,51	4,65	0,62	2,28	17,0	162	23,4	5,78	6,33	5,99	0,1634	5,64
3E	39,5	18,90	48,4	40,29	4,69	0,62	1,98	24,0	164	23,8	5,91	6,42	6,14	0,2297	5,83
4E	39,5	19,90	48,6	40,17	4,71	0,62	1,78	28,0	163	24,2	6,02	6,47	6,26	0,2675	5,93
5E	39,5	21,50	49,0	39,98	4,75	0,63	1,58	34,0	165	24,8	6,20	6,54	6,44	0,3237	6,08
6E	39,5	22,30	49,4	39,79	4,78	0,63	1,33	40,0	165	25,1	6,31	6,62	6,55	0,3796	6,22
7E	39,5	23,00	49,9	39,61	4,81	0,63	1,03	46,0	161	25,4	6,41	6,70	6,66	0,4351	6,36

	Q	h _a	H ₁	h ₁	F ₁	N	x ₂	x ₁	L _j	h ₂	Y	Y*	Y _N *	X ₁	Y _p
	[1/s]	[cm]	[cm]	[mm]	[-]	[-]	[m]	[cm]	[cm]	[cm]	[-]	[-]	[-]	[-]	[-]
8E	39,5	24,20	50,7	39,24	4,88	0,64	0,98	58,0	170	26,2	6,68	6,86	6,85	0,5450	6,61
9E	39,5	24,80	51,3	38,99	4,93	0,64	0,88	66,0	169	26,6	6,82	6,97	6,97	0,6174	6,77
10E	39,5	25,50	52,4	38,53	5,02	0,65	0,78	81,0	171	27,0	7,01	7,17	7,15	0,7515	7,05
1F	34,6	14,40	37,4	40,76	4,05	0,61	2,98	4,0	61	20,1	4,93	5,43	5,14	0,0449	4,69
2F	34,6	16,40	38,1	40,34	4,11	0,62	2,45	17,0	162	21,0	5,21	5,59	5,38	0,1893	5,04
3F	34,6	18,10	38,3	40,17	4,13	0,62	1,88	22,0	162	21,5	5,35	5,66	5,56	0,2443	5,17
4F	34,6	19,20	38,7	39,98	4,16	0,63	1,68	28,0	161	22,2	5,55	5,73	5,70	0,3098	5,32
5F	34,6	19,70	39,0	39,76	4,20	0,63	1,53	35,0	163	22,6	5,68	5,82	5,79	0,3857	5,49
6F	34,6	20,40	39,4	39,53	4,24	0,63	1,43	42,0	155	22,9	5,79	5,91	5,90	0,4609	5,64
7F	34,6	21,70	40,0	39,21	4,29	0,64	1,30	52,0	157	23,4	5,97	6,05	6,09	0,5672	5,85
8F	34,6	22,50	40,6	38,86	4,35	0,64	1,13	63,0	160	24,0	6,18	6,19	6,25	0,6827	6,06
9F	34,6	23,30	39,8	39,27	4,28	0,64	0,78	50,0	130	24,4	6,21	6,02	6,24	0,5461	5,81
1G	27,0	13,40	24,7	40,45	3,20	0,62	2,48	3,0	103	16,8	4,15	4,29	4,27	0,0449	3,74
2G	27,0	14,10	24,9	40,21	3,22	0,62	1,73	10,0	125	17,3	4,30	4,38	4,38	0,1490	3,93
3G	27,0	15,20	25,2	39,92	3,26	0,63	1,63	18,0	123	17,8	4,46	4,48	4,52	0,2666	4,14
4G	27,0	16,30	25,5	39,61	3,30	0,63	1,38	27,0	121	18,2	4,60	4,60	4,68	0,3973	4,36
5G	27,0	16,70	25,7	39,36	3,33	0,64	1,28	34,0	124	18,5	4,70	4,70	4,76	0,4978	4,52
6G	27,0	17,30	26,0	39,08	3,36	0,64	1,16	42,0	130	19,0	4,86	4,81	4,87	0,6114	4,68
7G	27,0	18,00	26,4	38,73	3,41	0,65	0,98	52,0	125	19,3	4,98	4,95	5,00	0,7515	4,87
8G	27,0	18,60	26,9	38,31	3,47	0,65	0,93	64,0	122	19,6	5,12	5,12	5,14	0,9169	5,07
9G	27,0	19,20	28,0	37,34	3,60	0,67	0,88	92,0	118	19,8	5,30	5,55	5,38	1,2917	5,53
1H	15,2	9,40	35,6	17,73	6,18	1,41	0,88	0,0	120	13,7	7,73	8,56	8,08	0,0000	7,17
2H	15,2	10,80	36,0	17,63	6,23	1,42	0,90	3,0	118	14,4	8,17	8,68	8,42	0,0478	7,39
3H	15,2	11,90	36,7	17,44	6,33	1,43	1,40	9,0	124	15,1	8,66	8,93	8,78	0,1424	7,86
4H	15,2	12,80	37,1	17,34	6,38	1,44	1,08	12,0	122	15,5	8,94	9,06	9,05	0,1892	8,09
5H	15,2	1,70	38,0	17,12	6,51	1,46	0,80	19,0	125	15,8	9,23	9,37	7,25	0,2971	8,61
6H	15,2	14,50	39,1	16,86	6,66	1,48	0,58	27,0	122	16,3	9,67	9,73	9,79	0,4180	9,19
7H	15,2	15,10	41,0	16,44	6,92	1,52	0,53	40,0	131	17,0	10,34	10,36	10,27	0,6094	10,05
8H	15,2	16,10	43,0	16,01	7,19	1,56	0,48	53,0	133	17,6	10,99	11,03	10,88	0,7942	10,86
9H	15,2	16,30	44,6	15,72	7,40	1,59	0,48	62,0	137	17,7	11,26	11,52	11,20	0,9183	11,40
10H	15,2	17,60	47,2	15,26	7,73	1,64	0,48	76,0	134	18,1	11,86	12,33	11,99	1,1051	12,26
1I	16,1	11,70	40,3	17,68	6,60	1,41	1,98	5,0	115	15,1	8,54	9,22	8,95	0,0746	7,92
2I	16,1	13,20	40,8	17,55	6,67	1,42	1,28	9,0	111	15,5	8,83	9,38	9,35	0,1336	8,22
3I	16,1	14,10	41,4	17,42	6,74	1,43	0,61	13,0	106	16,1	9,24	9,55	9,64	0,1921	8,53
4I	16,1	14,90	42,4	17,20	6,87	1,45	0,54	20,0	110	16,5	9,59	9,86	9,99	0,2932	9,05
5I	16,1	15,50	43,7	16,92	7,05	1,48	0,56	29,0	114	17,1	10,11	10,27	10,35	0,4206	9,70
6I	16,1	16,20	45,7	16,53	7,30	1,51	0,48	41,0	122	17,8	10,77	10,85	10,84	0,5861	10,50
7I	16,1	16,90	47,9	16,11	7,58	1,55	0,43	54,0	121	18,1	11,23	11,52	11,38	0,7597	11,31
8I	16,1	17,40	50,0	15,76	7,84	1,59	0,43	65,0	118	18,3	11,61	12,12	11,84	0,9019	11,98
9I	16,1	18,20	52,0	15,43	8,09	1,62	0,43	75,0	115	18,6	12,05	12,69	12,38	1,0274	12,60
10I	16,1	18,50	54,9	15,01	8,43	1,67	0,43	88,0	110	18,9	12,59	13,47	12,91	1,1853	13,41
1J	14,1	12,00	31,5	17,58	5,82	1,42	1,53	8,0	103	14,5	8,25	8,23	8,32	0,1378	7,23
2J	14,1	13,20	32,0	17,45	5,89	1,43	0,63	12,0	97	14,9	8,54	8,39	8,69	0,2057	7,54
3J	14,1	14,00	32,9	17,19	6,02	1,45	0,53	20,0	99	15,2	8,84	8,74	9,05	0,3394	8,12
4J	14,1	14,40	34,6	16,72	6,27	1,49	0,43	34,0	104	15,5	9,27	9,39	9,47	0,5667	9,07
5J	14,1	15,10	36,0	16,36	6,48	1,53	0,43	45,0	105	15,9	9,72	9,94	9,93	0,7394	9,75
6J	14,1	15,60	37,6	15,99	6,71	1,56	0,43	56,0	101	16,5	10,32	10,51	10,35	0,9069	10,40

	Q	h_a	H_1	h_1	F_1	N	x_2	x_1	L_j	h_2	Y	Y^*	Y_N^*	X_1	Y_p
	[l/s]	[cm]	[cm]	[mm]	[-]	[-]	[m]	[cm]	[cm]	[cm]	[-]	[-]	[-]	[-]	[-]
7J	14,1	16,10	38,6	15,76	6,86	1,59	0,43	63,0	93	16,8	10,66	10,90	10,68	1,0107	10,82
8J	14,1	16,50	40,2	15,42	7,08	1,62	0,43	73,0	94	17,0	11,02	11,47	11,09	1,1553	11,42
9J	14,1	16,80	42,3	15,02	7,37	1,66	0,43	85,0	90	17,3	11,52	12,20	11,56	1,3231	12,17
1K	11,0	10,00	19,8	17,61	4,52	1,42	1,98	4,0	72	11,8	6,70	6,44	6,74	0,0913	5,61
2K	11,0	10,40	20,0	17,51	4,56	1,43	1,58	7,0	72	12,0	6,85	6,56	6,89	0,1592	5,84
3K	11,0	11,40	20,3	17,37	4,62	1,44	0,98	11,0	71	12,4	7,14	6,73	7,21	0,2487	6,14
4K	11,0	11,80	20,6	17,20	4,69	1,45	0,58	16,0	66	12,8	7,44	6,96	7,41	0,3592	6,52
5K	11,0	12,20	21,0	17,02	4,76	1,47	0,63	21,0	66	13,1	7,70	7,17	7,61	0,4680	6,82
6K	11,0	12,60	21,8	16,67	4,91	1,50	0,48	31,0	69	13,4	8,04	7,60	7,92	0,6808	7,35
7K	11,0	13,00	22,9	16,21	5,12	1,54	0,43	44,0	69	13,7	8,45	8,19	8,32	0,9478	7,94
8K	11,0	13,40	24,0	15,78	5,33	1,58	0,43	56,0	71	13,8	8,74	8,89	8,72	1,1845	8,73
9K	11,0	13,80	25,7	15,21	5,64	1,64	0,43	72,0	70	14,0	9,20	10,01	9,25	1,4855	9,99

SERIES : 2.3

A2-9

	Q	h _{a,l}	h _{a,r}	H ₁	h ₁	F ₁	N	x _e	x ₂	x ₁	L _j	h ₂	Y	Y _N *	X ₁	Y _p
	[l/s]	[cm]	[cm]	[cm]	[mm]	[-]	[-]	[m]	[m]	[cm]	[cm]	[cm]	[-]	[-]	[-]	[-]
1 A	24,0	6,50	11,00	47,8	50,60	4,11	0,49	0,63	4,08	0,0	318	17,1	3,38	5,46	0,0000	3,57
2 A	24,0	7,90	12,10	48,3	50,28	4,15	0,50	0,48	3,73	5,0	213	18,1	3,60	5,54	0,0442	3,78
3 A	24,0	9,60	13,40	48,7	50,02	4,18	0,50	0,45	3,08	9,0	192	18,5	3,70	5,60	0,0792	3,94
4 A	24,0	11,50	15,20	49,3	49,69	4,22	0,50	0,48	2,73	14,0	187	19,8	3,98	5,67	0,1226	4,15
5 A	24,0	13,70	16,70	50,0	49,30	4,27	0,51	0,33	1,78	20,0	183	21,0	4,26	5,76	0,1741	4,39
6 A	24,0	15,10	18,50	50,5	48,97	4,32	0,51	0,28	1,88	25,0	178	22,3	4,55	5,84	0,2166	4,59
7 A	24,0	18,30	20,60	51,5	48,45	4,39	0,52	0,78	0,98	33,0	156	23,6	4,87	5,97	0,2837	4,90
8 A	24,0	20,05	22,70	52,3	48,00	4,45	0,52	0,53	1,08	40,0	153	24,6	5,13	6,08	0,3416	5,16
9 A	24,0	21,00	22,10	53,3	47,48	4,52	0,53	0,48	0,75	48,0	146	25,7	5,41	6,22	0,4067	5,44
10A	24,0	23,90	24,40	54,7	46,77	4,63	0,53	0,43	0,53	59,0	157	27,0	5,77	6,41	0,4945	5,80
1 B	20,0	11,30	9,10	35,0	50,32	3,45	0,50	3,50	0,58	5,0	143	15,8	3,14	4,59	0,0548	3,23
2 B	20,0	14,70	12,60	35,5	49,91	3,49	0,50	2,28	0,43	11,0	129	18,2	3,64	4,67	0,1199	3,47
3 B	20,0	17,60	15,40	36,1	49,35	3,55	0,51	1,68	0,38	19,0	127	19,8	4,01	4,79	0,2052	3,78
4 B	20,0	18,50	16,70	36,6	48,94	3,60	0,51	1,18	0,38	25,0	108	20,7	4,23	4,88	0,2682	4,01
5 B	20,0	17,80	19,70	37,2	48,46	3,65	0,52	0,83	0,41	32,0	120	21,2	4,36	4,98	0,3407	4,26
6 B	20,0	19,80	20,10	37,6	48,11	3,69	0,52	0,78	0,48	37,0	125	21,6	4,49	5,06	0,3917	4,43
7 B	20,0	20,70	19,50	38,0	47,77	3,73	0,52	0,91	0,38	42,0	120	22,2	4,65	5,14	0,4422	4,59
8 B	20,0	20,60	21,70	38,6	47,35	3,78	0,53	1,13	0,40	48,0	116	22,5	4,75	5,24	0,5020	4,77
9 B	20,0	21,60	22,70	39,9	46,39	3,90	0,54	0,82	0,38	62,0	130	23,3	5,02	5,47	0,6384	5,16
1 C	16,1	8,60	11,50	24,3	50,62	2,76	0,49	3,70	0,63	3,0	106	14,5	2,86	3,66	0,0431	2,62
2 C	16,1	12,20	13,70	24,7	50,02	2,81	0,50	2,68	0,58	11,0	109	15,5	3,10	3,77	0,1563	2,93
3 C	16,1	13,50	14,90	25,0	49,56	2,85	0,50	2,78	0,50	17,0	95	16,3	3,29	3,85	0,2397	3,16
4 C	16,1	14,60	15,80	25,2	49,33	2,87	0,51	1,73	0,48	20,0	93	17,2	3,49	3,89	0,2808	3,27
5 C	16,1	16,00	16,70	25,7	48,66	2,93	0,51	1,28	0,48	29,0	107	18,3	3,76	4,02	0,4024	3,57
6 C	16,1	17,20	18,20	26,4	47,75	3,01	0,52	1,43	0,41	41,0	99	19,2	4,02	4,21	0,5598	3,92
7 C	16,1	17,90	18,50	26,6	47,46	3,04	0,53	0,96	0,40	45,0	100	19,5	4,11	4,27	0,6112	4,02
8 C	16,1	18,50	19,20	27,0	47,01	3,08	0,53	0,98	0,45	51,0	104	19,7	4,19	4,36	0,6871	4,17
9 C	16,1	19,30	19,80	27,7	46,26	3,16	0,54	1,08	0,47	61,0	111	20,2	4,37	4,53	0,8110	4,40
1 D	12,0	10,60	9,70	15,6	51,02	2,03	0,49	3,26	0,66	0,0	88	12,1	2,37	2,72	0,0000	1,99
2 D	12,0	10,90	10,20	15,6	50,93	2,03	0,49	2,58	0,64	1,0	86	12,8	2,51	2,73	0,0214	2,03
3 D	12,0	11,30	11,20	15,7	50,65	2,05	0,49	1,53	0,62	4,0	77	13,2	2,61	2,77	0,0850	2,14
4 D	12,0	12,00	12,20	15,8	50,38	2,06	0,50	1,48	0,53	7,0	75	13,7	2,72	2,81	0,1480	2,26
5 D	12,0	12,70	12,80	16,0	49,67	2,11	0,50	1,18	0,43	15,0	63	14,0	2,82	2,93	0,3123	2,54
6 D	12,0	13,30	13,40	16,3	48,95	2,15	0,51	0,88	0,43	23,0	71	14,4	2,94	3,04	0,4716	2,79
7 D	12,0	13,70	13,70	16,5	48,42	2,19	0,52	0,88	0,43	29,0	72	14,7	3,04	3,13	0,5879	2,96
8 D	12,0	14,30	14,30	16,8	47,63	2,24	0,52	0,88	0,43	38,0	71	15,1	3,17	3,27	0,7575	3,17
9 D	12,0	14,80	14,70	17,4	46,15	2,35	0,54	0,88	0,43	55,0	80	15,3	3,32	3,56	1,0626	3,52
1 E	17,0	6,90	10,80	44,8	36,48	4,75	0,69	3,58	0,53	2,0	175	15,5	4,25	6,41	0,0209	4,21
2 E	17,0	8,50	12,70	45,5	36,17	4,81	0,69	3,28	0,48	7,0	165	16,1	4,45	6,52	0,0726	4,51
3 E	17,0	9,90	13,10	45,9	35,98	4,85	0,69	2,08	0,43	10,0	158	16,8	4,67	6,59	0,1033	4,68
4 E	17,0	12,10	15,00	46,5	35,73	4,90	0,70	1,88	0,48	14,0	137	18,1	5,07	6,69	0,1439	4,92
5 E	17,0	13,60	16,10	47,3	35,35	4,98	0,71	1,88	0,53	20,0	133	18,8	5,32	6,84	0,2040	5,28
6 E	17,0	14,40	17,00	48,0	35,10	5,03	0,71	1,78	0,48	24,0	132	19,5	5,56	6,94	0,2436	5,51
7 E	17,0	16,60	18,10	49,4	34,53	5,16	0,72	1,38	0,48	33,0	131	20,1	5,82	7,17	0,3312	6,01
8 E	17,0	17,60	19,10	49,9	34,34	5,20	0,73	1,18	0,48	36,0	126	20,6	6,00	7,25	0,3600	6,17
9 E	17,0	19,70	20,50	51,7	33,64	5,36	0,74	1,08	0,53	47,0	131	21,9	6,51	7,55	0,4634	6,73
10E	17,0	22,00	22,30	54,3	32,75	5,58	0,76	0,78	0,48	61,0	134	23,3	7,11	7,95	0,5907	7,38
11E	17,0	22,50	22,50	57,7	31,68	5,87	0,79	0,68	0,48	78,0	136	24,0	7,58	8,47	0,7387	8,11

Q	$h_{a,l}$	$h_{a,r}$	H_l	h_l	F_l	N	x_e	x_2	x_1	L_j	h_2	Y	Y_N^*	X_l	Y_p	
[l/s]	[cm]	[cm]	[cm]	[mm]	[-]	[-]	[m]	[m]	[cm]	[cm]	[cm]	[-]	[-]	[-]	[-]	
1 F	15,1	10,50	7,20	36,3	36,33	4,24	0,69	4,48	0,53	3,0	111	14,0	3,85	5,72	0,0358	3,86
2 F	15,1	11,10	8,00	36,6	36,14	4,28	0,69	3,28	0,58	6,0	114	14,7	4,07	5,79	0,0712	4,04
3 F	15,1	12,40	9,60	36,9	36,01	4,30	0,69	2,88	0,53	8,0	111	15,2	4,22	5,83	0,0947	4,15
4 F	15,1	13,80	11,20	37,7	35,55	4,38	0,70	2,48	0,51	15,0	118	16,0	4,50	6,00	0,1760	4,56
5 F	15,1	14,40	12,10	37,9	35,42	4,41	0,71	2,28	0,50	17,0	115	16,6	4,69	6,04	0,1989	4,68
6 F	15,1	15,20	13,00	38,3	35,22	4,44	0,71	2,18	0,48	20,0	113	17,4	4,94	6,12	0,2331	4,85
7 F	15,1	15,70	14,60	38,8	34,96	4,49	0,72	1,88	0,43	24,0	112	18,3	5,23	6,21	0,2782	5,07
8 F	15,1	17,20	15,50	39,5	34,57	4,57	0,72	1,38	0,48	30,0	113	18,7	5,41	6,36	0,3450	5,40
9 F	15,1	18,10	17,00	40,3	34,18	4,65	0,73	1,13	0,38	36,0	109	19,5	5,71	6,51	0,4107	5,70
10F	15,1	18,80	18,10	41,7	33,53	4,78	0,75	0,68	0,48	46,0	114	20,3	6,06	6,78	0,5176	6,18
11F	15,1	20,90	20,90	44,1	32,48	5,02	0,77	0,48	0,48	62,0	120	21,9	6,74	7,23	0,6824	6,86
1 G	13,2	7,90	10,80	28,3	36,70	3,66	0,68	3,33	0,53	3,0	111	13,2	3,60	4,94	0,0420	3,41
2 G	13,2	9,60	11,70	28,5	36,50	3,69	0,68	3,18	0,53	6,0	114	14,1	3,86	5,01	0,0837	3,58
3 G	13,2	10,90	12,80	29,1	36,09	3,76	0,69	2,78	0,48	12,0	110	14,8	4,10	5,14	0,1659	3,92
4 G	13,2	11,70	13,60	29,6	35,68	3,82	0,70	2,58	0,50	18,0	111	15,5	4,34	5,27	0,2467	4,25
5 G	13,2	13,20	14,40	29,9	35,48	3,85	0,70	2,38	0,46	21,0	109	16,2	4,57	5,34	0,2866	4,41
6 G	13,2	14,10	15,30	30,4	35,14	3,91	0,71	1,98	0,48	26,0	114	16,7	4,75	5,46	0,3522	4,67
7 G	13,2	15,40	16,10	30,9	34,80	3,97	0,72	1,48	0,43	31,0	117	17,5	5,03	5,58	0,4169	4,92
8 G	13,2	16,90	17,60	32,1	33,98	4,11	0,74	1,18	0,38	43,0	116	18,5	5,44	5,88	0,5681	5,45
9 G	13,2	18,50	18,70	33,4	33,23	4,25	0,75	0,53	0,53	54,0	102	19,5	5,87	6,17	0,7017	5,88
10G	13,2	19,80	19,80	36,7	31,46	4,62	0,79	0,53	0,53	80,0	108	20,4	6,49	6,91	0,9993	6,80
1 H	10,1	9,20	10,00	18,2	36,47	2,82	0,69	3,43	0,48	3,0	101	11,8	3,24	3,85	0,0581	2,78
2 H	10,1	9,80	10,70	18,3	36,24	2,85	0,69	2,69	0,53	6,0	94	12,2	3,37	3,91	0,1155	2,95
3 H	10,1	10,90	11,50	18,5	36,02	2,88	0,69	2,63	0,51	9,0	89	12,9	3,58	3,97	0,1723	3,11
4 H	10,1	11,60	12,30	18,8	35,57	2,93	0,70	2,08	0,48	15,0	90	13,4	3,77	4,11	0,2840	3,44
5 H	10,1	12,40	12,90	19,2	35,12	2,99	0,71	1,58	0,47	21,0	89	14,1	4,01	4,24	0,3933	3,74
6 H	10,1	13,20	12,80	19,4	34,90	3,02	0,72	1,28	0,48	24,0	87	14,3	4,10	4,31	0,4471	3,88
7 H	10,1	13,70	13,70	19,8	34,37	3,09	0,73	1,28	0,42	31,0	84	14,8	4,31	4,48	0,5701	4,17
8 H	10,1	14,60	14,60	20,3	33,85	3,16	0,74	1,08	0,48	38,0	86	15,6	4,61	4,65	0,6900	4,44
9 H	10,1	15,30	15,30	21,2	32,81	3,31	0,76	0,78	0,53	52,0	83	16,1	4,91	5,02	0,9201	4,92
10H	10,1	16,20	16,20	23,1	31,10	3,59	0,80	0,53	0,53	75,0	98	16,6	5,34	5,69	1,2716	5,66
1 I	8,2	9,80	8,70	12,6	37,77	2,16	0,66	2,08	0,58	1,0	79	10,7	2,83	3,01	0,0264	2,20
2 I	8,2	9,80	9,50	12,7	37,51	2,19	0,67	1,88	0,53	4,0	70	11,1	2,96	3,07	0,1049	2,37
3 I	8,2	10,40	10,40	12,9	37,01	2,23	0,68	0,78	0,58	10,0	68	11,7	3,16	3,19	0,2587	2,68
4 I	8,2	11,00	10,90	13,1	36,58	2,27	0,68	0,08	0,48	15,0	68	12,1	3,31	3,30	0,3835	2,93
5 I	8,2	11,40	11,30	13,3	36,07	2,32	0,69	0,08	0,08	21,0	69	12,4	3,44	3,43	0,5295	3,19
6 I	8,2	11,70	11,70	13,5	35,74	2,35	0,70	0,08	0,08	25,0	68	12,6	3,53	3,52	0,6245	3,34
7 I	8,2	12,20	12,20	13,6	35,31	2,39	0,71	0,08	0,08	30,0	68	12,9	3,65	3,64	0,7408	3,51
8 I	8,2	12,60	12,60	14,2	34,22	2,51	0,73	0,08	0,08	43,0	66	13,9	4,06	3,97	1,0304	3,92
9 I	8,2	13,20	13,20	15,4	32,23	2,75	0,78	0,08	0,08	67,0	70	13,5	4,19	4,67	1,5195	4,66
1 J	7,2	6,20	8,30	29,2	18,95	5,39	1,32	3,28	0,63	4,0	97	10,6	5,59	7,52	0,0696	5,11
2 J	7,2	7,30	8,90	29,8	18,81	5,45	1,33	3,13	0,63	7,0	95	11,0	5,85	7,67	0,1212	5,49
3 J	7,2	7,90	9,50	30,2	18,69	5,50	1,34	2,83	0,56	9,0	91	11,4	6,10	7,78	0,1552	5,73
4 J	7,2	8,70	10,30	30,5	18,57	5,55	1,35	2,78	0,54	11,0	89	12,1	6,51	7,89	0,1889	5,98
5 J	7,2	9,50	10,60	31,2	18,34	5,66	1,36	2,78	0,48	15,0	83	12,7	6,93	8,11	0,2554	6,46
6 J	7,2	10,60	11,50	31,6	18,22	5,72	1,37	2,58	0,45	17,0	85	13,1	7,19	8,23	0,2882	6,69
7 J	7,2	11,60	12,10	32,2	18,03	5,80	1,39	2,08	0,38	20,0	83	13,7	7,60	8,41	0,3368	7,04

Q	$h_{a,l}$	$h_{a,r}$	H_1	h_1	F_1	N	x_e	x_2	x_1	L_j	h_2	Y	Y_N^*	X_1	Y_p	
[1/s]	[cm]	[cm]	[cm]	[mm]	[-]	[-]	[m]	[m]	[cm]	[cm]	[cm]	[-]	[-]	[-]	[-]	
8 J	7,2	12,80	12,80	33,0	17,79	5,92	1,41	1,68	0,43	24,0	82	14,3	8,04	8,65	0,4006	7,49
9 J	7,2	13,70	13,70	34,3	17,42	6,11	1,43	0,43	0,43	30,0	83	15,1	8,67	9,04	0,4939	8,14
10J	7,2	14,40	14,40	36,4	16,86	6,42	1,48	0,43	0,43	39,0	82	15,6	9,25	9,67	0,6285	9,05
11J	7,2	15,40	15,40	39,4	16,16	6,84	1,55	0,43	0,43	50,0	88	16,3	10,09	10,51	0,7841	10,12
12J	7,2	16,50	16,50	43,3	15,38	7,37	1,63	0,43	0,43	62,0	85	17,0	11,05	11,55	0,9424	11,31
1 K	6,1	7,40	8,30	19,8	19,47	4,34	1,28	2,78	0,53	4,0	97	10,0	5,14	6,09	0,0866	4,26
2 K	6,1	8,40	9,30	20,4	19,43	4,36	1,29	2,28	0,50	7,0	95	10,6	5,46	6,21	0,1513	4,62
3 K	6,1	9,20	9,60	20,7	19,24	4,42	1,30	2,08	0,47	10,0	93	11,2	5,82	6,36	0,2147	4,97
4 K	6,1	10,00	10,50	20,9	19,12	4,46	1,31	1,38	0,47	12,0	90	11,7	6,12	6,46	0,2564	5,20
5 K	6,1	11,10	11,10	21,4	18,86	4,55	1,33	0,98	0,43	16,0	84	12,3	6,52	6,67	0,3387	5,63
6 K	6,1	11,60	11,60	22,3	18,42	4,72	1,36	0,43	0,38	23,0	86	12,6	6,84	7,06	0,4787	6,34
7 K	6,1	12,20	12,20	23,2	18,03	4,87	1,39	0,43	0,43	29,0	77	13,0	7,21	7,42	0,5946	6,90
8 K	6,1	12,90	12,90	24,4	17,51	5,09	1,43	0,43	0,43	37,0	70	13,5	7,71	7,93	0,7433	7,60
9 K	6,1	13,50	13,50	25,5	17,11	5,27	1,46	0,43	0,43	43,0	73	14,1	8,24	8,34	0,8503	8,10
10K	6,1	14,10	14,10	26,8	16,64	5,49	1,50	0,43	0,43	50,0	73	14,7	8,83	8,85	0,9702	8,68
11K	6,1	14,60	14,60	28,4	16,10	5,77	1,55	0,43	0,43	58,0	71	15	9,32	9,48	1,1007	9,37
1L	5,1	8,40	7,40	7,2	15,05	5,38	1,66	2,48	0,53	5,0	83	9,3	6,18	6,08	0,1099	3,20
2L	5,1	9,30	8,10	12,4	16,87	4,53	1,48	2,28	0,50	8,0	86	9,9	5,87	5,98	0,1904	4,06
3L	5,1	9,70	8,90	15,4	18,07	4,08	1,38	1,58	0,48	11,0	84	10,4	5,75	5,89	0,2753	4,68
4L	5,1	9,80	9,50	16,4	18,46	3,96	1,35	11,38	0,43	13,0	81	10,8	5,85	5,90	0,3307	5,00
5L	5,1	10,20	10,20	16,8	18,16	4,06	1,38	0,78	0,43	17,0	85	11,2	6,17	6,13	0,4270	5,42
6L	5,1	10,80	10,80	17,4	17,77	4,19	1,41	0,43	0,43	23,0	84	11,6	6,53	6,48	0,5685	6,00
7L	5,1	11,30	11,30	17,8	17,50	4,28	1,43	0,43	0,43	27,0	80	12,1	6,91	6,73	0,6601	6,36
8L	5,1	12,10	12,10	19,1	16,84	4,54	1,48	0,43	0,43	37,0	75	12,7	7,54	7,40	0,8795	7,21
9L	5,1	12,70	12,70	20,2	16,29	4,77	1,53	0,43	0,43	45,0	78	13,2	8,10	7,98	1,0449	7,87
10L	5,1	13,20	13,20	22,9	15,17	5,31	1,65	0,43	0,43	61,0	69	13,6	8,96	9,33	1,3483	9,29
1M	4,3	7,60	6,60	23,2	55,95	0,64	0,45	2,18	1,58	3,0	81	8,1	1,45	3,30	1,2555	5,16
2M	4,3	8,10	7,10	22,9	50,26	0,75	0,50	1,78	0,55	5,0	73	8,5	1,69	3,19	0,8812	5,02
3M	4,3	8,60	7,90	21,8	40,70	1,03	0,61	1,68	0,53	8,0	71	9,2	2,26	3,39	0,6813	5,03
4M	4,3	9,10	8,70	20,4	33,23	1,40	0,75	1,43	0,48	10,0	78	9,6	2,89	3,71	0,5800	5,04
5M	4,3	9,60	9,30	12,3	18,79	3,28	1,33	1,28	0,43	14,0	77	10,2	5,43	5,13	0,4369	4,61
6M	4,3	10,10	10,10	12,9	17,90	3,53	1,40	0,88	0,43	25,0	73	10,8	6,03	5,79	0,7502	5,56
7M	4,3	10,80	10,80	13,5	17,41	3,68	1,44	0,43	0,43	32,0	65	11,3	6,49	6,24	0,9398	6,12
8M	4,3	11,40	11,40	14,4	16,77	3,89	1,49	0,43	0,43	41,0	54	11,8	7,03	6,89	1,1702	6,83

APPENDIX 3

MEASUREMENTS OF CHAPTER 8

Appendix 3 includes the data of the experimental investigation presented in chapter 8. These tests were performed in sudden expanding channels with a central sill located at various positions. Table 3.1 indicates the main characteristics of the investigated geometries whereas the relevant notation is given in Fig. 3.1.

Table 3.1 : Sudden expanding channels with a central sill: Overall characteristics of experiments.

Series	b_2	B	shape	F_1	$S=s/h_1$		x_s		h_1		X_1	No. of runs
	[m]	[-]			[-]	from	to	from	to	from		
3.1	1.5	3	sym	3, 5, 7, 9	0.6	3	20	80	2.5	7.5	0.2	78
3.2	1.0	2	sym	3, 5, 7, 9	0.6	3	20	80	2.5	7.5	0.2	75
3.3	0.75	1.5	sym	3, 5, 7, 9	0.6	3	20	80	2.5	7.5	0.2	60

In addition to the symbols indicated in Fig. 3.1, the following non-dimensional terms are used :

$Y = h_2/h_1$: experimental sequent depths ratio

$Y^* = h_2^*/h_1$: sequent depths ratio according to Eq. (5.1)

$Y_P = h_{2,p}/h_1$: predicted sequent depths ratio Eq (5.26)

$X_1 = x_1/L_r^*$: non-dimensional toe position Eq. (5.3)

$X_s = x_s/L_r^*$: non-dimensional sill position according to Eq. (8.2)

$S = s/h_1$: non-dimensional sill height

A : evaluation of the lateral eddies vorticity.

p=stagnant, m=small, b=significant.

B: evaluation of the velocity distribution in the tailwater.

p=highly non-uniform; m=non-uniform; b=nearly uniform.

- C: evaluation of the tailwater waves.
 p =large with spray; m =no spray; b =small.
- D: evaluation of the jump symmetry.
 asy =stable asymmetric; fa =oscillating flow; s =symmetric.

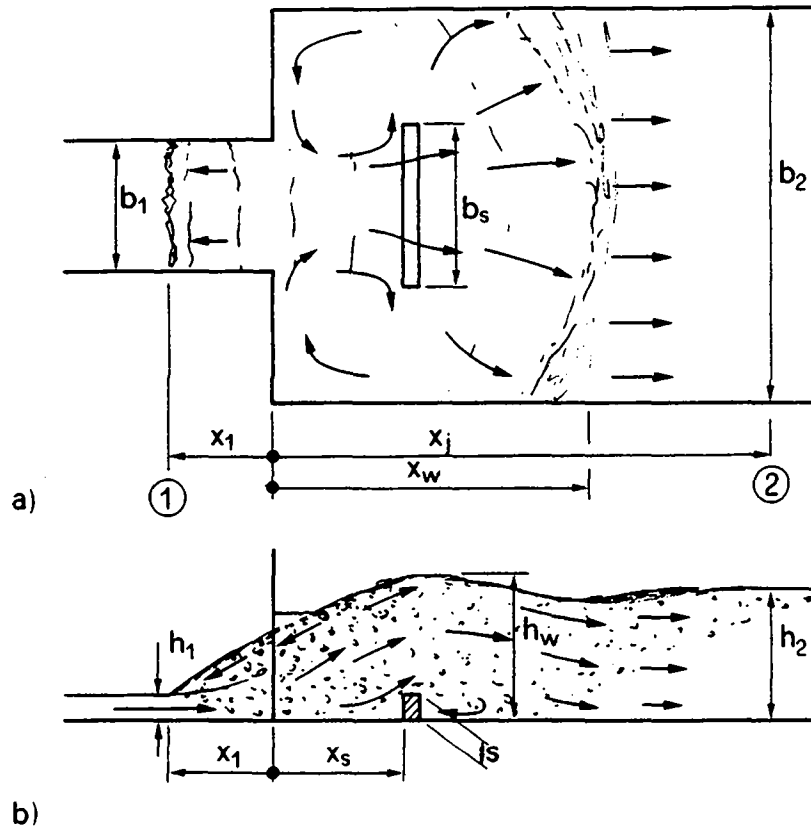


Fig. 3.1 : Relevant notation of sudden expansions with central sill investigated in chapter 8. a) Plan view; b) axial view.

SERIES : 3.1

A3 - 3

	Q	H ₁	h ₁	F ₁	x ₁	h ₂	h _w	x _w	Y	Y*	X ₁	Y _p	s	x _s	X _s	x _j	A	B	C	D
	[l/s]	[cm]	[cm]	[-]	[cm]	[cm]	[cm]	[cm]	[-]	[-]	[-]	[-]	[cm]	[cm]	[-]	[cm]				
1 A	56,0	104,0	2,51	8,99	26,0	22,1	24,3	95	8,81	12,23	0,196	9,17	5,0	40	0,30	260	m	p	p	fa
2 A	43,0	63,7	2,48	7,02	20,0	16,5	19,3	70	6,65	9,45	0,199	7,16	5,0	40	0,40	245	m	p	p	fa
3 A	31,0	33,7	2,51	4,99	14,0	12,2	15,9	65	4,87	6,57	0,201	5,08	5,0	40	0,57	200	m	p	p	asy
4 A	56,0	104,0	2,51	8,99	25,0	21,2	23,3	110	8,45	12,23	0,188	9,11	5,0	60	0,45	270	m	m	p	fa
5 A	43,0	63,7	2,48	7,02	19,0	16,8	18,8	100	6,77	9,45	0,189	7,10	5,0	60	0,60	240	p	p	p	fa
6 A	31,0	33,7	2,51	4,99	15,0	12,7	15,6	100	5,07	6,57	0,215	5,13	5,0	60	0,86	205	p	p	p	asy
7 A	56,0	104,0	2,51	8,99	24,0	22,0	26,0	105	8,77	12,23	0,181	9,05	5,0	80	0,60	270	m	p	p	fa
8 A	56,0	104,0	2,51	8,99	24,0	21,8	25,5	103	8,69	12,23	0,181	9,05	7,5	60	0,45	255	b	m	p	s-f
9 A	43,0	63,7	2,48	7,02	20,0	16,7	22,8	92	6,73	9,45	0,199	7,16	7,5	60	0,60	230	m	p	p	fa
10A	31,0	33,7	2,51	4,99	14,0	13,0	20,7	90	5,19	6,57	0,201	5,08	7,5	60	0,86	225	m	p	p	fa
11A	56,0	104,0	2,51	8,99	25,0	22,1	26,4	94	8,81	12,23	0,188	9,11	7,5	40	0,30	250	b	b	p	s
12A	43,0	63,7	2,48	7,02	20,0	16,8	23,1	80	6,77	9,45	0,199	7,16	7,5	40	0,40	230	b	m	p	s
13A	31,0	33,7	2,51	4,99	14,0	12,4	15,7	83	4,95	6,57	0,201	5,08	7,5	40	0,57	210	b	m	p	s
1 B	157,0	207,5	4,98	9,02	58,0	43,5	57,0	170	8,73	12,26	0,219	9,37	5,0	40	0,15	390	b	m	m	s
2 B	122,0	127,5	4,98	7,02	40,0	33,8	40,0	152	6,79	9,44	0,198	7,15	5,0	40	0,20	362	b	m	p	s
3 B	87,0	67,5	4,97	5,02	29,0	25,1	28,0	121	5,05	6,61	0,209	5,13	5,0	40	0,29	260	b	p	p	s
4 B	52,0	27,5	4,94	3,02	18,0	14,9	15,8	71	3,01	3,80	0,236	3,12	5,0	40	0,53	200	b	p	p	fa
5 B	157,0	207,5	4,98	9,02	55,0	42,9	54,0	175	8,61	12,26	0,208	9,29	5,0	60	0,23	390	m	b	m	s
6 B	122,0	127,5	4,98	7,02	40,0	33,8	39,8	160	6,79	9,44	0,198	7,15	5,0	60	0,30	360	b	b	m	s
7 B	87,0	67,5	4,97	5,02	31,0	24,5	27,5	149	4,93	6,61	0,223	5,19	5,0	60	0,43	275	m	m	p	fa
8 B	53,0	27,5	5,05	2,98	15,0	15,1	16,8	91	2,99	3,75	0,196	3,00	5,0	60	0,78	200	m	p	p	fa
9 B	157,0	207,5	4,98	9,02	55,0	43,7	47,0	200	8,77	12,26	0,208	9,29	5,0	80	0,30	390	m	m	m	fa
10B	122,0	127,5	4,98	7,02	40,0	33,5	32,0	170	6,73	9,44	0,198	7,15	5,0	80	0,40	340	p	m	m	asy
11B	157,0	207,5	4,98	9,02	55,0	43,9	59,2	151	8,81	12,26	0,208	9,29	7,5	40	0,15	390	b	m	m	s
12B	122,0	127,5	4,98	7,02	41,0	33,9	47,0	131	6,81	9,44	0,203	7,18	7,5	40	0,20	350	b	m	p	s
13B	87,0	67,5	4,97	5,02	29,0	23,9	27,7	103	4,81	6,61	0,209	5,13	7,5	40	0,29	280	m	p	p	s
14B	52,0	27,5	4,94	3,02	15,0	14,4	16,8	75	2,91	3,80	0,197	3,04	7,5	40	0,53	200	m	p	p	fa
15B	157,0	207,5	4,98	9,02	55,0	43,8	53,2	190	8,79	12,26	0,208	9,29	7,5	80	0,30	390	m	b	b	fa
16B	122,0	127,5	4,98	7,02	40,0	33,7	37,2	170	6,77	9,44	0,198	7,15	7,5	80	0,40	355	b	m	m	fa
17B	87,0	67,5	4,97	5,02	30,0	25,0	27,1	142	5,03	6,61	0,216	5,16	7,5	80	0,58	280	b	p	p	asy
18B	157,0	207,5	4,98	9,02	55,0	43,5	54,0	167	8,73	12,26	0,208	9,29	7,5	60	0,23	390	b	b	m	s
19B	122,0	127,5	4,98	7,02	41,0	33,9	38,0	150	6,81	9,44	0,203	7,18	7,5	60	0,30	345	b	b	p	s
20B	87,0	67,5	4,97	5,02	29,0	24,3	28,2	128	4,89	6,61	0,209	5,13	7,5	60	0,43	290	b	b	p	s
21B	53,0	27,5	5,05	2,98	14,0	14,7	16,1	90	2,91	3,75	0,183	2,97	7,5	60	0,78	205	m	p	p	fa
1 C	225,0	191,2	7,50	7,00	60,0	48,5	51,0	210	6,47	9,41	0,198	7,13	5,0	40	0,13	480	m	p	m	fa
2 C	160,0	101,2	7,46	5,01	40,0	32,5	38,0	171	4,36	6,61	0,192	5,06	5,0	40	0,19	360	m	p	m	fa
3 C	96,0	41,2	7,46	3,01	22,0	21,9	23,5	78	2,93	3,78	0,192	3,02	5,0	40	0,35	240	m	p	p	fa
4 C	225,0	191,2	7,50	7,00	59,0	51,0	57,0	201	6,80	9,41	0,195	7,11	5,0	60	0,20	440	b	b	m	s
5 C	160,0	101,2	7,46	5,01	40,0	35,7	36,1	191	4,78	6,61	0,192	5,06	5,0	60	0,29	368	m	p	m	fa
6 C	97,0	41,2	7,55	2,99	24,0	22,1	23,3	118	2,93	3,75	0,209	3,03	5,0	60	0,52	240	m	p	p	asy
7 C	225,0	191,2	7,50	7,00	60,0	51,2	53,2	210	6,83	9,41	0,198	7,13	5,0	80	0,26	430	b	b	m	s
8 C	225,0	191,2	7,50	7,00	65,0	50,9	54,0	212	6,79	9,41	0,214	7,23	5,0	60	0,20	475	b	m	b	s
9 C	160,0	101,2	7,46	5,01	42,0	35,1	34,0	192	4,70	6,61	0,201	5,10	5,0	60	0,29	360	m	s	m	fa
10C	97,0	41,2	7,55	2,99	32,0	22,6	24,0	129	2,99	3,75	0,279	3,15	5,0	60	0,52	230	m	s	p	fa
11C	225,0	191,2	7,50	7,00	60,0	51,2	57,0	200	6,83	9,41	0,198	7,13	7,5	80	0,26	425	m	m	m	s-f

Q	H ₁	h ₁	F ₁	x ₁	h ₂	h _w	x _w	Y	Y*	X ₁	Y _p	s	x _s	X _s	x _j	A	B	C	D	
[l/s]	[cm]	[cm]	[-]	[cm]	[cm]	[cm]	[cm]	[-]	[-]	[-]	[-]	[cm]	[cm]	[-]	[cm]					
12C	160,0	101,2	7,46	5,01	41,0	33,9	35,4	165	4,54	6,61	0,197	5,08	7,5	80	0,38	360	m	p	p	fa
13C	96,0	41,2	7,46	3,01	23,0	23,1	23,4	123	3,10	3,78	0,201	3,03	7,5	80	0,70	250	m	p	p	fa
14C	225,0	191,2	7,50	7,00	60,0	49,9	60,0	201	6,66	9,41	0,198	7,13	7,5	60	0,20	430	b	b	m	s
15C	160,0	101,2	7,46	5,01	41,0	35,1	41,3	160	4,70	6,61	0,197	5,08	7,5	60	0,29	350	b	b	p	s
16C	96,0	41,2	7,46	3,01	22,0	22,9	23,3	124	3,07	3,78	0,192	3,02	7,5	60	0,52	260	m	p	p	fa
17C	225,0	191,2	7,50	7,00	60,0	49,3	70,0	195	6,58	9,41	0,198	7,13	7,5	40	0,13	430	m	b	m	s
18C	160,0	101,2	7,46	5,01	41,0	35,5	45,2	150	4,76	6,61	0,197	5,08	7,5	40	0,19	350	b	b	p	s
19C	96,0	41,2	7,46	3,01	23,0	21,6	25,0	101	2,89	3,78	0,201	3,03	7,5	40	0,35	255	m	p	p	s-f

SERIES : 3.2

A3 - 5

	Q	H ₁	h ₁	F ₁	x ₁	h ₂	h _w	x _w	Y	Y*	X ₁	Y _p	s	x _s	X _s	x _j	A	B	C	D
	[l/s]	[cm]	[cm]	[-]	[cm]	[cm]	[cm]	[cm]	[-]	[-]	[-]	[-]	[cm]	[cm]	[-]	[cm]				
1 A	56,0	103,0	2,52	8,93	27,0	23,6	26,0	125	9,37	12,13	0,204	10,07	5,0	20	0,15	265	b	m	p	s
2 A	43,0	64,5	2,47	7,09	21,0	17,9	20,8	102	7,26	9,55	0,208	7,98	5,0	20	0,20	240	b	m	p	s
3 A	31,0	34,0	2,49	5,03	14,0	13,1	17,2	65	5,24	6,63	0,200	5,58	5,0	20	0,29	210	b	m	p	s
4 A	56,0	103,0	2,52	8,93	26,0	23,1	25,1	90	9,16	12,13	0,196	10,03	5,0	40	0,30	260	m	m	p	fa
5 A	43,0	64,5	2,47	7,09	19,0	18,1	20,1	65	7,35	9,55	0,188	7,90	5,0	40	0,40	235	p	p	p	fa
6 A	31,0	34,0	2,49	5,03	14,0	13,6	16,8	58	5,47	6,63	0,200	5,58	5,0	40	0,57	200	p	p	p	asy
7 A	56,0	103,0	2,52	8,93	25,0	24,7	27,0	175	9,79	12,13	0,189	9,99	7,5	40	0,30	255	b	m	p	s
8 A	43,0	64,5	2,47	7,09	21,0	17,7	23,8	158	7,18	9,55	0,208	7,98	7,5	40	0,40	220	b	b	p	s
9 A	31,0	34,0	2,49	5,03	14,0	13,1	20,5	83	5,24	6,63	0,200	5,58	7,5	40	0,57	200	b	b	p	s
10A	56,0	103,0	2,52	8,93	27,0	24,1	25,1	192	9,17	12,13	0,204	10,07	7,5	60	0,45	255	m	m	p	fa
11A	43,0	64,5	2,47	7,09	19,0	18,7	25,0	168	7,58	9,55	0,188	7,90	7,5	60	0,59	230	b	m	p	asy
12A	31,0	34,0	2,49	5,03	13,0	13,7	16,7	125	5,48	6,63	0,186	5,54	7,5	60	0,86	195	b	m	p	asy
1 B	157,0	207,5	4,98	9,02	60,0	48,8	61,5	165	9,79	12,26	0,227	10,30	5,0	40	0,15	385	b	b	p	s
2 B	122,0	128,0	4,97	7,04	39,0	35,1	42,0	148	7,07	9,47	0,193	7,86	5,0	40	0,20	355	b	b	p	s
3 B	87,0	67,5	4,97	5,02	29,0	26,1	29,2	110	5,25	6,61	0,209	5,59	5,0	40	0,29	260	b	p	p	fa
4 B	52,0	29,0	4,77	3,19	17,0	15,7	16,7	62	3,28	4,04	0,217	3,49	5,0	40	0,51	200	b	p	p	asy
5 B	157,0	207,5	4,98	9,02	54,0	46,2	57,1	170	9,27	12,26	0,204	10,18	5,0	60	0,23	395	b	b	m	s
6 B	122,0	128,0	4,97	7,04	41,0	36,9	43,0	158	7,42	9,47	0,203	7,90	5,0	60	0,30	350	b	b	m	fa
7 B	87,0	67,5	4,97	5,02	30,0	25,9	28,9	151	5,22	6,61	0,216	5,61	5,0	60	0,43	280	m	m	p	asy
8 B	53,0	29,0	4,87	3,15	14,0	15,7	17,6	96	3,22	3,98	0,177	3,39	5,0	60	0,76	220	m	p	p	asy
9 B	157,0	207,5	4,98	9,02	54,0	46,7	52,0	202	9,37	12,26	0,204	10,18	5,0	80	0,30	380	m	m	m	asy
10B	122,0	128,0	4,97	7,04	39,0	37,9	38,5	158	7,62	9,47	0,193	7,86	5,0	80	0,40	350	p	m	m	asy
11B	157,0	207,5	4,98	9,02	54,0	47,2	55,2	146	9,47	12,26	0,204	10,18	7,5	40	0,15	385	b	p	m	s
12B	122,0	128,0	4,97	7,04	40,0	36,4	48,8	130	7,33	9,47	0,198	7,88	7,5	40	0,20	350	b	b	p	s
13B	87,0	67,5	4,97	5,02	29,0	26,1	29,5	98	5,25	6,61	0,209	5,59	7,5	40	0,29	285	m	m	p	s
14B	52,0	29,0	4,77	3,19	14,0	16,1	18,6	58	3,37	4,04	0,178	3,44	7,5	40	0,51	210	m	p	p	fa
15B	157,0	207,5	4,98	9,02	54,0	49,2	57,0	195	9,88	12,26	0,204	10,18	7,5	80	0,30	395	m	b	b	fa
16B	122,0	128,0	4,97	7,04	40,0	38,0	41,3	150	7,64	9,47	0,198	7,88	7,5	80	0,40	340	b	m	p	asy
17B	87,0	67,5	4,97	5,02	29,0	26,7	28,8	130	5,37	6,61	0,209	5,59	7,5	80	0,58	260	b	p	p	asy
18B	157,0	207,5	4,98	9,02	54,0	46,7	56,7	165	9,37	12,26	0,204	10,18	7,5	60	0,23	390	b	b	m	s
19B	122,0	128,0	4,97	7,04	40,0	36,0	40,2	150	7,25	9,47	0,198	7,88	7,5	60	0,30	330	b	b	p	s
20B	87,0	67,5	4,97	5,02	28,0	26,6	30,5	127	5,35	6,61	0,202	5,57	7,5	60	0,43	270	b	m	p	fa
21B	53,0	29,0	4,87	3,15	14,0	16,2	17,7	85	3,32	3,98	0,177	3,39	7,5	60	0,76	205	m	p	p	asy
1 C	225,0	191,0	7,50	7,00	59,0	53,3	54,2	195	7,11	9,41	0,195	7,81	5,0	60	0,20	485	b	b	m	s
2 C	160,0	102,0	7,43	5,05	39,0	38,8	41,6	178	5,23	6,65	0,187	5,56	5,0	60	0,29	360	m	p	m	fa
3 C	96,0	41,0	7,49	2,99	22,0	23,0	24,4	115	3,07	3,76	0,193	3,24	5,0	60	0,53	250	m	p	p	asy
4 C	225,0	191,0	7,50	7,00	58,0	56,9	63,2	201	7,72	9,41	0,191	7,80	5,0	80	0,26	430	b	b	m	asy
5 C	160,0	102,0	7,43	5,05	40,0	38,1	38,5	190	5,13	6,65	0,191	5,57	5,0	80	0,38	375	m	p	m	asy
6 C	97,0	41,0	7,58	2,97	25,0	23,4	24,6	83	3,08	3,73	0,219	3,25	5,0	40	0,35	250	m	p	p	asy
7 C	225,0	191,0	7,50	7,00	60,0	54,6	56,0	209	7,28	9,41	0,198	7,83	5,0	80	0,26	425	b	b	m	fa
8 C	225,0	191,0	7,50	7,00	65,0	55,1	58,2	184	7,34	9,41	0,214	7,89	5,0	60	0,20	470	b	b	m	s
9 C	160,0	102,0	7,43	5,05	42,0	37,9	36,5	188	5,10	6,65	0,201	5,60	5,0	60	0,29	365	m	s	m	fa
10C	97,0	41,0	7,58	2,97	31,0	24,8	26,1	122	3,28	3,73	0,271	3,31	5,0	60	0,52	230	m	s	p	asy
11C	225,0	191,0	7,50	7,00	59,0	55,1	60,9	195	7,35	9,41	0,195	7,81	7,5	80	0,26	410	b	b	m	s
12C	160,0	102,0	7,43	5,05	39,0	38,0	39,8	188	5,12	6,65	0,187	5,56	7,5	80	0,38	370	m	p	p	asy

Q	H ₁	h ₁	F ₁	x ₁	h ₂	h _w	x _w	Y	Y*	X ₁	Y _p	s	x _s	X _s	x _j	A	B	C	D	
[l/s]	[cm]	[cm]	[-]	[cm]	[cm]	[cm]	[cm]	[-]	[-]	[-]	[-]	[cm]	[cm]	[-]	[cm]					
13C	96,0	41,0	7,49	2,99	21,0	23,4	25,1	135	3,13	3,76	0,184	3,22	7,5	80	0,70	260	■	p	p	asy
14C	225,0	191,0	7,50	7,00	61,0	53,5	61,1	195	7,14	9,41	0,201	7,84	7,5	60	0,20	420	b	■	■	s
15C	160,0	102,0	7,43	5,05	40,0	36,9	43,1	168	4,96	6,65	0,191	5,57	7,5	60	0,29	360	b	b	p	s
16C	96,0	41,0	7,49	2,99	21,0	23,1	24,3	115	3,09	3,76	0,184	3,22	7,5	60	0,53	260	■	p	p	fa
17C	160,0	102,0	7,43	5,05	41,0	39,4	49,3	182	5,31	6,65	0,196	5,59	7,5	40	0,19	360	b	■	p	s
18C	96,0	42,0	7,37	3,07	22,0	23,7	26,2	158	3,22	3,87	0,190	3,32	7,5	40	0,35	250	b	b	p	s

SERIES : 3.3

A3 - 7

Q	H ₁	h ₁	F ₁	x ₁	h ₂	h _w	x _w	Y	Y*	X ₁	Y _p	s	x _s	X _s	x _j	A	B	C	D	
[1/s]	[cm]	[cm]	[-]	[cm]	[cm]	[cm]	[cm]	[-]	[-]	[-]	[-]	[cm]	[cm]	[-]	[cm]					
1 A	56,0	103,0	2,52	8,93	25,0	25,4	25,1	83	10,07	12,13	0,189	10,79	2,5	20	0,15	250	m	m	p	s
2 A	43,0	64,5	2,47	7,09	20,0	19,6	20,1	69	7,95	9,55	0,198	8,54	2,5	20	0,20	240	m	m	p	s
3 A	31,0	34,0	2,49	5,03	15,0	14,4	16,8	60	5,77	6,63	0,215	5,99	2,5	20	0,29	190	b	b	p	s
4 A	56,0	103,0	2,52	8,93	26,0	24,6	27,0	121	9,75	12,13	0,196	10,82	2,5	40	0,30	260	b	m	p	asy
5 A	43,0	64,5	2,47	7,09	20,0	20,4	21,8	104	8,28	9,55	0,198	8,54	2,5	40	0,40	210	b	b	p	asy
6 A	31,0	34,0	2,49	5,03	15,0	14,8	20,5	64	5,93	6,63	0,215	5,99	2,5	40	0,57	200	b	b	p	asy
7 A	56,0	103,0	2,52	8,93	27,0	26,6	27,8	113	10,55	12,13	0,204	10,84	2,5	60	0,45	260	m	m	p	asy
8 A	43,0	64,5	2,47	7,09	21,0	20,4	25,0	98	8,26	9,55	0,208	8,57	2,5	60	0,59	225	b	m	p	asy
9 A	31,0	34,0	2,49	5,03	15,0	14,8	16,7	78	5,93	6,63	0,215	5,99	2,5	60	0,86	200	b	m	p	asy
10A	43,0	64,5	2,47	7,09	21,0	19,4	20,8	65	7,88	9,55	0,208	8,57	5,0	20	0,20	235	b	m	p	s
11A	31,0	34,0	2,49	5,03	15,0	14,1	17,2	60	5,67	6,63	0,215	5,99	5,0	20	0,29	210	b	m	p	s
12A	56,0	103,0	2,52	8,93	26,0	25,8	25,1	101	10,23	12,13	0,196	10,82	5,0	40	0,30	250	b	b	m	s
13A	43,0	64,5	2,47	7,09	21,0	19,7	20,1	88	7,99	9,55	0,208	8,57	5,0	40	0,40	245	b	b	p	s
14A	31,0	34,0	2,49	5,03	14,0	14,3	16,8	69	5,73	6,63	0,200	5,97	5,0	40	0,57	190	p	p	p	asy
15A	56,0	103,0	2,52	8,93	27,0	25,3	27,0	96	10,03	12,13	0,204	10,84	7,5	40	0,30	240	b	m	p	s
16A	43,0	64,5	2,47	7,09	19,0	19,2	23,8	93	7,79	9,55	0,188	8,51	7,5	40	0,40	210	b	b	p	s
17A	31,0	34,0	2,49	5,03	15,0	13,8	20,5	78	5,55	6,63	0,215	5,99	7,5	40	0,57	190	b	b	p	s
18A	56,0	103,0	2,52	8,93	28,0	26,2	25,1	103	10,39	12,13	0,211	10,87	7,5	60	0,45	270	m	m	p	fa
19A	43,0	64,5	2,47	7,09	21,0	20,4	25,0	86	8,26	9,55	0,208	8,57	7,5	60	0,59	240	b	m	p	asy
20A	31,0	34,0	2,49	5,03	14,0	13,5	16,7	69	5,41	6,63	0,200	5,97	7,5	60	0,86	200	b	m	p	asy
1 B	157,0	207,5	4,98	9,02	58,0	50,6	61,5	175	10,15	12,26	0,219	11,01	5,0	40	0,15	400	b	m	p	s
2 B	122,0	128,0	4,97	7,04	40,0	38,2	42,0	148	7,70	9,47	0,198	8,47	5,0	40	0,20	360	m	b	p	s
3 B	87,0	67,5	4,97	5,02	30,0	27,3	29,2	125	5,49	6,61	0,216	5,98	5,0	40	0,29	250	b	b	m	s
4 B	52,0	29,0	4,77	3,19	15,0	16,2	16,7	69	3,40	4,04	0,191	3,67	5,0	40	0,51	190	b	p	p	asy
5 B	157,0	207,5	4,98	9,02	53,0	51,9	57,1	174	10,41	12,26	0,200	10,95	5,0	60	0,23	385	b	b	m	s
6 B	122,0	128,0	4,97	7,04	38,0	40,3	43,0	161	8,11	9,47	0,188	8,45	5,0	60	0,30	340	b	m	m	fa
7 B	87,0	67,5	4,97	5,02	32,0	27,0	28,9	145	5,45	6,61	0,230	6,01	5,0	60	0,43	270	m	m	p	asy
8 B	53,0	29,0	4,87	3,15	14,0	16,9	17,6	84	3,47	3,98	0,177	3,61	5,0	60	0,76	210	m	p	p	asy
9 B	157,0	207,5	4,98	9,02	54,0	51,3	55,2	165	10,30	12,26	0,204	10,96	7,5	40	0,15	390	b	p	m	s
10B	122,0	128,0	4,97	7,04	41,0	38,7	48,8	151	7,79	9,47	0,203	8,48	7,5	40	0,20	340	b	b	p	s
11B	87,0	67,5	4,97	5,02	28,0	28,5	29,5	121	5,73	6,61	0,202	5,96	7,5	40	0,29	270	b	b	p	s
12B	52,0	29,0	4,77	3,19	16,0	16,2	18,6	74	3,40	4,04	0,204	3,68	7,5	40	0,51	200	m	p	p	fa
13B	157,0	207,5	4,98	9,02	55,0	53,0	56,7	178	10,63	12,26	0,208	10,97	7,5	60	0,23	400	b	b	m	s
14B	122,0	128,0	4,97	7,04	41,0	39,5	40,2	158	7,96	9,47	0,203	8,48	7,5	60	0,30	320	b	b	p	s
15B	87,0	67,5	4,97	5,02	28,0	28,1	30,5	146	5,66	6,61	0,202	5,96	7,5	60	0,43	250	b	m	p	fa
16B	53,0	29,0	4,87	3,15	16,0	16,2	17,7	92	3,32	3,98	0,203	3,63	7,5	60	0,76	190	m	p	p	asy
1 C	225,0	191,0	7,50	7,00	55,0	58,0	54,2	192	7,74	9,41	0,181	8,37	5,0	60	0,20	460	b	b	m	s
2 C	160,0	102,0	7,43	5,05	42,0	40,4	41,6	184	5,43	6,65	0,201	5,99	5,0	60	0,29	370	m	p	m	s
3 C	96,0	41,0	7,49	2,99	25,0	23,6	24,4	112	3,16	3,76	0,219	3,45	5,0	60	0,53	260	m	p	p	asy
4 C	97,0	41,0	7,58	2,97	25,0	24,1	24,6	100	3,19	3,73	0,219	3,43	5,0	40	0,35	250	m	p	p	asy
5 C	225,0	191,0	7,50	7,00	57,0	58,1	56,0	206	7,74	9,41	0,188	8,39	5,0	80	0,26	410	b	m	m	fa
6 C	225,0	191,0	7,50	7,00	63,0	56,5	58,2	200	7,53	9,41	0,208	8,44	5,0	60	0,20	460	b	b	m	s
7 C	160,0	102,0	7,43	5,05	45,0	42,3	36,5	185	5,69	6,65	0,215	6,02	5,0	60	0,29	370	m	s	m	fa
8 C	97,0	41,0	7,58	2,97	24,0	24,7	26,1	124	3,26	3,73	0,210	3,42	5,0	60	0,52	240	m	s	p	asy
9 C	225,0	191,0	7,50	7,00	57,0	58,7	60,9	195	7,82	9,41	0,188	8,39	7,5	80	0,26	400	b	b	m	s
10C	160,0	102,0	7,43	5,05	42,0	39,9	39,8	177	5,37	6,65	0,201	5,99	7,5	80	0,38	360	m	p	p	asy

Q	H ₁	h ₁	F ₁	x ₁	h ₂	h _w	x _w	Y	Y*	X ₁	Y _p	s	x _s	X _s	x _j	A	B	C	D	
[1/s]	[cm]	[cm]	[-]	[cm]	[cm]	[cm]	[cm]	[-]	[-]	[-]	[-]	[cm]	[cm]	[-]	[cm]					
11C	96,0	41,0	7,49	2,99	23,0	23,8	25,1	133	3,18	3,76	0,202	3,44	7,5	80	0,70	270	■	p	p	asy
12C	225,0	191,0	7,50	7,00	57,0	60,0	61,1	194	8,00	9,41	0,188	8,39	7,5	60	0,20	420	b	■	■	s
13C	160,0	102,0	7,43	5,05	41,0	41,3	43,1	158	5,56	6,65	0,196	5,99	7,5	60	0,29	370	b	b	■	s
14C	96,0	41,0	7,49	2,99	24,0	23,6	24,3	135	3,15	3,76	0,210	3,45	7,5	60	0,53	250	■	p	p	fa
15C	160,0	102,0	7,43	5,05	41,0	41,8	49,3	153	5,63	6,65	0,196	5,99	7,5	40	0,19	350	b	■	p	s
16C	96,0	42,0	7,37	3,07	23,0	23,6	26,2	90	3,21	3,87	0,199	3,53	7,5	40	0,35	260	b	b	p	s

REFERENCES

- Arbhabhira, A. & Abella, A.U. (1971): Hydraulic Jump within Gradually Expanding Channel. Proc. ASCE, *J. Hydraulics Division* 97(HY1): 31-42. Discussions 1971, 97(HY9): 1567-1570; 1971, 97(HY10): 1788-1790; 1972, 98(HY9): 1717-1719.
- Arbhabhira, A. & Wan, W.-C. (1975): Characteristics of a Circular Jump in a Radial Wall Jet. *J. Hydraulic Research* 13(3): 239-257.
- Bakhmeteff, B.A. & Matzke, A.E. (1936): The Hydraulic Jump in Terms of Dynamic Similarity. *Trans. ASCE* 100: 630-680.
- Ball, J.W. (1963): Construction finishes and high-velocity flow. Proc. ASCE, *J. Hydraulics Division*, 89: 91-110.
- Ball, J.W. (1976): Construction from surface irregularities in high velocity. Proc. ASCE, *J. Hydraulics Division*, 102(HY9): 1283-1297.
- Bretz, N.V. (1987): Ressaut Hydraulique Forcé par Seuil. Thesis No. 699, presented to the Swiss Federal Institute of Technology, Lausanne (EPFL). Appeared also as *Communication No. 2*, Laboratoire de Constructions Hydrauliques, EPFL, ed. R. Sinniger, Lausanne, Switzerland.
- Bundschi, F. (1928): Das Wasserauflauten. *Bauingenieur* 9(27): 493-497.
- Chow, V.T. (1959): *Open Channels Hydraulics*, McGraw-Hill: New York.
- Cvetkov, P.K. (1952): Hydraulische Berechnung eines in Strömungsrichtung sich verbreiternden Tosbeckens. *Hydrotechnisches Bauwesen*: H10.
- Einwachter, J. (1932): Berechnung der Deckwalzenbreite des freien Wassersprunges. *Wasserkraft und Wasserwirtschaft* 27(21): 245-249.
- Elevatorsky, E.A. (1959): *Hydraulic Energy Dissipators*. McGraw-Hill Book Company: New York-Toronto-London.
- France, P.W. (1981a): An Investigation of a Jet-Assisted Hydraulic Jump. *J. Hydraulic Research* 19(4): 325-337; 1982, 20(4): 363-364.

France, P.W. (1981b): Analysis of the Hydraulic Jump within a Diverging Rectangular Channel. *Proc. Institution Civil Engineers Part 2*, 71(Jun): 369-378. Discussion 1981, 71(Dec): 237-239.

Frank, J. (1943): Der Wechselsprung und die Bemessung der Tosbecken an Wehren. *Wasserkraft und Wasserwirtschaft* 38(3): 49-57.

Gerndt, R.D. (1971): Beitrag zur Untersuchung der Bewegungsvorgänge in Tosbecken mit geradliniger, allmählicher Erweiterung. *Thesis* presented to the Technical University of Aachen; appeared also as *Mitteilung* No. 3, Institut für Wasserbau, Technical University Aachen, ed. Prof. Borkenstein, Aachen: 1971.

Hager, W.H. (1985a): B-Jumps at Abrupt Channel Drops. *Proc. ASCE, J. Hydraulic Engineering*, 111(5): 861-866.

Hager, W.H. (1985b): Hydraulic Jump in Non-Prismatic Rectangular Channels. *J. Hydraulic Research* 23(1): 21-35. Discussion 1985, 23(4): 386-389.

Hager, W.H. (1986): Discharge Measurement Structures, *Communication 1*, Laboratoire de Constructions Hydrauliques EPFL, ed. R. Sinniger, Switzerland.

Hager, W.H., & Bremen, R. (1989): Viscosity Effects on Classical Hydraulic Jump. *J. Hydraulic Research* 27,

Hager, W.H., Bremen, R. & Kawagoshi, N. (1989): Classical Hydraulic Jump : Sequent Depth *J. Hydraulic Research* 27(5): 565-585.

Hager, W.H., Bremen, R. & Kawagoshi, N. (1990): Classical Hydraulic Jump : Length of Roller *J. Hydraulic Research* 28, to be published.

Hager, W.H. & Sinniger, R. (1985): Flow Characteristics of the Hydraulic Jump in a Stilling Basin with an Abrupt Bottom Rise. *J. Hydraulic Research* 23(2); 101-113. Discussion 1986, 24(3): 207-215.

Harleman, D.R.F: (1959): Discussion to Rouse, et al. (1959), *Trans. ASCE*. Vol. 124: 959-962.

Hartung, F. (1972): Gestaltung von Hochwasserentlastungsanlagen bei Talsperrendämmen. *Wasserwirtschaft* 62(1/2): 39-51.

Herbrand, K. (1970): Der räumliche Wechselsprung - literaturstudie. Bericht Nr. 18, Versuchsanstalt für Wasserbau der Technischen Universität München, Oscar v. Miller Institut, ed. F. Hartung, München.

Herbrand, K. (1971): Das Tosbecken mit seitlicher Aufweitung. *Bericht* Nr. 21, Versuchsanstalt für Wasserbau der Technischen Universität München, Oscar v. Miller Institut, ed. F. Hartung, München.

Herbrand, K. (1973): The Spatial Hydraulic Jump. *J. Hydraulic Research* 11(3): 205-217. Discussion 1974, 12(3): 389-400.

Herbrand, K. & Knauss, J. (1973): Computation and Design of Stilling Basins with Abruptly or Gradually Enlarged Boundaries. Commission Internationale des Grands Barrages ICOLD, 11e Congrès, Madrid, Q.41, R.4, 57-79.

Karki, K.S. (1976): Supercritical Flow over Sills. Proc. ASCE, *J. Hydraulics Division* 102(HY10): 1449-1459. Discussions 1977(HY5): 584-585; 1977, 103(HY10): 1245-1247; 1978, 104(HY4): 571.

Kawagoshi, N. & Hager, W.H. (1990): Wave Type Flow at Abrupt Drops - I. Flow Geometry. *J. Hydraulic Research* to be published.

Khalifa, A.M. & McCorquodale, J.A. (1979): Radial Hydraulic Jump. Proc. ASCE, *J. Hydraulics Division* 105(HY9): 1065-1078).

Koloseus, H.J. & Ahmad, D. (1969): Circular Hydraulic Jump. Proc. ASCE, *J. Hydraulics Division* 95(HY1): 409-422. Discussion 1969, 95(HY6): 2197-2200; 1970, 96(HY7): 1610-1611.

Kusnetzow, S.K. (1958): Die Fliessbewegung bei plötzlicher Verbreiterung des Strombettes. *Gidrotechnicheskoe Stroitel'stvo (Russ.)* 27(H6): 34-37.

Macha, L. (1963) : Untersuchungen über die Wirksamkeit von Tosbecken. *Dissertation* TU Berlin, appeared also as *Mitteilung* No. 61 (Teil 1) and No 62 (Teil 2), Institut für Wasserbau und Wasserwirtschaft, TU Berlin: Berlin.

Magalhaes, A. Pinto de (1979): Bacias de Dissipação de Energia Divergentes em Planta de Secção Rectangular e com Fundo Horizontal. Laboratorio Nacional de Engenharia Civil (LNEC), *Memoria* No. 529: Lisboa.

Magalhaes, de M. & Minton, P. (1975): Design Implications of Hydraulic Jumps of Sudden Enlargements. *Proc. Instn. Civ. Engrs.* Part 2. 59(March): 169-174.

Mason, P.J. (1982): The choice of Hydraulic Energy Dissipator for Dam Outlet Works Based on a Survey of Prototype Usage. *Proc. Institution Civil Engineers*, London, part. 1, 72(May): 209-219. Discussions 74(Feb): 123-126.

Mazumder, S.K. & Sharma, A. (1983): Stilling Basins with Diverging Side Walls. *XX IAHR-Congress, Moscow*, 7; 490-492.

Mazumder, S.K., & Naresh, H.S. (1988): Use of Appurtenances for Economic and Efficient Design of Jump-Type Dissipator Having Diverging Side Walls for Flumed Canal Falls. *J. Institution of Engineers, India* 68(May): 284-290.

McCorquodale, J.-A. & Regts, E.H. (1968): A Theory for the Forced Hydraulic Jump. *Trans. Engineering Institute Canada* 11(C-1, Aug): 1-9.

Nettleton, P.C. & McCorquodale, J.A. (1983): Radial Stilling Basins with Baffles. *6th Canadian Hydrotechnical Conference, Ottawa, Ont., June 2 and 3*: 651-670.

Nettleton, P.C. & McCorquodale, J.A. (1989): Radial Stilling Basins with Baffles Blocks. *J. of Civil Engineering*, 16: 489-497.

Noseda, G. (1963): La Formazione del Risalto Lungo una Corrente Veloce in Espansione. *VIII Convegno di Idraulica, Pisa*, A4:1-11.

Noseda, G. (1964): Un Fenomeno di Instabilità del Risalto Lungo una Corrente Veloce in Espansione. *L'Energia Elettrica* 41(4): 249-254.

Oosterholt, G.A. (1944): An Investigation of the Energy Dissipated in a Surface Roller. *Appl. Sci. Res.* A1: 107-130.

Peterka, A.J. (1954): *Spillway tests confirm model-prototype conformance*. United States Department of the Interior. Bureau of Reclamation. Engineering Monograph, 16: Denver, Colorado.

Peterka, A.J. (1958): *Hydraulic Design of Stilling Basins and Energy Dissipators*. US Department Interior, Bureau of Reclamation, Engineering Monograph, 25: Denver, Col. (Appeared also as 7th printing in 1983).

Pezzoli, G. (1969): La Stabilità del Risalto Idraulico negli Alvei Non Prismatici. *L'Energia Elettrica* 46(11): 753-758.

Paderi, F. (1964): Il Calcolo del Risalto Idraulico in Canale Divergente a Fondo Orizzontale. *Giornale del Genio Civile*: 760-772.

Paderi, F. (1966): Equazioni Adimensionali e Abaco Generale per il Calcolo del Risalto Idraulico in Canale Divergente Prismatico o Convergente, a Sezione Rettangolare e a Fondo Orizzontale. *Giornale del Genio Civile* : 635-651.

Rajaratnam, N. (1964): The Forced Hydraulic Jump. *Water Power* 16(Jan): 14-19; 16(Feb): 61-65.

Rajaratnam, N. (1965): The Hydraulic Jump as a Wall Jet. Proc. ASCE, *J. Hydraulics Division* 91(HY5): 107-132. Discussion 1966, 92(HY3): 110-123; 1967, 93(HY1): 74-76.

Rajaratnam, N. (1967): Hydraulic Jumps. In *Advances in Hydrosiences*, 4:197-280, ed. V.T: Chow, Academic Press: New York.

Rajaratnam, N. & Subramanya, K. (1968): Hydraulic Jumps below Abrupt Symmetrical Expansions. Proc. ASCE, *J. Hydraulics Division* 94(HY2): 481-503. Discussion 1969, 95(HY2): 723-724; 1970, 96(HY2): 579.

Rajaratnam, N. & Subramanya, K. (1968): Profile of the Hydraulic Jump. Proc. ASCE, *J. Hydraulics Division* 94(HY3): 663-673. Discussion 1969, 95(HY1): 546-557; 1969, 95(HY2): 725-727; 1970, 96(HY2): 579-580.

Riegel, R.M. & Beebe, J.C. (1917): The Hydraulic Jump as a Means of Dissipating Energy. Miami Conservancy District. *Technical Reports* Parts III: Dayton (Ohio).

Rouse, H., Bhootha, B.V. & Hsu, E.Y. (1951): Design of Channel Expansions. *Trans. ASCE* 116: 326-346.

Rouse, H. & Jezdinsky, V. (1965): Cavitation and Energy Dissipation in Conduit Expansions. *XI IAHR Congress Leningrad*, 1(28): 1-7.

Rouse, H. Tien To Siao & Nagaratnam, S. (1959): Turbulence Characteristics of the Hydraulic Jump. *Trans. ASCE* 124: 926-966.

Rubatta, A. (1963): Il Risalto Idraulico in Canale Divergente. *L'Energia Elettrica* 40(10): 783-790.

Rubatta, A. (1964): Il Risalto Idraulico in Canale Convergente. *L'Energia Elettrica* 41(5): 329-334.

Safranez, K. (1929): Untersuchungen über den Wechselsprung. *Bauingenieur* 10(37): 649-651; 10(38): 668-677.

Sarma, K.V.N. & Newham, D.A. (1973): Surface profiles of Hydraulic Jump for Froude Numbers less than Four. *Water Power* 25(Apr): 139-142.

Schröder, R. (1957): Untersuchungen über Diskontinuierliche Abflussvorgänge in Freispiegelgerinnen. *Dissertation* TU Berlin; appeared also as *Mitteilung* No. 48, Institut für Wasserbau, TU Berlin: Berlin.

Schröder, R. (1963): Die Turbulente Strömung im Freien Wechselsprung. Habilitationsschrift. *Mitteilung* No. 59, Institut für Wasserbau und Wasserwirtschaft, TU Berlin, ed. H. Press: Berlin.

Sharma, H.R. (1963): Der räumliche Wechselsprung und seine Probleme. *Wissenschaftliche Zeitschrift der Technischen Universität Dresden* 12(6): 1731-1738.

Sharma, H.R. (1965): Der geknickte Wechselsprung. *Wissenschaftliche Zeitschrift der Technischen Universität Dresden* 14(1): 73-79.

Torres, W.J. (1979): On the Designing of Forcel Spatial Hydraulic Jump Energy Dissipators. XVIII IAHR-Congress, Cagliari, 4(C.a.): 55-62.

Unny, T.E. (1960): *Der Räumliche Wechselsprung*. Dissertation TU Dresden.

Unny, T.E. (1961): The Spatial Hydraulic Jump. Proc. of the 9th *Convention of Internat. Association for Hydraulic Research IAHR*, Belgrad.

CURRICULUM VITAE

Nom, prénom : BREMEN Roger
Date de naissance : 20 juin 1963
Nationalité : allemande
Etat civil : célibataire
Adresse : Av. Menton 4, 1005 Lausanne

Formation scolaire :

1969-1974 Ecole primaire de Giubiasco (Tessin).
1974-1982 Liceo classico e scientifico di Bellinzona (Tessin).
Obtention d'une maturité cantonale type C.
1982-1987 Etudes à l'Ecole Polytechnique Fédérale de Lausanne.
Le travail pratique de diplôme a été consacré à l'étude de l'écoulement dans des canaux collecteurs.
Meilleure moyenne générale (9.3/10) de la volée de génie civil 1986/1987.

Diplôme : Ingénieur civil EPF (1987)

Activité professionnelle :

1987-1990 Travail de doctorat (en cours) auprès du Laboratoire de Constructions Hydrauliques de l'EPFL.
L'étude porte sur les bassins amortisseurs avec élargissement.
Pendant cette période, plusieurs publications touchant différents domaines de l'hydraulique ont été publiées dans des revues spécialisées

Lausanne, le 30 avril 1990

